CATALOG OF APOLLO 15 ROCKS

Part 2. 15306—15468

Curatorial Branch Publication 72
JSC 20787
October 1985

GRAHAM RYDER
(Lunar and Planetary Institute;
Northrop Services, Inc.)

National Aeronautics and
Space Administration

Lyndon B. Johnson Space Center
Houston, Texas

CATALOG OF APOLLO 15 ROCKS

Part 2. 15306—15468

GRAHAM RYDER
(Lunar and Planetary Institute;
Northrop Services, Inc.)

October 1985

CATALOG OF APOLLO 15 ROCKS

CONTENTS:

15306 REGOLITH BRECCIA ST. 7 134.2 g

INTRODUCTION: 15306 is a typical glassy regolith breccia. It contains glass as balls and shards, many undevitrified; some lithic (undevitrified) fragments; and numerous mineral fragments in a glassy, opaque brown matrix. It contains one clast which is probably a pristine highlands igneous lithology. Macroscopically, it is brownish-gray, subangular and coherent (Fig. 1). Its surface is irregular and has a few zap pits. 15306 was collected with the soil sample at the rake site on the north-east rim of Spur Crater.

PETROLOGY: 15306 is a regolith breccia (Fig. 2). It has an opaque, brown, glassy matrix. According to Wentworth and McKay (1984) it is subporous, with a density of 2.34 gm/cm^3. Glass spheres and shards are prominent, and include green, yellow, orange, and colorless varieties. Most are undevitrified, but a few are brown because of devitrification. Best and Minkin (1972) included 15306 glass in a series of analyses of Apollo 15 glass, but tabulated only one glass analysis. Much of 15306 consists of mineral fragments.

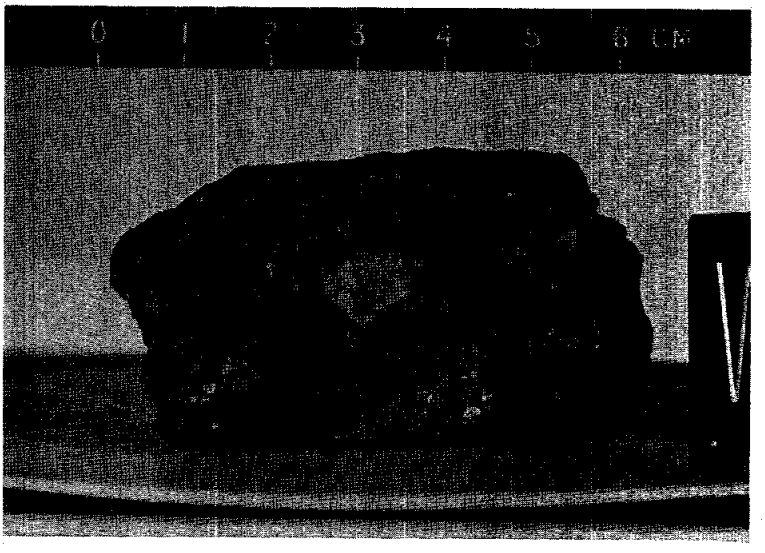

Figure 1. Macroscopic view of 15306,0 following breakage of some splits from the visible side. Prominent clast in center is labelled "A". S-71-44401.

Figure 2. Photomicrograph of 15306,6, general matrix view. Transmitted light. Width about 2mm.

Lithic clasts are generally sparse and small. One depicted in Figure 2 is apparently a plagioclase-poikilitic mare basalt. Warren and Wasson (1980) described and chemically analyzed two clasts, both highlands, one of which is probably pristine. The "probably pristine" clast (CL21) is about 8 x 7 mm in surface expression. It consists modally of about 55% plagioclase, 25% orthopyroxene, 20% olivine, and 1% opaques. Most of the plagioclase is maskelynitized, with the maskelynite slightly more calcic ($An_{94.1}$) than non-maskelynitized plagioclase ($An_{93.2}$). The mafic grains are less than 0.3 mm across and are scattered. Mineral compositions are shown in Figure 3. Metal compositions suggest that the clast is pristine; although the chemical analysis suggest contamination, this might be from 15306 matrix which is difficult to separate from the clast. A second clast (CL25), 5 x 5 mm, is not pristine. It is a noritic anorthosite containing 79% plagioclase, and is essentially a polymict breccia with some granulitic texture. Mineral compositions are shown in Figure 4 and show a wide variation.

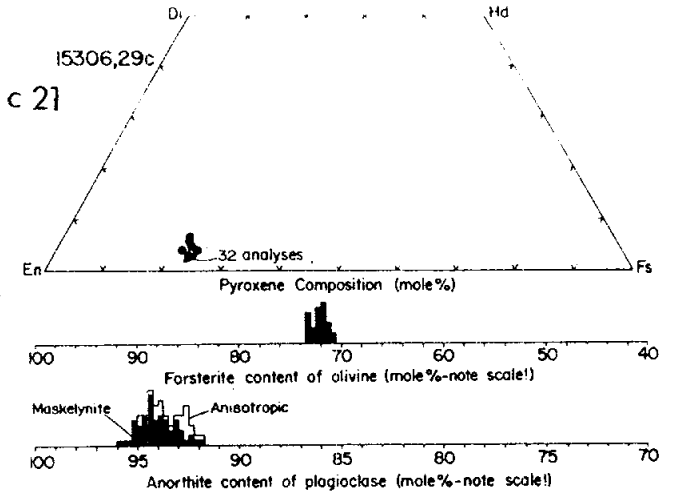

Figure 3. Mineral compositions in C21 (Warren and Wasson, 1980).

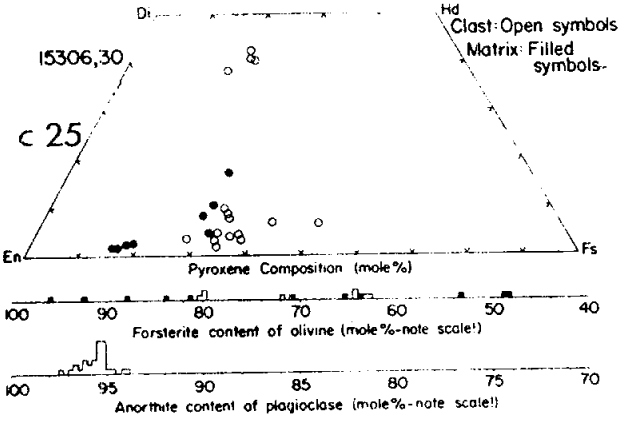

Figure 4. Mineral compositions in C25 (Warren and Wasson, 1980).

CHEMISTRY: Only C, N, and S analyses have been reported for the bulk matrix (Table 1). Two clasts were analyzed for major and trace elements (Table 1); their rare earth patterns are shown in Figure 5. The chemistry suggests that both clasts are contaminated with meteoritic material, but Warren and Wasson (1980) suggest that CL21 is "probably pristine", on the basis of homogeneous mineral compositions and metal compositions, even though its siderophiles are high and its rare earth pattern is essentially that of KREEP. The non-pristine clast CL25 also has a KREEP rare earth pattern.

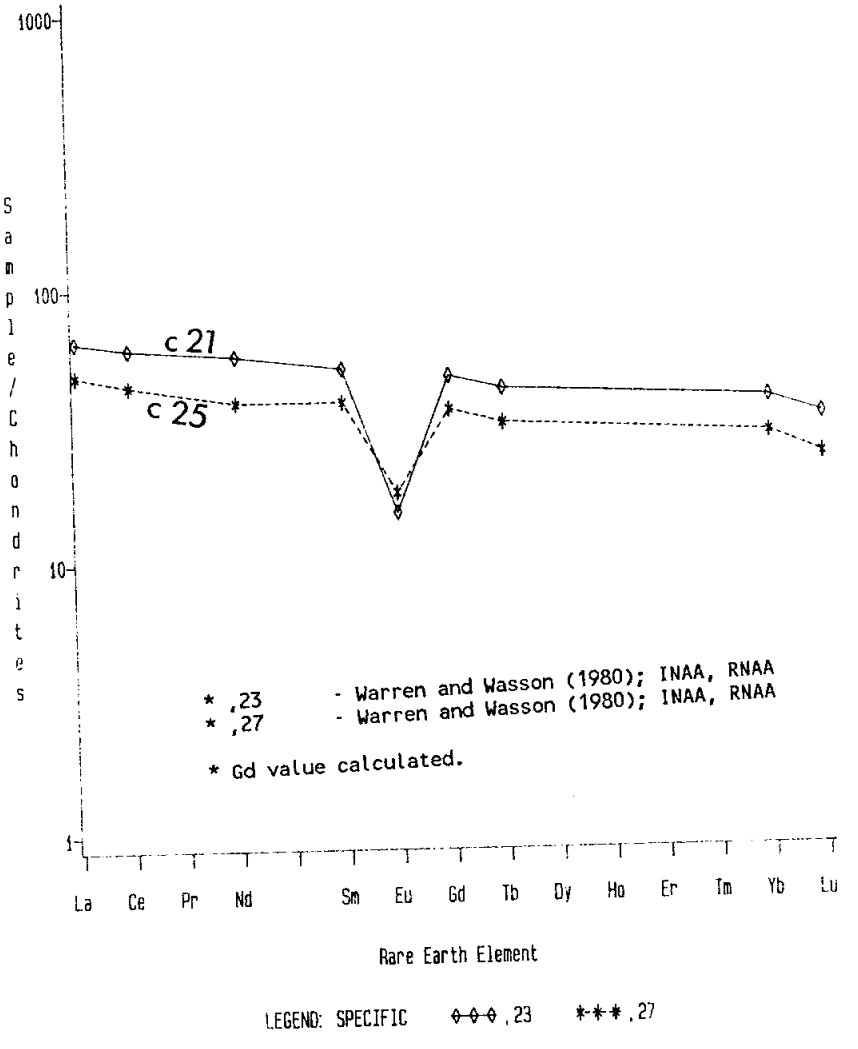

Figure 5. Rare earths in two clasts in 15306.

PROCESSING AND SUBDIVISIONS: Although 15306 is coherent, it was fractured and a few pieces fell off, and early allocations made from them. One of those fragments (,4) was used to make the matrix thin sections ,5 and ,6, with much of potted butt ,4 remaining. One of the allocations for the clasts analyzed by Warren and Wasson was made from a clast in ,1 (CL25). The probably pristine clast (CL21) was labelled "B" in data packs and was scraped from ,0. The genealogy of those two samples is shown in Figure 6. The clasts visible in Figure 1 include "A" (large, center) which was sampled but stored and not allocated. The two other small ones to the right in Figure 1 are "C" and "D" respectively and have not been allocated.

Figure 6. Genealogy of two 15306 clasts allocated to Wasson, with current masses and locations.

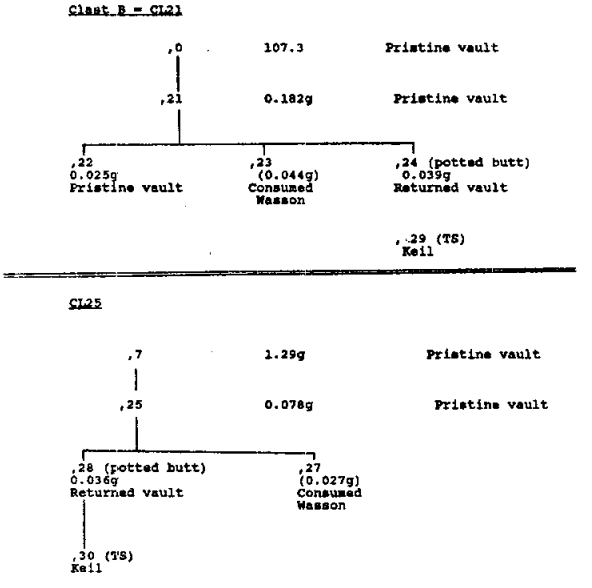

TABLE 15306-1. Chemical analyses of matrix (,11) and two clasts (,23 and ,27)

		Matrix ,11	(CL21) ,23	(CL25) ,27
Wt %	SiO2		47.3	45.8
	TiO2		1.8	0.43
	Al2O3		18.0	27.8
	FeO		8.9	4.6
	MgO		12.9	4.6
	CaO		10.1	16.0
	Na2O		0.427	0.495
	K2O		0.050	0.197
	P2O5			
(ppm)	Sc		16.3	8.8
	V			
	Cr		2790	642
	Mn		1040	520
	Co		28.7	17.2
	Ni		26	29
	Rb			
	Sr			
	Y			
	Zr		480	290
	Nb			
	Hf		10.7	5.5
	Ba		420	1640
	Th		4.4	3.3
	U		1.6	0.81
	Pb			
	La		21.4	16.0
	Ce		53	39
	Pr			
	Nd		34	23
	Sm		9.18	6.93
	Eu		1.05	1.24
	Gd			
	Tb		2.0	1.5
	Dy			
	Ho			
	Er			
	Tm			
	Yb		7.7	5.7
	Lu		1.13	0.81
	Li			
	Be			
	B			
	C	170		
	N	83		
	S	810		
	F			
	Cl			
	Br			
	Cu			
	Zn		0.45	1.52
(ppb)	I			
	At			
	Ga		2.7	3.3
	Ge		0.0089	0.027
	As			
	Se			
	Mo			
	Tc			
	Ru			
	Rh			
	Pd			
	Ag			
	Cd		<0.005	0.006
	In		4.0	2.6
	Sn			
	Sb			
	Te			
	Cs			
	Ta		2500	660
	W			
	Re			0.063
	Os			
	Ir		0.61	1.54
	Pt			
	Au		0.36	0.21
	Hg			
	Tl			
	Bi			
		(1)	(2)	(2)

References and methods:

(1) Cripe and Moore (1975), Moore and Lewis (1976); combustion-titration, combustion and gas chromatography.

(2) Warren and Wasson (1980); INAA, RNAA, microprobe fused bead.

15307 HOLLOW GLASS SPHERE ST. 7 1.3 g

INTRODUCTION: 15307 is a fragile, hollow glass sphere, with a lip (Fig. 1). It is dark green/black. Its surface is smooth with very few zap pits, and one half is shiny, the other dusty (Fig. 1). The sample is broken slightly, revealing its hollowness, and at least where it is broken the walls are extremely thin. It has never been processed or allocated. It was observed by the astronauts on the lunar surface and put into the container containing the soil from which it was taken (Bailey and Ulrich, 1975). In the lab it was retrieved and given a separate rock number. The sample was collected with the soil sample at the rake site on the north-east rim of Spur Crater.

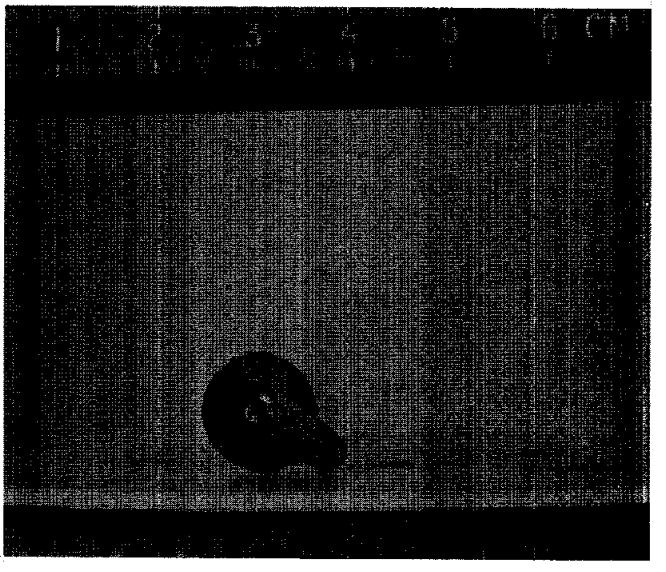

Figure 1. Glass sphere 15307. S-71-43037

15308 GLASSY IMPACT MELT (?) ST. 7 1.7 g

INTRODUCTION: 15308 is a dark, fine-grained highlands breccia which appears to be a glassy impact melt containing a few highlands clasts (Fig. 1). It would appear that the prominence of one of the clasts in some thin sections is the cause of the previous designation of the rock as a feldspathic, coarse highlands lithology, i.e., anorthositic norite (e.g., Simonds et al., 1975; Dowty et al., 1973b). The glass is of aluminous basaltic composition. The sample is coherent, uniform, lacks zap pits, and the matrix contains perhaps 1% tiny vugs. Macroscopically the breccia looks like the dark portion of 15455 and 15445, to which it is chemically quite similar. The sample was collected with the soil sample at the rake site on the north-east rim of Spur Crater.

PETROLOGY: There is some confusion as to the nature of 15308. According to Dowty et al. (1973b) it is a severely shocked anorthositic norite with some parts almost completely melted--relatively unshocked areas have a coarse "primary" texture with large plagioclase crystals. Simonds et al. (1975) referred to it as a calaclastic annealed rock with either a poikilitic or a granulitic texture (similar to 77017 or 76235) and about 70% plagioclase. Neither of these descriptions appears to be compatible with the macroscopic description of the rock as a dark, aphanitic breccia, nor with the bulk rock chemical analysis (following section). It is probable that the glassy melt matrix of thin section 15308,2 (Fig. 2) is the dominant lithology of the rock. The melt is brown, partly feathery crystallized or devitrified glass, and with few mineral clasts, which are mainly plagioclase. This melt contains about 50 or 60% plagioclase (which agrees with the bulk rock chemical analysis, following section). 15308,2 contains four main lithic clasts, all plagioclase-rich breccias. The largest (Fig. 2) corresponds with the Dowty et al. (1973b) description of the anorthositic norite lithology, and is similarly shot through with troilite. It contains relict but fine-grained cumulate textures (curvilinear boundaries) and ilmenite occurs in grains as big as the plagioclase and pyroxenes , i.e., about 500 microns; each ilmenite grain consists of numerous individual blebby patches. The anorthositic norite of Dowty et al. (1973B) contains armalcolite, Zr-armalcolite, troilite, and ilmenite, in addition to the dominant plagioclase and orthopyroxene. Iron metal is absent. Dowty et al. (1972) mentioned veins with troilite on grain boundaries. Small augites with exsolution lamellae are present in the anorthositic norite in 15308,2. Mineral analyses for the anorthositic norite were presented by Hlava et al. (1973) and Nehru et al. (1973, 1974) and are shown in Figure 3. Hlava et al. (1973) included analyses of olivine. The MgO in the ilmenite (5.5% to 6.9%) is much higher than in ilmenites in ferroan anorthosites such as 15362 (Nehru et al., 1974), and the spinel compositions contrast with those in mare basalts. The other three lithic clasts immersed in the glassy matrix of 15308,2 are all very plagioclase-rich breccias, clearly of highlands origin.

CHEMISTRY: A bulk rock analysis was made by Murali et al. (1977), from dark chips and fines selected to represent the bulk rock (Table 1). The analysis is fairly similar to melts such as 15455 and 15359. It has an aluminous basaltic composition, and a KREEP rare-earth pattern, although at low abundances of rare earths (Fig. 4). The analysis contrasts sharply with the more aluminous, less magnesian defocussed beam analysis by Dowty et al. (1973b) (Table 2) which, as explained above, probably represents a large white clast.

PROCESSING AND SUBDIVISIONS: ,1 was chipped from ,0 (Fig. 1). It contains a prominent white clast, and was consumed in making thin sections ,1; ,2; ,5; and ,6. The chemical analysis (,3) was made from chips and fines produced during this chipping. ,0 is now 1.34 grams.

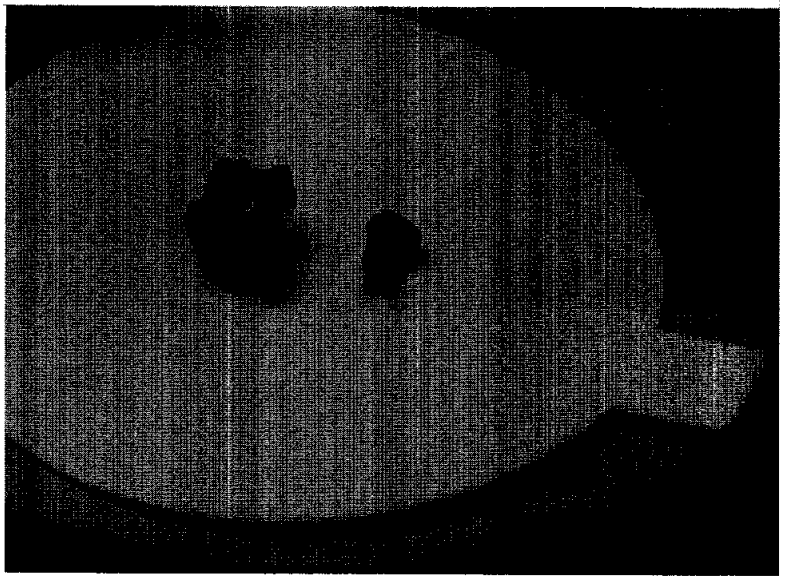

Figure 1. Macroscopic view following chipping into ,0 and ,1. A white clast is prominent on the chipped face of ,0. S-71-58133

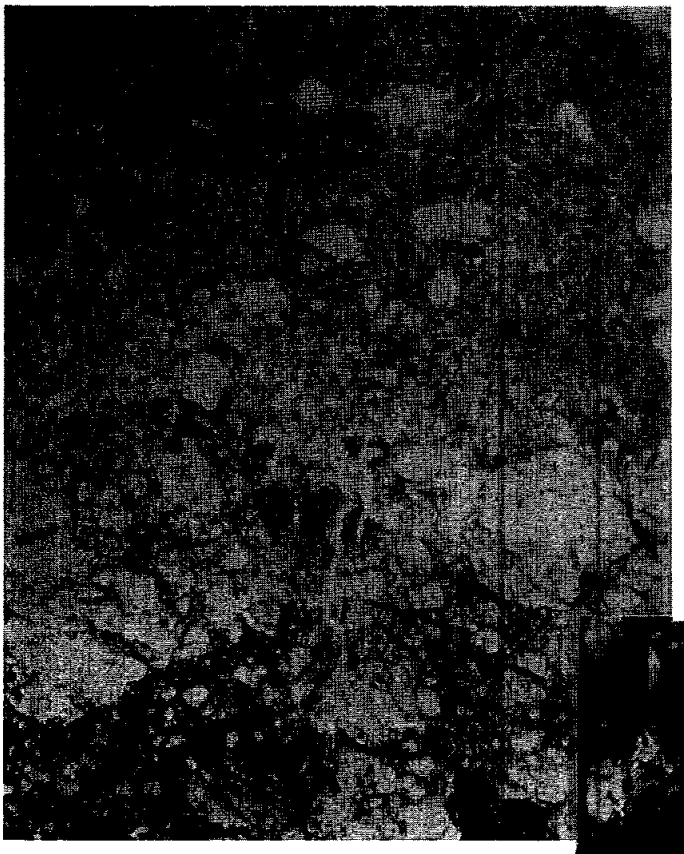

Fig. 2a

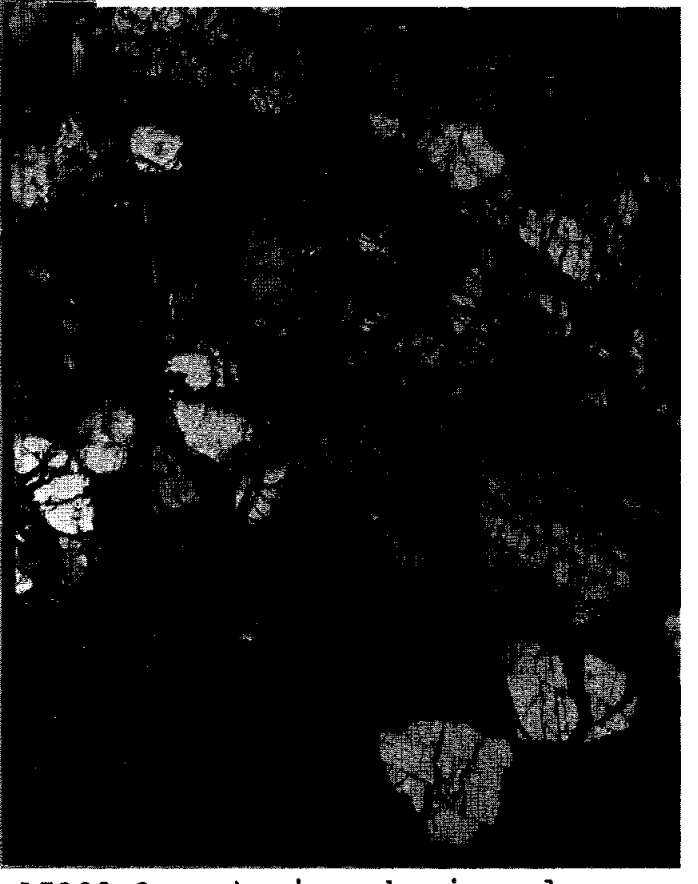

Fig. 2b

Figure 2. Photomicrographs of 15308,2. a) view showing glassy melt matrix (top), and ilmenite-bearing, cataclastic anorthositic norite clast (bottom). Transmitted light. Width about 2 mm. b) view of part of the anorthositic norite clast, showing cataclasis, relict "cumulate" textures, and ilmenite (black, lower center). Crossed polarizers. Width about 600 microns.

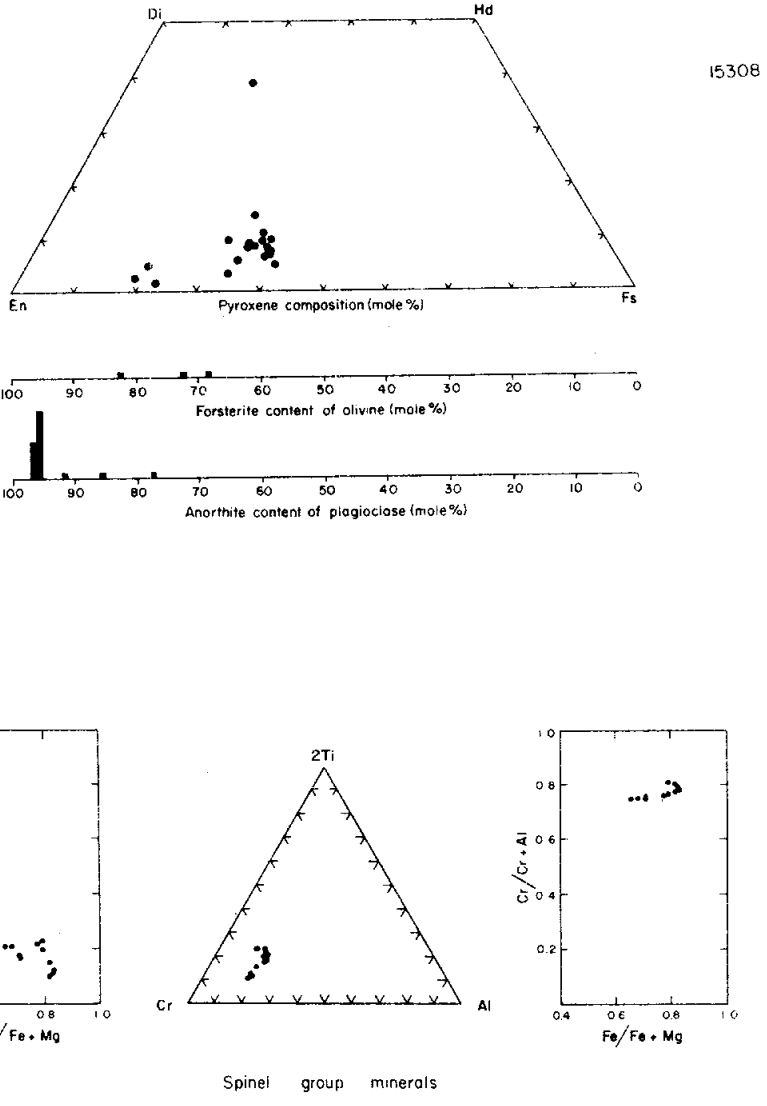

Figure 3. Mineral compositions for 15308, probably mainly anorthositic norite clast (Dowty et al., 1973b).

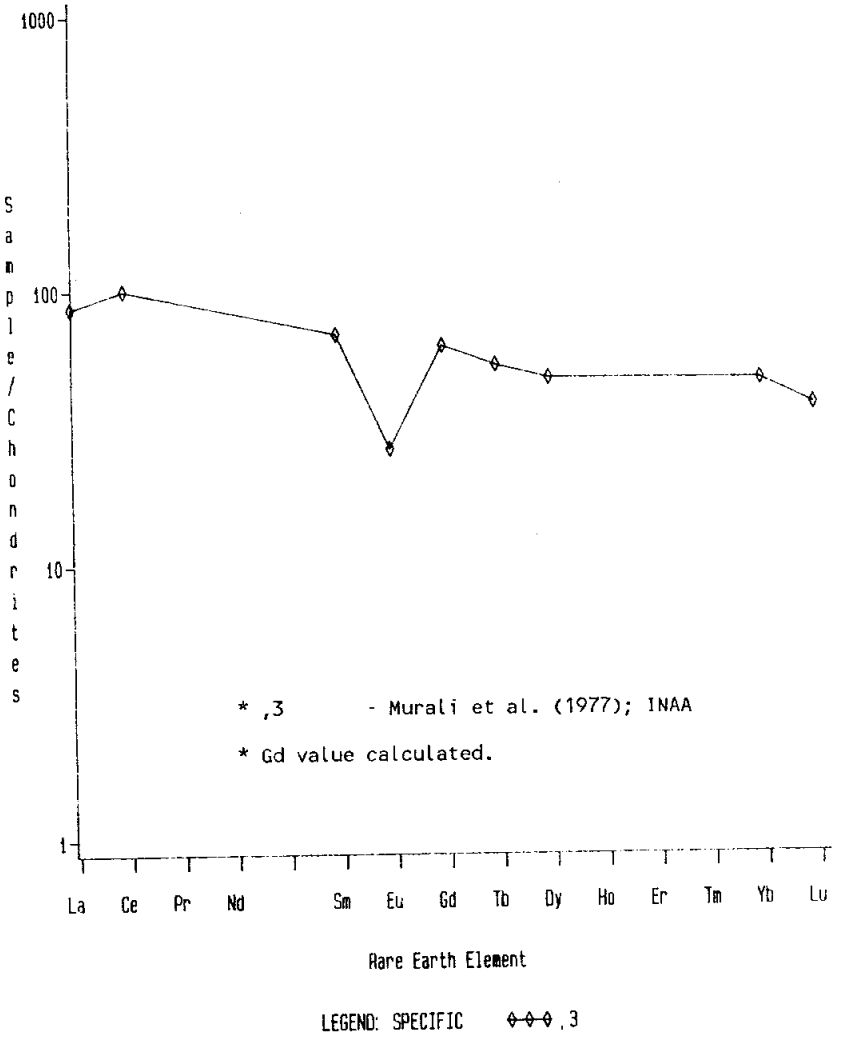

Figure 4. Bulk rock rare earths.

TABLE 15308-1. Chemical analysis of bulk rock

		,3
Wt %	SiO2	
	TiO2	1.3
	Al2O3	18.7
	FeO	8.7
	MgO	13.4
	CaO	10.1
	Na2O	0.58
	K2O	0.26
	P2O5	
(ppm)	Sc	14.5
	V	41
	Cr	1080
	Mn	810
	Co	23
	Ni	149
	Rb	
	Sr	
	Y	
	Zr	405
	Nb	
	Hf	10.7
	Ba	277
	Th	5.1
	U	
	Pb	
	La	28.6
	Ce	88
	Pr	
	Nd	
	Sm	12.5
	Eu	1.82
	Gd	
	Tb	2.5
	Dy	15
	Ho	
	Er	
	Tm	
	Yb	9.3
	Lu	1.28
	Li	
	Be	
	B	
	C	
	N	
	S	
	F	
	Cl	
	Br	
	Cu	
	Zn	
(ppb)	I	
	At	
	Ga	
	Ge	
	As	
	Se	
	Mo	
	Tc	
	Ru	
	Rh	
	Pd	
	Ag	
	Cd	
	In	
	Sn	
	Sb	
	Te	
	Cs	
	Ta	1400
	W	
	Re	
	Os	
	Ir	
	Pt	
	Au	1.2
	Hg	
	Tl	
	Bi	
		(1)

TABLE 15308-2. Microprobe defocussed beam analysis of 15308 white clast(?) (Dowty et al., 1973b)

Wt%	SiO2	44.1
	TiO2	1.24
	Al2O3	27.3
	FeO	5.9
	MgO	6.7
	CaO	13.3
	Na2O	0.63
	K2O	0.17
	P2O5	0.11
ppm	Mn	700
	Cr	3150

Reference and method:

(1) Murali et al. (1977); INAA

15315 REGOLITH BRECCIA ST. 7 35.6 g

INTRODUCTION: 15315 is a regolith breccia (Fig. 1) containing abundant glass and mineral fragments, and much less abundant lithic fragments, in a glassy, porous matrix. Green glass spherules are prominent. The sample is grey-brown, blocky, but rounded and fractured, and was originally dust-covered. One large zap pit was visible through the dust. It was collected as part of the rake sample from the north-east rim of Spur Crater.

PETROLOGY: 15315 consists of abundant green glass debris, some devitrified, and many mineral fragments (Fig. 2) in a fine-grained, porous, glassy matrix. Dowty et al. (1973b) described it as a polymict breccia, consisting almost entirely of glass, but stated that the matrix was light-colored. While green glass is dominant, clear, yellow, and some orange glass is also present. Glass analyses were presented by Hlava et al. (1973), and Bunch et al. (1972) referred to 15315 in a column of green glass analyses. Hlava et al. (1973) also presented analyses of glass in green glass chondrules, and of the olivine within them. Lithic fragments are rare and small but include crystalline materials. Basalts containing cinnamon-brown pyroxene (mare basalts?) are visible macroscopically. The several-millimeter across clast in Figure 1 does not exist in thin sections.

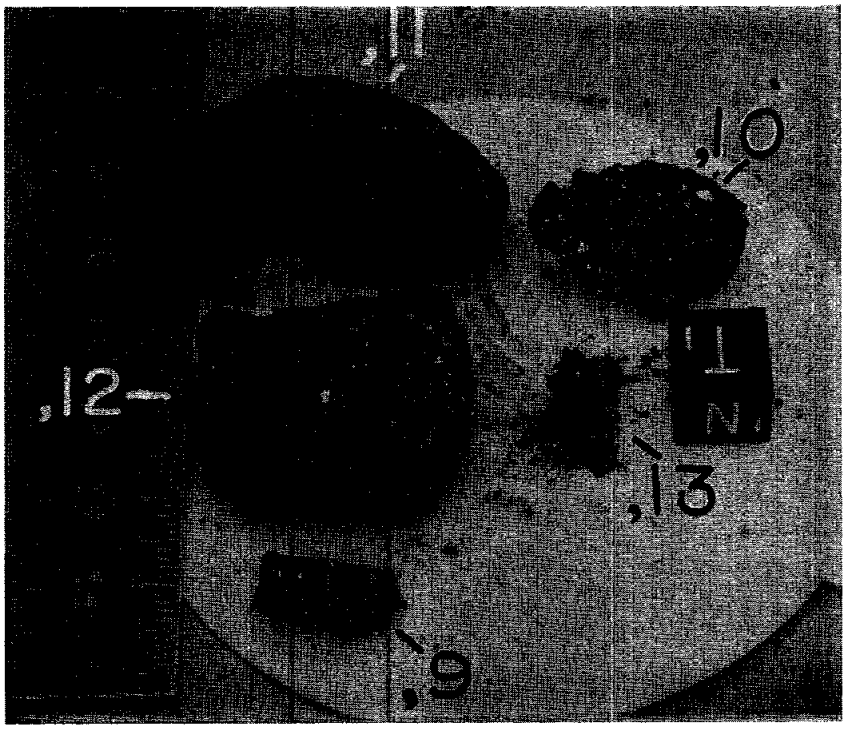

Figure 1. Major subdivisions and macroscopic view of 15315. S-72-53914

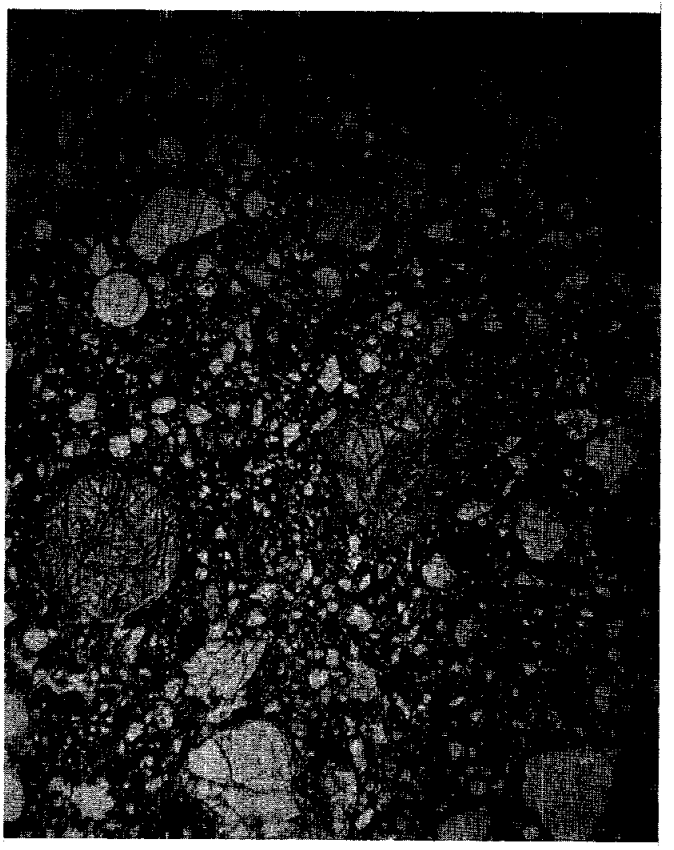

Figure 2. Photomicrograph of 15315,4. Transmitted light. Width about 2 mm.

MAGNETICS: Cisowski and Fuller (1983) used the saturation remanence normalization method to estimate a paleomagnetic intensity, finding NRM_{200}/IRM_{200} to be 1.2×10^{-3}.

PROCESSING AND SUBDIVISIONS: Small chips were originally removed from ,0 (Fig. 3). Part of ,2 was used to make thin sections ,4 and ,16. Subsequently ,0 was subdivided and renumbered into several large pieces (Fig. 1), of which ,11 (16.35 g) and ,12 (12.49 g) are the largest.

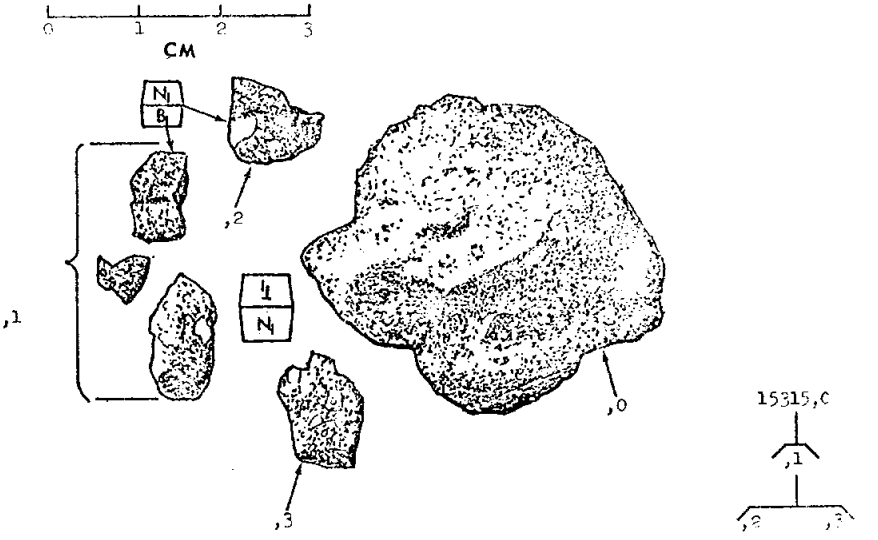

Figure 3. Original chipping of 15315.

15316 REGOLITH BRECCIA ST. 7 6.1 g

INTRODUCTION: 15316 is a glassy, porous, regolith breccia, containing glass, mineral, and lithic debris in a fine-grained, brown, opaque matrix. In contrast with many other regolith breccias at Station 7, 15316 has more shocked clasts, and less distinct, reacted-appearing clast boundaries. Macroscopically it is similar to other grey-brown regolith breccias (Fig. 1). It appeared to have no zap pits. 15316 was collected as part of the rake sample from the north-east rim of Spur Crater.

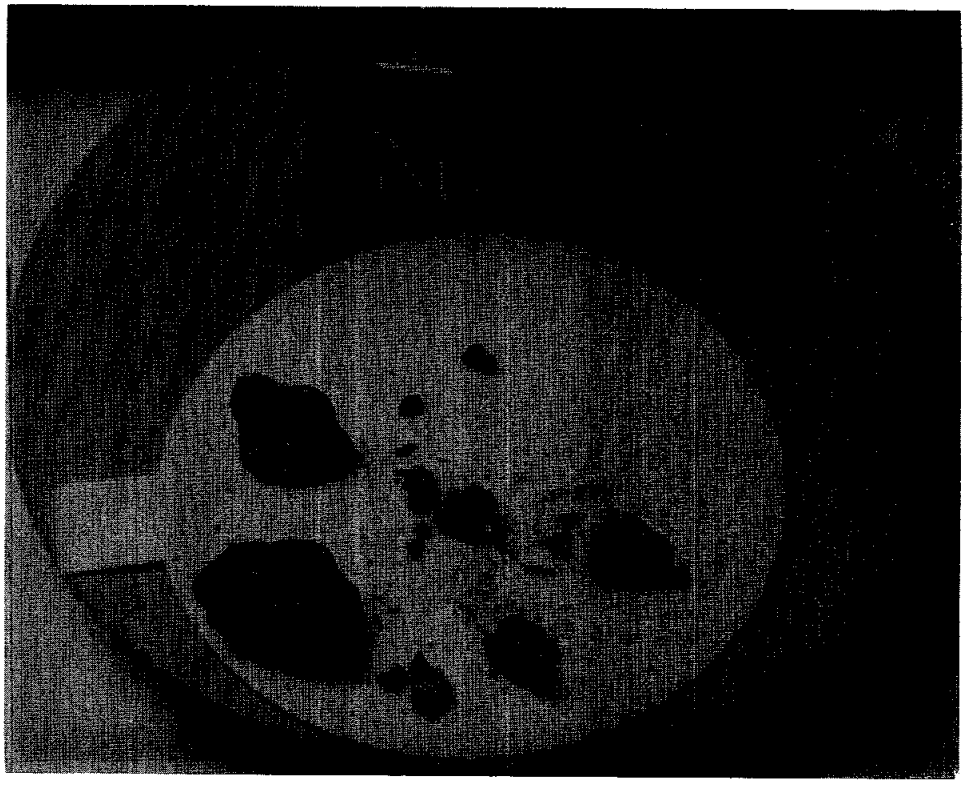

Figure 1. Post-split view of 15316. S-71-57206

PETROLOGY: 15316 appears similar to other glassy regolith breccias (Fig. 1) but in thin section it has a darker, more denser-appearing matrix, and clast boundaries are less distinct (Fig. 2). Nonetheless it is porous, and much of the glass is not devitrified. Steele et al. (1977) found it to consist of 10% glass, 5% lithic clasts (anorthosite), 40% mineral clasts, 40% fine matrix, and 5% pore-space. They noted the reaction between the matrix and mineral clasts, and that the anorthosite clast (visible in Figure 2) was shocked. They also noted an unusual, small metal intergrowth (Fe-metal + Cr-containing sulfide) of possible meteoritic origin. The anorthosite has low-iron, high-Ca plagioclase, and small, minor pyroxene (~En_{72-74},Wo_{3-6}). They also plotted an analysis of an exsolved pyroxene matrix fragment ($En_{70}Wo_3$). Steele et al. (1972b) reported that the mineral clasts included olivine (~Fo_{87}) and pink spinel, and a wide range of pyroxene compositions (Fig. 3). These pyroxenes include both mare and highlands compositions.

Other lithic clasts include small mare basalt and fine-grained, brown glassy breccias. Glasses are dominantly green glass spheres, but small lapilli-like glasses are also present.

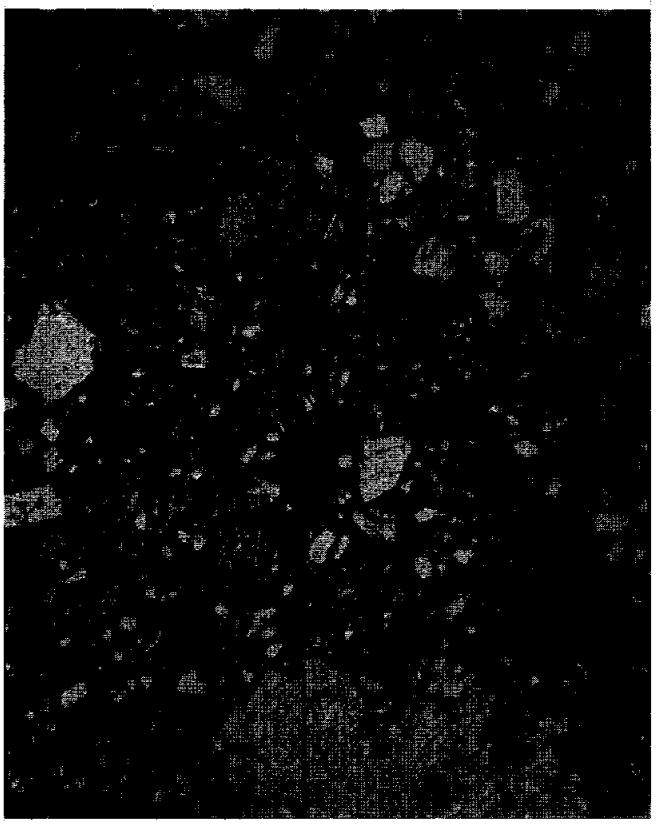

Figure 2. Photomicrograph of 15316,2, general view. Clast in bottom center is shocked anorthosite described by Steele et al. (1977). Transmitted light. Width about 2 mm.

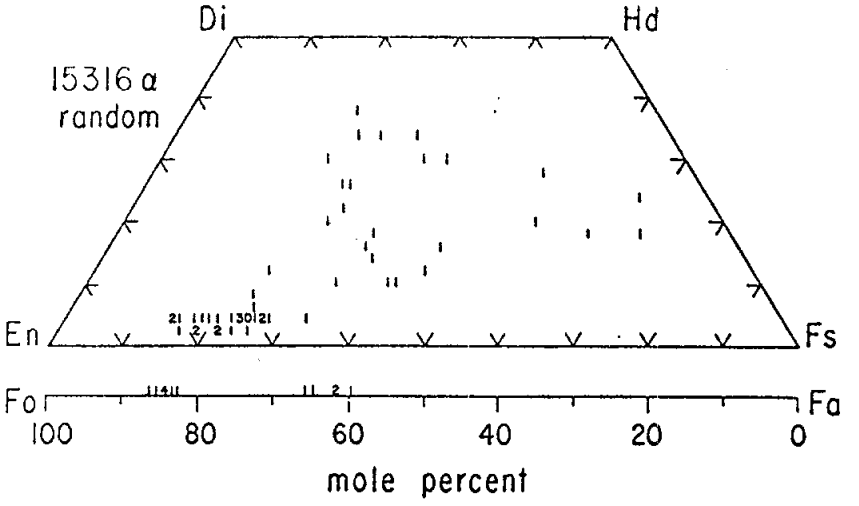

Pyroxenes and olivines in low-glass breccia 15316. (D = 13)

Figure 3. Compositions of mafic minerals in 15316 (Steele et al., 1972b).

PROCESSING AND SUBDIVISIONS: 15316 was chipped (Fig. 4). ,0 is now 3.61 g, and ,1 is 1.95 g. ,2 was mainly used to produce thin sections ,2 and ,6 with small potted butts ,8 and ,9 remaining.

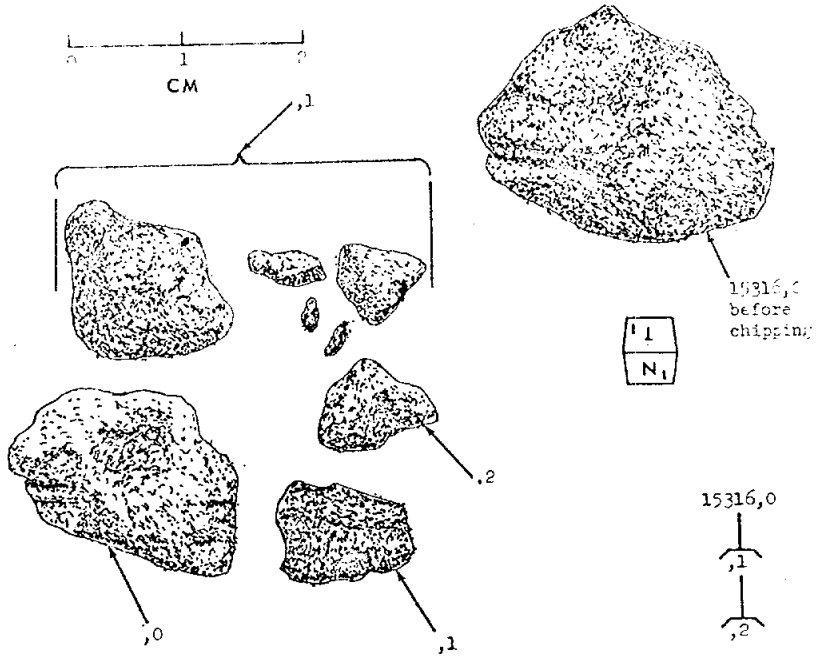

Figure 4. Splitting of 15316.

15317 REGOLITH BRECCIA ST. 7 0.6 g

INTRODUCTION: 15317 is a small, dusty sample which appears to be a typical regolith breccia (Fig. 1). It has never been subdivided or allocated. It was collected as part of the rake sample from the north-east rim of Spur Crater.

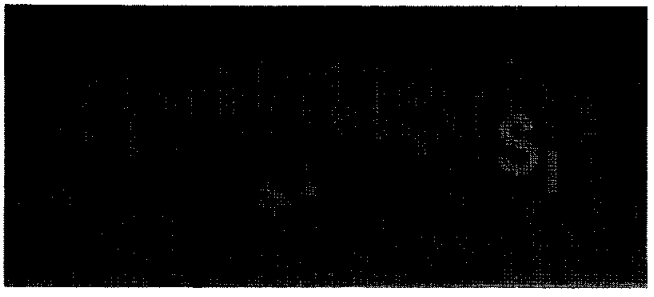

Figure 1. Sample 15317. S-71-49363

15318 REGOLITH BRECCIA ST. 7 5.4 g

INTRODUCTION: 15318 is a glassy regolith breccia, containing varied glass, mineral, and lithic debris in a fine, glassy but friable matrix (Fig. 1). Mare basalt debris is present. The sample is gray-brown, rounded, and was dusty, with two large zap pits on one side. The sample was collected as part of the rake sample from the north-east rim of Spur Crater.

PETROLOGY: 15318 is a porous, glassy, regolith breccia (Fig. 2). Most glass is undevitrified, but some is devitrified. Green glass is most common, but pale yellow glass is prominent, some as spheres, and red/orange glass occurs as very small and sparse spheres and fragments. Dowty et al. (1973b) described 15318 as a polymict microbreccia, and noted the many mineral clasts, which are mostly feldspar. Lithic clasts include shocked and re-crystallized fragments which appear noritic. The clasts in Figure 2b include a mare basalt (lower center), and a feldspathic breccia, possibly granulitic (upper center). Small KREEP basalt fragments are also present.

Hlava et al. (1973) reported analyses of glasses ranging from aluminous, highlands impact glasses to mare volcanic glasses. Their analysis of a red/orange glass was used as a starting composition for melting experiments by Kesson (1975, 1977). The composition might represent one of the least fractionated, most primitive high-Ti mare basalts. Olivine is the liquidus phase to at least 22 Kb, but at pressures of 25 to 30 Kb should be replaced by pyroxene. Delano (1980b) also analysed red glasses in 15318, as well as 15425, 15426, and 15427, finding three distinct groups. Experiments on the most-magnesian group indicated multiple saturation at depths of over 400 km in the moon. The specific analyses from 15318 were not identified. Delano (1980a, 1981) analyzed yellow glasses in the same four samples, again without specifying which analyses were from 15318. The yellow glasses form two groups, one volcanic, the other impact in origin.

PROCESSING AND SUBDIVISIONS: 15318 had one end chipped off (Fig. 1) to produce ,1, part of which was made into thin sections ,2; ,6; and ,8. A potted butt remains. ,0 is now 4.4 g.

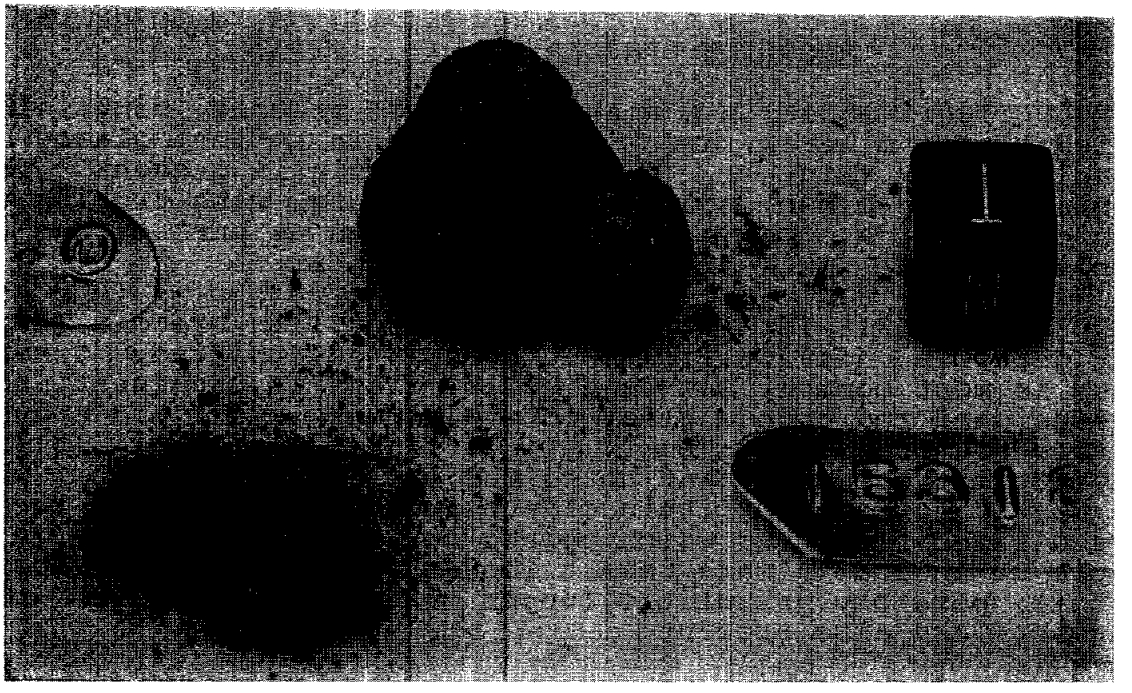

Figure 1. Post-split view of 15318,0 (left) and ,1 (right). S-71-59126

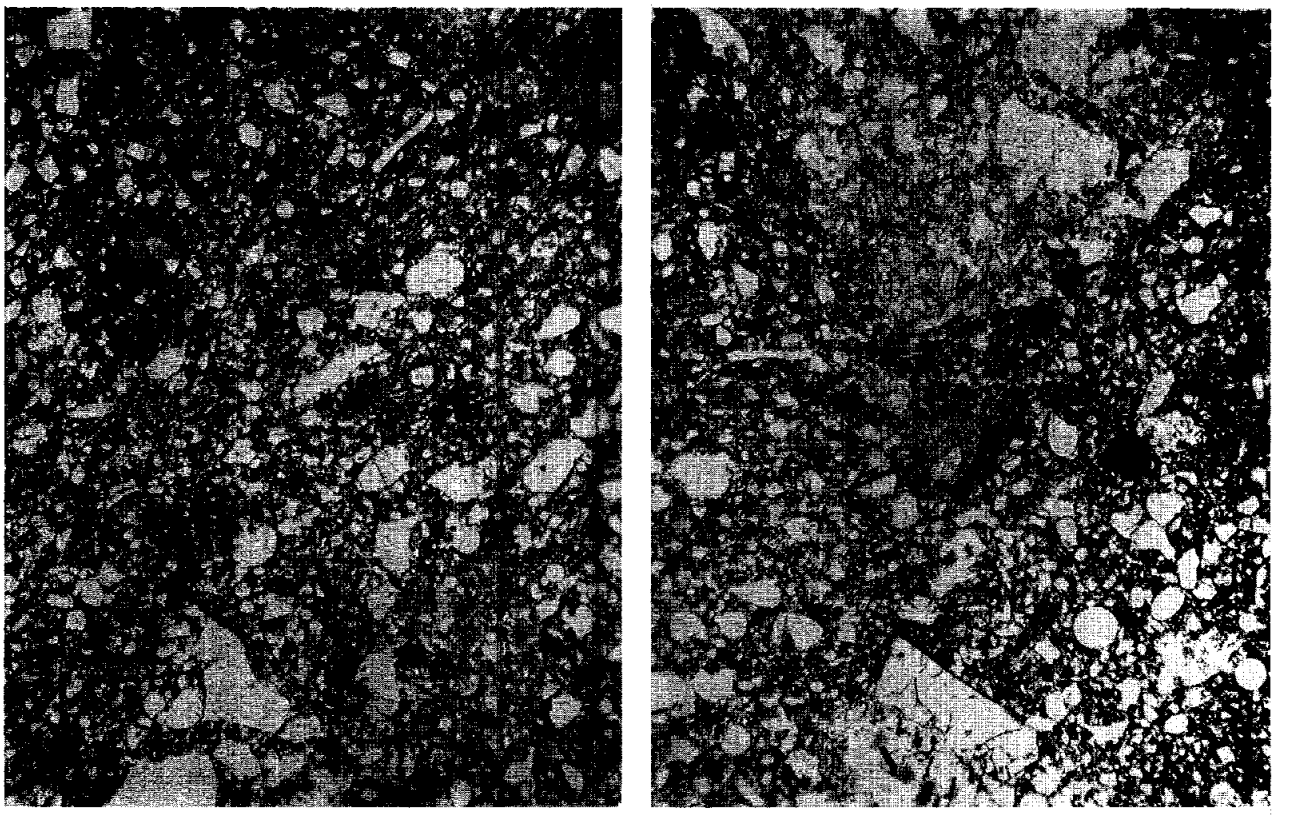

Figure 2. Photomicrographs of 15318,6. Transmitted light. Widths about 2 mm. b) shows two clasts, a mare basalt (lower) and a feldspathic breccia (upper).

15319 REGOLITH BRECCIA ST. 7 8.0 g

INTRODUCTION: 15319 is a friable regolith breccia (Fig. 1) with a greenish matrix with abundant spherules in at least one part. It is not a purely green glass clod, as several pale-colored clasts are visible, but it is lower in incompatible elements than most other analyzed regolith breccias. It has no obvious zap pits. It was collected as part of the rake sample from the north-east rim of Spur Crater.

CHEMISTRY: S.R. Taylor et al. (1973) analyzed a bulk matrix sample for minor and trace elements (Table 1, Fig. 2). The sample has among the lowest incompatible element abundances of Apollo 15 regoliths or regolith breccias, with the possible exception of some green glass clods. S.R. Taylor et al. (1973) modelled its composition as a mixture of 37.8% highland basalt and 62.2% low-K Fra Mauro basalt, but such a modelling would appear to have no physical significance for 15319. Indeed, these figures seem to be essentially reversed, given the low incompatibles in 15319. S.R. Taylor et al. (1972) and S.R. Taylor (1973) plotted some of the data, and these plots indicate that chemically 15319 contains about 75% "highland basalt".

PROCESSING AND SUBDIVISIONS: Several chips were removed from ,0, but only ,2 (Fig. 1) was allocated. No thin sections have ever been made. ,0 is now 7.06 grams.

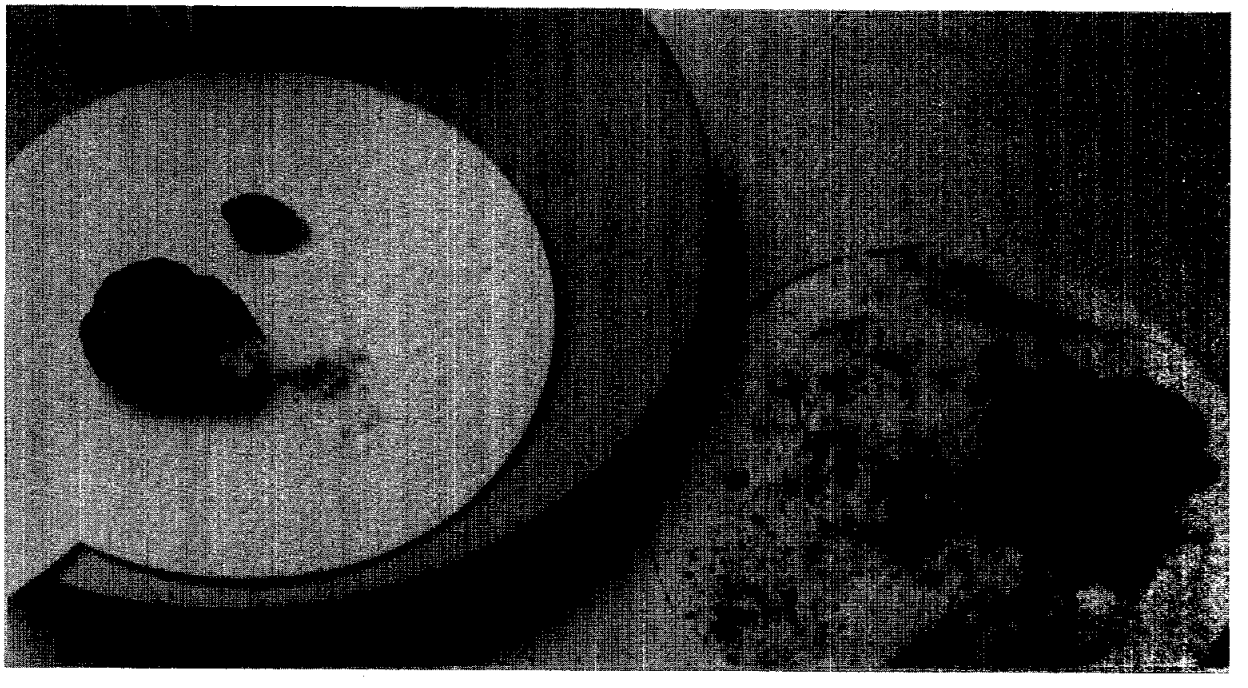

Figure 1. Post split view of 15319, showing ,0 and its daughter ,2 (left) and the chips, fragment, and fines which are ,1 (right).

TABLE 15319-1. Bulk analysis of 15319,2

Wt%	SiO2	
	TiO2	
	Al2O3	
	FeO	
	MgO	
	CaO	
	Na2O	
	K2O	
	P2O5	
(ppm)	Sc	33.0
	V	140.0
	Cr	2400
	Mn	
	Co	48.0
	Ni	248
	Rb	2.0
	Sr	
	Y	35.0
	Zr	156.0
	Nb	10.1
	Hf	3.5
	Ba	134
	Th	1.8
	U	0.5
	Pb	2.5
	La	9.8
	Ce	26.0
	Pr	3.8
	Nd	16.8
	Sm	5.6
	Eu	1.05
	Gd	7.1
	Tb	1.14
	Dy	6.9
	Ho	1.67
	Er	4.7
	Tm	0.74
	Yb	4.5
	Lu	0.69
	Li	
	Be	
	B	
	C	
	N	
	S	
	F	
	Cl	
	Br	
	Cu	11.0
	Zn	
(ppb)	I	
	At	
	Ga	4400
	Ge	
	As	
	Se	
	Mo	
	Tc	
	Ru	
	Rh	
	Pd	
	Ag	
	Cd	
	In	
	Sn	180
	Sb	
	Te	
	Cs	100
	Ta	
	W	180
	Re	
	Os	
	Ir	
	Pt	
	Au	
	Hg	
	Tl	
	Bi	
		(1)

References and methods:

(1) S.R. Taylor et al. (1973); spark source mass spec, emission spec.

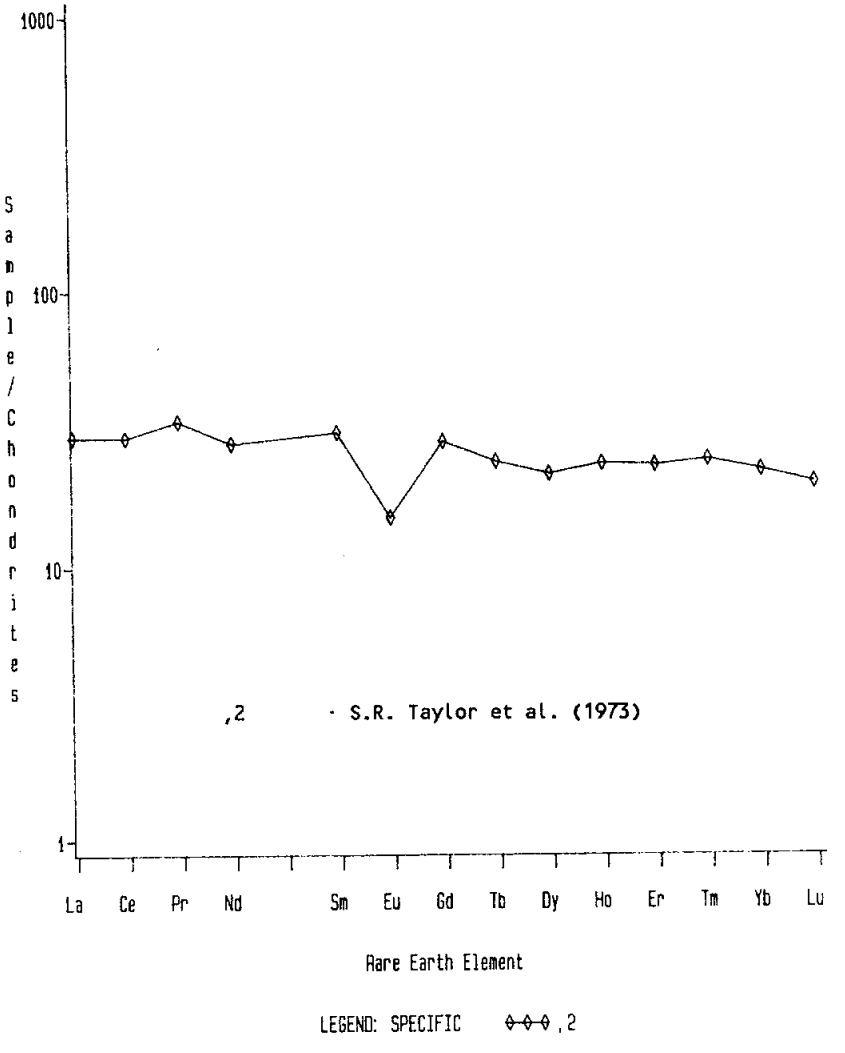

Figure 2. Rare earths in 15319,2.

15320 REGOLITH BRECCIA ST. 7 4.7 g

INTRODUCTION: 15320 is a regolith breccia containing a few pale-colored clasts (Fig. 1). It was dusty and had no visible zap pits. It has never been subdivided but was used for a magnetic measurement. It was collected as part of the rake sample from the north-east rim of Spur Crater.

MAGNETICS: Gose et al. (1972) measured the natural remanent magnetization of the entire sample using the Develco cryogenic magnetometer. They found that 15320 was more magnetic than igneous rocks (mare basalts), with an NRM intensity between 10^{-4} and 10^{-5} emu/g.

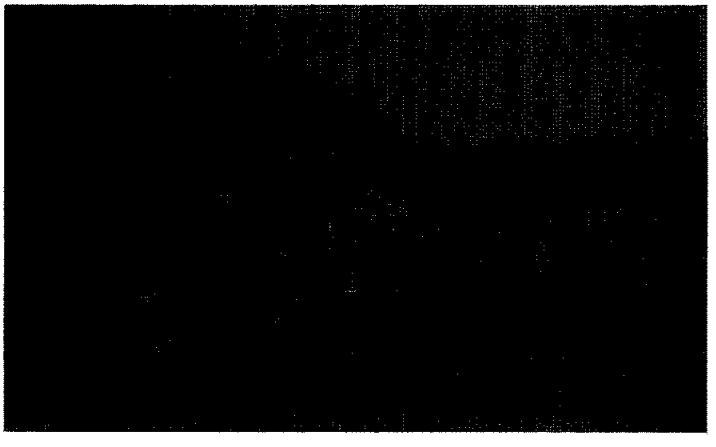

Figure 1. Sample 15320. S-71-49377

15321 REGOLITH BRECCIA ST. 7 0.3 g

INTRODUCTION: 15321 is a regolith breccia (Fig. 1) which is slabby, angular, and dusty. No zap pits were obvious on its surface. It has never been subdivided or allocated. It was collected as part of the rake sample from the north-east rim of Spur Crater.

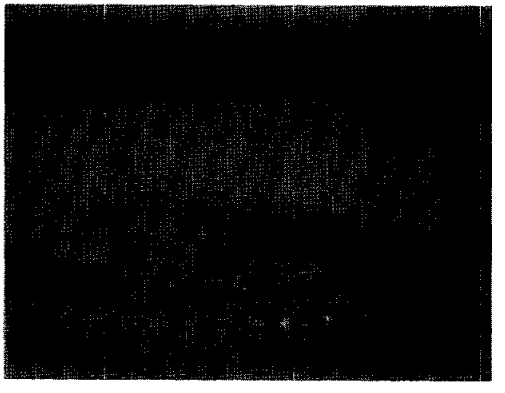

Figure 1. Sample 15321. S-71-49805

15322 REGOLITH BRECCIA ST. 7 8.4 g

INTRODUCTION: 15322 is a glassy regolith breccia with mineral and lithic as well as glass debris. A pale-colored clast is prominent on one surface, and one area is coated with a vesicular glass (Fig. 1). The sample is moderately coherent, gray-brown, and blocky. It was collected as part of the rake sample from the north-east rim of Spur Crater.

PETROLOGY: 15322 is a regolith breccia containing abundant glass and mineral fragments (Fig. 2) and some lithic fragments which include KREEP basalts, anorthosites, and highland breccias. The matrix is porous and brown-gray. The glasses include green, colorless, and yellow fragments and spheres, some of which are devitrified. Steele et al. (1977) found the sample to contain 30% glass, 5% lithic fragments, 30% mineral clasts , and 35% finer matrix. Pyroxene and olivine analyses (Fig. 3) have a wide range of compositions, and indicate mare basalt, KREEP basalt, and an ultrabasic (to explain Fo_{89} grains) components. Steele et al. (1977) reported brief mineral data for a KREEP basalt clast, and for an exsolved pyroxene fragment. Steele et al. (1972b) reported a "gabbroic anorthosite ?" clast ($En_{70-75}Wo_{3-6}$) and a "variolitic basalt ?" clast ($En_{76}Wo_6$ and more iron- and calcium-rich compositions).

PROCESSING AND SUBDIVISIONS: Chips were taken from 15322 (Figs. 1, 4) and one (,1) was taken to make thin sections ,1 and ,6. The prominent clast (Fig. 1) is not in the thin sections. All pieces other than daughters of ,1 remain with ,0.

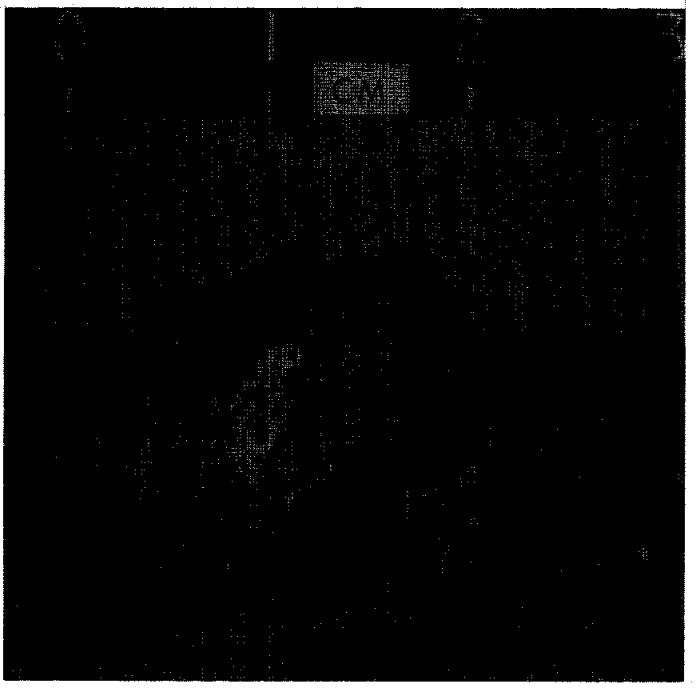

Figure 1. Post-split view of 15322, with ,1 at far right. S-71-49615

Figure 2. General view of 15322,6. Transmitted light. Width about 2 mm.

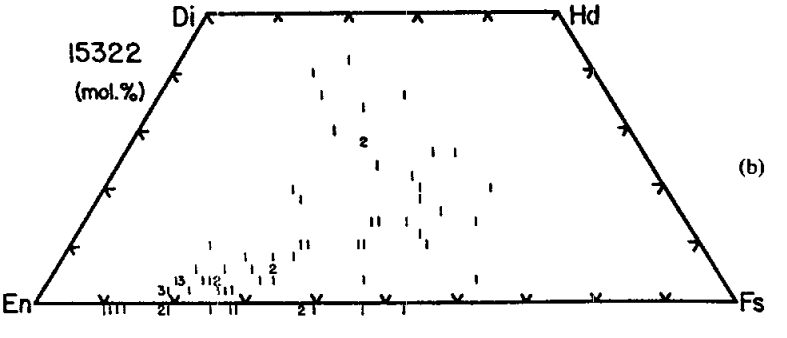

Figure 3. Compositions of pyroxenes and olivines in 15322,1 (Steele et al., 1977).

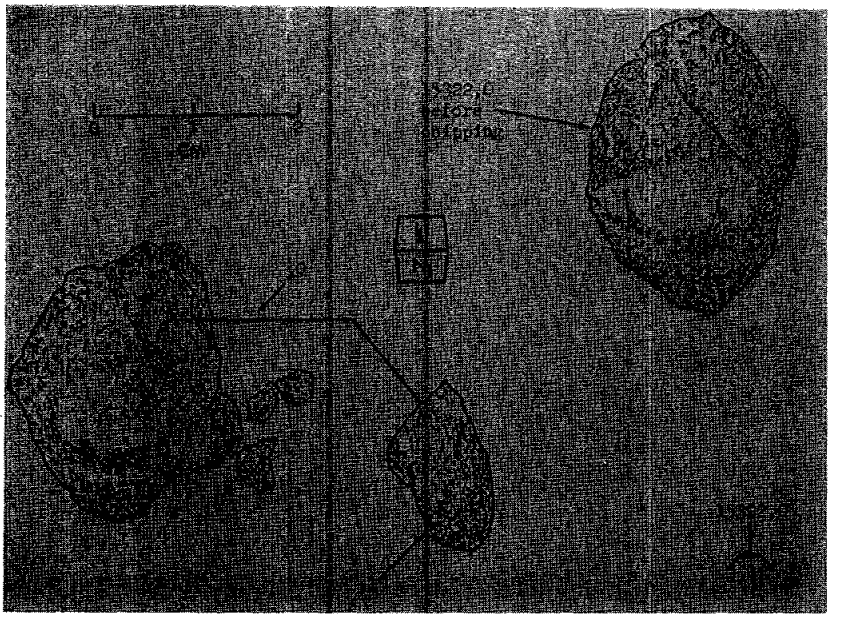

Fig. 4a

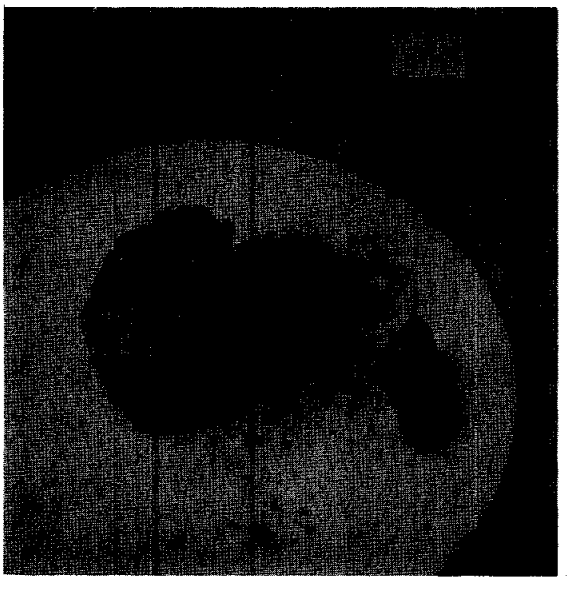

Fig. 4b

Figure 4. Chipping of 15322 a) diagram; b) photograph S-71-57225.

15323 REGOLITH BRECCIA ST. 7 4.4 g

INTRODUCTION: 15323 is a glassy regolith breccia (Fig. 1), more coherent and less porous than many others from Spur Crater. It contains small lithic clasts, as well as mineral and glass fragments, and has a vesicular glass coat in part. The glass coat has some zap pits, but more occur on the breccia. It was collected as part of the rake sample from the north-east rim of Spur Crater.

PETROLOGY: 15323 is a regolith breccia (Fig. 2), with a brown, opaque, glassy matrix which is less porous than most of its ilk. It contains many clear, yellow, and orange glass spherules and fragments (Dowty et al., 1973b), as well as green glass. It also contains highlands breccia fragments and KREEP basalts. Hlava et al. (1973) reported about 30 glass analyses, which include aluminous highlands and mare glasses. They also reported compositions of pyroxene, olivine, plagioclase (Fig. 3) and Si-K-rich residual glass in a high-alumina basalt fragment. Their olivine analysis is listed as $Fo_{16.5}$ but should be $Fo_{85.5}$. Their defocussed beam analysis for the fragment is consistent with a KREEP basalt (Al_2O_3 19.4%, K_2O 0.6%). The glass coat is vesicular, colorless/gray, and faintly banded (Fig. 2b).

PROCESSING AND SUBDIVISIONS: Because of its coherency, 15323 was sawn to produce ,1 and ,2 (Figs. 1, 4). ,0 is now 3.39 g. ,2 was partly used to make thin sections ,7 and ,8.

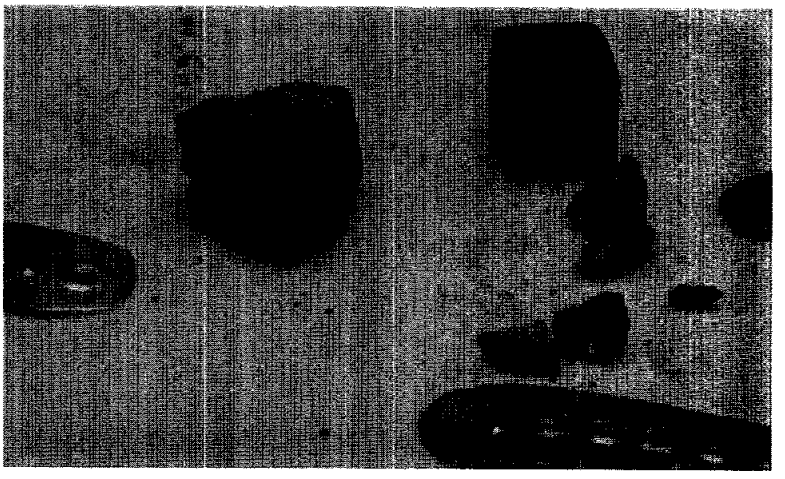

Figure 1. Post-sawing view of 15323. S-71-59575

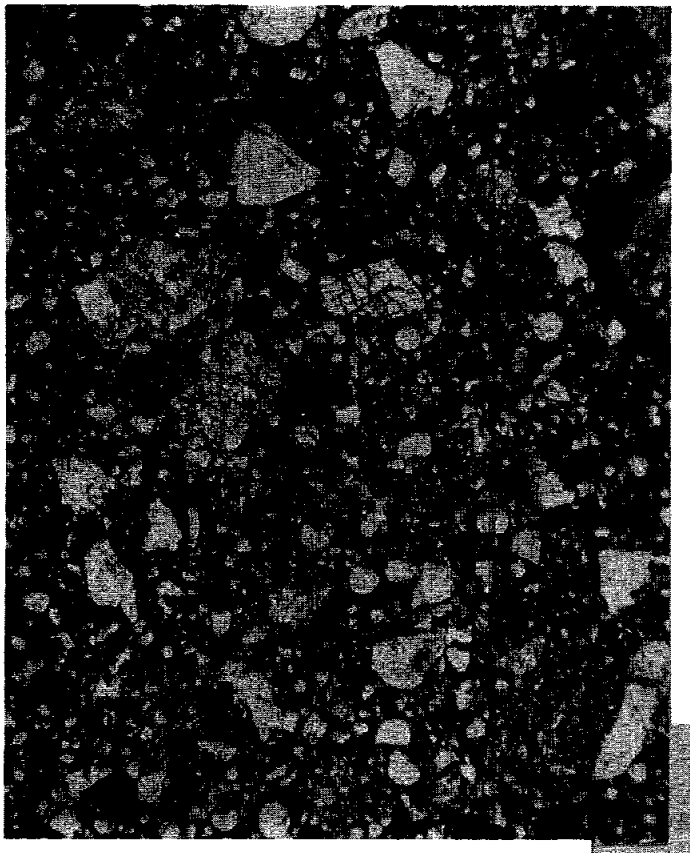

Fig. 2a

Fig. 2b

Figure 2. Photomicrographs of 15323,8. Transmitted light. Widths about 2 mm. a) general matrix, showing small highlands breccia fragments (left center); b) general matrix, showing vesicular glass coat (top, left) and prominent KREEP basalt fragment (top, right).

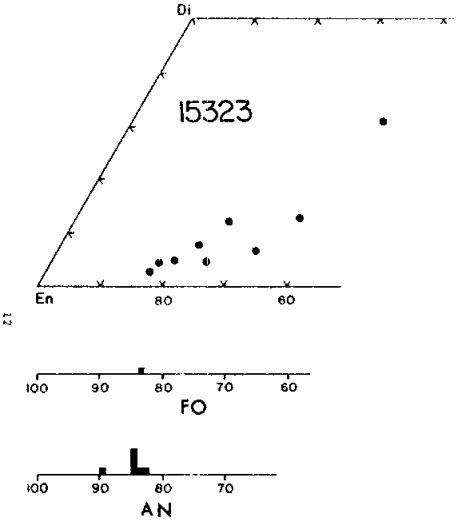

Figure 3. Compositions of minerals in clast of KREEP basalt. (Hlava et al., 1973)

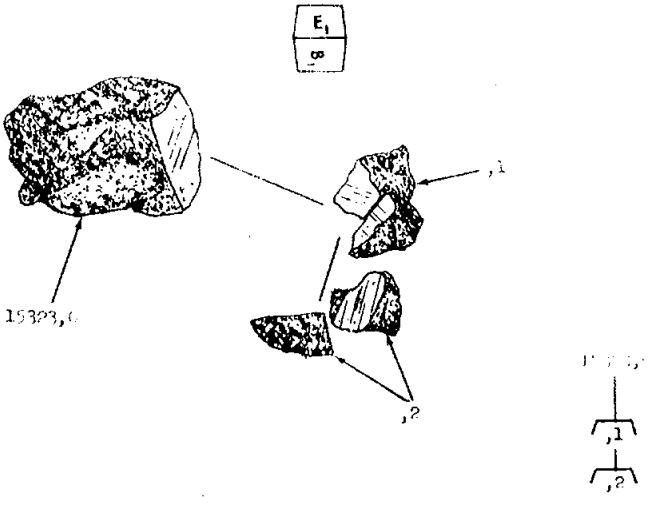

Figure 4. Sawing of 15323.

15324 REGOLITH BRECCIA ST. 7 32.3 g

INTRODUCTION: 15324 is a regolith breccia, less porous than most others at Spur Crater but more porous than 15323. It contains glass, mineral, and lithic debris in a glassy matrix. Green glass spheres are prominent macroscopically. It is low in incompatible elements compared to many other A15 regolith breccias. It has a lumpy, irregular surface but zap pits are apparently absent. It was collected as part of the rake sample from the north-east rim of Spur Crater.

PETROLOGY: 15324 is a brown, glassy regolith breccia (Fig. 2). It contains abundant glass and glassy debris, including spheres, of colorless, green, yellow, and some orange glass. Mineral fragments include cataclastic and shocked plagioclases, exsolved pyroxene, and a large twinned pyroxene. Lithic fragments are sparse and include glassy and feldspathic breccias. The matrix is not as porous as many other breccias, but is more porous than 15323.

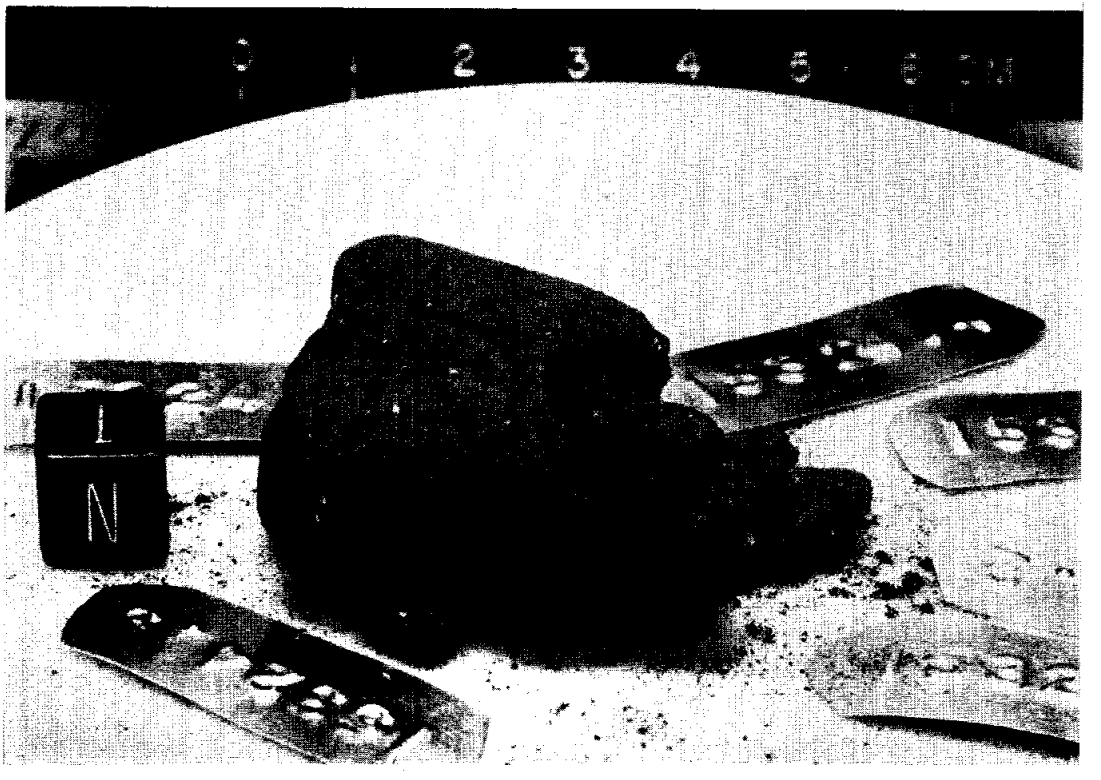

Figure 1. Post split view of 15324. S-71-59559

CHEMISTRY: An analysis for bulk rock minor and trace elements was reported by S.R. Taylor et al. (1973) (Table 1, Fig. 3). The incompatible elements are very low for a regolith breccia, but not as low as 15319. S.R. Taylor et al. (1973) modelled the analysis as a mixture of 37.8% highlands basalt and 62.2% low-K Fra Mauro, but this modelling has little physical significance. The component percentages are probably reversed (i.e., should be 62.2% highlands basalt), given the low incompatible element abundances, consistent with the diagrams of S.R. Taylor (1973) and S.R. Taylor et al. (1972) which indicate about 65% highland basalt component.

PROCESSING AND SUBDIVISIONS: 15324 was chipped and split (Figs. 1, 4). ,2 was partly used to make thin sections ,8; ,9; and ,10, while ,4 was used for the chemical analysis. All other pieces remain unused. ,0 is now 21.43 grams.

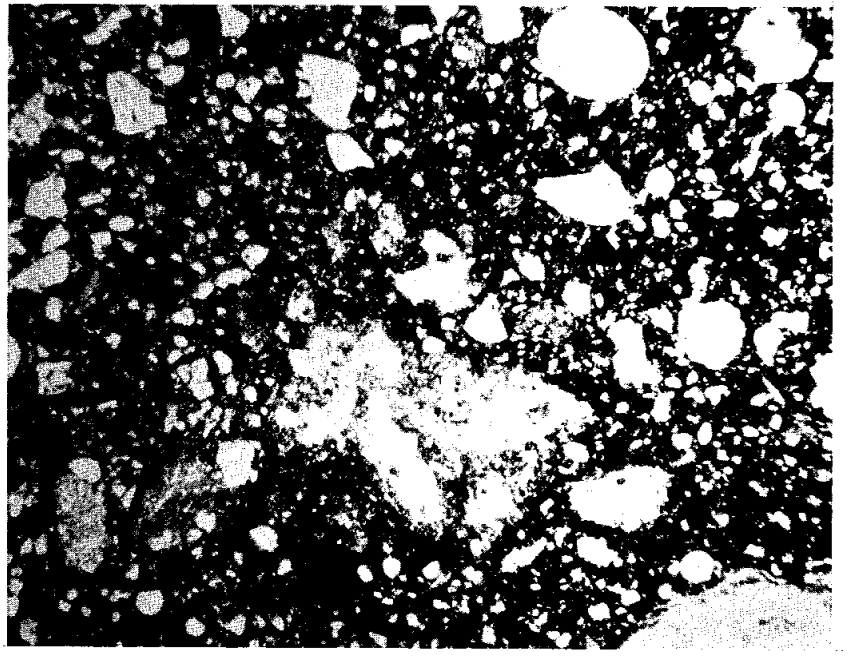

Figure 2. General matrix view of 15324,9. Transmitted light. Width about 2 mm.

TABLE 15324-1. Bulk chemical analysis

		,4
Wt%	SiO2	
	TiO2	
	Al2O3	
	FeO	
	MgO	
	CaO	
	Na2O	
	K2O	
	P2O5	
(ppm)	Sc	36.0
	V	130.0
	Cr	2500
	Mn	
	Co	48.0
	Ni	248
	Rb	2.6
	Sr	
	Y	47.0
	Zr	200.0
	Nb	15.0
	Hf	3.5
	Ba	160
	Th	1.79
	U	0.43
	Pb	2.3
	La	13.6
	Ce	31.0
	Pr	4.4
	Nd	18.3
	Sm	5.7
	Eu	1.07
	Gd	7.2
	Tb	1.09
	Dy	6.8
	Ho	1.64
	Er	4.7
	Tm	0.73
	Yb	4.4
	Lu	0.68
	Li	
	Be	
	B	
	C	
	N	
	S	
	F	
	Cl	
	Br	
	Cu	11.0
	Zn	
(ppb)	I	
	At	
	Ga	5000
	Ge	
	As	
	Se	
	Mo	
	Tc	
	Ru	
	Rh	
	Pd	
	Ag	
	Cd	
	In	
	Sn	190
	Sb	
	Te	
	Cs	100
	Ta	
	W	130
	Re	
	Os	
	Ir	
	Pt	
	Au	
	Hg	
	Tl	
	Bi	
		(1)

References and methods:

(1) S.R. Taylor et al. (1973); spark source mass spec.; emission spec.

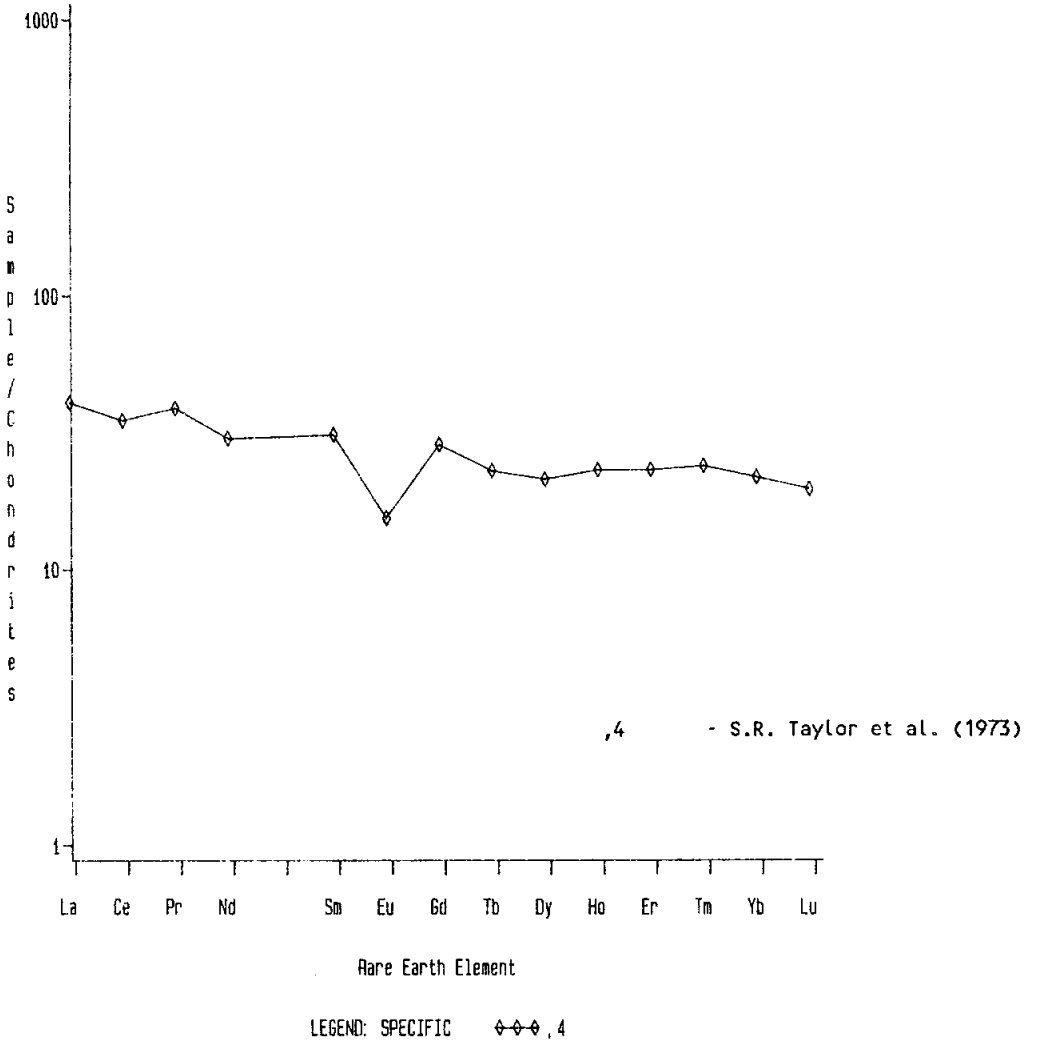

Figure 3. Rare earths in 15324,4

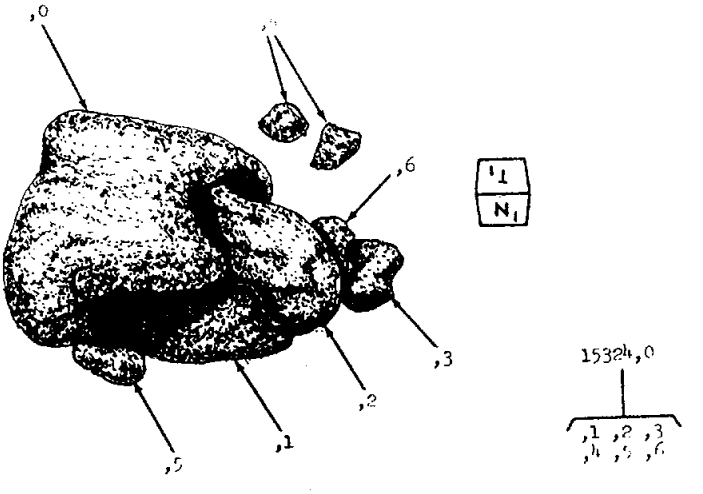

Figure 4. Chipping of 15324.

15325 REGOLITH BRECCIA, GLASS-COATED ST. 7 57.8 g

INTRODUCTION: 15325 is a glassy regolith breccia, conspicuous by the vesicular pale green glass coat which covers more than half its surface (Fig. 1a). Most of the breccia surface exposed is slickensided, and small patches of the glass coat overlie, hence post-date, the slickensides (Fig. 1b). The breccia itself contains glass, mineral, and debris in a glassy matrix. Some of the glass coat has zap pits, especially 100 micron diameter pits at one end, but no pits are present outside the glass area. 15325 was collected as part of the rake sample from the north-east rim of Spur Crater.

Fig. 1a

Figure 1. Pre-chip photos of 15325. Area marked with arrow on 1b is source of ,1 and ,2. (a) S-76-26844; b) S-76-26840.

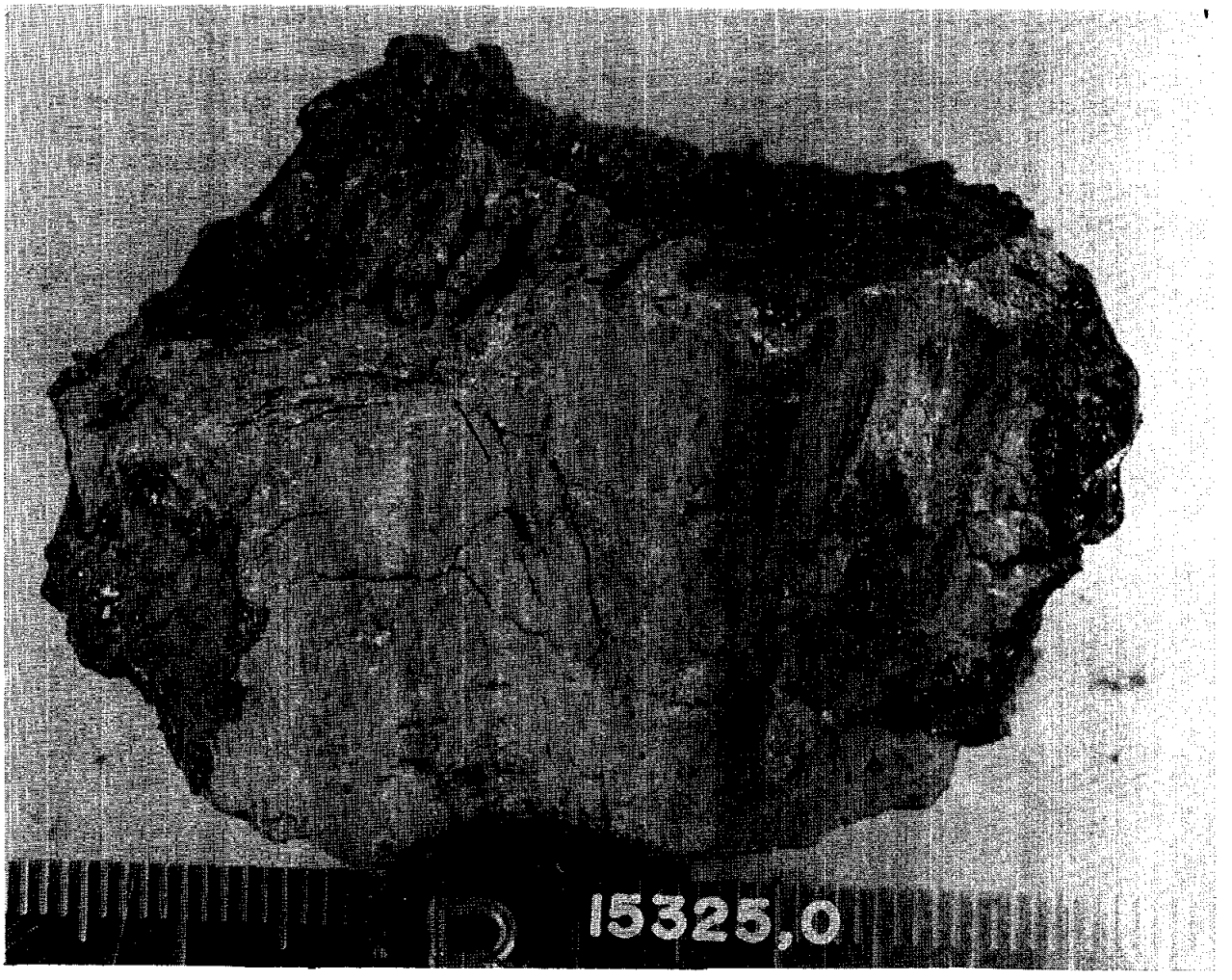

Fig. 1b

PETROLOGY: 15325 is a glassy breccia (Fig. 2) with a dense glassy matrix with a porosity lower than most Spur Crater regolith breccias. It has a vaguely foliated or sheared appearance in thin sections. It contains abundant glass debris, including green, colorless, yellow, and red. Lithic clasts are small and include varied feldspathic breccias, glassy breccias, and KREEP basalts. The glass coat does not appear in thin sections.

Figure 2. Photomicrograph of general matrix in 15325,4. Transmitted light. Width about 2 mm.

CHEMISTRY: Wanke et al. (1977) reported an analysis of the bulk breccia, including major, minor, and trace elements (Table 1, Fig. 3). The composition is not unusual for a Spur Crater regolith breccia.

PROCESSING AND SUBDIVISIONS: ,1 and ,2 were chipped from the slickensided area indicated in Figure 1. ,1 was partly used in producing thin sections ,4 and ,5. ,2 was used for the chemical analysis. The glass coat has not been allocated.

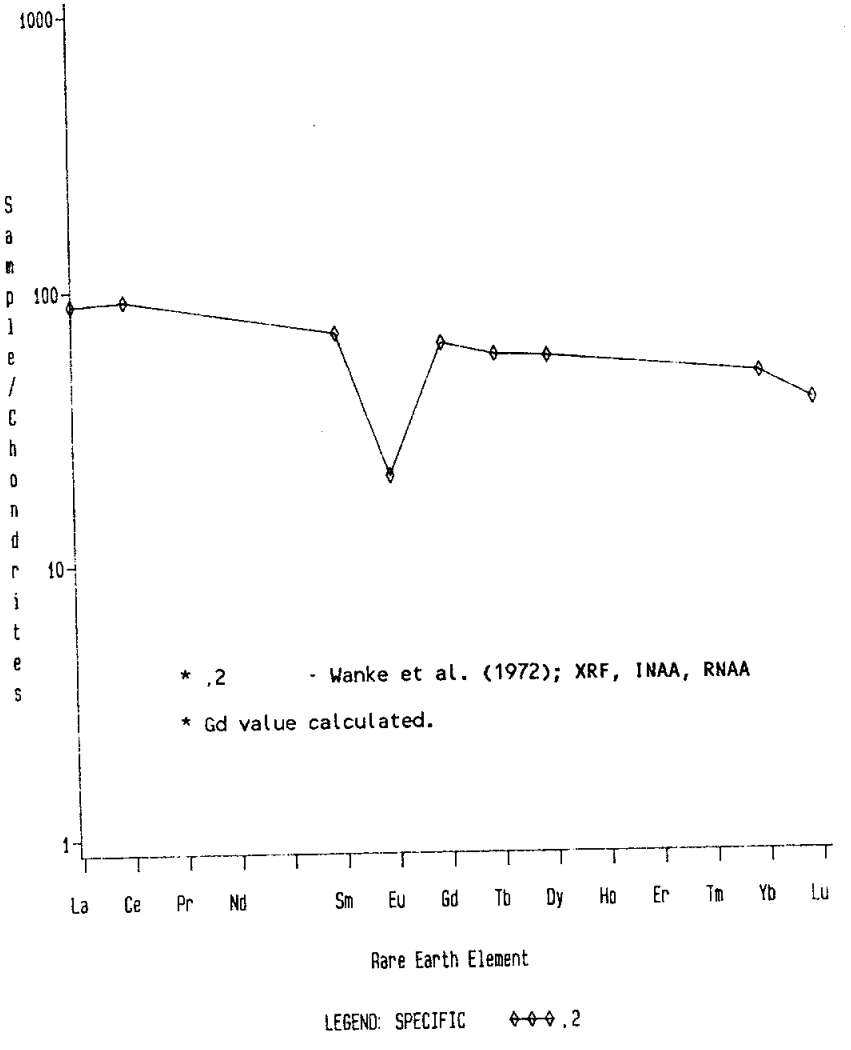

Figure 3. Rare earths in bulk rock 15325 (Wanke et al., 1977).

TABLE 15325-1. Bulk chemical analysis

		,2
Wt %	SiO2	48.4
	TiO2	1.28
	Al2O3	16.5
	FeO	12.7
	MgO	10.8
	CaO	11.1
	Na2O	0.510
	K2O	0.246
	P2O5	0.247
(ppm)	Sc	23.3
	V	77.4
	Cr	2270
	Mn	1225
	Co	35.7
	Ni	180
	Rb	
	Sr	138
	Y	96
	Zr	405
	Nb	29
	Hf	10.0
	Ba	290
	Th	4.68
	U	
	Pb	
	La	29.5
	Ce	81.1
	Pr	
	Nd	
	Sm	12.6
	Eu	1.45
	Gd	
	Tb	2.71
	Dy	18.0
	Ho	
	Er	
	Tm	
	Yb	9.76
	Lu	1.32
	Li	
	Be	
	B	
	C	
	N	
	S	450
	F	
	Cl	
	Br	
	Cu	
	Zn	
(ppb)	I	
	At	
	Ga	
	Ge	
	As	
	Se	
	Mo	
	Tc	
	Ru	
	Rh	
	Pd	
	Ag	
	Cd	
	In	
	Sn	
	Sb	
	Te	
	Cs	
	Ta	1270
	W	
	Re	
	Os	
	Ir	
	Pt	
	Au	
	Hg	
	Tl	
	Bi	
		(1)

References and methods:

(1) Wanke et al. (1972); XRF, INAA, RNAA.

15326 REGOLITH BRECCIA ST. 7 2.5 g

INTRODUCTION: 15326 is a glassy regolith breccia (Fig. 1) poor in lithic fragments, and rich in glass spheres. It was dusty but with abundant green material visible. It has a few zap pits. It was collected as part of the rake sample from the north-east rim of Spur Crater.

Figure 1. Post-chip view of 15326. Largest piece is ,0; second largest is ,1, used for thin sections.

PETROLOGY: 15326 is a regolith breccia which is very rich in glass spheres (Fig. 2), mainly green, and very poor in lithic and mineral fragments. Steele et al. (1977) reported 50% glass, 45% fine matrix, only 5% mineral fragments, and no lithic fragments. The glasses are mainly spheres or devitrified spheres. The fine matrix is opaque, brown, and glassy, and is moderately porous.

PROCESSING AND SUBDIVISIONS: Chips taken from ,0 (Fig. 1) include the largest ,1, which was used to make thin sections ,1 and ,6, with potted butts remaining. The other chips were not numbered separately, remaining with ,0.

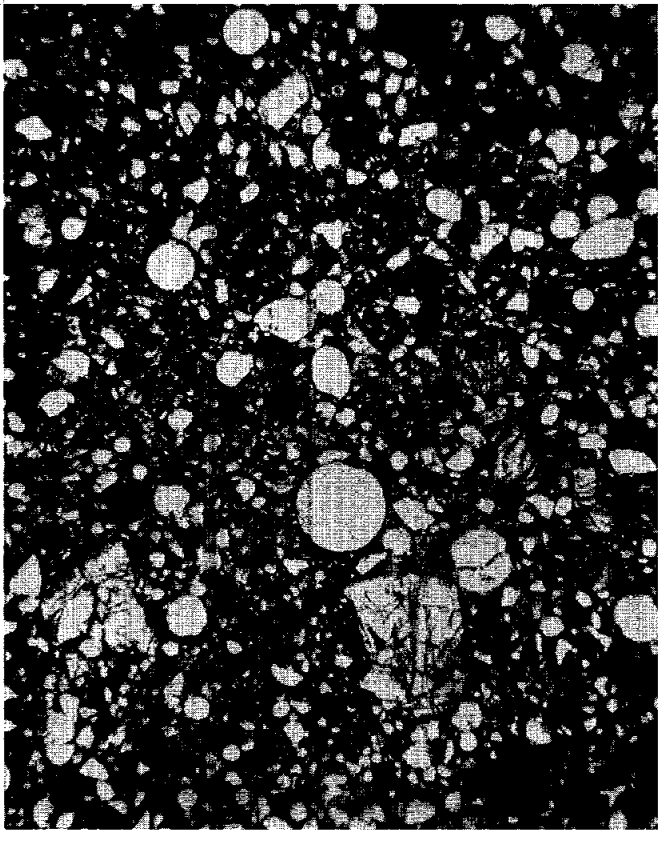

Figure 2. Photomicrograph of general matrix of 15326,6. Transmitted light. Width about 2 mm.

15327 CLAST-RICH GLASSY MELT BRECCIA ST. 7 12.4 g

INTRODUCTION: 15327 is a coherent, dark, polymict breccia with a prominent white clast (Fig. 1). 15327 is very unusual. It consists of dominantly coarse clasts (larger than 0.5 mm) embedded in a pale, clear, microvesiculated glass which also appears to occur partly as a surface coat glass. The white clast appears to be a pristine cumulate spinel-bearing troctolitic anorthosite. Zap pits are present, including a 3 mm one in the white clast (Fig. 1). 15327 was collected as part of the rake sample from the north-east rim of Spur Crater.

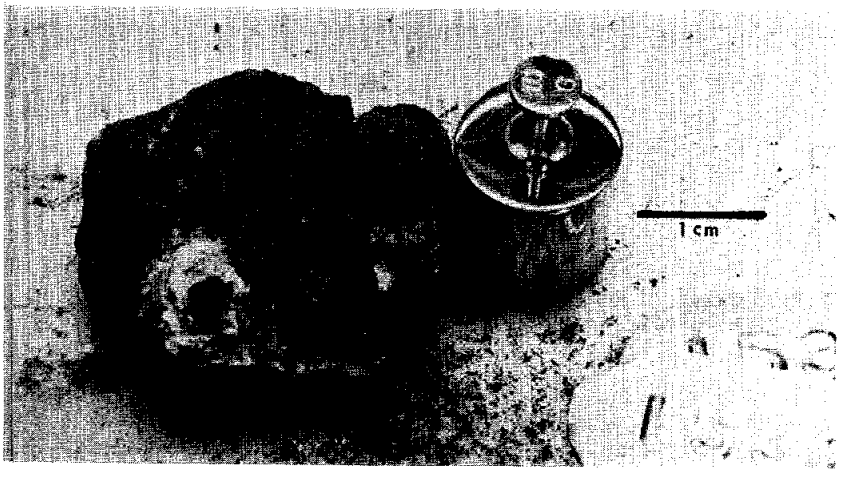

Figure 1. Post-saw view of 15327. S-71-59204

PETROLOGY: 15327 is a polymict glassy breccia, but it is not a regolith breccia. The glass matrix is clear and continuous (Fig. 2a) in contrast with the opaque, multigenerational matrix of regolith breccias. It occupies about 10% or less of the sample. Glass forms a coat in places (Fig. 2b) but this could be a separate glass. Dowty et al. (1973b) described 15327 as a polymict microbreccia whose clasts are mainly lithic and mineral fragments. Feldspar is predominant, but large pyroxenes and spinels are also present. All the minerals have a mosaic extinction. Hlava et al. (1973) presented analyses of glass fragments; green glass compositions are rare but a variety of glass compositions exists.

Clasts are of two main varieties, one a series of impact melts, the other pieces of an apparently single noritic/troctolitic anorthosite. The impact melts are dominantly crystalline and range from plagioclase-phyric (Fig. 2c) to microsubophitic and micropoikitic. The anorthosite fragments appear to be fragments strung out from the larger white clast visible in Figure 1. Hlava et al. (1973) presented mineral analyses for the large fragment in ,7, showing a restricted set of mineral compositions: calcic plagioclase ($An_{96-97.5}$, Fe <0.08%), magnesian olivine (Fo_{89}); and magnesian pyroxene, diopside ($En_{49}Wo_{48}$) with some orthopyroxene (Fig. 3). Most fragments are very plagioclase-rich; a defocussed beam analysis by Dowty et al. (1973b) has 32.3% Al_2O_3. Several fragments have good to excellent cumulate textures preserved, with curving grain boundaries; the fragments have been lightly shocked but not cataclasized. One fragement in ,9 has an excellent cumulate texture (Fig. 2d), has olivine and plagioclase which appear the same as those in other fragments, but has the added distinction of containing pink spinel as the dominant phase, occuring as two grains with a curving boundary. The spinel is only faintly pink, partly because the section is thin. Coupled with the presence of spinel as large (up to about 400 microns) mineral fragments elsewhere in 15327, this suggests that the large white clast in 15327 is actually a spinel-troctolitic anorthosite, akin to those in 15445. Simonds et al. (1975) referred to 15327 as a cataclastic annealed coarse-grained rock, but this designation is not in accord with either the macroscopic observations nor with any of the thin sections.

PROCESSING AND SUBDIVISIONS: Because 15327 was so coherent, it was sawn, the butt end providing ,1 and ,2 (Fig. 1). ,2 became the stub for thin sections ,7 to ,10. No other subdivisions or allocations have been made.

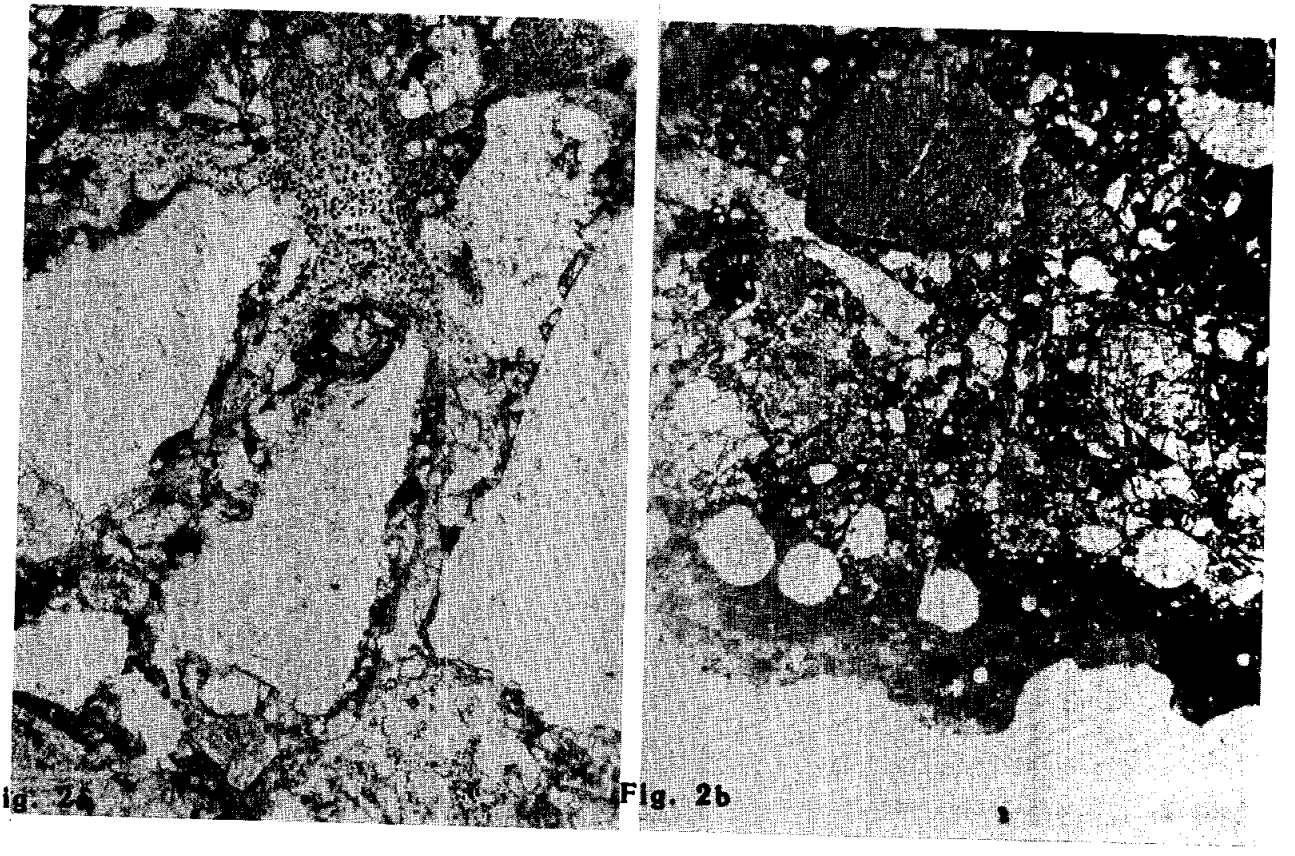

Fig. 2a

Fig. 2b

Figure 2. Photomicrographs of 15327. a) 15237,9, showing clasts of the anorthosite immersed in a continuous, clear, microvesiculated glass. Transmitted light. Width about 600 microns. b)15327,10, showing polymict breccia with glass matrix and vesicular glass coat. Transmitted light. Width about 2 mm. c) 15327,10, showing fragments of plagioclase-phyric impact melts embedded in glass. Transmitted light. Width about 2 mm. d) 15327,9, showing spinel cumulate clast. Transmitted light. Width about 600 microns. O = olivine, $ = spinel, P = plagioclase.

Fig. 2c

Fig. 2d

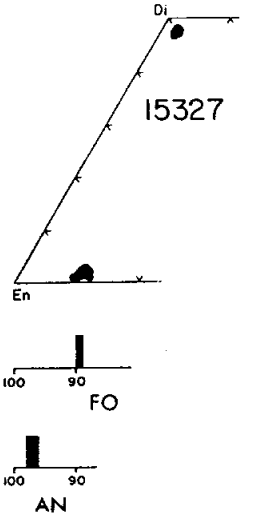

Figure 3. Compositions of minerals in anorthosite clast in 15327,7. (Hlava et al., 1973).

15328 REGOLITH BRECCIA ST. 7 0.3 g

INTRODUCTION: 15328 is a dusty breccia, with small mineral fragments visible and the general appearance of a regolith breccia (Fig. 1). It is slabby and lacks zap pits. It has never been processed or allocated. It was collected as part of the rake sample from the north-east rim of Spur Crater.

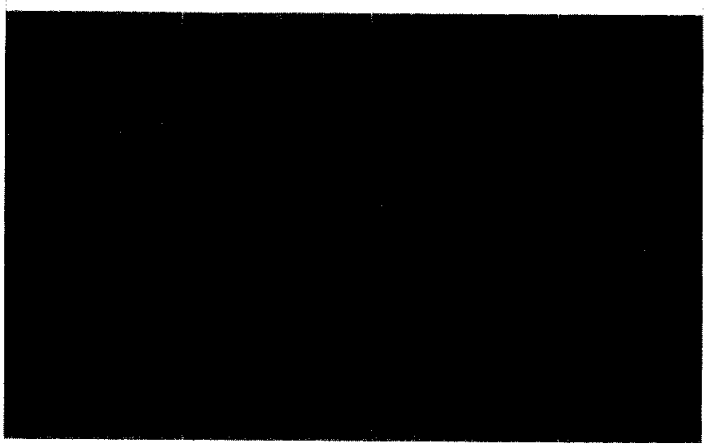

Figure 1. Sample 15328. S-71-49511

15329 REGOLITH BRECCIA, GLASS-COATED ST. 7 2.2 g

INTRODUCTION: 15329 is a regolith breccia with a partial bubbly glass coat (Fig. 1). It is fairly coherent though moderately porous, and has a population dominated by glass and glassy melt breccias, but including KREEP basalts. The sample has possible zap pits on one small area of glass, but pits are not obvious on the breccia surface. The sample was collected as part of the rake sample from the north-east rim of Spur Crater.

PETROLOGY: 15329 is a dense-looking, shocked, and moderately porous regolith breccia, with a partial glass coat (Fig. 2). The glasses include spheres and fragments of clear, green, brown, yellow, and red glass. According to Steele et al. (1977) the sample consists of 50% glass, 5% lithic fragments (anorthosites and KREEP basalts), 30% mineral clasts, and 15% fine matrix. The fine matrix and the glass are difficult to distinguish and the mineral clasts are mostly plagioclase. Opaque, messy, glassy breccias are prominent lithic clasts, and KREEP basalts are present (Fig. 2a). Two KREEP basalts are tabulated by Steele et al. (1977) with some mineral data.

The glass coat (Fig. 2b) is vesicular, very pale-green-gray, and faintly banded.

PROCESSING AND SUBDIVISIONS: Because of its coherency 15329 was sawn, producing chips (,1) and a sawn piece (,2) (Fig. 1). These were combined as ,2 and entirely used to produce thin sections ,6 to ,8. ,0 is now 1.44 grams.

Figure 1. Post-sawing view of 15329. S-71-59555

Fig. 2a

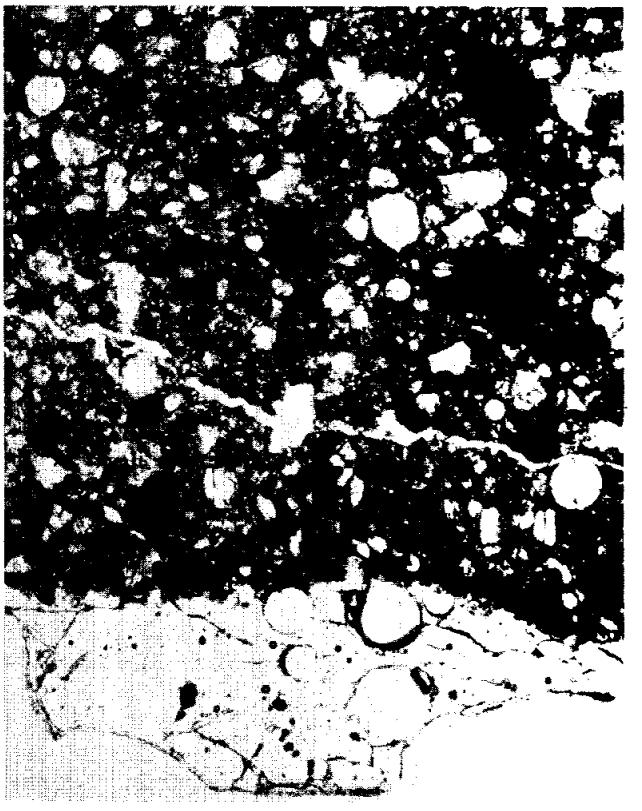

Fig. 2b

Figure 2. Photomicrographs of 15329,7, transmitted light. a) general view showing dark glassy breccias (top right, etc.), colorless glass (lower center), and two KREEP basalt fragments (bottom left and right). Width about 2 mm. b) general view showing glass coat (top). Width about 1.25 mm.

15330 REGOLITH BRECCIA ST. 7 57.8 g

INTRODUCTION: 15330 is a tough, glassy, gray-brown, and not very porous regolith breccia (Fig. 1). It contains glass, mineral, and lithic debris including feldspathic breccias, but KREEP basalts are not present or are inconspicuous. It is also low in incompatible element abundances compared with most local regolith breccias. It has zap pits on all sides, including large (greater than 5 mm) ones. Clasts larger than about 4 mm are not present (Fig. 1). 15330 was collected as part of the rake sample from the north-east rim of Spur Crater.

PETROLOGY: 15330 is a clean-looking regolith breccia (Fig. 2) in which the numerous mineral fragments are generally little shocked. Nonetheless, it is not very porous. It contains abundant glass, including devitrified glass, glassy breccias, and the matrix. Colorless, green, yellow, and orange glasses exist as spheres and shards. Some green glass is devitrified. The lithic clasts include the glassy breccias and highlands feldspathic breccias (mainly fine-grained impact melts or granoblastic rocks), and one looks like a noritic anorthosite cumulate. Small mare basalt fragments are present but KREEP basalt fragments appear to be absent.

CHEMISTRY: Wanke et al. (1977) reported a bulk analysis for major, minor, and trace elements (Table 1, Fig. 3). The sample is not remarkable in major element composition, but is rather lower in incompatible elements than local regolith breccias.

MAGNETICS: Gose et al. (1972) determined a natural remanent magnetic intensity of a little less than 10^{-4} emu/g, using a Develco cryogenic magnatometer. This value is higher than that for igneous rocks (mare basalts).

PROCESSING AND SUBDIVISIONS: Gose et al. (1972) made their measurement using the entire sample. Subsequently it was chipped (Fig. 1). Only ,4 (for chemistry), and ,5 (for thin sections ,8 and ,9) has been used, and much of ,5 remains. ,0 is now 47.3 g.

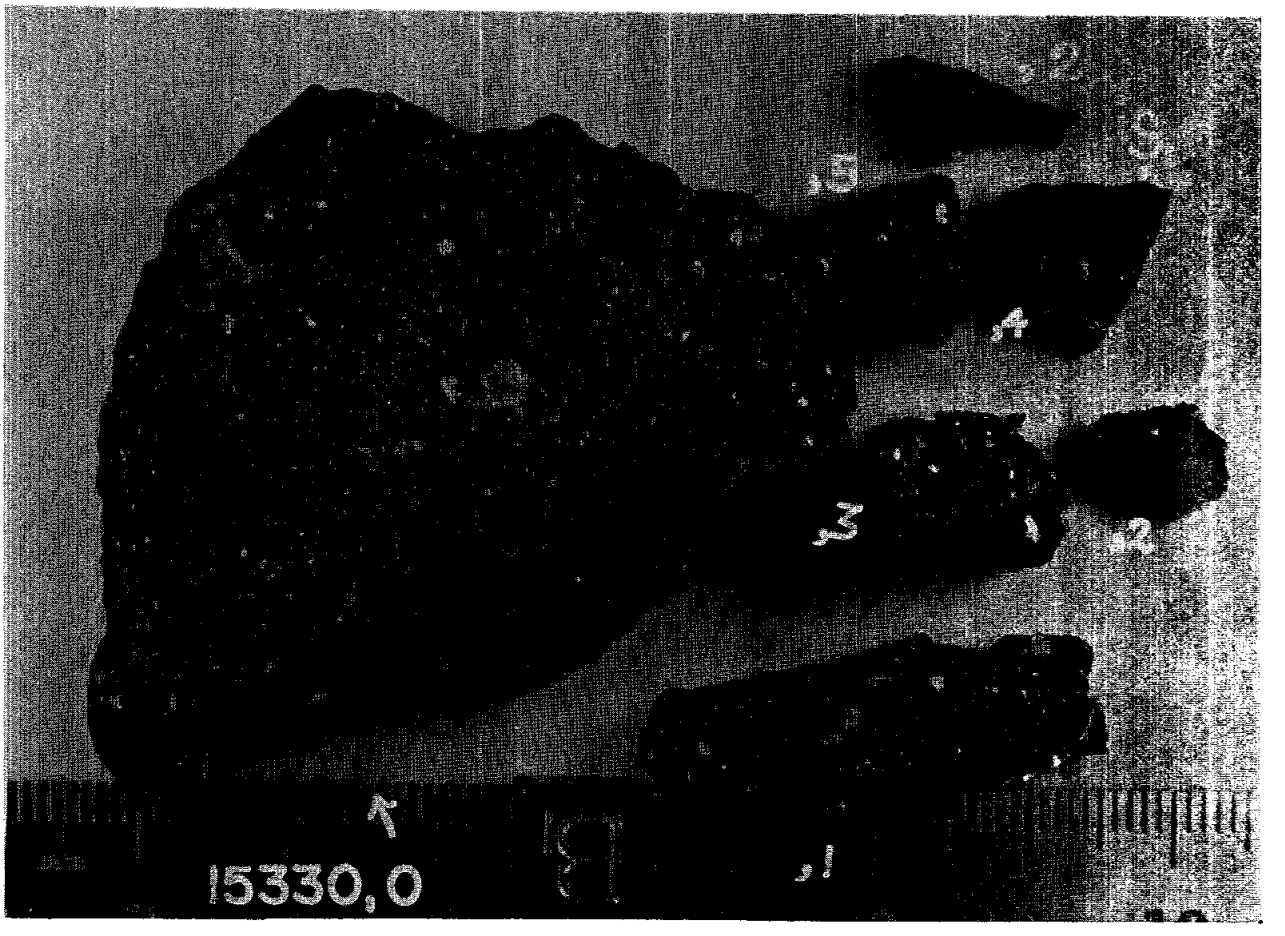

Figure 1. Post chip view of 15330,0 and its daughters.
S-76-26373

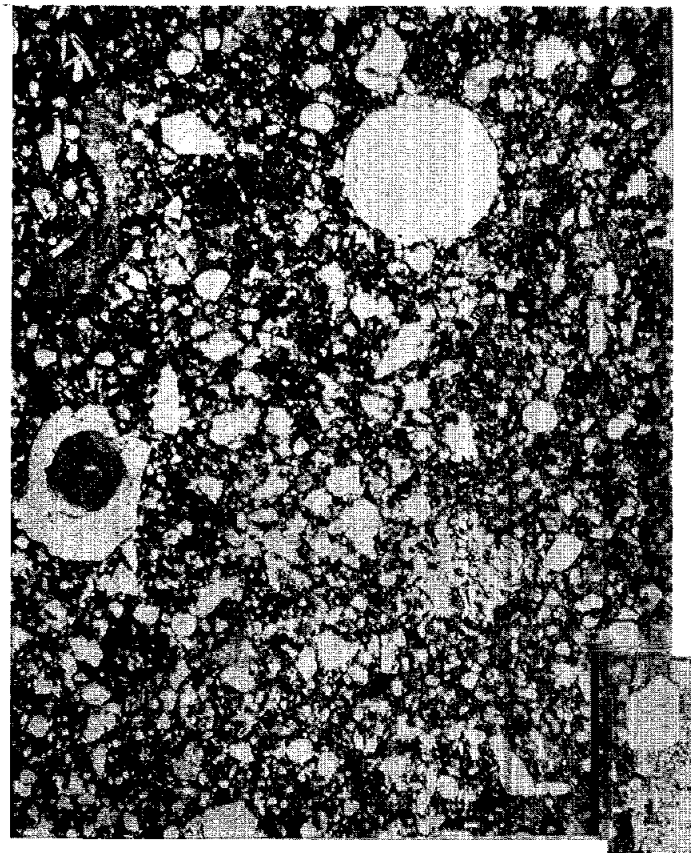

Fig. 2a

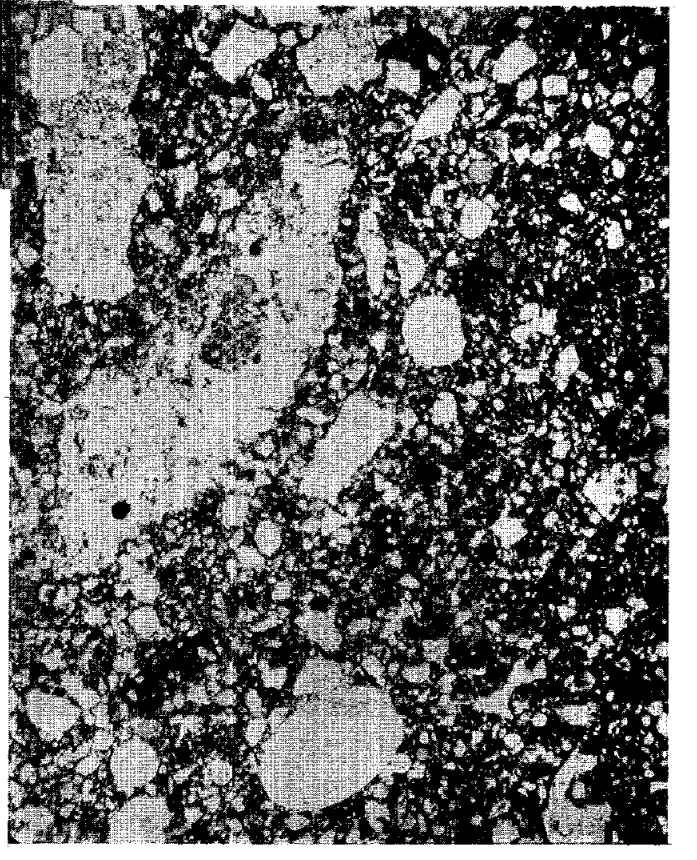

Fig. 2b

Figure 2. Photomicrographs of 15330,8. Transmitted light. Widths about 2 mm. a) shows a devitrified sphere within yellow glass (left), a yellow glass sphere (top center), and a small mare (?) basalt (lower right center). b) shows a crystalline feldspathic breccia (top left), and a glassy breccia (left center). Both show other glass spheres and mineral fragments.

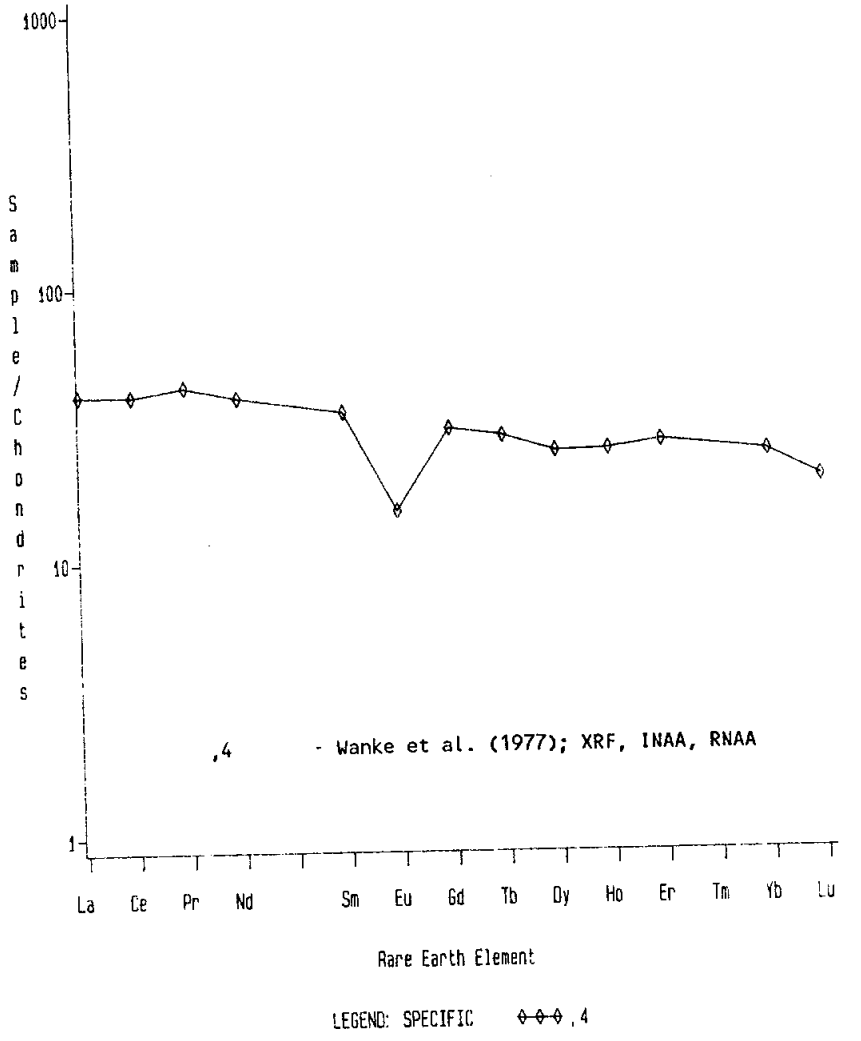

Figure 3. Rare earths in bulk 15330.

TABLE 15330-1. Bulk chemical analysis

		,4
Wt %	SiO2	46.22
	TiO2	1.12
	Al2O3	16.3
	FeO	12.7
	MgO	11.7
	CaO	11.7
	Na2O	0.404
	K2O	0.125
	P2O5	0.135
(ppm)	Sc	25.4
	V	86.8
	Cr	2300
	Mn	1300
	Co	46.6
	Ni	300
	Rb	2.81
	Sr	118
	Y	57
	Zr	196
	Nb	12
	Hf	4.72
	Ba	136
	Th	2.2
	U	0.58
	Pb	
	La	13.5
	Ce	35.7
	Pr	4.90
	Nd	24
	Sm	6.36
	Eu	1.06
	Gd	7.63
	Tb	1.35
	Dy	8.02
	Ho	1.8
	Er	5.45
	Tm	
	Yb	5.01
	Lu	0.68
	Li	9.8
	Be	1.91
	B	
	C	
	N	
	S	850
	F	51
	Cl	16.4
	Br	0.084
	Cu	11.2
	Zn	42.4
(ppb)	I	
	At	
	Ga	4990
	Ge	
	As	24
	Se	480
	Mo	
	Tc	
	Ru	
	Rh	
	Pd	
	Ag	
	Cd	
	In	
	Sn	
	Sb	
	Te	
	Cs	130
	Ta	650
	W	250
	Re	1.2
	Os	
	Ir	
	Pt	
	Au	2.9
	Hg	
	Tl	
	Bi	
		(1)

References and methods:

(1) Wanke et al. (1977); XRF, INAA, RNAA.

15331 REGOLITH BRECCIA ST. 7 2.6 g

INTRODUCTION: 15331 is a regolith breccia (Fig. 1) containing glass and mineral fragments, and prominent small lithic fragments, mainly breccias. The sample was a dark slabby fragment with one glassy slickensided surface. Spall areas suggested that one end had been exposed, but zap pits were not obvious. 15331 was collected as part of the rake sample from the north-east rim of Spur Crater.

PETROLOGY: 15331 is a glassy regolith breccia (Fig. 2). Neither thin section (,2 and ,6) is of high quality, and the porosity and fine matrix texture are impossible to evaluate. Colorless, green, yellow, and orange glasses occur as spheres and shards. Steele et al. (1977) tabulated 15331,2 as 35% glass, 20% lithic fragments (mare, anorthosite, and breccia), 25% mineral fragments, and 30% fine matrix. They noted several anorthosite clasts, and one large holocrystalline lithic clast. They tabulated two clasts; A had 20% pyroxene ($En_{\sim 58}Wo_{10-30}$) and 80% plagioclase (low iron, high calcium) with a fine grain size. B was a variolitic mare basalt. They plotted an exsolved pyroxene fragment (Mg' about 62). Steele et al. (1972b) reported grains of olivine (Fo_{87}) and pink spinel in the matrix.

PROCESSING AND SUBDIVISIONS: 15331 was chipped to produce ,1 and ,2 (Fig. 3). ,2 was used to make thin sections ,2 and ,6, with small potted butts remaining. ,0 is now 1.69 g.

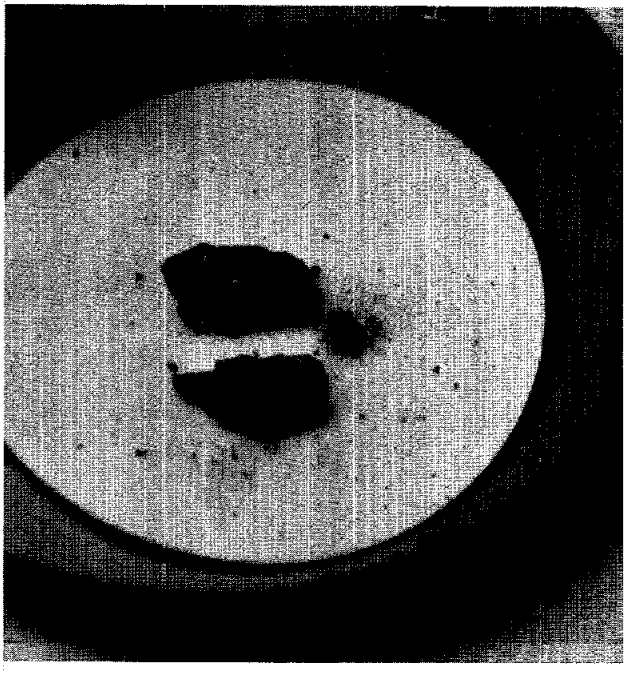

Figure 1. Post split view of 15331,0 and ,1 before ,1 was split into two pieces. S-71-57235

Figure 2. General matrix of 15331,2. Transmitted light. Width about 2 mm.

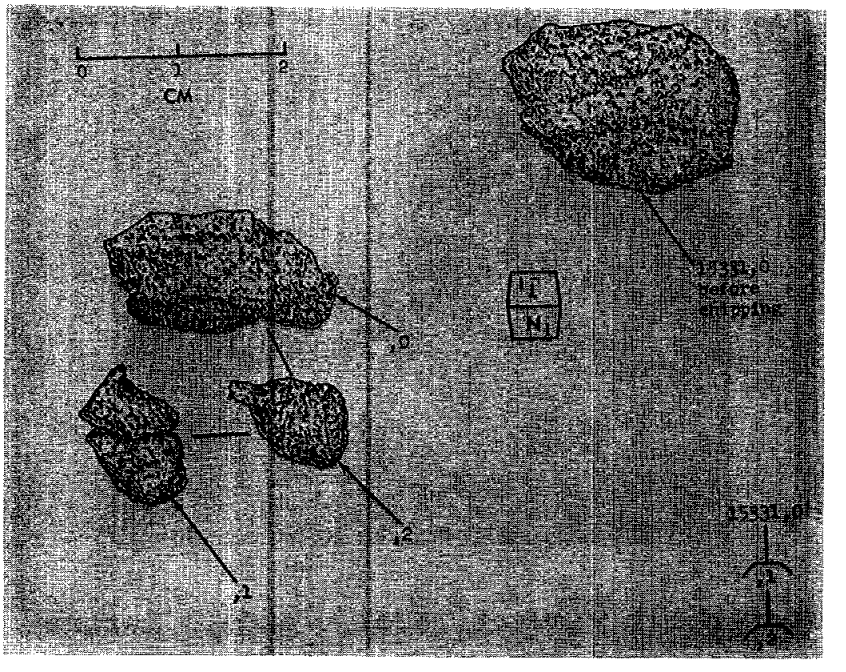

Figure 3. Chipping of 15331.

15332 AGGLUTINATE ST. 7 2.3 g

INTRODUCTION: 15332 is a dark agglutinate with abundant vesicles (Fig. 1). Pale clasts are visible within it, and a 1-mm zap pit occurs on one such clast. The sample was collected as part of the rake sample from the north-east rim of Spur Crater.

PETROLOGY: 15332 is an agglutinate (Fig. 2), consisting of a brownish and grayish glass which is very vesicular and enclosing small lithic clasts and many mineral clasts (Dowty et al., 1973b). The glass is faintly banded and contains minute Fe-metal spherules. Hlava et al. (1973) tabulated glass compositions. The agglutinate glass is aluminous, essentially low-K Fra Mauro (Table 1). Other glasses (spherules, etc.) include high-alumina highlands and low-alumina mare varieties. Hlava et al. (1973) also reported analyses of plagioclase in an ANT fragment (An about 90) and in a high-alumina basalt fragment (An about 95); they wrongly listed the An contents as Ab contents.

PROCESSING AND SUBDIVISIONS: A single chip (,1) was taken (Fig. 1) and partly used to make thin sections ,3; ,4; and ,5.

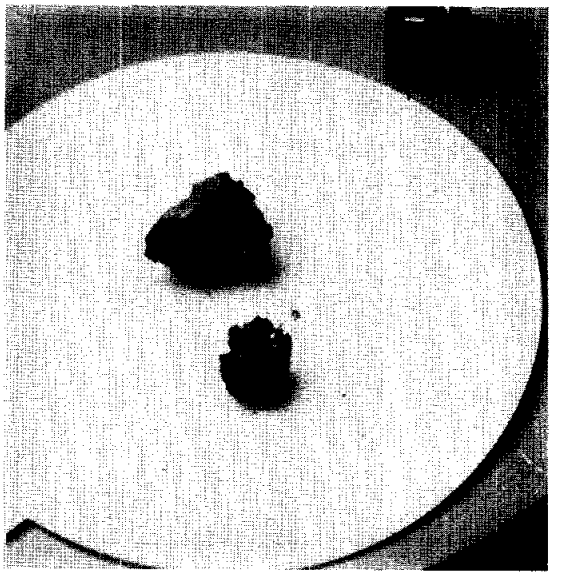

Figure 1. Post-split view of 15332. S-71-57219

Figure 2. General view of 15332,3. Transmitted light. Width about 2 mm. The vesicles are prominent.

TABLE 15332-1. Compositions of matrix glass in 15332 (Hlava et al., 1973)

	Melt Matrix			Spherule and fragmental inclusions									
	12	10	8	16	15	13	6	4	5	9	1	2	3
SiO_2	46.7	46.4	46.8	50.0	50.8	51.4	50.5	49.7	49.4	50.6	46.3	43.2	44.2
TiO_2	1.39	1.40	1.43	1.53	1.75	2.04	2.98	1.72	1.74	4.2	.38	13.5	3.2
Al_2O_3	16.9	16.5	16.5	16.5	15.6	14.8	14.1	13.8	13.8	9.9	7.1	7.1	8.5
Cr_2O_3	.19	.20	.12	.18	.23	.24	.11	.21	.22	.10	.41	.48	.33
FeO	10.8	11.1	11.4	9.1	9.4	9.7	11.3	12.0	12.1	15.4	19.8	21.0	21.0
MnO	.18	.19	.14	.17	.19	.17	.20	.22	.23	.24	.35	.33	.36
MgO	10.2	10.4	10.4	8.9	8.5	8.7	7.0	10.0	11.1	6.1	17.0	11.7	11.5
CaO	11.3	11.3	11.1	10.5	9.9	9.7	9.8	10.4	9.9	9.0	8.5	8.1	9.2
BaO	.07	.04	.09	.09	.10	.11	.21	.07	.09	.21	.03	.12	.08
Na_2O	.59	.49	.56	.63	.79	.64	.93	.63	.59	1.03	.07	.51	.36
K_2O	.27	.24	.24	.49	.64	.51	.82	.41	.48	1.05	.03	.15	.09
P_2O_5	.26	.25	.26	.24	.20	.22	.22	.25	.23	.21	.20	.17	.22
ZrO_2	.08	.08	.21	.17	.17	.33	.14	.09	.58	.15	.03	.09	.09
Total	98.93	98.59	98.85	98.48	98.27	98.40	98.50	99.55	100.03	98.72	100.40	99.45	99.21
CIPW Molecular Norms													
q	--	--	--	6.35	5.74	7.81	6.65	2.44	.96	7.70	--	--	--
z	.08	.08	.20	.15	.16	.16	.32	.13	.14	.56	.03	.09	.09
or	1.45	1.45	1.45	3.85	3.91	3.12	5.07	2.48	2.88	6.62	.18	.96	.56
ab	5.40	4.50	5.12	1.58	7.33	5.95	8.73	5.78	5.37	9.87	.64	4.93	3.40
an	43.54	43.06	42.54	43.84	38.33	37.25	33.33	34.33	34.01	20.57	19.16	17.89	22.37
di	9.56	10.13	9.56	6.86	8.97	9.01	13.13	13.46	11.49	20.80	17.73	19.48	19.35
hy	31.72	32.13	30.55	34.48	32.39	33.04	27.85	38.20	42.00	26.97	35.86	22.38	34.39
ol	5.54	5.93	7.91	--	--	--	--	--	--	--	25.02	13.15	14.22
cm	.22	.23	.14	.21	.27	.28	.13	.24	.25	.12	.46	.57	.39
il	1.98	2.00	2.03	2.21	2.52	2.94	4.34	2.45	2.46	6.36	.54	20.21	4.80
ap	.56	.54	.56	.52	.44	.48	.49	.54	.49	.47	.43	.39	.49
Group	AHAB	AHAB	AHAB	AHAB	AHAB	AHAB	AHAB	AHAB	AHAB	MISC	FP	IOB	PIC

15333 REGOLITH BRECCIA (?) ST. 7 0.3 g

INTRODUCTION: 15333 is a breccia with the macroscopic properties of a regolith breccia (Fig. 1). It was dusty and slabby, with no pits obvious. It has never been subdivided or allocated. It was collected as part of the rake sample from the north-east rim of Spur Crater.

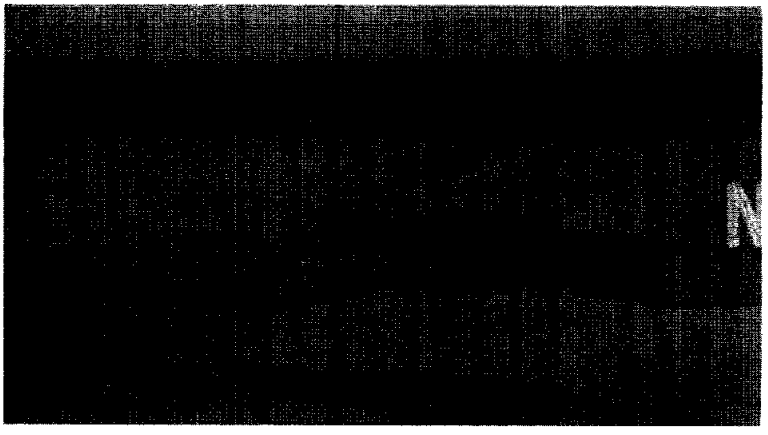

Figure 1. Sample 15333. S-71-49641

15334 REGOLITH BRECCIA ST. 7 7.5 g

INTRODUCTION: 15334 is a polymict breccia with the macroscopic properties of a regolith breccia (Fig. 1). It has two small glass surface patches. Zap pits are not obvious anywhere. The sample was subdivided (Figs. 1, 2) but the only split was (unproductively) allocated, and returned. The sample was collected as part of the rake sample from the north-east rim of Spur Crater.

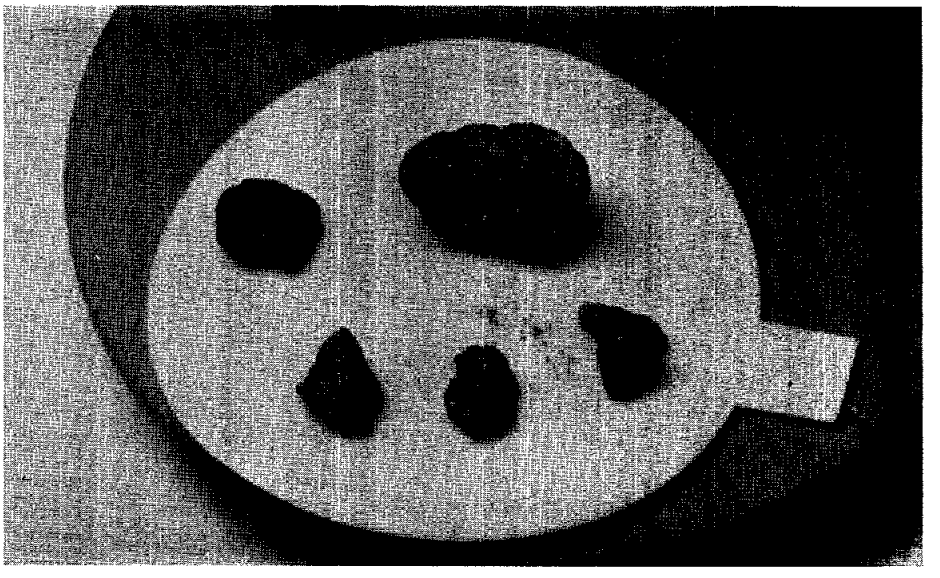

Figure 1. Post-split view of 15334. S-71-57233

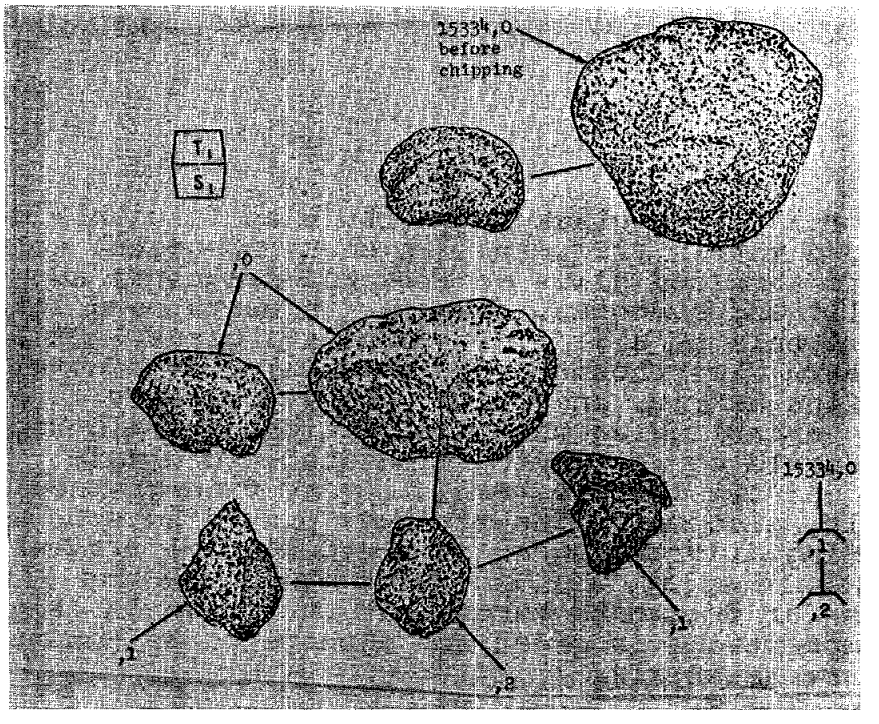

Figure 2. Chipping of 15334.

15335 REGOLITH BRECCIA ST. 7 6.0 g

INTRODUCTION: 15335 is a moderately friable, brown-gray regolith breccia (Fig. 1). It had apparent fresh fracture surfaces on both ends, and glassy slickensides on one surface. No zap pits were obvious. The sample was collected as part of the rake sample from the north-east rim of Spur Crater.

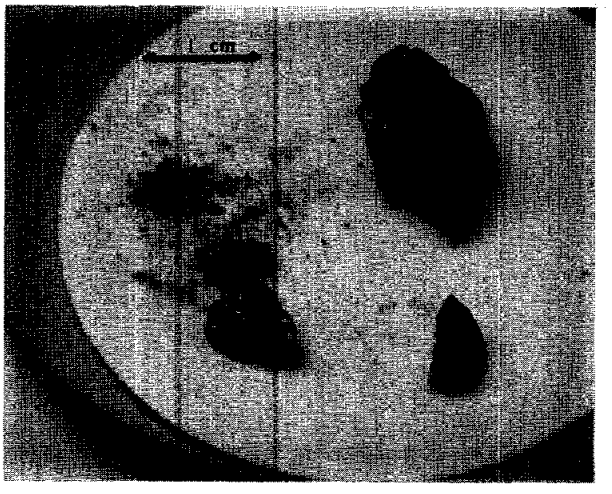

Figure 1. Post-chip view of 15335. S-71-57215

PETROLOGY: 15335 is a glassy regolith breccia with a dense-looking, brown matrix (Fig. 2). It contains green, colorless, yellow, and orange/red glass spheres and fragments as well as glassy lapilli and breccias, mineral fragments, and lithic fragments. Steele et al. (1977) found 40% glass, 10% lithic fragments (mare, anorthosite, and breccia), 15% mineral fragments, 25% fine matrix, and 10% porosity (porosity is actually difficult to establish as the thin sections are plucked and bubbled). Steele et al. (1977) tabulated two clasts: A with 80% plagioclase and 20% olivine (Fo_{88-90}), very fine-grained, and B, a mare basalt, also very fine-grained; providing some mineral data, including diagramming an exsolved mineral fragment (about $En_{55}Wo_{12}$). Steele et al. (1972b) showed pyroxene and olivine compositions for fragments throughout their sample (Fig. 3). The range of compositions is great and appears to be dominated by KREEP and mare materials.

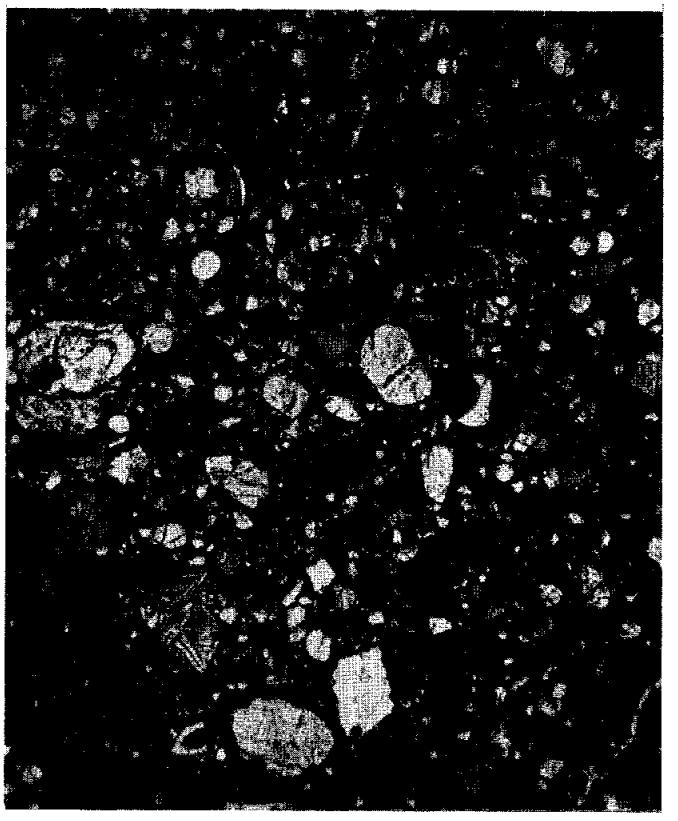

Figure 2. Photomicrograph of general matrix of 15335,6. Transmitted light. Width about 2 mm.

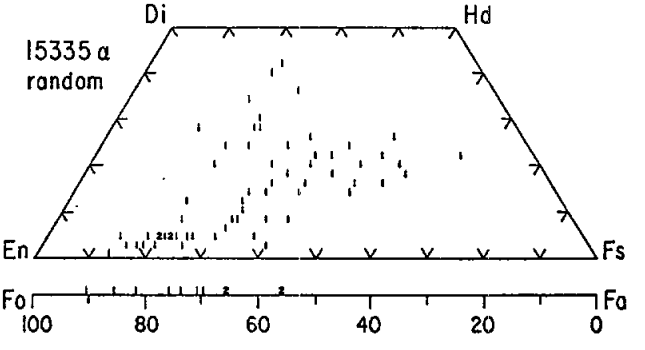

Pyroxenes and olivines in high-glass breccia 15335.

Figure 3 Pyroxenes and olivines in 15335 (Steele et al., 1972b).

PROCESSING AND SUBDIVISIONS: 15335 was chipped (Figs. 1 and 4). ,2 was used to produce thin sections ,2 and ,6, with potted butts remaining. ,0 is now 4.75 g.

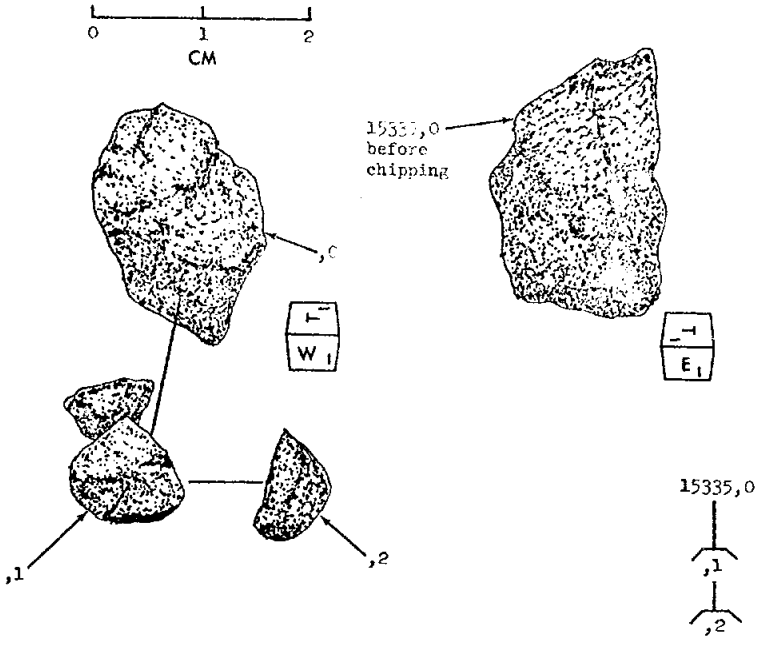

Figure 4. Chipping of 15335.

15336 REGOLITH BRECCIA (?), GLASS-COATED ST. 7 0.2 g

INTRODUCTION: 15336 is a light-colored breccia chip which is half-coated with a vesicular glass (Fig. 1). Possibly it is an agglutinate. It has never been subdivided or allocated. It was collected as part of the rake sample from the north-east rim of Spur Crater.

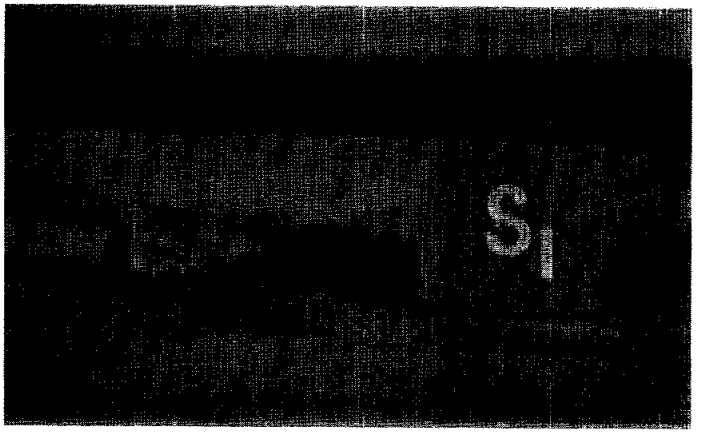

Figure 1. Sample 15336. The vesicular glass is on the bottom on this view. S-71-49633

15337 REGOLITH BRECCIA ST. 7 4.3 g

INTRODUCTION: 15337 is a regolith breccia with a dark glassy matrix (Fig. 1). It is gray-brown, glassy, and had possible spalls but no obvious zap pits. It was collected as part of the rake sample from the north-east rim of Spur Crater.

Figure 1. Post-split view of 15337,0 (right) and ,2 (left). S-71-57223

PETROLOGY: 15337 is a regolith breccia which is very heterogeneous compared with most (Fig. 2), and partly foliated. It was described by Dowty et al. (1973b) as a polymict microbreccia with a dark glassy matrix. Some patches are much darker and glassier than others, and there are many glassy schlieren and rounded glassy breccias. Spherules and fragments include clear, green, yellow, and sparse red/orange glass. "Chondrules" of Dowty et al. (1973b) are partly crystallized (or devitrified) glass spheres. Hlava et al. (1973) reported several analyses of glass of several colors, and including both aluminous and mare glasses. A vesicular glass vein occurs in one locality (Fig. 2). Lithic clasts are mainly breccias, but one appears to be an anorthositic norite with a cumulate texture.

Fig. 2a

Fig. 2b

Figure 2. Photomicrographs of 15337,4. Transmitted light. Widths about 2 mm. a) general matrix showing schlieren; b) matrix and vesicular glass vein.

PROCESSING AND SUBDIVISIONS: ,1, a chip removed from ,0, avoided a small white but prominent clast (Fig. 3). ,1 was split to produce ,2 (shown in Figure 1) which was partly used to produce thin sections ,4 and ,5. ,0 is now 3.2 g.

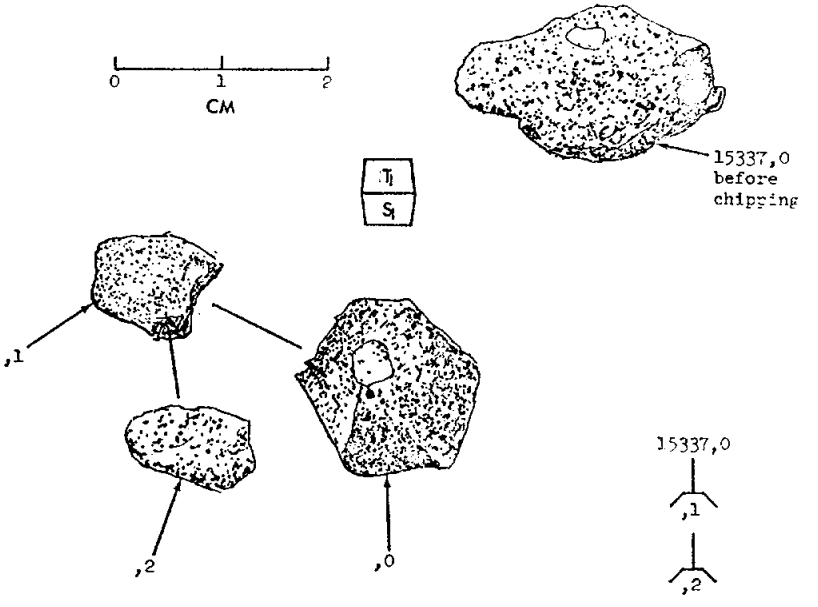

Figure 3. Chipping of 15337.

15338 REGOLITH BRECCIA ST. 7 11.1 g

INTRODUCTION: 15338 is a gray-brown regolith breccia (Fig. 1). It is dusty. Zap pits up to 4 mm diameter occur on at least one end, and a coarse surface texture is apparent there. The sample has never been subdivided or allocated. It was collected as part of the rake sample from the north-east rim of Spur Crater.

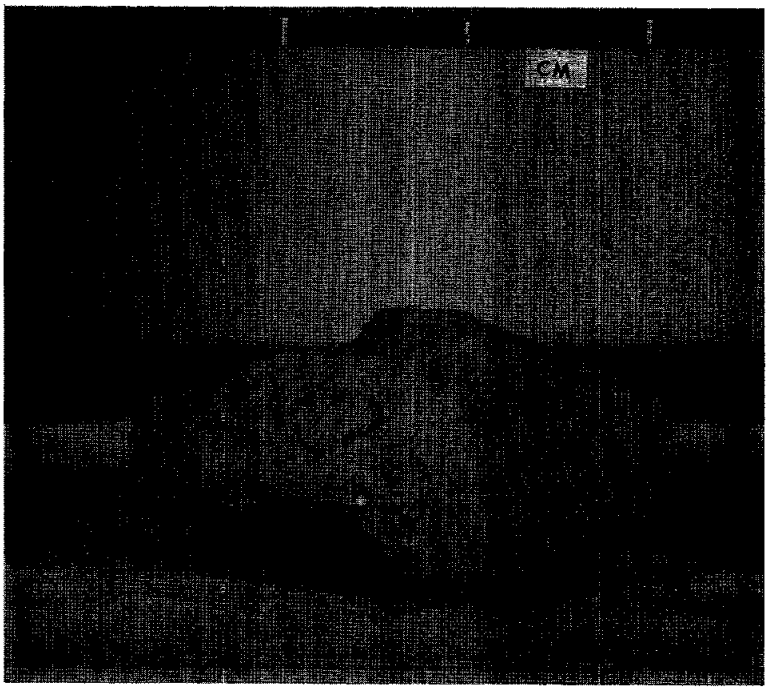

Figure 1. Sample 15338. S-71-49653

15339 REGOLITH BRECCIA (?) ST. 7 0.4 g

INTRODUCTION: 15339 is a tiny breccia fragment which has the macroscopic characteristics of a dust-covered regolith breccia. It has never been subdivided or allocated. It was collected as part of the rake sample from the north-east rim of Spur Crater.

Figure 1. Sample 15339. S-71-49607

15340 GLASS/REGOLITH BRECCIA (?) ST. 7 0.9 g

INTRODUCTION: 15340 appears to be dominantly vesicular glass with regolith breccia either embedded within it or acting as a substratum (Fig. 1). The sample was very dusty, and because of that no zap pits were obvious. The sample has never been subdivided or allocated. It was collected as part of the rake sample from the north-east rim of Spur Crater.

Figure 1. Sample 15340. S-71-49507

15341 REGOLITH BRECCIA ST. 7 1.6 g

INTRODUCTION: 15341 is a regolith breccia with a fine-grained, glassy matrix and few lithic clasts. It was dusty, fairly friable, and had at least two zap pits larger than 1-mm across on one side. Its angular shape appears to be a product of fresh fractures forming its sides. It was collected as part of the rake sample from the north-east rim of Spur Crater.

Figure 1. Angular, dusty sample 15341, pre-processing. S-71-49624

PETROLOGY: 15341 is a glassy regolith breccia (Fig. 2). It contains spheres of green, yellow, colorless, and red glass, and shards of brown, devitrified glassy material. Lithic clasts are small, and include anorthosites, highlands impact melts, and a mare (?) basalt. Mineral fragments include shocked and unshocked examples. According to Steele et al. (1977), 15341 consists of 20% glass, 5% lithic material (anorthosite), and 60% fine matrix.

PROCESSING AND SUBDIVISIONS: 15341 was chipped to produce ,1 from which thin sections ,1 and ,6 were made, with small potted butts remaining. During processing ,0 broke up into several pieces because of the friability.

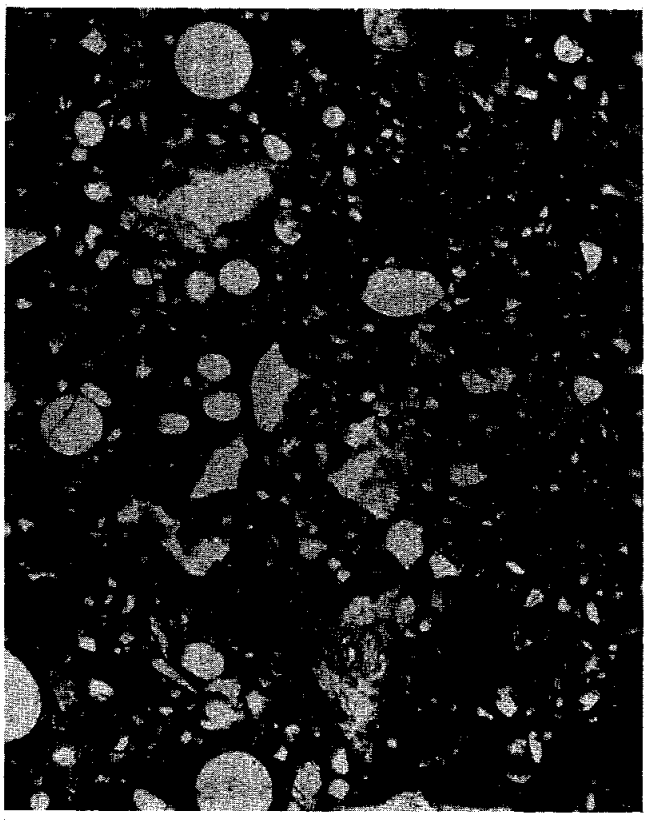

Figure 2. General matrix photomicrograph of 15341,1. Transmitted light. Width about 2 mm.

15342 REGOLITH BRECCIA ST. 7 7.5 g

INTRODUCTION: 15342 is a regolith breccia with a dark glassy matrix (Fig. 1). It was dusty and moderately friable. Its texture and possible spalls suggested exposure, but zap pits were not obvious. 15342 was collected as part of the rake sample from the north-east rim of Spur Crater.

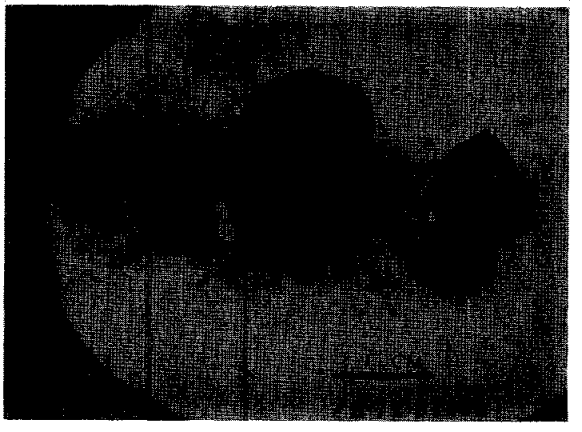

Figure 1. Post split view of 15342, with ,0 to the left. ,1 comprises the small chip and half of the third chip; ,2 is the top half of the third chip.

PETROLOGY: 15342 is a dark glassy matrix regolith breccia (Fig. 2) (Dowty et al., 1973b), similiar to 15337. It contains glass spherules and fragments, and small lithic fragments. Bunch et al. (1972) listed 15342 with 15315 as a "Green glass breccia" for which a green glass composition of unstated derivation was given. Hlava et al. (1973) presented analyses of several glasses, including one very aluminous (28% Al_2O_3) glass and green, orange, and colorless mare glasses.

PROCESSING SUBDIVISIONS: Chips were removed from one side of ,0 (Fig. 1). Part of one of the chips, ,2, was partly used to produce thin sections ,4 and ,5. ,0 is now 5.79 g.

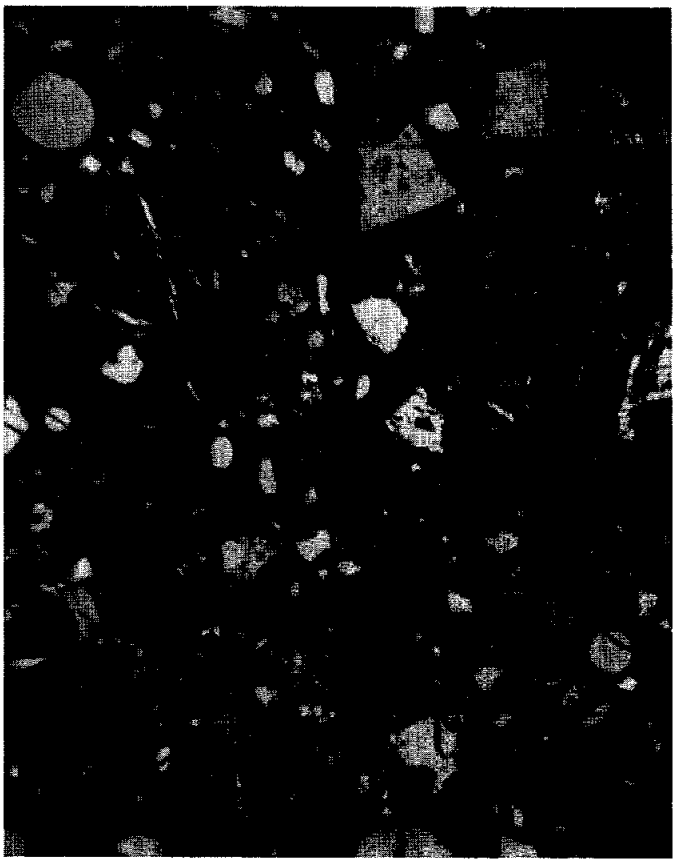

Figure 2. Photomicrograph of 15342,4. Transmitted light. Width of view ~1.25 mm.

15343 REGOLITH BRECCIA ST. 7 6.9g

INTRODUCTION: 15343 is a regolith breccia (Fig. 1) which is fairly shocked and heterogeneous, with a dark glassy matrix. It appears distinctively speckled with white clasts. It was dusty and had no obvious pits. It was collected as part of the rake sample from the north-east rim of Spur Crater.

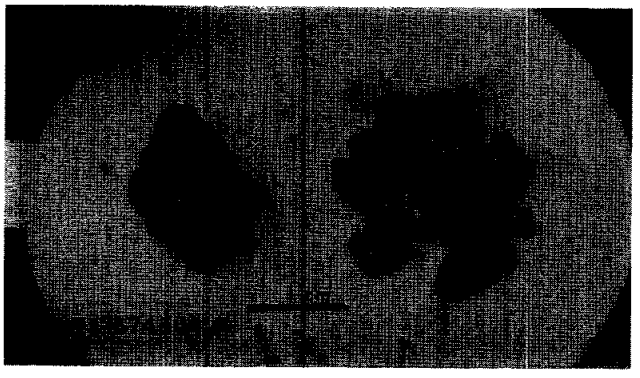

Figure 1. Post-chip view of 15343,0 and ,1.

PETROLOGY: 15343 is a fairly heterogeneous, glassy regolith breccia (Fig. 2). According to Dowty et al. (1973b) it is similar to 15337, with a moderately dark glass matrix, and has a few small feldspathic (ANT) lithic clasts. Several of the mineral clasts are shocked. Glasses include yellow, green, colorless, and orange/red. Hlava et al. (1973) presented analyses of glasses which are all mare in origin.

PROCESSING AND SUBDIVISIONS: Several chips were removed from ,0 (Fig. 1). One was numbered ,2 and partly used to produce thin sections ,4 and ,5. The remaining chips were designated ,1 (2.32g); ,0 is now 4.07 g.

Figure 2. General view of matrix of 15343,4. Transmitted light. Width about 2 mm.

15344 REGOLITH BRECCIA, GLASS-COATED ST. 7 7.9 g

INTRODUCTION: 15344 is a glassy regolith breccia, at least half-coated with a green-black vesicular glass (Fig. 1). No zap pits were evident on the glass, but one large pit (mm-sized) was present at the edge of the glass, chipping it away. The sample was dusty. It was collected as part of the rake sample from the north-east rim of Spur Crater.

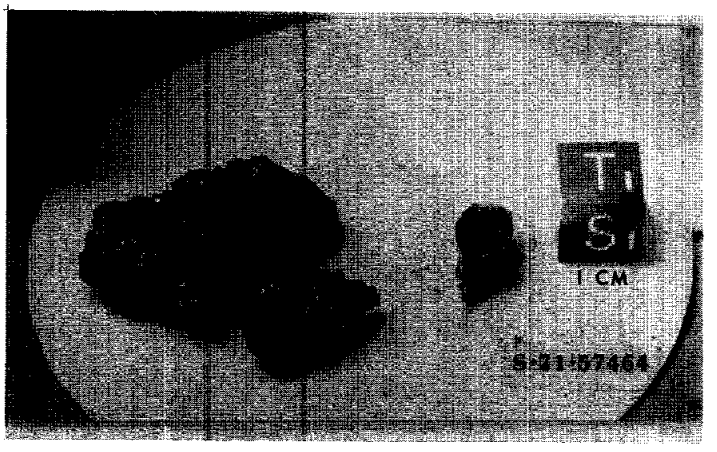

Figure 1. Post split view of vesicular glass-coated sample 15344. ,2 is the chip on the right. S-71-57464

PETROLOGY: 15344 is a regolith breccia coated with vesicular glass (Fig. 2). The coating glass is greenish with a smooth exterior surface. The regolith breccia is heterogeneous. Steele et al. (1977) found that it consisted of 15% glass, 35% lithic material (dominated by a single large KREEP basalt), 35% mineral fragments, and 15% fine matrix (glassy). They tabulated the presence of the KREEP basalt clast, providing some mineral data. It is a few millimeters across and consists of pyroxene, plagioclase, and mesostasis, with an igneous texture. It is coarse-grained, but not as coarse as 15386. Steele et al. (1977) tabulated selected mineral analyses for this KREEP clast, and Steele et al. (1980) reported ion probe analyses for minor elements (Li, Mg, K, Ti, Sr, and Ba), in its plagioclases--its Sr (420 ppm) is high but on the same trend as other lunar rocks. Steele et al. (1972a) plotted plagioclase compositions for 15344, not all from the KREEP basalt but representing more calcic, plutonic highlands samples as well. Mare plagioclases are not present among those analyzed (but mare basalts do occur as small clasts in the rock, along with feldspathic breccias). Glasses include red spheres as well as green, colorless, and yellow varieties.

PROCESSING AND SUBDIVISIONS: 15344 was chipped (Fig. 1). One chip ,2 was used to make thin sections ,2 and ,6, with small potted butts remaining.

Fig. 2a

Fig. 2b

Figure 2. Photomicrographs of 15344,6. Transmitted light. Widths about 2 mm. a) general matrix (left) and glass coat (right); b) matrix (lower right), KREEP basalt clast described by Steele et al. (1977) (center), and glass coat (top).

15345 VESICULAR GLASS/BRECCIA CLASTS ST. 7 12.3 g

INTRODUCTION: 15345 is a mass of vesicular glass with clasts (mainly regolith breccias) immersed in it (Fig. 1). The glass forms less than half of the sample excluding vesicles. One side has a good population of microcraters and two probable secondary "glass splash" impacts. Portions of the glass have a metallic luster. The sample was collected as part of the rake sample from the northeast rim of Spur Crater.

PETROLOGY: 15345 consists of several-millimeter-sized pieces of rock, mainly regolith breccias, immersed in a vesicular, greenish glass (Fig. 2). Almost 1/3 to 1/2 of the solid sample is glass. The soil breccias are brown and very glassy but most of the glass is devitrified. Lithic clasts in the regolith breccias include mare and KREEP basalts and crystalline feldspathic breccias. Small basaltic fragments occur immersed by themselves in the glass.

CHEMISTRY: S.R. Taylor et al. (1973) provided minor and trace element data for a bulk rock(?) split of 15345,3 (Table 1, Fig. 3). The sample is rather normal-looking for an Apollo 15 regolith breccia despite its glass and regolith breccia mixed origin. It is like 15455-dark and on S.R. Taylor et al.'s (1973) mixing analysis contains no highland basalt component, whereas S.R. Taylor et al. (1972) and S.R. Taylor (1973) show simple diagrams suggesting that it has almost 15% highland basalt. The physical meaning of these mixing analyses is unknown.

PROCESSING AND SUBDIVISIONS: 15345 was coherent, and the end of it was sawn to produce ,1 (Fig. 1). Pieces were chipped from ,1 to make a thin section (,8 from ,2) and for the chemical analysis (,3). ,0 is now 9.90 g; ,1 is now 1.00 g.

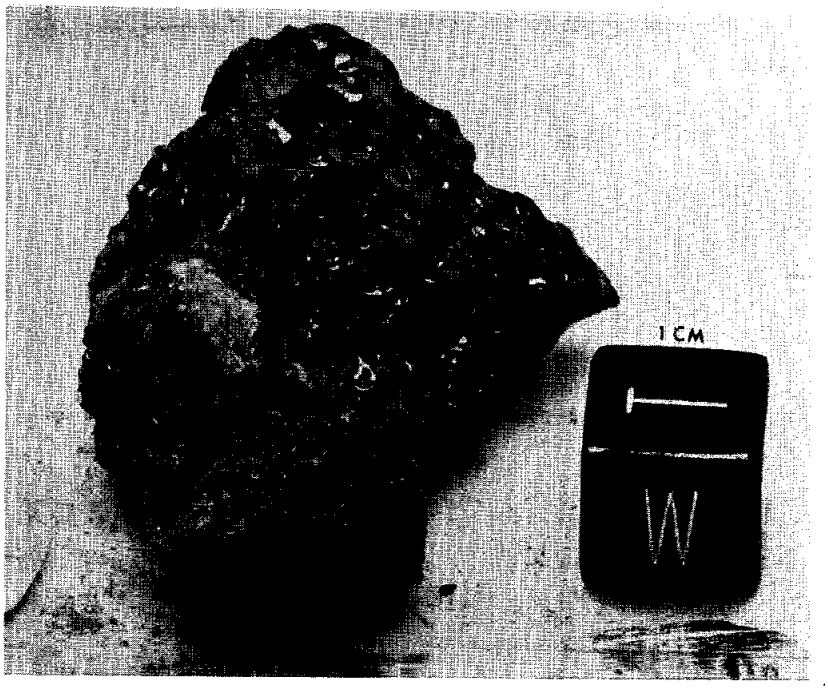

Figure 1. Post-sawing view of 15345. ,1 is at the front. S-71-59209

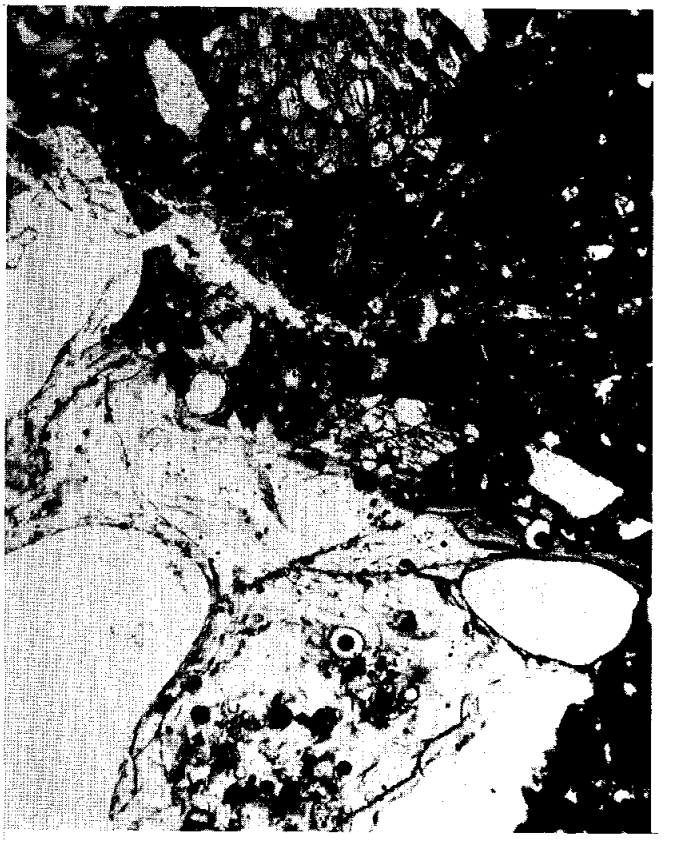

Figure 2. General view of 15345,8, with a mare basalt clast (top) enclosed in a regolith breccia, in turn enclosed in vesicular glass. Transmitted light. Width about 2 mm.

TABLE 15345-1. Bulk chemical analysis

		,3
Wt %	SiO2	
	TiO2	
	Al2O3	
	FeO	
	MgO	
	CaO	
	Na2O	
	K2O	
	P2O5	
(ppm)	Sc	17.0
	V	190.0
	Cr	1800
	Mn	
	Co	27.0
	Ni	160
	Rb	5.5
	Sr	
	Y	91.0
	Zr	415.0
	Nb	29.0
	Hf	8.8
	Ba	330
	Th	4.94
	U	1.3
	Pb	3.6
	La	27.0
	Ce	73.0
	Pr	10.2
	Nd	41.8
	Sm	12.5
	Eu	1.47
	Gd	15.8
	Tb	2.51
	Dy	15.6
	Ho	3.62
	Er	10.7
	Tm	1.6
	Yb	9.5
	Lu	1.5
	Li	
	Be	
	B	
	C	
	N	
	S	
	F	
	Cl	
	Br	
	Cu	28.0
	Zn	
(ppb)	I	
	At	
	Ga	2600
	Ge	
	As	
	Se	
	Mo	
	Tc	
	Ru	
	Rh	
	Pd	
	Ag	
	Cd	
	In	
	Sn	180
	Sb	
	Te	
	Cs	210
	Ta	
	W	250
	Re	
	Os	
	Ir	
	Pt	
	Au	
	Hg	
	Tl	
	Bi	
		(1)

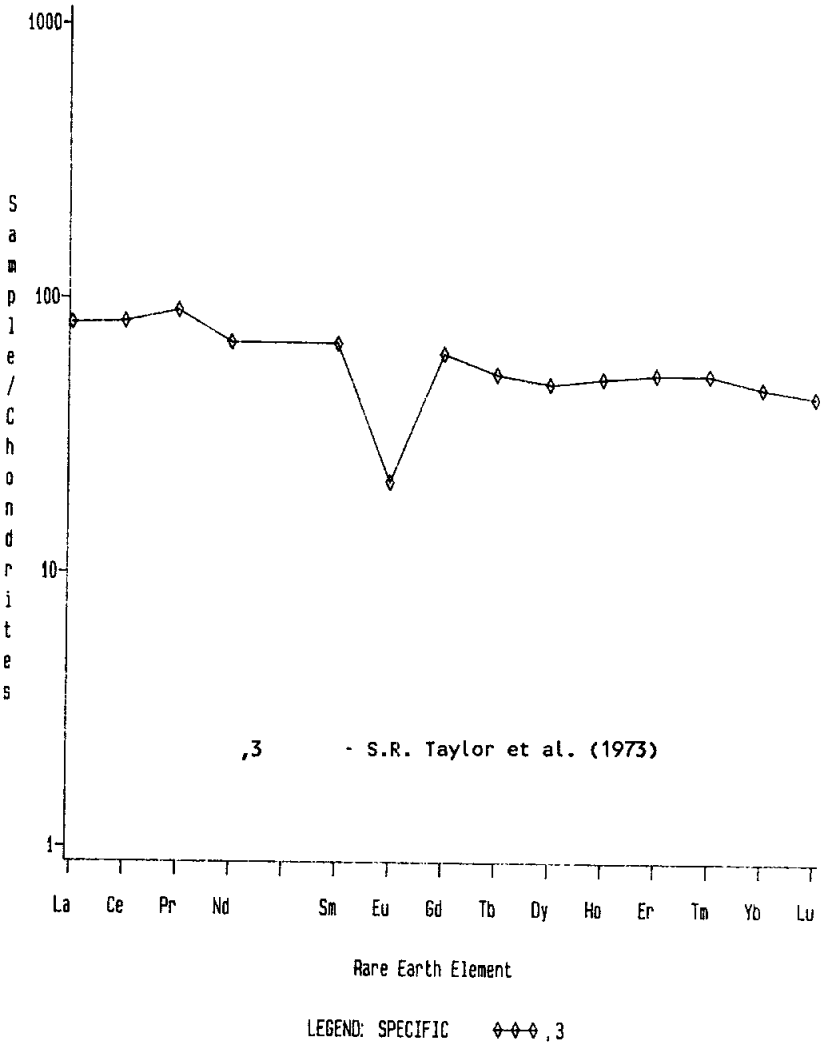

Figure 3. Rare earths in 15345,3.

References and methods:

(1) S.R. Taylor et al. (1973); spark source mass spec., emission spec.

15346 REGOLITH BRECCIA ST. 7 3.1 g

INTRODUCTION: 15346 is a regolith breccia, with many glass spheres, a large proportion of unshocked mineral fragments, and few lithic fragments (Fig. 1). It is moderately friable. Its texture and spalling suggested exposure, but zap pits were not obvious; the glass spherules were distinctively abundant macroscopically. 15346 was collected as part of the rake sample from the north-east rim of Spur Crater.

PETROLOGY: 15346 is a regolith breccia (Fig. 2). Dowty et al. (1973b) described it as a polymict breccia similar to 15316, i.e., with a light-colored glass matrix. Hlava et al. (1973) provided 60 glass analyses, which are dominantly mare, with the maximum alumina content being 16.4%. Glasses include green, colorless, yellow, and red/orange.

PROCESSING AND SUBDIVISIONS: 15346 was chipped (Figs. 1 and 3), and ,2 was partly used to make thin sections ,4 and ,5.

Figure 1. Post-split view of 15346. S-71-57467

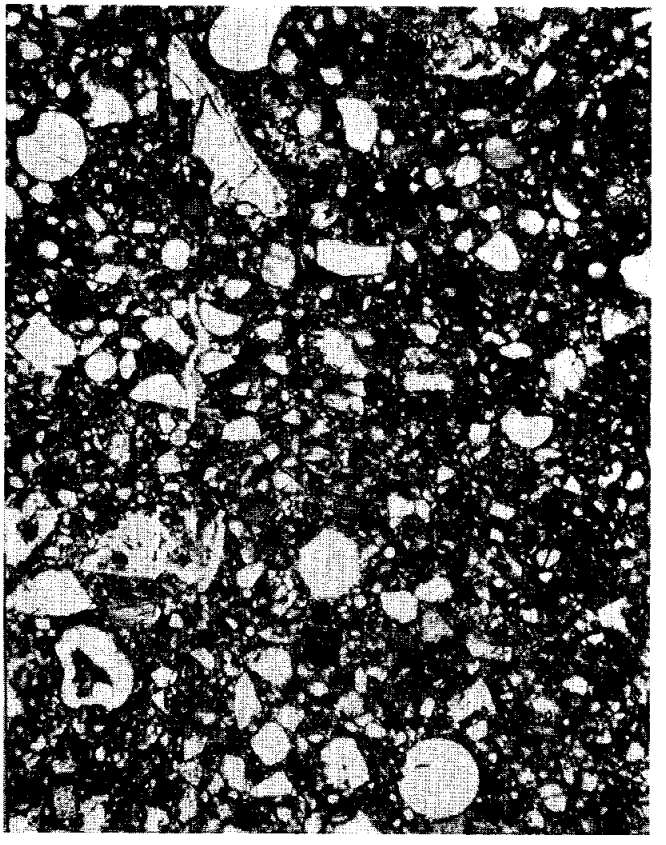

Figure 2. Photomicrograph view of 15346,4. Transmitted light. Width about 2 mm.

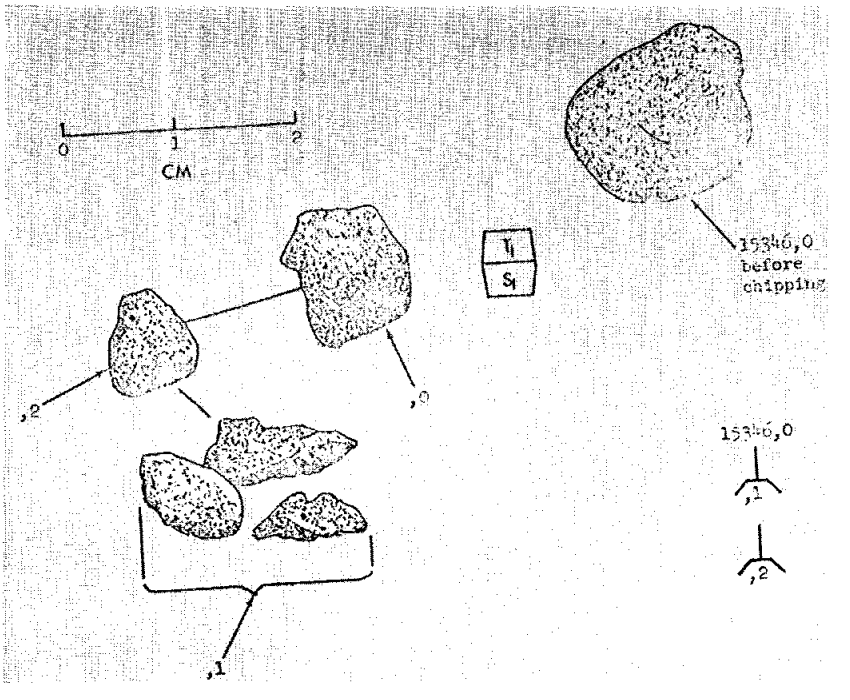

Figure 3. Chipping and numbering of 15346.

15347 REGOLITH BRECCIA ST. 7 3.2 g

INTRODUCTION: 15347 is a regolith breccia, less glassy than most (Fig. 1), but with a brown glassy matrix and an obvious mare component. Although its surface had a suggestion of spalls, zap pits were not obvious. It was collected as part of the rake sample from the north-east rim of Spur Crater.

PETROLOGY: 15347 is a regolith breccia (Fig. 2). It has a brown glassy matrix. It contains fewer glass spheres than many regolith breccias, but mare basalt clasts are prominent; one is a pyroxene-vitrophyre. Steele et al. (1977) found 15347 to consist of 15% glass and 35% fine-grained matrix, with 5% lithic fragments, 40% mineral fragments, and 5% porosity. The lithic clasts include mare, anorthositic, and breccia fragments. Steele et al. (1972b) showed pyroxene compositions (Fe-Ca-rich) from three igneous clasts, and Steele et al. (1977) tabulated four fine, variolitic mare clasts, plotting their compositions on a quadrilateral diagram. Steele et al. (1972) also plotted general olivine and pyroxene compositions from 15347 (Fig. 3) showing a wide range and indicating mare and KREEP components.

PROCESSING AND SUBDIVISIONS: Several chips were taken from ,0 (Figs. 1 and 4). ,2 was used to make thin sections ,2 and ,6, with small potted butts remaining. ,0 is now 1.92 g; ,1 is 0.57 g.

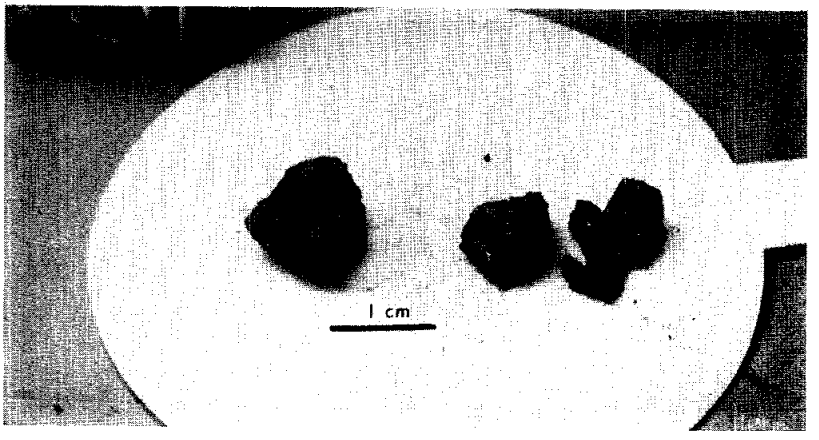

Figure 1. Post-split view of 15347. S-71-57445

Figure 2. General matrix of 15347,6. Transmitted light. Width about 2 mm.

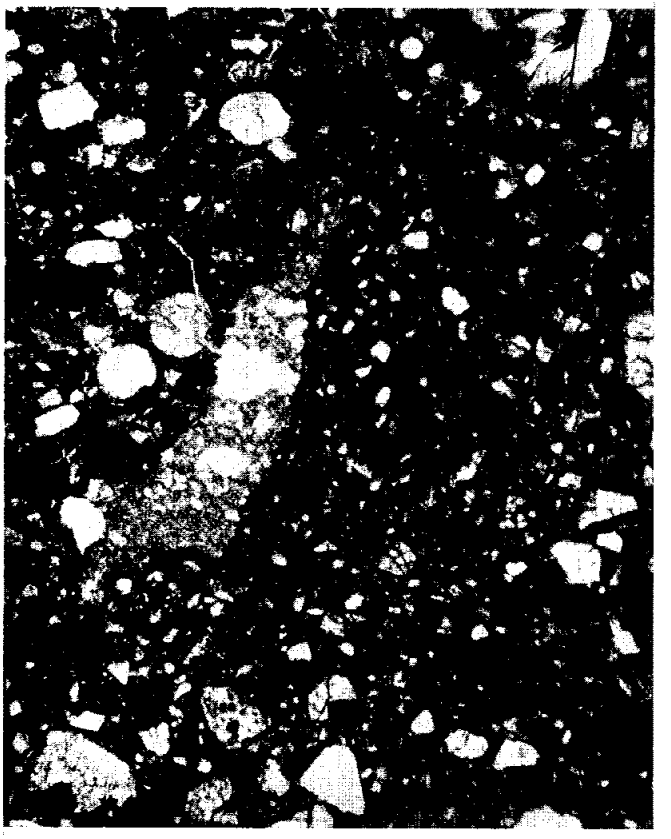

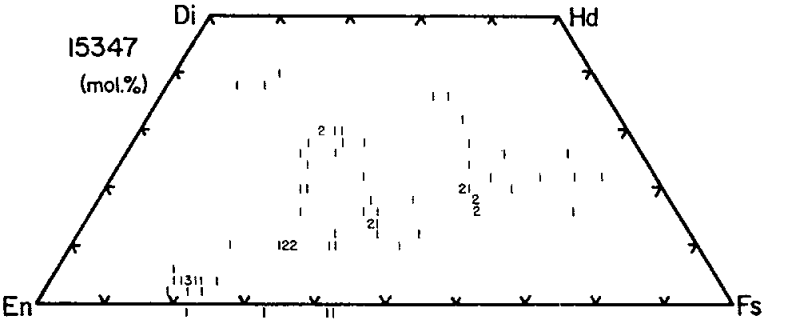

Figure 3. Compositions of pyroxenes and olivines in the 15347 matrix (Steele et al., 1977).

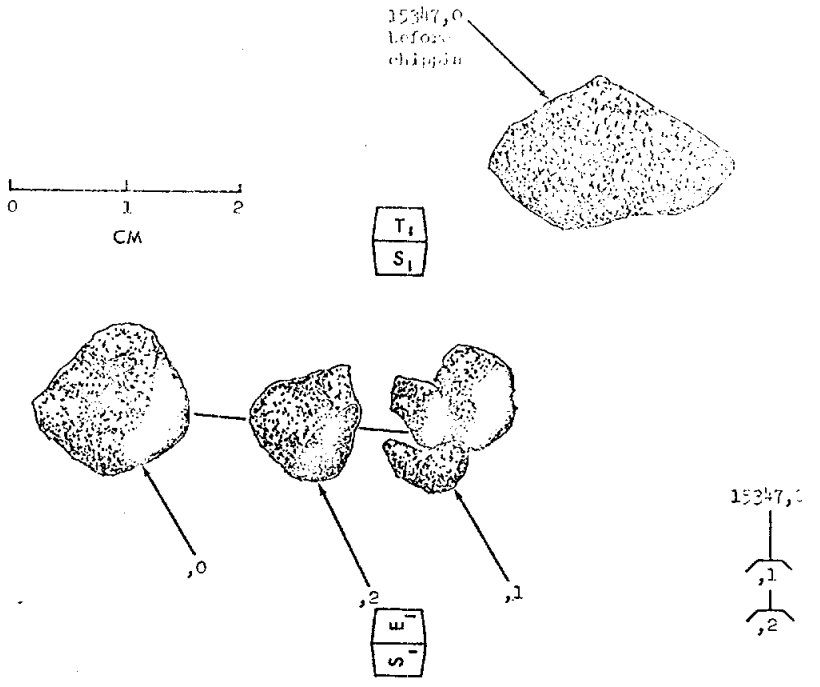

Figure 4. Chipping and numbering of 15347.

15348 REGOLITH BRECCIA (?) ST. 7 0.3 g

INTRODUCTION: 15348 is a small, dusty fragment which looks like a regolith breccia (Fig. 1). It has no obvious zap pits. One red mineral or glass grain was visible. The sample has never been subdivided or allocated. 15348 was collected as part of the rake sample from the north-east rim of Spur Crater.

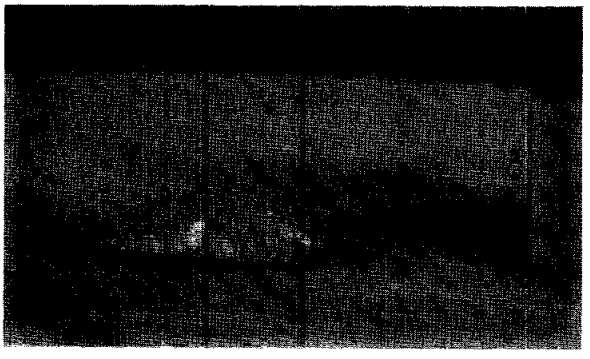

Figure 1. Sample 15348. S-71-49673

15349 REGOLITH BRECCIA ST. 7 2.3 g

INTRODUCTION: 15349 is a regolith breccia with a dark glassy matrix, fairly heterogeneous, and moderately friable (Fig. 1). One side is slickensided, but no zap pits are obvious. 15349 was collected as part of the rake sample from the north-east rim of Spur Crater.

PETROLOGY: 15349 is a heterogeneous regolith breccia (Fig. 2) with glass forming a dark matrix. Dowty et al. (1973b) stated that it is similar to 15337, with some clear glass veins. Glass spheres include green, colorless, yellow, and red (one about 300 microns). Glassy, irregular lapilli are present, and brown glassy devitrified material is not uncommon. Hlava et al. (1973) provided analyses of seven green glasses, and of plagioclase (An_{95}, Fe about 0.2) and pyroxenes ($En_{77}Wo_3$) from an ANT fragment. Lithic clasts include anorthositic and feldspathic crystalline breccias, but are not common.

PROCESSING AND SUBDIVISIONS: Chipping is shown in Figure 1. ,2 was partly used to make thin sections ,4 and ,5. ,0 is now 1.16 g.

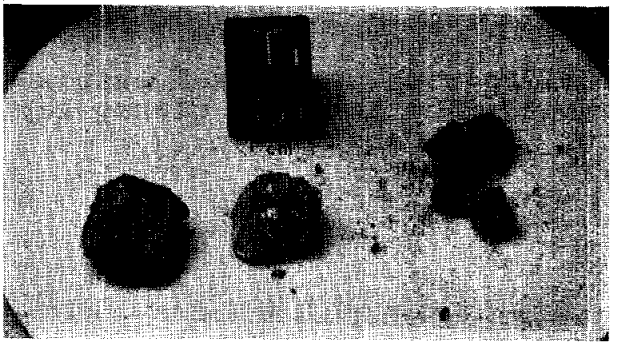

Figure 1. Post split view of 15349. ,0 is on left, ,2 is in middle, and the four chips composing ,1 are on the right.

Figure 2. Photomicrograph of general matrix of 15349,4. Pale fragment at bottom is a glassy lapillus. Transmitted light. Width about 2 mm.

15350 REGOLITH BRECCIA ST. 7 2.9 g

INTRODUCTION: 15350 is a glassy regolith breccia with an opaque glassy matrix, green glass balls, yellow glass, and a variety of small lithic clasts. The sample was angular, moderately coherent, lacked zap pits, and was dusty (Fig. 1). It was collected as part of the rake sample from the north-east rim of Spur Crater.

Figure 1. Pre-split, dusty view of 15350. S-71-49693

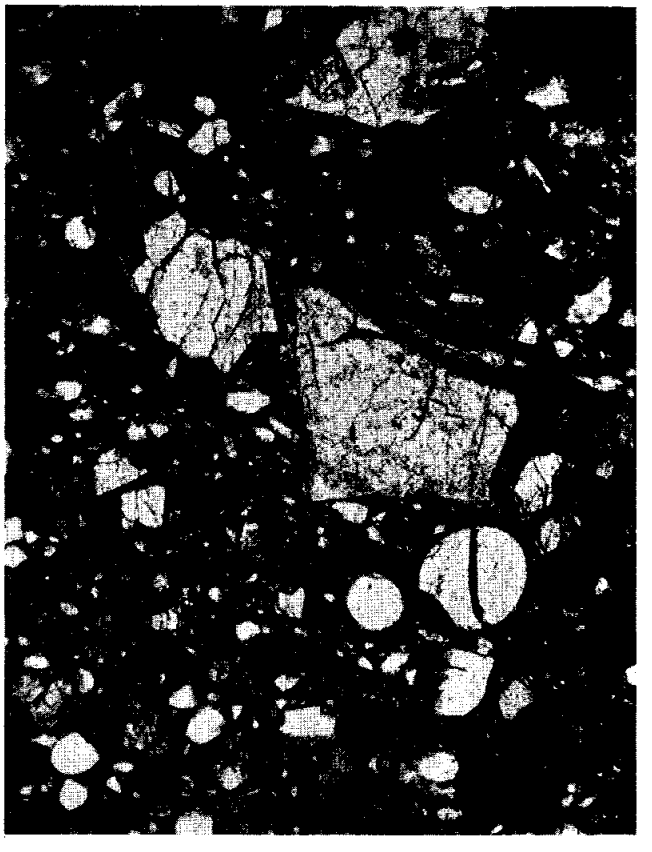

Figure 2. General matrix photomicrograph of 15350,6. Transmitted light. Width about 2 mm.

PETROLOGY: 15350 is a regolith breccia (Fig. 2). According to Steele et al. (1977), 15350,2 consists of 65% glass or fine matrix (which are difficult to distinguish), 30% mineral clasts, and 5% lithic clasts. They listed two KREEP basalt and one mare basalt clast studied for which they provided pyroxene data (Fig. 3). Steele et al. (1972a) plotted some pyroxene analyses (Ti vs. Al), and some plagioclase analyses. The mineral fragments include exsolved pyroxenes. Thin section ,6 contains green glass balls and pieces, including devitrified examples; balls, shards, and irregularly-shaped pieces of yellow glass; and colorless shards and balls. The lithic clasts include glassy and melt-matrix breccias, and highlands, plagioclase-rich breccias, all of which are small. The matrix of 15350 is porous, though Steele et al. (1977) state that it is not.

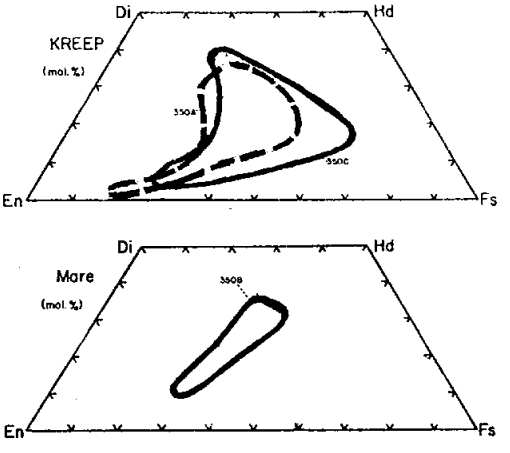

Figure 3. Pyroxenes in three clasts in 15350,2 (Steele et al., 1977).

PROCESSING AND SUBDIVISIONS: Chips were removed from ,0 (now 2.1 g) (Fig. 4). ,2 was made into thin sections ,2 and ,6, with potted butts ,8 and ,9 remaining. ,1 is 0.16 g.

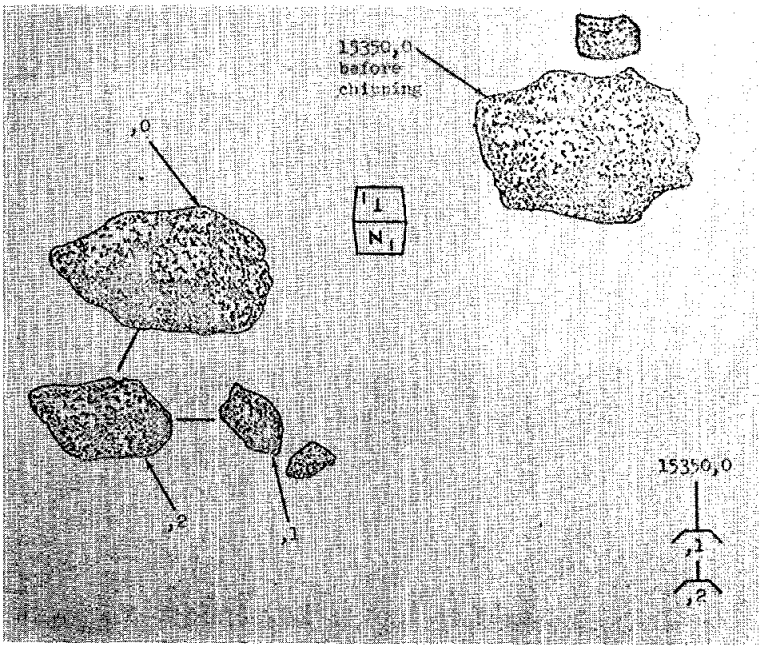

Fig. 4a

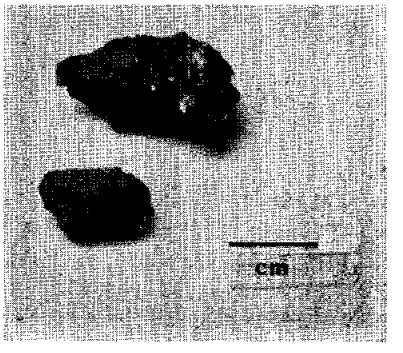

Fig. 4b

Figure 4. Splitting of 15350 (a) diagram; (b) photograph prior to splitting ,1 from ,2. S-71-57490

15351 REGOLITH BRECCIA ST. 7 4.2 g

INTRODUCTION: 15351 is a glassy regolith breccia containing green and yellow glass materials and a glassy matrix. It was angular and dusty (Fig. 1). It was collected as part of the rake sample from the north-east rim of Spur Crater.

Figure 1. Pre-split view of 15351. S-71-49699

PETROLOGY: 15351 is a regolith breccia with an opaque matrix (Fig. 2). It contains green glass balls and shards, a yellow-orange shard and other yellow glass debris, and other glasses. It contains mineral fragments and small lithic fragments, some of which are highlands and some mare basalts. Steele et al. (1977) found it to contain 15% glass, 5% lithic clasts (breccias), 15% minerals, and 65% fine matrix, which is very dark. Although they state it is non-porous, it is in fact quite porous.

PROCESSING AND SUBDIVISIONS: Chipping of 15351 produced several fragments (Fig. 3). ,0 is now 3.02 g, and ,1 consists of 0.65 g and is more than one piece. From ,2, thin sections ,2 and ,6 were made, with potted butts ,8 and ,9 remaining.

Figure 2. General matrix photomicrograph of 15351,6. Transmitted light. Width of view about 2 mm.

Fig. 3a

Fig. 3b

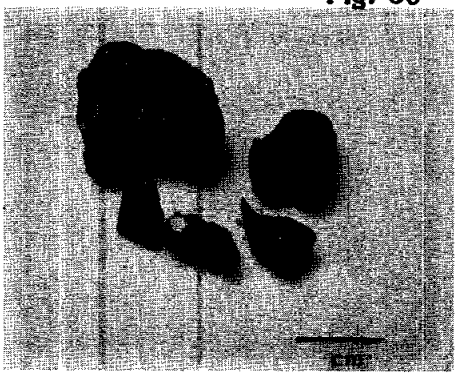

Figure 3. Splitting of 15351. a) diagram; b) photograph. S-71-57488

15352 REGOLITH BRECCIA, GLASS-COATED ST. 7 2.9 g

INTRODUCTION: 15352 is a regolith breccia, containing green and yellow glass balls, other glass debris, lithic fragments, and mineral fragments in an opaque glassy matrix. It is thickly coated and intruded with a dark vesicular glass (Fig. 1). The glass appeared to have no zap pits, but was dusty. 15352 was collected as part of the rake sample from the north-east rim of Spur Crater.

Figure 1. Pre-split view of 15352. S-71-49675

PETROLOGY: The breccia portion of 15352 is a glassy regolith breccia (Fig. 2) containing green, yellow, and colorless glasses as balls, shards, and irregular lapilli, as well as lithic and mineral debris. The lithic fragments appear to be dominantly KREEP basalts and highlands breccia fragments, all of which are small (less than 1 mm). The mineral fragments include exsolved pyroxenes, but plagioclase is dominant (Dowty et al., 1973b). Hlava et al. (1973) provided analyses of many glasses, including green glass and other mare glasses (all of which are olivine-normative), and high-alumina basalt glasses. Some of the aluminous glasses are KREEPy and most are colorless. Prinz et al. (1973) reported microprobe and ion microprobe analyses of six homogeneous high-alumina basalt glasses (in the text they refer to the sample as 15353, but in the tables correctly refer to 15352). Their study was to gain insight into the origin of low-alkali high-aluminous basalt and its relationship to alkali high-alumina basalt.

The glass coat, which may dominate the mass of the sample, is vesicular, and in thin sections is greenish-grey and banded (Fig. 2). It penetrates the breccia as thin veins in several places. Hlava et al. (1973) did not state which, if any, of their glass analyses are of the glass coat.

Figure 2. Photomicrograph of 15352,4, showing dark regolith breccia (upper left) containing glass balls and lithic fragments; and the vesicular glass coat (lower right). The dark circular objects in the lower center are sectioning artifacts.

PROCESSING AND SUBDIVISIONS: Chips were removed from ,0, which is now 1.95g. Most of ,2 (Fig. 3) was used to produce thin sections ,4; ,5; ,6; and ,7.

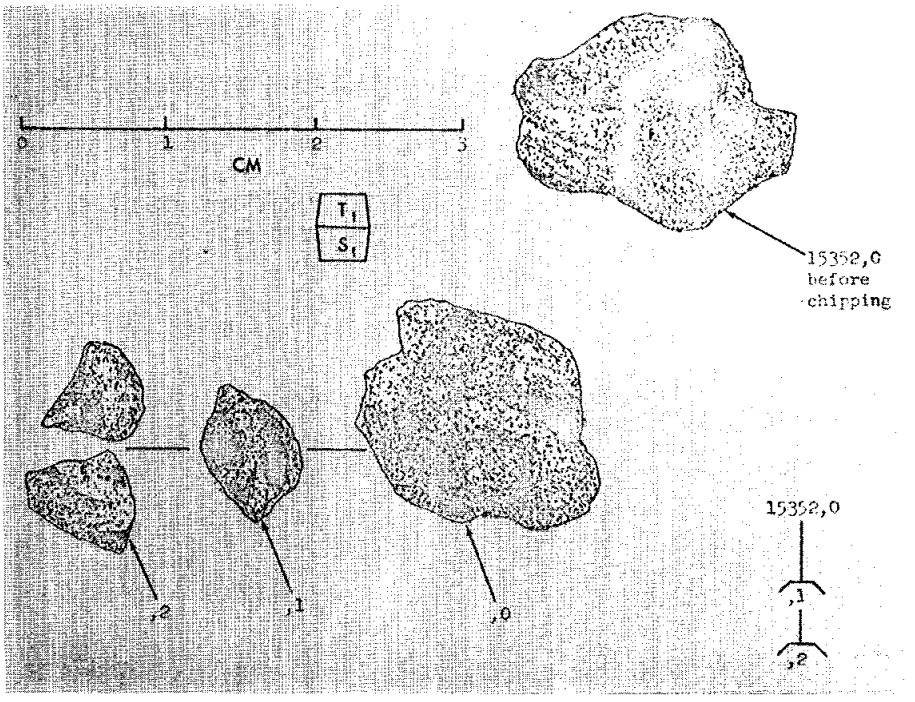

Fig. 3a

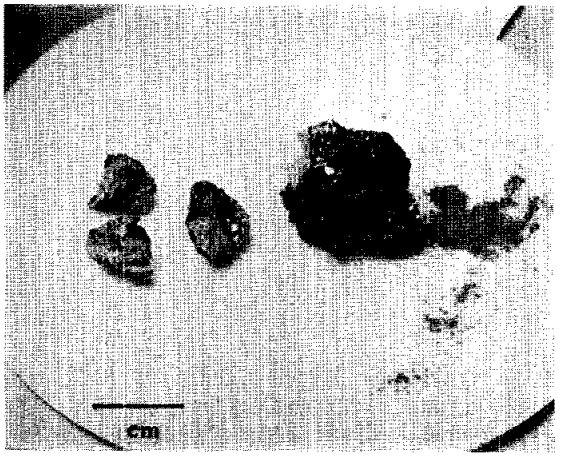

Fig. 3b

Figure 3. Chipping of 15352. a) diagram; b) photograph. S-71-57471

15353 REGOLITH BRECCIA ST. 7 10.6 g

INTRODUCTION: 15353 is a regolith breccia, containing glass, lithic, and mineral debris in a dark, glassy matrix. The lithic clasts include olivine-normative mare basalt and highlands material. The sample was dusty and fairly angular (Fig. 1). No zap pits were obvious. 15353 was collected as part of the rake sample from the north-east rim of Spur Crater.

Figure 1. Post-chip view of 15353. S-71-57479

PETROLOGY: 15353 is a glassy regolith breccia (Fig. 2). Steele et al. (1977) reported that it contained 35% glass, 15% lithic clasts, 20% mineral clasts, and 30% fine matrix. The glasses include green, yellow, and colorless glass balls. The lithic clasts include mare basalts and breccia fragments. One large clast (A of Steele et al., 1977) is an olivine-bearing basalt (Fig. 2) with 50% equigranular plagioclase, 45% pyroxene, and some ilmenite. A second clast (B of Steele et al., 1977) contains plagioclase with low iron and is an Fe-rich (En ~50) highlands lithology. Several small fragments are impact melts. (Prinz et al., 1973, erroneously referred to 15353 in their text as the source of their glass data, but their sample was 15352.)

PROCESSING AND SUBDIVISIONS: 15353 was split by chipping (Figs. 1 and 3). ,0 is now 7.75 g and ,1 is 2.26 g. ,2 was used to produce thin sections ,2 and ,7, with potted butts ,9 and ,10 remaining.

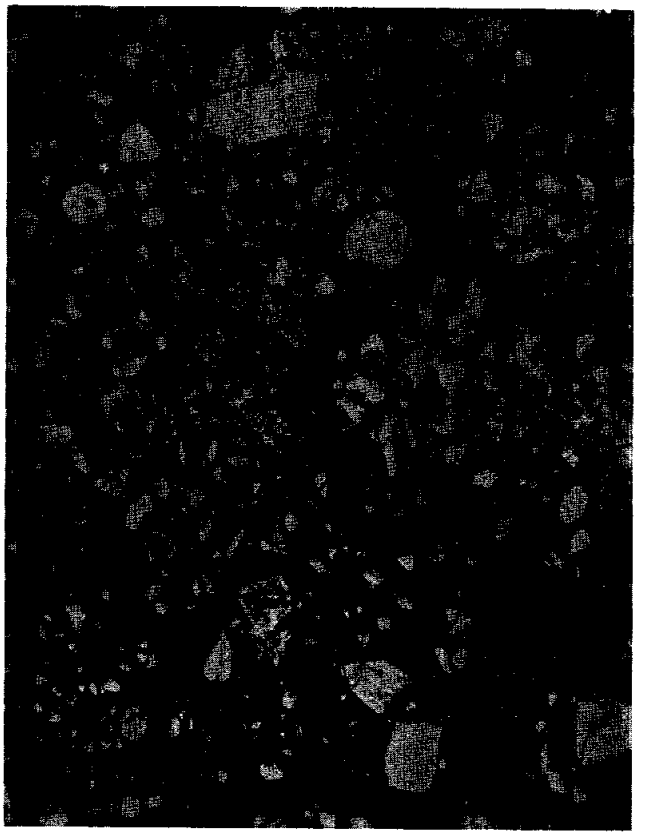

Figure 2. Photomicrograph of general matrix of 15353,2. Clast in upper right is clast A of Steele et al. (1977), a mare basalt. Transmitted light. Width about 2 mm.

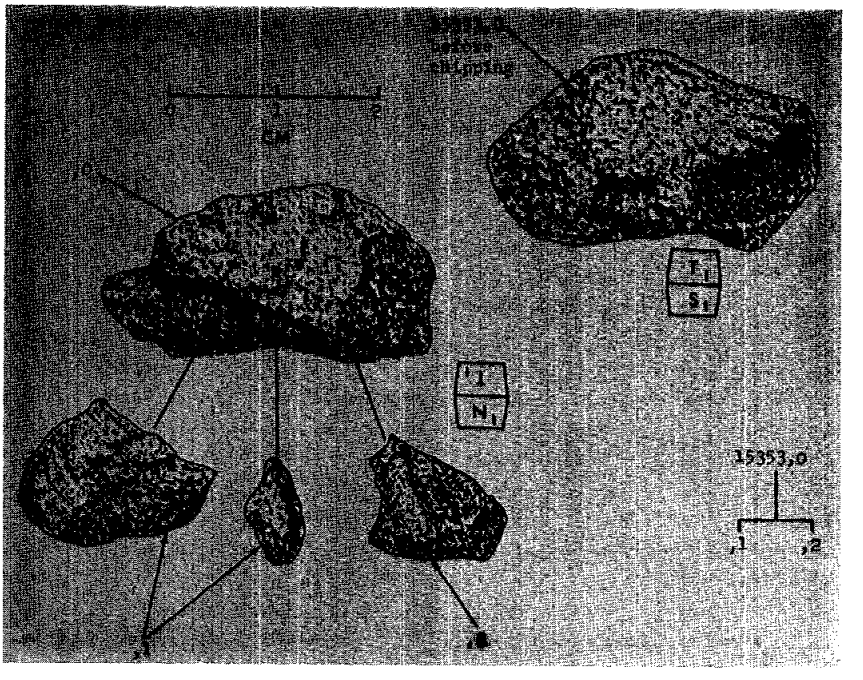

Figure 3. Chipping of 15353.

15354 REGOLITH BRECCIA (?) ST. 7 0.3 g

INTRODUCTION: 15354 appears to be a regolith breccia, which was dust-coated (Fig. 1). Tiny white clasts and colored fragments (glass?) are embedded in a dark matrix. The sample has never been subdivided or allocated. It was collected as part of the rake sample from the north-east rim of Spur Crater.

Figure 1. Macroscopic view of 15354. S-71-49709

15355 REGOLITH BRECCIA ST. 7 5.2 g

INTRODUCTION: 15355 is a coherent glassy breccia of regolith origin, containing green glass balls, glassy lapilli, and other surficial materials. The sample was dust covered (Fig. 1), and a glass patch at one apex appears to be the result of a rock-breaking impact. This patch and the surrounding breccia show zap pits. The sample was collected as part of the rake sample from the north-east rim of Spur Crater.

PETROLOGY: 15355 is a brown glassy matrix regolith breccia (Fig. 2) which is moderately porous. It contains green glass balls, some of which are devitrified, and other brownish glass and lapilli. No obvious KREEP or mare basalt clasts are present, and there are few lithic fragments at all. One appears to be a highlands breccia. Mineral fragments are common.

PROCESSING AND SUBDIVISIONS: One end (,1) was sawn from 15355 and used to make thin sections ,6; ,7; and ,8, with a potted butt remaining. ,0 is now 4.41 g. (The cutting plans in the data pack for this rock erroneously show a slablet ,2 sawn from ,0.)

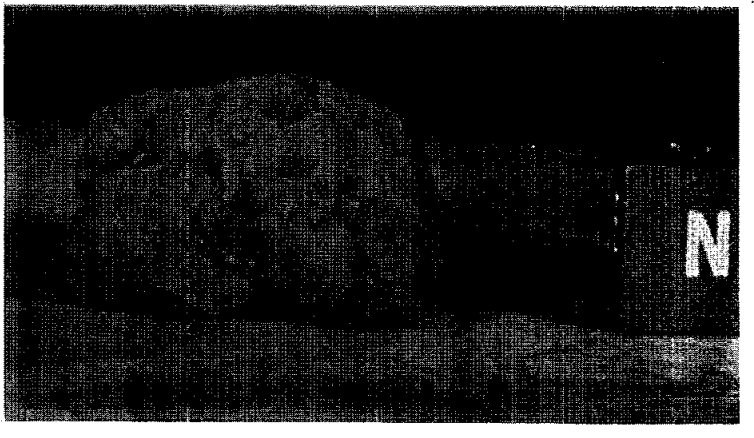

Figure 1. Macroscopic pre-split view of 15355. S-71-49683

Figure 2. General photomicrograph view of 15355,6, showing glass balls and glassy lapilli. Transmitted light. Width about 2 mm.

15356 FINE-GRAINED IMPACT MELT ST. 7 2.0 g

INTRODUCTION: 15356 is a fine-grained, clast-bearing impact melt of high alumina basalt composition, and with apparently high alkali (K_2O ~0.6%). It is dark gray, aphanitic, and coherent (Fig. 1) and had dust coating two sides. It appeared to lack zap pits. 15356 was collected as part of the rake sample from the north-east rim of Spur Crater.

PETROLOGY: 15356 is a fine-grained, clast-bearing impact melt (Fig. 2). Simonds et al. (1975) described it as an ultrafine, subophitic impact melt with mineral clasts, containing about 50% plagioclase. Dowty et al. (1973b) described it as a breccia of alkalic high-alumina basalt composition, containing plagioclases, pyroxenes, and olivines (Fig. 3), as well as minor metal, K-rich glass, Ba-K-feldspar, Zr-armalcolite, rutile, and ilmenite. Mineral analyses were presented by Nehru et al. (1973, 1974) and Hlava et al. (1973). Nehru et al. (1974) noted that the rock contains homogeneous pink spinel, but lacks chromite. They suggested that the restricted mineral compositions in the sample indicated that 15356 was a monomict breccia. The metal grains, containing 0.4 to 0.5% Co and ~5% Ni, indicate meteoritic contamination of the sample.

In thin section ,3 (Fig. 2), the olivines are clasts, as are some of the plagioclases, while the pyroxene and the remaining plagioclases form the melt groundmass. The pyroxenes form small poikilitic phases (Fig. 2c) enclosing plagioclases. In a few patches the melt has a subophitic texture. The metal forms blebs and the ilmenites are needle-like. There are no lithic fragments. Some of the plagioclase clasts have a sieved, melted, and assimilated appearance.

CHEMISTRY: The only chemical analysis is the microprobe defocussed beam analysis of thin section 15356,4 by Dowty et al. (1973b) (Table 1), which indicates a high-alumina basalt and high-incompatible elements composition (K_2O 0.58%, P_2O_5 0.34%) of the sample.

PROCESSING AND SUBDIVISIONS: The sample was chipped (Fig. 4), and thin sections ,3 and ,4 were made from ,1. Only 0.01 g remains of ,1. ,0 exists as several small fragments with a mass of 1.38 g.

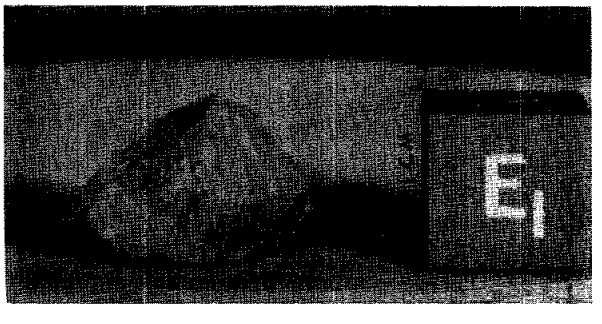

Figure 1. Pre-split of 15356. S-71-49372

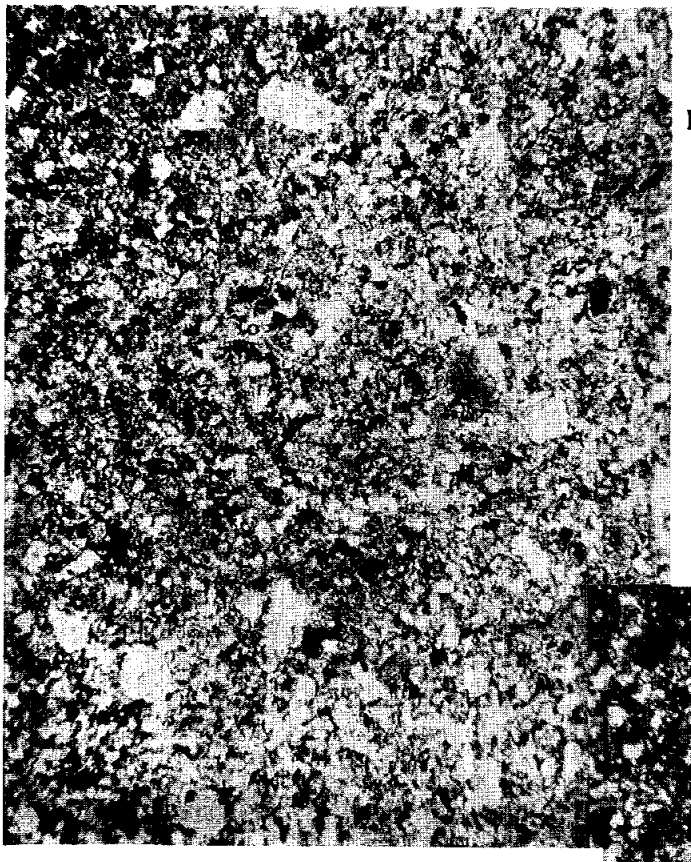

Fig. 2a

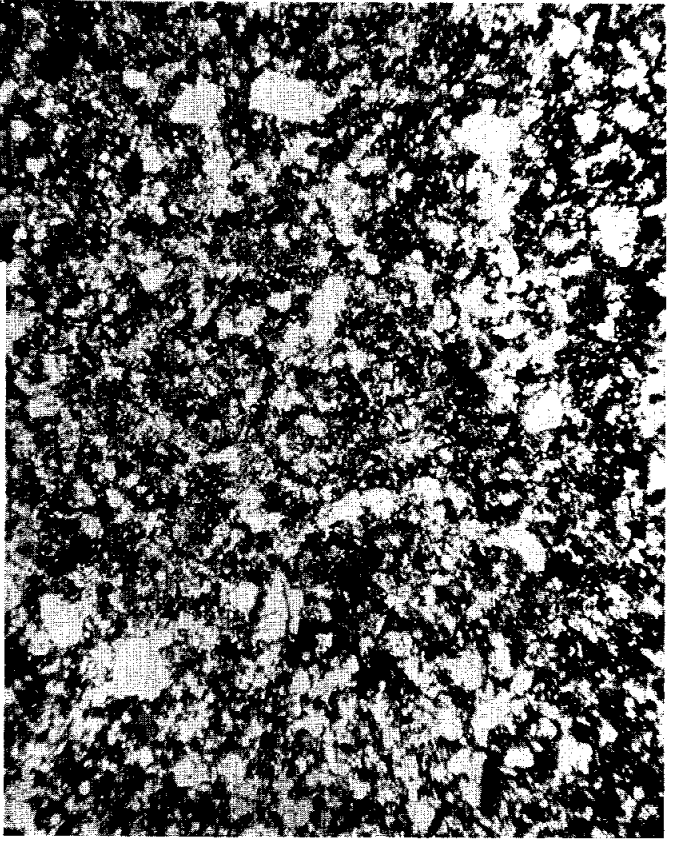

Fig. 2b

Figure 2. Photomicrographs of 15356,3. a) general view showing fine-grained, regular texture and clasts. Transmitted light. Width about 2 mm. b) as (a), crossed polarizers. c) groundmass view showing tiny pyroxene oikocrysts (e.g., elongated, mottled, pale-colored objects) and clasts (e.g., clear objects). Crossed polarizers. Width about 600 microns. d) reflected light view of groundmass, showing pyroxenes (pale-grey), plagioclases (darker grey) and metal (white). Width about 125 microns.

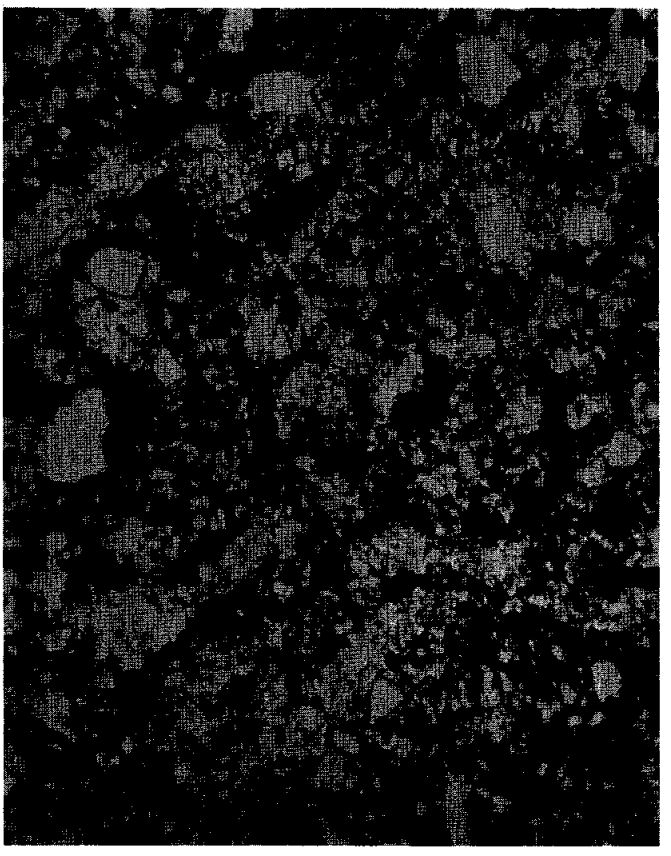

Fig. 2c

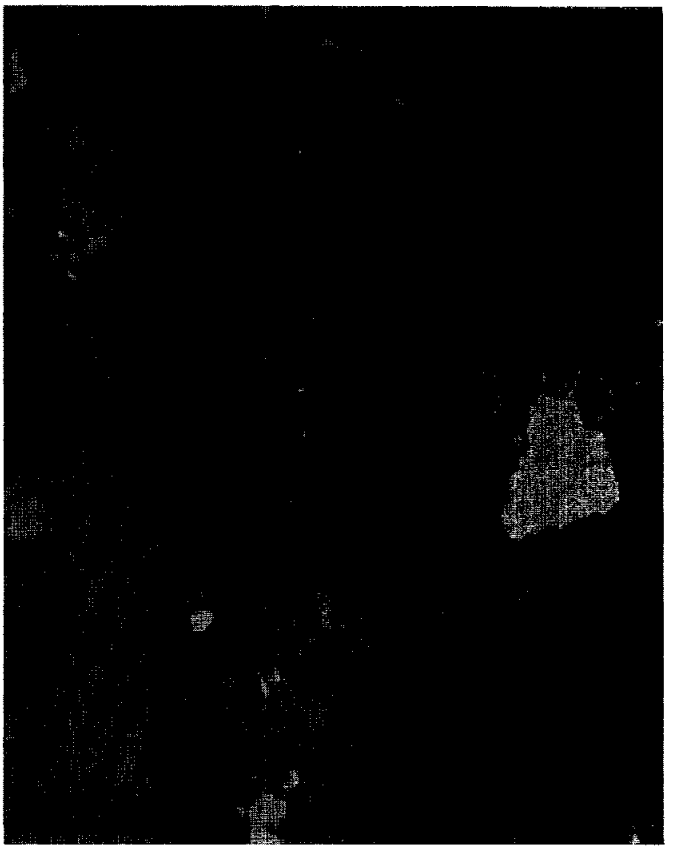

Fig. 2d

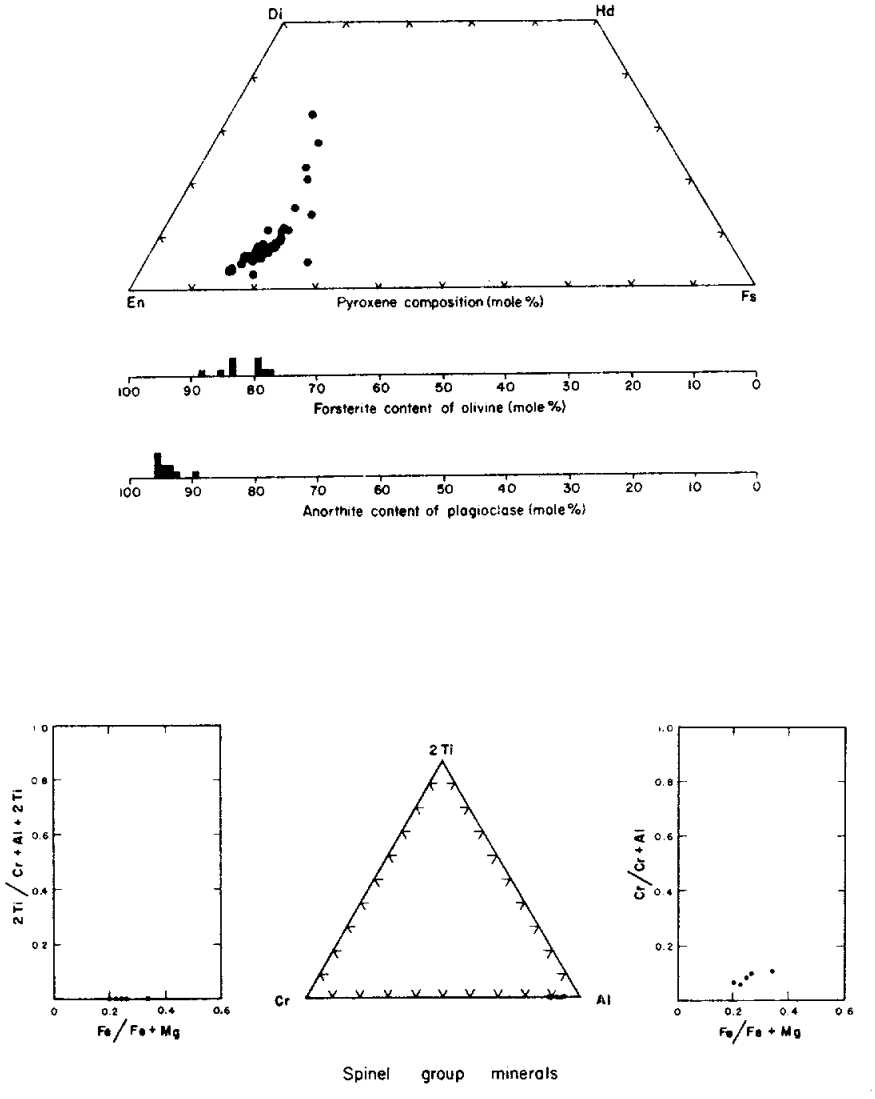

Figure 3. Compositions of minerals in 15356 (from Dowty et al., 1973b). Olivines and spinels are clasts, most plagioclases analysed are probably clasts.

TABLE 15356-1. Defocussed beam microprobe analysis of 15356,4. (Dowty et al., 1973b)

Wt%	SiO2	45.6
	TiO2	1.12
	Al2O3	20.0
	FeO	7.5
	MgO	13.7
	CaO	10.2
	Na2O	0.68
	K2O	0.58
	P2O5	0.34
ppm	Cr	1200
	Mn	850

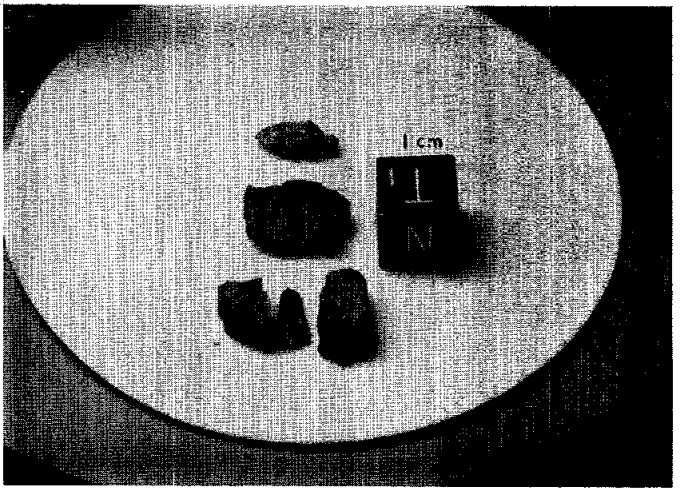

Figure 4. Photograph of chipping of 15356. The larger piece, nearest the scale cube, is ,1. The rest are ,0. S-71-57966

15357 FINE-GRAINED IMPACT MELT ST. 7 11.8 g

INTRODUCTION: 15357 is a fine-grained, coherent impact melt (Fig. 1), containing mineral clasts and a few lithic clasts of highland origin. It is angular, was dusty, and appeared to have zap pits on at least one surface. 15357 was collected as part of the rake sample from the north-east rim of Spur Crater.

PETROLOGY: 15357 is a poikilitic impact melt with mineral clasts (Simonds et al. (1975). It is finer-grained than 15356 and the oikocrysts much less distinct (Fig. 2). According to Steele et al. (1977), the sample is a non-porous breccia, lacking glass and containing 5% lithic clasts and 95% mineral clasts, and the lithic clasts are anorthositic. One clast (or possibly coarser matrix patch) in 15357,9 has a subophitic texture (Fig. 2d). Most mineral clasts are plagioclase and olivine, but include pyroxene, of which some are exsolved. Some olivines and several plagioclases have a polygonal texture. Steele et al. (1972a, b) reported mineral chemical data. The plagioclase is of highland origin (An_{97-85}, Fe <0.2%) and the pyroxenes have a very limited range (Fig. 3) of about $En_{71}Wo_3$.

CHEMISTRY: Helmke and Haskin (1972) reported an analysis of split ,3, without supplying the data other than to state that the rare earths are at about 80x chondritic abundances, hence the sample contains a significant KREEP component.

PROCESSING AND SUBDIVISIONS: Several small pieces were chipped from ,0 (now 9.1 g) as shown in Figure 4. ,2 was used to make thin sections ,2 and ,9, leaving potted butt ,12. ,3 was subdivided for the chemical analysis.

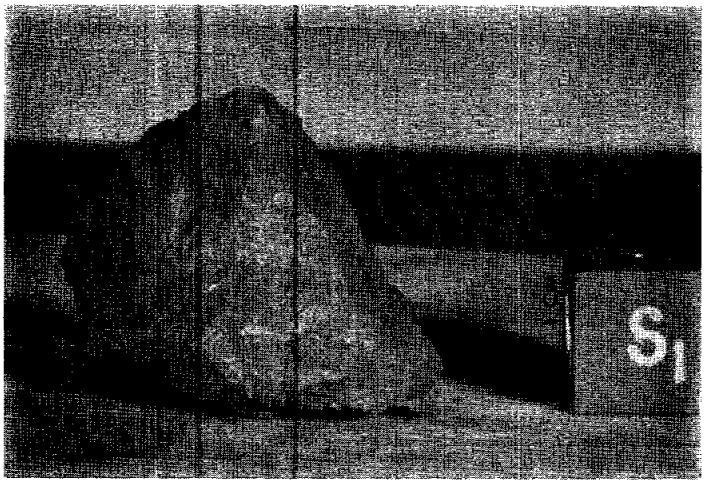

Figure 1. Pre-split view of 15357. S-71-49353

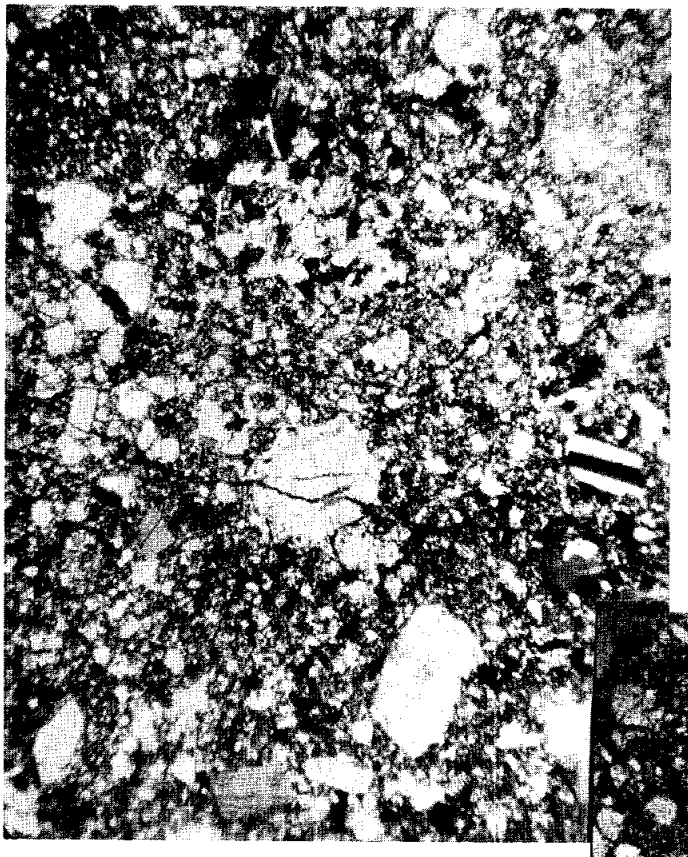

Fig. 2a

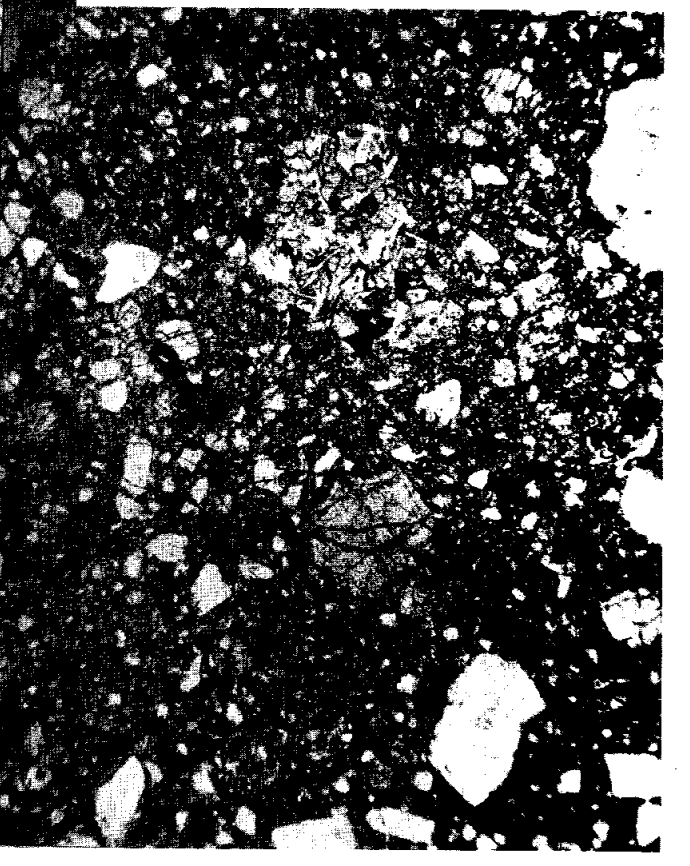

Fig. 2b

Figure 2. Photomicrographs of 15357,9. a) general view showing mineral clasts and fine-grained groundmass with subophitic patch, top center. Transmitted light. Width about 2 mm. b) same as (a). Crossed polarizers, showing exsolved pyroxene, center. c) subophitic clast or patch in (a). Crossed polarizers. Width about 600 microns. d) reflected light view of very fine poikilitic melt matrix. Width about 125 microns.

Fig. 2c

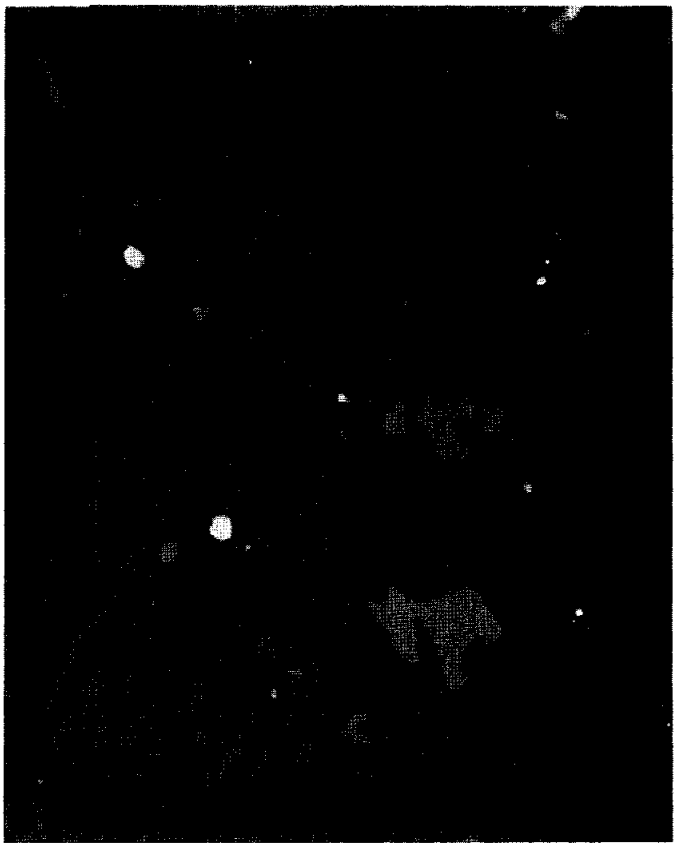

Fig. 2d

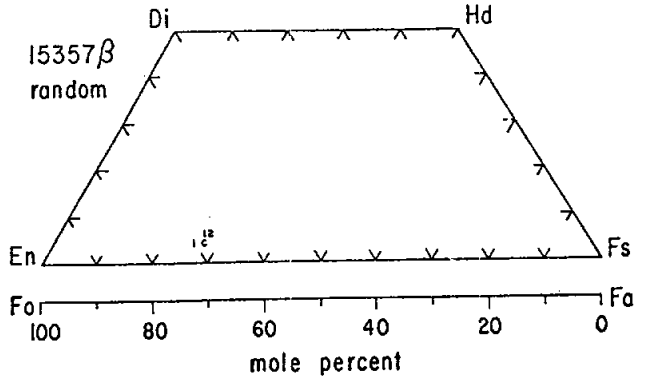

Pyroxenes in 15357 KREEP breccia. (C = 12)

Figure 3. Compositions of pyroxenes in 15357 (Steele et al., 1972b).

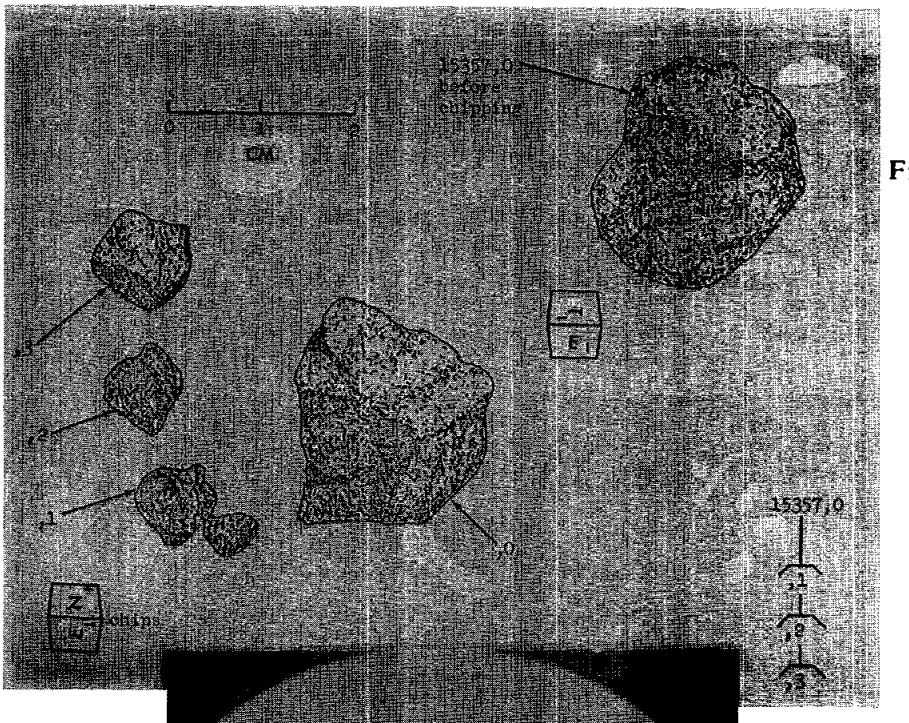

Fig. 4a

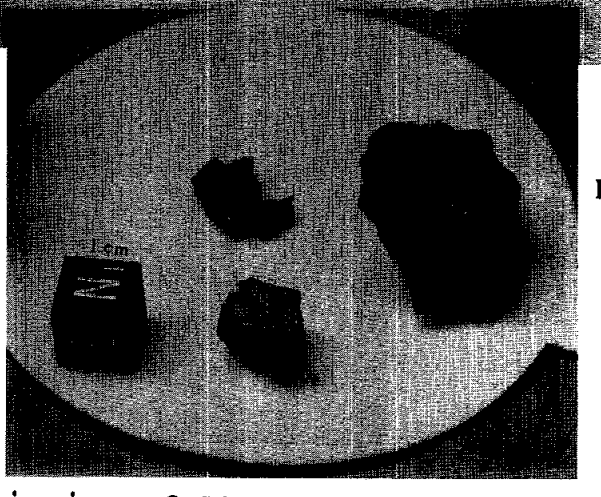

Fig. 4b

Figure 4. Chipping of 15357. a) drawing of splits. b) photograph of splits. S-71-57970

15358 GLASSY BRECCIA WITH KREEP BASALT CLASTS ST. 7 14.6 g

INTRODUCTION: 15358 is a brown, vesicular glass, rather agglutinate-like. It contains dominantly KREEP-basalt clasts. The sample was angular and tough, and very dusty (Fig. 1). Vugs or vesicles occur in the glass, but no zap pits were obvious. The sample was collected as part of the rake sample from the north-east rim of Spur Crater.

PETROLOGY: 15358 consists dominantly of a brown vesicular glass, containing clasts (Fig. 2a). The lithic clasts are dominantly KREEP basalts, with a range of textures fromspherulitic/vitrophyric (Fig. 2b) to intersertal. All show abundant clear orange interstitial (residual) glass suggesting rapid cooling of their parent flows. None contain mineral clasts or textures suggestive of impact melt. One other lithic clast is a brown devitrified glass. Virtually all other clasts are mineral clasts.

Dowty et al. (1973b) described 15358 as a polymict microbreccia, and noted the KREEP chemistry of the clast depicted in Figure 2b. Hlava et al. (1973) listed plagioclase, pyroxene, and opaque mineral analyses, referring to the sample as high-alumina basalt; presumably all of the analyses are from a KREEP basalt clast.

PROCESSING AND SUBDIVISIONS: Several pieces were chipped from the parent (Fig. 3). ,0 is now 11.4 g; ,1 is now 2.12 g. Thin sections ,6 and ,7 were made from ,4, of which 0.21 g remains.

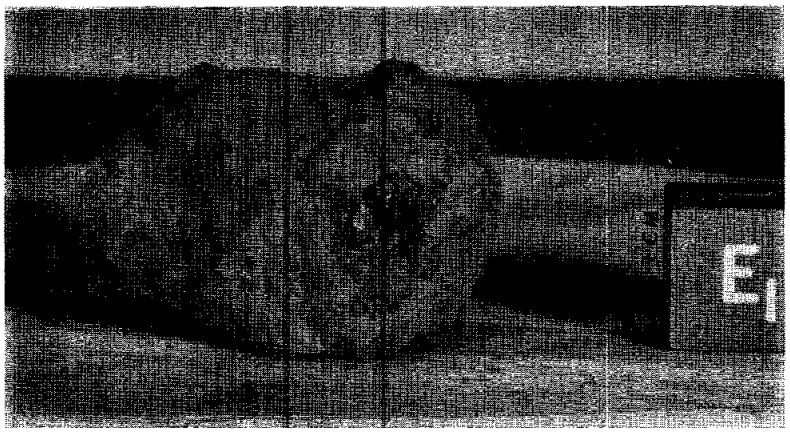

Figure 1. Pre-split view of dusty sample 15358. S-71-49346

Fig. 2a

Fig. 2b

Figure 2. Photomicrographs of 15358,6. a) general view showing dark, glassy, vesicular matrix and dominant KREEP basalt clasts. Transmitted light. Width about 2 mm. b) large spherulitic/vitrophyric KREEP basalt clast. Transmitted light. Width about 2 mm.

Fig. 3a

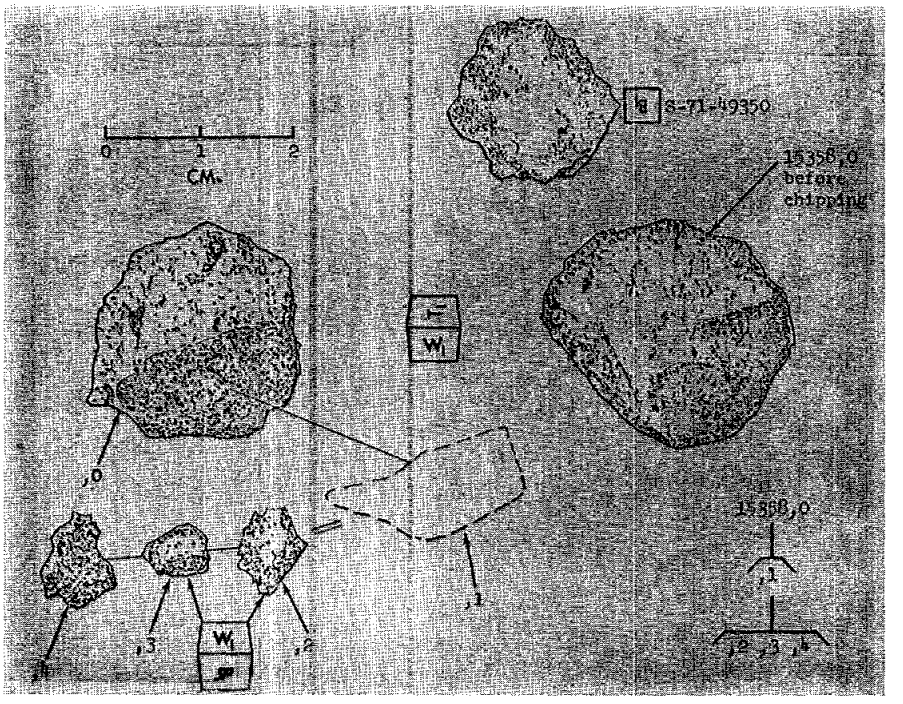

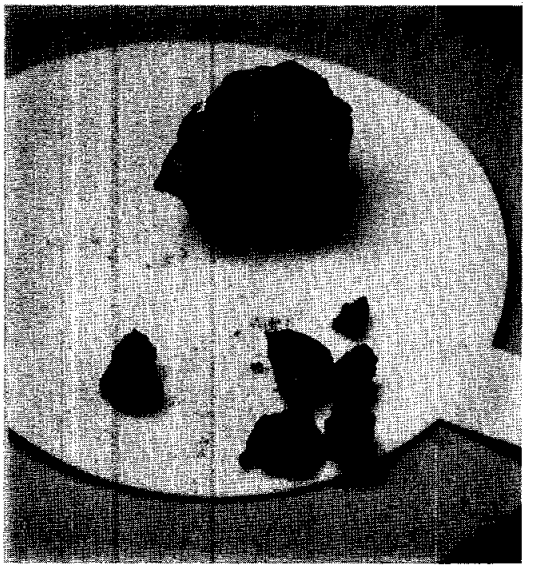

Figure 3. Splitting of 15358,6. a) diagram. b) photograph. S-71-57983

15359 FINE-GRAINED IMPACT MELT ST. 7 4.2 g

INTRODUCTION: 15359 is a fine-grained micropoikilitic impact melt containing mineral clasts. It has a texture rather like the melt portion of 15445, and a high-alumina basalt composition. It is a dark, angular, aphanitic sample (Fig. 1), which had no zap pits but was dusty. It was collected as part of the rake sample from the north-east rim of Spur Crater.

PETROLOGY: 15359 is a very fine-gained, clast-rich melt (Fig. 2) very similar to the melt groundmass of 15445, except that euhedral melt olivines do not appear to be present. It contains mineral clasts of olivine and plagioclase, with some flame-textured plagioclase (devitrified maskelynite) and polygonal olivine (Fig. 2). Some clasts have coronas or overgrowths. The melt itself is plagioclase-rich, contains a little mesostasis glass, stubby ilmenite, and metal/sulfide blebs. The texture is not entirely uniform, with some patches containing ilmenite which is acicular.

While Simonds et al. (1975) referred to 15359 as a very fine-grained subophitic impact melt, Dowty et al. (1973b) referred to it as a (monomict?) microbreccia of alkali high-alumina basalt composition. However, it is not as alkalic as Apollo 15 KREEP basalts (Tables 1, 2). Dowty et al. (1973b) provided mineral compositional data (Fig. 3), and Hlava et al. (1973) tabulated microprobe analyses of pyroxenes, plagioclases, olivines, and metal. Most of the data for olivine and plagioclase is probably of clasts. Nehru et al. (1973, 1974) reported analyses of chromite, ulvospinel, and ilmenite, which are present as small grains. The metals (0.8 to 1.2% Co; 4.4 to 7.4% Ni) indicate meteoritic contamination.

CHEMISTRY: A chemical analysis was reported by Murali et al. (1977) (Table 1). The rare earths are shown in Figure 4. A microprobe defocussed beam analysis by Dowty et al. (1973b) (Table 2) is in general agreement with the Murali et al. (1977) analysis. The composition is similar to that of 15445 and 15455 except a little less magnesian and richer in rare earth elements. The rare earths have a KREEP pattern.

PROCESSING AND SUBDIVISIONS: 15359 was split by chipping (Fig. 5). ,0 is now 4.2 g. Part of ,1 was used for chemical analysis, and part of ,2 was used to make thin sections ,4 and ,6.

Figure 1. Pre-split view of 15359. S-71-49795

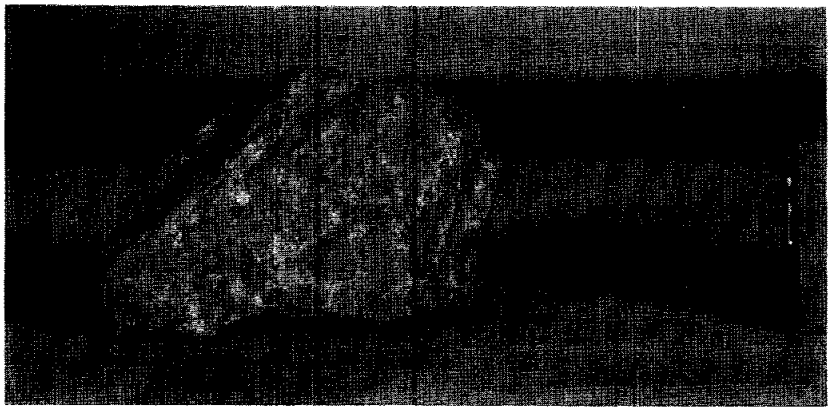

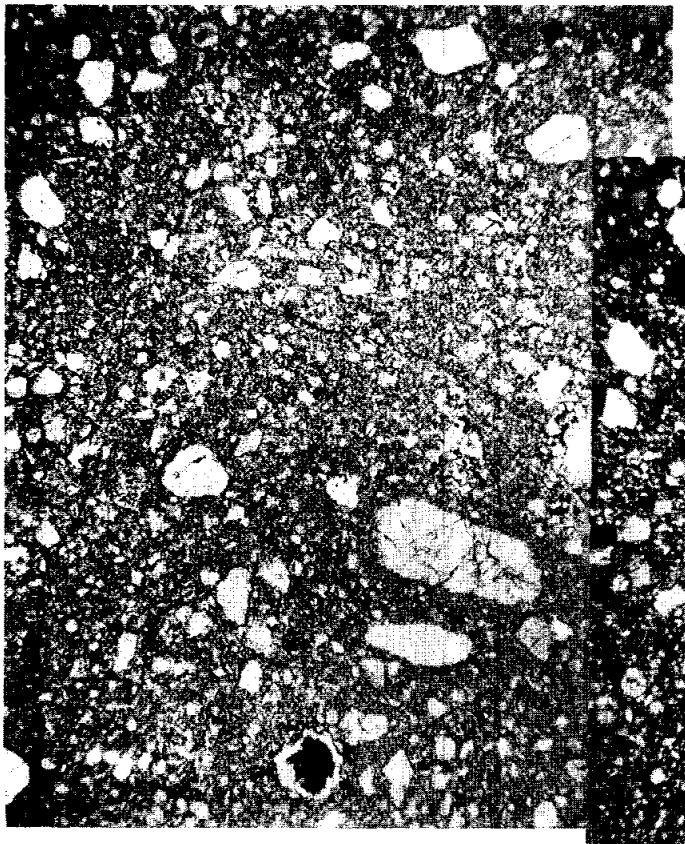

Fig. 2a

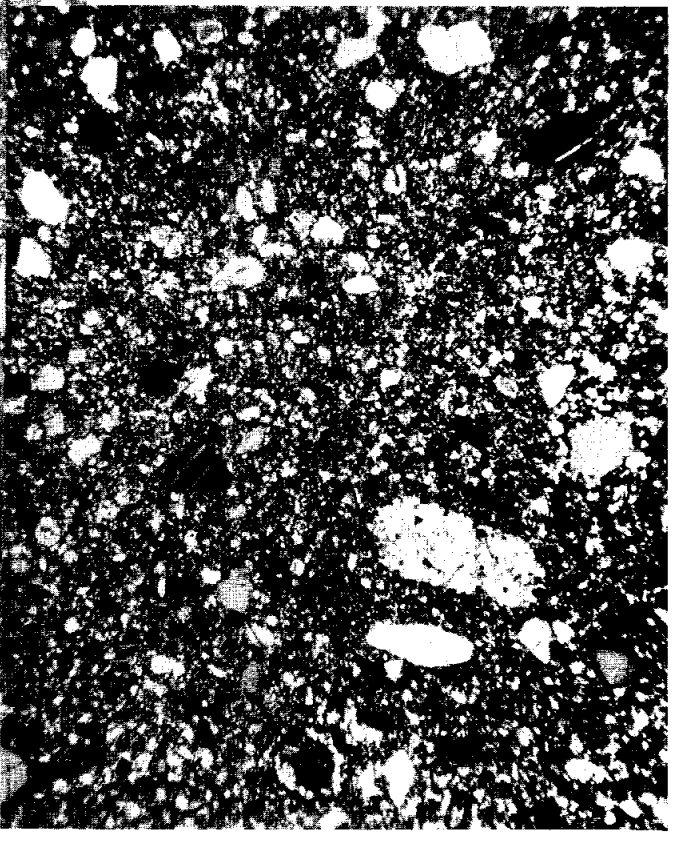

Fig. 2b

Figure 2. Photomicrograph of 15359,4. a) general view, showing fine-grained, generally uniform matrix, and clasts. Clast in lower center has a corona or overgrowth. Transmitted light. Width about 2 mm. b) as (a), crossed polarizers. c) flame-textured plagioclase clast and polygonalized olivine clast. Crossed polarizers. Width about 1.25 millimeters. d) reflected light view of groundmass. Width about 125 microns.

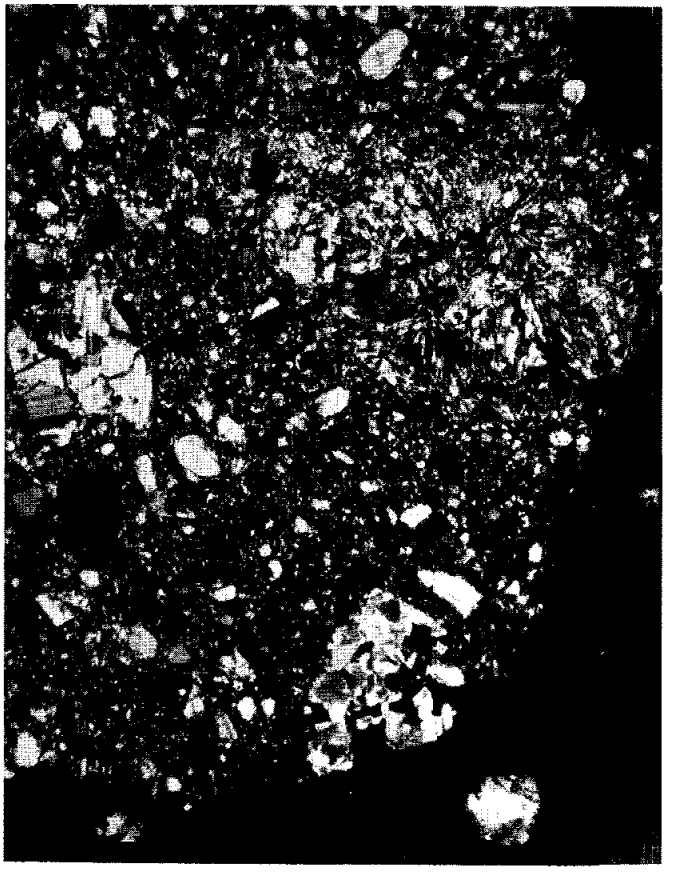

Fig. 2c

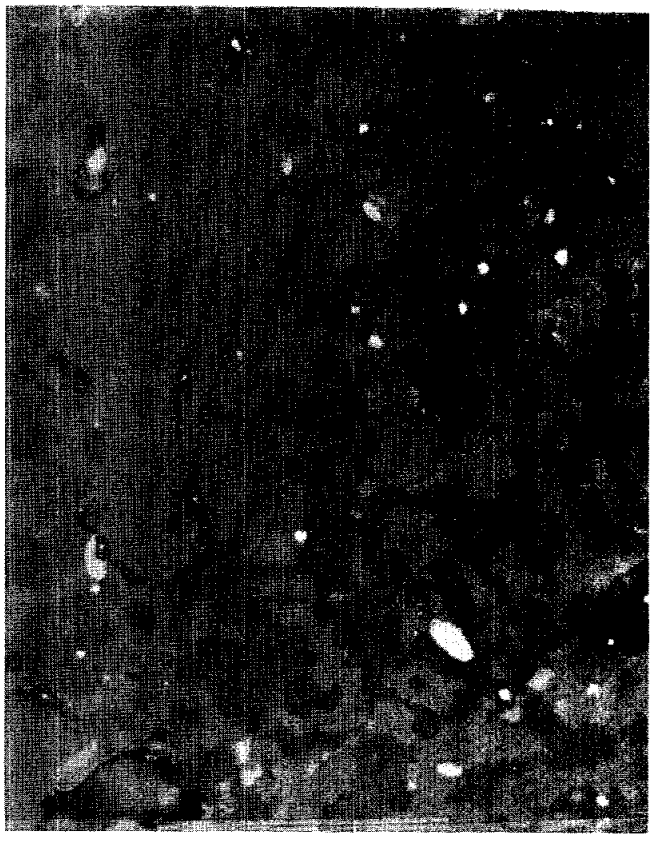

Fig. 2d

TABLE 15359-1. Chemical analyses of 15359,5

Wt %	SiO2	
	TiO2	0.5
	Al2O3	19.8
	FeO	8.3
	MgO	12.2
	CaO	11.7
	Na2O	0.59
	K2O	0.19
	P2O5	
(ppm)	Sc	15.2
	V	43
	Cr	1260
	Mn	870
	Co	20
	Ni	137
	Rb	
	Sr	
	Y	
	Zr	781
	Nb	
	Hf	15.0
	Ba	270
	Th	7.2
	U	
	Pb	
	La	40.0
	Ce	111
	Pr	
	Nd	
	Sm	17.7
	Eu	1.57
	Gd	
	Tb	3.5
	Dy	22
	Ho	
	Er	
	Tm	
	Yb	11.6
	Lu	1.60
	Li	
	Be	
	B	
	C	
	N	
	S	
	F	
	Cl	
	Br	
	Cu	
	Zn	
(ppb)	I	
	At	
	Ga	
	Ge	
	As	
	Se	
	Mo	
	Tc	
	Ru	
	Rh	
	Pd	
	Ag	
	Cd	
	In	
	Sn	
	Sb	
	Te	
	Cs	
	Ta	1800
	W	
	Re	
	Os	
	Ir	
	Pt	
	Au	
	Hg	
	Tl	
	Bi	
		(1)

References and Methods:

(1) Murali et al. (1977); INAA

TABLE 15359-2. Defocussed beam microprobe bulk rock analysis (Dowty et al., 1973b)

Wt %	SiO2	48.6
	TiO2	1.08
	Al2O3	18.0
	FeO	9.6
	MgO	11.0
	CaO	10.3
	Na2O	0.66
	K2O	0.19
	P2O5	0.05
ppm	Mn	800
	Cr	2200
	Zr	1050

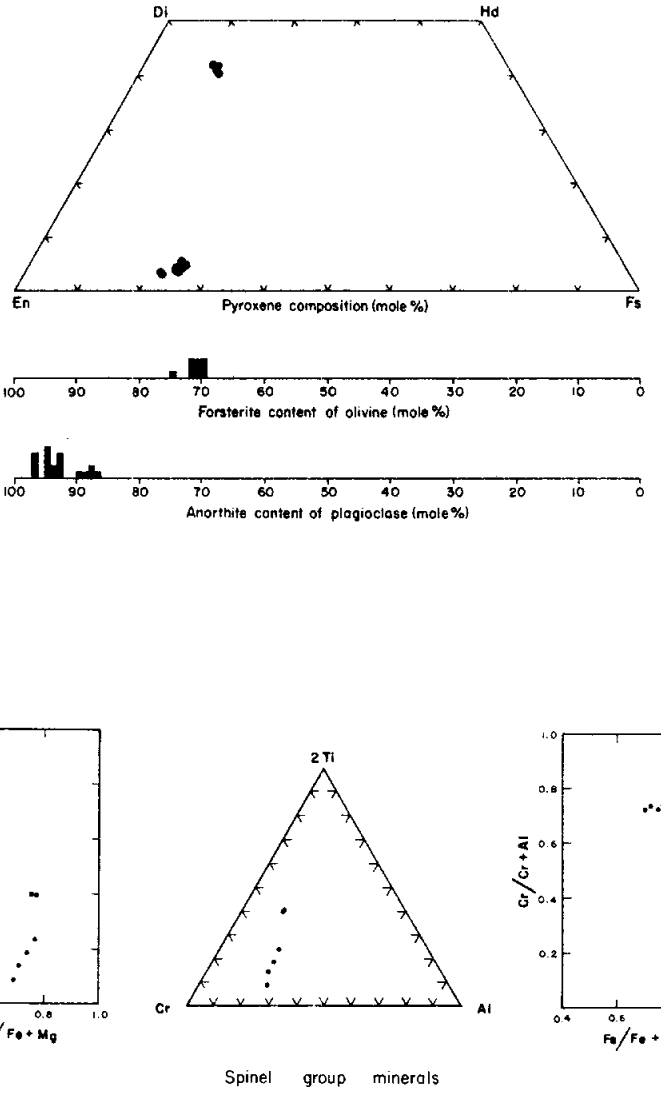

Figure 3. Compositions of minerals in 15359 (Dowty et al., 1973b).

Figure 4. Rare earths in 15359 (Murali et al., 1977).

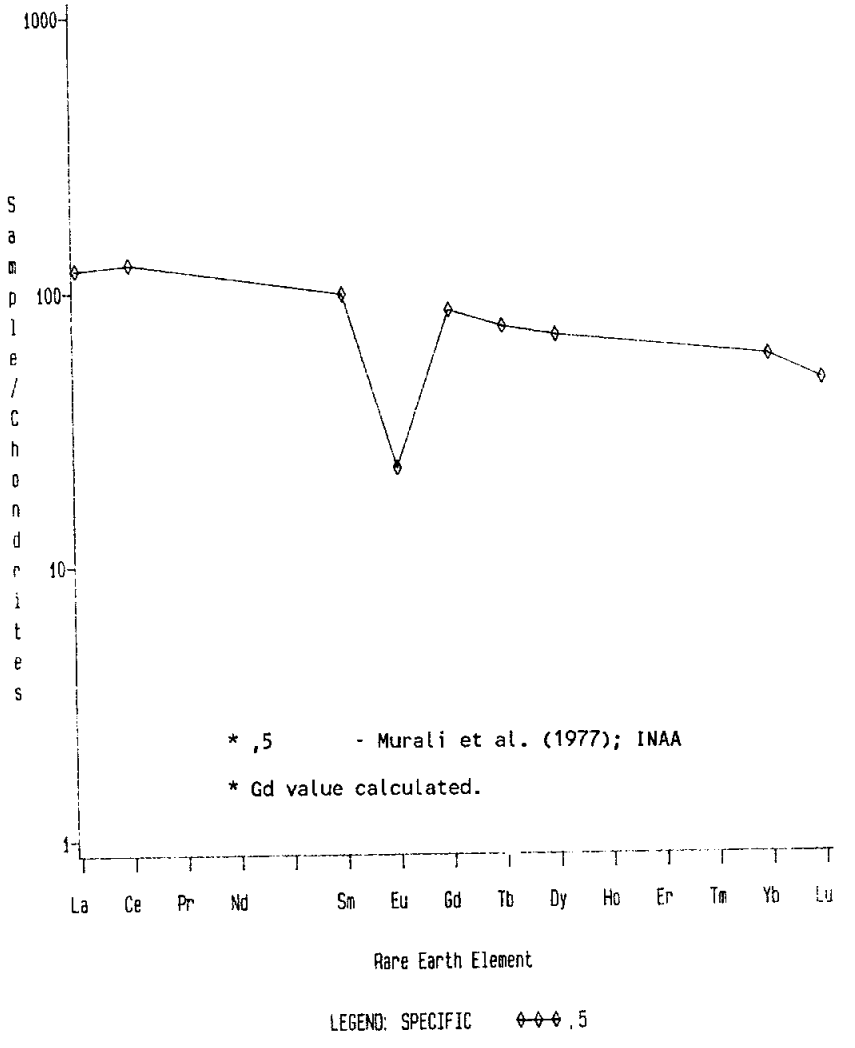

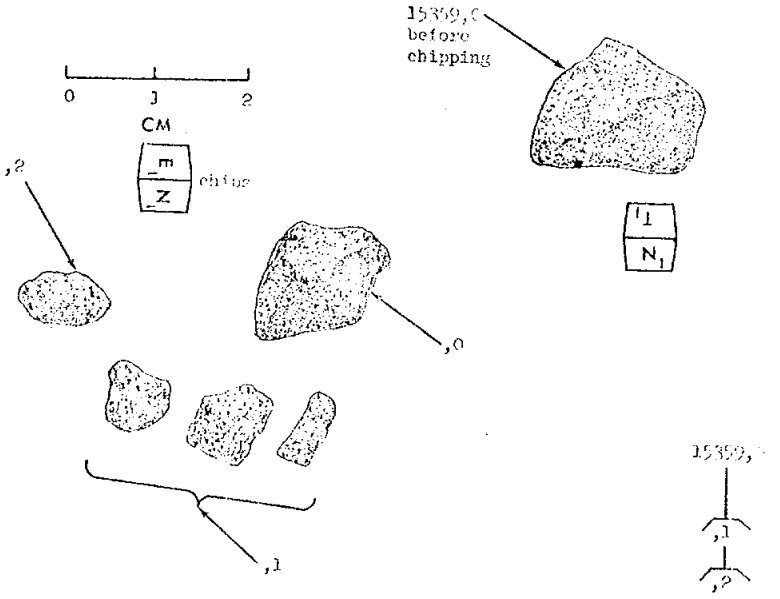

Figure 5. Chipping diagram for 15359.

15360 REGOLITH BRECCIA ST. 7 9.3 g

INTRODUCTION: 15360 is a brown-glassy matrix regolith breccia with a variety of small lithic clasts. It is coated on two opposing sides by vesicular glass and contains one larger white clast (Fig. 1). All depressions were originally dust-filled. Zap pits were not positively identified on the glass. 15360 was collected as part of the rake sample from the north-east rim of Spur Crater.

PETROLOGY: The dominant dark matrix of 15360 is a brown glassy regolith breccia, containing a variety of lithic clasts, mineral fragments, and glasses (Fig. 2). According to Steele et al. (1977), the sample consists of 20% glass, 5% lithic clasts, 30% mineral clasts, and 45% matrix, without porosity. The fragments show many shock effects. The glasses include green, yellow, and reddish examples. Steele et al. (1977) described three lithic clasts, one KREEP, one mare, and one ultrabasic. The ultrabasic one is depicted in Figure 2c. It is nearly all shocked olivine, with some plagioclase, pyroxene, and chromite. The olivine (Fo_{91}, CaO 0.03%) is similar to that in the spinel-troctolite clast in 15445 but this clast lacks Mg-spinel and appears to be unique. The mare clast was identified by its high-Fe, high-Ca plagioclase and its pyroxene compositions, and the KREEP by its low-Fe, low-Ca plagioclase and its pyroxene compositions (pyroxene quadrilateral plots for both are shown in Steele et al., 1977). Few lithic clasts are larger than 500 microns, except the white one visible in Figures 1 and 3 which does not occur in the thin sections.

PROCESSING AND SUBDIVISIONS: 15360 was chipped to produce ,0 (6.68 g), ,1 (1.87 g), and ,2 (Fig. 3). From ,2, the thin sections ,2 and ,6 were made (potted butts ,8 and ,9 remaining).

Figure 1. Macroscopic view of 15360, showing predominately the vesicular glass coat and the large white unsampled clast. S-71-49661

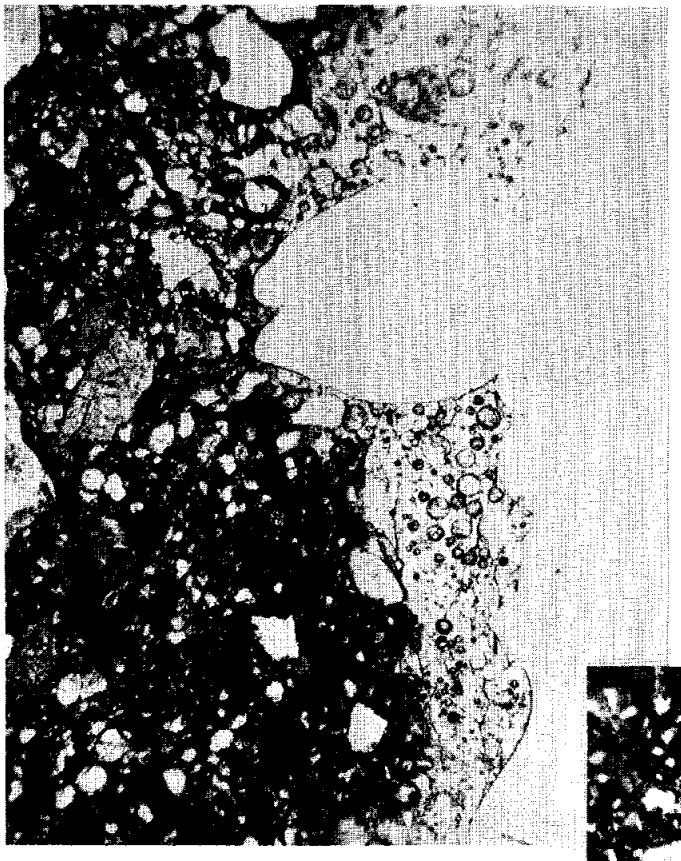

Fig. 2a

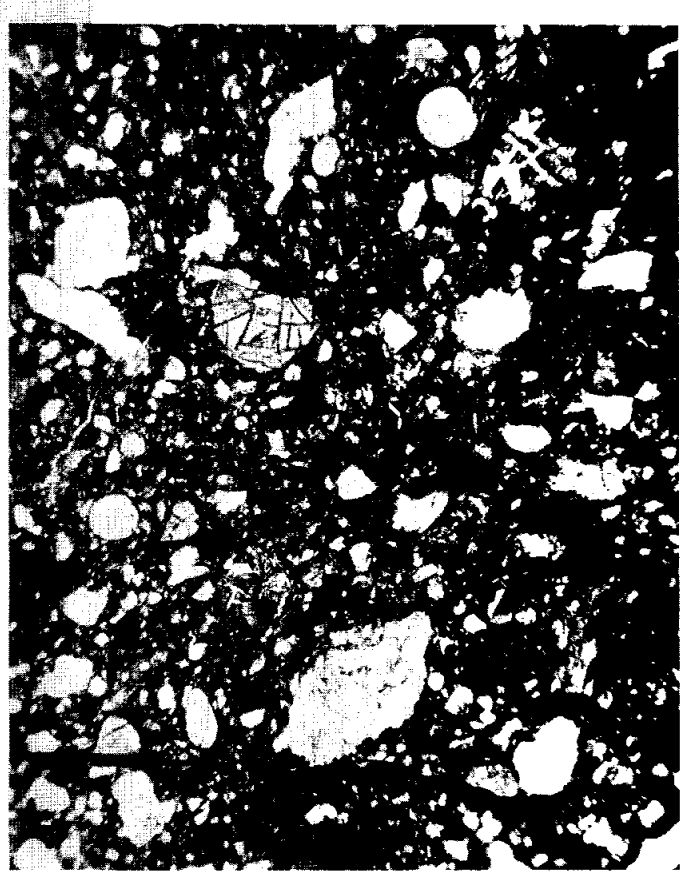

Fig. 2b

Figure 2. Photomicrographs of 15360. a) 15360,6, showing vesicular clear glass coat and interior opaque glassy breccia. Transmitted light. Width about 2 mm. b) 15360,2 showing opaque matrix, glass balls, and the ultrabasic clast (lower center). Transmitted light. Width about 2 mm. c) ultrabasic clast in 15360,2. Crossed polarized light. Width about 300 microns.

Fig. 2c

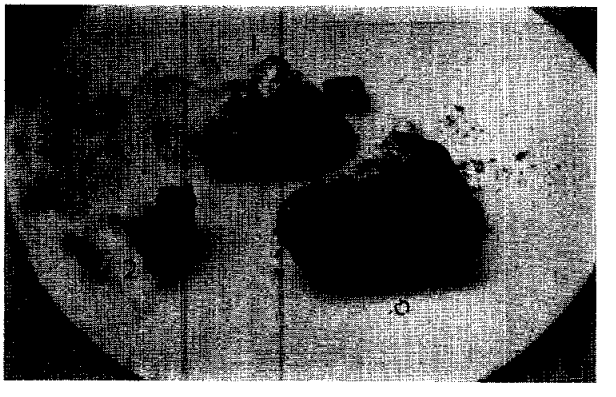

Figure 3. Chipping of 15360. Smallest chip is ,2, from which thin sections were made. S-71-57943

15361 ANORTHOSITE ST. 7 0.9 g

INTRODUCTION: 15361 is a white angular breccia, apparently an anorthosite (Fig. 1). It is dust-covered with possible zap pits. It has not been subdivided or allocated. 15361 was collected as part of the rake sample from the north-east rim of Spur Crater.

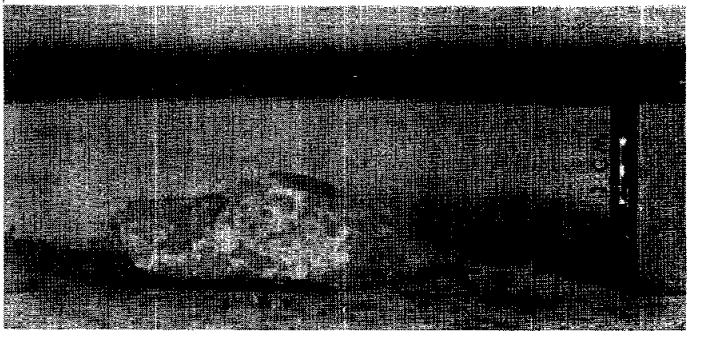

Figure 1. Macroscopic view of 15361. S-71-49337

15362 CATACLASTIC ANORTHOSITE ST. 7 4.2 g

INTRODUCTION: 15362 is a friable white sample consisting almost entirely of plagioclase (Fig. 1). It appears to be a cataclastic anorthosite from a pristine, igneous precursor. It is extremely brecciated but relict grains several millimeters across are present. Most surfaces were dusty, but a few microcraters were positively identified. 15362 was collected as part of the rake sample from the north-east rim of Spur Crater.

PETROLOGY: 15362 consists almost entirely of plagioclase grains, with relics up to a few millimeters across but most occurring as finer-grained material (Fig. 2). Many plagioclases are deformed. A description was given by Dowty et al. (1972), including mineral compositional data, and further mineral analyses were given by Dowty et al. (1973b), Nehru et al. (1973, 1974), Hlava et al. (1973), Hansen et al. (1979), Steele et al. (1980), Steele and Smith (1979), and Meyer (1979). According to Dowty et al. (1972), the texture is varied, and includes opaque, shock-produced plagioclase veins. It is far more cataclasized than 15415. The sample contains accessory pyroxene and ilmenite, and chromite and troilite were also observed. Plagioclase compositions are $An_{96.7 \pm 0.6}$, and x-ray precession studies indicated that the structure is ordered. The twins are predominantly pericline. Steele and Smith (1979), Meyer (1979), and Steele et al. (1980) measured trace elements in the plagioclases with the ion microprobe (Table 1). Hansen et al. (1979) measured some minor elements in plagioclase with the microprobe, finding an Ab (3.1 mol %), similar to previous studies, and 0.036% MgO, 0.067% FeO, and 0.014% K_2O as an average of 23 analyses.

The less than 2% pyroxene present includes augite and hypersthene, with augite predominating more than 3 to 1 (Dowty et al., 1972). Smaller grains within plagioclases are only augite; larger ones (up to 500 microns) between plagioclases are intergrowths. Compositions are shown in Figure 3 and have a narrow range. X-ray precession studies on augite allowed the cell dimensions to be determined and showed no evidence for exsolved, epitaxial low-Ca pyroxene. The opaque minerals were discussed by Nehru et al. (1974) and complete microprobe analyses were listed by them and by Nehru et al. (1973). Chromite (9.1% Al_2O3 average) is low in TiO_2 and MgO, and is homogeneous. The troilite was too small to analyze.

The high plagioclase content suggests that 15362 is a cumulate, a member of the ferroan anorthosite suite, but there is no longer any textural evidence for an igneous origin. The mineralogy (low-Ca pyroxene, high-Ca in augite, the pericline twinning) suggests that the sample was held at high subsolidus temperatures for some time.

CHEMISTRY: Chemical analyses listed in Table 2 are consistent with a very plagioclase-rich sample, a member of the ferroan, low-K anorthosite suite. The rare earths are shown in Figure 4.

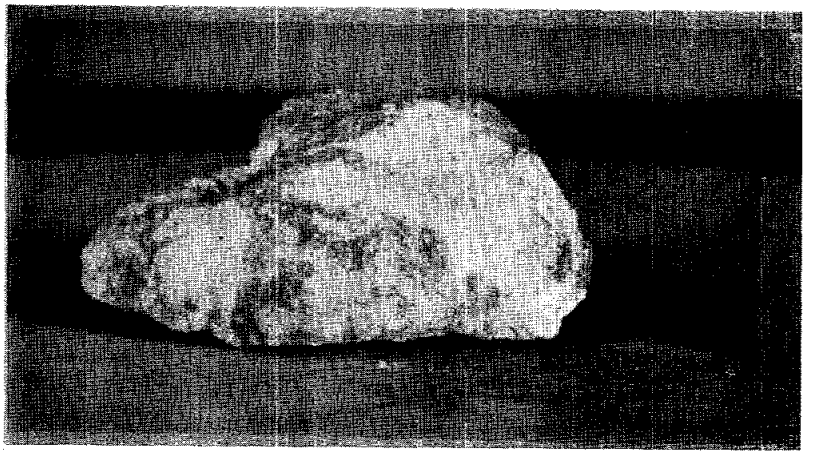

Figure 1. Pre-split view of 15362. S-71-49629

TABLE 15362-1. Minor elements in plagioclases in 15362 (ppm)

	a	b	c
Li	1.5	2.2	1.83
Mg	300	288	232
K	—	—	108
Ti	—	91	48
Sr	—	200	179
Ba	40	26	8.2
Mol % Ab	—	—	3.5

a,b: Meyer (1979)
c: Steele et al. (1980), average of many analyses.

Fig. 2a

Fig. 2b

Figure 2. Photomicrographs of 15362,11, crossed polarizers, widths about 2 mm. a) predominantly coarse grains. b) predominantly fine-grains.

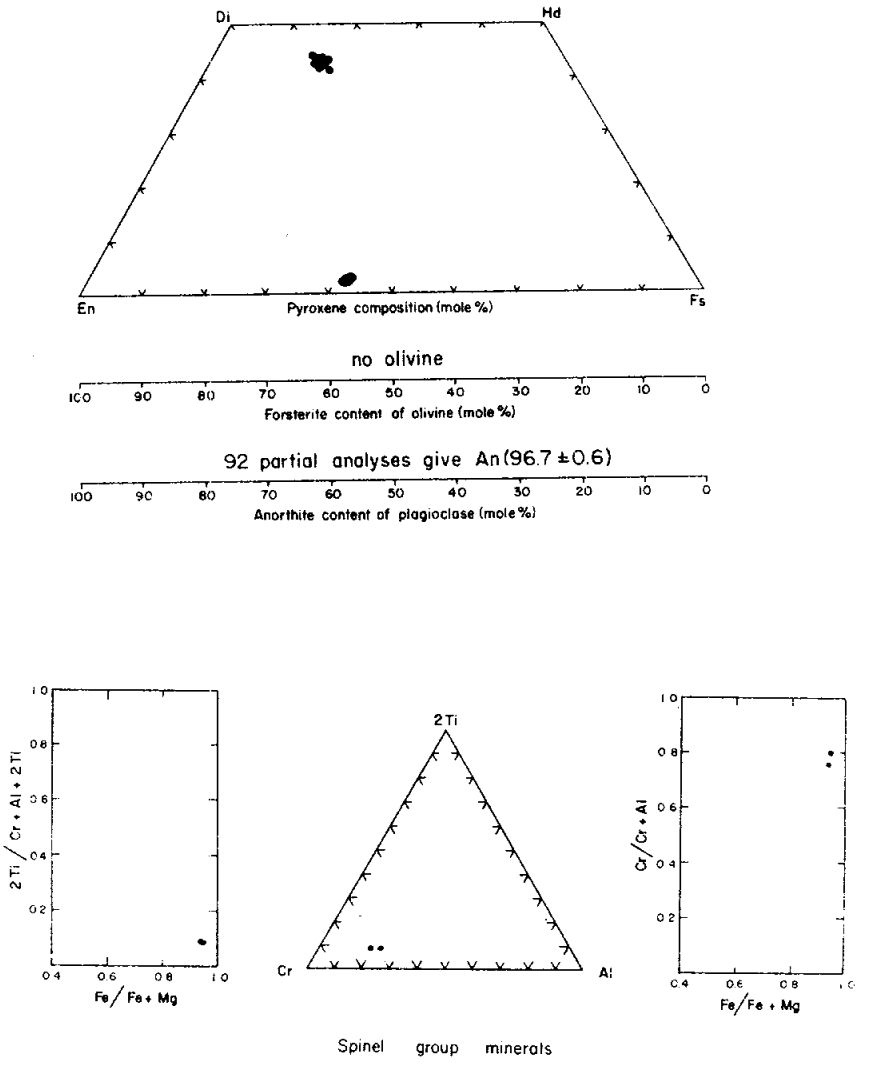

Figure 3. Compositions of minerals in 15362, from Dowty et al. (1973b).

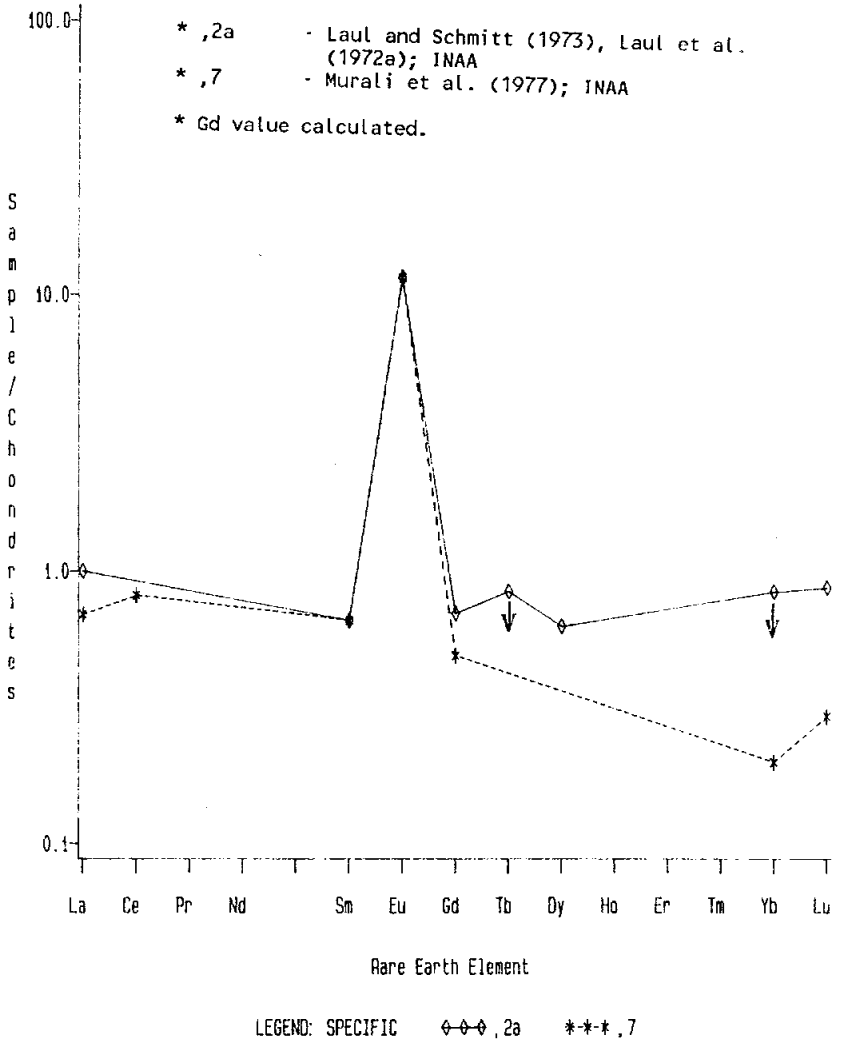

Figure 4. Rare earths in 15362.

Laul and Schmitt (1972a) suggested that, by comparison with 15415, 15362 was contaminated with 0.2% KREEP. However, the rare earth pattern of 15362 is flatter than that for 15415, and would not appear to indicate contamination at all. The low Co and Ni abundances would are consistent with a lack of meteoritic contamination, but determinations of the highly siderophile element abundances (Ir, Au, etc.) have not been made.

RADIOGENIC ISOTOPES AND GEOCHRONOLOGY: Alexander and Kahl (1974) studied Ar isotopes. The release diagram (Fig. 5) does not show a good plateau, uncertainties are large because of the low K content, and there is evidence of recent gas loss. The simplest interpretation is that material older than 4.1 b.y. was extensively but not completely outgassed around 3.9 b.y., but this is not unique. The sample is probably older than 3.98 ± 0.06 b.y. The behaviour of the K/Ca ratio with release is consistent with release of gas from a single mineral phase.

EXPOSURE HISTORY: The study of Alexander and Kahl (1974) gave an Ar exposure age of 428 ± 43 m.y.

PROCESSING AND SUBDIVISIONS: Four chips were taken from ,0, which is now 2.95 g. ,1 was partly consumed to make the two thin sections ,6 and ,11. Two of the others (,2 and ,3) were allocated for analysis. (The cutting picture on file in the 15362 data pack is erroneous, showing the sawing of an entirely different sample.)

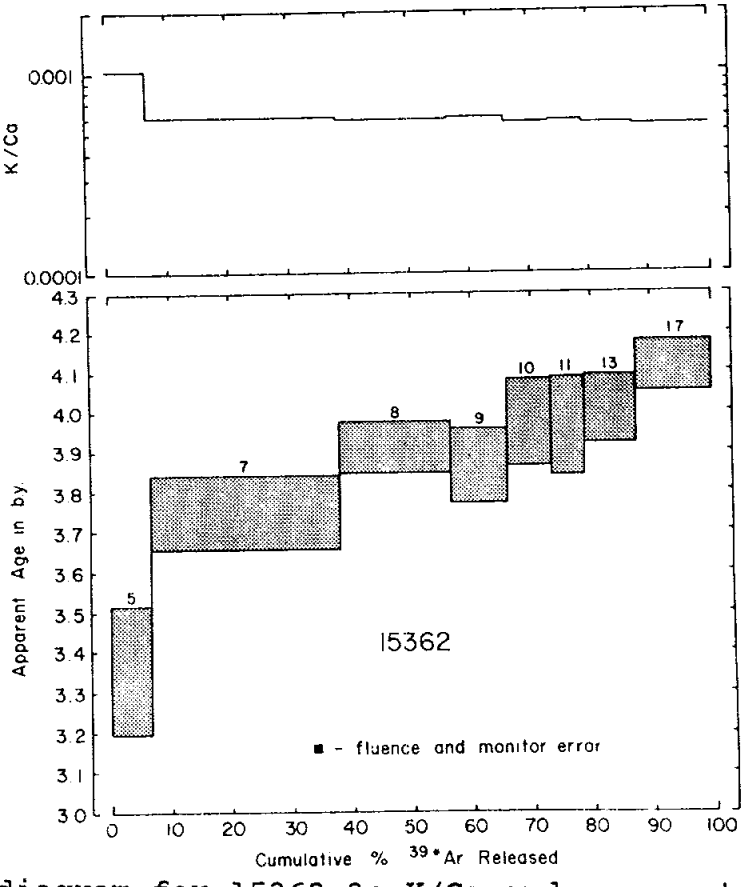

Figure 5. Ar release diagram for 15362,3; K/Ca and apparent age (Alexander and Kahl, 1974).

TABLE 15362-2. Chemical analyses of 15362

		,2(a)	,7	,3
Wt %	SiO2			
	TiO2	0.2		
	Al2O3	35.4	32.3	
	FeO	0.57	0.23	
	MgO		0.3	
	CaO	18.4	17.0	22.7(b)
	Na2O	0.347	0.39	
	K2O	<0.02	0.011	0.012
	P2O5			
(ppm)	Sc	1.6	0.7	
	V	<28		
	Cr	80	30	
	Mn	110	40	
	Co	1.4	0.31	
	Ni		10	
	Rb			
	Sr			
	Y			
	Zr	<70		
	Nb			
	Hf	0.10	0.05	
	Ba			
	Th			
	U			
	Pb			
	La	0.33	0.23	
	Ce		0.72	
	Pr			
	Nd			
	Sm	0.12	0.12	
	Eu	0.80	0.80	
	Gd			
	Tb	<0.04		
	Dy	0.20		
	Ho			
	Er			
	Tm			
	Yb	<0.17	0.04	
	Lu	0.027	0.006	
	Li			
	Be			
	B			
	C			
	N			
	S			
	F			
	Cl			
	Br			
	Cu			
	Zn			
(ppb)	I			
	At			
	Ga			
	Ge			
	As			
	Se			
	Mo			
	Tc			
	Ru			
	Rh			
	Pd			
	Ag			
	Cd			
	In			
	Sn			
	Sb			
	Te			
	Cs			
	Ta			
	W			
	Re			
	Os			
	Ir			
	Pt			
	Au			
	Hg			
	Tl			
	Bi			
		(1)	(2)	(3)

References and methods:

(1) Laul and Schmitt (1973), Laul et al. (1972a); INAA.
(2) Murali et al. (1977); INAA
(3) Alexander and Kahl (1974); from Ar isotopes.

Notes: (a) values in Laul and ScHmitt (1973) supercede some of those from Laul et al. (1972a).
(b) unrealistically high.

15363 ANORTHOSITE ST. 7 0.5 g

INTRODUCTION: 15363 is a flat, tabular white chip, apparently a crushed anorthosite (Fig. 1). One edge is slightly rounded and may be pitted, but no distinct pits occur on the sample, which is a little dust-covered. It has not been subdivided or allocated. 15363 was collected as part of the rake sample from the northeast rim of Spur Crater.

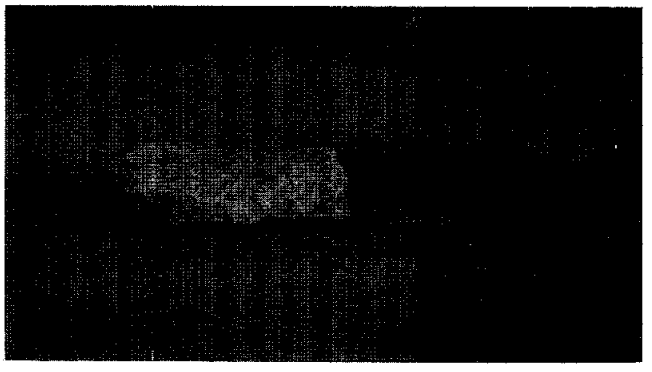

Figure 1. Macroscopic view of 15363. S-71-49523

15364 ANORTHOSITIC (MONOMICT?) BRECCIA ST. 7 1.5 g

INTRODUCTION: 15364 is a plagioclase-rich, fine-grained fragmental breccia (Fig. 1). It lacks mare, KREEP, green glass, or other breccia clasts and appears to have a restricted olivine-bearing feldspathic highlands provenance. It has some mineral features distinct from ferroan anorthosites.

15364 macroscopically appears to have about 10% mafics, and to be coated in grey dust. No distinct zap pits were seen, but the corners were slightly rounded. It was collected as part of the rake sample from the north-east rim of Spur Crater.

PETROLOGY: 15364 was described by Steele et al. (1977), and mineral chemical data were given in Steele et al. (1972a, b), Hansen et al. (1979), and Smith et al. (1980a, b). The sample lacks glass, and consists of 20% lithic clasts and 80% mineral clasts, which are dominantly plagioclase (Fig. 2a). The lithic clasts are crystalline, generally poikilitic varieties in which the olivine encloses plagioclases (Figs. 2b-d). Overall the plagioclases are calcic (An_{97-95}) and low in Fe (<0.15%); olivine is ~Fo_{70}; and pyroxene is ~$En_{75}Wo_3$.

Steele et al. (1977) described the clast shown in Figure 2b (their clast A). It has euhedral, chemically unzoned plagioclase enclosed poikilitically in olivine. The olivine is Fo_{72} with 0.10% CaO, pyroxene is $En_{73}Wo_4$, and the plagioclase is An_{97}. Chromite is also present. Discrepancies between these analyses and later ones (below) occur. Precise analyses of the Al, P, Ca, Ti, Cr, and Mn in four olivine grains were made by Smith et al. (1980a). The Ti in the olivines is higher than in ferroan anorthosites (Smith et al., 1980a, b, label the sample as ,2 but the thin section is ,1). Hansen et al. (1979) analysed plagioclases in the clast, with the microprobe, for MgO (0.046%), FeO (0.057%), and K_2O (0.040%), with a mol % Ab of 5.2%. The K_2O contents are at the low end of the Mg-suite, but the high end of the ferroan anorthsotic suite. The orthopyroxene is reported as Mg_{76}. The plagioclases were also analyzed by Smith et al. (1980b) with the ion probe, for Li (7.3 ppm), Mg (355 ppm), K (550 ppm), Ti (100 ppm), Sr (275 ppm), and Ba (80 ppm), with mol % Ab of 5.9%. The Ba is higher than in ferroan anorthosite plagioclase. The chromite is Ti-rich. Steele et al. (1977) also found a clast B to be similar to clast A except that it contained no euhedral plagioclase.

PROCESSING AND SUBDIVISIONS: Only a small chip ,1 was removed from ,0, for thin sections ,1; ,7; and ,14. ,0 (1.22 g) was temporarily allocated for a magnetic study.

Figure 1. Pre-split view of 15364. S-71-49611

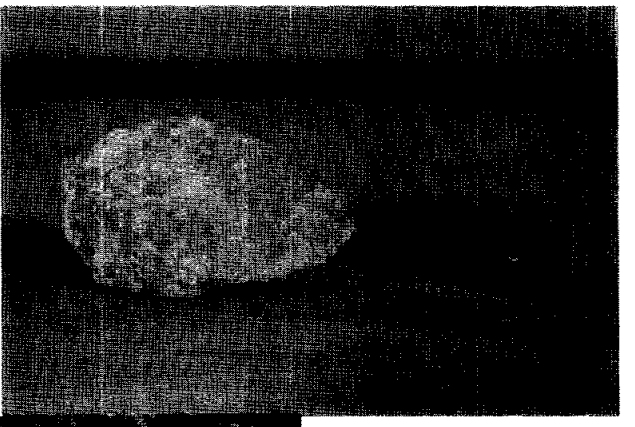

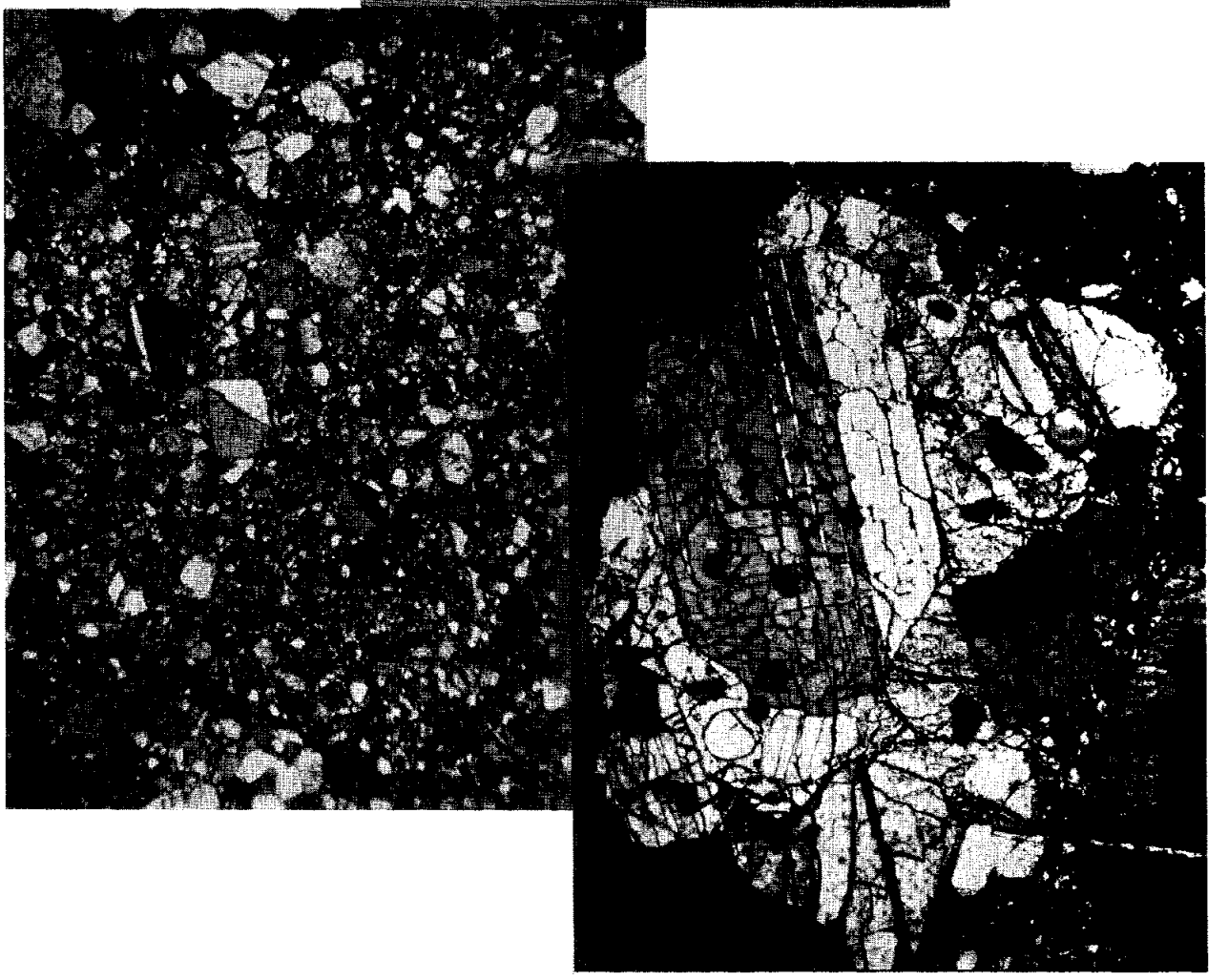

Figure 2. Photomicrograph of 15364. a) general matrix view of 15364,7, showing fine grain-size and brecciated nature. Crossed polarizers, width about 2 mm. b) Clast A of Steele et al. (1972) in 15364,1, showing euhedral plagioclase. Crossed polarizers, width about 600 microns. c) polygonal plagioclase-olivine clast in 15364,7. Crossed polarizers, width about 300 microns. d) poikilitic olivine-plagioclase clast in 15364,1. Transmitted light, width about 600 microns.

Fig. 2c

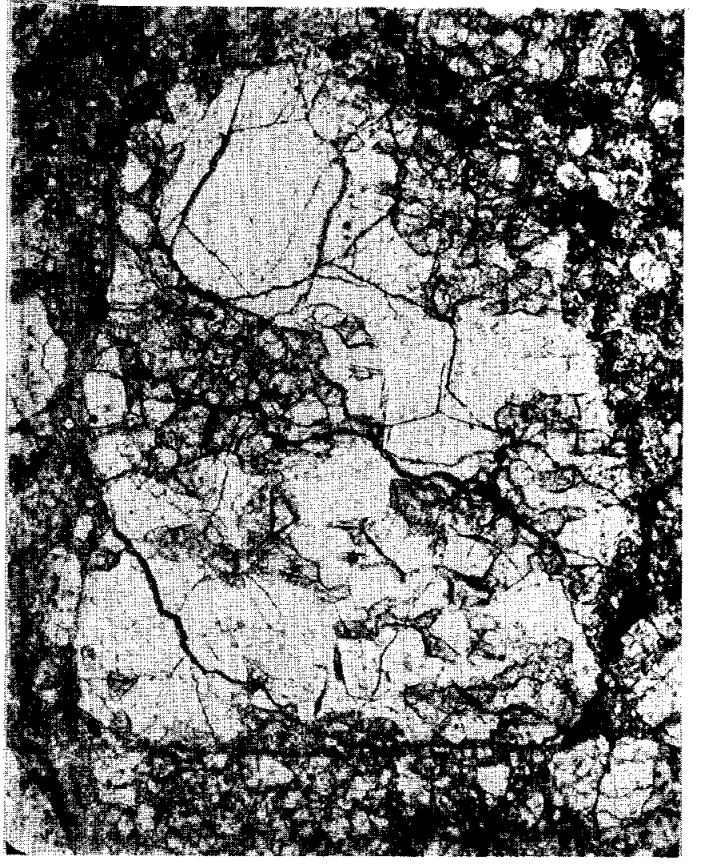

Fig. 2d

15365 INDURATED GREEN GLASS CLOD ST. 7 2.9 g

INTRODUCTION: 15365 is a clod of green glass spherules and other green glass material (Fig. 1), but differs in being more indurated and having more devitrified material than other clods. Its surface was moderately and irregularly pitted and dusty. It was collected as part of the rake sample from the north-east rim of Spur Crater.

Figure 1. Pre-split view of 15365. S-71-49181

TABLE 15365-1. Defocussed beam microprobe bulk analysis of 15365,1 (Bunch et al., 1972)

Wt%	SiO2	43.8
	TiO2	0.44
	Al2O3	7.7
	FeO	21.4
	MgO	15.7
	CaO	8.6
	Na2O	0.12
	K2O	<0.02
	P2O5	0.02
ppm	Mn	2300
	Cr	3200

PETROLOGY: 15365 is a compacted or lithified green glass clod (Fig. 2), in which the outlines of most spherules and chondrules have been obscured (Dowty et al., 1973b). However, it is entirely a green glass clod, like other clods (Bunch et al., 1972). Microprobe analyses of the bulk rock (Table 1), individual glasses, and green glass chondrules are given in Bunch et al. (1972) and Hlava et al. (1973) . Compared to other green glass clods, 15365 contains more coarsely devitrified spherules and more finely devitrified brownish glass, and a lower porosity with a more continuous glassy matrix.

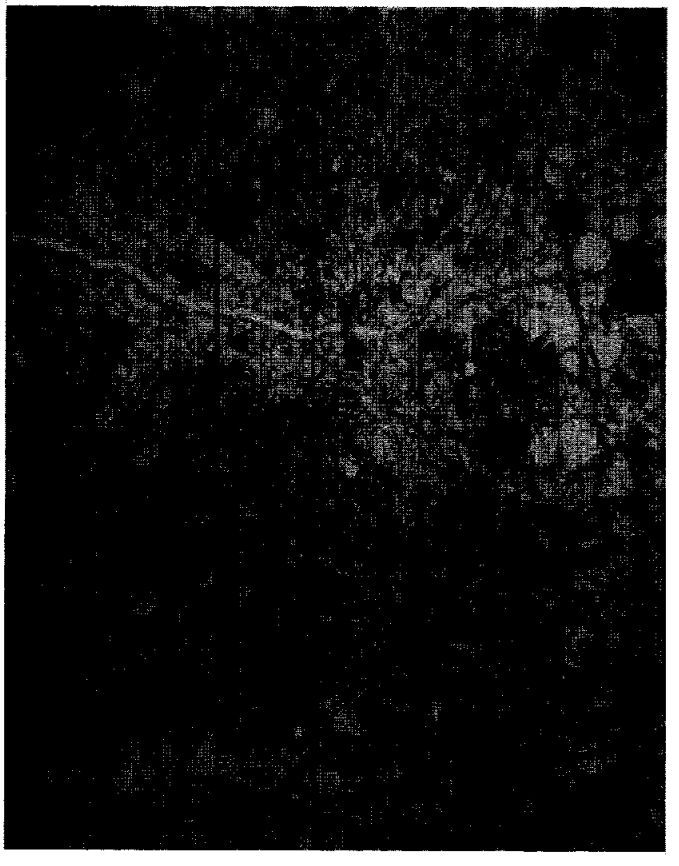

Figure 2. Photomicrograph of 15365,4, general view. Several spherules have crystals (devitrification) and the dark patches are finely-devitrified glasses. Transmitted light. Width about 2 mm.

PROCESSING AND SUBDIVISIONS: Two chips were split from ,0 (now 1.28 g) (Fig. 3). From ,1, both thin sections ,4 and ,5 were made. ,2 is a 0.97 g chip.

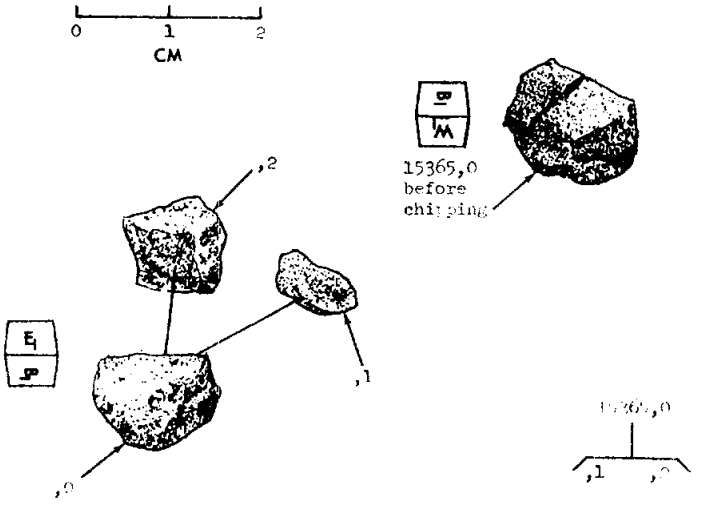

Figure 3. Chipping of 15365. ,1 was used for thin sections.

15366 GREEN GLASS CLOD ST. 7 3.3 g

INTRODUCTION: 15366 is a friable to moderately coherent clod of green glass materials (Fig. 1). It was collected as part of the rake sample from the north-east rim of Spur Crater.

Fig 1

Figure 1. Pre-split view of 15366. S-71-49150

PETROLOGY: 15366 consists of green glass balls, shards, and other related glass (Fig. 2), and is friable. Most glasses are not devitrified; and most balls are less than 300 microns across. Steele et al. (1972b) gave a composition for the glass (Table 1) which is the same as other green glasses; the finest material has the same composition as the coarser.

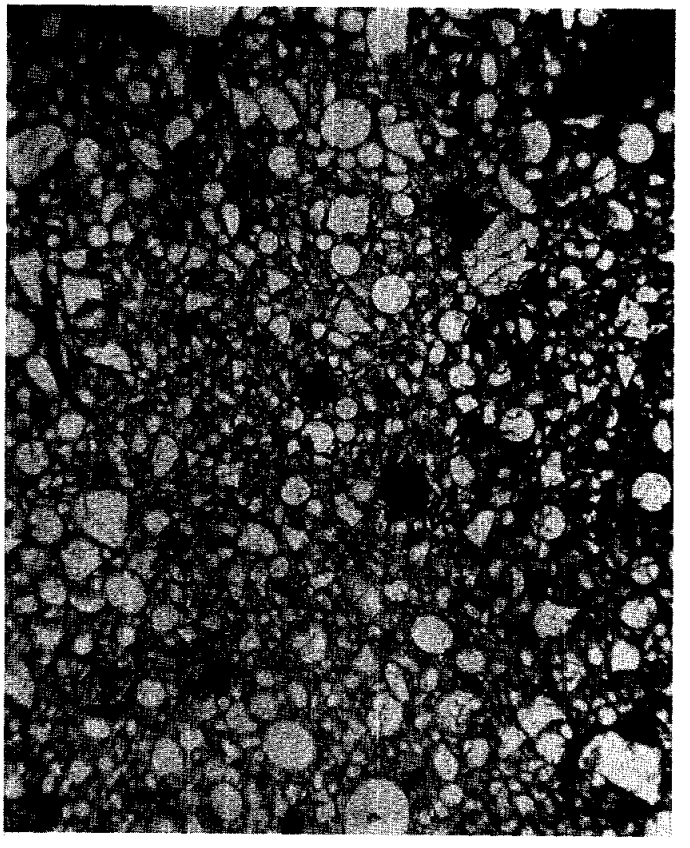

Figure 2. Photomicrograph of 15366,1. Transmitted light. Width about 2 mm.

TABLE 15366-1. Composition of glass in 15366,1. (Steele et al., 1972b)

Wt%	SiO2	46.4
	TiO2	0.40
	Al2O3	7.5
	FeO	20.3
	MgO	18.1
	CaO	8.1
	Na2O	0.10
	K2O	0.07
ppm	Cr	3500

PROCESSING AND SUBDIVISIONS: A single chip was taken from ,0 (now 2.36 g) (Fig. 3), and used to make thin sections ,1 and ,6.

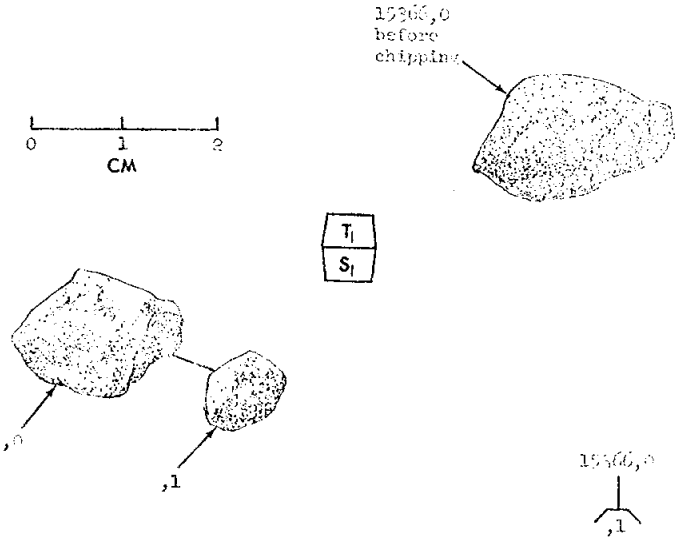

Figure 3. Splitting of 15366.

15367 GREEN GLASS CLOD ST. 7 1.1 g

INTRODUCTION: 15367 is a friable clod of green glass spherules in a fine matrix of green glass materials (Fig. 1). It has never been subdivided or allocated. It was collected as part of the rake sample from the north-east rim of Spur Crater.

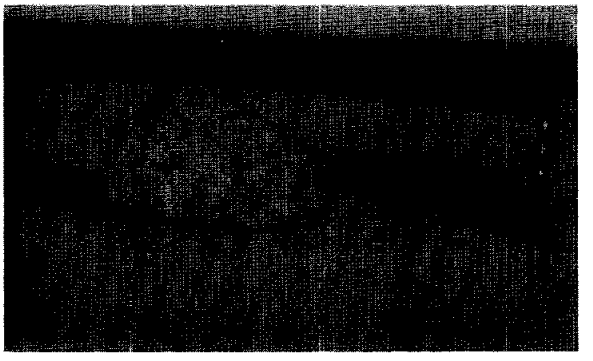

Figure 1. Macroscopic view of 15367. S-71-49046

15368 GREEN GLASS CLOD ST. 7 0.40 g

INTRODUCTION: 15368 is a friable clod of green glass spherules in a fine matrix of green glass materials (Fig. 1). It has never been subdivided or allocated. It was collected as part of the rake sample from the north-east rim of Spur Crater.

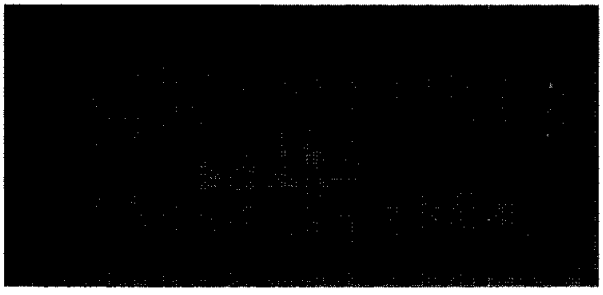

Figure 1. Macroscopic view of 15368. S-71-49086

15369 GREEN GLASS CLOD ST. 7 2.5 g

INTRODUCTION: 15369 is a friable clod of green glass material (Fig. 1), with green spherules and fragments in a matrix of grey-green powder. It was dusty with no obvious zap pits, although individual spherules in the container appeared to have pits. 15369 was collected as part of the rake sample from the north-east rim of Spur Crater.

Figure 1. Pre-chip view of 15369. S-71-49164

PETROLOGY: The entire sample consists of green glass balls, shards, and other debris (Fig. 2), with only a little devitrification such as finely-devitrified brown glass. The sample is porous.

PROCESSING AND SUBDIVISIONS: Thin sections ,7 and ,8 were made from a chip ,6. ,0 is now 1.65 g.

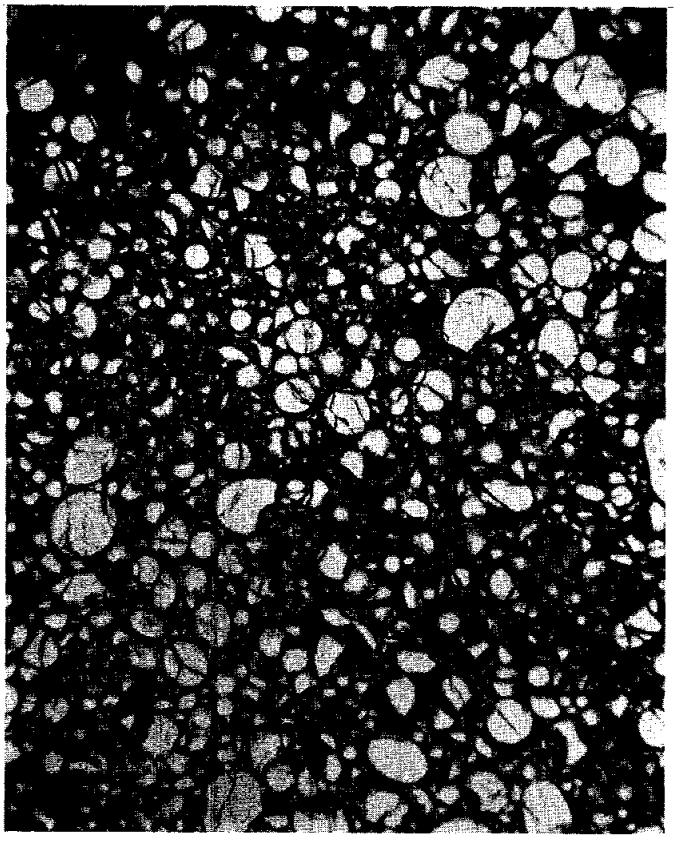

Figure 2. Photomicrograph of 15369,7. Transmitted light. Width about 2 mm.

15370 GREEN GLASS CLOD ST. 7 2.9 g

INTRODUCTION: 15370 is a friable clod (Fig. 1) of green glass spherules. It was collected as part of the rake sample from the north-east rim of Spur Crater.

PETROLOGY: 15370 consists almost entirely of green glass spherules (mainly less than 200 microns across) and broken spherules (Fig. 2a), which are held together by a small amount of (green glass?) matrix (Dowty et al., 1973b). The only anisotropic material appears to be devitrified glass, which is brown colored. The sample is porous with angular fragments making up the finest portions. A bulk analyses by microprobe defocussed beam (Table 1) shows the rock to be identical in composition with typical green glass from the landing site, with a norm containing 42% olivine, 37% pyroxene, and 20% plagioclase.

PROCESSING AND SUBDIVISIONS: Only a chip from which two thin sections (,3 and ,5) were produced has been separated from ,0, which has a mass of 2.17 g.

Figure 1. Macroscopic view of original ,0, showing dusty coating and visible balls. S-71-49154

TABLE 15370-1. Defocussed beam microprobe bulk analysis of 15370,1 (Bunch et al., 1972)

Wt %	SiO2	43.2
	TiO2	0.40
	Al2O3	7.1
	FeO	21.0
	MgO	18.5
	CaO	8.2
	Na2O	0.07
	K2O	<0.02
	P2O5	0.03
ppm	Cr	3600
	Mn	1600
		99.26

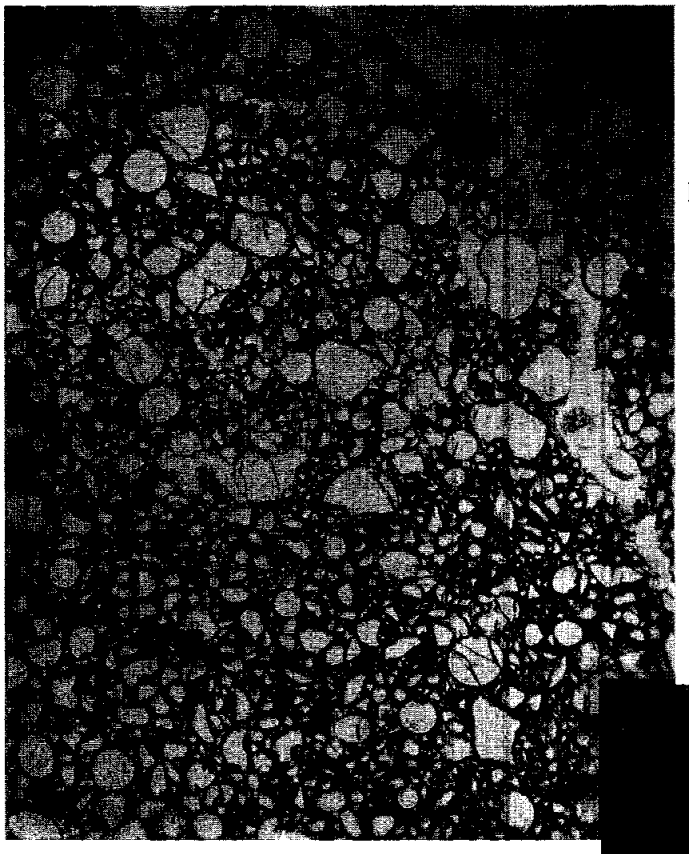

Fig. 2a

Fig. 2b

Figure 2. Photomicrographs of 15370,3. a) general view showing glass balls and shards. Opaque beads in near top right corner are devitrified glass. Width ~2 mm. Transmitted light. b) reflected light view showing porosity of matrix and angularity of smallest grains. Width ~125 microns.

15371 GREEN GLASS CLOD ST. 7 0.5 g

INTRODUCTION: 15371 is a clod consisting entirely of green glass material (Fig. 1). It is extremely friable and has entirely disaggregated. It was collected as part of the rake sample from the northeast rim of Spur Crater.

PETROLOGY: Macroscopically, 15371 is identical with green glass clods 15370, etc. (Fig. 1). Two thin sections ,12 and ,13 appear as grain mounts with polished surfaces. The particles are virtually all green glass spherules, beads, and fragments (Fig. 2) with rare devitrified examples. Most of the intact balls are less than 200 microns across; finer-grained matrix material, as occurs in 15370, is absent from the thin sections, presumably as a result of the sectioning procedure.

PROCESSING AND SUBDIVISIONS: The sample disaggregated during handling, and the thin sections (,12 and ,13) were made from such disaggregated material. Apart from the thin sections, only 0.149 g remains (,0).

Figure 1. Sample 15371,0 prior to disaggregation. S-71-49176

Figure 2. Transmitted light photomicrograph of 15371,13. Width about 2 mm.

15372 GREEN GLASS CLOD ST. 7 0.8 g

INTRODUCTION: 15372 is macroscopically similar to green glass clod samples 15370, etc., and is equally friable (Fig. 1). It has never been subdivided or allocated. It was collected as part of the rake sample from the north-east rim of Spur Crater.

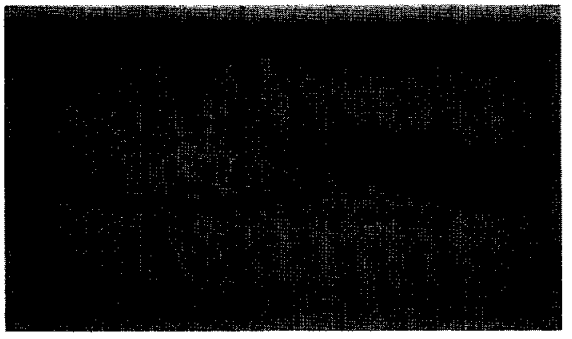

Figure 1. Macroscopic view of 15372. S-71-49042

15373 GREEN GLASS CLOD ST. 7 0.6 g

INTRODUCTION: 15373 is macroscopically similar to green glass clod samples 15370, etc., and is equally friable (Fig. 1). It has never been subdivided or allocated. It was collected as part of the rake sample from the north-east rim of Spur Crater.

Figure 1. Macroscopic view of 15373. S-71-49082

15374 GREEN GLASS CLOD ST. 7 1.0 g

INTRODUCTION: 15374 is macroscopically similar to green glass clod samples 15370, etc., and is equally friable (Fig. 1). It has never been subdivided or allocated. It was collected as part of the rake sample from the north-east rim of Spur Crater.

Figure 1. Macroscopic view of 15374. S-71-49190

15375 GREEN GLASS CLOD ST. 7 0.4 g

INTRODUCTION: 15375 is macroscopically similar to green glass clod samples 15370, etc., and is equally friable (Fig. 1). It has never been subdivided or allocated. It was collected as part of the rake sample from the north-east rim of Spur Crater.

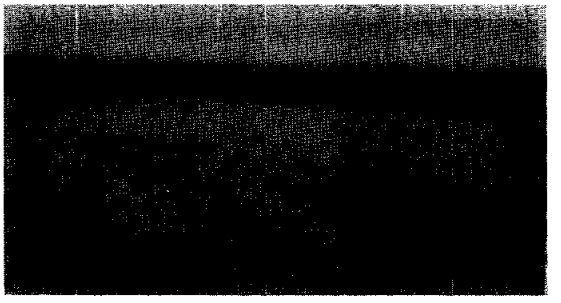

Figure 1. Macroscopic view of 15375. S-71-49094

15376 GREEN GLASS CLOD ST. 7 1.0 g

INTRODUCTION: 15376 is a friable clod (Fig. 1) of green glass spherules, macroscopically similar to 15370, etc. It was collected as part of the rake sample from the north-east rim of Spur Crater.

PETROLOGY: 15376 consists of green glass spherules and a few chondrules very loosely held together (Dowty et al., 1973b). Thin section ,3 (Fig. 2) has a uniform grain-size and is from a sieved fraction. A bulk analysis by microprobe defocussed beam (Table 1) shows the rock to be identical in composition with typical green glass from the landing site, with a norm containing 42% olivine, 37% pyroxene, and 20% plagioclase, the same as clod 15370.

PROCESSING AND SUBDIVISIONS: 15376 was substantially dissected for the making of thin sections, and ,0 is disaggregated and is only 0.39 g. Six small thin sections were made from ,1, and are sieve fractions.

Figure 1. Macroscopic view of 15376,0 prior to disaggregation. S-71-49092

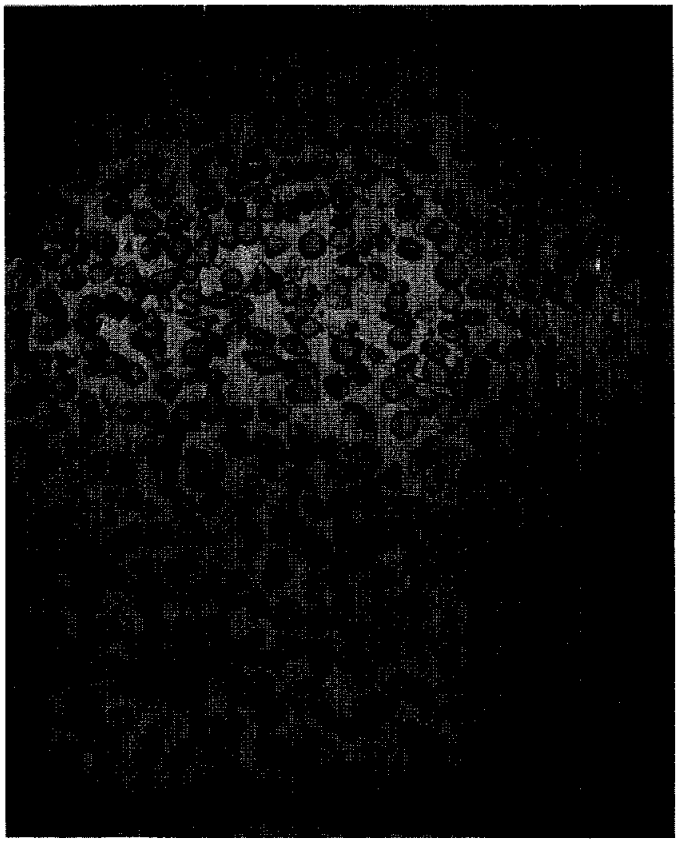

Figure 2. Photomicrograph of 15376,2, consisting almost entirely of green glass. Transmitted light. Width about 2 mm.

Table 15376-1. Defocussed beam microprobe bulk analysis of 15376,1 (Bunch et al., 1972)

Wt %	SiO2	43.6
	TiO2	0.43
	Al2O3	7.0
	FeO	21.5
	MgO	18.7
	CaO	8.3
	Na2O	0.08
	K2O	<0.02
	P2O5	0.03
ppm	Cr	3500
	Mn	1800
		100.51

15377 GREEN GLASS CLOD ST. 7 0.5 g

INTRODUCTION: 15377 is macroscopically similar to green glass clod samples 15370, etc., and is equally friable (Fig. 1). It has never been subdivided or allocated. It was collected as part of the rake sample from the north-east rim of Spur Crater.

Figure 1. Macroscopic view of 15377. S-71-49158

15378 REGOLITH BRECCIA ST. 7 3.3 g

INTRODUCTION: 15378 is a glassy-matrix regolith breccia which is somewhat friable. It contains lithic clasts, including KREEP basalts, mineral fragments, and glass balls, shards, and lapilli. Apart from green glass, any mare component is inconspicuous. One large lithic clast is conspicuous (Fig. 1). The sample lacks zap pits and has slickensides on at least one side. It was collected as part of the rake sample from the north-east rim of Spur Crater.

PETROLOGY: Brief reports of the petrography of 15378 were made by Steele et al. (1972a, 1977), with microprobe analyses of minerals. The sample is a glassy, opaque breccia (Fig. 2). According to Steele et al. (1977) thin section ,2 consists of 20% glass, 5% lithic clasts, 30% mineral fragments, and 45% fine matrix, without porosity. However, thin section ,6 does appear to be porous (Fig. 2b). The sample contains several igneous-textured clasts, including KREEP basalts (for which mineral data are given by Steele et al., 1977), and fine-grained breccia fragments.

Plagioclase mineral clasts are calcic (An_{95-97}) with less than 0.2% Fe, indicating a non-mare source other than KREEP (Steele et al., 1972a). Pyroxene mineral data is diagrammed by Steele et al, 1972a) and is highland in origin. The mineral fragments in ,6 include opaque minerals.

The large lithic fragment conspicuous in Figure 1 consists of light brown, yellow, and white minerals, but does not occur in the thin sections. One red-brown fragment larger than 1 mm is visible macroscopically.

PROCESSING AND SUBDIVISIONS: ,1 was chipped from the parent, then subsplit into ,1 and ,2 (Fig. 3). From ,2 the three thin sections ,2; ,3; and ,6 were made, all general matrix. The large lithic fragment appears to remain both in ,0 (2.47 g) and in ,1, which was originally chipped to contain it.

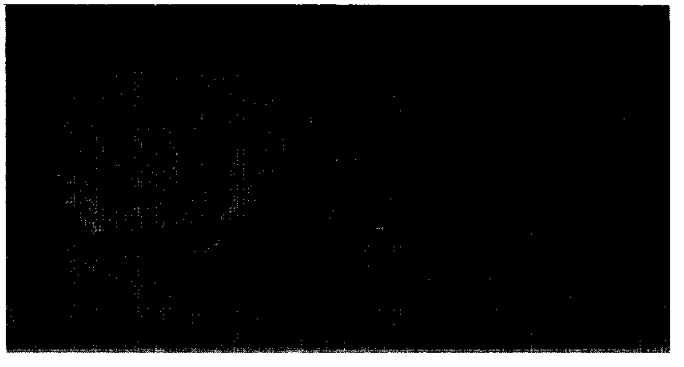

Figure 1. Macroscopic view of unprocessed sample, showing general dark matrix (right), and lithic clast (left). S-71-49078

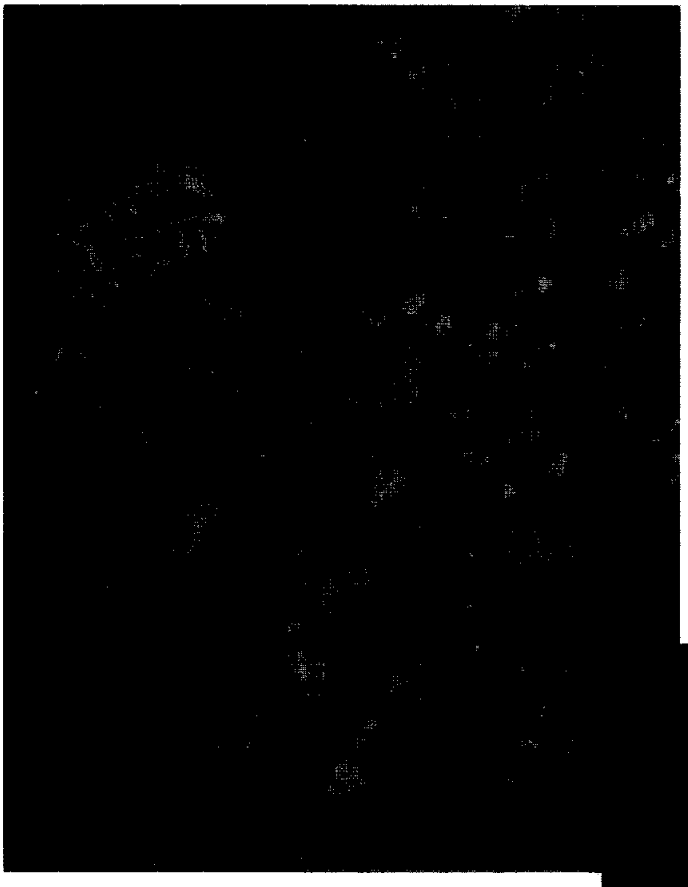

Fig. 2a

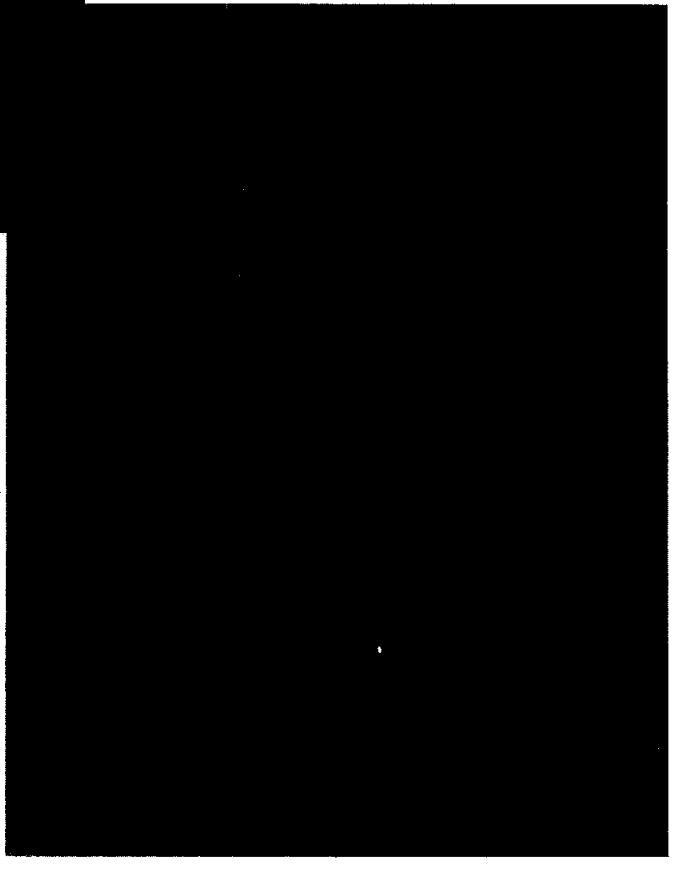

Fig. 2b

Figure 2. Photomicrographs of 15378,6. a) general matrix showing green glass balls, KREEP basalt (upper left), and glass lapilli (lower left) in an opaque matrix. Transmitted light. Width about 2 mm. b) reflected light view showing porosity of matrix, green glass ball, and lithic and mineral fragments. Width about 125 microns.

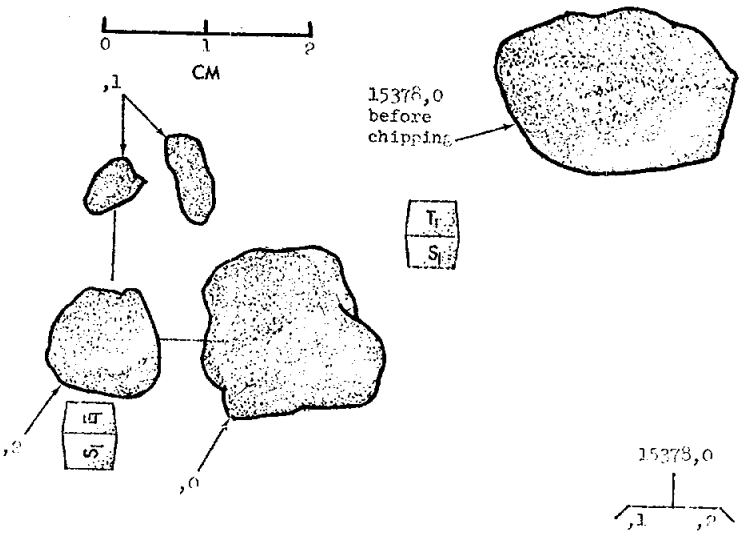

Figure 3. Chipping of 15378.

15379 FINE-GRAINED OLIVINE-NORMATIVE MARE BASALT ST. 7 64.3 g

INTRODUCTION: 15379 is a fine-grained olivine-normative basalt, with whole-rock Rb-Sr isotopic characteristics similar to other Apollo 15 mare basalts. It is highly shocked, with glass veins, and is friable as a result. It was collected as part of the rake sample from the north-east rim of Spur Crater. Its surface was very dusty and appeared to have no zap pits (Fig. 1).

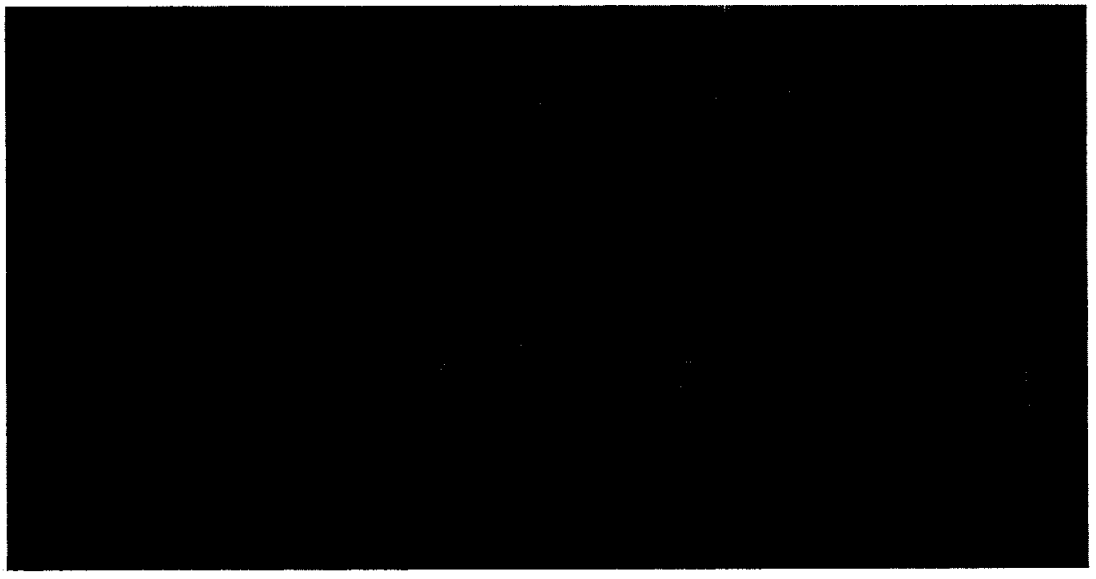

Figure 1. Macroscopic view of original sample 15379,0, mainly dust-covered. S-71-49170

PETROLOGY: 15379 is a fine-grained mare basalt (Fig. 2a) containing about 20% stubby-angular, and partly "hollow" plagioclase, abundant brownish pyroxene, and at least some olivine. According to Papanastassiou and Wasserburg (1973) the opaque phase is ilmenite. In the thin sections, all from a single chip, the basalt is heavily shocked. The plagioclase is milky under binoculars rather than translucent; it is not maskelynitized but its twins are deformed. The pyroxene is very shattered and much has closely-spaced deformation lamellae. Analyses of mafic minerals were diagrammed by Steele et al. (1972a) (Fig. 3).

The rock has crosscutting veins of an opaque glass (Fig. 2b), and pods of bubble-containing glass are present (Papanastassiou and Wasserburg, 1973). The glass shows evidence of flow and contains partly-assimilated crystals, and is probably melted rock, not foreign material.

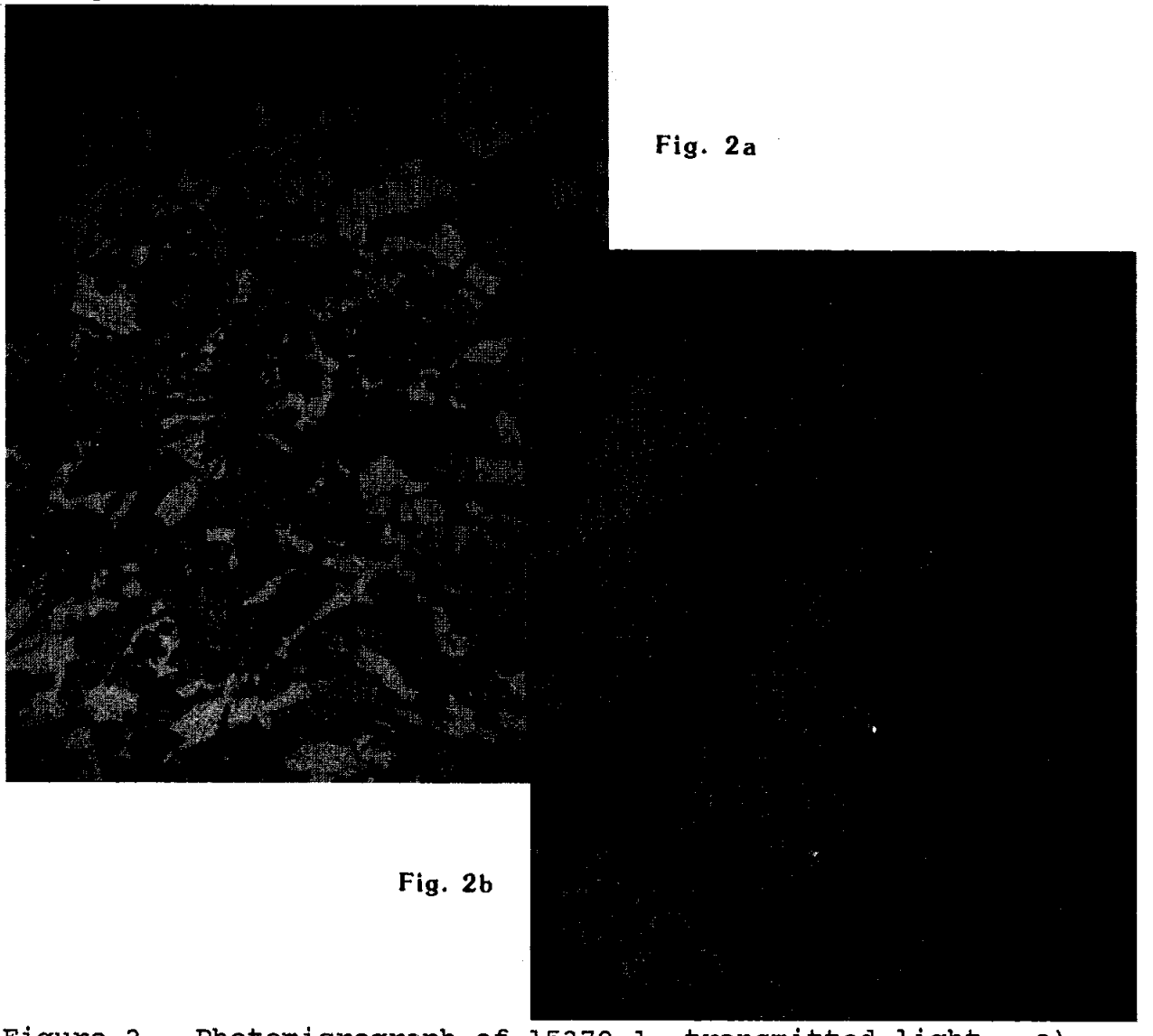

Fig. 2a

Fig. 2b

Figure 2. Photomicrograph of 15379,1, transmitted light. a) general view; width about 2 mm. b) opaque glass injected veins cutting and surrounding mineral grains; width about 300 microns.

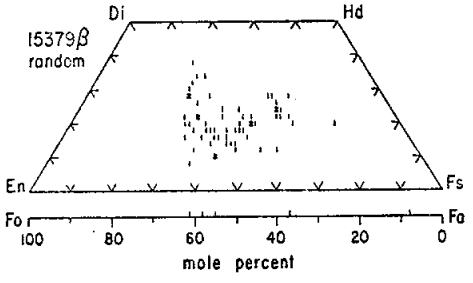

Figure 3. Composition of pyroxenes and olivines in 15379 (Steele et al., 1972a).

TABLE 15379-1. Chemical analyses

		,2	,3	,5	,5	,0
Wt %	SiO2	44.60				
	TiO2	2.51	2.3	2.29		
	Al2O3	8.27	9.3			
	FeO	22.9	22.6			
	MgO	10.75	10	8.6		
	CaO	9.55	9.1			
	Na2O	0.27	0.278	0.26		
	K2O	0.06	0.049	0.050		0.048
	P2O5	0.12				
(ppm)	Sc	38	42			
	V	250	220			
	Cr	4380	4060			
	Mn	2250	2085			
	Co	67	49			
	Ni	120				
	Rb	<1		0.827	0.836	
	Sr	130		98.5	97.4	
	Y	28				
	Zr	74	<190	86.3		
	Nb	12				
	Hf		3.1	2.2		
	Ba	70	60	51.5		
	Th					0.49
	U			0.133		0.15
	Pb					
	La	<10	4.9	5.64		
	Ce		14	14.6		
	Pr					
	Nd			10.3		
	Sm		3.6	3.18		
	Eu		0.93	0.980		
	Gd			3.67		
	Tb		0.7			
	Dy		4.7	4.42		
	Ho					
	Er			2.92		
	Tm					
	Yb	4.3	2.3	2.11		
	Lu		0.33	0.304		
	Li	6.9		8.1		
	Be	<1				
	B					
	C					
	N					
	S					
	F					
	Cl					
	Br					
	Cu	17				
	Zn					
(ppb)	I					
	At					
	Ga	4700				
	Ge					
	As					
	Se					
	Mo					
	Tc					
	Ru					
	Rh					
	Pd					
	Ag					
	Cd					
	In					
	Sn					
	Sb					
	Te					
	Cs					
	Ta		400			
	W					
	Re					
	Os					
	Ir					
	Pt					
	Au					
	Hg					
	Tl					
	Bi					
		(1)	(2)	(3)	(4)	(5)

References and Methods:

(1) Christian et al. (1972), Cuttitta et al. (1973); XRF, semi-micro chem., opt. em. spec.
(2) Laul and Schmitt (1973); INAA
(3) Church et al. (1972), Nyquist et al. (1972, 1973), Weismann and Hubbard (1975); isotope dilution, mass spec.
(4) Papanastassiou and Wasserburg (1973); isotope dilution, mass spec.
(5) O'Kelley et al. (1972); gamma ray spectroscopy

CHEMISTRY: Chemical analyses are listed in Table 1 and the rare earths are plotted in Figure 4. The analyses are quite consistent and demonstrate that the sample is an intermediate member of the olivine-normative mare basalt group. Christian et al. (1972) and Cuttitta et al. (1973) listed an excess reducing capacity of +0.58, and analyzed for, and found no, Fe_2O_3. The Cu data is listed in Cuttitta et al. (1973) as 0.17 ppm instead of 17 ppm.

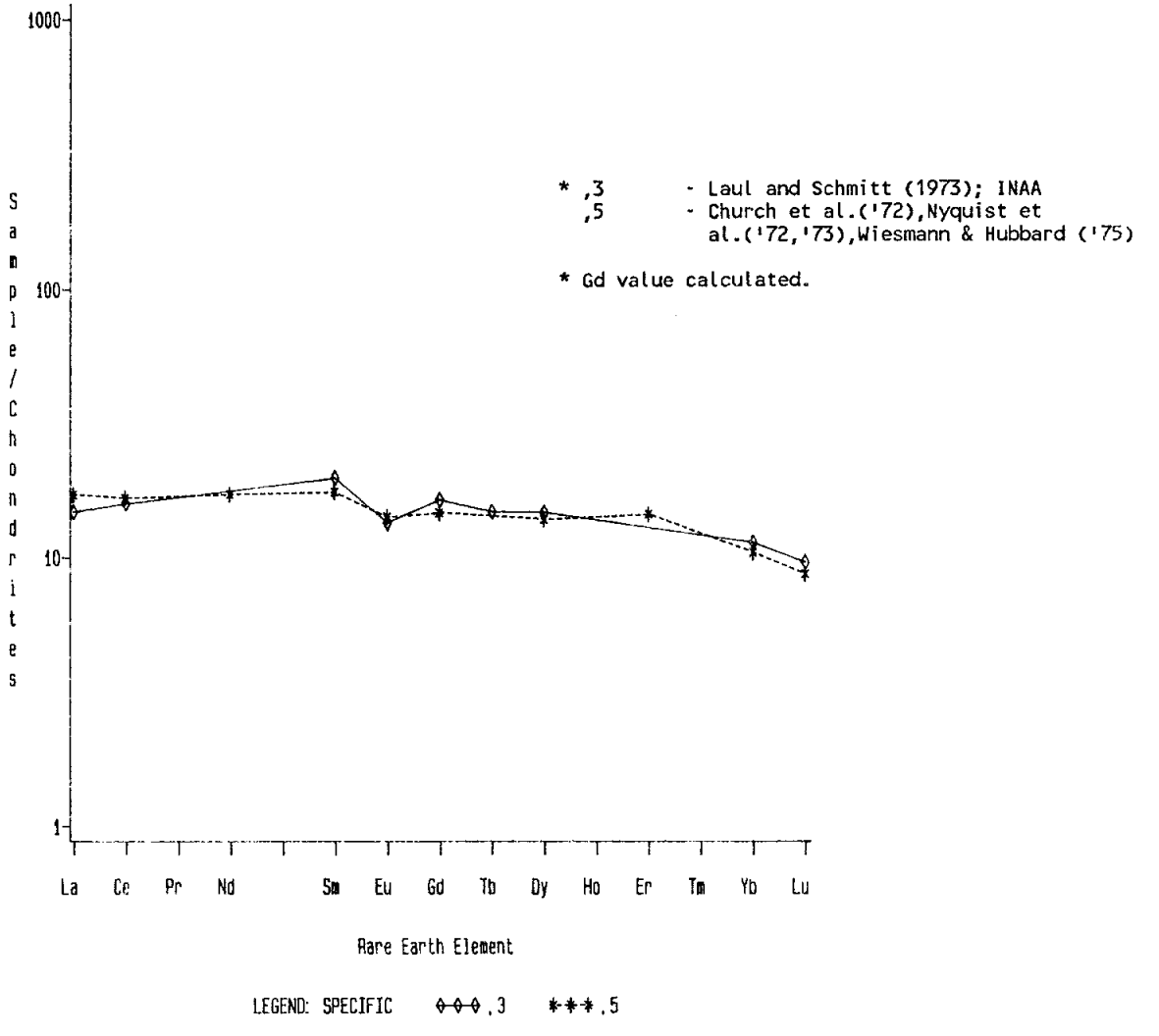

Figure 4. Rare earths in 15379.

RADIOGENIC ISOTOPES: Nyquist et al. (1972, 1973) and Papanastassiou and Wasserburg (1973) reported Rb-Sr isotopic data on aliquots of the same solution of a whole rock sample split from ,5 (Table 2). These data show that the sample must be similar in both age and initial Sr isotopic ratio to other Apollo 15 mare basalts.

TABLE 15379-2. Rb-Sr isotopic data for aliquots of 15379,5 (total rock)

Rb (ppm)	Sr (ppm)	$^{87}Rb/^{86}Sr$	$^{87}Sr/^{86}Sr$	T_{BABI}	Reference
0.827	98.5	0.0243±7	0.70057±11	4.21 b.y.	Nyquist et al. (1972, 1973)
0.836	97.4	0.02486±10	0.70048±5	4.23 b.y.	Papanastassiou and Wasserburg (1973)

EXPOSURE: Eldridge et al. (1972) reported cosmogenic nuclide disintegration data for ^{22}Na, ^{26}Al, and ^{54}Mn. The ^{26}Al data suggest that 15379 was ejected and exposed only 0.8 to 1.3 m.y. ago.

PROCESSING AND SUBDIVISIONS: A few pieces were chipped off from ,0 (Fig. 5) and all further subdivisions made from them. ,0 now is 58.6 g. Three thin sections (,1; ,6; and ,7) were made from ,1, with the potted butt numbered ,12.

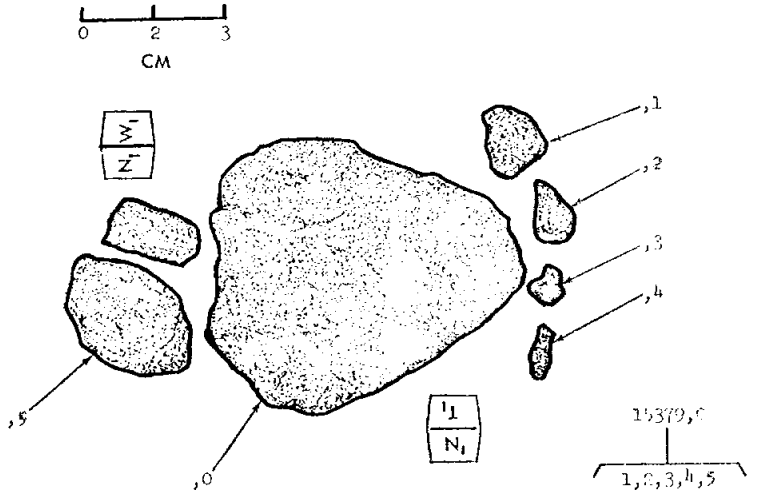

Figure 5. Chipping of 15379.

15380 FINE-GRAINED OLIVINE-NORMATIVE MARE BASALT ST. 7 5.2 g

INTRODUCTION: 15380 is a fine-grained olivine-normative basalt (Fig. 1). It is shocked, with glass veins, and is petrographically and chemically very similar to shocked basalt 15379. It was originally dust-covered except for one freshly-fractured face, and was quite probably a part of 15379 prior to collection. It was collected as part of the rake sample from the north-east rim of Spur Crater.

Figure 1. Macroscopic view of dust-covered 15380, pre-splitting. S-71-49038

PETROLOGY: 15380 is an olivine-bearing mare basalt and appears very similar to 15379 in grain size, texture, and shock features (Fig. 2). It consists of about 20% stubby, angular, and partly "hollow" plagioclases, abundant brownish pyroxenes, and at least some olivines, which are generally equant. The basalt is heavily shocked, with deformation lamellae in mineral grains, cross-cutting fractures along which slip has taken place (visible in Figs. 2a, b), and veins of opaque glass (Fig. 2b). The opaque phases include chromite and ilmenite, and some cristobalite is present.

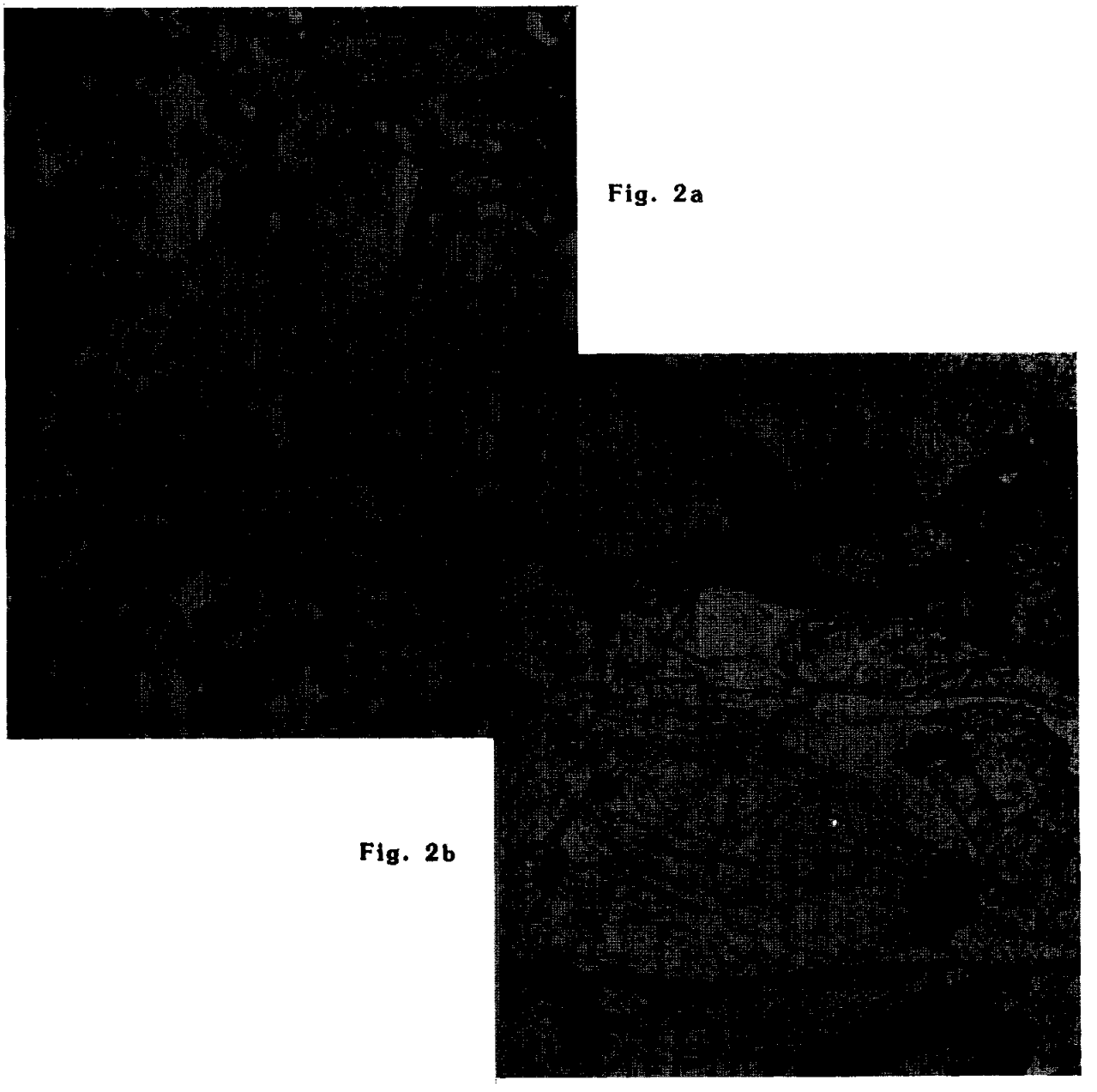

Fig. 2a

Fig. 2b

Figure 2. Transmitted light photomicrographs of 15380,3. a) general view, width about 2 mm. Microfaults, partly glass lined, are visible in lower center, showing offsets. b) glass veins surrounding offset portion of basalt, width about 300 microns.

TABLE 15380-1.
Chemical analyses

		,2
Wt %	SiO2	46.1
	TiO2	2.55
	Al2O3	8.33
	FeO	22.8
	MgO	10.2
	CaO	9.85
	Na2O	0.258
	K2O	0.057
	P2O5	
(ppm)	Sc	44
	V	
	Cr	4600
	Mn	2170
	Co	49
	Ni	
	Rb	<0.9
	Sr	
	Y	
	Zr	
	Nb	
	Hf	2.1
	Ba	
	Th	
	U	
	Pb	
	La	4.21
	Ce	11.2
	Pr	
	Nd	9.1
	Sm	3.14
	Eu	0.81
	Gd	4.1
	Tb	0.69
	Dy	4.65
	Ho	0.93
	Er	2.6
	Tm	
	Yb	2.05
	Lu	0.279
	Li	
	Be	
	B	
	C	
	N	
	S	
	F	
	Cl	
	Br	
	Cu	
	Zn	3±2
(ppb)	I	
	At	
	Ga	3500
	Ge	
	As	
	Se	
	Mo	
	Tc	
	Ru	
	Rh	
	Pd	
	Ag	
	Cd	
	In	
	Sn	
	Sb	
	Te	
	Cs	43
	Ta	
	W	
	Re	
	Os	
	Ir	
	Pt	
	Au	
	Hg	
	Tl	
	Bi	
		(1)

Reference and method:

(1) Helmke et al. (1973); atomic absorption, INAA

CHEMISTRY: The single analysis of 15380 (Table 1) shows it to be an olivine-normative mare basalt. The analysis is almost identical with that of the texturally-similar 15379, except that the rare earths in 15380 (Fig. 3) are a little lower. The sample appears to be an intermediate member of the olivine-normative suite. The silica abundance (Table 1) seems to be a little high.

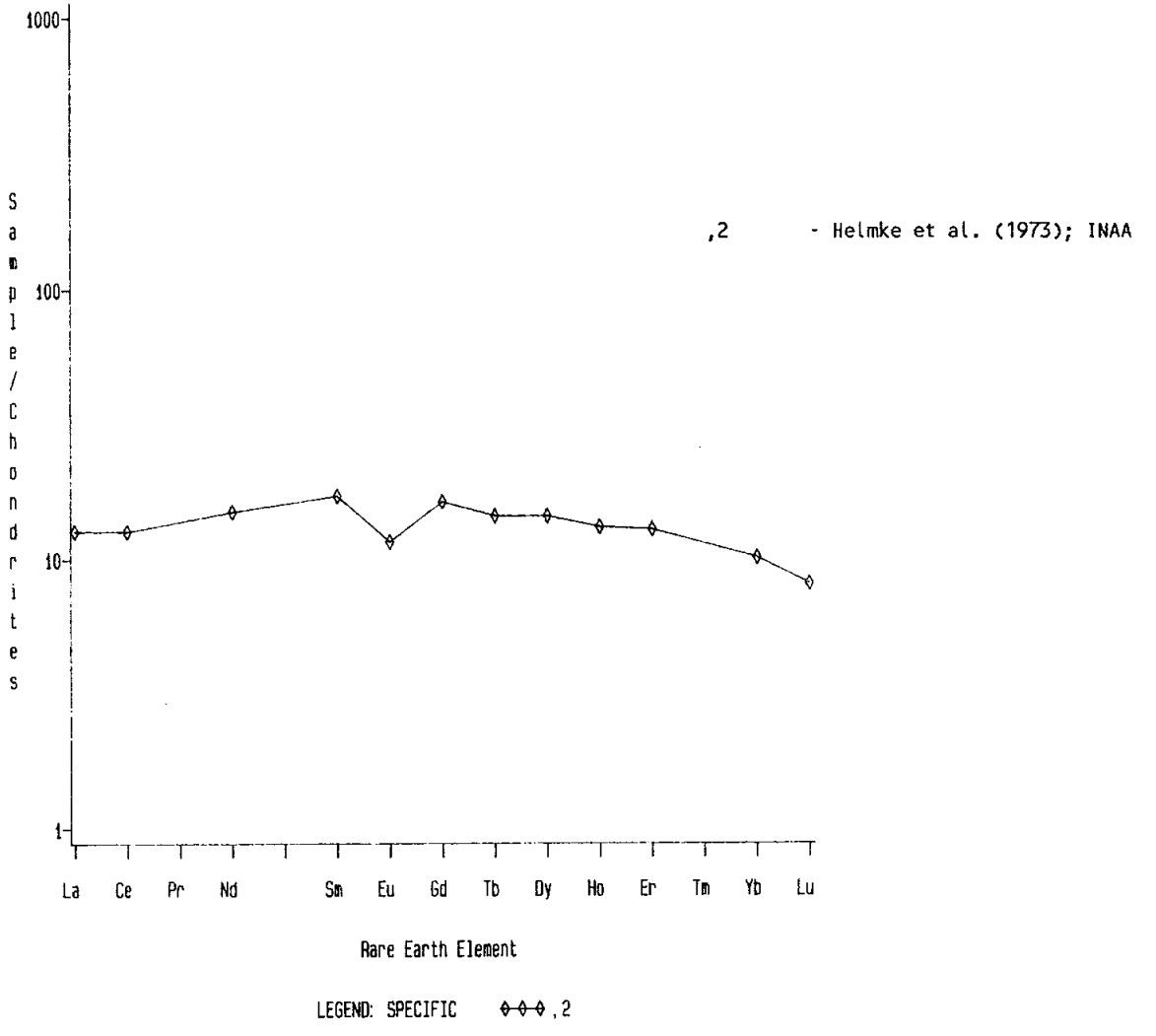

Figure 3. Rare earths in 15380,2.

PROCESSING AND SUBDIVISIONS: 15380 was substantially chipped (Fig. 4). ,0 is now 4.13 g. ,2 was used for the chemical analysis, and ,3 was made into thin sections ,3; ,4; and ,8 (potted butt ,12 remaining).

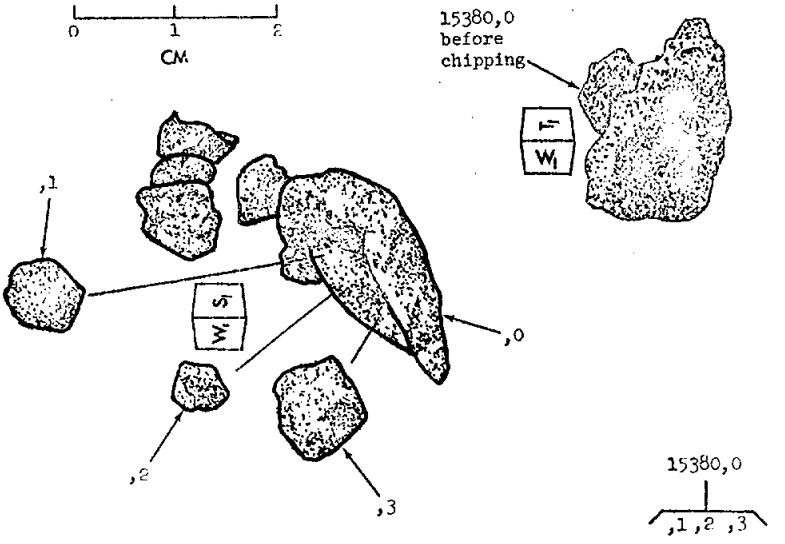

B_1 WORK ORIENTATION (LRL "MUG" PHOTOGRAPHY)

Figure 4. Chipping of 15380.

15381 FINE-GRAINED (OLIVINE-NORMATIVE MARE?) BASALT ST. 7 0.3 g

INTRODUCTION: 15381 is a small fragment of a fine-grained basalt macroscopically similar to olivine-normative mare basalts (Fig. 1). It is dust-covered. It was collected as part of the rake sample from the north-east rim of Spur Crater. It has never been subdivided or allocated.

Figure 1. Macroscopic view of 15381. S-71-49056

15382 KREEP BASALT ST. 7 3.2 g

INTRODUCTION: 15382 (Fig. 1) is a fragment of pristine (volcanic) basalt with KREEP rare-earth element abundances and patterns. It is finer-grained than the otherwise-similar 15386. Like other KREEP basalts, it is older (~3.9 b.y.), more feldspathic, and more alkaline than Apollo 15 mare basalts. It is an angular, tough sample, collected as part of the rake sample from the north-east rim of Spur Crater.

Figure 1. Pre-split view of 15382. Scale in centimeters. S-72-32747

PETROLOGY: 15382 is different from other volcanic rock samples at the Apollo 15 site except 15386, but it is typical of many even-smaller-particles found in Apennine Front materials, mare plains regolith samples, and breccias 15405 and 15205. It has a clast-free, basaltic texture (Simonds et al., 1975). It has been described, and had mineral and bulk (defocussed beam microprobe) analyses reported by Dowty et al. (1973b, 1976), Crawford and Hollister (1977), and Hollister and Crawford (1977). Microprobe mineral and glass analyses were also reported by Hlava et al. (1973), and opaque mineral data were presented and discussed by Nehru et al. (1973, 1974).

According to Dowty et al. (1973b, 1976), 15382 consists of 4% silica phase, 49% plagioclase, 34% pyroxene, 5% opaque minerals, and 8% miscellaneous (mainly mesostasis). Crawford and Hollister (1977) found only 32.9% plagioclase and 41.9% pyroxene. The mesostasis areas contain cristobalite, ilmenite, glass, phosphates (whitlockite and apatite), tranquillityite, armalcolite, and baddeleyite. Olivine is not present. The texture is intergranular to subophitic with plagioclase laths ~0.2 x 0.8 mm, often curved in the manner apparently confined to this type of basalt, and forming an interlocking mass (Fig. 2). The sample is finer-grained than 15386, and appears to have crystallized by single-stage, rapid cooling.

Figure 2. Portion of thin section 15382,6. Transmitted light. Width about 2.7 mm. S-79-27741

Pyroxene compositions form a smooth trend from high-Mg, low Ca cores to pigeonite rims, with some subcalcic augite (<10%) (Fig. 3). The cores are orthopyroxene with up to 4% Al_2O_3. The orthopyroxene to pigeonite transition is sharp, and some cores are euhedral (Crawford and Hollister, 1977). Plagioclases are generally zoned from An_{86} to An_{80}, although Dowty et al. (1976) reported that a few plagioclase cores are as calcic as An_{95} (Fig. 4). FeO increases from 0.25 in the center to 0.5% at the edge (Dowty et al., 1976) (see also Fig. 5). Glass inclusions in the rims of plagioclase are unique (Crawford and Hollister, 1977).

Nehru et al. (1973, 1974) found that chromite is generally absent and that the dominant opaque phases are ulvospinel and ilmenite, dominantly in mesostasis areas. A few chromite cores do occur in ulvospinel, which is high in Cr and low in Al. Ilmenite has low MgO (1-3%). The rare metal phase contains less than 1% Ni. Engelhardt (1979) tabulated ilmenite paragenesis.

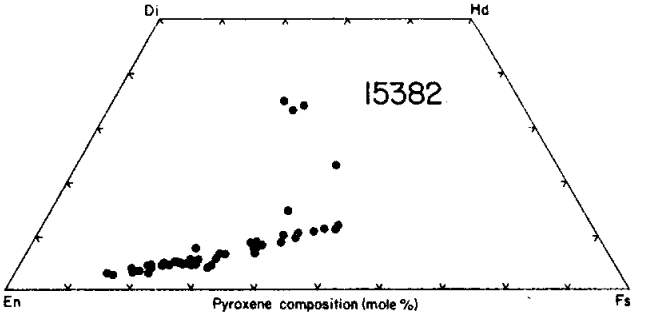

Figure 3. Compositions of pyroxenes in 15382 (Dowty et al., 1976).

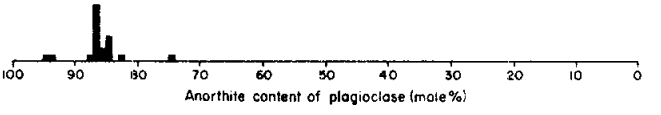

Figure 4. Compositions of plagioclases in 15382 (Dowty et al., 1976).

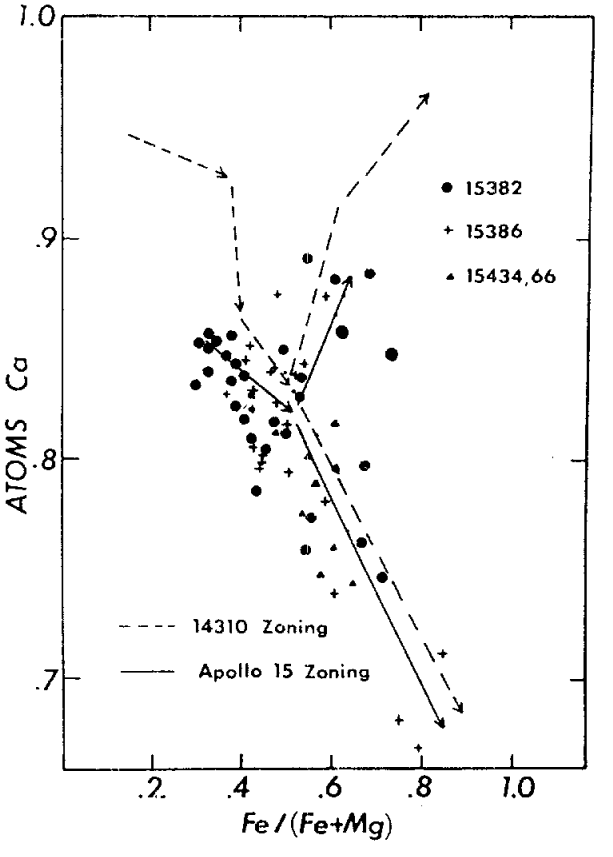

Figure 5. Compositions of plagioclases in 15382 (Crawford and Hollister, 1977).

Crawford and Hollister (1977) and Hollister and Crawford (1977) both described and discussed silicate liquid immiscibility in 15382. They suggested that an Fe-rich melt separated early in crystallization, after formation of core orthopyroxenes and plagioclases, i.e., after only about 20% crystallization. To reach the proposed field of immiscibility plagioclase must have crystallized alone early, a process inconsistent with the textural and compositional evidence for a cotectic melt. Hence, Hollister and Crawford (1977) propose a disequilibrium process. They relate the immiscible Fe-rich melt to mare basalts. Because these authors believed that rock 14310, a KREEP basalt, is volcanic, they suggested that 15382 experienced metal loss in an earlier stage of fractionation to reduce the siderophile content, and that the magma for 15382 rose more slowly to the surface such that evidence for high pressure minerals (as they claimed for 14310) was erased. This view is not widely held; rather, the low siderophiles are generally considered indigenous and the high siderophiles in 14310 considered to be meteoritic contamination.

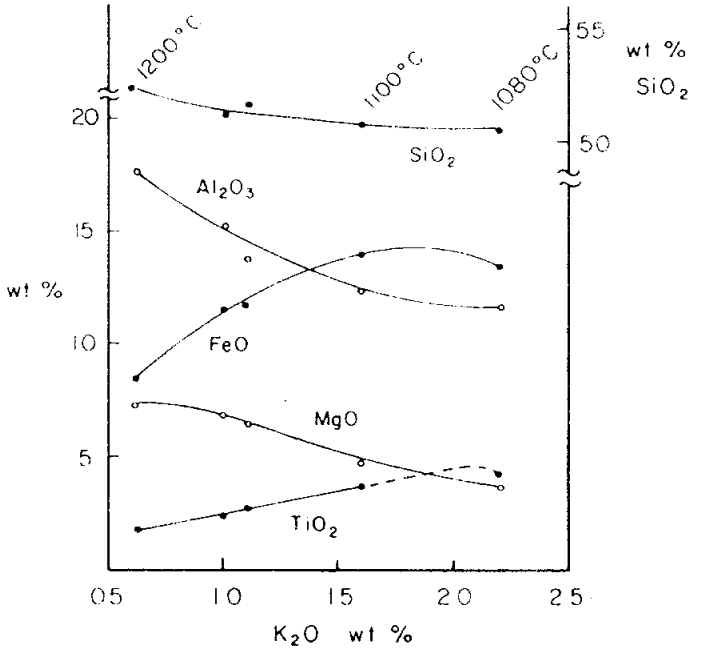

Figure 6. Liquid line of descent for 15382, experimental data (Hess et al., 1978). All liquids below 1180°C coexist with low-Ca px and plag. Ilmenite crystallizes between 1100°C and 1080°C. Immiscible liquids occur at 1035°C.

TABLE 15382-1. Chemical analyses

		,9	,0	,14	,15	a	b	,9	,14	,14b
Wt %	SiO_2									
	TiO_2	2.17		2.2						
	Al_2O_3	14.9		16.4						
	FeO	9.2		10.0						
	MgO	7.4		9.8						
	CaO	7.1		10.4				7.1		
	Na_2O	0.85		0.81						
	K_2O	0.632	0.59	0.53				0.38	0.550	
	P_2O_5									
(ppm)	Sc			19.0						
	V			60						
	Cr			2120						
	Mn			1110						
	Co			17						
	Ni			28	18					
	Rb	16.1			16.0				14.1	
	Sr	195							183	
	Y									
	Zr	1170		966						
	Nb									
	Hf	32.7		27						
	Ba	793		610						
	Th		10.5	1.0a						
	U	3.72	3.1		3.3					5.94
	Pb									
	La	79.5		68.1						
	Ce	212		218						
	Pr									
	Nd	127				111.8	107.2			
	Sm	35.2		29.7		31.06	29.84			
	Eu	2.77		2.72						
	Gd	42.9								
	Tb			6.2						
	Dy	45.7		40						
	Ho									
	Er	28.1								
	Tm									
	Yb	24.0		19.2						
	Lu	3.43		2.70						
	Li									
	Be									
	B									
	C									
	N									
	S									
	F									
	Cl									
	Br				0.142					
	Cu									
	Zn				2.6					
(ppb)	I									
	At									
	Ga									
	Ge				47.1					
	As									
	Se				72					
	Mo									
	Tc									
	Ru									
	Rh									
	Pd				⩽0.6					
	Ag				0.44					
	Cd				86.6					
	In				2.66					
	Sn									
	Sb				0.17					
	Te				1.0					
	Cs				725					
	Ta			3100						
	W									
	Re				0.0089					
	Os				0.018					
	Ir				0.0132					
	Pt									
	Au				0.0033					
	Hg									
	Tl				3.2					
	Bi				0.29					
		(1)	(2)	(3)	(4)	(5)	(5)	(6)	(7)	(8)

References for Table 15382-1

References and methods:

(1) Hubbard et al. (1973), Nyquist et al. (1972, 1973), Church et al. (1972); isotope dilution mass spec, colorimetry, AA.
(2) Schonfeld et al. (1972), O'Kelley et al. (1976); gamma ray spec.
(3) Murali et al. (1977); INAA.
(4) Gros et al. (1976); RNAA.
(5) Lugmair and Carlson (1978); isotope dilution, mass spec.
(6) Stettler et al. (1973); Ar, irradiation.
(7) Papanastassiou and Wasserburg (1976); isotope dilution, mass spec.
(8) Papanastassiou and Waserburg (1977), Tera and Wasserburg (1976); isotope dilution, mass spec., abundance calculated by summing 208, 207, and 206 proportions given.

Notes:

(a) appears to be typographical error.
(b) erroneously listed as ,114 by Tera and Wasserburg (1976).

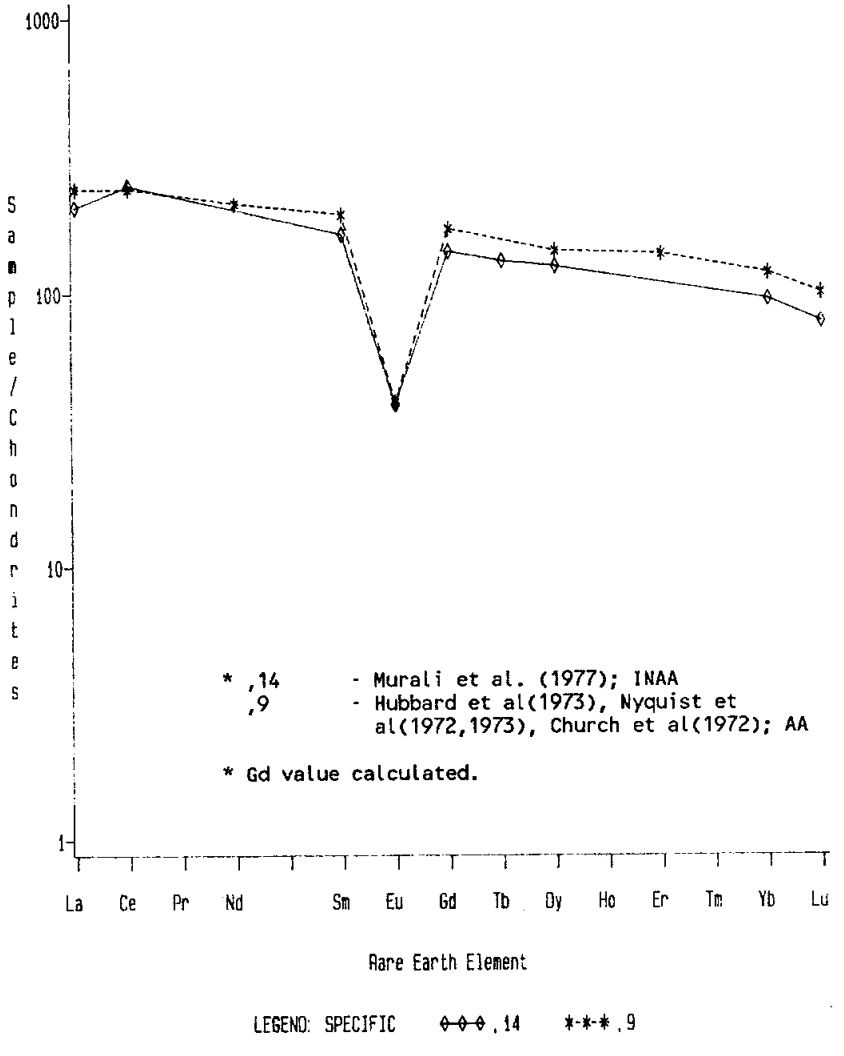

Figure 7. Rare earth element data for 15382.

Hess et al. (1978) conducted equilibrium and controlled cooling experiments on the composition for 15382 determined by Dowty et al. (1976). This analysis is more aluminous than the more conventional analyses (Table 1), but preliminary experiments on that composition yielded similar results. The liquid line of descent is shown as Figure 6; the data is tabulated in Hess et al. (1978). The basalt is saturated at the liquidus (1180-1185°C) with both plagioclase (An_{86}) and pyroxene ($En_{76}Wo_5$). The pyroxene is more evolved (Al-poorer, Ca-richer, Mg-poorer) than observed in the basalt itself. The high-Al pyroxene and the An_{95} grain of Dowty et al. (1976) may then be relics of an earlier magma stage. Ilmenite crystallizes between 1100 and 1080°C, and silicate liquid immiscibility takes place at 1035°C. The liquid line of descent is one of iron enrichment and not silica enrichment, toward a ferrobasaltic composition, and not toward the silica-pyroxene-plagioclase eutectic. A granitic to monzodiorite composition is produced by silicate liquid immiscibility.

CHEMISTRY: Chemical analyses are listed in Table 1, and rare earths are plotted in Figure 7. Two microprobe defocussed beam analyses are listed separately in Table 2. The analyses are in general agreement, and distinguish 15382 from mare basalts, regolith breccias, and anorthosites. The major element chemistry is that of a cotectic (plag + low-Ca px) basalt. The incompatible abundances and patterns are those of KREEP. Gros et al. (1976) note that volcanic KREEP, as shown by 15386, does not have intrinsically high siderophiles such as had been claimed by some authors for KREEP sample 14310.

TABLE 15382-2. Microprobe defocussed beam analyses

	,7[a]	,6,7,17[b]
SiO2	52.4	52.53
TiO2	1.78	1.29
Al2O3	17.8	18.44
Cr2O3	0.21	----
FeO	8.6	8.27
MnO	0.10	----
MgO	7.1	7.01
CaO	9.9	10.30
Na2O	0.96	----
K2O	0.57	0.46
P2O5	0.55	----
	99.97	98.3

(a) Dowty et al. (1973b, 1976)
(b) Hollister and Crawford (1977)

RADIOGENIC ISOTOPES AND GEOCHRONOLOGY: Rb-Sr isotopic data for whole-rock samples was reported by Nyquist et al. (1972, 1973) and Papanastassiou and Wasserburg (1976a, b) (Table 3), without specific comment. Papanastassiou and Wasserburg (1976b) determined a Rb-Sr isochron which yielded an age of 3.90 ± 0.02 b.y. with an initial $^{87}Sr/^{86}Sr$ of 0.700241; the data on which this is based has not been published. This age and initial Sr (corrected for interlaboratory bias) are identical with those determined for 15386 by Nyquist et al. (1975).

TABLE 15382-3. Rb-Sr whole rock isotopic data

Rb	Sr	$^{87}Rb/^{86}Sr$	$^{87}Sr/^{86}Rb$	T_{BABI}	Reference
16.1	195	0.240	0.71383±6	4.29	Nyquist et al. (1973)
14.1	183	0.2228	0.71266±6	4.29	Papanastassiou and Wasserburg (1976)

$\lambda = 1.39 \times 10^{-11}$ yr-1

Lugmair et al. (1976) discussed results for Sm-Nd whole rock data for 15386,14,9002, showing the evolution of ^{143}Nd (ϵ) against time. The data define an intercept with a lunar "chondritic" evolution (represented by rock 15555, which is no longer preferred for such a purpose) at 4.72 ± 0.1 b.y., which requires a two-stage evolution. The data conflict with models relating KREEP to the source materials of mare basalts. Lugmair and Marti (1975) and Lugmair and Carlson (1978) reported whole rock Sm-Nd isotopic data for two small aliquots of ,14,9002 (Table 4). It is not stated whether the data discussed in Lugmair et al. (1976) is any or all of the data subsequently reported. The data are very similar to all other KREEP samples (e.g., Figure 8) in both Sm/Nd and isotopic ratios, which indicate a moonwide process to make KREEP at 4.36 ± 0.06 b.y. (T_{ICE} ages). The specific T_{ICE} ages for 15382 are given in Table 4. The data in this case are referred not to 15555 but to the meteorite Juvinas, yielding T_{ICE} (at which the intercept with chondritic evolution defined by Juvinas occurs). In the T_{JUV} age, the initial $^{143}Nd/^{144}Nd$ of Juvinas is used in a fashion similar to BABI in the Rb-Sr system, and this model age has less physical reality than T_{ICE}.

TABLE 15382-4. Sm-Nd whole rock isotopic data (Lugmair and Carlson, 1978)

	Sm ppm	Nd ppm	$^{147}Sm/^{144}Nd$	$^{147}Nd/^{144}Nd$	T_{ICE}	T_{JUV}
a	31.06	111.8	.1679	.511889±21	4.38±.14	4.59±.02
b	29.84	107.2	.1683	.511894±16	4.42±.11	4.58±.02

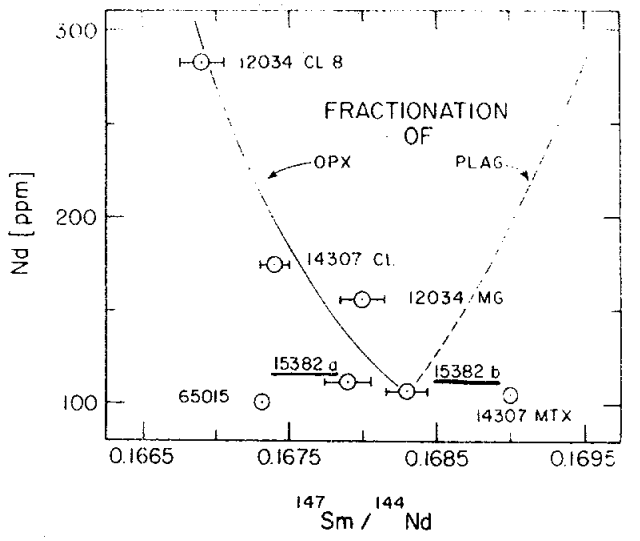

Figure 8. Sm-Nd isotopic data for whole rock samples (Lugmair and Carlson, 1978).

Stettler et al. (1973) and Turner (1973) reported similar ^{40}Ar-^{39}Ar plateau ages of 3.90 ± 0.05 b.y. and 3.91 ± 0.04 b.y. respectively (Fig. 9), based on intermediate temperature plateaus. Turner et al. (1973) reported a 26% Ar loss, which does not allow a well-defined K-Ar age.

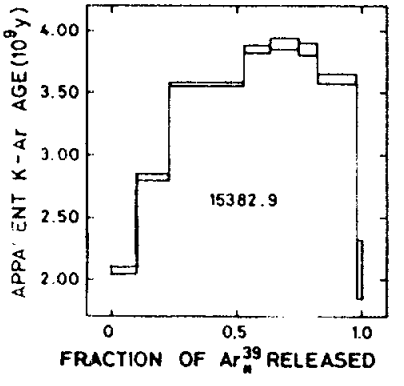

Fig. 9a

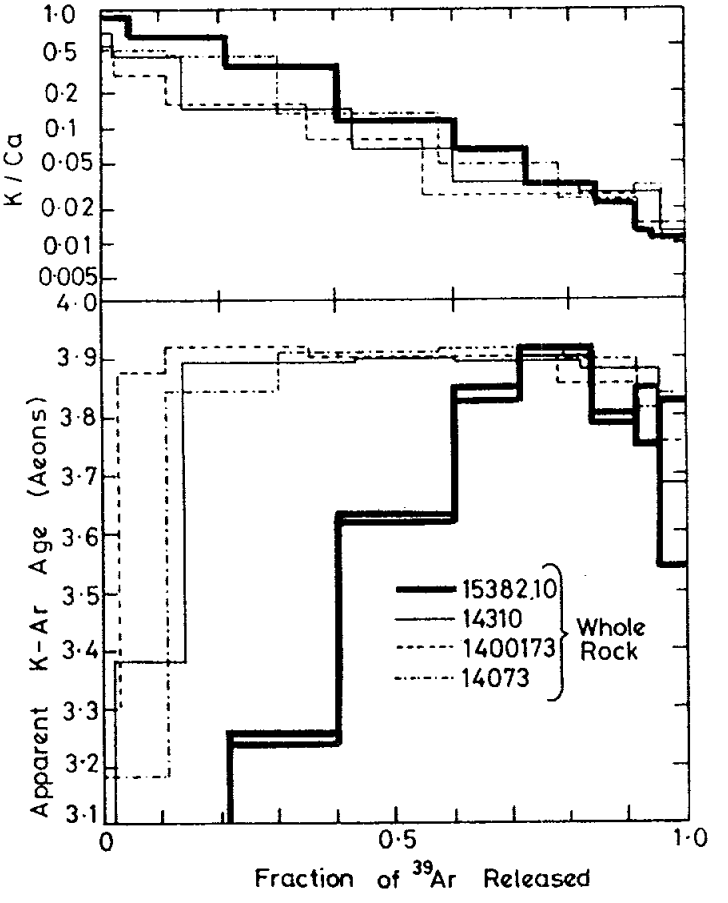

Fig. 9b

Figure 9. ^{40}Ar-^{39}Ar release diagrams for 15382 whole rock samples. a) Stettler et al., 1973. b) Turner et al., 1973.

Tera and Wasserburg (1976) reported whole rock Pb isotopic data without comment, (,14, erroneously listed as ,114), and Papanastassiou and Wasserburg (1976) reported the same data plus data for plagioclase. The data are nearly concordant at 4.38 b.y. Assuming the crystallization age of 3.90 ± 0.02 b.y. also gives an upper intersection of about 4.4 b.y. The plagioclase is highly radiogenic and has $^{207}Pb/^{206}Pb$ nearly identical to that of the total rock because quintessence (mesostasis) dominates both samples.

Haines and Weiss (1978) reported fission track data for a subsample of ,14. The average track retention age is 3.2 ± 0.3 b.y., significantly lower than the ^{40}Ar-^{39}Ar and Rb-Sr ages for this sample. The data are consistent with either complete erasure of tracks at 3.2 b.y. (which seems more likely to the authors on thermal grounds) or later partial erasure from a lower temperature event.

RARE GAS AND EXPOSURE: Stettler et al. (1973) and Turner et al. (1973) report ^{38}Ar exposure ages of 230 and 240 m.y. respectively. O'Kelley et al. (1976) reported ^{26}Al values consistent with saturation, indicating exposure to cosmic rays for at least two million years or so.

PROCESSING AND SUBDIVISIONS: A slab was originally cut from this very small sample (Fig. 10). ,2 was made into a potted butt and entirely used for the only thin sections ,6; ,7; and ,17. ,1 is 0.27 g. ,0 was subsequently subdivided to leave mainly ,11 (0.68 g chips and fines) and ,12 (0.81 g chip), with ,14 allocated for P.I. subdivisions.

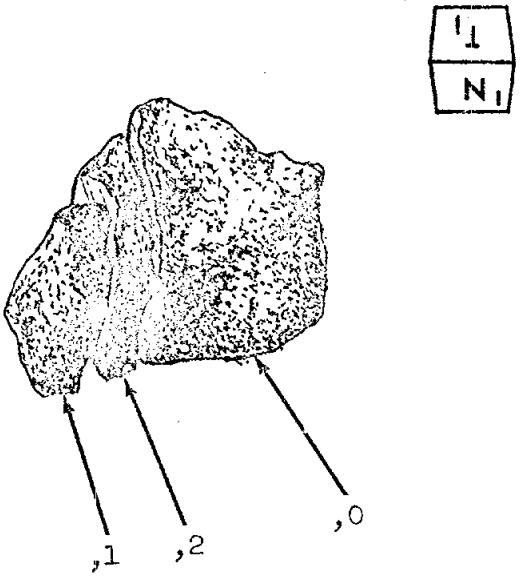

Figure 10. 1971 cutting diagram of completed sawing of 15382.

15383 GLASS WITH MONOMICT (BASALT) CLAST ASSEMBLAGE 1.4 g

INTRODUCTION: 15383 is a distinct, coherent rock. It consists of a matrix of a single, shock-produced glass with rounded fragments of a single rock type, apparently a basalt. Macroscopically the basalt is similar to mare basalts, but appears thoroughly microfractured. 15383 is partly caked with dust and is subangular (Fig. 1). Its surface has no zap pits. It was collected as part of the rake sample from the north-east rim of Spur Crater.

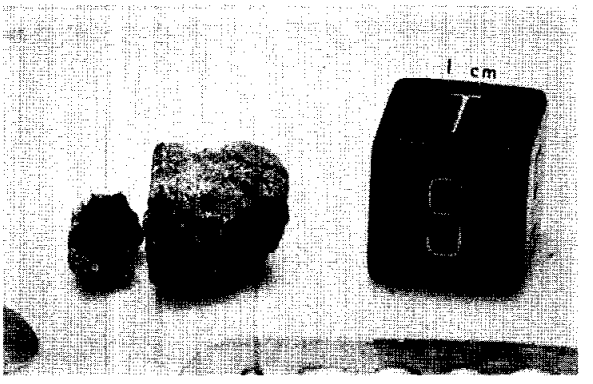

Figure 1. Post-sawing view of ,1 (left) and ,0. S-71-59122

PETROLOGY: About half of 15383 consists of a very pale-brown, clear, continuous glass (Fig. 2), containing lithic relics. These relics are all rounded, indicating submersion in a very hot glass, suggesting shock production of the glass. Further, the relics all contain deformation features, such as kinked twin lamellae and strains. The original mineralogy was pyroxene-rich and appears to have been a mare-basalt of some kind. Plagioclases formed stubby to lathy, angular, in some places hollow grains (Fig. 2). Other phases present include chromite, ilmenite, and "sieved" fayalite. The pyroxene is unexsolved. Most of the rounded relics are less than half a millimeter across, but they include examples up to 2 millimeters or so.

Fig. 2a

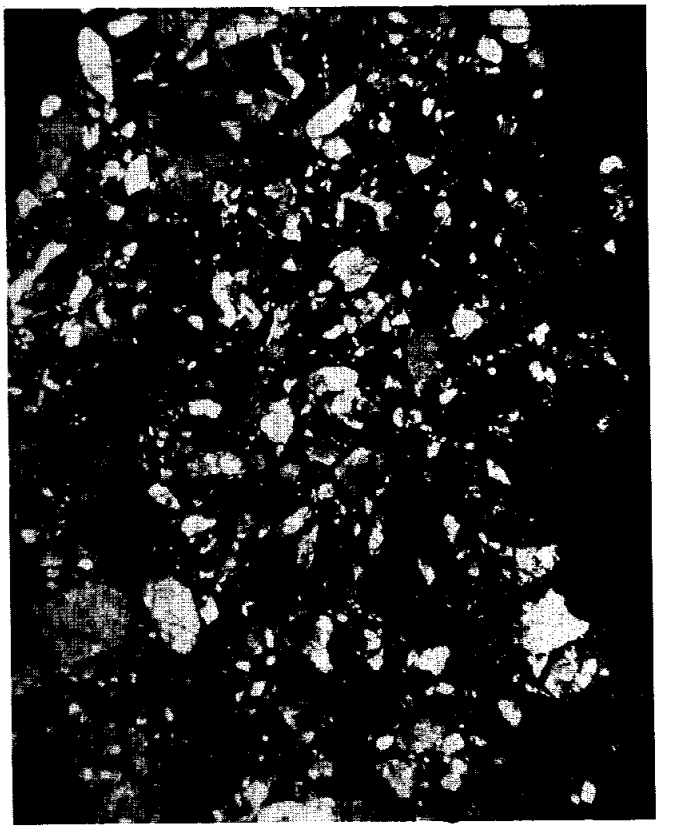

Fig. 2b

Fig. 2c

Figure 2. Photomicrographs of 15383,7. a) general view showing rounded fragments. Transmitted light. Width about 2 mm. b) same view as (a), in crossed polarizers, showing isotropic glass and strain in same minerals. c) view of one rounded clast showing its igneous mineralogy and texture, and surrounding glass. Transmitted light, width about 300 microns.

PROCESSING AND SUBDIVISIONS: A single piece (,1) was sawn from this coherent rock (Fig. 3), and consumed in producing thin sections ,4 and ,7. No other splits have been made. ,0 is now 1.16 g.

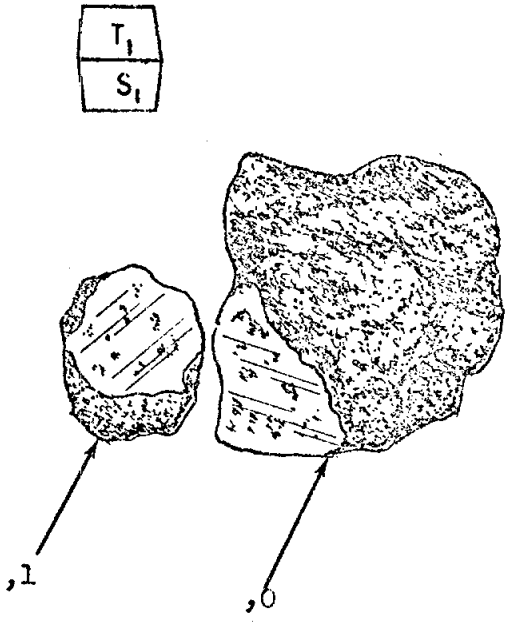

Figure 3. Sawing of 15383.

15384 MEDIUM-GRAINED OLIVINE-NORMATIVE MARE BASALT ST. 7 1.4 g

INTRODUCTION: 15384 is an olivine-bearing, medium-grained mare basalt with a granular texture. It is angular and coherent (Fig. 1), with a greyish dust coat originally on its surface. It has no zap pits. It was collected as part of the rake sample from the north-east rim of Spur Crater.

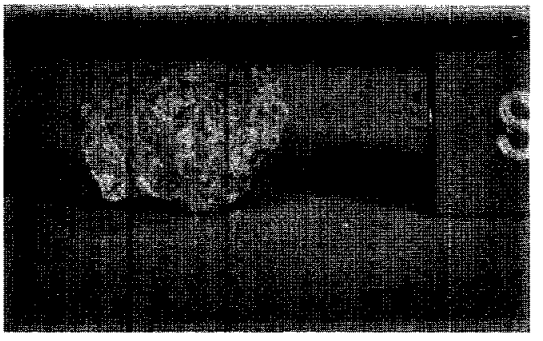

Figure 1. Pre-split view of 15384. S-71-49130

PETROLOGY: 15384 is a granular, olivine-bearing basalt (Fig. 2a,b). Compared with 15379, it is a little coarser, contains some better-developed plagioclase laths, and the mafic minerals are much more equant. Some of the olivines contain silicate melt inclusions and chromite, and some of the pyroxene and plagioclase is intergrown in a rather graphic texture (Fig. 2c). The sample is slightly shocked but lacks deformation lamellae and glass veins.

Fig. 2a

Fig. 2b

Fig. 2c

Figure 2. Photomicrographs of 15384,7. a) general view in transmitted light, showing mafic nature and basaltic texture. Width about 2 mm. b) same view as (a), in crossed polarizers, showing granular texture of mafic minerals. c) "graphic" intergrowth of pyroxene (grey) and plagioclase (extinct), crossed polarizers. Width about 300 microns.

PROCESSING AND SUBDIVISIONS: 15384 was substantially chipped (Fig. 3) but only ,2 was further processed, to provide thin sections ,6; ,7; and ,8. ,1 (0.205 g); ,3 (0.090 g); and ,4 (0.100 g) are the only remaining pieces other than the potted butt ,2 (0.570 g).

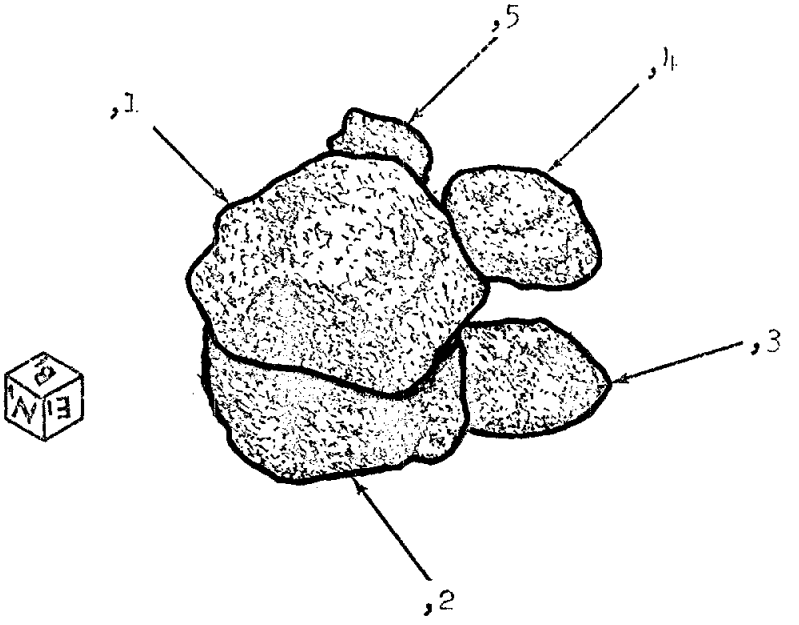

Figure 3. Chipping of 15384.

15385 FELDSPATHIC PERIDOTITE (MARE BASALT) ST. 7 8.7 g

INTRODUCTION: 15385 (Fig. 1) is a coarse mare basalt, texturally similar to coarser-grained variants of the olivine-normative basalts but perhaps even coarser (Fig. 2). It differs in having higher MgO, a feature it shares with 15387, which is also similar to 15385 in other respects. Its argon age (3.39 ± 0.05 b.y.; Husain, 1974) is the same as that of other Apollo 15 mare basalts. It was a friable sample. It was collected as part of the rake sample from the northeast rim of Spur Crater.

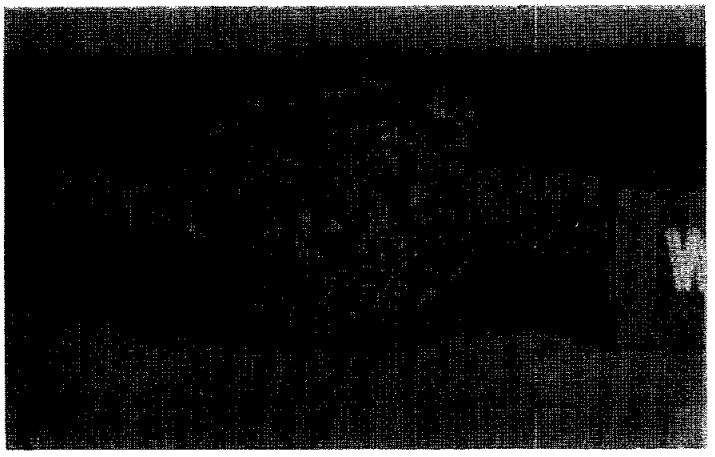

Figure 1. Macroscopic view of 15385,0 as originally documented. S-71-49189

Fig. 2a

Fig. 2b

Fig. 2c

Fig. 2d

Figure 2. Photomicrographs of 15385. widths 2 mm. (a, b) showing large anhedral pyroxenes, poikilitic plagioclases, and small euhedral olivines. The olivine just below center contains two large silicate melt inclusions. (c, d) showing large anhedral pyroxene with interior sharp zoning/overgrowth and enclosing olivine and chromite, and difference in texture of a single olivine grain in plagioclase (euhedral) and in pyroxene (embayed).

PETROLOGY: 15385 was described by Dowty et al. (1973a, b), who referred to it as feldspathic peridotite, forming a group of two with 15387. The name peridotite is somewhat of a misnomer, implying a plutonic rock, but the ranges of the mineral compositions (Fig. 3), lack of pyroxene exsolution, and high-Ca in olivine show the sample to be extrusive or of very shallow origin. Mineral analyses have been published by Dowty et al. (1973c) and Nehru et al. (1973, 1974). The mode has 42% pyroxene, 30% olivine, 24% plagioclase, 3% opaques, and 1% residual phases. Conspicuous are the large (1 to 2 mm) olivine crystals, which according to Dowty et al. (1973a) are anhedral. However, many olivines have well-developed crystal faces, especially where they are enclosed in or project into plagioclases (Figs. 2a, b). Where they are enclosed by pyroxenes, they tend to be anhedral or even embayed (Fig. 2c, d). Many contain silicate inclusions, and most are magnesian (Fo_{52-68}). Pyroxenes are large and blocky, and contain many small euhedral opaque phases. Some (Figs. 2c, d) contain sharp boundaries with an overgrowth of more pyroxene. The pyroxenes are more magnesian than those in olivine-normative or quartz-normative Apollo 15 basalts, and few are Fe-rich (Fig. 3). Both olivine and pyroxene suggest a cumulate origin. The plagioclase is poikilitic, enclosing olivines. The ilmenite contains more MgO than other Apollo 15 mare basalts, on average (3-5%); the metal, which is in early-formed grains, has high Ni contents, more than 5%. The spinel shows the best evidence for a chromite-ulvospinel compositional gap among Apollo 15 mare basalts. Chromite is small and euhedral; ulvospinel is subhedral to anhedral. According to Dowty et al. (1973a), 15385 and 15387 could be cumulates from a melt with an Fe/(Fe+Mg) similar to ol-normative basalts; about 25% olivine plus 65% olivine-phyric basalt would roughly produce 15385.—The geographic limitation to Spur Crater constrains models of origin which relates these basalts to olivine-phyric basalts (e.g., by subsurface differentiation), which are not found at Spur Crater.

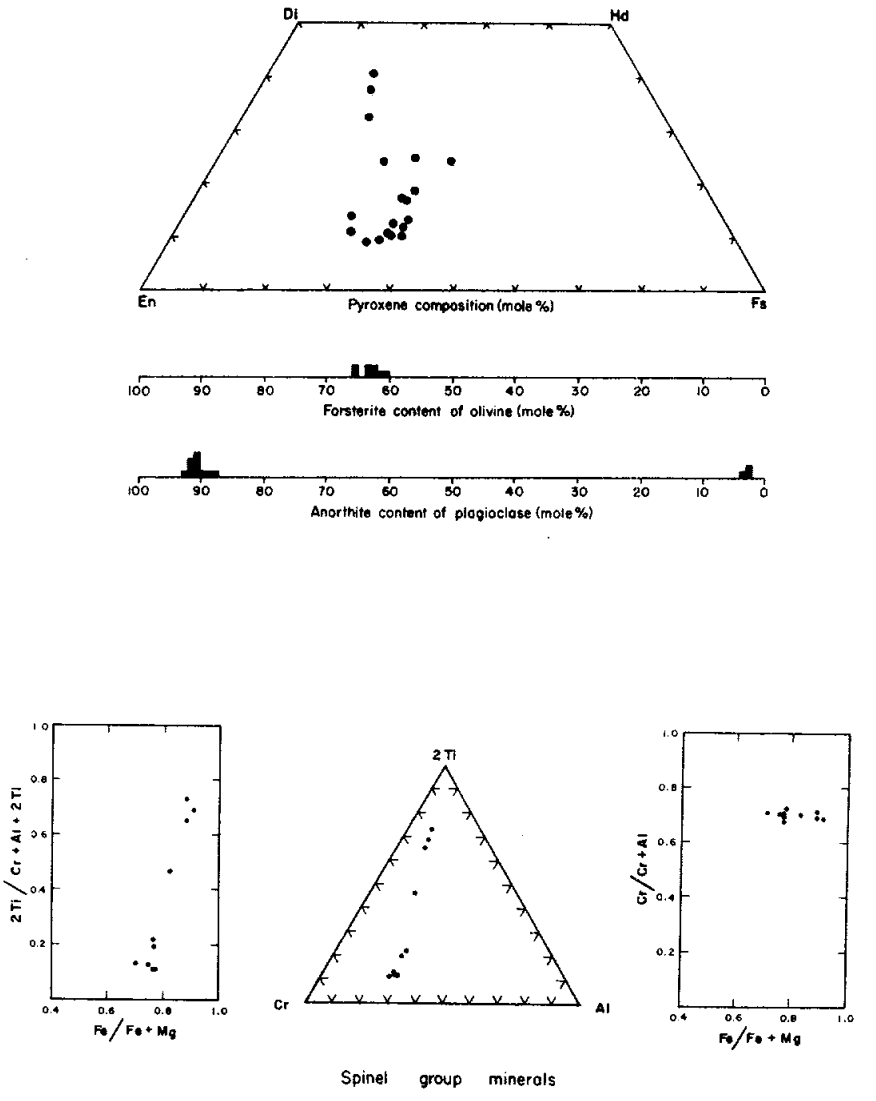

Figure 3. Composition of minerals in 15385 (Dowty et al., 1973b)

CHEMISTRY: Chemical analyses are listed in Table 1 and the rare earths shown in Figure 4. Conspicuous are the high MgO and low Al_2O_3. While the high TiO_2 rare earths, and other incompatible elements demonstrate that the sample is not a mantle clino-pyroxenite, they also show that the sample is not just another Apollo 15 basalt with added olivine (with or without pigeonite) (Rhodes and Hubbard, 1973), and that, if 15385 is a cumulate, its parent had higher rare earths than other Apollo 15 basalts. (However, the analysis of Ma et al. (1976), with lower rare earths and lower iron, is more in line with an origin of olivine accumulation, although those authors do not point that out.) Rb is as high as quartz-normative Apollo 15 mare basalts, but Sr is even lower than olivine-normative Apollo 15 mare basalts.

TABLE 15385-1. Chemical analyses

			,2	,7	,3
Wt %	SiO2	41.4	40.72		
	TiO2	1.99	2.68	1.7	
	Al2O3	8.8	4.81	6.8	
	FeO	21.2	25.27	23.1	
	MgO	16.9	17.66	18.2	
	CaO	7.3	6.48	6.8	7.42
	Na2O	0.32	0.15	0.216	
	K2O	<0.01	0.06	0.033	0.032
	P2O5	0.03	0.08		
(ppm)	Sc			39	
	V			187	
	Cr	5550	4272	5030	
	Mn	1850	2480	1820	
	Co			64	
	Ni			138	
	Rb		1.113		
	Sr		79.0		
	Y				
	Zr		106		
	Nb				
	Hf		3.3	2.2	
	Ba		63.8	57	
	Th		0.62		
	U		0.18		
	Pb				
	La		6.96	4.0	
	Ce		18.0		
	Pr				
	Nd		13.4		
	Sm		4.51	2.6	
	Eu		0.873	0.67	
	Gd		6.08		
	Tb			0.57	
	Dy		5.89	2.3	
	Ho				
	Er		3.19		
	Tm				
	Yb		2.72	1.7	
	Lu			0.29	
	Li		5.6		
	Be				
	B				
	C				
	N				
	S		1000		
	F				
	Cl				
	Br				
	Cu				
	Zn				
(ppb)	I				
	At				
	Ga				
	Ge				
	As				
	Se				
	Mo				
	Tc				
	Ru				
	Rh				
	Pd				
	Ag				
	Cd				
	In				
	Sn				
	Sb				
	Te				
	Cs				
	Ta			1840a	
	W				
	Re				
	Os				
	Ir				
	Pt				
	Au				
	Hg				
	Tl				
	Bi				
		(1)	(2)	(3)	(4)

References for Table 15385-1

References and method:

(1) Dowty et al. (1973); defocussed beam microprobe.
(2) Rhodes and Hubbard (1973), Wiesmann and Hubbard (1975); XRF, isotope dilution/mass spec.
(3) Ma et al. (1976); INAA.
(4) Husain et al. (1972), Husain (1974); from Ar, irradiation, heating, mass spec.

Note:

(a) anomalously high, should be treated with caution.

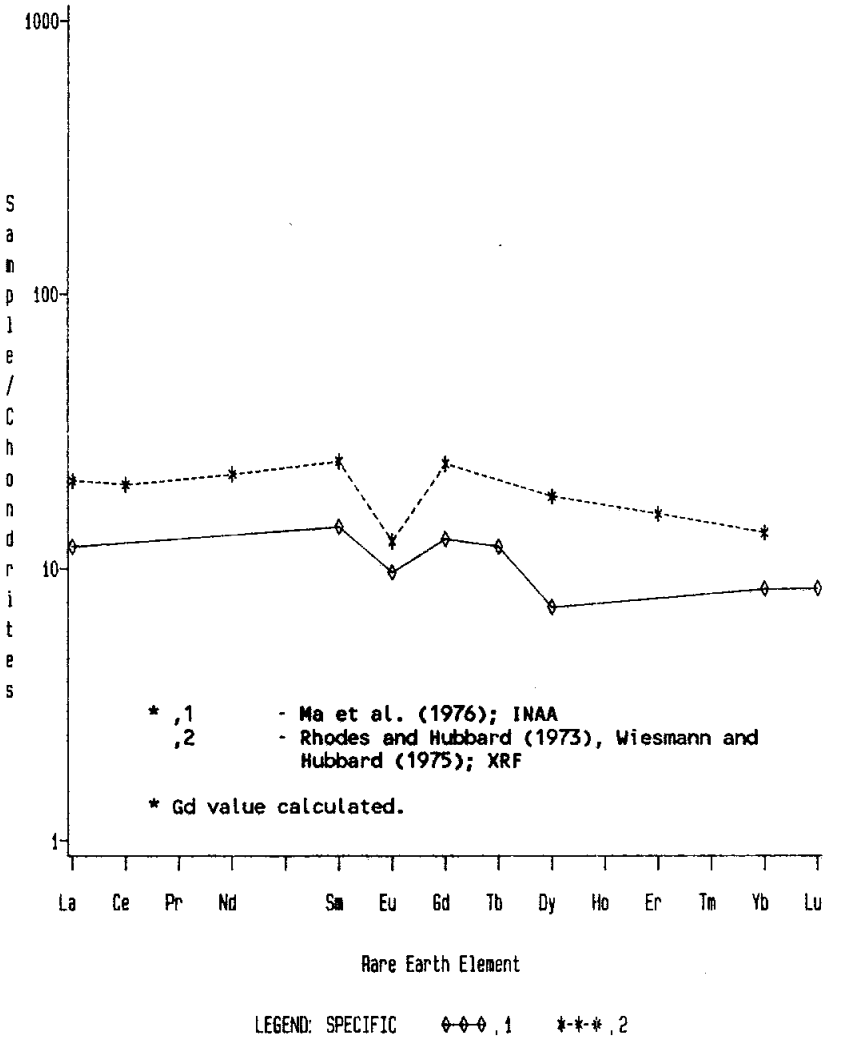

Figure 4. Rare earths in 15385.

GEOCHRONOLOGY AND RADIOGENIC ISOTOPES: Husain et al. (1972) and Husain (1974) performed stepwise heating on split ,3 (Fig. 5). There was little argon loss from the sample (3.5%). The ages presented are 3.32 ± 0.06 for ^{40}Ar-^{39}Ar and 3.28 b.y. for K-Ar (Husain et al., 1972), and 3.39 ± 0.05 b.y. for ^{40}Ar-^{39}Ar and 3.33 ± 0.03 b.y. for K-Ar (Husain, 1974). The age is (within error) the same as other Apollo 15 mare basalts, although Husain (1974) uses it to indicate a range of ages of Apollo 15 basalts.

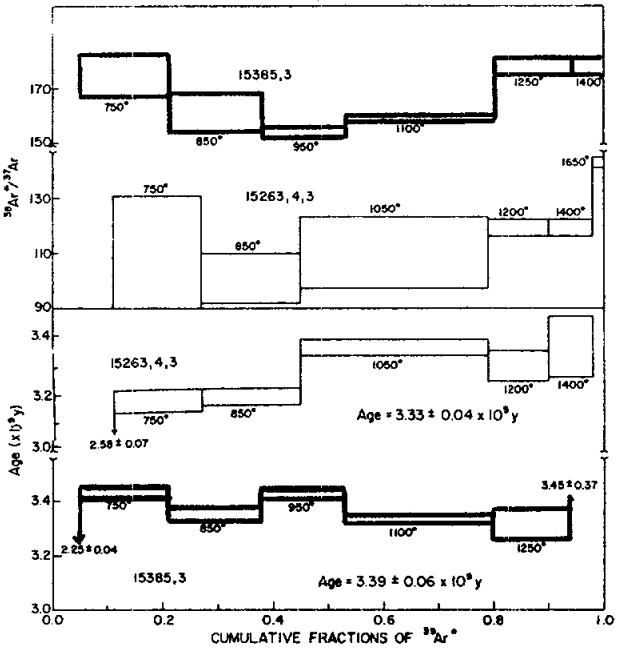

Figure 5. Argon release diagram (Husain, 1974)

Wiesmann and Hubbard (1975) reported a bulk rock $^{87}Sr/^{86}Sr$ of 0.70134 ± 10, higher than other Apollo 15 mare basalts, but the data plot within analytical error on the same isochron as other Apollo 15 mare basalts.

EXPOSURE: Husain et al. (1972) and Husain et al. (1974) determined Ar exposure ages of 270 ± 14 m.y. and 298 ± 12 m.y. respectively for ,3.

PROCESSING AND SUBDIVISIONS: The splits (,1; ,2; ,3) were chipped from ,0 for early allocations (Fig. 6), with thin sections ,9 and ,13 being produced from ,1. In 1984 two more small pieces (,17) were taken from ,0 for chemical analyses.

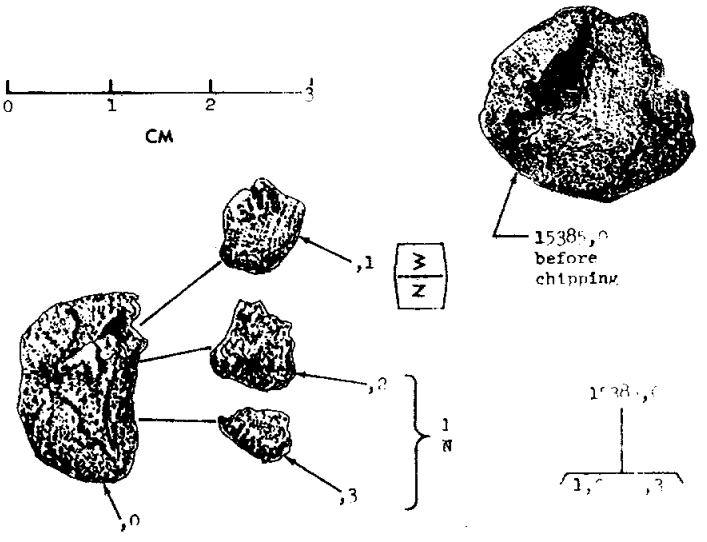

Figure 6. Chipping of 15385.

15386 KREEP BASALT ST. 7 7.5 g

INTRODUCTION: 15386 (Fig. 1) is a fragment of pristine (volcanic) basalt with KREEP rare-earth element abundances and patterns. It is coarser-grained than the otherwise-similar 15382. Like other KREEP basalts, it is older (~3.9 b.y.), more feldspathic, and more alkaline than Apollo 15 mare basalts. It is a tough sample, collected as part of the rake sample from the northeast rim of Spur Crater.

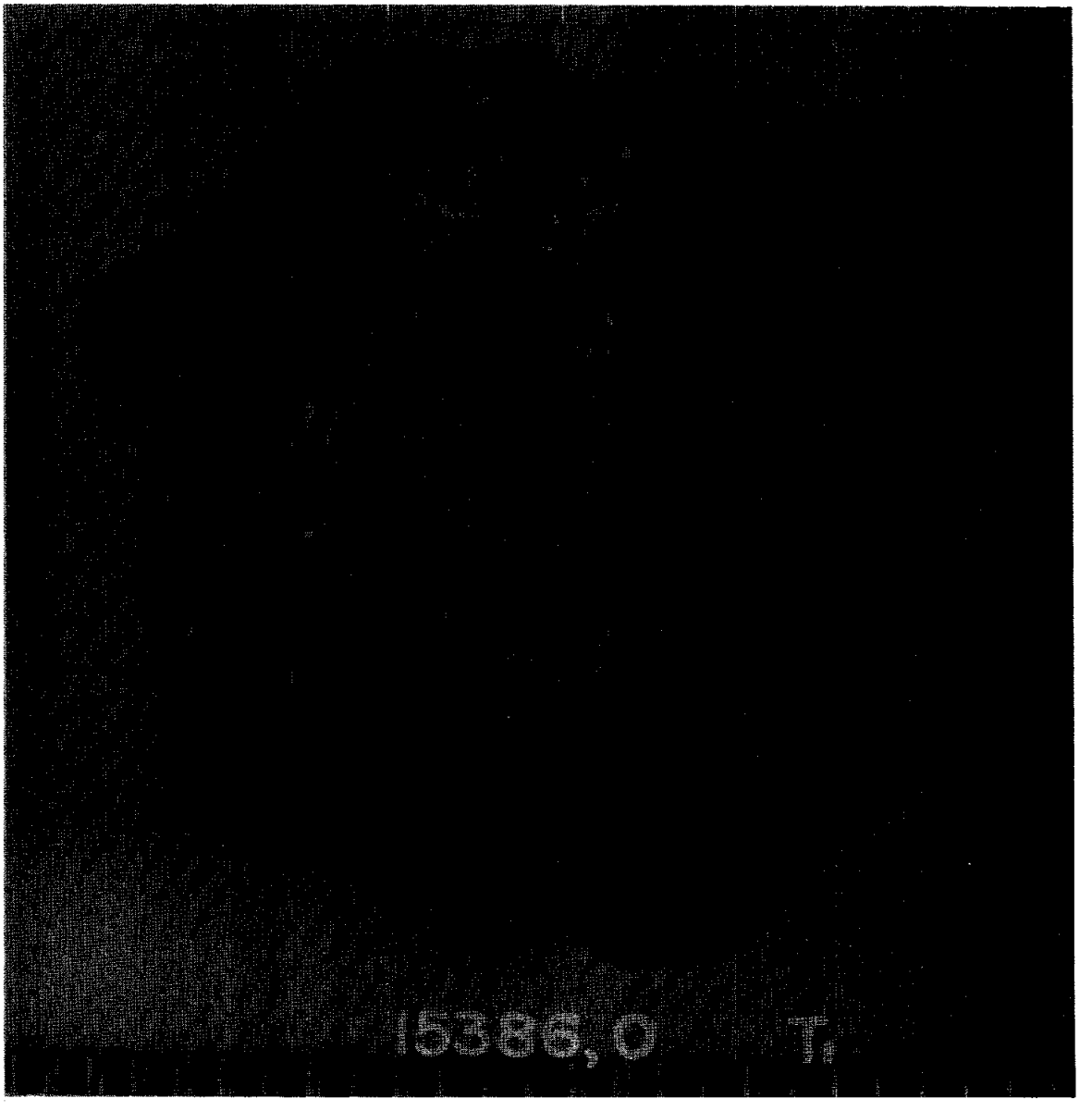

Figure 1. Macroscopic view of 15386,0 as it was in 1976 (S-76-24072). It has since been further subdivided.

PETROLOGY: 15386 is different from other volcanic rock samples at the Apollo 15 site except 15382, but is typical of many even-smaller particles found in Apennine Front materials, mare plains regolith samples, and breccias 15405 and 15205. However, according to Steele et al. (1972a) it is not a common clast-type within Spur Crater breccias. It has a subophitic to intersertal texture (Fig. 2). Descriptions and mineral analyses have been given by Steele et al. (1972a), Crawford et al. (1977), and Takeda et al. (1978, 1984). According to Steele et al. (1972a) it contains 35% plagioclase laths, 50% interstitial pyroxene, 10% cristobalite, 3% plates of ilmenite, and minor sulfide, iron-metal, and phosphates. There is no olivine. According to Simonds et al. (1975) 15386 contains about 50% plagioclase. Plagioclase and pyroxene crystallized simultaneously, and rapid cooling led to the small grain size, the lack of exsolutions, and the compositional range of the pyroxenes (below).

Figure 2. Transmitted light photograph of 15386,3. Width ~2 mm.

The pyroxenes have a wide range of Mg/Fe (Fig. 3). They have been most thoroughly investigated by Takeda et al. (1978). The cores are clear orthopyroxene, overgrown with rims of pigeonite which have numerous cracks. The pigeonite is untwinned, contains patches of augite, and is rimmed by augite. X-ray diffraction studies show that the core orthopyroxene shares (100) with pigeonite, and weak reflections show that augite shares a common (001) in the pigeonite. Takeda et al. (1978) found zoning trends similar to those found by Steele et al. (1972a) and tabulated some representative analyses. Core orthopyroxenes contain up to 4.1% Al_2O_3 and 1.28% Cr_2O_3.

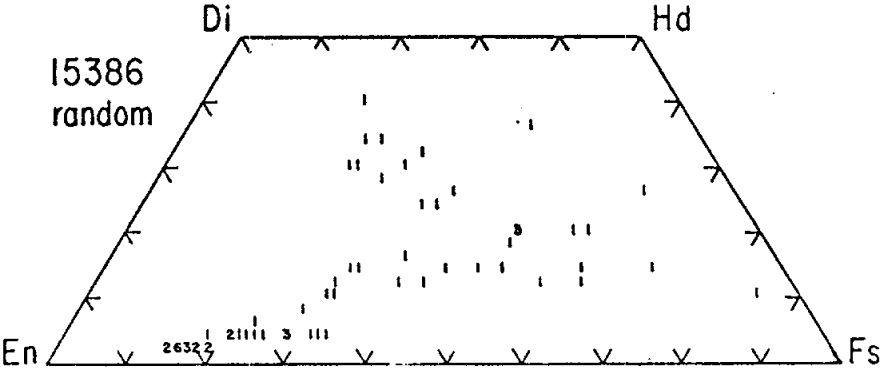

Figure 3. Compositions of pyroxenes in 15386 (Steele and Smith, 1972a).

The plagioclases are Na-rich and zoned, An_{85-70} (Steele et al., 1972a). Their Fe contents are lower than mare basalts and not on their trend (Fig. 4), but are similar to other KREEP basalts including 14310 (Fig. 5).

Takeda et al. (1984) studied the dark brown mesostasis, which is common as triangular interstices (~0.4 x 0.2 mm) and is characteristic of this basalt type, using microprobe, SEM, and ATEM techniques. Fe-rich pyroxene composes 48%, plagioclase 13%, silica 12%, silica/K-spar intergrowths 3%, ilmenite 11%, whitlockite 7%, troilite 2%, iron-metal 1%, and zirconolite 1% of the mesostasis. An unidentified Ca-rich phase is also present. A whitlockite analysis showed that most of the bulk rock Ce content can be accounted for by whitlockite.

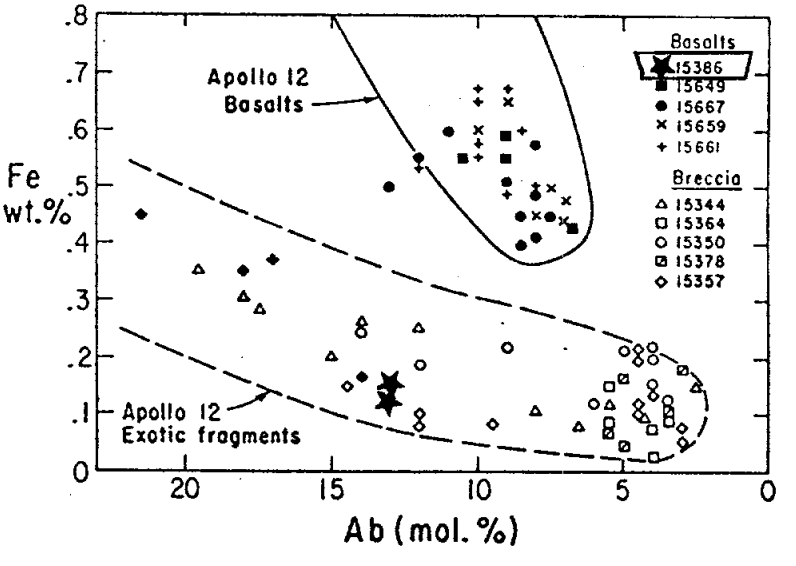

Figure 4. Compositions of plagioclases in 15386 (Steele and Smith, 1972a).

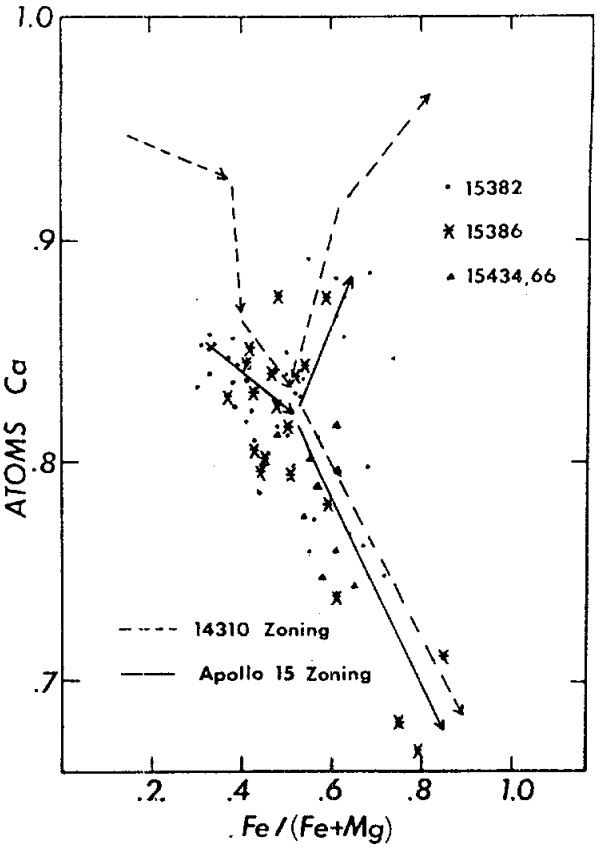

Figure 5. Compositions of plagioclases in 15386 (Crawford and Hollister, 1977).

The bulk composition of 15386 lies on the plagioclase-pyroxene cotectic in the Ol-Pl-Si system (McKay and Weill, 1976) and the source flow was probably a fractional crystallization product of a more primitive liquid. The composition, textures, and pristine chemistry (below) all suggest that 15386 is a volcanic flow, not an impact melt, but this interpretation is not universally held.

Crystallization experiments on 15386-like or related compositions were conducted by Irving (1977a, b), Rutherford et al. (1980), and Dickinson and Hess (1982). Irving (1977a, b) used a synthetic composition similar to that determined by Rhodes and Hubbard (1973) (Table 1) to conduct experiments at pressures up to 5 Kb. The liquidus temperature increased from 1135 ± 10°C at 5 Kb. Although plagioclase (An_{75}) and low-Ca pyroxene coexist within 70°C of the liquidus at all pressures, there is no multiple saturation within the pressures of the crust or upper mantle, and the sample apparently evolved by the fractional crystallization of subcalcic pyroxene and calcic plagioclase. Rutherford et al. (1980) used a similar composition but slightly richer in FeO and Na_2O, and were especially interested in ilmenite saturation. In contrast with Irving (1977a, b), their liquidus temperature was almost unaffected by pressure (1 atmosphere, and 5 Kb), and the charge was saturated with both pyroxene and plagioclase within 30°C of the liquidus. Ilmenite saturation was attained with 5% TiO_2 in the liquid between 1087o and 1080°C at 1 atmosphere, and with 6% TiO_2 in the liquid between 1115° and 1090°C at 5 Kb. The data are used by Rutherford et al. (1980) to constrain the origin of both KREEP and of high-Ti mare basalt sources. Dickinson and Hess (1982) used a liquid composition produced by the crystallization of the Rutherford et al. (1980) starting material to investigate whitlockite saturation. 4.45% P_2O_5 was needed for saturation at 1200°C, decreasing to 2.44% at 1047°C.

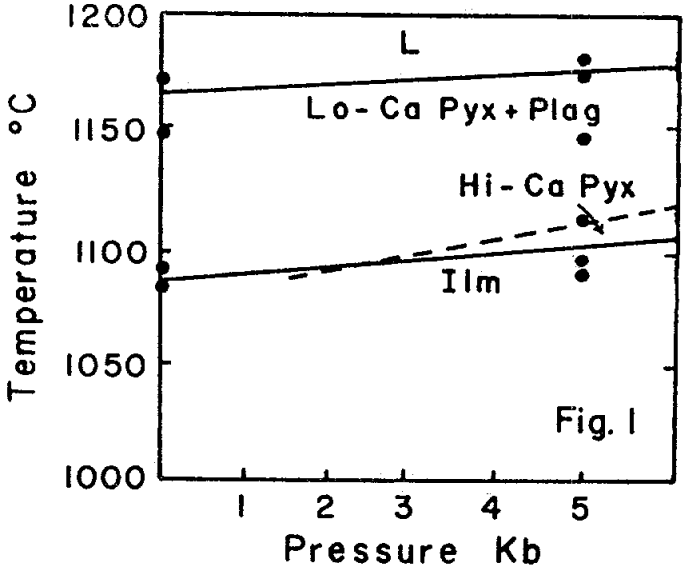

Figure 6. Crystallization experiment results for 15386 (Rutherford et al., 1980).

CHEMISTRY: Chemical analyses are listed in Table 1 and the rare earths plotted in Figure 7. The data are generally consistent except that the analysis of Warren et al. (1978) has higher MgO and lower rare earths than does that of Rhodes and Hubbard (1973) and Hubbard et al. (1974). In Warren et al. (1978), the Ge units are wrongly listed as ppm instead of ppb, and in Warren and Wasson (1978) the Cd and In units are wrongly listed as ppm instead of ppb.

The low In indicates that 15386 is a volcanic rock, not a meteorite-contaminated impact melt, but the Ge and Au abundances are somewhat high and require special explanations (Warren et al., 1978). The rare earth element pattern is the common KREEP pattern.

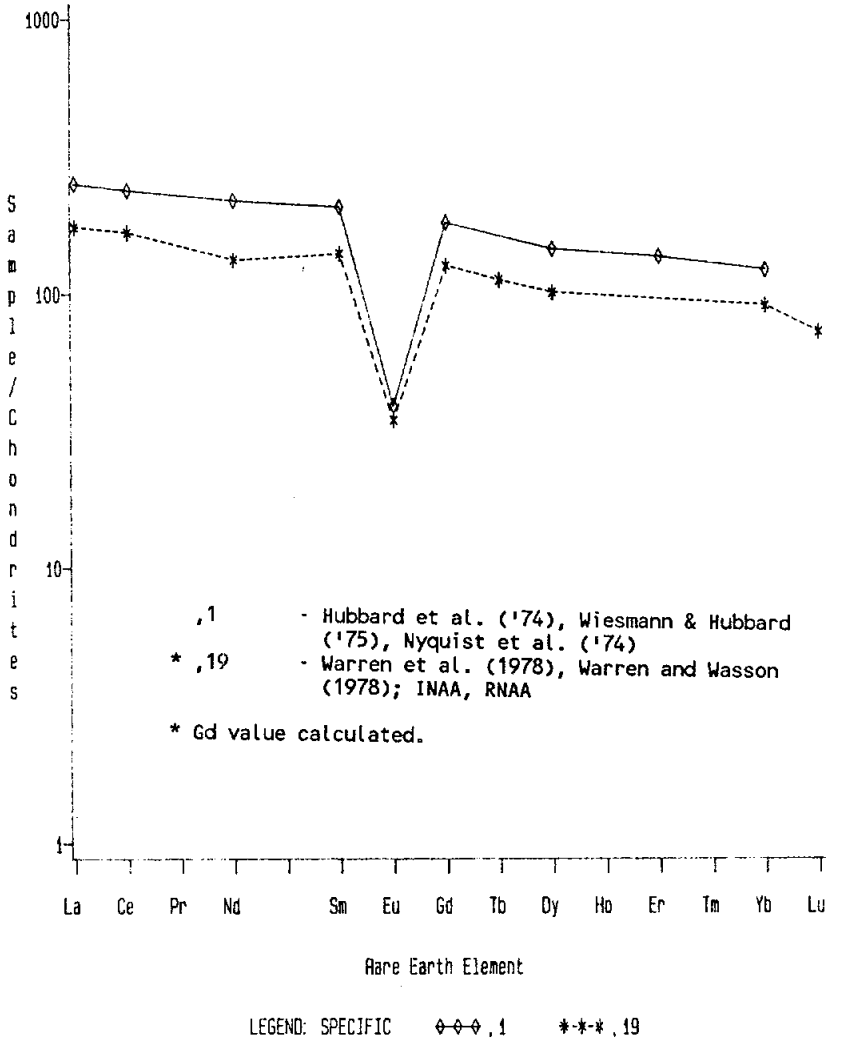

Figure 7. Rare earth element data for 15386.

TABLE 15386-1. Chemical analyses

		,19	,1	,1	,0	,25,27	,35	?
Wt %	SiO2		50.83					
	TiO2	1.9	2.23					
	Al2O3	15.3	14.77					
	FeO	10.2	10.55					
	MgO	10.5	8.17					
	CaO	9.5	9.71					
	Na2O	0.811	0.73					
	K2O	0.50	0.67	0.685	0.59			
	P2O5		0.70					
(ppm)	Sc	22.0						
	V	62						
	Cr	2430		2124				
	Mn	1150	1240					
	Co	23						
	Ni	12.5						<30
	Rb	14		18.46				
	Sr			187.4				
	Y							
	Zr	970						
	Nb							
	Hf	21					26.228	
	Ba	650		837				
	Th	10.0			11.80			
	U	2.8			3.30			
	Pb							
	La	58		83.5				
	Ce	147		211				
	Pr							
	Nd	80		131		129.6		
	Sm	25.5		37.5		36.0		
	Eu	2.4		2.72				
	Gd			45.4				
	Tb	5.3						
	Dy	32		46.3				
	Ho							
	Er			27.3				
	Tm							
	Yb	18.2		24.4				
	Lu	2.48					3.193	
	Li			27.2				
	Be							
	B							
	C							
	N							
	S		900					
	F							
	Cl							
	Br							
	Cu							
	Zn	3.5						
(ppb)	I							
	At							
	Ga	6200						
	Ge	61(a)						
	As							
	Se							
	Mo							
	Tc							
	Ru							
	Rh							
	Pd							
	Ag							
	Cd	10						
	In	1.8						
	Sn							
	Sb							
	Te							
	Cs	800						
	Ta	2400						
	W							
	Re							
	Os							
	Ir	0.061						
	Pt							
	Au	0.22(a)						
	Hg							
	Tl							
	Bi							
		(1)	(2)	(3)	(4)	(5)	(6)	(7)

References and methods:

(1) Warren et al. (1978), Warren and Wasson (1978); INAA, RNAA.
(2) Rhodes and Hubbard (1973); XRF
(3) Hubbard et al. (1974), Wiesmann and Hubbard (1975), Nyquist et al. (1974); isotope dilution, mass spec.
(4) O'Kelley et al. (1976); gamma ray spec.
(5) Carlson and Lugmair (1979a, b); isotope dilution, mass spec.
(6) Unruh and Tatsumoto (1984); isotope dilution, mass spec.
(7) Blanchard, unpublished; INAA

Notes:

(a) authors believe abundance high.

RADIOGENIC ISOTOPES AND GEOCHRONOLOGY: Nyquist et al. (1974) reported Rb and Sr whole rock isotopic data and followed this with a Rb-Sr internal isochron (Nyquist et al., 1975) (Table 2). The isochron, using the whole rock data, plagioclase separate, and mesostasis plus pyroxene separate gives an age of 3.94 ± 0.01 b.y. (= 1.39 x 10^{-11} yr^{-1}) or 3.86 b.y. (= 1.42 x 10^{-11} yr^{-1}), with initial $^{87}Sr/^{86}Sr$ = 0.70038 ± 3 (Fig. 8).

15386 is resolved from 15434, a particle of KREEP basalt separated from soil, in initial Sr isotopes, but not in age (Nyquist et al., 1975). The age is the same as 15382. The data indicate some precursor event represented more or less by the model ages, and a second melting event at the crystallization age.

TABLE 15386-2. Rb-Sr Isotopic Data (Nyquist et al., 1975)

Split	Rb ppm	Sr ppm	$^{87}Rb/^{86}Sr$	$^{87}Sr/^{86}Sr$
WR	18.46	187.4	0.285 ± 2	0.71640 ± 7
Plag	1.25	323.8	0.0112 ± 1	0.70102 ± 10
Mes + Px	43.04	129.8	0.959 ± 7	0.75441 ± 14

TABLE 15386-3. Rb-Sr Model Ages
(b.y., ± 0.04)

	T_{BABI}	T_{LUNI}
λ = 1.39 x 10^{-11} yr^{-1}	4.25	4.28
λ = 1.42 x 10^{-11} yr^{-1}	4.15	4.18

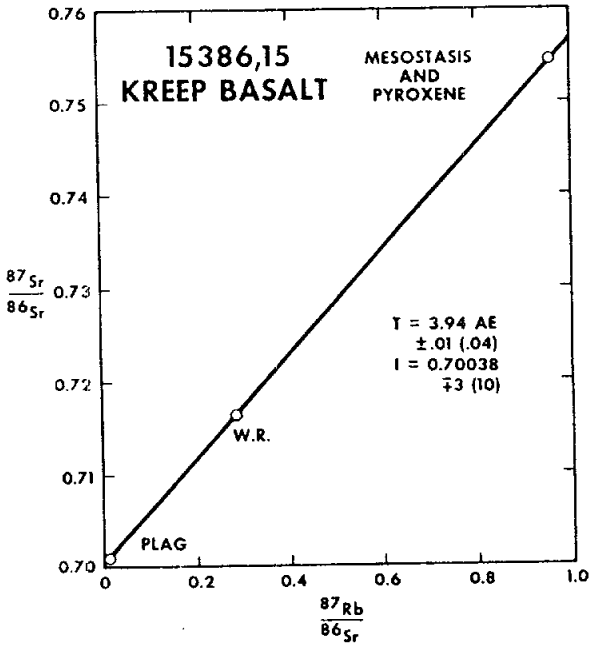

Figure 8. Rb-Sr isochron (Nyquist et al., 1975).

Carlson and Lugmair (1979a) reported whole-rock and mineral-separate Sm and Nd isotopic data for 15386. The isochron (crystallization) age of 3.85 ± 0.08 b.y. (Fig. 9) is indistinguishable from the Rb-Sr isochron age. (A preliminary report had 3.87 ± 0.12 b.y., Carlson and Lugmair, 1979b.) The subchondritic initial $^{143}Nd/^{144}Nd$ requires that the KREEP rare earth pattern was established much earlier -- 4.36 b.y., similar to other KREEP model ages.

Unruh and Tatsumoto (1983) reported Lu and Hf isotopic data for 15386 and other KREEP samples; unlike Sm-Nd data, there is a large range in the isotopic ratios for different KREEP samples. The data are discussed in terms of mare basalt sources and KREEP genesis without specific reference to 15386.

EXPOSURE: O'Kelley et al. (1976) reported ^{26}Al disintegration count data. The ^{26}Al is saturated, indicating a surface exposure of at least one or two million years.

PROCESSING AND SUBDIVISIONS: Originally splits ,1 and ,2 were chipped off one end for allocations (Fig. 10). ,2 was made into thin sections, and all thin sections are from ,2. Subsequent allocations were made by further chipping of ,0, which is now 3.6 g.

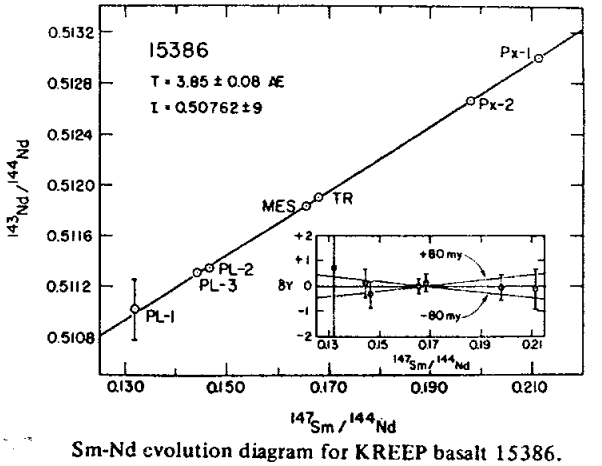

Sm-Nd evolution diagram for KREEP basalt 15386. The slope of the best fit line through the data points corresponds to an age of 3.85 ± 0.08 AE ($\lambda = 6.54 \times 10^{-12}$ yr^{-1}) in good agreement with that indicated by the Rb-Sr system

Figure 9. Sm-Nd isochron (Carlson and Lugmair, 1979a).

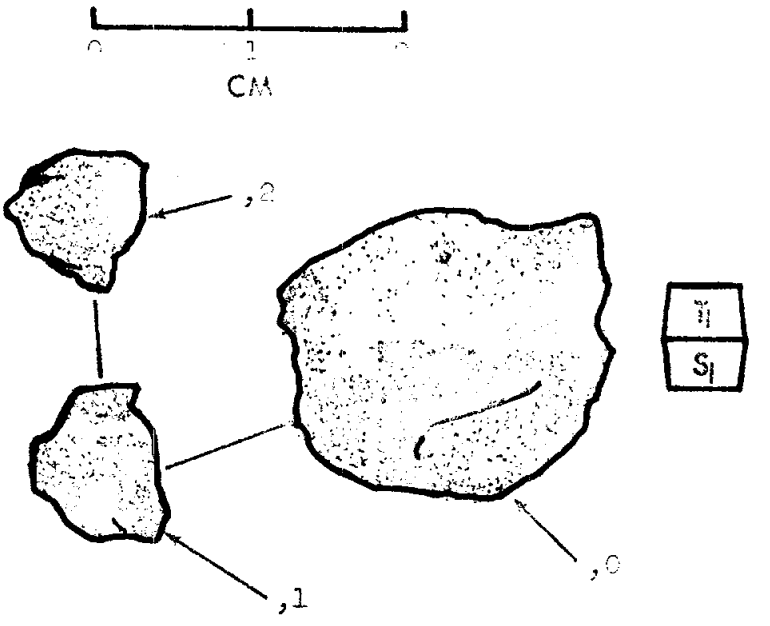

Figure 10. Initial processing of 15386.

15387 FELDSPATHIC PERIDOTITE (MARE BASALT) ST. 7 2.0 g

INTRODUCION: 15387 (Fig. 1) is a coarse mare basalt, texturally similar to coarse-grained variants of olivine-normative basalts but richer in olivine and perhaps even coarser. It is very similar to 15385. It was collected as part of the rake sample from the northeast rim of Spur Crater. Because 15387 was friable, it is possible that the two samples are part of a once single piece which broke up prior to, during, or after collection.

PETROLOGY: 15387 was described by Dowty et al. (1973a, b), who referred to it as feldspathic peridotite, forming a group of two with 15385. The name peridotite is somewhat of a misnomer, implying a plutonic rock, but the ranges of the mineral compositions (Fig. 2), lack of pyroxene exsolution, and high-Ca in olivine show the sample to be extrusive or of very shallow origin. Microprobe mineral analyses have been published by Dowty et al. (1973c) and Nehru et al. (1973, 1974. The mode is only slightly different from 15385: 38% pyroxene, 34% olivine, 22% plagioclase, 5% opaques, and 1% residual phases. The petrographic description is the same as that for 15385, and the mineral chemistry is almost the same (Fig. 2), with a slightly wider reported range of silicate mineral compositions extending to more fractionated compositions.

CHEMISTRY: Only defocussed beam microprobe analyses of 15387 have been made (Table 1). These are very similar to the corresponding analysis for 15385. Bunch et al. (1972) suggested that an ultramafic composition like 15387 is parental to the Apollo 15 green glass, but noted that the higher TiO_2 content of 15387 precludes such a composition itself from being parental.

PROCESSING AND SUBDIVISIONS: Only one chip (,1) was removed from ,0 and two thin sections (,7; ,8) and one grain mount (,6) were made from it.

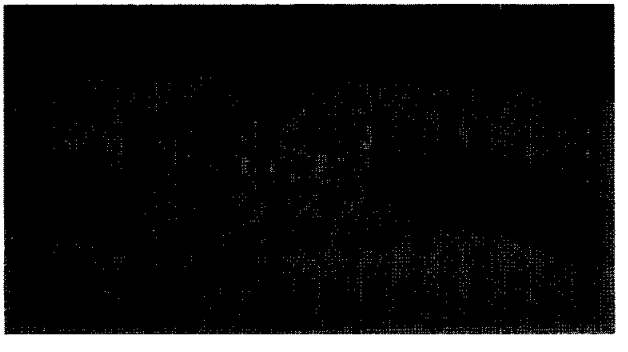

Figure 1. Macroscopic view of 15387,0 before processing (S-71-49050).

Figure 2. Compositions of minerals in 15387 (Dowty et al., 1973b).

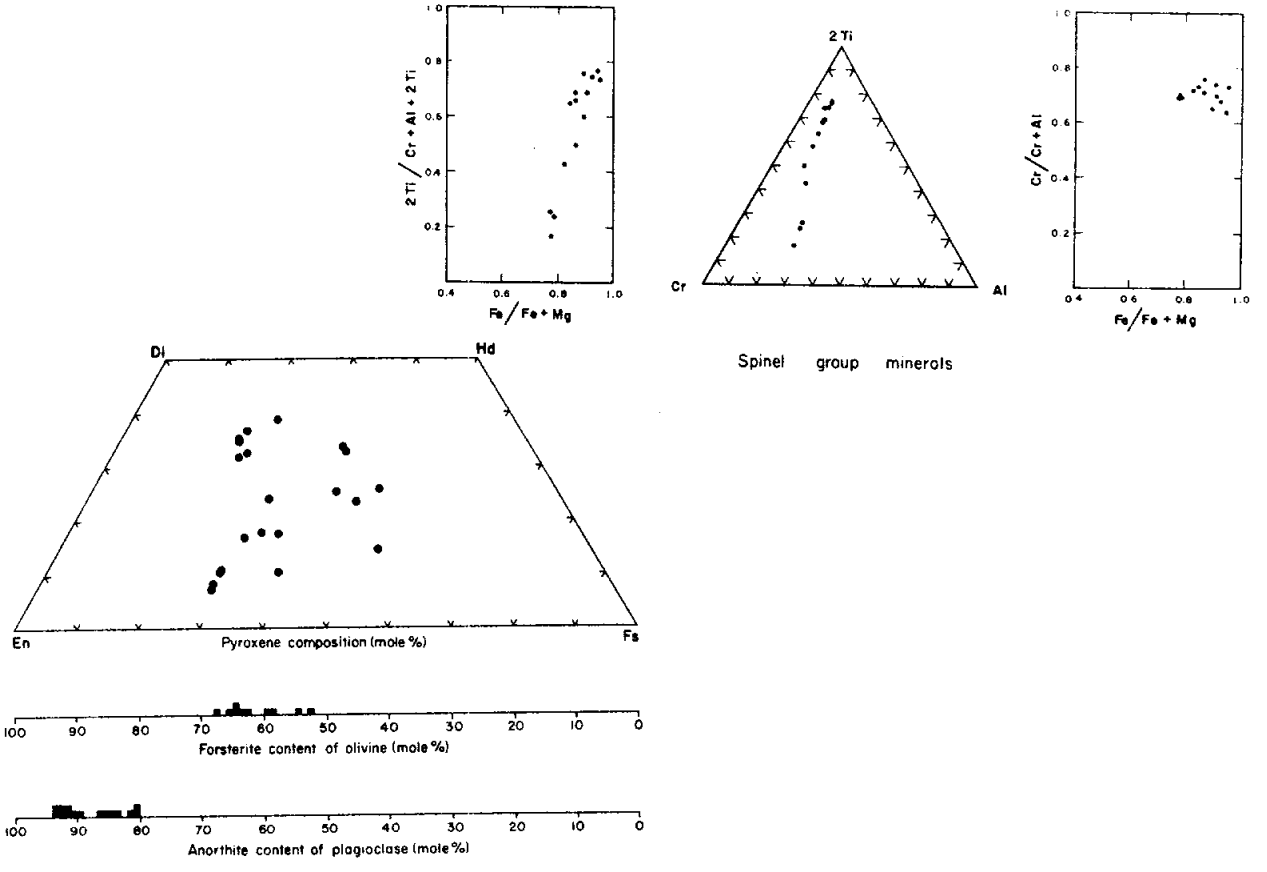

TABLE 15387-1. Chemical analyses

		,1	
Wt %	SiO2	41.9	41.8
	TiO2	1.12	1.44
	Al2O3	10.0	7.7
	FeO	22.5	23.9
	MgO	17.1	18.1
	CaO	7.5	7.0
	Na2O	0.27	0.28
	K2O	0.01	0.01
	P2O5	0.03	0.04
ppm	Cr	3700	3700
	Mn	2100	2200
		(1)	(2)

References and methods:

(1) Bunch et al. (1972); Microprobe defocussed beam
(2) Dowty et al. (1972); Microprobe defocussed beam

15388 FELDSPATHIC MICROGABBRO (MARE BASALT) ST. 7 9.0 g

INTRODUCTION: 15388 is a coarse, mare-type basalt which appears to be unique both in its greater abundance of feldspars than most mare basalts, and in its texture. Large, oriented pyroxene phenocrysts are embedded in a finer-grained mass of plagioclase and pyroxene which are intergrown (Fig. 1). 15388 was collected as part of the rake sample from the northeast rim of Spur Crater.

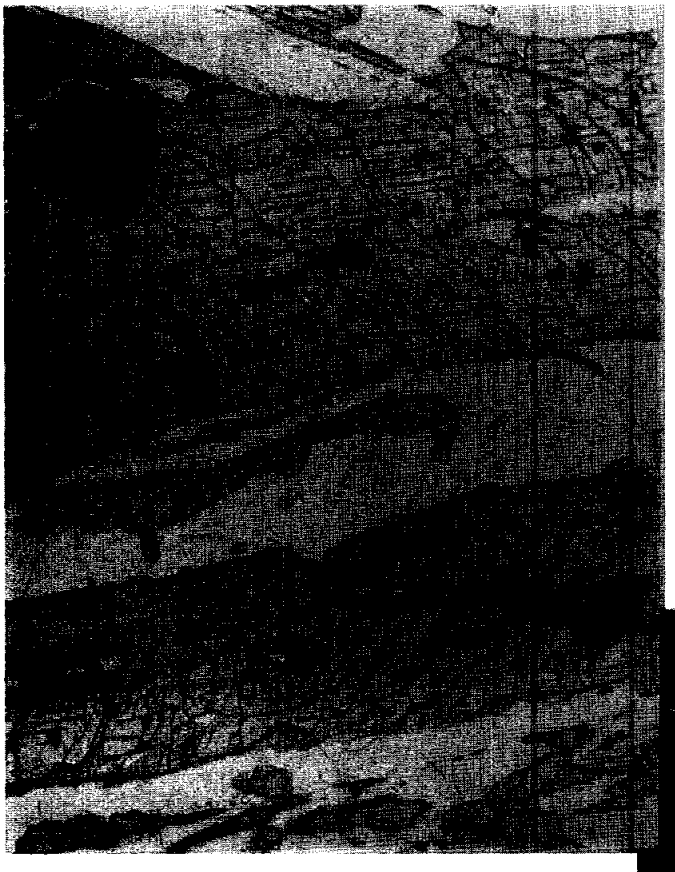

Fig. 1a

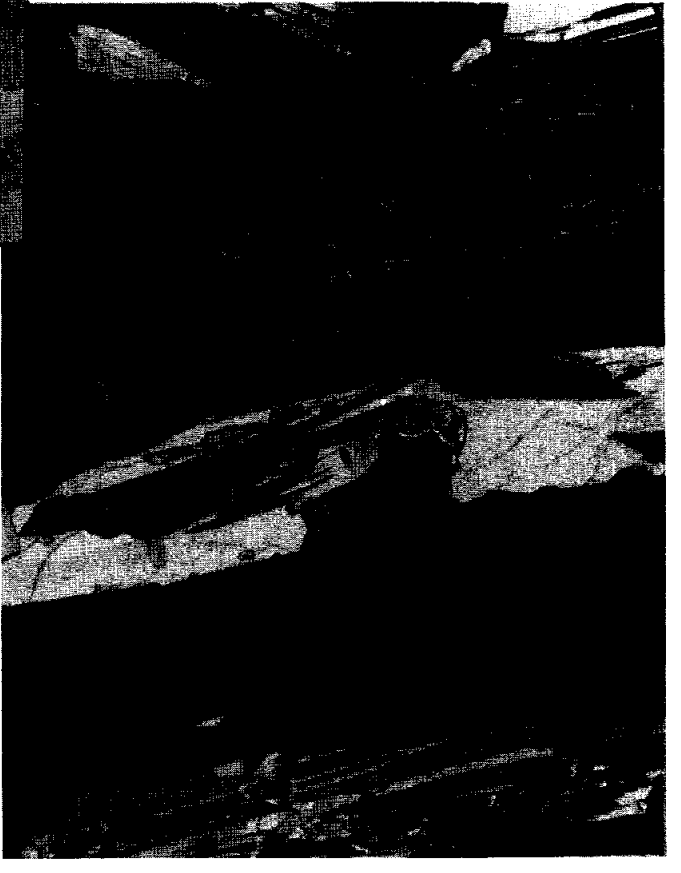

Fig. 1b

Fig. 1c

Fig. 1d

Figure 1. Photomicrographs of 15388,11, width 2 mm. a, b show parts of large, parallel pyroxene phenocrysts containing ilmenite, and interstitial plagioclase. c, d show the texture of the inter-phenocryst area, with pyroxene and plagioclase intergrown in a somewhat graphic texture.

PETROLOGY: 15388 has been described by Dowty et al. (1973a, b) who referred to it as feldspathic microgabbro, a unique sample. Microprobe mineral analyses have been published by Dowty et al. (1973c) and Nehru et al. (1973, 1974). It contains 57% pyroxene, 36% plagioclase, 6% opaque phases, and 1% cristobalite and mesostasis (the pyroxene is erroneously listed as 51% in Dowty et al., 1973b), and its mineral chemistry shows that it is a mare basalt. A pronounced orientation is determined principally from the large pyroxene crystals (Figs. 1a, b), at least in the small area of the thin section. In the remainder, plagioclase poikilitically encloses pyroxene, although this is really an intergrowth because the pyroxene is generally optically continuous over several apparent individuals. Olivine does not appear to be present. Pyroxenes (Fig. 2) show a range in compositions, as do plagioclases (An_{95-80}). Nehru et al. (1973, 1974) described and analysed the ilmenite and spinel group minerals. Cr-ulvospinel is present in minor amounts and is unique among Apollo 15 mare basalts. It occurs as inclusions in ilmenite, which is the major opaque phase. Most of the ilmenite contains less than 1% MgO. 15388 is possibly related to an Apollo 15 olivine basalt parent, by the removal of olivine from that parent, and subsequent accumulation of pyroxene and plagioclase to make the 15388 lithology.

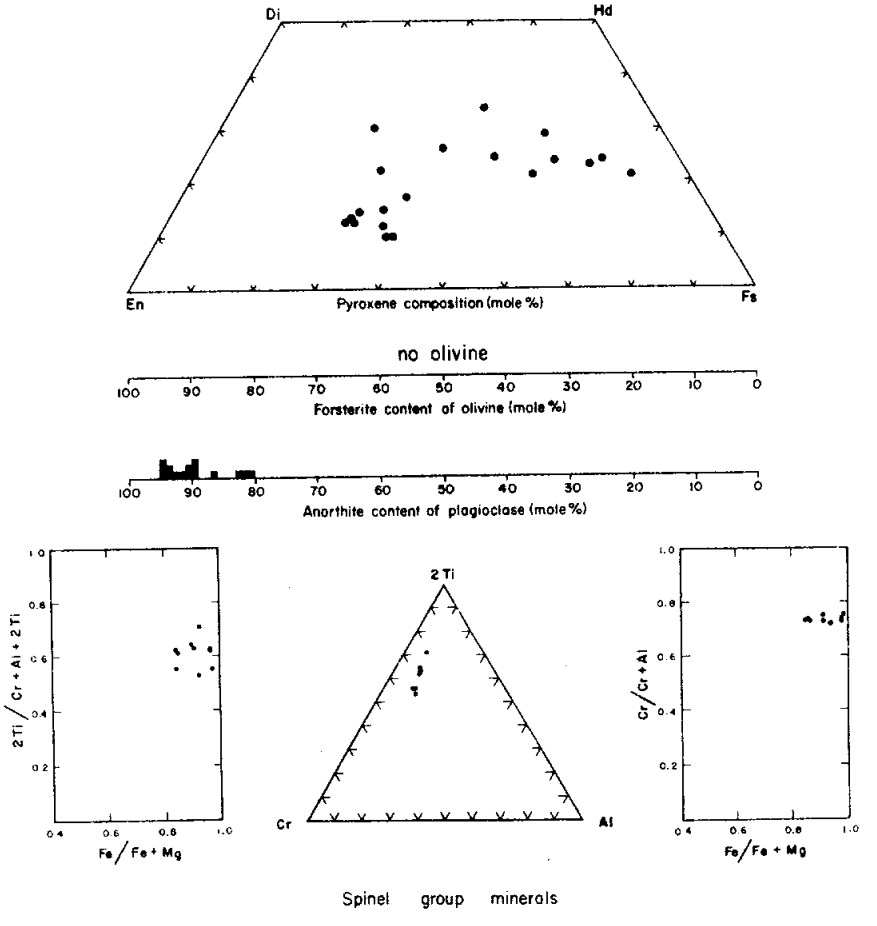

Figure 2. Mineral compositions in 15388, from Dowty et al. (1973b).

TABLE 15388-1. Chemical analyses

		,3	,7
Wt %	SiO2		
	TiO2	1.1	5.1
	Al2O3	15.4	12.8
	FeO	15.1	17.6
	MgO	10	7.7
	CaO	11.7	10.5
	Na2O	0.428	0.416
	K2O	0.024	0.032
	P2O5		
(ppm)	Sc	42	43
	V	180	150
	Cr	2700	2350
	Mn	1540	1720
	Co	37	27
	Ni		<36
	Rb		
	Sr		
	Y		
	Zr	<180	
	Nb		
	Hf	0.9	1.2
	Ba		29
	Th		
	U		
	Pb		
	La	1.2	1.6
	Ce	4.2	
	Pr		
	Nd		
	Sm	1.2	1.5
	Eu	0.89	0.91
	Gd		
	Tb	0.3	0.36
	Dy	2.5	3.4
	Ho		
	Er		
	Tm		
	Yb	1.6	1.6
	Lu	0.22	0.29
	Li		
	Be		
	B		
	C		
	N		
	S		
	F		
	Cl		
	Br		
	Cu		
	Zn		
(ppb)	I		
	At		
	Ga		
	Ge		
	As		
	Se		
	Mo		
	Tc		
	Ru		
	Rh		
	Pd		
	Ag		
	Cd		
	In		
	Sn		
	Sb		
	Te		
	Cs		
	Ta	300	320
	W		
	Re		
	Os		
	Ir		
	Pt		
	Au		
	Hg		
	Tl		
	Bi		
		(1)	(2)

TABLE 15388-2. Microprobe defocussed beam bulk analysis (Dowty et al., 1973b)

Wt %	SiO2	45.7
	TiO2	2.57
	Al2O3	10.9
	FeO	17.2
	MgO	10.1
	CaO	9.7
	Na2O	0.39
	K2O	<0.01
	P2O5	0.02
ppm	Cr	2000
	Mn	1550

References and methods:

(1) Laul and Schmitt (1973); INAA.
(2) Ma et al. (1976); INAA.

CHEMISTRY: Chemical analyses are listed in Table 1 and Table 2 and rare earth elements shown in Figure 3. The sample shows higher Al than most mare basalts, in agreement with the petrographic observations. It showed the first observed positive Eu anomaly among mare basalts, which suggests accumulation of plagioclase and little occlusion of residual magma (Laul and Schmitt, 1973). Laul and Schmitt (1973) also suggest the possibility of the fusion of nearly pure mafic and plagioclase cumulates, although the meaning of this is ambiguous and not further described. The severe discrepancies among the analyses for TiO2 is a reflection of the coarse-grain size, the heterogenous distribution of ilmenite, and the small size of the samples analyzed.

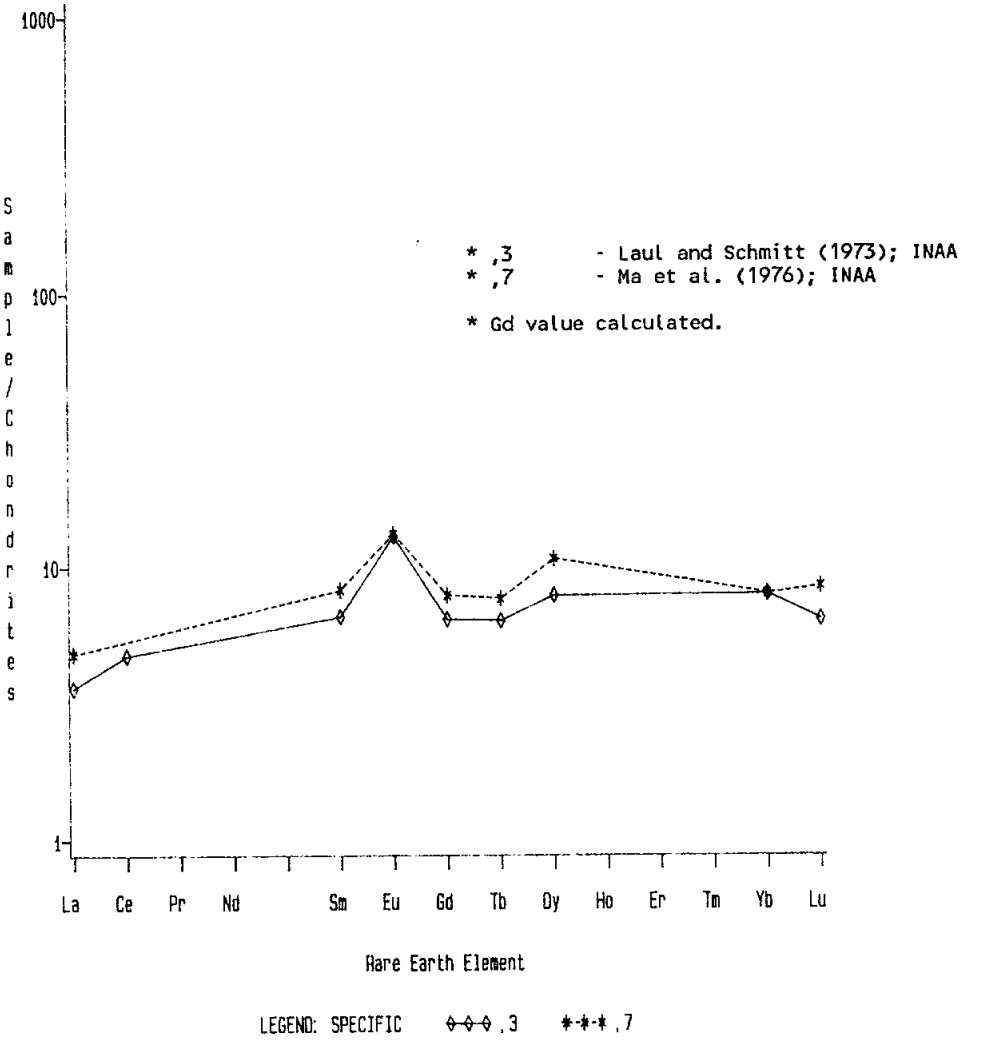

Figure 3. Rare earths in 15388.

TRACK AND EXPOSURE: Bhandari et al. (1972, 1973) tabulated the track density for a surface chip. The track density is 5x106 cm^{-2}, and a "suntan" exposure age of less than 1 m.y. was derived.

PROCESSING AND SUBDIVISIONS: A piece was sawn from ,0 and then resawn to provide ,1 and ,2 (Fig. 4). ,0 now has a mass of 5.24 g. Thin sections ,10; ,11; ,12 were produced from ,2, and the chemical analyses were of pieces of ,1.

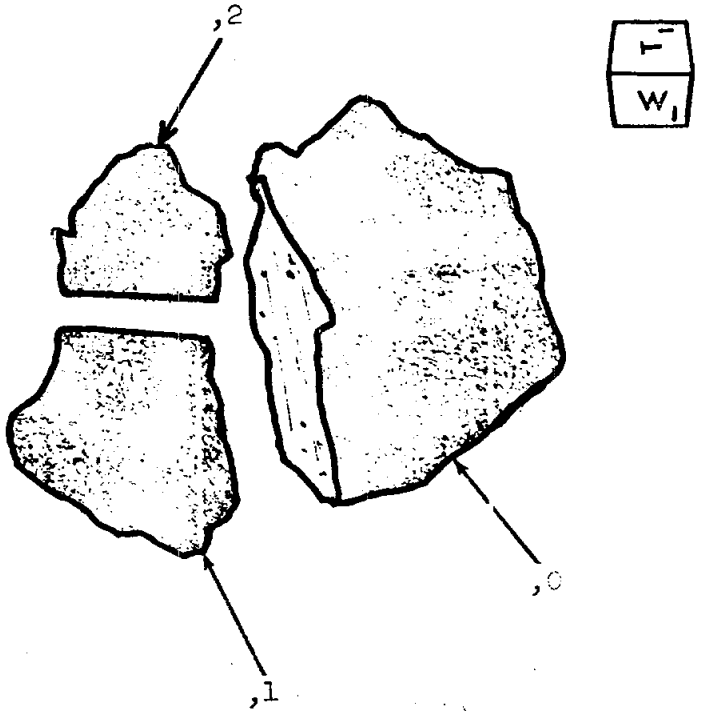

Figure 4. Sawing of 15388.

15389 AGGLUTINATE ST. 7 2.8 g

INTRODUCTION: 15389 (Fig. 1) is a large agglutinate containing mineral and breccia fragments. It was collected as part of the rake sample on the northeast rim of Spur Crater.

PETROLOGY: 15389 is a bubbly agglutinate consisting of a glassy to cryptocrystalline matrix enclosing mineral and lithic fragments (Fig. 2). The matrix is almost all opaque, but a few clast-free, gray glassy areas are present. The lithic clasts are dominantly fine-grained feldspathic breccias ranging from porous regolith breccia and feldspathic granulites to impact melts. There are many mineral fragments and some glass fragments, but the opaque mineral content is low. Steele et al. (1977) tabulated 15389 as consisting of 75% glass, 5% lithic clasts (breccias) and 20% vesicles. No analyses have been published, but the sample appears to be dominantly but not exclusively of highland derivation.

PROCESSING AND SUBDIVISIONS: A single chip (,1) was taken and two thin sections (,1 and ,6) were made from it.

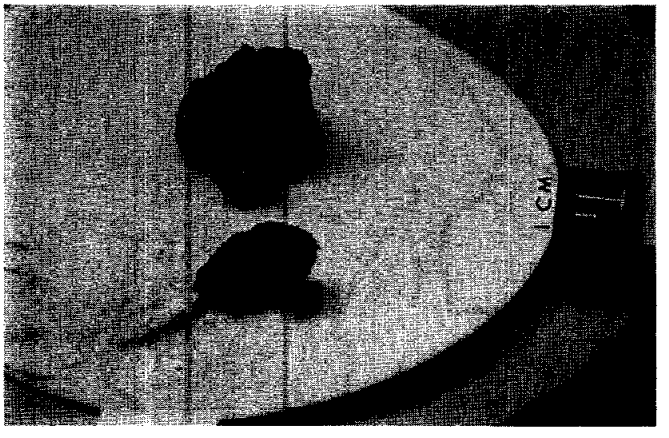

Figure 1. Macroscopic view of 15389. S-71-58127

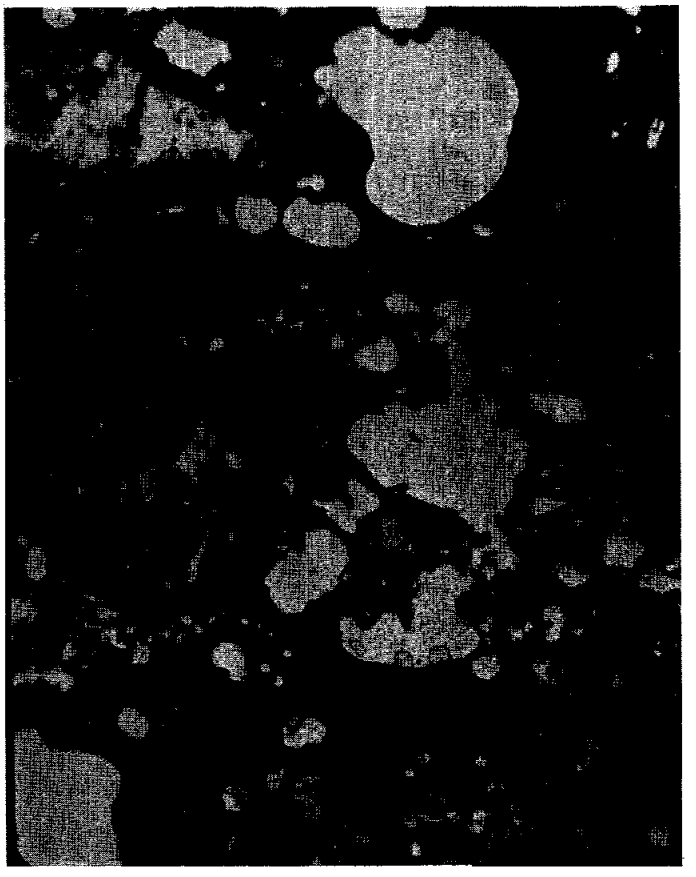

Figure 2. Photomicrograph of 15389,6. Transmitted light. Width about 2 mm.

15390 VESICULAR GLASS AND BRECCIA ST. 7 3.5 g

INTRODUCTION: 15390 is a dark vesicular glass with breccia either enclosed in or adhering to it (Fig. 1). Part of the glass appears to be frosted rather than fresh or shiny, and it is dusty in places. The sample was broken up during processing (Fig. 2) but no work has been done on the sample. It was collected as part of the rake sample on the north-east rim of Spur Crater.

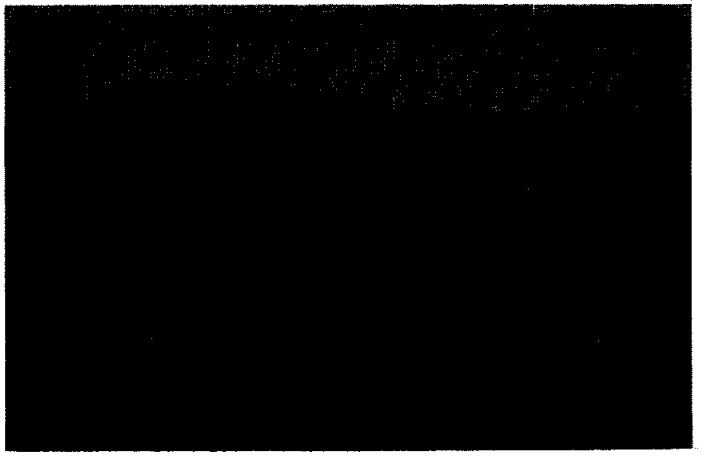

Figure 1. Pre-chipping view of 15390. S-71-49140

Figure 2. Chipping of 15390. ,0 is 2.3 g; ,1 is 0.56 g; and ,2 is 0.56 g.

15391 GLASS (WITH BRECCIA CLASTS?) ST. 7 0.30 g

INTRODUCTION: 15391 is a glass chip (Fig. 1). It appears to be a little vesicular and dusty, and may contain some breccia clasts. It has never been subdivided or allocated. It was collected as part of the rake sample on the north-east rim of Spur Crater.

Figure 1. Macroscopic view of 15391. S-71-49126

15392 GLASS ST. 7 0.40 g

INTRODUCTION: 15392 is a glass chip (Fig. 1). It is vesicular and dusty. It has never been subdivided or allocated. It was collected as part of the rake sample on the north-east rim of Spur Crater.

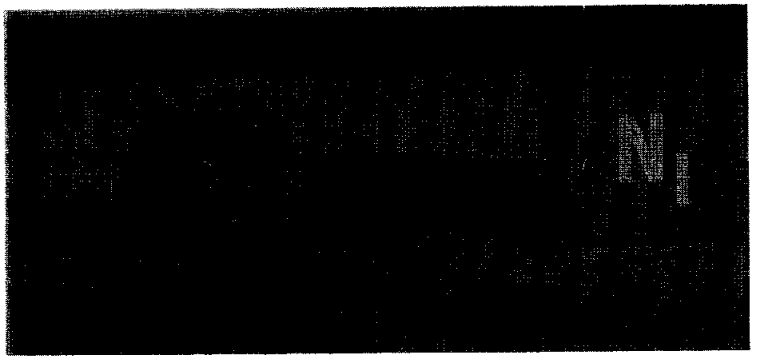

Figure 1. Macroscopic view of 15392. S-71-49136

15405 FINE-GRAINED IMPACT MELT (KREEP) ST. 6A 513.1 g

INTRODUCTION: 15405 is a fine-grained impact melt, of KREEP basalt composition and variolitic texture. It has a clast population limited to A15 KREEP basalts and quartz-monzodiorites ("QMD"), among the most rare-earth enriched of lunar samples, which are probably closely related to each other. Most radiogenic isotope systems of the QMD were disturbed ~0.6 to 1.2 b.y. ago, and possibly the impact melt was formed at that same time. Lead ages on zircons in QMD indicate an age of 4.37 b.y. (Compston et al. 1984).

15405 was the only rock sample collected at Station 6A, the highest location explored on the Apennine Front. It was chipped from the top of a distinctive isolated boulder which was sighted and identified as a sampling target en route to Station 6. The 3 m-long boulder has a prominent soil fillet on the upslope side and soil was present on top of the boulder: these greenish soils were also sampled.

The sample is blocky and angular, and extremely tough, with a medium gray to dark gray matrix (Figs. 1, 2). Although described as fractured in the Apollo 15 Lunar Sample Information Catalog (1974), it really resembles a block of a lava or welded slablets (Imbrium Consortium 1976; Marvin subsection p. 76). Although described in PET (1972) as closely resembling 15445 and 15455 from Spur Crater, 15405 is actually quite different in melt composition, texture, and clast population. It was originally studied cursorily in a Consortium headed by Murthy, and later studied by the Imbrium Consortium, whose reports are abbreviated below as ICR 1 (=1976) and ICR 2 (=1977).

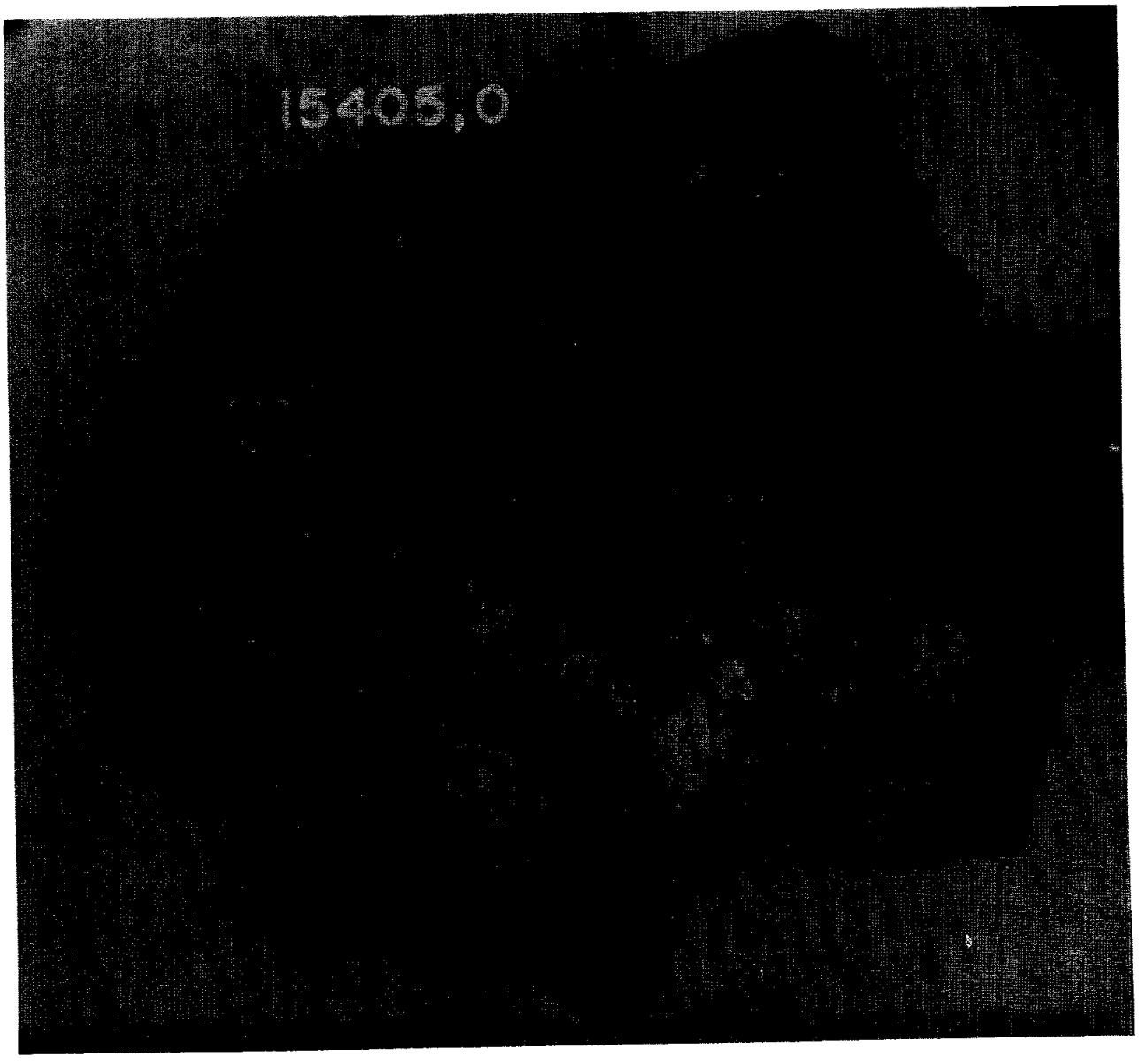

Figure 1. 15405,0 prior to sawcut in 1975; sawcut slab outlined.

PETROLOGY: The matrix, which makes up about 95% of the rock, is fine-grained and vesicular (Fig. 2). Mineral clasts and small (<1 mm) light-colored lithic clasts are common; a few lithic clasts are up to 1 cm. An important type of clast is speckled black-and-white (Fig. 3), and is an igneous KREEP-rich quartz-monzodiorite. Slabbing of the rock shows many clasts to be strung out as schlieren, sometimes quite porous, and the sample exhibits flow banding and lenticular fissureS (ICR 2, Marvin subsection, p. 19) (Fig. 2).

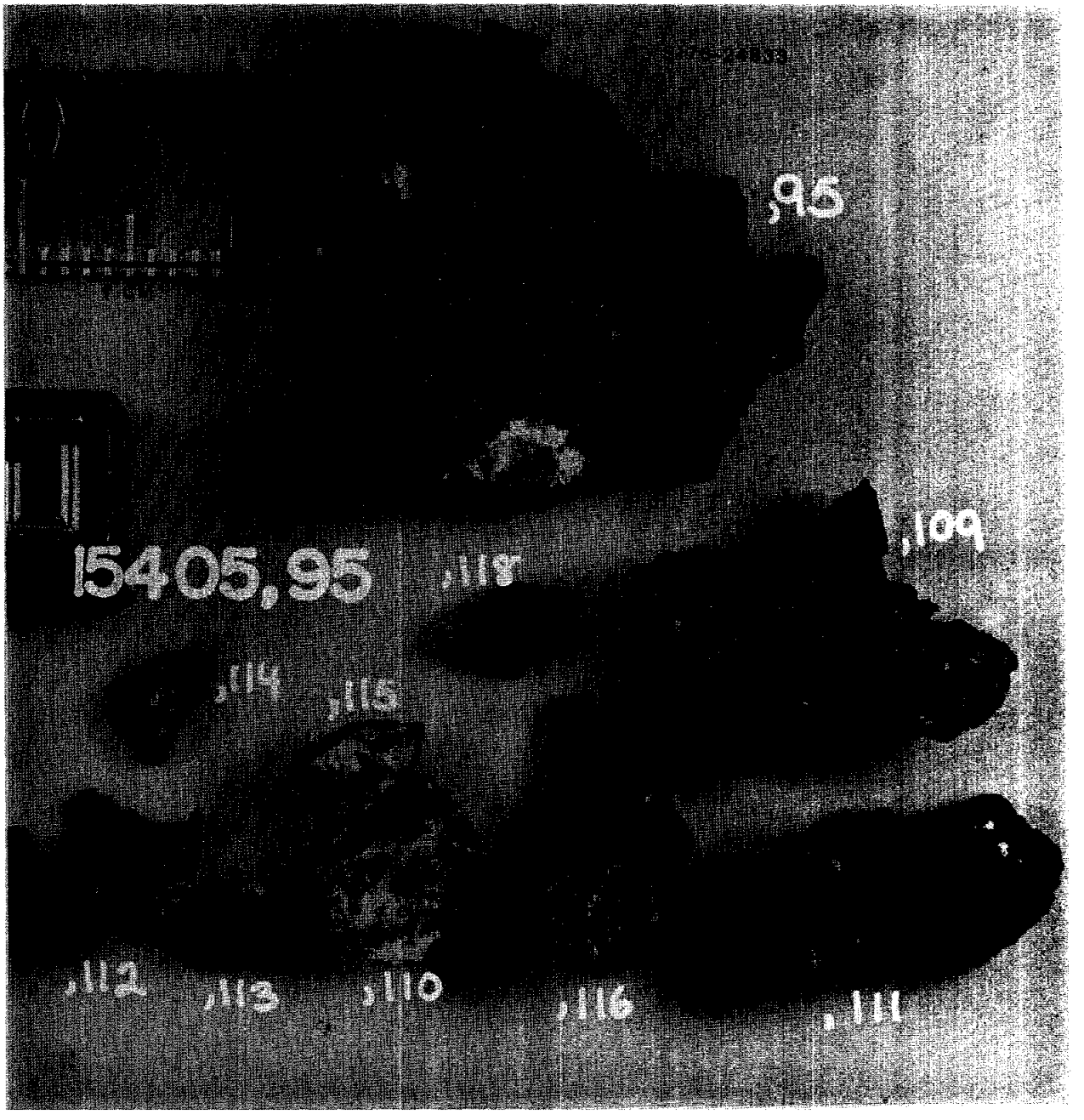

Figure 2. Subdivisions of slab 15405,95. Prominent white clasts are quartz-monzodiorite.

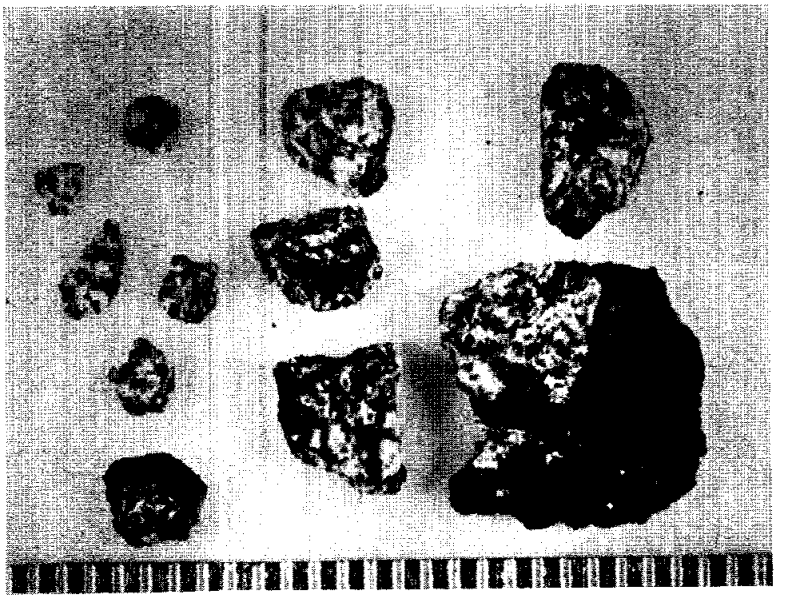

Figure 3. Quartz-monzodiorite clast A fragments. Scale is millimeters.

The petrography of the matrix and the clasts has been described by the Imbrium Consortium (ICR 1, subsections Marvin p. 76, Ryder and Bower p. 77, Taylor p. 94; and ICR 2, subsections Marvin p. 19, Ryder and Bower p. 20) and Ryder (1976). The matrix is an opaque, fine-grained, rather uniform, variolitic impact melt (Fig. 4) with a major and trace element composition similar to A15 KREEP basalts. It was classified as a subophitic impact melt by Simonds et al. (1975).It consists of plagioclase, pyroxene, and ilmenite laths with interstitial angular patches of glass. The melt texture does not define the foliation, which is instead defined only by some clast orientation and by the lenticular fissures and schlieren.

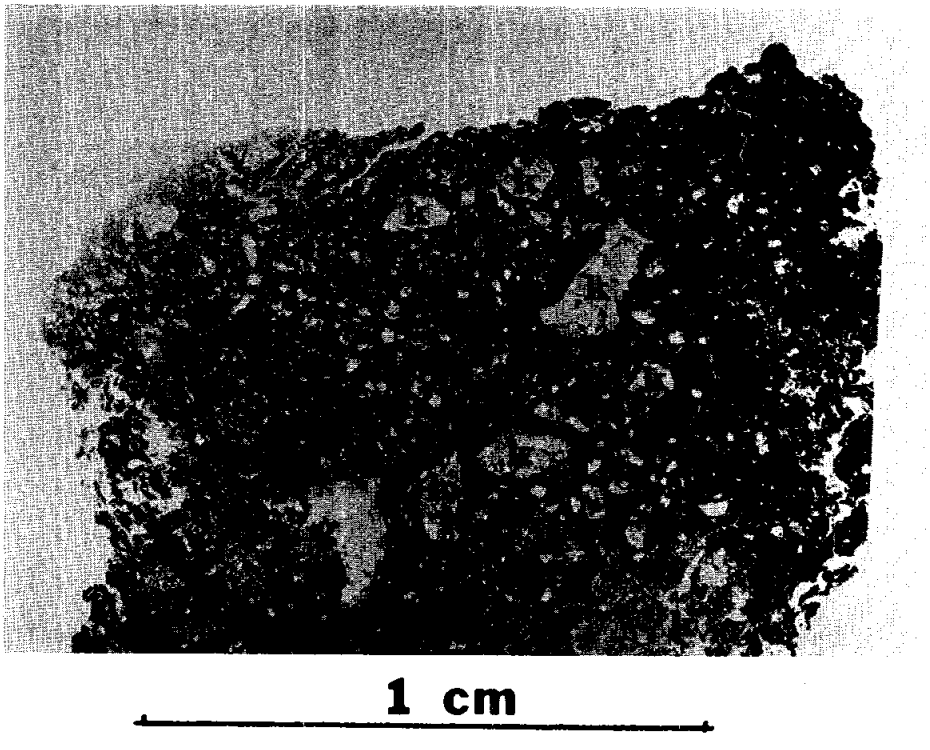

Fig. 4a

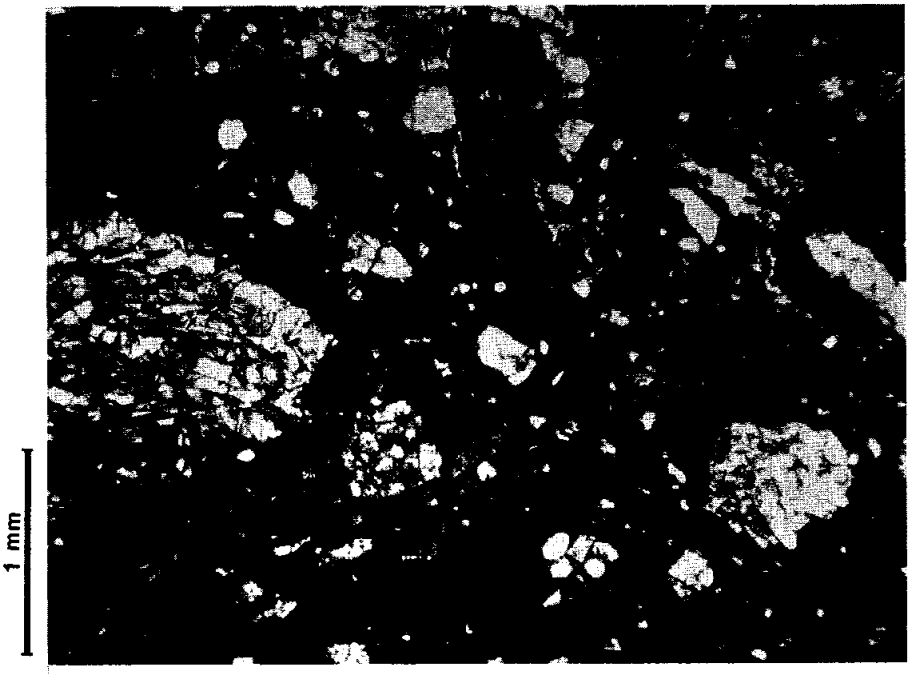

Fig. 4b

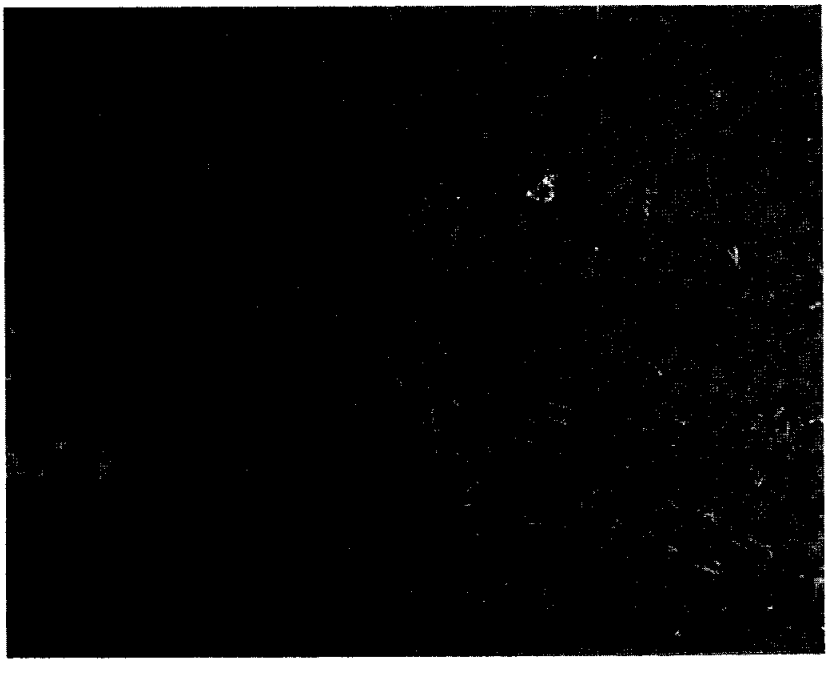

Fig. 4c

Figure 4. Photomicrographs of matrix of 15405. a) whole thin section 15405,12, transmitted light. K = KREEP basalt. g = QMD ("granite"). o = olivine-vitrophyre. b) 15405,11, transmitted light. c) melt matrix, 15405,11. Reflected light.

Lithic clasts are of two main types: A15 KREEP basalts with a variety of textures (Fig. 5), and quartzmonzodiorites (QMD), a more silicic, coarser-grained lithology (Fig. 6). Other clasts, such as granitic fragments (Ryder 1976) and Fe-metal rich fragments (ICR 2, Ryder and Bower subsection, p. 20) appear to be unrepresentative fragments of quartzmonzodiorite or at least closely related to them. The only other lithic clast-type identified in thin sections is a single small olivine-vitrophyric melt-rock (Fig. 4). Other rock types such as mare basalts, anorthosites, breccias, or glass are conspicuously absent. Virtually all the individual mineral fragments in the matrix are pyroxenes and plagioclases derived from A15 KREEP basalts or quartzmonzodiorites (Fig. 8).

Fig. 5a

Fig. 5b

Fig. 5c

Figure 5. Photomicrographs of KREEP basalt clasts, all to same scale, transmitted light.

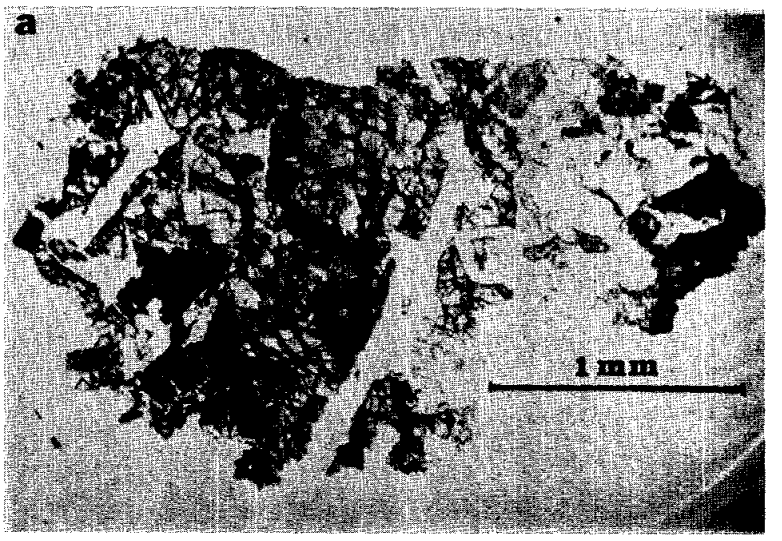

Fig. 6a

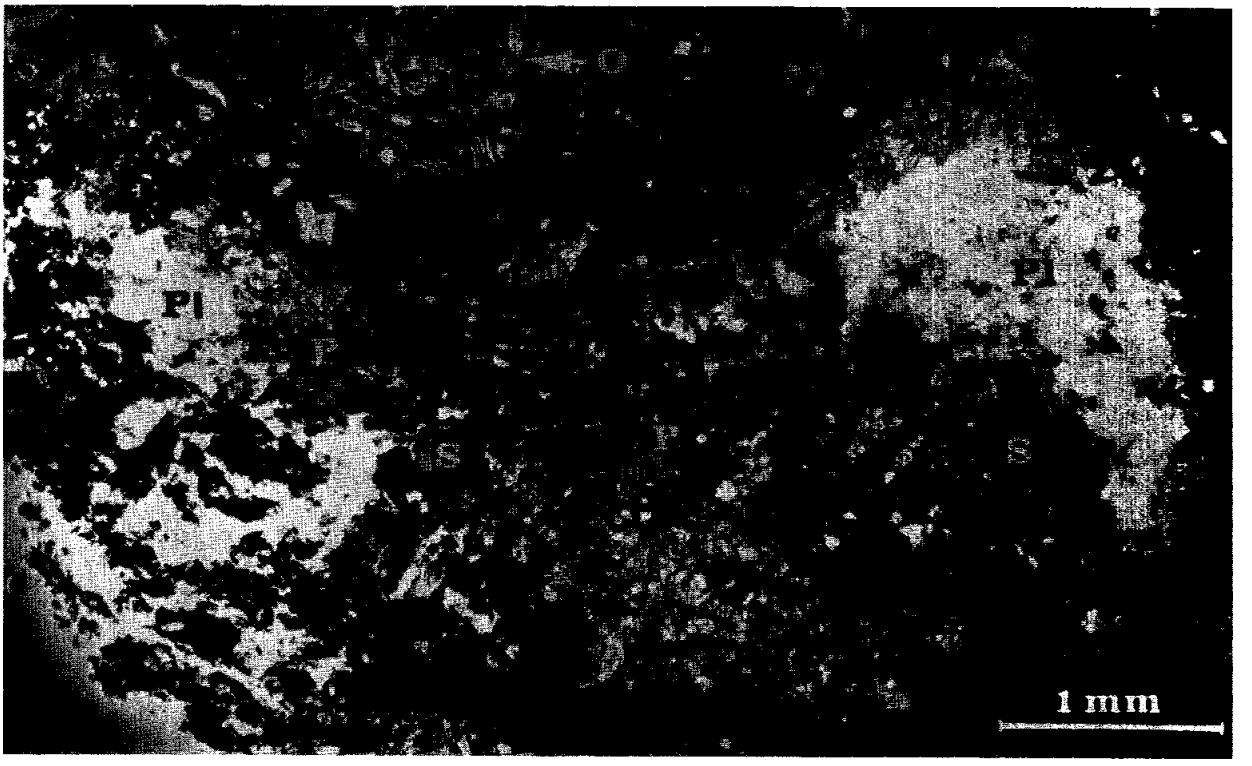

Fig. 6b

Figure 6. General photomicrographs of QMD. a) 15405,56, whole thin section, transmitted light. b) fragment in 15405,12 ("granite"). s = silica phase. Pl = plagioclase. p = pyroxene. o = olivine-vitrophyre

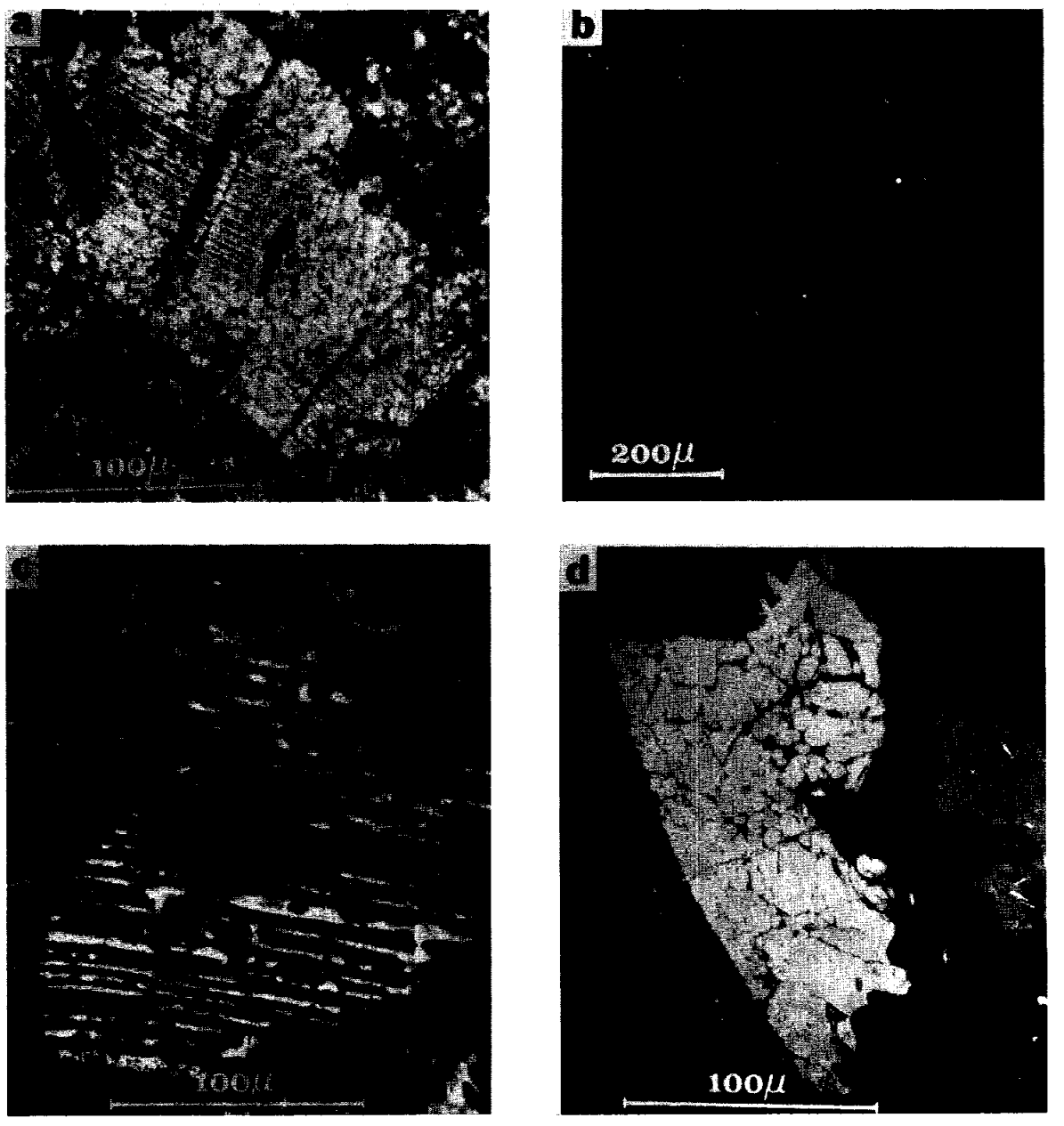

Figure 7. Photomicrographs of phases in QMD. a) exsolved ferroaugite (transmitted light); b) silica (dark gray with curved fractures), plagioclase (dark gray), and pyroxene (light gray) (reflected light); c) silica-potassium feldspar intergrowth (crossed polarizers); d) ilmenite (bright) with Si-K fine-grained mesostasis (reflected light).

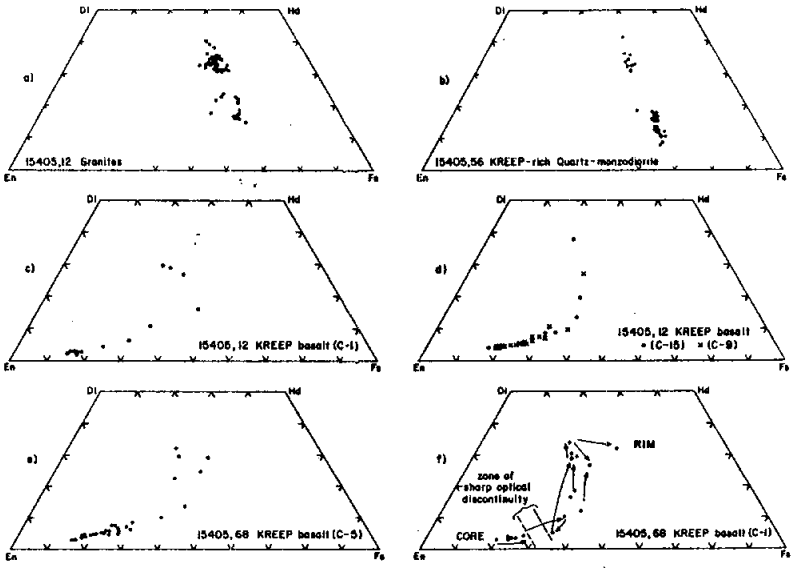

Figure 8. Compositions of pyroxenes in 15405 clasts.

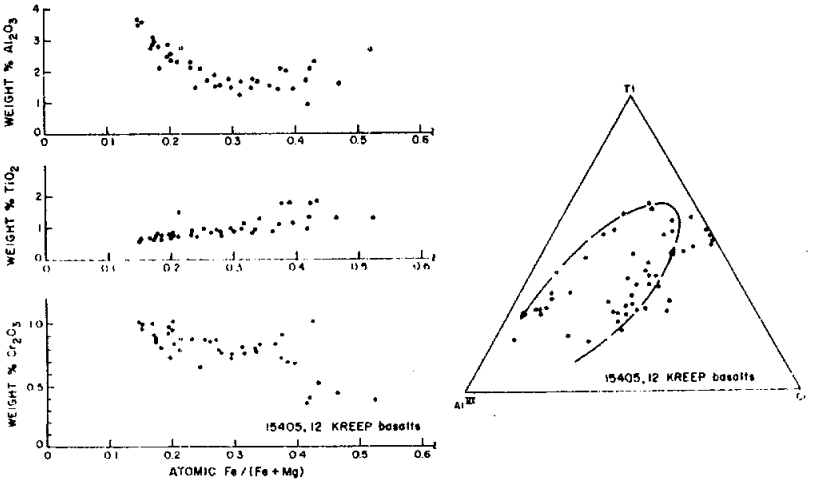

Figure 9. Minor elements in pyroxenes in 15405 KREEP basalts.

The KREEP basalt fragments are described by the Imbrium Consortium (ICR 1, Ryder and Bower subsection, p. 77) and, briefly, by Ryder (1976). They are texturally and mineralogically similar to other A15 KREEP basalts (Figs. 5, 8, 9, 11). They have a wide range of textures and grain-sizes, and consist mainly of plagioclase, zoned pyroxenes, and interstitial phases including cristobalite, ilmenite, phosphates, iron metal, and glass. Two small crystals of Mg-olivine have been identified in these basalts.

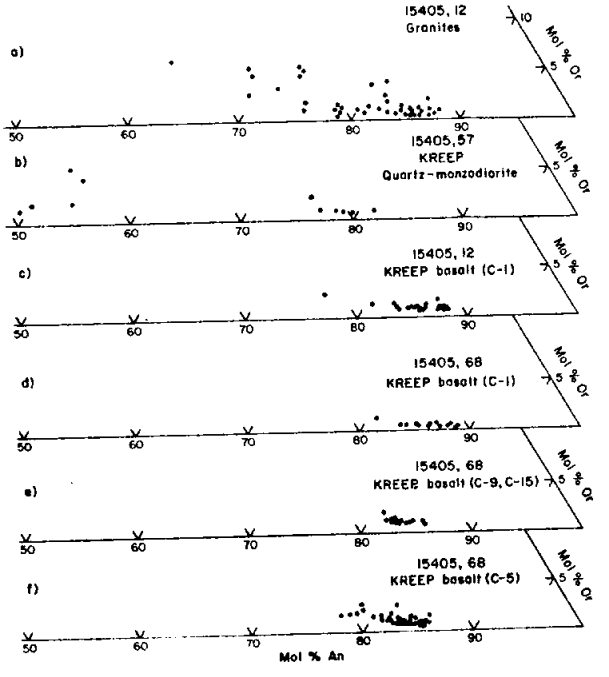

Figure 10. Minor elements in pyroxenes in 15405 QMD.

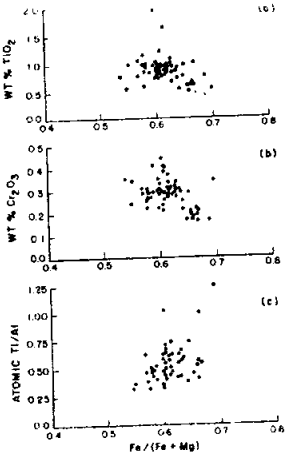

Figure 11. Compositions of plagioclases in 15405.

The quartzmonzodiorite clasts (Ryder 1976; G. Taylor et al. 1980; ICR 1, ICR 2), are less abundant than KREEP basalt clasts, but tend to be larger (e.g. Fig. 3). They tend to be more brecciated than the basalts (Fig. 6b); those with a better preserved texture are coarse basaltic, with plagioclase laths. However, they are not just coarse KREEP basalts--they have much more cristobalite and potash feldspar, have more equilibrated and iron-rich exsolved pyroxenes, and have plagioclase which is more sodic (Figs. 6, 7, 8, 10, and 11). The silica and potash feldspar phases are intergrown (Fig. 7c). Zircon, phosphate, and ilmenite are prominant, and fayalite and Fe-metal are present in some fragments. The mineral compositions (analyses or analysis plots in Ryder, 1976; G. Taylor et al., 1980; Takeda et al., 1981; and ICR 1, ICR 2) are similar to those in the end-products of KREEP basalt crystallization. G. Taylor et al. (1980) estimate a mode of ~35% each of pyroxene and plagioclase, 10-15% each of silica and potash feldspar, ~0.5 to 1.0% each of zircon, ilmenite, whitlockite, and minor chromite and Fe-metal (<0.02% Ni, 0.2% Co). Zircon chemical data is provided by Compston et al. (1984). The distinction originally made between "granites" and quartz-monzodiorites (Ryder, 1976) is probably not real, as the two types have identical mineral compositions; the "granites" are probably unrepresentative fragments of quartzmonzodiorites (ICR 2, Ryder and Bower subsection, p. 20).

The quartzmonzodiorites were deformed by shock and shock heating, disturbing the radiogenic isotope systems (below) and even melting pyroxenes in places (Takeda et al., 1981). Takeda et al. (1981) studied the composition, exsolution, inversion, and deformation of the pyroxenes using analytical TEM, single-crystal XRD, and microprobe techniques. In agreement with previous workers, Takeda et al. (1981) found that the quartzmonzodiorites contain two pyroxenes--a pigeonite and a subcalcic augite--each exsolved. Individual grains are homogeneous (except for exsolution) but there are slight differences among grains. Deformation is heterogeneous, and includes mechanical twinning, dislocations, and shock-heat-produced melting.

Ryder (1976), Nyquist et al. (1977), and Irving (1977b) suggested that QMD formed by fractional crystallization of a KREEP basalt magma. In contrast, Rutherford et al. (1976) suggested that silicate liquid immiscibility also played a part. This possibility was discussed by Ryder (1976) and G. Taylor et al. (1980) who found the chemical evidence to be largely against immiscibility. Ryder (1976) suggested a close relationship between the QMD and the KREEP basalt fragments in 15405 because of the chemical similarities and lack of other kinds of fragments in the samples.

CHEMISTRY: Analyses of matrix or bulk rock are listed in Table 1, and of clasts (mainly QMD) in Table 2. Rare earths for all analyzed lithologies are plotted in Figure 12. Table 3 lists microprobe-derived analyses of matrix and QMD.

The matrix/bulk rock has major and incompatible element abundances very like those of pristine KREEP basalts 15382 and 15386, and is presumably mainly derived from material like the KREEP basalt clasts within the matrix. There are discrepancies among analyses, probably resulting in part from varied clastic materials among splits, and in part from small sample sizes. The analysis by Laul and Schmitt (1972, 1973) of sawdust produced during rock processing has high MgO (and, by difference, low SiO_2) and is perhaps less reliable than other analyses. The matrix has siderophile element abundances elevated over those of pristine KREEP basalts (e.g., Ir ~1 ppb) indicating meteoritic contamination, but at rather low levels cf. most highlands breccias (Ir 5-10 ppb). The two different splits analyzed by Anders' group were assigned to separate projectile groups (2 and 3H; Hertogen et al., 1977) on siderophile ratios.

KREEP basalt clasts were only specifically analyzed in bulk with microprobe defocussed beam (Ryder and Bower, ICR 1) but the white clast fragment (A-1) analyzed by Ganapathy et al. (1973) has trace elements (Table 2) similar to the matrix and KREEP basalts rather than to QMD. While the Ir abundance (0.343 ppb) of the clast is non-pristine, it is very low and the sample was not assigned to any meteoritic projectile group (Hertogen et al., 1977). The remaining analyses in Table 2 are specifically of QMD fragments. These analyses demonstrate the evolved nature (Mg ~0.35; light REEs 500 to 700 x chondrites, among the highest reported for lunar samples) which lead to QMD being dubbed "super-KREEP" by Nyquist et al. (1977; ICR 2). The QMD is nearly uniformly enriched in REE abundances relative to the 15405 matrix, except for a deeper Eu anomaly. The analyses are quite consistent given the coarse grain size, and are consistent with the Nyquist et al. (ICR 2) contention that the high rare earth abundances well-represent bulk rock and do not result from an unrepresentative overabundance of some exotic mineral such as whitlockite. Siderophile element abundances demonstrate a lack of meteoritic contamination, and there is no doubt that QMD is an igneous rock type. Its major element composition places the lithology close to the Qz-Plag-Px eutectic in the Silica-Forsterite-Anorthite system. Nyquist et al. (1977, ICR 2) found the major and trace element abundances to be consistent with an origin by ~64% crystallization of KREEP basalt or by 34% partial melting of a KREEP basalt (quartz-normative) source, and that immiscibility is not involved in the petrogenesis, a conclusion also reached by G. Taylor et al. (1980).

TABLE 15405-1. Chemical analyses of bulk rock or matrix

		a	,5,A-5	,26	,63	,62	,59	,49	,117
Wt %	SiO2			51.49					
	TiO2	1.2		1.80					
	Al2O3	13.8		15.44					
	FeO	12.8		11.17					
	MgO	14		7.33					
	CaO	10.3		9.98				7.6	
	Na2O	0.547		0.81					
	K2O	0.40		0.82				1.4	0.7120
	P2O5		0.72		0.57				
(ppm)	Sc	23		23					
	V	91		22					
	Cr	2050		1500					
	Mn	1420		1500					
	Co	36		9.8					
	Ni			43	83				
	Rb		25.6	29	27.4				20.5
	Sr			190					168
	Y			360					
	Zr	500		1100					
	Nb			80					
	Hf	16.2							
	Ba	480		1200					767
	Th	10					16.2		
	U	2.3	5.105		4.690	3.1	3.93		
	Pb			6.0			9.64		
	La	46		55					78.7
	Ce	114							197
	Pr								
	Nd								120
	Sm	20.9							34.2
	Eu	1.45							2.27
	Gd								40.3
	Tb	3.6							
	Dy								44.2
	Ho								
	Er								28.0
	Tm								
	Yb	14		32					23.5
	Lu	2.1							3.32
	Li			24					36.8
	Be			9.7					
	B								
	C								
	N								
	S								
	F								
	Cl					53.3			
	Br		0.140		0.129	0.223			
	Cu			6.8					
	Zn		4.1	4.1	4.2				
(ppb)	I					0.6			
	At								
	Ga			4000					
	Ge		94		62.6				
	As								
	Se		89		78				
	Mo								
	Tc								
	Ru								
	Rh								
	Pd				1.7				
	Ag		2.9		2.22				
	Cd		16		17.7				
	In		1.0		1.47				
	Sn								
	Sb		0.81		1.06				
	Te		2.2		4.9				
	Cs		1160		1120				
	Ta	2000							
	W								
	Re		0.147		0.121				
	Os				1.16				
	Ir		1.64		1.28				
	Pt								
	Au		0.93		0.525				
	Hg				3.4				
	Tl		4.3		0.25				
	Bi		0.19						
		(1)	(2)	(3)	(4)	(5)	(6)	(7)	(9)

TABLE 15405-2. Chemical analyses of clasts

		,5,A-1	,86	,88(WRI)	,90	,87d	,85	,85	,152
Wt %	SiO2								(55.4)e
	TiO2								2.6
	Al2O3								11.9
	FeO							15.1	14.1
	MgO								3.8
	CaO				6.4				8.9
	Na2O							0.87	0.81
	K2O				2.8		1.71	1.8	2.1
	P2O5								
(ppm)	Sc							30.7	29
	V								33
	Cr							1220	1510
	Mn								1400
	Co							7.8	8.0
	Ni		<2						
	Rb	20.7	39.0			35.89	40.6		
	Sr					190.1	154		
	Y								
	Zr								1620
	Nb								
	Hf							51	44.7
	Ba						1490		1900
	Th			85.8				43	39.4
	U	4.105	11.500	17.4					11.1
	Pb			14.0					
	La						224	210	
	Ce						555	560	
	Pr								
	Nd						328		
	Sm						92.0	93	77.4
	Eu						2.69	2.52	2.75
	Gd						110		
	Tb							19.7	14.9
	Dy						116		101
	Ho								
	Er						71.7		
	Tm								
	Yb						60.9	65	55.2
	Lu						8.06	9.0	8.2
	Li						40.9		
	Be								
	B								
	C								
	N								
	S								
	F								
	Cl								
	Br	0.120	0.220						
	Cu								
	Zn	4.9	6.3					60	
(ppb)	I								
	At								
	Ga								
	Ge	160	345						
	As								
	Se	104	89						
	Mo								
	Tc								
	Ru								
	Rh								
	Pd		<0.9						
	Ag	2.5	2.15						
	Cd	9.8	18.9						
	In	1.0	45.2c						
	Sb	0.35	1.40						
	Te	1.9	9.4						
	Cs	920b	1190					1100	
	Ta							13,000	10,100
	W								
	Re	0.059	0.046						
	Os		0.007						
	Ir	0.343	0.0060						
	Pt								
	Au	0.25	0.051						
	Hg								
	Tl	3.7	5.8						
	Bi	0.21	0.31						
		(2)	(4)	(6)	(7)	(8)	(9)	(10)	(11)

References and methods for Tables 1 and 2:

(1) Laul and Schmitt (1973); INAA
(2) Ganapathy et al. (1973); RNAA
(3) Christian et al. (1976); XRF, etc.
(4) Gros et al. (ICR 1, 1976)
(5) Jovanovic and Reed (ICR 1, 1976); leaching; INAA
(6) Tatsumoto and Unruh (ICR 1, 1976); ID/MS
(7) Bernatowicz et al. (1978); argon isotopes
(8) Nyquist et al. (ICR 1); ID/MS
(9) Nyquist et al. (ICR 2); ID/MS
(10) Blanchard, unpublished; INAA
(11) Taylor et al. (1980); INAA

Notes:

(a) sawdust
(b) corrected value from Higuchi et al. (1975)
(c) doubtful value, contamination ?
(d) less than 44 micron fraction after grinding and sieving
(e) SiO2 by difference

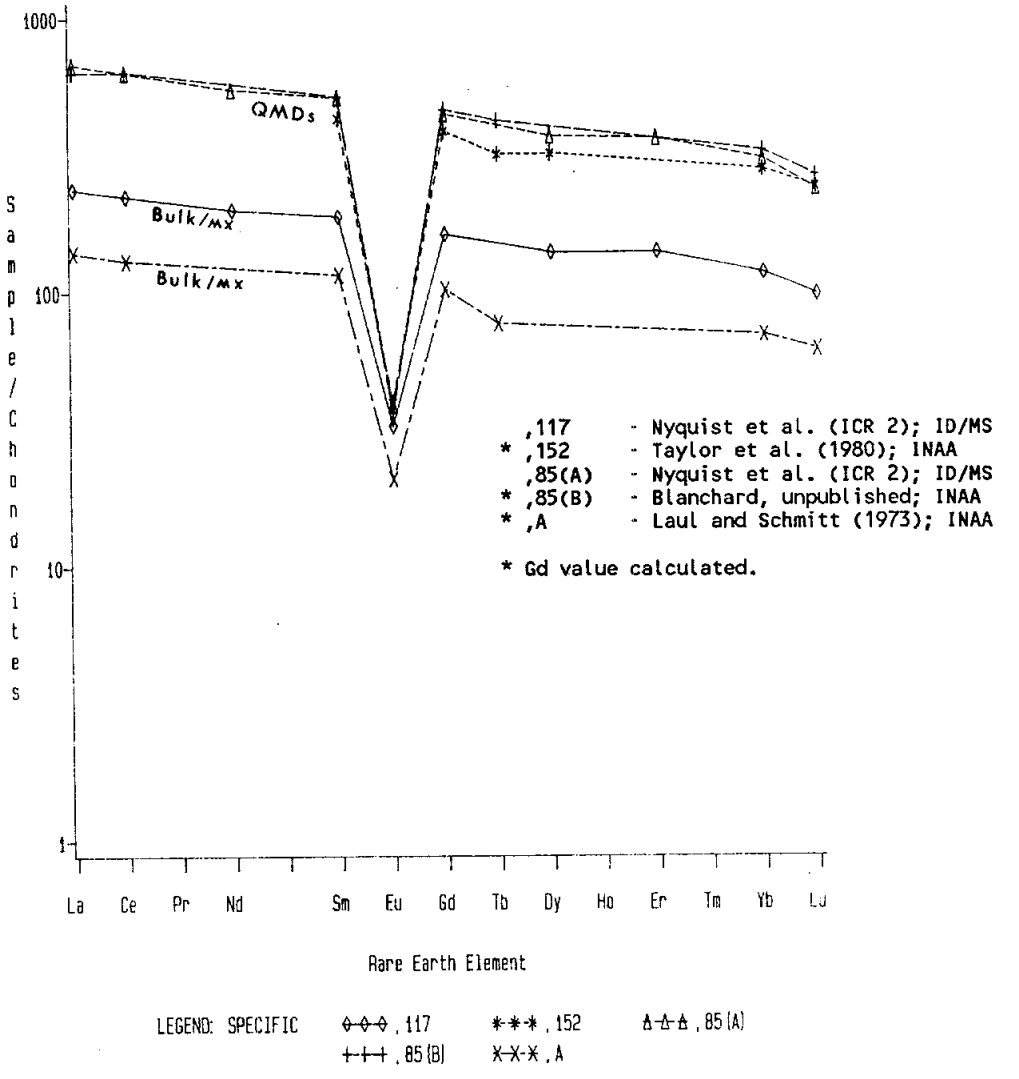

Figure 12. Rare earths in 15405 bulk rock/matrix, and QMD fragments.

TABLE 15405-3. Microprobe analyses of matrix and QMD in 15405

			Ts,12
Wt %	SiO2	57.4	49.7
	TiO2	1.1	1.6
	Al2O3	13.2	14.6
	FeO	11.2	10.7
	MgO	3.4	8.3
	CaO	9.0	11.8
	Na2O	1.0	0.84
	K2O	1.9	0.67
	P2O5	0.4	0.54
ppm	Cr		4300
	Mn		1200
	Zr	3000	
	Ba		1400
	La	183	
	Ce	413	
	Nd	287	
		(1)	(2)

References and methods:
(1) Ryder (1976); microprobe defocussed beam
(2) Taylor (ICR 1); mode/microprobe

STABLE ISOTOPES: Clayton et al. (1973) analyzed the oxygen isotopic composition of a matrix sample and a clast from 15405. The $\delta^{18}O$ of the matrix is 5.70‰, of the clast is 6.0‰. The clast is described as a "shocked troctolite with a salt-and-pepper appearance" and is almost certainly in fact a quartz-monzodiorite sample. A sample specifically of quartzmonzodiorite analyzed by Clayton (ICR 2) gave a $\delta^{18}O$ of 5.68‰, in no way exceptional for lunar rocks. The value demonstrates (by comparison with other lunar samples) that there is very little effect on the oxygen isotopic composition resulting from the igneous differentiation which produced acid rocks such as 15405 QMD and 12013.

GEOCHRONOLOGY AND RADIOGENIC ISOTOPES: The isotopic systems are generally disturbed, but indicate an age for the QMD greater than 4.0 b.y., likely greater than 4.2 b.y., and an age for the matrix melt of about 1 b.y. There is no indication of the 3.8 to 3.9 b.y. age which normally characterizes highlands breccias and A15 KREEP basalts.

Nyquist et al. (ICR 1; ICR 2; 1977) reported Rb-Sr isotopic data for the quartzmonzodiorite, including mineral separates, and for the melt matrix. The quartzmonzodiorite separates show that the Sr is extremely radiogenic, but scatters, with no linear array defined (Fig. 13). This provides only loose constraints on chronology, the whole rock data corresponding with a model age of 5.3 b.y. demonstrating open-system behaviour for the rock as a whole. Because the Sr is so radiogenic, the model age should approximate the true age. Correcting for Rb loss by assuming original K/Rb ratios, Nyquist et al. (ICR 2; 1977) found that the whole rock age could not be older than 4.4 b.y., and for a typical Apollo 15 KREEP K/Rb, the age would be $\sim$ 4.2 b.y. (Fig. 14). Younger ages cannot be excluded, but for the QMD and matrix to lie on a 3.9 b.y. isochron would require lower original K/Rb and greater Rb loss.

Bernatowicz et al. (ICR 2; 1977; 1978) attempted to date both the QMD and the matrix using the ^{40}Ar-^{39}Ar method. The QMD (,90) contains large amounts of trapped ^{36}Ar, which they believe to be a terrestrial atmospheric contamination. An intermediate temperature release plateau (800°-1100°C), in which 60% total ^{39}Ar was released, indicates a significant heating event at 1.29 $\pm$ 0.04 b.y. (Fig. 15a); there is however a large ^{40}Ar correction. The low temperature, low age may result from post-heating diffusion; the high temperature, high age may represent incomplete degassing of the QMD during the heating. For the matrix sample (,49) the correction for trapped ^{40}Ar is much more severe and precludes a clear age estimate. Qualitatively the releases are similar to those for the QMD, and in agreement with a 1.3 b.y. old heating event (Fig. 15b).

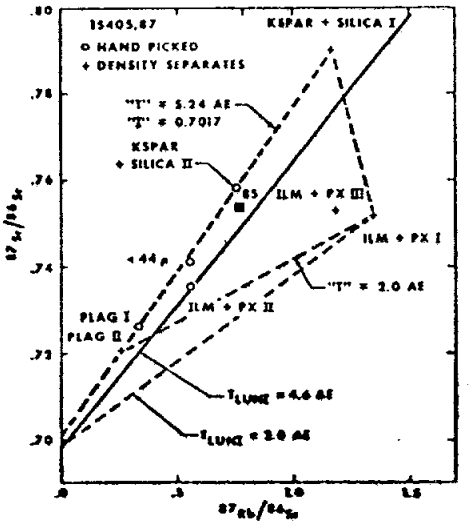

Figure 13. QMD Rb-Sr data (Nyquist et al., 1977).

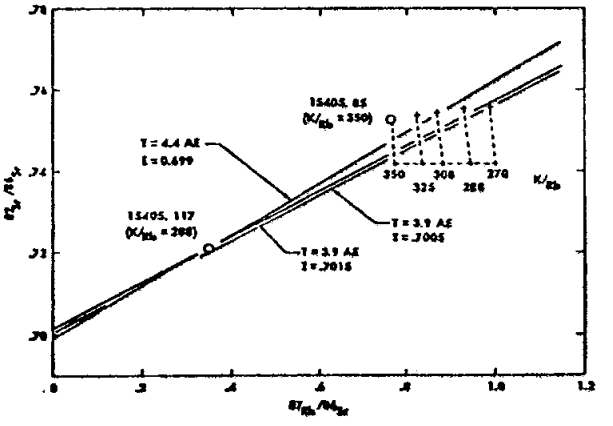

Figure 14. "Corrected" 15405 Rb-Sr isochron (Nyquist et al., 1977).

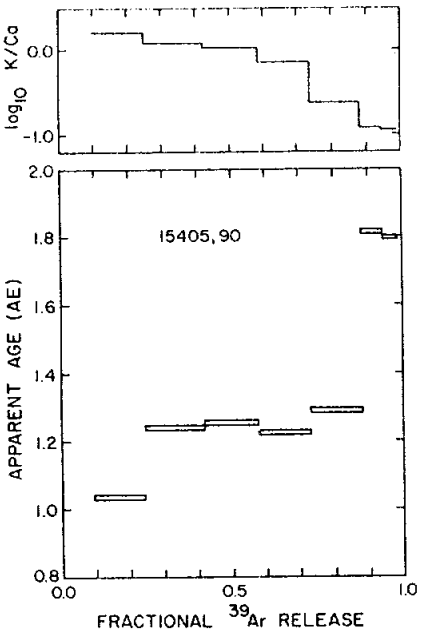

Fig. 15a

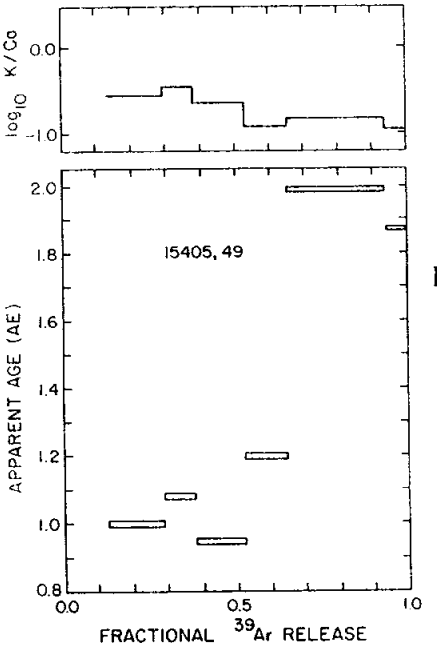

Fig. 15b

Figure 15. Ar release diagrams a) QMD ,90; b) matrix ,49 (Bernatowicz et al., ICR 2).

Tatsumoto and Unruh (ICR 1; 1976) and Unruh and Tatsumoto (1977) reported U, Th, and Pb isotopic data for whole rock and mineral separates of the QMD and for the matrix. The QMD contains the highest U and Th thus far analyzed for a lunar sample, and rather radiogenic Pb. The matrix is not so radiogenic and its U, Th, and Pb characteristics are typical of KREEP basalts. The U-Pb evolution (Fig. 16) demonstrates a complicated clast history with at least three events, including an event at 0.6 to 1.2 b.y. which disturbed the system. Making the assumption that U-Pb was closed during all but one of the recent disturbances leads to an age of 4.0 ± 0.1 b.y. for the QMD; this is merely a model age, with the additional disadvantage that it is poorly defined. A line joining the whole rock QMD and 15405 matrix points interceding concordia at ~4.2 and ~1.9 b.y. ago, substantially different from the "cataclysm" line characteristic of most highlands breccias.

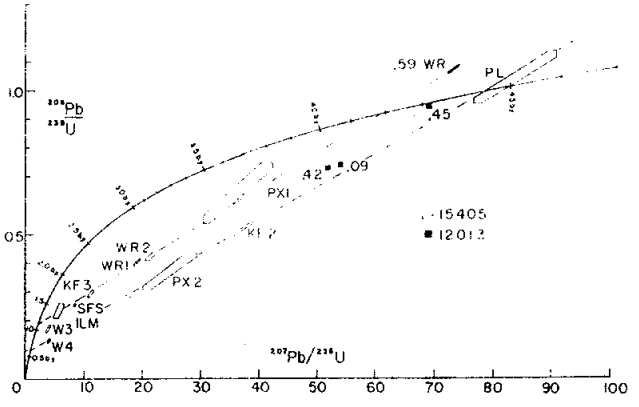

$^{206}Pb/^{238}U$ vs. $^{207}Pb/^{235}U$ evolution diagram for mineral separates and whole-rock analyses of 15405,88 and a whole-rock analysis of 15405,59. The data are corrected for meteorite primordial Pb ($^{206}Pb/^{204}Pb = 9.307$, $^{207}Pb/^{204}Pb = 10.294$; Tatsumoto *et al.*, 1973) so the upper concordia intercepts of the broken lines do not have any age significance. The lower intercepts and the scatter in the data indicate a young event (or events) of about 0.6–1.2 b.y. WR1 plots in a different place than previously reported in our abstracts (Tatsumoto and Unruh, 1976; Unruh and Tatsumoto, 1976) due to an erroneously calculated Pb concentration. Hexagons correspond to the calculated uncertainties for the data.

Figure 16. U-Pb evolution for 15405 materials (Tatsumoto and Unruh, 1976).

Compston et al. (1984) used a high resolution microprobe (SHRIMP) to analyze U,Th, and Pb in four zircon grains for the QMD. One is strongly discordant (60% Pb loss), the remainder vary from a few percent to 25% Pb loss. The locus of loss corresponds to an event at 1.4 b.y. Extrapolation to concordia gives an intersection at 4.365 ± .030 b.y., and one spot in one zircon contained Pb which can be interpreted as signifying the presence of a significantly older inclusion within the zircon. Highly radiogenic Pb was also found in plagioclase. As with the other isotopic systems, there is no record of the 3.8 or 3.9 b.y. event common to most highland breccias.

Podosek and Walker (ICR 1) found that fission tracks in a whitlockite in a chip of QMD correspond with a heating event 0.5 to 1.5 b.y. ago.

RARE GAS, TRACKS, AND EXPOSURE: Drozd et al. (1976) and Podosek and Walker (ICR 1) reported Ne, Kr, and Xe isotopic ratios for one matrix sample. The ^{21}Ne exposure age is 6 m.y., that of ^{81}Kr is 11.4 ± 1.1 m.y. The sample does not contain fission xenon in excess of that expected from in situ decay of ^{238}U and ^{244}Pu, and does not contain large amounts of solar wind gas. Bernatowicz et al. (1977, 1978) reported Ar isotopic ratios and abundances for samples of matrix and a QMD clast for varied temperature releases (see GEOCHRONOLOGY section).

Fleischer and Hart (1972, 1973) measured track density, track stability, and U in a matrix sample. Pyroxene and feldspar have an average density of $(2.82 \pm 0.54) \times 10^5$ tracks per cm^2. Most grains are distorted and this density is for undistorted areas. The density is low indicating a brief surface residence time--equivalent of 5 to 6 m.y. at 6 cm depth and 0.5 to 0.6 m.y. at 1 cm deep. Podosek and Walker (ICR 1) also measured tracks in a matrix sample, finding an approximately 10 m.y. surface exposure age.

PROCESSING AND SUBDIVISIONS: Early subdivision was made from loose and chipped pieces (Fig. 17). The 38.5 g chip ,5 was allocated to Murthy for consortium study; sawdust from its subdivision by Murthy was used by Laul and Schmitt (1972, 1973). Thin sections (,2, 3, 10-,16) were made from fragment ,1.

Subdivisions for the Imbrium Consortium are documented by Marvin (ICR 1, ICR 2), and included chipping ,0 and picking from ,8, a collection of chips and fines, for matrix, exterior surface, and quartzmonzodiorite separations. Subsequently the main piece ,0 was sawn (Figs. 1, 2) to produce slab ,95, from which many allocations were made. A summary of all the thin sections cut from 15405 is shown in Table 4.

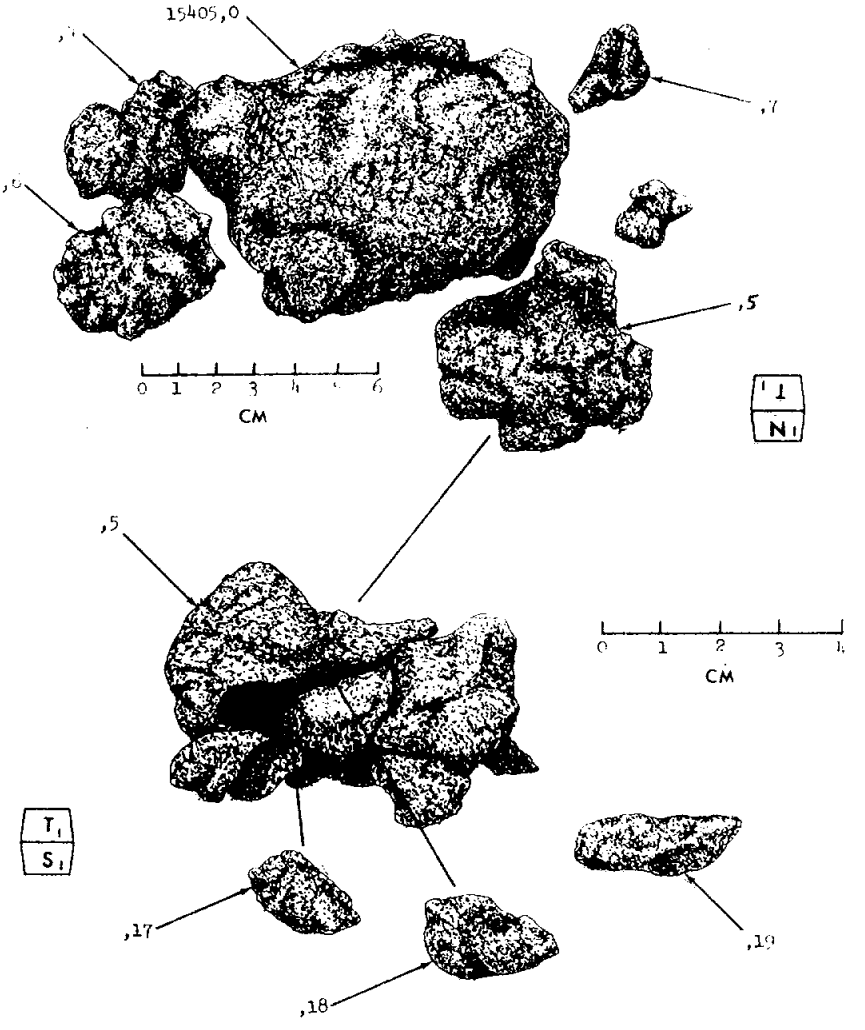

Figure 17. Original splitting of 15405.

TABLE 15405-4. Thin sections of 15405

NUMBER	LINEAGE AND PARENTAGE	DESCRIPTION
,2 ,3 ,10-,16 ,33 ,34 ,35	,1 ⟵ ,0 ,29 ⟵ ,6	matrix and clasts matrix and clasts
,54 ,55 ,56 ,57	,50 ⟵ ,8 ⟵ ,0 ,52 ⟵ ,8 ⟵ ,0	matrix and clasts quarzmonzodiorite
,68 ,69 ,70	,61 ⟵ ,7 ⟵ ,0	matrix and clasts
,145 ,146 ,147	,138 ⟵ ,95 ⟵ ,0	matrix and clasts. ,145 contains QMD
,166	,86 ⟵ ,6 ⟵ ,0	quartzmonzodiorite

15415 FERROAN ANORTHOSITE ST. 7 269.4 g

INTRODUCTION: 15415 ("Genesis Rock") consists almost entirely of anorthite, and is a coarse-grained, ferroan crystalline rock with a complex cataclastic and metamorphic history. It was originally a plagioclase cumulate from a liquid with a near-chondritic rare earth pattern and rare earth abundances perhaps 10x chondrites. The source of the 15415 parent liquid was separated from a chondritic Rb/Sr reservoir very early in lunar history. Ar-Ar ages of ~4.0 b.y. probably represent later heating events, not original igneous crystallization.

15415 is a pale, blocky, angular to subrounded sample, which was originally partly dust-covered (Fig. 1). Some individual pieces are tough, but penetration fracturing makes some portions friable. The surface was hackly on fresh faces; zap pits were present on only one (S) surface. 15415 was collected from the northern lip of Spur Crater, where it was perched on a clump which was sampled as 15435 to 15437. It is generally believed (e.g., Wilshire et al., 1972) that 15415 was a clast in a friable soil breccia or clod represented by the clump. It rested on a gentle slope of several degrees to the south towards the bottom of Spur Crater. It was especially noted by the Apollo 15 crew as "something close to anorthosite, because it's crystalline and .... just almost all plag." (Bailey and Ulrich, 1975).

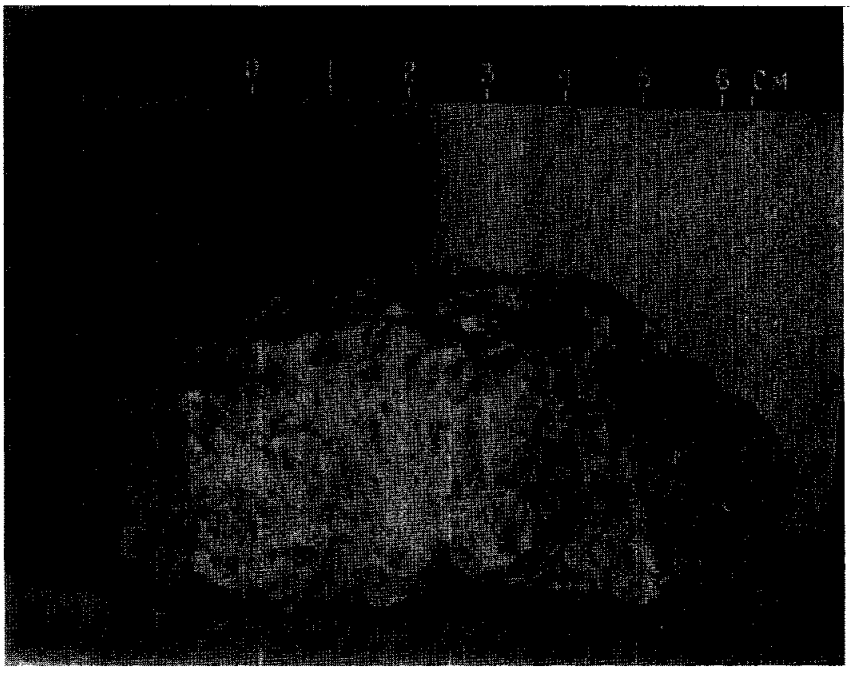

Figure 1. Pre-split view of ,0, showing white anorthosite and gray dust. S-71-44998

PETROLOGY: 15415 consists almost entirely of anorthite crystals, with minor iron-rich mafic minerals consisting mainly of diopsidic augite, and traces of hypersthene, ilmenite, and a silica mineral. The plagioclase content may be greater than 99%, but the textural heterogeneity precludes an accurate modal determination from single subsamples. The textures (Fig. 2) demonstrate a complex cataclastic and metamorphic history, following an origin by accumulation from a plagioclase-saturated magma.

Fig. 2a

Figure 2. Photomicrographs of 15415, all crossed polarizers, all widths about 2 mm except g and h, whose widths are about 300 microns. a) 15415,19, general view: polygonal grains with curving boundaries, fracturing, and mechanical twins. b) 15415,15: bands of small polygonal plagioclases cutting single large plagioclase. c) 15415,19: cataclasized, annealed region. d) 15415,94: large shock deformed plagioclase crystals. e) 15415,92: pyroxenes (arrows) along plagioclase grain boundaries. Large plagioclase in bottom left shows parallel fractures and mechanical twins. f) 15415,19: large plagioclase at bottom shows inclusions of plagioclase (e.g., arrows); rectangle in top center shows augite at triple junction. g) 15415,19: blow-up of rectangle in (f) showing two augites at plagioclase grain boundaries. h) 15415,19: pyroxene inclusions in large plagioclase.

Fig. 2b

Fig. 2c

Fig. 2d

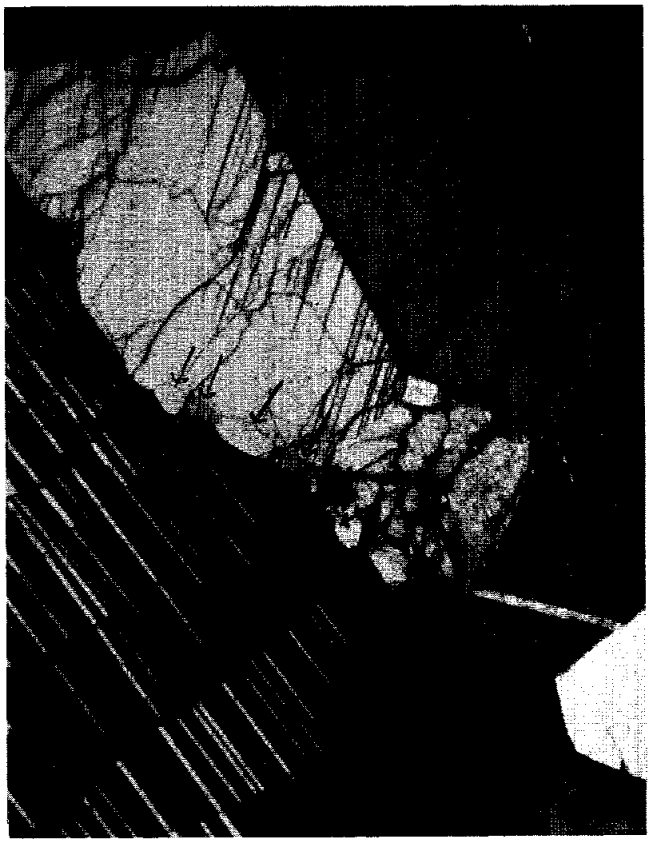

Fig. 2e

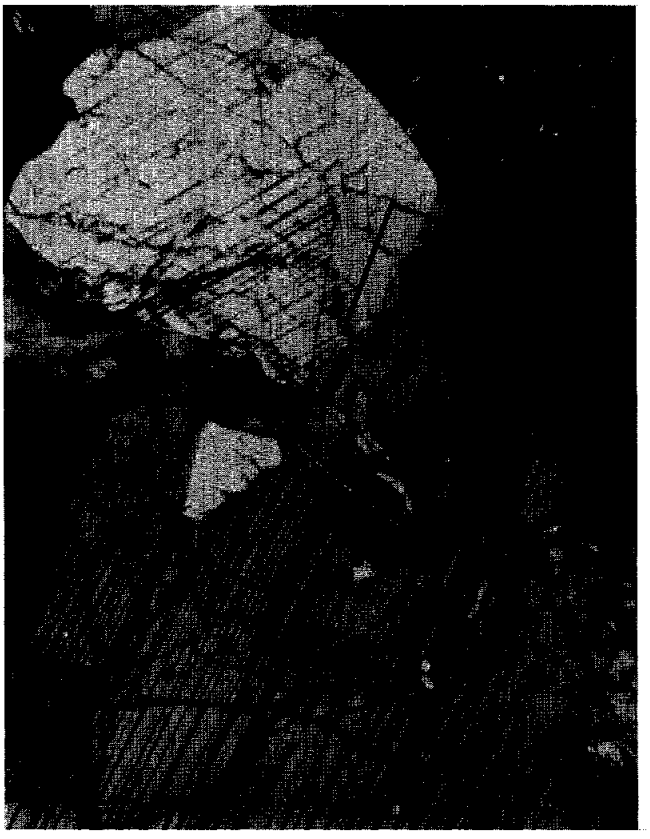

Fig. 2f

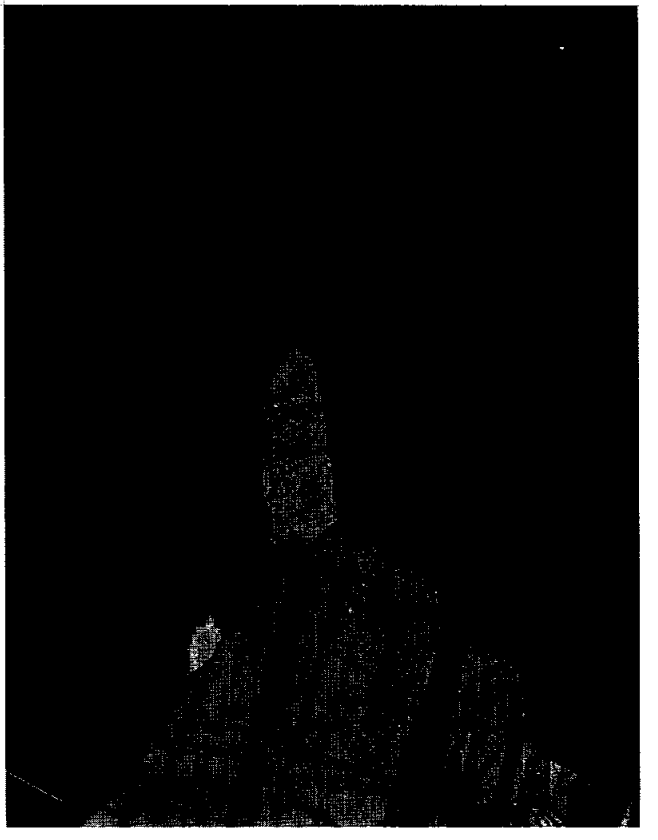

Fig. 2g

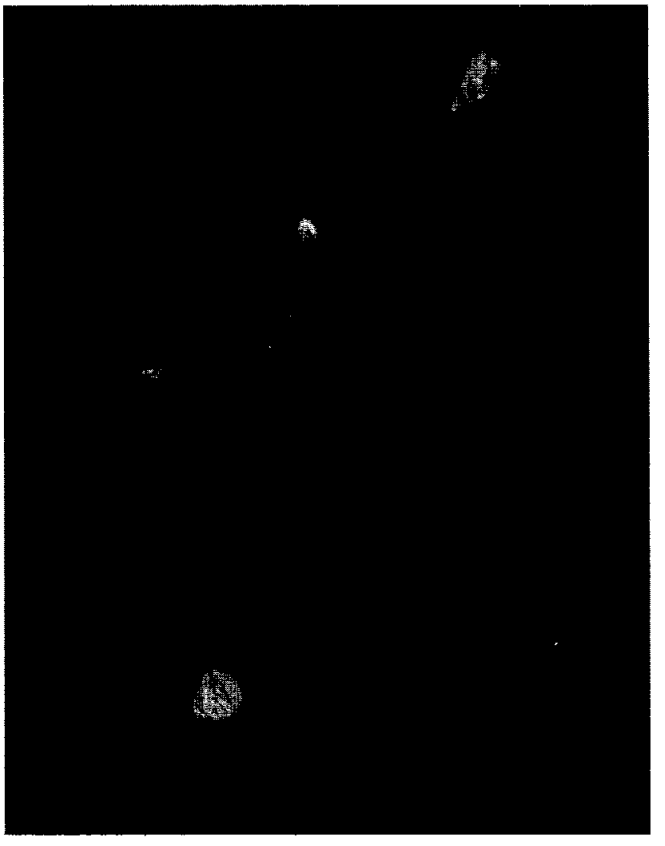

Fig. 2h

Comprehensive descriptions and interpretations were provided by James (1972), Hargraves and Hollister (1972), Steele and Smith (1971), Wilshire et al. (1972), and Stewart et al. (1972), and are in essential agreement. Dixon and Papike (1975) included 15415 in their Group 1, the group of least-shock-damaged anorthosites. The plagioclase is highly inequigranular, with the largest grains up to 3 cm (as seen in hand specimen) and down to below resolution. In thin section, the largest grains are anhedral and form a coarse granular mosaic. Intermediate-sized grains (1.3 to 0.1 mm) form polygons with plane or smoothly-curving boundaries, in patches which cut the larger grains. Both textural types are cut by pervasive shear fractures and contain abundant deformation features, including extinction variation and mechanical twinning. Both primary and deformation twinning include pericline and albite twins. Diopsidic augite forms equant inclusions in plagioclase; polygons along grain boundaries; polygons intergrown with polygonal plagioclase; and then septa between large plagioclase grains. All are tiny (less than

200 microns), and some show exsolution (both pigeonite and orthopyroxene recognized). Augite shows the same deformation features as plagioclase, but not so abundantly developed. Hargraves and Hollister (1972) found that four augite grains in their thin section had their optic planes and c-axes more or less parallel, suggestive of the grains being a single poikilitic crystal. Hypersthene forms rare discrete grains; there is no optical evidence that it crystallized as pigeonite according to Hargraves and Hollister (1972), whereas Stewart et al. (1972) specifically noted pigeonite as well as orthopyroxene. Ilmenite occurs within pyroxene grains, and the silica occurs in several modes, included in plagioclase for example. Wilshire et al. (1972) tentatively identified traces of apatite and olivine, but neither phase has been confirmed. Hewins and Goldstein (1975) found and analyzed three minute grains of Ni- and Co-free iron metal.

Microprobe data is generally consistent. The plagioclase compositions are calcic and homogeneous (Table 1), although Hargraves and Hollister (1972) used step-scanning to find a slight compositional variation. A single analysis (An_{96-8}) listed by Dixon and Papike (1975) is consistent with the data in Table 1. Hansen et al. (1979) also reported precise microprobe analyses for MgO (0.05 ± 0.006%), FeO (0.102 ± 0.011%), and K_2O (0.023 ± 0.005%) (uncertainties 1 sigma), averages for 30 analyses of plagioclase. Ion microprobe analyses for several trace elements are listed in Table 2. The data are fairly consistent with each other and with other analyses (e.g., isotope dilution for plagiophile elements, microprobe for K, Mg). Palme et al. (1984) reported INAA analyses for five plagioclase separates (Table 3), showing the low abundances of rare earths and transition metals. Schurmann and Hafner (1972) performed Mossbauer analysis on carefully handpicked plagioclases, finding two distinct Fe^{2+} peaks, with a spectra indistinguishable from lunar basalt plagioclases. The data indicate a rapid crystallization and cooling event at some time later than the plutonic crystallization; heating to 1000°C for two days produced no change. They determined $Fe^{3+}/(Fe^{2+} + Fe^{3+})$ to be 0.04. Niebuhr et al. (1973) used electron spin resonance on three millimeter-sized anorthite single crystals to confirm that about 1% of the iron is ferric (in the tetrahedrally co-ordinated Al^{3+} position).

Lally et al. (1972), Heuer et al. (1972a,b), and Nord et al. (1973) reported and discussed HVEM crystallographic data. Plagioclase grains showed undeformed albite and pericline twins, and all contain 1 to 2% augite inclusions. A thin section showed fracture and deformation of twins; many regions were free of deformation, but others showed deformation and recovery (dense arrays of dislocations, etc.). The c-type domains are large and easily imaged. Strong "c" and "d" type diffraction spots indicated P $\bar{1}$ symmetry; samples were heated to observe the I $\bar{1}$ to P $\bar{1}$ phase transition. Czank et al. (1973) made precession photographs of the (b*c*) reciprocal lattice plane in plagio-

TABLE 15415-1. An-contents of plagioclases

Reference	Average	Range
James (1972)	96.6 ± 1.2	
Hargraves and Hollister (1972)		96-98
Steele and Smith (1971)	97.6	96.7-99.0
Lally et al. (1972)		93-95
Stewart et al. (1972)	96.5	
Hansen et al. (1979)	96.1	

TABLE 15415-2. Trace elements in plagioclase, ion probe analyses (ppm)

Reference	Ab %	Li	Mg	K	Ti	Sr	Ba
Meyer et al. (1974)		1.6	280	190	90	177	9
Steele et al. (1980)	4.3	2.0	305	60	75	200	6.5
Meyer (1979)		2.6	300				13
Meyer (1979)		1.7	300	91		190	10

TABLE 15415-3. INAA analyses of five plagioclase separates (Palme et al., 1984)

Weight, mg.		42.5	34.5	265	615	816
Na	ppm	2670	2570	4014	4320	4300
Sr	ppm	191	212	246	220	232
Eu	ppb	790	740	1290	1280	1270
Ba	ppm	6	7	21	22	22
La	ppb	140	120	364	391	385
Sm	ppb	38	35	108	103	112
Yb	ppb	<14	<14	32	23	28
Lu	ppb	--	<2	2.4	1.6	2
Fe	ppm	1130	1050	1200	690	852
Sc	ppb	157	155	270	120	216
Cr	ppm	3.6	1	8.5	1.9	3.6
Co	ppb	320	358	88	12	15
Mn	ppm	--	--	40	24	29

clase. Strong c-reflections are consistent with a high An content and a slow cooling rate. Stewart et al. (1972) reported optical properties and powder diffraction data. They also reported single crystal x-ray and electron diffraction results, finding the space group to be P1, and the properties indicate a high degree of short and long range order.

Pyroxene compositions were reported by James (1972), Hargraves and Hollister (1972), Steele and Smith (1971), Stewart et al. (1972), and Evans et al. (1978). Data are consistent (Fig. 3), generally about $En_{40}Wo_{45}$ for host augites, and about $En_{57}Wo_3$ for exsolved hypersthene. Stewart et al. (1972) interpreted the first crystallized pyroxene to have been augite, followed by pigeonite; both became more Fe-rich by fractional crystallization. They estimated crystallization at 1150°C for one augite, and 1030°C for a pigeonite, from comparison homogenization experiments. Evans et al. (1978) made a detailed study of the crystal structure and thermal history of a single crystal of untwinned orthopyroxene, giving crystallographic data. They found a space group Pbca, and a high degree of order expected for metamorphishm at 500°C, or even lower. There was no post-metamorphic thermal event which disordered it, so the 4.05 b.y. Ar-Ar age (Turner, 1972; Husain et al., 1972) is interpreted as the age of termination of the metamorphism. Post-4.05 b.y. events, which produced only a little Ar loss, had no effect on the pyroxene ordering. Smith and Steele (1974) described the pyroxene occurrences and compositions, and found that the (Fe/Mg) augite(Fe/Mg) orthopyroxene is 0.55, like terrestrial granulites, and unlike the 0.73 or so of terrestrial igneous rocks, again suggesting meta-morphism. The Mg/Fe distribution between ilmenite and low-Ca pyroxene suggests 650°C to 800°C. Smith and Steele (1974) suggested that plagioclase exsolved pyroxene plus silica plus ilmenite, questioning the assumption of any primary pyroxene. If the pyroxene were primary, the parent magma for 15415 would have atomic Mg/(Mg+Fe) of about 0.4; if exsolved, then parental Mg/(Mg+Fe) would be about 0.8, a very significant difference.

Roedder and Weiblen (1972) reported that a large number of inclusions, most less than 1 micron across, outline the main fractures. The inclusions were too small for positive identification, but some appear to be gas (sic) (which is probably a typographic error and intended to be glass), others presumably pyroxene. Simmons et al. (1975) used 15415,91 to illustrate shock-induced cracks which are subparallel, trans-granular fractures. They believed that the granulated grain boundaries were a product of cataclasis (tectonic) rather than impact.

CHEMISTRY: Chemical analyses for bulk rock 15415 are listed in Table 4, and the rare earths plotted in Figure 4. The main features of the data are the high alumina and low iron, the high iron/magnesium ratio, the low abundance of rare earths, and the lack of meteoritic siderophile contamination, features remarked

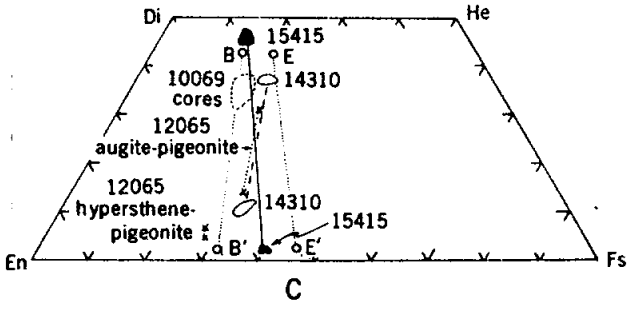

Fig. 3a

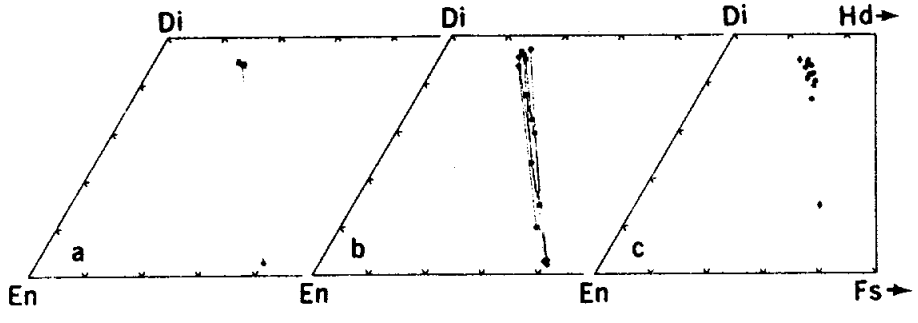

Fig. 3b

Figure 3. Compositions of pyroxenes in 15415. a) from Hargraves and Hollister (1972); b) from James (1972).

TABLE 15415-4. Chemical analyses of bulk samples

		,123	,0	,11	,11	,11	,12(e)	,177	,177			,40 P-1	,40P-2	,40C	,0	,?
Wt %	SiO2	44.08					44.94									
	TiO2	0.02		0.025	0.016		0.02									
	Al2O3	35.49					35.72		35.5							
	FeO	0.23					0.21	0.199	0.202							
	MgO	0.09		0.16			0.53		<0.5							
	CaO	19.68					20.58		21.0							
	Na2O	0.34		0.38	0.38		0.38	0.364	0.356							
	K2O	<0.01	0.012	0.015	0.014	0.015	0.017					0.0151			0.015	
	P2O5	0.01														
(ppm)	Sc						0.40	0.437	0.434							
	V															
	Cr				63		19.0	19.3	20.3							
	Mn	0					42		47							
	Co						0.26	0.194	0.190							
	Ni						3	12.2	13.3							
	Rb			0.17	0.15(a)							0.217				0.19
	Sr	184		178	172		173	202	198			173.3				240.5
	Y															
	Zr															
	Nb															
	Hf						0.017	0.011	0.014							
	Ba			6.2	6.28		6.5	6	6							
	Th		<0.030		0.027					0.0036	0.0034		0.0064	0.0037	0.0035	0.028
	U		0.0024		0.0098	0.0125	0.0015			0.0017	0.0014		0.0034	0.0014	0.00087	<0.005
	Pb									0.268	0.246		0.18	0.28	0.16	
	La				0.118		0.21	0.130	0.133							
	Ce			0.32	0.35			0.320	0.330							
	Pr															
	Nd			0.20	0.175											
	Sm			0.049	0.046		0.062	0.056	0.054							
	Eu			0.807	0.806		0.82	0.805	0.805							
	Gd			0.062	0.050											
	Tb							0.0100	0.0070							
	Dy			0.063	0.044		0.054									
	Ho															
	Er				0.019											
	Tm															
	Yb			0.045	0.035		0.035	0.029	0.028							
	Lu				0.0034		0.0041	0.0036	0.0061							
	Li			1.0	2.0											
	Be															
	B															
	C															
	N															
	S		0													
	F															
	Cl						150									
	Br															
	Cu						57.9									
	Zn						31.8									
(ppb)	I															
	At															
	Ga						3100									
	Ge						20									
	As						4.1									
	Se															
	Mo															
	Tc															
	Ru															
	Rh															
	Pd															
	Ag															
	Cd															
	In															
	Sn															
	Sb															
	Te															
	Cs															
	Ta							31	25							
	W						260									
	Re															
	Os															
	Ir															
	Pt															
	Au						0.77									
	Hg															
	Tl															
	Bi															
		(1)	(2)	(3)	(4)	(5)	(6)	(7)	(7)	(8)	(8)	(8)	(9)	(9)	(9)	(10)	(11)

TABLE 15415-4. Continued

	,?	,42	,42	,12	,45	,44	,9	,9	,7	,7
SiO2										
TiO2										
Al2O3										
FeO										
MgO								19.6		
CaO										
Na2O							0.013		0.016	0.014
K2O										
P2O5										
Sc										
V										
Cr										
Mn										
Co										
Ni										
Rb	0.16			0.11						
Sr	173.4									
Y										
Zr										
Nd										
Hf										
Ba										
Th										
U		0.0066	0.031							
Pb										
La										
Ce										
Pr										
Nd										
Sm										
Eu										
Gd										
Tb										
Dy										
Ho										
Er										
Tm										
Yb										
Lu										
Li		15								
Be										
B					15	3				
C										
N										
S										
F		<0.7								
Cl		0.50(b)								
Br		0.057(b)	0.097(b)	2.3						
Cu										
Zn				0.26						
I		1.1(c)								
At										
Ga										
Ge				1.2						
As										
Se				0.23						
Mo										
Tc										
Ru			<0.5							
Rh										
Pd										
Ag				1.73						
Cd				0.57						
In				0.178						
Sn										
Sb				0.067						
Te		68		2.1						
Cs				23						
Ta										
W										
Re				0.00084						
Os			3.5							
Ir				<0.010						
Pt										
Au				0.117(d)						
Hg										
Tl				0.09						
Bi				0.097						
	(11)	(12)	(12)	(13)	(14)	(15)	(16)	(17)	(18)	(18)

References to Table 15415-4

References and methods:

(1) LSPET (1972); XRF
(2) LSPET (1972); gamma ray spectroscopy
(3) Wiesmann and Hubbard (1975), Nyquist et al. (1972a,b); isotope dilution, mass spec
(4) Wiesmann and Hubbard (1975), Hubbard et al. (1971), Nyquist et al. (1972b); isotope dilution, mass spec
(5) Church et al. (1972); isotope dilution, mass spec
(6) Wanke et al. (1975); XRF, INAA, RNAA
(7) Haskin et al. (1981); INAA
(8) Tatsumoto et al. (1972); isotope dilution, mass spec
(9) Tera et al. (1972); isotope dilution, mass spec
(10) Keith et al. (1972); gamma ray spectroscopy
(11) Wasserburg and Papanastassiou (1971); isotope dilution, mass spec
(12) Reed and Jovanovic (1972), Jovanovic and Reed (1977); Activation (neutron and photon)
(13) Morgan et al. (1972a,b), Ganapathy et al. (1973); RNAA
(14) Moore et al. (1973); combustion, gas chromatography
(15) Desmarais et al. (1973); combustion, gas chromatography
(16) Husain et al. (1972); from Ar isotopes
(17) Husain (1974); from Ar isotopes
(18) Turner (1972); from Ar isotopes

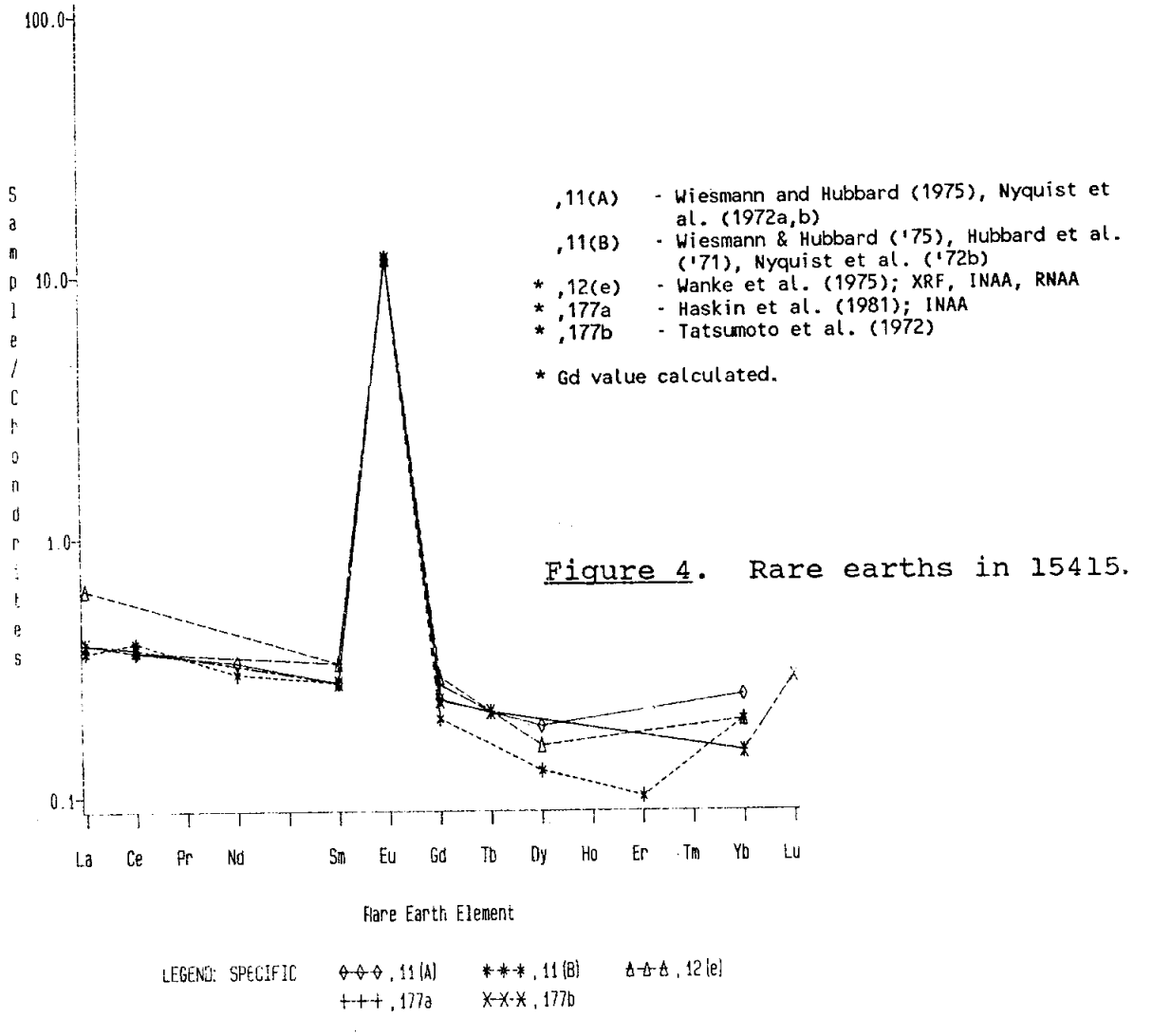

Figure 4. Rare earths in 15415.

upon by various authors. Haskin et al. (1981) analyzed two subsamples for rare earths, finding good agreement except for Lu. They suggested that Lu has anomalous behaviour (not Yb as had been suggested earlier), and also found that La was anomalous among all laboratories. Otherwise the rare earths in 15415 are "appealingly simple". Haskin et al. (1981), Hubbard et al. (1972), and Palme et al. (1984) calculated parental liquids with roughly chondritic rare earth element patterns and abundances ~10x chondrites. A small positive Eu anomaly in some calculations is very sensitive to the distribution coefficient used and may not be real. 15415 has rather primitive rare earth abundances, although its Fe/Mg is higher than many other (mainly Apollo 16) ferroan anorthosites. Palme et al. (1984) performed INAA analysis of five plagioclase separates (Table 3).

15415 is outstandingly low in volatiles and siderophiles (Morgan et al., 1972b). Six of eight volatiles show a constant normalized pattern of $7.2 \pm 0.8 \times 10^{-4}$ x chondrites (Morgan et al., 1976). The data of Reed and Jovanovic (1972) also show low volatiles. The low siderophiles are a standard for demonstrating the presence of meteoritic siderophiles in other samples, e.g., Apollo 11 anorthosites (Morgan et al., 1972a). While the sample contains very little U and Th, the Pb value is disproportionately high (Tatsumoto et al., 1972). Much of the Pb is easily leachable (Tera et al., 1972). The low Th/U (Tatsumoto et al., 1972; Silver, 1976) reflects the concentration of plagioclase in the absence of large ion lithophile element enrichment.

DesMarais et al. (1973, 1974) provided data on carbon compounds released on combustion, and on H contents. Both total C (see also Moore et al., 1973), and total H abundances are much lower than values for lunar fines. Simoneit et al. (1973) studied the gas release pattern under vacuum with pyrolysis. At low temperatures, H_2O and CO_2 are the absorbed species; at higher temperature low levels of only CO are evolved bimodally. All nitrogen analyses are at background levels.

STABLE ISOTOPES: Oxygen isotopic determinations were made by Epstein and Taylor (1972) who reported δO^{18} (°/oo) of 6.05 ± 0.04, and by Clayton et al. (1972, 1973) and Clayton and Mayeda (1975) who reported δO^{18} (°/oo) for plagioclase of 5.78, 5.71, and 5.84 respectively. These values are similar to other lunar rocks and as expected for igneous processes. Clayton and Mayeda (1975) also reported a δO^{17} (°/oo) of 2.88, hence 15415 lies on the terrestrial/lunar mass fractionation line.

Epstein and Taylor (1972) reported a δSi^{30} (°/oo) of -0.18, similar to other lunar igneous rocks.

RADIOGENIC ISOTOPES AND GEOCHRONOLOGY: ^{40}Ar-^{39}Ar studies by Husain (1972) and Husain et al. (1972a,b), and Turner (1972) give ages of 4.09 ± 0.19 b.y. and 4.05 ± 0.15 b.y. As stated by Turner (1972), there is no evidence of a real plateau, and the age is an "asymptotic high temperature" age, giving a lower limit

of 3.9 b.y. to the crystallization age. Husain et al. (1972a) interpreted the age to mean that 15415 was a fragment of 4.1 b.y. old crust, virtually unaffected by post-crystallization thermal effects. However, the sample is probably much older. The sample is retentive, with most radiogenic ^{39}Ar released above 900°C. The Ar losses over the last 4.0 b.y. are 13% (Turner, 1972) or 4% (Husain, 1972a,b). K/Ca is constant with temperature, consistent with release of Ar from a monomineralic rock.

Whole rock Rb-Sr data were provided by Wasserburg and Papanastassiou (1971) and Papanastassiou and Wasserburg (1973), by Nyquist et al. (1972a,b; 1973) and Wiesmann and Hubbard (1975) and by Tatsumoto et al. (1972) (Table 5). These data establish I_o to be less than or equal to BABI. It is clear that 15415 has extremely low Rb/Sr and in the last 4.6 b.y. has never been exposed to an environment with Rb/Sr as high as even the low values observed in low K Apollo 11 mare basalts (Wasserburg and Papanastassiou, 1971). Material forming the rock must have separated from a reservoir with Rb/Sr = 0.0035 (e.g., Apollo 11 rocks) within 3.5×10^8 years of the formation of the Moon, but no precise statement of age is possible. However, the data demonstrate a maximum formation interval for the Moon of 3 m.y. after the solar system (Rb/Sr = 0.6) had the composition of BABI close to 4.6 b.y. ago (Wasserburg and Papanastassiou, 1971).

U, Th-Pb isotopic data were presented by Tera et al. (1972), and by Tatsumoto et al. (1972) and Nunes et al. (1973). According to Tera et al. (1972) the bulk of the Pb is easily leachable, and is very heterogeneous isotopically. A highly radiogenic Pb is the one easily leached, leaving a residue of primodial Pb; the radiogenic Pb was added post-crystallization. There is no direct evidence for an ancient crust; rather the Pb represents 4.0 b.y. old material. Nunes et al. (1973) noted the complexities in interpretation of ages from the Pb data; if there are components other than in situ radiogenic Pb and modern (terrestrial) Pb, then a simplastic U-Pb age interpretation is not strictly valid.

RARE GASES AND EXPOSURE: Husain et al. (1972a,b) and Husain (1974) reported a ^{38}Ar exposure age of 90 ± 10 m.y., and Turner (1972) a ^{38}Ar exposure age of 112 m.y. While these are similar to a ^{81}Kr-Kr exposure age of 104 ± 15 m.y. by Eugster et al. (1984), the latter found that 15415 had experienced a multistage exposure. They reported detailed analyses for rare gas isotopes. Their investigation was hampered by strongly diffusive losses from their sample, e.g., 98% ^3He_c missing, 40% of radiogenic ^{40}Ar missing, so that the abundances of cosmogenic components do not appear to be reliable. The shielding depth at collection for their subsplit was about 10g/cm^2.

Keith et al. (1972) and Keith and Clark (1974) reported disintegration count data for cosmogenic nuclides. The lack of Fe in the sample led to very low activities for ^{54}Mn, ^{56}Co, and ^{22}Na. The ^{26}Al is unsaturated (Keith and Clark, 1974; Yokoyama et al., 1974) indicating rapid erosion and an exposure of 1.61

TABLE 15415-5. Rb-Sr isotopic data for whole-rock 15415

Reference		Rb	Sr	$^{87}Rb/^{86}Sr$	$^{87}Sr/^{86}Sr$	$I_{4.6\ b.y.}$	$I_{4.6\ b.y.}$ (a)
Wasserburg and Papanastassiou (1971)	15415-A	0.196	240	0.0024	0.69926±12	0.69910±12	--
Wasserburg and papanastassiou (1971)	15415-B(b)	0.145	173	0.0027	0.69914±5	0.69898±5	—
Nyquist et al. (1972a,b; 1973)	15415,1	0.17	177	0.0028	0.69938±18	0.69920±18	0.69908±18
Nyquist et al. (1972a,b; 1973)	15415,11	0.142	172	0.0024	0.69926±5	0.69910±5	0.69898±5
Tatsumoto et al. (1972)	15415	0.217	173.3		0.69914		

(a) corrected for interlaboratory bias to C.I.T. data.
(b) preferred value, more precise and larger sample.

TABLE 15415-6. Elastic wave velocities (Km/sec)

Pressure Kb	0	0.5	1.0	1.5	2	3	4	5	6	7	9	(10)*	Reference
S	—	2.0	2.5	2.90	3.26	3.42	3.54	3.56	3.58	3.61	—	3.69	Chung, 1973
P	—	5.0	5.6	6.02	6.40	6.65	6.70	6.78	6.83	6.85	—	6.87	Chung, 1973
P	5.98	6.20	6.28	—	6.43	6.56	—	6.75	—	6.89	7.01	—	Mizutani and Newbigging, 1973

(+0.51, -0.34) m.y. based on a one-step elevation to the surface, and representing only the most recent surface residence time.

PHYSICAL PROPERTIES: Gose et al. (1972) and Pearce et al. (1972, 1973) studied the magnetic properties of 15415. As received the sample was weakly magnetic, with a NRM intensity about 1 x 10^{-6} emu/g, which is two orders of magnitude less than breccias. Alternating field demagnetization is very weak and difficult to measure (sample only 2 g). There seems to be a stable component of about 2 x 10^{-7} emu/g (Fig. 5), extremely weak by comparison with mare basalts and breccias, presumably because there is so little iron. There is no systematic change in direction; the scatter in Figure 5 probably results from the intensity being so close to the detection limit rather than from instability.

Seismic velocities were measured by Chung (1973) and by Mizutani and Newbigging (1973) (Table 6). The data agree well except at low pressure, and the differences presumably result from varied fracturing of the sub-samples. The velocities are less than for terrestrial anorthosites because of the numerous fractures and microcracks in 15415.

Chung and Westphal (1973) reported dielectric spectra data. The high frequency dielectric constant (K') is 4, which is low, and the high frequency dissipation factor (tan δ) is about 0.001, also low.

Hoyt et al (1972) reported on thermoluminescence studies of 15415, giving glow curves (photons detected vs. temperature). The thermoluminescence sensitivity is extremely low, and the glow curve stage is very different from those of fines. Materials such as 15415 can contribute very little to the thermoluminescence of lunar fines.

Spectral reflectance data were reported by Adams and McCord (1972) and Charette and Adams (1977). Both spectra are dominated by the Fe^{2+} plagioclase band at 1.3 microns, but whereas Adams and McCord (1972) found no pyroxene band structure, Charette and Adams (1977) found a two-pyroxene composite band, and a feature near 0.6 microns that could result from very thin plates of ilmenite in the pyroxene.

PROCESSING AND SUBDIVISIONS: 15415 has been substantially subdivided and widely allocated. Apart from small loose chips, 15415 was originally subdivided by prying off one end (,34) and sawing off another (,33) (Fig. 6). ,33 was entirely subdivided by further sawing to produce the main chips shown in Figure 6. Most allocations were made from the subdivisions of ,33; ,34 was also allocated. In 1975, 30% of ,0 was allocated for remote storage, so it was sawn, with resulting subdivisions shown in Figure 7. ,139 (26.9 g) and ,140 (28.6 g) are stored at Brooks. ,143 now has a mass of 89.7 g and is the largest intact piece of 15415. Ten thin sections were made from each of chip ,3 and from ,55, and one from ,46. Other principal investigator-made thin sections, grain mounts, and TEM foils exist.

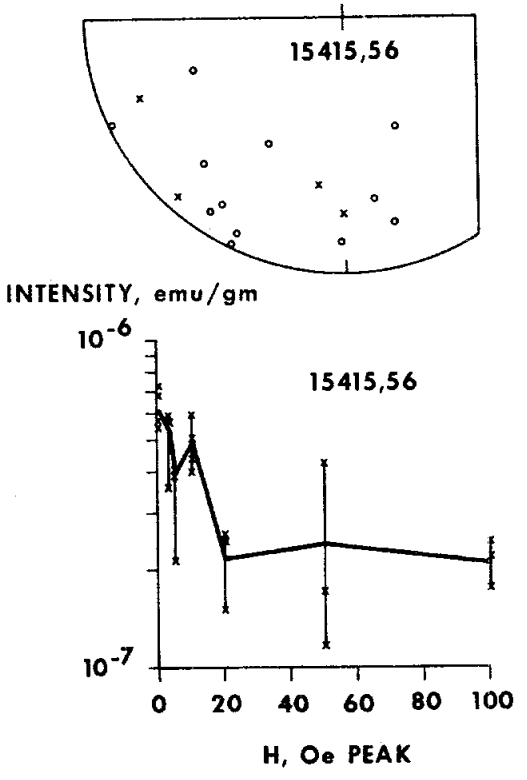

AF demagnetization of anorthosite sample 15415,56. No systematic changes in direction were observed. Error bars on intensity curve represents absolute error for repeat measurements. (The same definition applies to all similar figures.)

Figure 5. AF demagnetization of 15415,56.

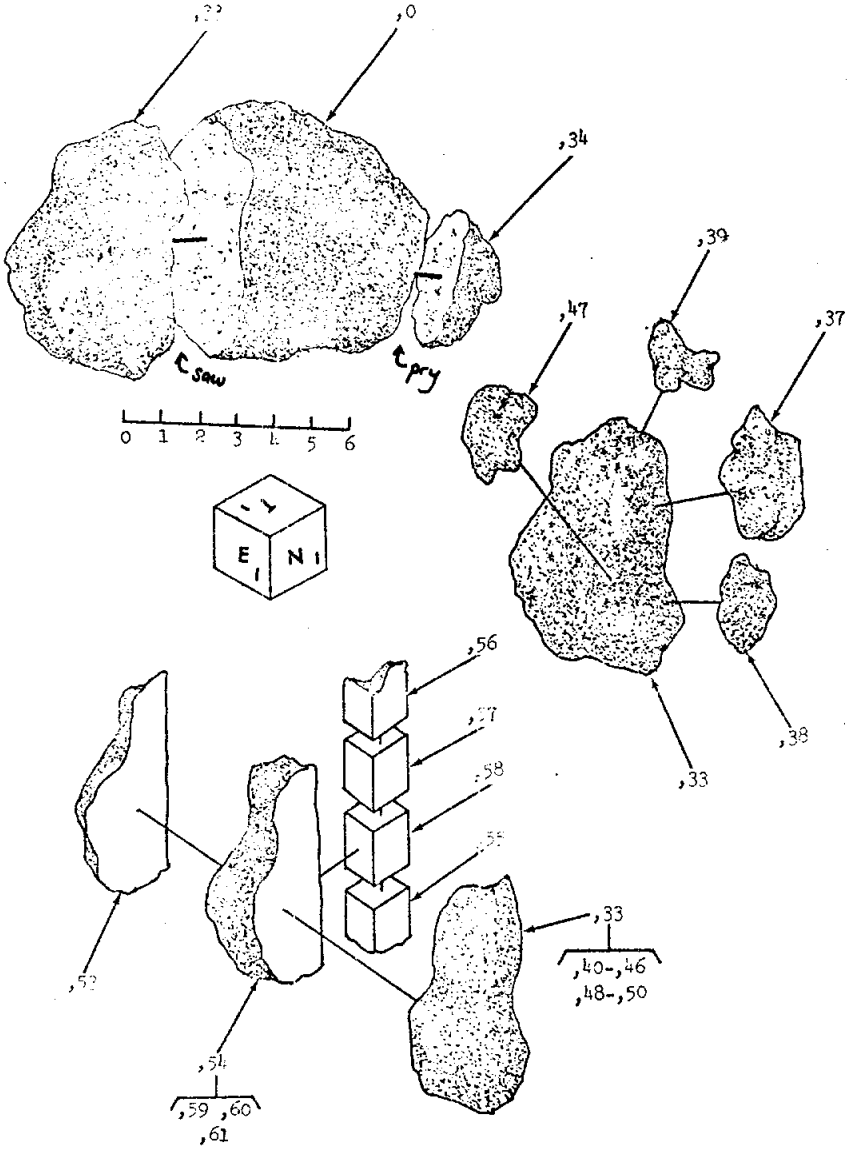

Figure 6. Original subdivision of 15415.

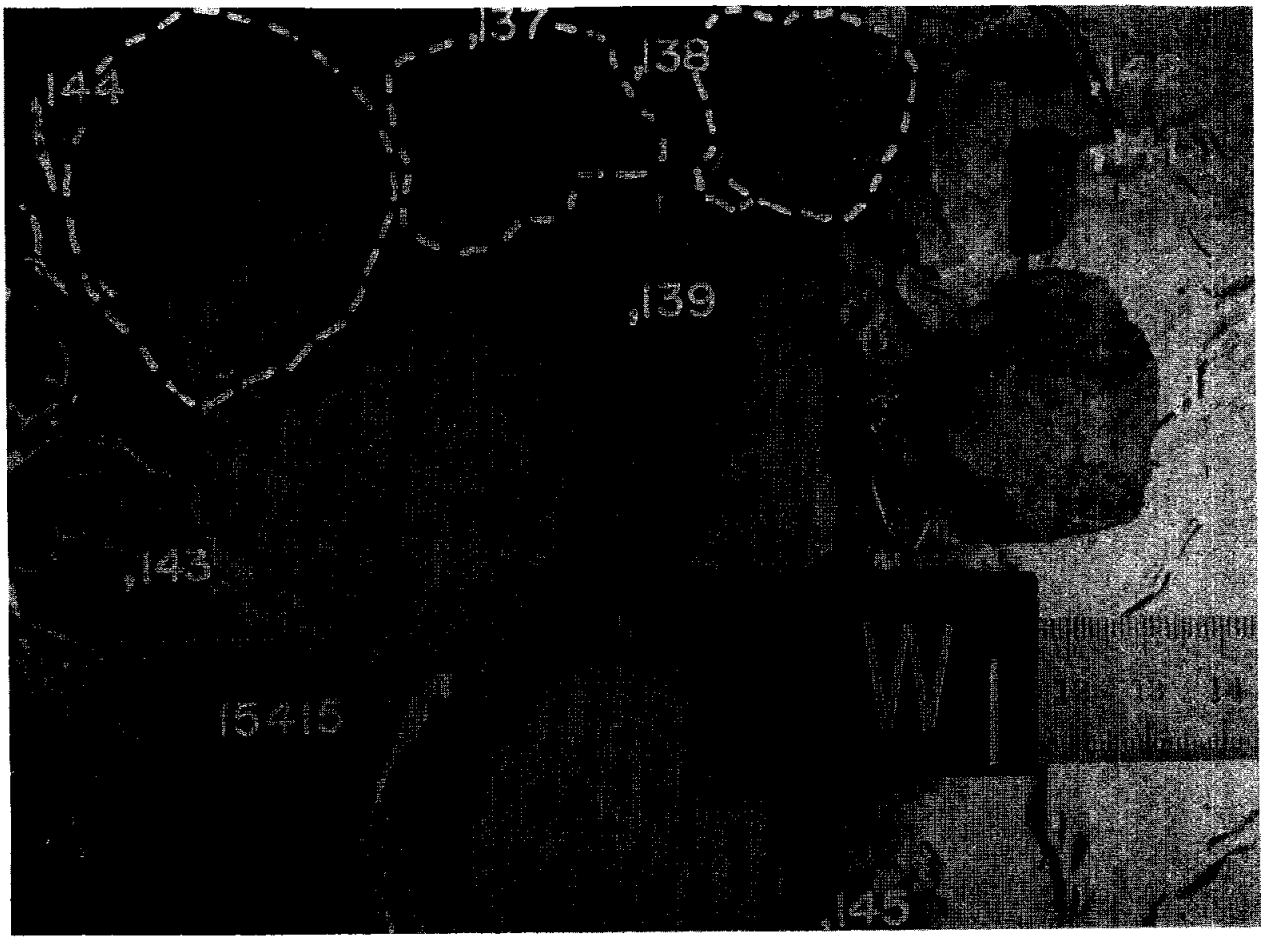

FIgure 7. 1975 subdivision of ,0. S-75-32659.

15417 REGOLITH BRECCIA ST. 7 1.3 g

INTRODUCTION: 15417 is a moderately friable regolith breccia containing glass, and small mineral and lithic clasts (Fig. 1). It is light brownish gray and rounded, with a smooth surface and no zap pits. It was collected from the north rim crest of Spur Crater along with soil 15410-15414, and very close to samples 15418 and 15419.

PETROLOGY: 15417 is a regolith breccia (Fig. 2) with a porous matrix, which contains brown glass. It is rather fine-grained compared with many other regolith breccias, with few clasts in the thin section 15417,4 larger than a few hundred microns across. Glass spheres are present but not in such large quantities as many other regolith breccias. Sewell et al. (1974) provided energy-dispersive defocussed beam microprobe analyses of clasts in 15417,4, including metamorphosed basalts, feldspathic basalts, and breccias, and also mare glasses (including eight green glasses), and some mineral analyses. 15417 appears to have a diverse set of sources. Gleadow et al. (1974), a companion study to Sewell et al. (1974), also listed 15417 among their studied samples, but provided no specific data.

PROCESSING AND SUBDIVISIONS: Only ,1 was chipped from ,0 (Fig. 1), and partly used to make the only thin section ,4. ,0 is now 0.95 g.

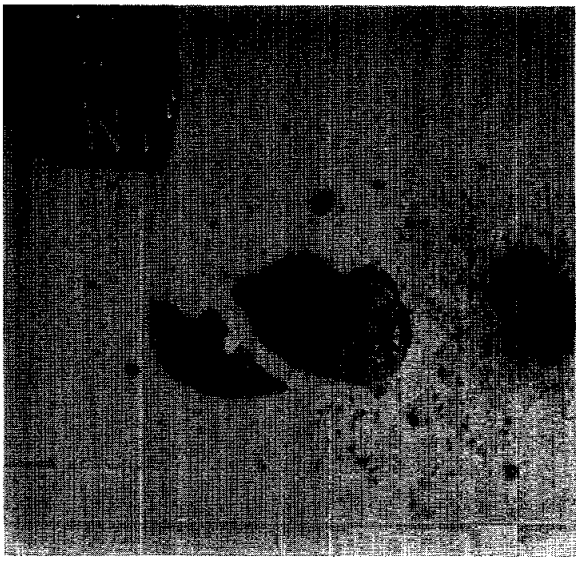

Figure 1. Post-chip view of 15417,0 (right) and 15417,1 (left). S-71-60168

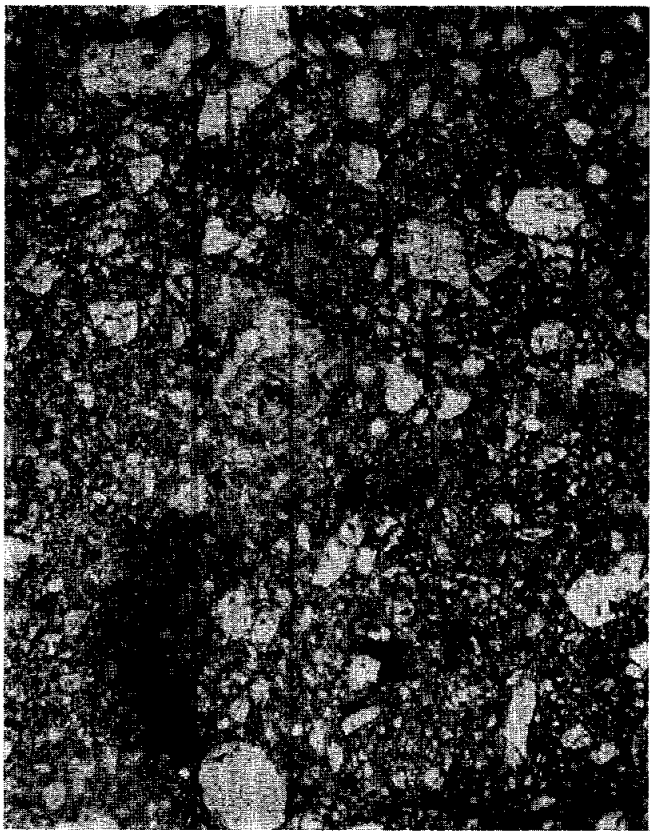

Figure 2. Photomicrograph of 15417,4, general view. Transmitted light. Width about 2 mm.

15418 SHOCKED/MELTED BRECCIA ("ANORTHOSITIC GABBRO") ST. 7 1141.0 g

INTRODUCTION: 15418 is an aluminous breccia ("anorthositic gabbro"), texturally unique among Apollo 15 samples. Its brecciated interior was shocked and shock-heated, and its rind vesiculated and melted. It contains a few large white clasts and was shocked ~4.0 b.y. ago. It was originally studied in a consortium headed by Tatsumoto.

15418 was collected from the summit of the subdued rim crest of Spur Crater, near several other rocks bigger than 10 cm, and may represent material from as deep as 20 m in the crater. The sample is blocky, subrounded, gray, and tough, with prominent exterior vesicles (Figs. 1, 2). It has zap pits on all sides and was moderately buried. Its lunar orientation is known.

PETROLOGY: 15418 is considered an important sample as a unique aluminous breccia ("gabbroic anorthosite", ~70% plag.) and as such was described and depicted by PET (1972). Photomicrographs are shown in Figure 3. The PET (1972) description is only of the exterior, melted portion of the rock. The only comprehensive studies have been by Heuer's group (Heuer et al. 1972, Christie et al. 1973, and an especially detailed description by Nord et al. 1977) who studied the interior as well as the exterior, using optical, microprobe, and SEM methods. The interior was also studied by Sewell et al. (1974) who provided microprobe analyses, and Gleadow et al. (1974) who provided a description. The interior has a fragmental nature with some large crystals of plagioclase (~5 mm) and less common olivines (2 mm) in a finer-grained, fragmental and recrystallized matrix (Fig. 3d,e), which consists of olivine, orthopyroxene, clinopyroxene, and plagioclase. All are shocked, with aggregate extinction, but each fragment consists of a polycrystalline aggregate. TEM studies show evidence for their crystallization from glass or from partial recovery from heavily deformed preexisting crystals. The plagioclase (clasts and matrix) have a limited compositional range (An_{96-97}), and so do mafic grains (Fig. 4) (Nord et al., 1977). Similar analyses were also presented by Ahrens et al. (1973) and Sewell et al. (1974). (Note that the latter authors inverted the headings of the clinopyroxene and orthopyroxene analyses.) Some of the plagioclases have a spherulitic or fibrous (wheat-sheaf) texture, from the devitrification of an originally glassy feldspar. Intracrystalline pores (100-1000 Å) are also common, and might result from volatiles or from the density contrast between devitrified and undevitrified glass. The exterior (Nord et al. 1977, PET 1972) is different, and includes an outer zone of flow-banded glass -- several subzones occur (Fig. 3a,b,c). Nord et al. (1977) summarized the history of the sample as shown in Table 1: an initial slow-cooled equilibration followed by brecciation. A second impact produced shock deformation, melting of the surface, and injection of glass along cracks. Following this, heating devitrified the

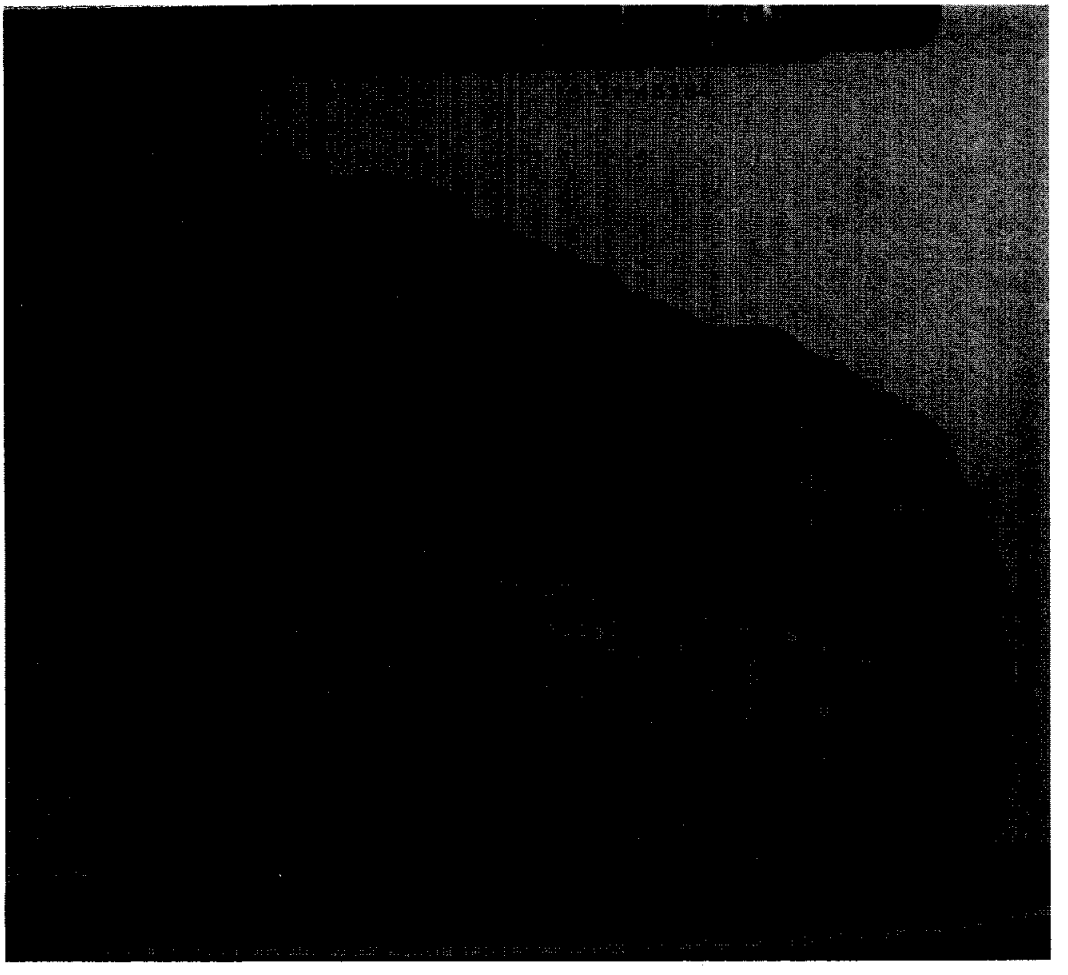

Figure 1. Macroscopic view of 15418 showing exterior vesicles and zap pits.

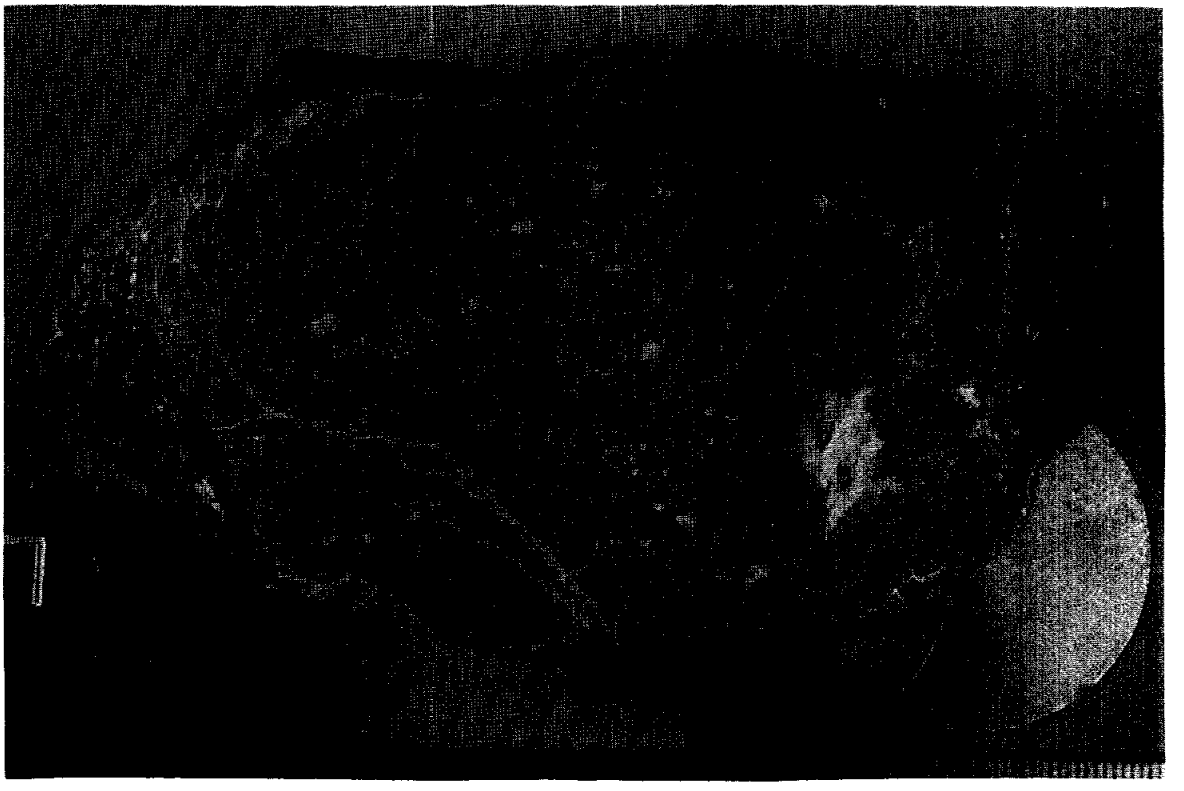

Figure 2. Sawn surface of end piece ,27, showing plagioclase-rich clasts, fine-grain-size, overall homogeneity, small vesicles, and concentration of vesicles at rim (especially on right hand side).

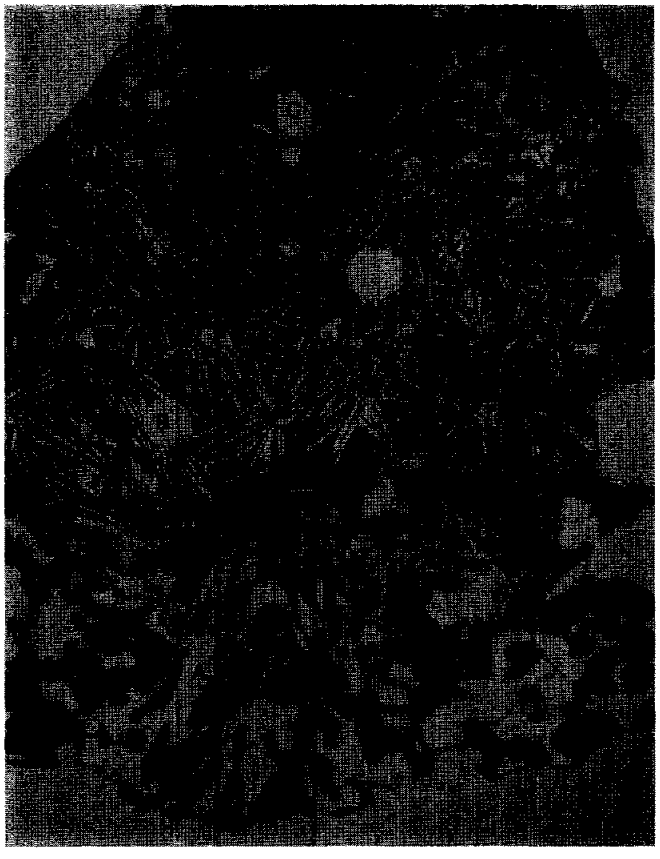

Fig. 3a

Figure 3. Photomicrographs, all to same scale except (c):
(a) 15418,8, exterior rind, with zones A, B, C described by Nord et al. 1977. Transmitted light.
(b) 15418,17, more common exterior as manifested in thin sections and showing some similarities with the interior of the rock. White is plagioclase, dark is plag + px, all shocked and recrystallized. Transmitted light.
(c) 15418,17, detail of (b): lighter gray is mafic phases, darker gray is plagioclase. Reflected light.
(d) 15418,98, interior of 15418 showing fragmental and recrystallized texture; bottom left is a single larger plagioclase crystal. Transmitted light.
(e) 15418,98, same field as (d) but crossed polarizers, showing polycrystalline nature of grains.

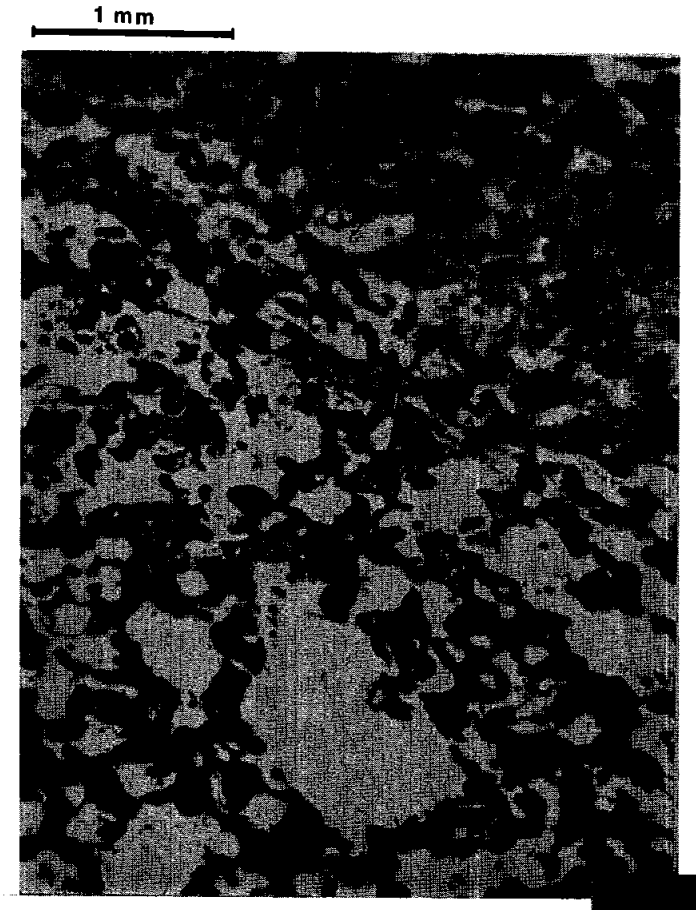

Fig. 3b

Fig. 3c

Fig. 3d

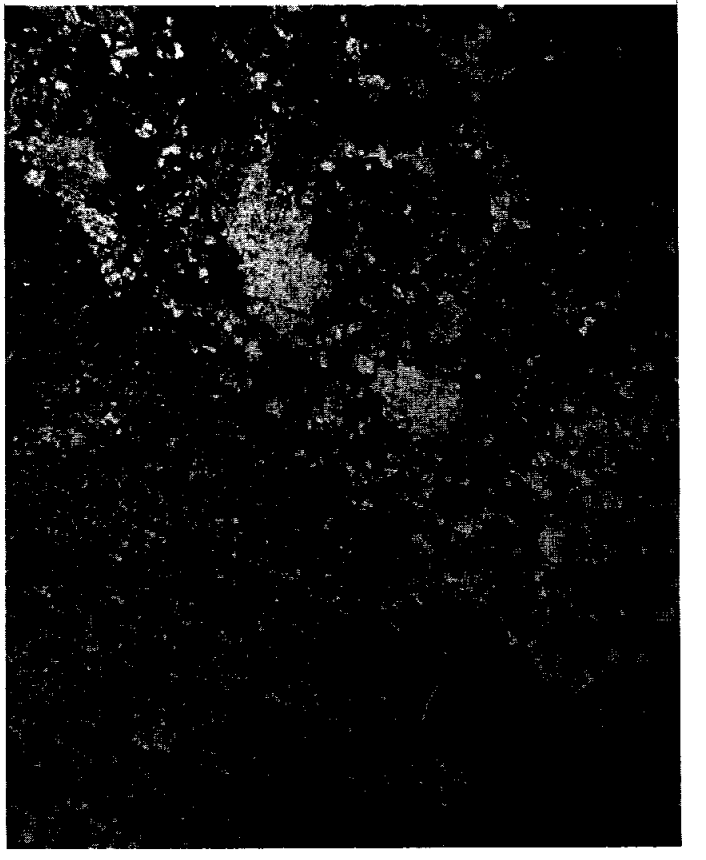

Fig. 3e

TABLE 15418-1. Summary of mechanical and thermal history of 15418 (Nord et al., 1977)

Event	Mechanical effects	Thermal effects	Processes and resulting textures
I		Initial crystallization and slow cooling.	Coarse-grained texture. Chemical equilibration approached.
II a.	Fracturing and brecciation.	First impact event.	Brecciated structure.
b.		Shock heating	Recrystallization giving rise to present hornfelsic grain structure Chemical equilibrium established or undisturbed?
III a.	Shock deformation and ejection with partial melting of surface.	Second impact event.	Partial shock vitrification and high local deformation. Fractures filled with impact-produced melt from rock surface.
b.		Shock heating	Devitrification of thetomorphic and melt glasses. Recovery and partial recrystallization of deformation structure. Element distribution unchanged.
IV	Transport (farming) by small impacts.		Some cracking with little or no effects on fabric.

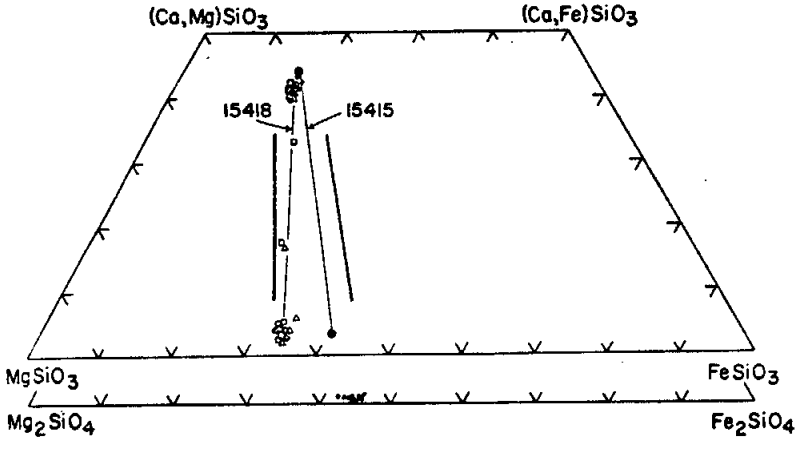

Figure 4. Pyroxenes and olivines in 15418,17 (Nord et al., 1977).

thetomorphic and melt glasses, and caused some recovery of the silicates. Subsequent small-scale impact produced minor cracking. A similar history is deduced by Richter et al. (1976) who studied microcracks in exterior samples, finding several episodes of cracking as shown by cross-cutting relationships. Some are open, others are sealed with glass with a composition similar to the bulk rock (they quoted the Bansal et al. 1972 analyses as for 15415,51 instead of 15418,51). Glass in fractures was injected but shows no flow-banding; at the edges the glassy plagioclase of the host has crystallized. Open cracks were subjected to differential strain analysis (DTA). The crack closure pressures are similar to other lunar samples, but the porosity is low, and the cracks were produced in mild shock events.

Hutcheon et al. (1972) also used HVEM to study what was mainly a single large clast of plagioclase. It was highly deformed with an heterogeneous distribution of deformation, and abundant recrystallization. They found gas bubbles but no pre-existing (i.e., formed prior to the rock) solar flare tracks. Huffman et al. (1974) and Schwerer et al. (1973) tabulated Mossbauer and magnetic studies of the sample. Magnetic studies showed 0.067% metallic iron. Mossbauer studies showed none, all iron being in silicates: 59.5% in pyroxene, 40.4% in olivine, none in oxides or sulfides.

Studies of glass of 15418 composition were made by Cukiermann and Uhlmann (1972), Uhlmann et al. (1974), and Yinnon (1980). They studied flow characteristics, measuring viscosity v. temperature, reliable data only being obtained above 1270°C (no crystals) and below 835°C. At intermediate temperatures crystallization took place during the time required to measure viscosity. Uhlmann et al. (1974) also shows the variation of crystal growth rate with temperature. Yinnon et al. (1980) conducted differential thermal analysis (DTA) experiments, and plotted the crystallization temperature against the heating rate.

CHEMISTRY: Analyses are listed in Table 2, and rare earths plotted in Figure 5. Authors generally merely noted the aluminous and low-potassic nature of the sample. Some of the analyses are on sawdust from the slabbing. The major elements and rare earths are consistent among analyses, but some variation occurs in some trace elements e.g. between the two splits analyzed by Ganapathy et al. (1973). This difference is said to be a more probable result of different mineralogies than to have anything to do with vesicularity (Ganapathy et al. 1973).

Allen et al. (1973a,b) analyzed for ^{204}Pb and for Fe metal; the tentative vaules for ^{204}Pb in Allen et al. (1973b) were replaced. Hubbard et al. (1972) reported the same data as PET (1972) but differ in Na_2O (0.21% instead of 0.31%) and K_2O (0.05% instead of 0.03%). Their quote of 0.93% instead of 0.03% for P_2O_5 is undoubtedly a printing error.

TABLE 15418-2. Chemical analyses of bulk rock

			,51a		,30-08	,30-08	,5	,51	,30-07A	,49	,30,03	,30-07A	
Wt %	SiO2	44.97	44.2						45.53				
	TiO2	0.27	0.27	0.37					0.29		0.23	0.272	
	Al2O3	26.73	26.6	26.4					25.98				
	FeO	5.37	6.65	7.5					6.66				
	MgO	5.38	5.08	5.3					6.09				
	CaO	16.10	16.0	15.8					15.63				
	Na2O	0.31	0.27	0.282					0.31		0.32	0.30	
	K2O	0.03	0.013	0.011					0.03		0.0200	0.0236	0.0104
	P2O5	0.03							0.03				
(ppm)	Sc			12.7						7.0			
	V			42						18.0			
	Cr	750		1900						1150	614	628	
	Mn	620		660					770				
	Co			77						10.0			
	Ni									54.0			
	Rb		0.17					0.162			0.361	0.489	
	Sr	152	140					140.1			148		
	Y									5.4			
	Zr	67		180							30	35	
	Nb												
	Hf			0.8						0.16	0.8	0.6	
	Ba		19.2	70						20.0	24.4	28.9	
	Th									0.10	0.28	0.34	0.102
	U		0.045		0.016	0.036					0.078	0.094	0.043
	Pb									0.14			
	La		1.07	1.2						1.06	1.73	2.19	
	Ce		3.31							2.4		6.78	
	Pr									0.33			
	Nd		2.09							1.41	3.15	3.75	
	Sm		0.688	0.69						0.43	0.940	1.16	
	Eu		0.726	0.73						0.69	0.764	0.762	
	Gd		1.25							0.67	1.25		
	Tb			0.18						0.12			
	Dy		1.12	1.2						0.8	1.49	1.84	
	Ho									0.19			
	Er		0.85							0.59	1.04	1.24	
	Tm									0.1			
	Yb		0.74	0.81						0.6	0.907	1.12	
	Lu		0.120	0.12						0.09	0.143	0.176	
	Li				16						2.3	2.6	
	Be												
	B												
	C						11						
	N												
	S	300	400(b)						300				
	F												
	Cl				1.11								
	Br				0.52	0.39							
	Cu									2.0			
	Zn												
(ppb)	I				1.6								
	At												
	Ga									2200			
	Ge												
	As												
	Se												
	Mo												
	Tc												
	Ru					3.4							
	Rh												
	Pd												
	Ag												
	Cd												
	In												
	Sn												
	Sb												
	Te				6.3								
	Cs												
	Ta			90									
	W												
	Re												
	Os					9.3							
	Ir												
	Pt												
	Au												
	Hg												
	Tl												
	Bi												
		(1)	(2)	(3)	(4)	(4)	(5)	(6)	(7)	(8)	(9)	(9)	(10)

TABLE 15418-2 Continued

		,30-08	,30-05Dc	,30-06d	,50				
Wt %	SiO2								
	TiO2								
	Al2O3								
	FeO								
	MgO								
	CaO				15.54				
	Na2O								
	K2O				0.0066				0.0152
	P2O5								
(ppm)	Sc								
	V								
	Cr								
	Mn								
	Co								
	Ni								
	Rb		0.80	0.03					0.263
	Sr								134.6
	Y								
	Zr								
	Nb								
	Hf								
	Ba								
	Th					0.1272	0.1377	0.2077	
	U		0.185	0.024		0.0380	0.0394	0.0578	
	Pb					0.138	0.132	(1.927e)	
	La								
	Ce								
	Pr								
	Nd								
	Sm								
	Eu								
	Gd								
	Tb								
	Dy								
	Ho								
	Er								
	Tm								
	Yb								
	Lu								
	Li								
	Be								
	B								
	C								
	N								
	S								
	F								
	Cl								
	Br		0.055	0.075					
	Cu								
	Zn	2.74	0.82	0.49					
(ppb)	I								
	At								
	Ga								
	Ge		65	17					
	As								
	Se		56	25					
	Mo								
	Tc								
	Ru								
	Rh								
	Pd								
	Ag		0.59	1.4					
	Cd		1.7	2.4					
	In		0.29	0.18					
	Sn								
	Sb		0.50	0.16					
	Te		3.7	1.9					
	Cs		40	8					
	Ta								
	W								
	Re		0.38	0.13					
	Os								
	Ir		5.4	2.2					
	Pt								
	Au		1.00	0.26					
	Hg								
	Tl		0.21	0.095					
	Bi	<1.09	0.16	0.29					
		(11)	(12)	(12)	(13)	(14)	(14)	(14)	(14)

References to Table 15418-2

References and Methods:

(1) PET (1972); XRF, AAS
(2) Bansal et al. (1972); XRF, ID
(3) Laul et al. (1972a), Laul and Schmitt (1972); INAA
(4) Reed and Jovanovic (1972); RNAA
(5) Moore et al. (1972, 1973)
(6) Nyquist et al. (1972, 1973); ID/MS
(7) Hubbard et al. (1974); XRF
(8) S.R. Taylor et al. (1973); SSMS, ES
(9) Wiesmann and Hubbard (1975); ID/MS
(10) Keith et al. (1972); Gamma-ray spectroscopy
(11) Allen et al. (1973); leaching, RNAA
(12) Ganapathy et al. (1973); RNAA
(13) Stettler et al. (1973); MS
(14) Tatsumoto et al. (1972); ID/MS

Notes:

(a) sawdust
(b) from Hubbard et al. (1974)
(c) vesicular exterior
(d) dense interior
(e) indicates sawing contamination

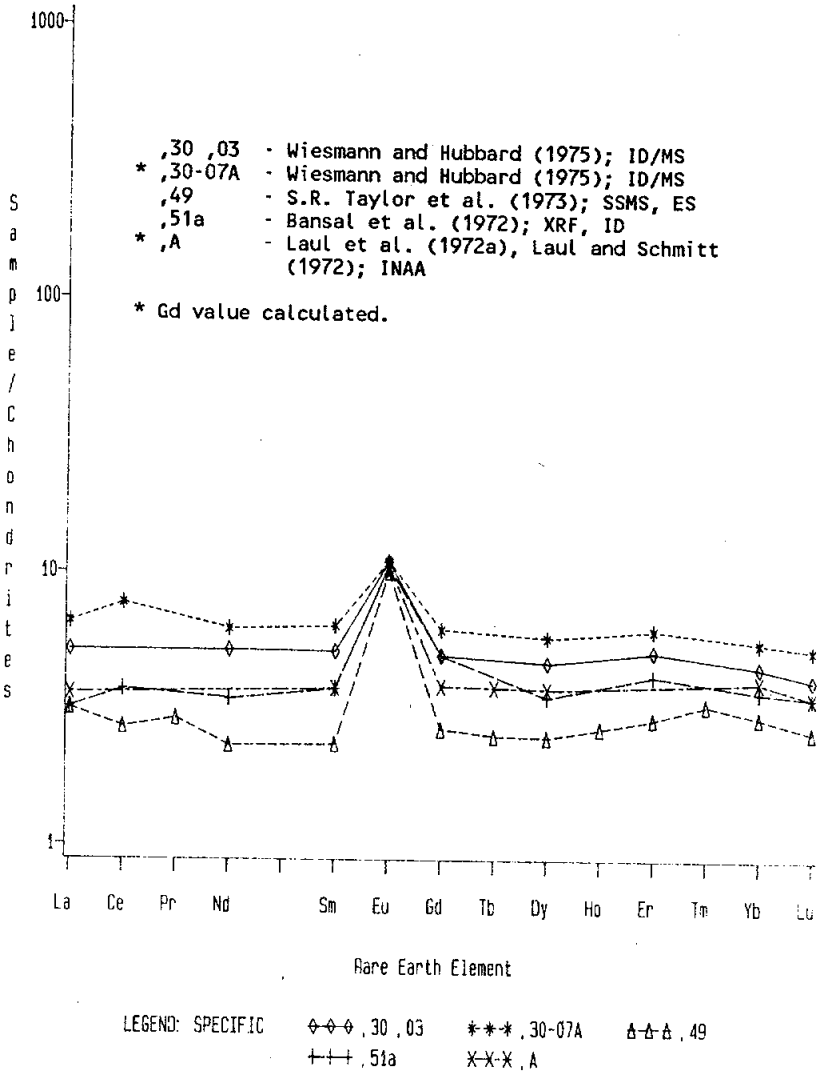

Figure 5. Rare earths in 15418.

RADIOGENIC ISOTOPES AND GEOCHRONOLOGY: Rb and Sr whole rock isotopic data is presented by Nyquist et al. (1972, 1973), Wiesmann and Hubbard (1975) and Tatsumoto et al. (1972) (Table 3). The data are reasonably consistent.

Stettler et al. (1973) did ^{40}Ar-^{39}Ar dating on the sample (Fig. 6) finding a high temperature plateau at 3.99 ± 0.07 b.y., and an intermediate temperature release age of 4.04 ± 0.06 b.y. The constancy of the Ca/K ratio indicates that the potassium is in plagioclase, not in an accessory phase.

Tatsumoto et al. (1972) reported Pb isotopic ratios and $^{238}U/^{204}Pb$ for one sample, and $^{232}Th/^{238}U$ for three samples including sawdust. The sample lies above concordia indicating lead enrichment relative to uranium in the sample analyzed. The data point for the sawdust is below concordia if the Pb value of the rock is used instead of the sawdust value (whose very high lead is sawcut contaminant).

EXPOSURE: Stettler et al. (1973) determined an exposure age of 250 m.y. using the ^{38}Ar method. Keith and Clark (1972) provided data on cosmogenic nuclides (with low ^{54}Mn, ^{56}Co, and ^{22}Na because of the calcic, mafic-poor nature of the sample). ^{26}Al is saturated, merely indicating exposure longer than 2 m.y. MacDougall et al. (1973) found no solar flare tracks in the sample.

PHYSICAL PROPERTIES: Nagata et al. (1972a,b, 1973, 1975) tabulated basic magnetic properties (hysteresis measurements) and NRM data. Kamacite is the major ferromagnetic constituent, with 4% Ni in the metal. The sample has an unusually small paramagnetic susceptibility. Demagnetization of ,46 revealed a hard component with an intensity of 1×10^{-6} emu/gm, with a direction reasonably constant for fields greater than 100 Oe.rms. Thermal demagnetization indicated an NRM attributable to a TRM acquired by cooling from 300°C at most. The observed NRM of ,41 could be obtained with an impact pressure of 50 kb in a magnetic field of ~8000 gammas.

Todd et al. (1973) and Wang et al. (1973) tabulated seismic (Vp and Vs) measurement as a function of pressure (Table 4), finding the values similar to those for lunar igneous (mare) rocks. Ahrens et al. (1973) made Hugoniot measurements (Figs. 7,8), tabulating the data (Table 5) resulting from shock experiments. O'Keefe and Ahrens (1975) discuss the equation of state, and 15418 became the standard for lunar crustal impact modelling because of these data and its composition.

Schwerer et al. (1973, 1974) measured the electrical conductivity of 15418 in reducing and oxidizing atmospheres as a function of temperature (Figs. 9, 10) as well as produced Mossbauer spectra. Baldridge et al. (1972) measured the thermal expansion coefficients from -100°C to +200°C.

TABLE 15418-4. Seismic velocities (Km/Sec) as a function of pressure (Todd et al. 1972) for 15418,43

bars	1	100	250	500	750	1000	1500	2000	3000	4000	5000
P	4.85	5.00	5.20	5.50	5.77	6.02	6.33	6.50	6.64	6.69	6.75
S	2.82	2.88	2.97	3.08	3.19	3.28	3.42	3.50	3.58	3.63	3.69

TABLE 15418-3. Whole rock Rb-Sr isotopic data (not adjusted for interlaboratory bias)

Reference	Split	$^{87}Sr/^{86}Sr$	$^{87}Rb/^{86}Sr$
Nyquist et al. (1972, 1973)	,51 sawdust	0.69934 ± 5	0.0034 ± 3
Wiesmann and Hubbard (1975)	,30,03	0.69948 ± 12	
Tatsumoto et al. (1972)	,28,30, and/or ,51	0.69954 0.69965	

Shot No.	Initial Density (g/cm^3)	Flyer Plate Velocity (km/sec)	Elastic Shock Velocity (km/sec)	Free-Surface Velocity (km/sec)	Hugoniot Elastic Limit (kb)	Final Shock Pressure (kb)	Final Shock Density (g/cm^3)
270	2.821	1.618[a] ±0.005	5.88 ±0.09	0.84	70 ± 4	204 ± 4	3.82 ± 0.07
276	2.834	1.318[a] ±0.001	6.02 ±0.12	*	*	155 ± 4	3.69 ± 0.08
268	2.813	2.166[a] ±0.005	6.30 ±0.01	0.60	65 ± 10	282 ± 6	4.25 ± 0.04
269	2.822	1.992[a] ±0.005	6.10 ±0.05	*	*	261 ± 5	4.07 ± 0.04
279	2.846	1.139[b] ±0.005	5.94 ±0.10	0.49	42 ± 5	88 ± 3	3.22 ± 0.06
280	2.823	0.850[b] ±0.0015	6.04 ±0.05	0.56	48 ± 5	65 ± 2	3.08 ± 0.05
281	2.812	0.803[b] ±0.002	6.18 ±0.02	0.61	53 ± 2	63 ± 1	3.03 ± 0.01
277	2.821	1.020[a] ±0.005	5.99 ±0.04	0.84	71 ± 10	129 ± 7	3.37 ± 0.06
287	2.823	1.17[a] ±0.006	6.24 ±0.11	0.65	57 ± 6	148 ± 8	3.48 ± 0.08
288	2.806	1.108[a] ±0.005	6.14 ±0.02	0.80	69 ± 11	145 ± 7	3.38 ± 0.04

[a]Polycrystalline W, 19.3 g/cm^3.
[b]Aluminum alloy, 2024.
*Not measured.

TABLE 15418-5. Hugoniot data for lunar sample 15418 (Ahrens et al., 1972a).

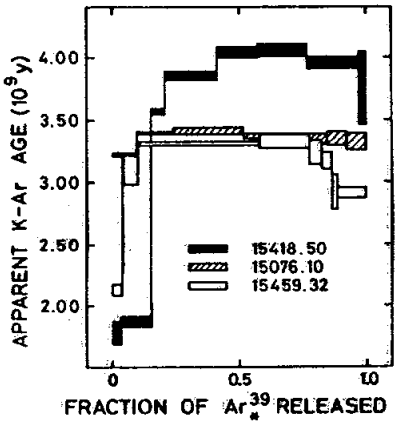

Figure 6. Ar release for 15418 and other samples (Stettler et al., 1973).

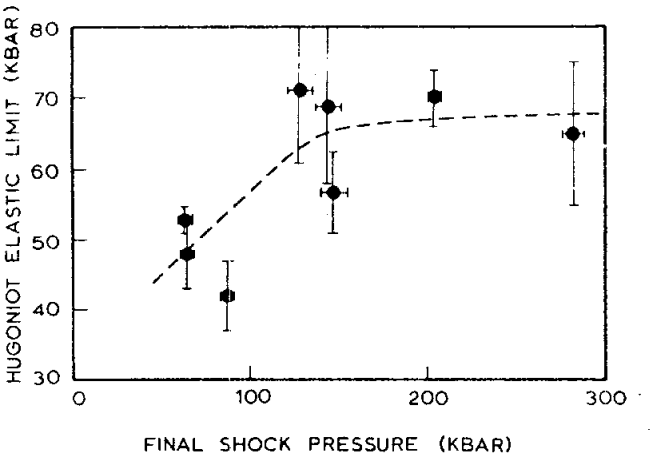

Figure 7. Hugoniot elastic limits as a function of shock pressure (Ahrens et al., 1973).

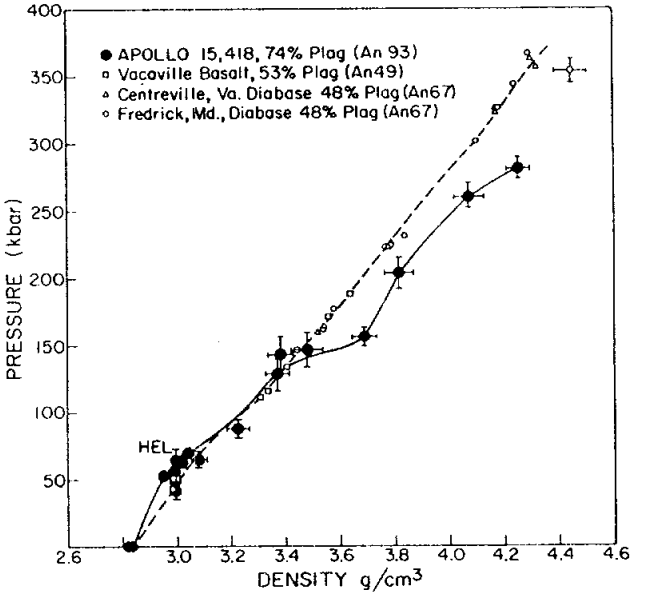

Figure 8. Hugoniot data for 15418 and several terrestrial analogs (Ahrens et al., 1973).

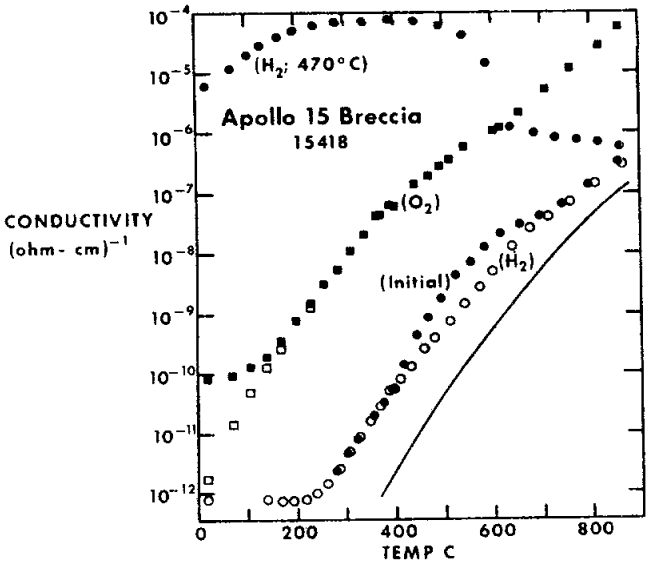

Electrical conductivity (dc) of lunar breccia (Apollo 15418) measured during initial heating, in reducing (H_2) and oxidizing (O_2) atmospheres, and in a reducing atmosphere after oxidation followed by low-temperature reduction (H_2; 470°C). Solid curve represents equivalent d-c leakage conductivity.

Figure 9. Electrical conductivity measurements (Schwerer et al., 1973).

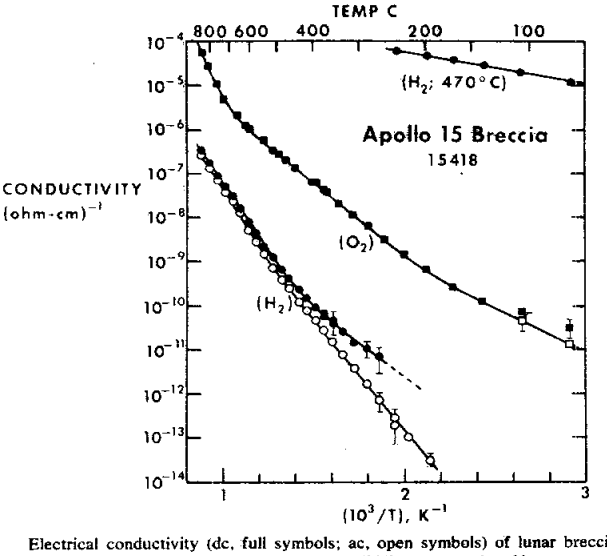

Electrical conductivity (dc, full symbols; ac, open symbols) of lunar breccia (Apollo 15418) in various atmospheres (*see* Fig. 4). Solid lines are results of least-squares fit to Equation 1 (*see* text).

Figure 10. Electrical conductivity measurements (Schwerer et al., 1973).

PROCESSING AND SUBDIVISIONS: Two chips, 1 and ,2 were originally taken from the exterior for allocation, including potted butt ,6 for thin sections ,8 and ,10 to ,26 (Fig. 11). Subsequently the rock was sawn, providing two end pieces which remain more or less intact: ,27 (321.3 g) now in remote storage, and ,0 (526.3 g) (Fig. 12). The slab piece ,28 was substantially subsawn, and ,28 and ,30 substantially split and allocated under the Tatsumoto Consortium and later studies. ,37 became a second potted butt, for thin sections ,152 to ,155. Thin section ,98 was made from ,47, an interior part of the slab taken from ,36.

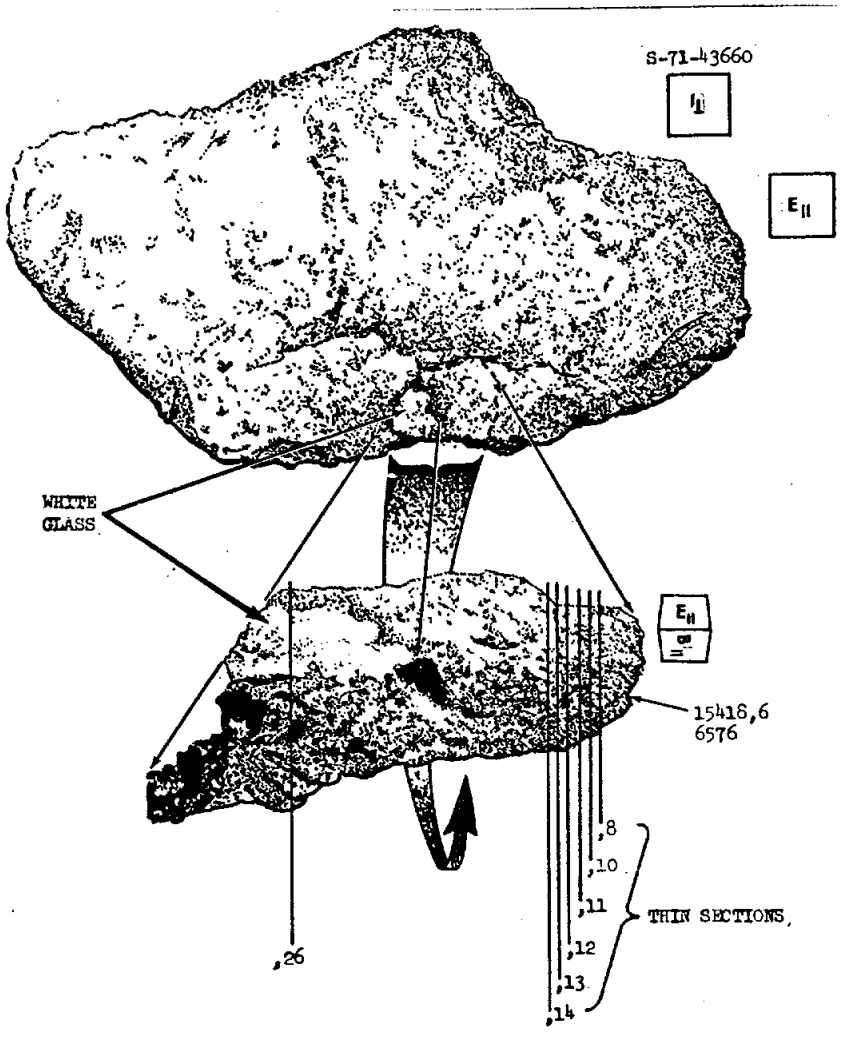

Figure 11. Potted butt ,6 and its thin sections.

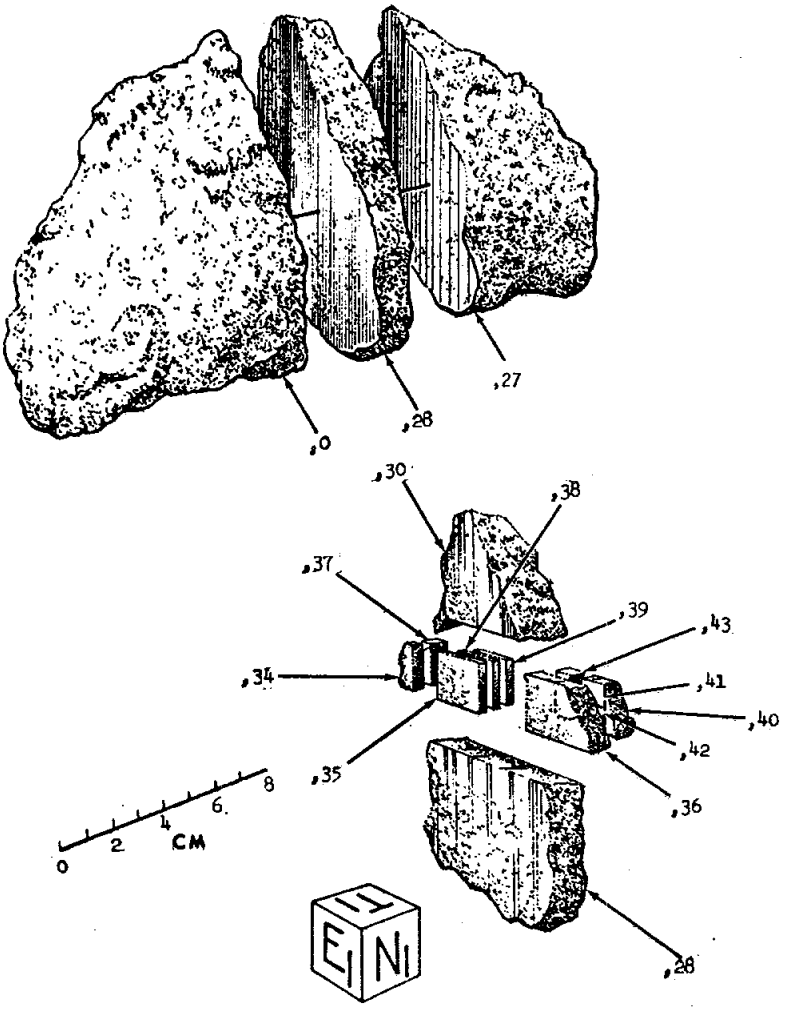

Figure 12. Main sawing subdivision of 15418.

15419 REGOLITH BRECCIA, GLASS-COATED ST. 7 17.7 g

INTRODUCTION: 15419 is a medium light gray regolith breccia, moderately coherent and partly coated with a deep brown glass (Fig. 1). The glass contains about 35% vesicles up to 3 mm in diameter, and is an entity entirely separate from the rock, which it penetrates in thin stringers. Small clasts including basalts, breccias, and plagioclase and other mineral fragments are visible. The sample was collected at the same locality as 15418, which lay on top of it, near sample 15417 on the north lip of Spur Crater. It has never been subdivided or allocated.

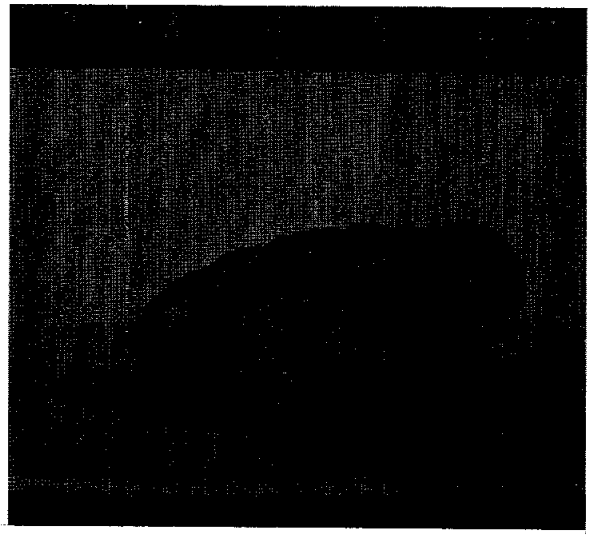

Figure 1. Sample 15419. S-71-43653

15425 GREEN GLASS CLODS ST. 7 136.3 g

INTRODUCTION: 15425 is an extremely friable greenish clod (Fig. 1) in which the green material is the common Apollo 15 volcanic (pyroclastic) green glass. The sample is really a regolith clod with green glass concentrations varying considerably from place to place. Zones extremely rich in green glass are present and grade over short distances into fairly normal-looking regolith zones in which yellow and red glasses and lithic and mineral debris are common.

The clod is light-greenish gray, blocky, and subrounded. It was removed from the sample bag and processed as four pieces. The surface is smooth and too friable to have retained any patina or zap pits; the four pieces have disintegrated into several smaller pieces.

Two clods were collected from the north rim of Spur Crater and are labelled on lunar surface photographs and diagrams as 15425 and 15426 (Fig. 2). The samples were part of a small cluster of fragments each as much as 25 cm across, and were collected because of their green tint, similar to materials observed but not collected at St. 6A. No small crater is clearly related to the rock cluster. The CDR suggested that all the fragments in the cluster were part of a big fragment which broke when it hit (Bailey and Ulrich, 1975). They have generally been interpreted to be ejecta from a depth of perhaps 20 m beneath the surface (LSPET, 1972). The two clods were placed in the same bag and extracted as several pieces which were grouped in a now unknown manner and numbered 15425, 15426, and 15427, with fine material (<1 cm) residue numbered 15421 to 15424. According to data packs, it is likely that all three contain pieces of both of the original clods sampled, and all show variability in concentrations of green glass. Many studies have produced observations and conclusions without discriminating to which particular of the three samples specific data refers. Hence data from all three samples are most usefully considered together.

PETROLOGY: Macroscopically 15425 is fine-grained, with 95% of the material being a light greenish-gray or greenish brown, and with particle sizes less than 0.1 mm. The largest piece contains obvious rock clasts and does not have an exposure of light greenish-gray material. Matrices range from greenish to grayish in a patchy fashion, and the less green varieties, at first considered to be dust-coatings, are the dominant matrix. In general, the green zones appear as clasts (up to a cm or so) in the grayish-brown material. ,4, a piece originally about 15 g, consists of 70 to 80% of a very fine brown-gray matrix, 10% white clasts up to approximately 1 mm, 10% green glass, and less than 1% amber or brown glass. With the green material in the fine matrix, the total green material is 30 to 40%. ,2 (12 g) and ,5 (16 g) appear to be very similar. Few pieces as big as 1 cm appear to be as rich in green glass as some subsamples of 15426 and 15427, although ,7 (2 g) might have as much as 80% green glass.

Figure 1. Four original pieces numbered 15425. S-71-43591

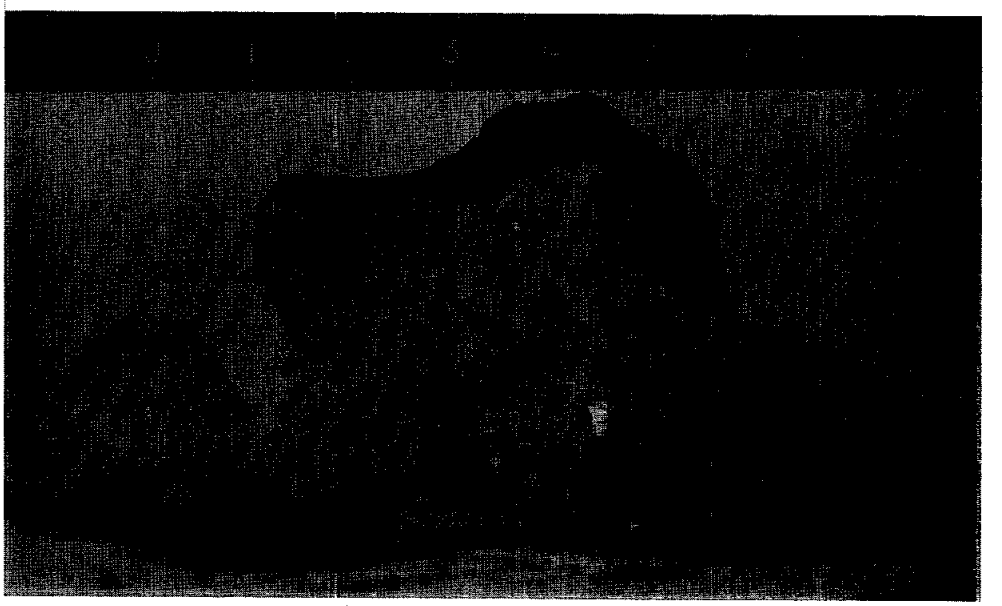

Nagle (1981) found that clods of 15425 were light colored with enough green glass to give a greenish tint, and all the pieces were friable. They showed differences in textural properties, in crystallization states, and in lithic association, and were all poorly sorted. Nagle (1981) drew comparisons with clods in core 15007 which are purer, with more unbroken spheres. 15425 was like 15427 in that numerous particles were crystallized; in 15426 there were more particles with quench crystallites, and the clods in core 15007 had more glassy spheres. (However, these observations are probably more subsample specific than generalizations about the entire samples.) Nagle's (1981) work on 15425 was on a thin section, but his designations of (,67) and (-7) are erroneous, as no such thin sections exist.

All the thin sections are from a single chip, and are of a porous regolith breccia. It contains abundant green glass, including partly crystallized varieties, in a fine-grained, dark brown matrix (Fig. 3). Homogeneous volcanic yellow and red glass spheres, and heterogeneous yellow impact glasses are present. Lithic fragments include coarse highlands materials, including anorthositic and noritic fragments, as well as feldspathic impact melts and agglutinitic-looking glass. In some sections there are zones which are virtually entirely green glass, and these grade very sharply into more typical-looking regolith material. These zones appear to be essentially clasts in the remainder of the rock.

Butler et al. (1972) noted that chondrules (=green glass vitrophyres) are abundant in thin section 15425,16. Agrell et al. (1973) described glass from 15425, 15426, and 15427. All three contain green spheres, subordinate brown spheres, and other glasses of mare derivation. Agrell et al. (1973) listed an analysis of an evolved interstitial glass in an olivine chondrule (= green glass vitrophyre) in 15425, and noted four spheres isochemical with green glass spheres but with a granular crystalline mosaic texture. The average composition for five devitrified spheres is similar to general green glass analyses.

Delano (1979) analyzed clear green glasses in 15425, 15426, 15427, and 15318 with the microprobe for major elements and Ni, finding several different compositional groups; data for 15425 was not specified. Meyer et al. (1975) showed SEM photographs of a green glass sphere and its micromound surface texture from 15425,26. Butler and Meyer (1976) also showed a SEM photograph of a green sphere.

Delano (1980b) analyzed volcanic red glass (TiO_2 about 13.8 wt%) in 15425 as well as 15318, 15426, and 15427. Ni was in all cases below the detection limit of 50 ppm. He found three subgroups related by a prominent chemical trend. Experiments on this composition indicate that trend to originate from shallow (less than 5 kb) fractionation, and the most primitive glass to have originated at about 480 km depth.

Delano (1980a) and Delano et al. (1981) analyzed yellow impact glasses (TiO_2 about 4.8%) in 15425, 15426, 15427, and 15318; chemical data for 15425 was not distinguished. The glasses form a compositional cluster, unlike other impact glasses and distinct from the volcanic yellow glass. About 90% are angular fragments, with schlieren and lithic clasts, not spherules. Delano et al. (1981) considered that the glasses were exotic to the Apollo 15 site and were derived from Eratosthenian-age lavas in Mare Imbrium. However, yellow impact glasses from 15426 and 15427 were dated as 3.35 b.y. old by Spangler and Delano (1984).

Fang et al. (1982) inferred glass cooling rates for 15425, which they describe as a weakly coherent breccia containing a modest fraction of interstitial glass. Their composition for 15425 has 51.14% SiO_2, and 6.66% MgO, is of unknown derivation, and is quite different from 15426 or other likely regolith breccia compositions. The inferred cooling rates necessary for glass formation are higher than can be obtained for radiation, hence, such glasses formed in separate bodies; the breccia formed by subsequent compaction which did not include heating above the liquidus. In view of the unusual composition used, the application of the results to 15425 is questionable.

Nagle (1982) stated erroneously that 15425 was a rake sample and from a crater bottom; in fact it is neither.

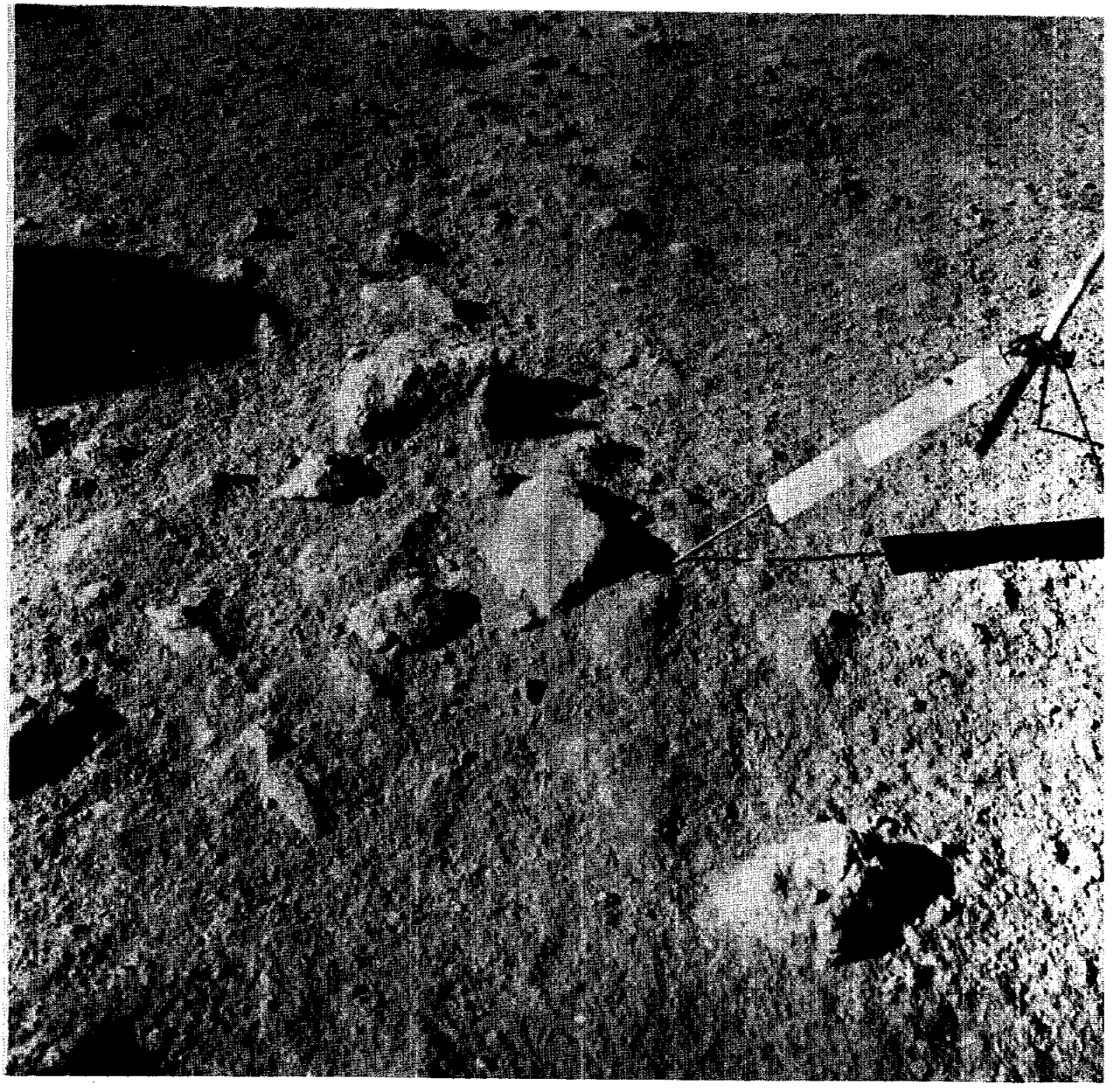

Fig. 2a

Figure 2. Presampling environment of samples 15421-15427 a) surface photograph AS15-86-11666; b) sketch map.

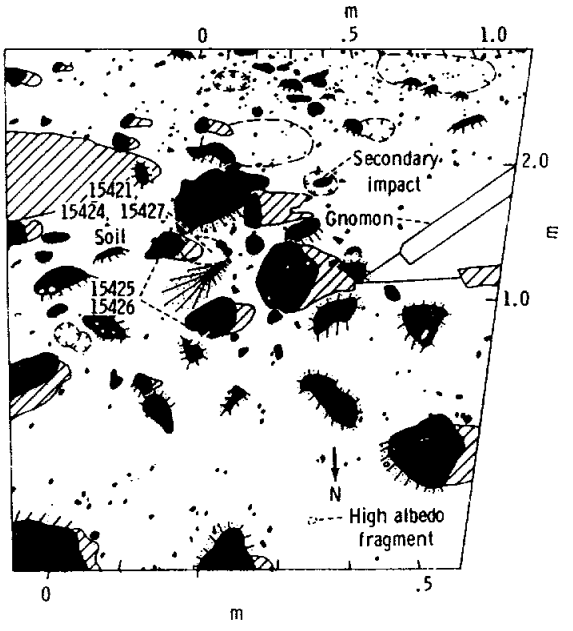

Fig. 2b

CHEMISTRY: No bulk analysis for 15425 has been reported; analyses of individual glasses are included in the reports above. Chemical studies of the surfaces of glasses in 15425 were made by Meyer et al. (1975), Butler and Meyer (1976), Butler (1978), and Cirlin and Housley (1979). Meyer et al. (1975) found that of 50 handpicked droplets studied in 15425,26, only one had large Zn and Pb signals (ion microprobe) and surficial micromounds; SEM-EDX data showed that Zn and S were present in the micromounds but not in the underlying glass. Hence the surficial micromound film is a major site for volatile species. Meyer et al. (1975) consequently deduced a cogenetic origin for the spheres and the surficial volatiles, consistent with a lava fountaining mechanism. The surface Pb has no corresponding U and Th, i.e., it is unsupported. Butler and Meyer (1976) found that S was the most abundant element in the surface coat of the green spheres. 96% of all spheres showed detectable S; for other elements the proportions are: Zn, 79%; Cl, 51%; K, 16%; Cu, 42%; Ni, 17%; and P, 8%. A Zn vs. S plot shows that the ratio is varied from grain to grain (Fig. 4), but is constant for an individual grain (Fig. 5). Butler (1978) showed an SEM photograph and a Zn intensity map of a green droplet in 15425,26. Four brown glass droplets (= yellow volcanic glass) with S and Zn coats were also found, with nearly identical compositions (TiO_2 about 3.6%). Cirlin and Housley (1979) used a scanning Auger microprobe to investigate the surface of green and brown (= yellow volcanic) glasses in 15425, providing data for Zn/S. The volatiles in the outer few atomic layers vary considerably from one droplet to another, but the variation in individual droplets is much smaller. The Zn/S ratio deviates from 1, indicating that the carrier is not merely a ZnS phase . No K was observed in any of the five green glasses, whereas three brown (= yellow volcanic) glasses did show K.

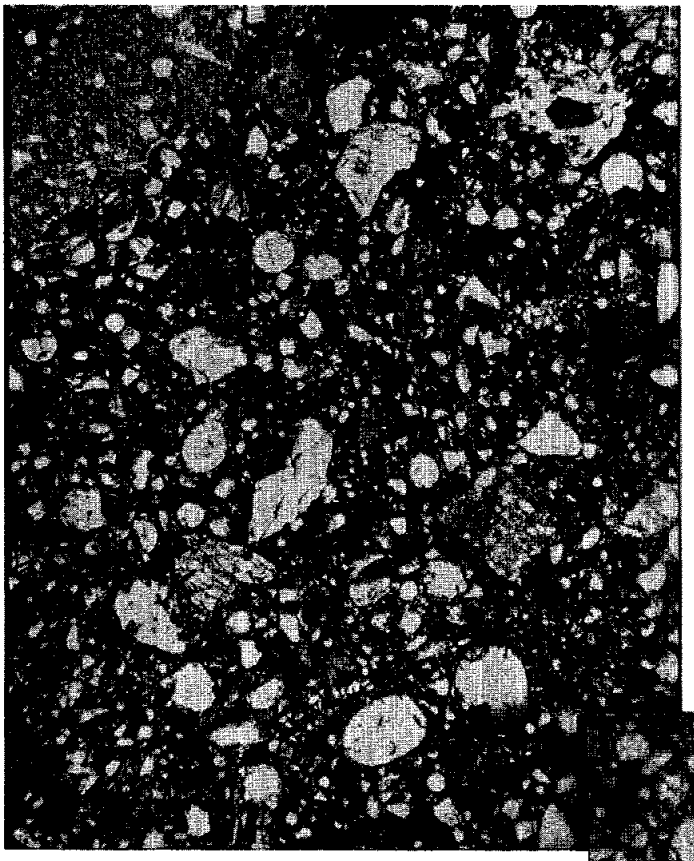

Fig. 3a

Fig. 3b

Figure 3. Photomicrographs of 15425,10. Transmitted light. Widths about 2 mm. a) typical friable regolith, with glass and lithic clasts; b) shows zone at top which is a pure green glass and its partly crystallized products.

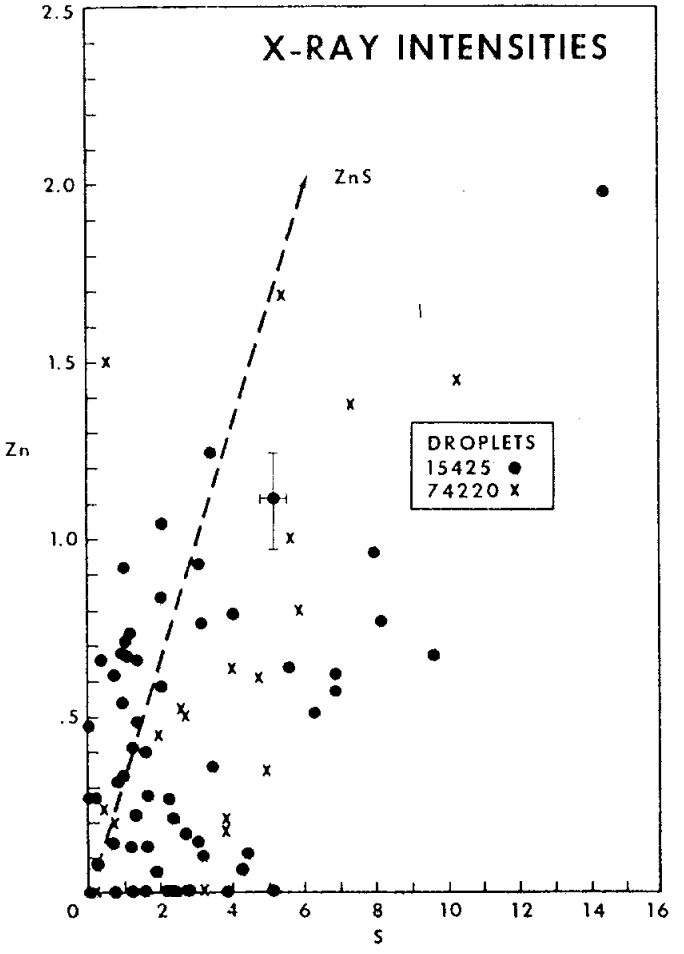

Figure 4. Zn vs. S x-ray intensities for 20x20 micron areas on green glass droplets from 15425,26 (Butler and Meyer, 1976).

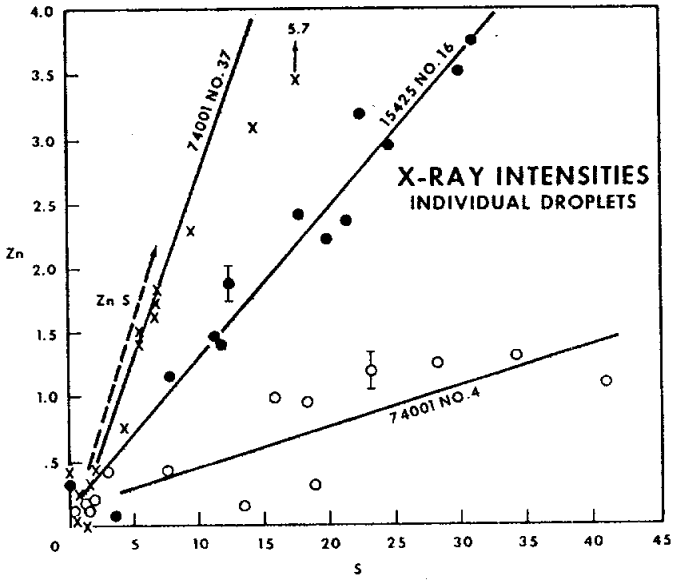

Figure 5. Zn vs. S x-ray intensities for spots on an individual green glass sphere from 15425,26 (Butler and Meyer, 1976).

RADIOGENIC ISOTOPES AND GEOCHRONOLOGY: The only radiogenic isotope study for 15425 is for Pb isotopes in the surficial volatile coat of green glasses by Meyer et al. (1975). Isotopic ratios were determined for individual spheres and the data are probably not diluted by any Pb component supported by U or Th inside the glass; the surficial Pb has apparently been unsupported by U or Th. Only one data point from 15425 was used. Because the ratios of the isotopes to ^{204}Pb could not be determined as well as ^{206}Pb, the data were unconventionally plotted on a $^{208}Pb/^{206}Pb$ vs. $^{207}Pb/^{206}Pb$ diagram (Fig. 6). A constant lunar Th/U ratio of 3.8 was assumed. The data for 15425 agree in a general way with the age determined by Podosek and Huneke (1973), and is consistent with a model in which there was no differentiation in the source region from 4.53 to 3.4 b.y.; the surficial Pb evolved in a $^{204}Pb/^{238}U$-rich source inside the Moon.

PROCESSING AND SUBDIVISIONS: The initial four pieces constituting 15425 soon disintegrated because of their friability into several smaller pieces which were stored as ,1 to ,8 (range 2 g - 77 g), and are probably now in even smaller pieces. ,8 was potted and produced all the thin sections (,10 to ,19). ,4 was subdivided for a few allocations (and is now 4.8 g), and a grain mount was also made from it. ,7, which was believed to be richer in green glass than most, gave birth to ,30 which was sieved and partly consumed.

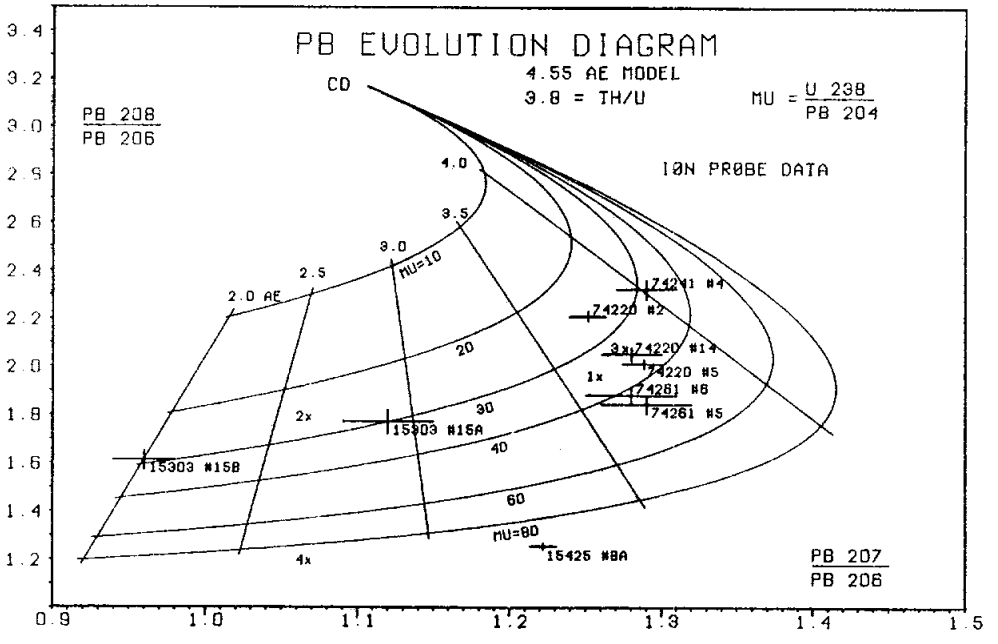

Lead evolution diagram for unsupported lead in Apollo 15 green and Apollo 17 orange glass samples. Only the best ion probe data from Table 2 are plotted here. CD = isotope ratio for primordial lead as measured in Canyon Diablo troilite, μ = mu = today's ratio for $^{238}U/^{204}Pb$ for the source region. Point 1 is Silver's (1974b) value for the lead volatilized from 74220 at 600°C. Point 2 is Silver's (1974a) value for the bulk sample 74220. Point 3 is Silver's bulk value corrected for lead evolved from 3.5 b.y. to present. Point 4 is lead ratio measured for bulk sample of 15426 by Barnes *et al.* (1974). Growth curves for lead isotopes assuming a single-stage evolution in a reservoir with Th/U = 3.8 and variable $^{238}U/^{204}Pb$. The new decay constants for U and Th were used (Tatsumoto *et al.*, 1972).

Figure 6. Pb evolution diagram for green and orange glass droplets (ion microprobe data) (Meyer et al., 1975).

15426 GREEN GLASS CLODS ST. 7 223.6 g

INTRODUCTION: 15426 is an extremely friable greenish clod (Fig. 1) in which the green material is the common Apollo 15 volcanic (pyroclastic) green glass. The sample is really a regolith clod with green glass concentrations varying considerably from place to place. Volcanic yellow and red glasses and yellow impact glasses and some other mineral and lithic debris are present. Green glasses from this sample and 15427 have been dated as ~3.4 b.y. old, yellow volcanic glasses as ~3.6 b.y. old, and yellow impact glasses as ~3.35 b.y. old. Rare gas exposure ages are about 300 m.y.

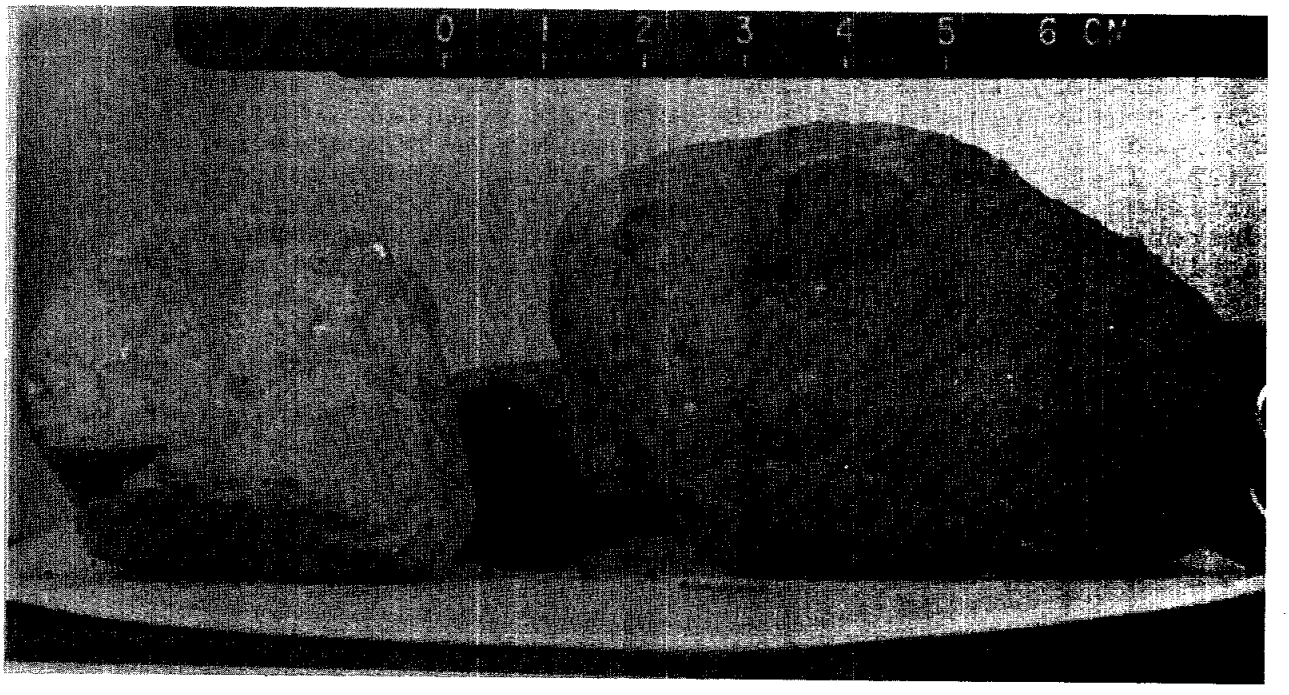

Figure 1. Macroscopic view of 3 pieces of 15426 as removed from the sample bag. ,1 is to right; ,26 is at rear. S-71-43586

The clod is light grayish yellow-green, and is blocky, rounded, and very friable. It was removed from the sample bag and processed as three pieces. It is not entirely homogeneous as some pieces contain more than 90% spherules and are very green, while others contain a smaller proportion of spherules and are grayer. For instance, ,2, from which several thin sections were made, is a spherule-rich polymict regolith breccia, whereas ,29 from which several other thin sections were made consists predominantly of green volcanic glass and yellow impact glass to the general exclusion of other debris. ,26 is a large piece which consists almost entirely of green glass spheres (Fig. 2). The surfaces of pieces of 15426 are too friable to have retained any patina or zap pits. Because of its purity and extreme friability, 15426,26 is a restricted access sample.

15426 was collected with clods 15425 and 15427 and fines from the north rim of Spur Crater (see cataloging of 15425 for numbering and site characteristics). Many studies have produced observations and conclusions without discriminating to which particular of the three samples specific data refer. Hence data from all three samples are most usefully considered together.

PETROLOGY: Macroscopically 15426 is fine-grained and is striking in its abundance and visibility of green glass spherules. Ovoids and broken glasses are much less abundant. As noted above, the sample is not homogeneous, with considerable green glass concentration variations from place to place. Plagioclase, mafic silicates, and small rock clasts are also visible in small amounts. Morris (1976) found that ,97 had an I_s/FeO of 0.3, and McKay et al. (1984) found an I_s/FeO of 0 to 1 for ,126. These are extremely low maturities; it is not clear how much these samples were typical 15426 or purer green 15426. Nagle (1981) observed 15426,26 macroscopically, and drew comparisons with 15425, 15427, and core 15007 green clods. 15426 contained more particles with quench crystallites, whereas 15425 and 15427 had numerous crystallized particles and 15007 had more glassy particles (the observations are probably more subsample specific than sample specific).

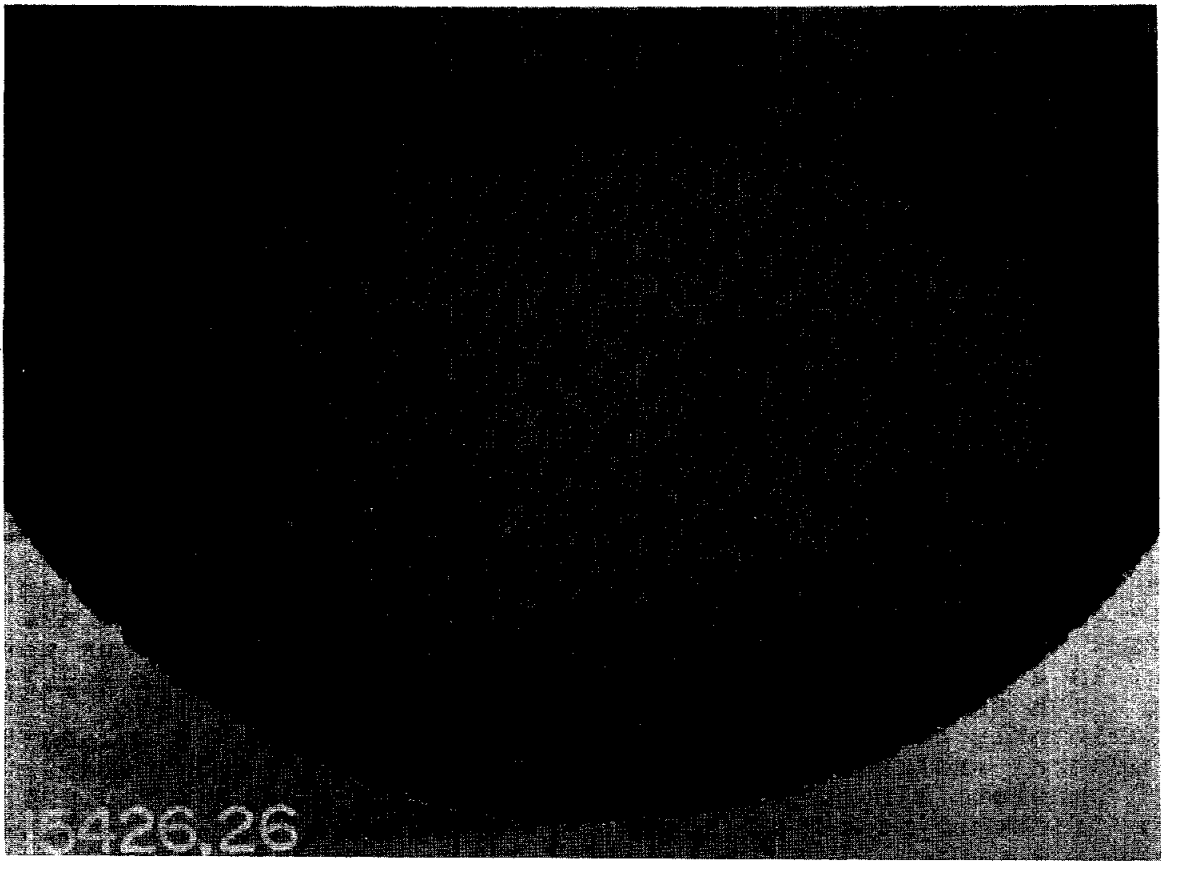

Fig. 2a

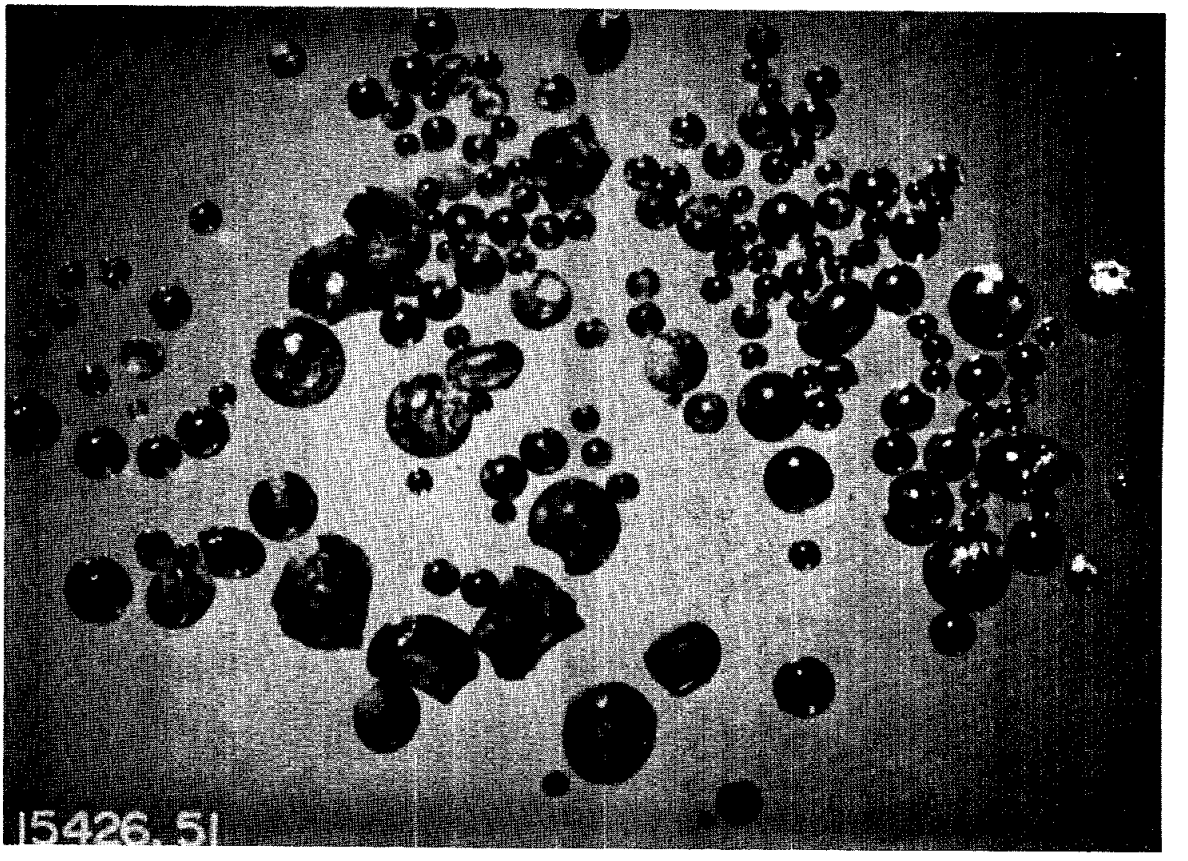

Fig. 2b

Figure 2. a) 15426,26. S-80-42656
b) Particles of green glass from 15426,6.

No comprehensive descriptions of 15426 petrography have ever been published, as most studies have concentrated on the glasses themselves. Thin sections from piece ,2 are of a polymict regolith breccia, not a pure green clod (Fig. 3a). The breccia is porous, contains agglutinitic glass, and not only green but also red and yellow glass spheres, as well as heterogeneous yellow glasses. Lithic clasts are present, including feldspathic crystalline fragments and possibly mare (or KREEP?) basalts, as well as coarse plagioclase and mafic mineral fragments. Thin sections from ,29 are less polymict, and are dominated by a mixture of green volcanic glasses and yellow impact glasses (Fig. 3b). Rare lithic (small, plutonic?) and plagioclase fragments are scattered. Wood and Ryder (1977) found thin section ,19 to be a more mature regolith breccia than a 15427 sample, containing rock, mineral, and glass clasts, with 68% of the sample being a "matrix" of less than 25 micron grain size. Both mare and highland mineral fragments were identified. Desmarais et al. (1973) found 5% agglutinates in the greater-than-105 micron fraction of a split from a green-enriched clod.

Fig. 3a

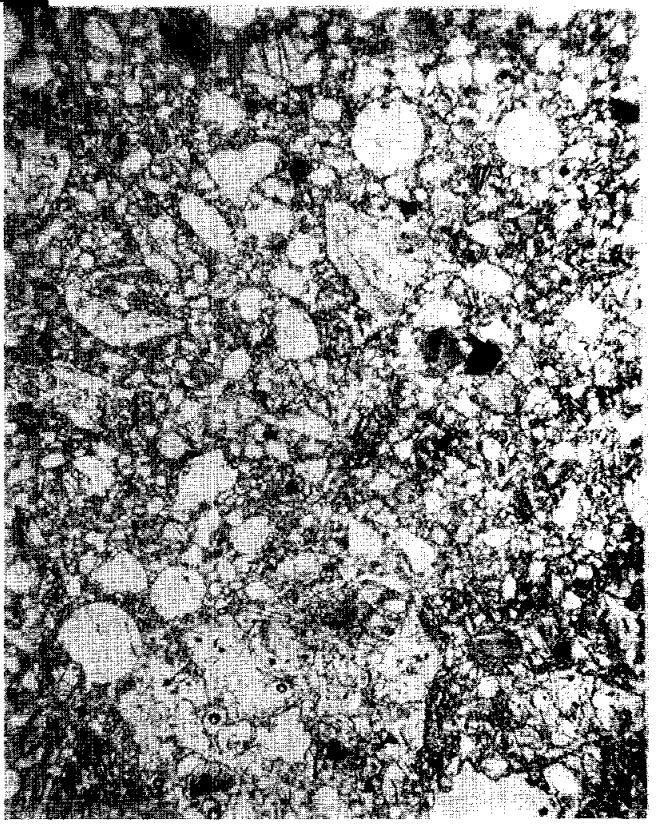

Fig. 3b

Figure 3. Photomicrographs of 15426. Transmitted light. Widths about 2 mm. a) 15426,17, showing regolith-like nature; b) 15426,70, showing mix of green glass spheres and yellow impact glasses.

Butler et al. (1972) noted that "chondrules" (= partly crystallized green glass) are abundant in thin sections from ,2 (they list thin section ,19 erroneously as from 15436), and depicted a "plag-px-glass" chondrule with a diameter of 0.35 mm. Agrell et al. (1972) described glasses from 15425, 15426, and 15427, with SEM observations of spheres and composite aggregates indicating a multiplicity of collisions and adhesions. They ascribed to the green glasses an impact origin, in which the final stage produced low velocity microcraters and minor abrasions. An absence of high velocity micrometeorite impacts indicates that the glasses, unlike many other types, were not exposed at the surface.

Green glasses have received the most intensive study, following early recognition of this glass type at the Apollo 15 site as common and significant (e.g., Ridley et al., 1973b). Desmarais et al. (1974) determined a mean grain size of $\phi = 3.2$ for green glasses, and Morgan and Wandless (1974) found $\phi = 3.25$, coarser than Apollo 17 yellow glass. Butler (1978) listed a microprobe analysis of a green glass droplet, recognizing its volcanic nature, and Delano (1979) precisely analyzed green glasses in 15425, 15426, and 15427 for major elements and Ni with the microprobe. These glasses defined two main arrays and five individual groups. Data from 15426 was not specified. Delano and Lindsley (1982) analyzed glasses from groups B and C in 15426 for P, Mn, Ti, and Cr to provide additional petrogenetic constraints, and suggested that the fractionation trends are difficult to understand in terms of any silicate and oxide assemblage, and speculated that igneous processes other than crystal-liquid fractionation might have occurred. Wood and Ryder (1977) discussed the enigma of the green glass compositional variation, which caused problems for both igneous and impact origin concepts. Basu et al. (1979) studied green glass vitrophyres in 15426 and 15427 (and other regoliths) providing microprobe data on glass and olivine compositions. Grove (1981) discussed data for 15426 green glasses, incorrectly attributing the Hlava et al. (1973) data to 15426, and assuming that all of the Delano (1979) analyses were from 15426. His discussion related the observed chemical trends to sulfide fractionation as part of the petrogenesis of green glasses. Griscom et al. (1973, 1975) and Friebele et al. (1974) conducted ESR/FMR studies on separated green glass balls, finding a spectrum interpreted as arising entirely from "magnetite-like" phases (total ~0.01 wt %) (Fig. 4). Cusps and discontinuties in the spectrum show a behaviour typical of many titanomagnetites but unknown for Fe-iron. The "magnetite-like" phase is probably a ferric iron spinel. Burns and Dyar (1982) made a Mossbauer spectral study of handpicked green spherules, and found no Fe^{3+} in either it or a synthetic glass made at fO_2 of 10^{-14} atmospheres. Earlier work on a synthetic glass made at fO_2 of 10^{-11} atmospheres had shown significant Fe^{3+}. The spectrum showed olivine crystallites to be present; significant changes of coordination about Fe^{3+} ions occur in the glass during olivine crystallization.

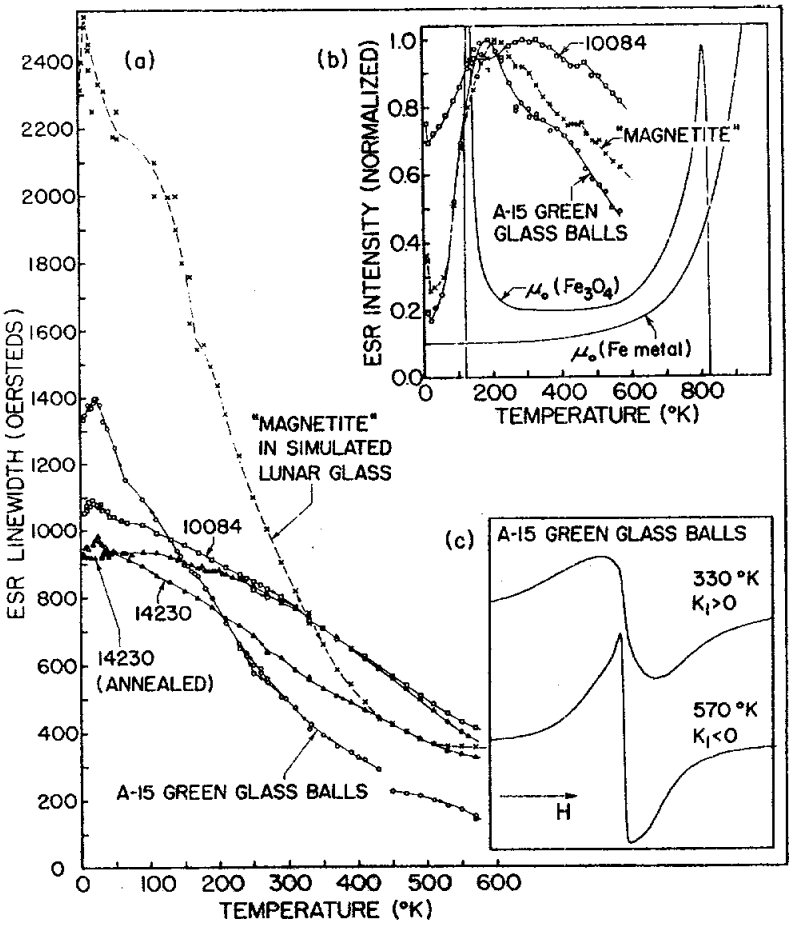

Figure 4. Temperature dependance of ESR (a) linewidth and (b) intensity for 15426 glass balls and other materials (Griscom et al., 1973).

Delano (1980b) analyzed red volcanic glasses (TiO_2 ~13.8%) in 15426,72 as well as in samples from 15318, 15425, and 15427, for major elements and Ni using the microprobe. Data for 15426 were not specified. Ni was always less than the detection limit of 50 ppm. Three subgroups were identified, related to each other by a prominent chemical trend. Experiments on this composition indicates that trend to originate from shallow (less than 5 kb) fractionation, and the most primitive glass to have originated at about 480 km depth.

Wood and Ryder (1977) reported an average composition for five homogeneous yellow glasses in 15426,19; these glasses are the volcanic yellow glasses of Delano and Livi (1981). Delano (1980a), Delano et al. (1981) and Spangler and Delano (1984) analyzed yellow impact glasses (TiO_2 ~4.8%) in 15426 as well as 15425, 15427 and 15318; chemical data for 15426 were not distinguished. The glasses form a compositional cluster, unlike other impact glasses, and are distinct from the volcanic yellow glass. About 90% are angular fragments, with schlieren and lithic clasts, not spherules. Delano et al. (1981) considered that the glasses were exotic to the Apollo 15 site and were derived from Eratosthenian-age lavas in Mare Imbrium. However, such yellow impact glasses from 15426 (and 15427) were dated as 3.35 b.y. old by Spangler and Delano (1984). Delano et al. (1982) depicted yellow impact glass in 15426,72, containing three large single crystal clasts (olivine and pyroxene) and smaller inclusions of volcanic green glass, orthopyroxene, and olivine. All clast-glass contacts are sharp.

Ridley et al. (1973) quoted 15426 erroneously at the start of their paragraph 4; all their data and observations are for 15427.

CHEMISTRY: Chemical analyses are tabulated separately as bulk clods (Table 1); sized fractions of bulk clods (Table 2); green glass composites (Table 3); and brown (= yellow volcanic) glass composites (Table 4). Rare earth data for a very green bulk clod sample and for green glass composites and brown (yellow volcanic) glass are shown in Figure 5.

Only one clod analyses, that of Keith et al. (1972), represents bulk rock and that is for only K, U, and Th; all the other clods were selectively green-enriched portions of the rock. The data of Keith et al. (1972) is similar in U and Th to that of Taylor et al. (1973) for fines 15421, the less-than-1-mm bag residue from 15425, 15426, and 15427, and probably represents bulk rock. All other analyses are variously lower in U. Most of the analyses listed were reported without significant discussion. The "bulk" analyses labelled ,118 are all from the very green-glass rich sample ,26; most others from another green-glass rich sample ,27, and that of Korotev (1984 unpublished) is from a split of ,1. The iron in the bulk clod analyzed magnetically by Pearce et al. (1973) also suggests it was almost pure green glass. Th, Rb, Pb, and S are also lower in these "bulk" clods than in the Taylor et al. (1973) analysis of 15421 fines. These "bulk" analyses are enriched over the green glass composites in U and Th, and other incompatibles, but not by very much, nor are the refractory siderophiles greatly enriched compared with pure green glass, and Ni is not enriched at all. The major elements of Korotev (1984, unpublished) are a little higher in Al and Ti and a little lower in Mg than pure green glass. Morgan and Wandless (1984) found that the abundances of refractory siderophile elements Os, Re, and Ir are uniform, averaging 7.8 x 10^{-4} x Cl chondrites. Volatile siderophile elements and chalcogens are much more abundant. With appropriate corrections for an indigenous lunar contribution, the siderophile abundances resemble the Group 1L meteoritc component ascribed to Imbrium (Hertogen et al., 1976), but may also reflect direct derivation from a "primitive" lunar mantle.

TABLE 15426-1. Analyses of bulk clod samples

		,0	,36	,31	,118	,118	,35	,33	,32	,30	,97	,126
(wt %)	SiO2											0.50
	TiO2											9.7
	Al2O3										19.4	17.9
	FeO											15.1
	MgO											8.5
	CaO											0.22
	Na2O											
	K2O	0.11										
	P2O5											
(ppm)	Sc											33.5
	V											124
	Cr											3360
	Mn											1805
	Co											69.6
	Ni				116	163						210
	Rb		0.584									
	Sr		40.59									66
	Y											70
	Zr											
	Nb											
	Hf											2.6
	Ba											59
	Th	1.89	0.4203									0.9
	U	0.41	0.1134		0.061	0.081	0.125					0.23
	Pb		1.248									
	La											4.99
	Ce											13
	Pr											
	Nd											8
	Sm											2.43
	Eu											0.478
	Gd											
	Tb											0.51
	Dy											
	Ho											
	Er											
	Tm											
	Yb											2.10
	Lu											0.304
	Li											
	Be											
	B											
	C			23				2.5	21	7		
	N								42	29		
	S								340			
	F											
	Cl											
	Br											
	Cu											
	Zn				26	24	51					
(ppb)	I											
	At											
	Ga											
	Ge											
	As											
	Se				109	106	125					
	Mo											
	Tc											
	Ru											
	Rh											
	Pd				<1.5							
	Ag				21	14	25					
	Cd				110	89	118					
	In						5.6					
	Sn											
	Sb				2.9	0.9	0.89					
	Te											60
	Cs											270
	Ta											
	W											
	Re				0.031	0.032	0.034					
	Os				0.42	0.41						
	Ir				0.32	0.28	0.32					<2
	Pt											<2
	Au				0.52	0.34						
	Hg											
	Tl				3.0	2.0	4.2					
	Bi				2.7		1.7					
		(1)	(2)	(3)	(4)	(4)	(4)	(5)	(6)	(7)	(8)	(9)

References and methods:

(1) Keith et al. (1972); gamma ray spectroscopy
(2) Barnes et al. (1973); isotope dilution, mass spectrometry, and some variations
(3) Desmarais et al. (1973); pyrolysis, gas chromatography
(4) Morgan and Wandless (1984); RNAA
(5) Modzeleski et al. (1972); vacuum pyrolysis, mass spectrometry
(6) Moore and Lewis (1972, 1976), Moore et al. (1973), Cripe and Moore (1974); combustion, gas chromatography
(7) Wszolek et al. (1972); pyrolysis, mass spectrometry
(8) Pearce et al. (1973); magnetic
(9) Korotev (1984 unpublished); INAA

TABLE 15426-2. Analyses of sized fractions of bulk green-rich clods

		,35(A)	,35(B)	,35(C)	,35(D)	,35(E)
Wt %	SiO2					
	TiO2					
	Al2O3					
	FeO					
	MgO					
	CaO					
	Na2O					
	K2O					
	P2O5					
(ppm)	Sc					
	V					
	Cr					
	Mn					
	Co	48				
	Ni		160	183	146	96
	Rb	0.47				
	Sr					
	Y					
	Zr					
	Nb					
	Hf					
	Ba					
	Th					
	U	0.095	0.112	0.075	0.065	0.066
	Pb					
	La					
	Ce					
	Pr					
	Nd					
	Sm					
	Eu					
	Gd					
	Tb					
	Dy					
	Ho					
	Er					
	Tm					
	Yb					
	Lu					
	Li					
	Be					
	B					
	C					
	N					
	S					
	F					
	Cl					
	Br	0.136				
	Cu					
	Zn	80	10.4	11.4	20	80
(ppb)	I					
	At					
	Ga					
	Ge	196				
	As					
	Se	174	43	61	85	334
	Mo					
	Tc					
	Ru					
	Rh					
	Pd		<2.5	<0.8	1.69	<2.5
	Ag	39	5.6	7.9	13.8	53
	Cd	183	34	49	72	283
	In	9.3				
	Sn					
	Sb	1.58	0.21	1.00	1.16	0.83
	Te	16				
	Cs	27				
	Ta					
	W					
	Re	0.047	0.014	0.0421	0.0130	0.048
	Os		0.28	0.42	0.26	0.68
	Ir	0.41	0.190	0.30	0.166	0.43
	Pt					
	Au		0.141	0.144	0.21	1.23
	Hg					
	Tl	6.9	1.41	0.90	1.75	8.0
	Bi	2.4	<0.7	26	8.9	64
		(1)	(2)	(2)	(2)	(2)

TABLE 15426-3. Analyses of bulk separated green glass spherules

		,38	,35	,31	,74	?(A)	?	?	(c)	?	,48(D)
Wt %	SiO2	45.6									
	TiO2	0.29				0.38	0.33				
	Al2O3	7.67				7.5	7.7				
	FeO	19.7				20.0	20.1				
	MgO	16.6				17.5	18				
	CaO	8.72				8.5	8.1			8.4	
	Na2O	0.12				0.133	0.144			0.014	
	K2O	<0.06					0.018				
	P2O5										
(ppm)	Sc	43				37.5	39				
	V	150				165	170				
	Cr	2800				3660	3860				
	Mn	1600				2020	1960				
	Co	72	77			74.8	80				
	Ni	170				153		154			
	Rb	0.34	0.46								
	Sr										
	Y	7.2									
	Zr	22.0									
	Nb	1.5									
	Hf	0.42				0.57	0.7				
	Ba	17.0									
	Th	0.08									
	U	0.02	0.120		0.050			0.0218	0.049		
	Pb	0.53									
	La	1.4				1.2	1.25				
	Ce	3.8									
	Pr	0.53									
	Nd	2.2									2.2
	Sm	0.76				0.83	0.78				0.73
	Eu	0.21				0.24	0.24				
	Gd	0.91									
	Tb	0.15				0.21	0.18				
	Dy	1.1									
	Ho	0.27									
	Er	0.8									
	Tm	0.15									
	Yb	0.93				0.97	0.92				
	Lu	0.14				0.14	0.16				
	Li										
	Be										
	B										
	C			25							
	N										
	S										
	F										
	Cl										
	Br		0.040								
	Cu	3.5									
	Zn		19								
(ppb)	I										
	At										
	Ga	4700									
	Ge		37					9.0			
	As										
	Se		69								
	Mo										
	Tc										
	Ru										
	Rh										
	Pd										
	Ag		8.9								
	Cd		46								
	In		1.3								
	Sn	120									
	Sb		0.12								
	Te		3.3								
	Cs		24								
	Ta										
	W	140									
	Re		0.020					0.0058			
	Os										
	Ir		0.22					0.117			
	Pt										
	Au		0.188								
	Hg										
	Tl		1.13								
	Bi		0.38								
		(1)	(2)	(3)	(4)	(5)	(5)	(6)	(7)	(8)	(9)

TABLE 15426-4. Analyses of brown glass composites

		,35	,33?	,33?(c)
Wt %	SiO2			
	TiO2		3.7	
	Al2O3		8.5	
	FeO		23.2	
	MgO		12.5	
	CaO		9.0	
	Na2O		0.40	
	K2O		0.09	
	P2O5			
(ppm)	Sc		43.5	
	V		116	
	Cr		3780	
	Mn		2120	
	Co	60	65.2	
	Ni			
	Rb	2.0		
	Sr			
	Y			
	Zr			
	Nb			
	Hf		5.1	
	Ba			
	Th			
	U	0.915		0.72
	Pb			
	La		9.6	
	Ce			
	Pr			
	Nd			
	Sm		6.8	
	Eu		1.51	
	Gd			
	Tb		1.4	
	Dy			
	Ho			
	Er			
	Tm			
	Yb		4.5	
	Lu		0.62	
	Li			
	Be			
	B			
	C			
	N			
	S			
	F			
	Cl			
	Br	0.045		
	Cu			
	Zn	18		
(ppb)	I			
	At			
	Ga			
	Ge	64		12
	As			
	Se	101		
	Mo			
	Tc			
	Ru			
	Rh			
	Pd			
	Ag	8		
	Cd	<48		
	In	1.2		
	Sm			
	Sb	0.3(a)		9.2(b)
	Te	12		
	Cs	174		
	Ta		700	
	W			
	Re	0.029		0.0166
	Os			
	Ir	0.38		0.143
	Pt			
	Au	0.195		0.66(b)
	Hg			
	Tl	1.77		
	Bi	<2.8		
		(1)	(2)	(3)

References for Table 15426-2

References and methods:

(1) Ganapathy et al. (1973); RNAA
(2) Morgan and Wandless (1984); RNAA

Notes:

(A) finest portion "matrix", mainly green glass spheres
(B) sieved >240 microns from bulk
(C) sieved 270-72 microns from bulk
(D) sieved 72-37 microns from bulk
(E) sieved <37 microns from bulk

References for Table 15426-3

References and methods:

(1) S.R. Taylor et al. (1972, 1973), S.R. Taylor (1972); spark source mass spectrography; emission spectrography; microprobe
(2) Ganapathy et al. (1973); RNAA
(3) Desmarais et al. (1973); pyrolysis, gas chromatography
(4) Fleischer and Hart (1974); tracks of neutron-induced ^{235}U fissions
(5) Ma et al. (1981); INAA
(6) Morgan and Wandless (1984); RNAA
(7) Simoneit et al. (1973); fission tracks
(8) Podosek and Huneke (1973); argon isotopes
(9) Lugmair and Marti (1977, 1978); isotope dilution, mass spectrometry

Notes:

(A) weighted mean of 55 green glasses analyzed individually
(B) combined from analyses of several green glass groups
(C) average of 100 green glass spheres
(D) combined leached, whole sphere, and broken sphere fractions with unleached yellow-green devitrified fractions, all of which show no significant difference.

References for Table 15426-4

References and methods:

(1) Ganapathy et al. (1973); RNAA
(2) Ma et al. (1981); INAA
(3) Morgan and Wandless (1984); RNAA

Notes:

(a) low precision, ±0.2
(b) high from contamination, according to authors.
(c) etched

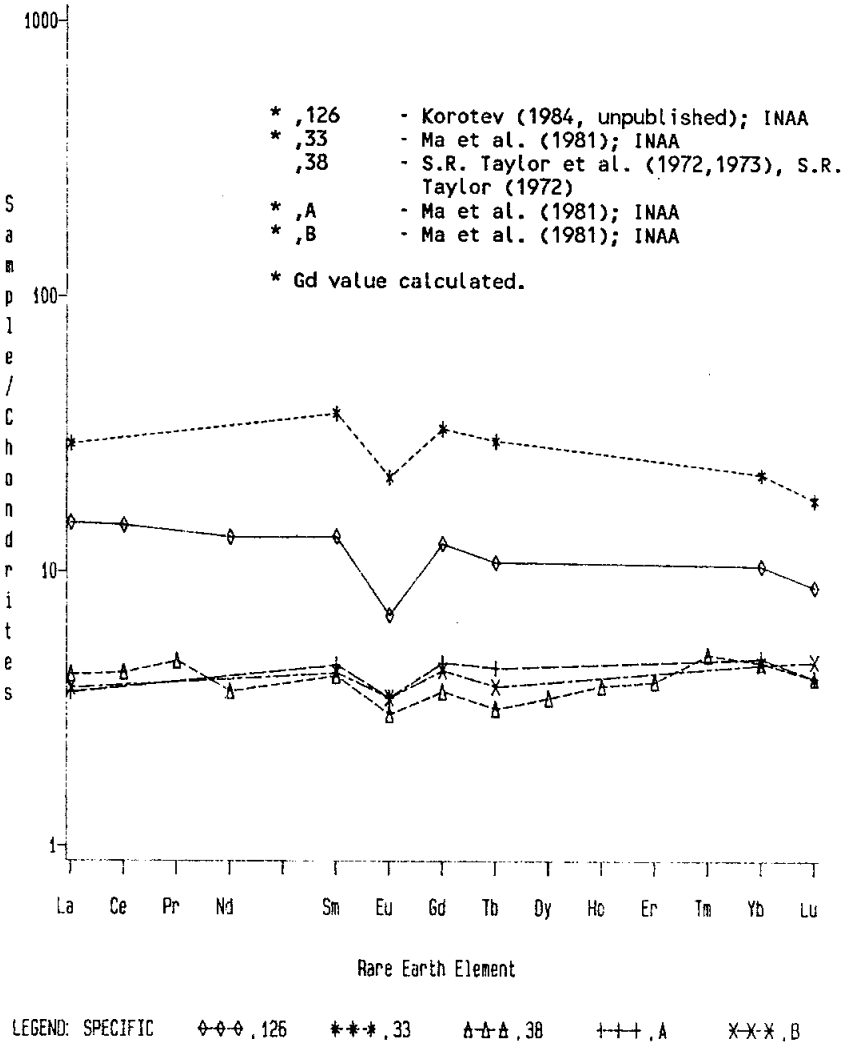

Figure 5. Rare earths in 15426 green glass and yellow glass.

Desmarais et al. (1973) reported carbon as its contribution from CH_4 (0.4 ppm C), CO (15.0) and CO_2 (8), with the total C of 23 ppm, similar to other soils, and to the green glass itself. A similar C abundance was found by Modzeleski et al. (1972) and Wszolek et al. (1972) using methods criticised by Desmarais et al. (1973) (also separate CO, CO_2, CH_4 determinations) as less efficient in releasing all C than is combustion. Desmarais et al. (1974) also analyzed for hydrogen, finding 12 ± 0.5 micromoles/g, which is lower than most mature cores and fines (40-70). Two-thirds of the hydrogen is released between 450 and 1050°C. The surface correlated H is 42 ± 14 micromoles H/cm², the volume correlated only 2 ± 5 micromoles H/g (cf. total H of 12 micromoles/g). Wszolek et al. (1972) measured gases released by dissolution (DF dissolution) finding very small quantities of CD_4, CH_4, and C_3D_6, with total deuterocarbons only 1 or 2 % their abundances in other soils. They find their data for C and N (little surface implanted) to be consistent with an origin from 20 m within Spur Crater. Simoneit et al. (1973) used the same green-glass enriched clod to study release of other gases by pyrolysis, showing diagrams for H_2O, N_2, CO, NO, and H_2S release. They found very low amounts of these products; H_2O, NO, and CO2 were released at low temperatures (<400°C), whereas H_2S, N_2, and CO were released at 1200-1300°C, probably on melting of the sample.

Sieved fractions (Table 2) indicate that the log abundance of volatile elements is correlated with surface area (Morgan and Wandless, 1984). The correlation lines are parallel (Fig. 6) in spite of differences in volatility, indicating control by a single major phase, e.g., ZnS. The refractory siderophiles Os, Re, and Ir have a complex distribution versus surface area and appear to have two components. The distributions indicate that similar volatile species were involved, possibly carbonyl or carbonyl halides. The "finer matrix" of Ganapathy et al. (1973) is similar to an average of the Morgan and Wandless (1984) fractions for most elements, but its size is unknown as it was handpicked, not sieved. From it, Ganapathy et al. (1973) inferred that the matrix was enriched in volatiles, and that the volatiles and siderophiles are of lunar origin, perhaps condensed on the spheres in the impact [sic] which produced them.

Analyses of green glass composites of materials separated from the clods are generally consistent with each other (Table 3). The major element chemistry is basaltic but more magnesian than any other mare basalts, and the rare earths are primitive and barely fractionated, with a small Eu anomaly. Refractory siderophiles are low and similar to those of Apollo 15 low-Ti mare basalts. Fleischer and Hart (1972, 1973) originally determined a U abundance of 5.1 ± 1.5 ppb for three green glass spherules, but later revised their data to about 50 ppb (Fleischer and Hart, 1974). Desmarais et al. (1978) analyzed for carbon contributions from different compounds, finding 0.14 ppm C from CH_4, 18.0 from CO, and 6.7 from CO_2, similar to the bulk clod (which was rather green glass rich). They claim that this demonstrates that molten material can retain some C. Desmarais et al. (1974) made hydrogen measurements, finding 10 ± 2.5 micromoles/g for the 149-1000 micron fraction of glass, similar to the bulk clod also analyzed.

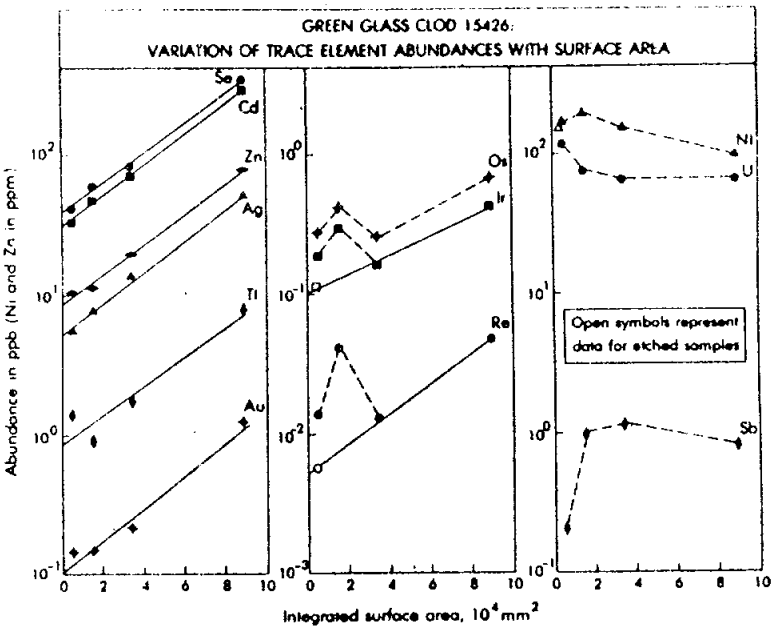

Figure 6. Trace elements and surface area for green glass (Morgan and Wandless, 1984).

Ma et al. (1981) made a chemical study of individual green glass spheres (<1 mg); 175 were analyzed for Na and Mn, and 55 for majors, transition metals, and rare earths. The data showed them to belong to several different groups (not equivalent to the Delano (1979) groups based on microprobe major element data), whose petrogenetic signficance was discussed by Ma et al. (1981). Morgan and Wandless (1984) used the same samples to characterise the groups in refractory siderophiles and volatiles. They also found a correlation of Ni and U, counter to geological experience but in accord with the anticorrelation of Ni with Mg found by Delano (1979). The argon isotopic studies by both Huneke et al. (1973) and Podosek and Huneke (1973) and Spangler et al. (1984) indicate that the K/Ca ratios of the exterior few microns of the green glasses are higher than the interiors, and this is almost certainly a result of higher K in the exteriors of the spheres.

Brown (=yellow volcanic) glasses are distinct from the green glasses and form a tight cluster (Delano and Livi, 1981). They are lower in MgO, and richer in TiO_2 (~3.8%) and incompatible elements. Their siderophile abundances demonstrate them to be uncontaminated with meteoritic meterial. Ma et al. (1981) analyzed five such glasses individually and inferred that despite their tight clustering they consist of groups related by mixing and fractionation lines. Brown glass data were presented but not discussed by Ganapathy et al. (1973) and by Morgan and Wandless (1984).

STABLE ISOTOPES: Clayton et al. (1972, 1973), and Clayton and Mayeda (1975) measured oxygen isotopic ratios in a subsplit of a green glass-enriched clod. The low δO^{18} (Table 5) is a result of the high pyroxene and olivine components of the melt. The δO^{18} and δO^{17} values show that the samples lie on an Earth-Moon mass fractionation line.

Barnes et al. (1973) determined K isotopic ratios: $^{39}K/^{41}K$ of 14.018 and 14.004, and $^{40}K/^{41}K$ of 0.001845 and 0.001830. These data do not show fractionation effects, whereas regoliths do, hence 15426 is not merely a compacted soil.

TABLE 15426-5. Oxygen isotopes in ,42, a green glass enriched portions

WR δO^{17}	WR δO^{18}	Spheres δO^{18}	Reference
	5.41	5.27	Clayton et al. (1972)
	5.46	5.32	Clayton et al. (1973)
2.60	5.27		Clayton and Mayeda (1975)

RADIOGENIC ISOTOPES/GEOCHRONOLOGY: Hussain (1972) reported the first age determination for green glass spherules. Using the ^{40}Ar-^{39}Ar method he derived an age of 3.79 ± 0.08 b.y., consistent with an origin in the Imbrium impact. No details of the analysis have ever been published. The age is inconsistent with ^{40}Ar-^{39}Ar studies by Huneke et al. (1973) and Podosek and Huneke (1973) and by Spangler et al. (1984), in which ages similar to other Apollo 15 mare basalts were determined. The former study provided an age of 3.38 ± 0.06 b.y. for a composite of green glasses. The age was determined from the three higher temperature releases in which most of the ^{39}Ar was released, and in which corrections for trapped ^{40}Ar are small (Fig. 7). At the lowest temperature releases trapped ^{40}Ar is significant. The data are considered very reliable and irreconcilable with the age by Husain (1972). Spangler et al. (1984) used the laser microprobe for argon releases and dated six glasses from green glass group A (Delano, 1979) as an average 3.41 ± 0.12 b.y. old and three from group D as an average 3.35 ± 0.18 b.y. old. The samples include examples from both 15426 and 15427. There is no significant difference among these ages or with the age determined by Huneke et al. (1973) and Podosek and Huneke (1973). The method produced low amounts of argon, but the low blanks and internal checks give confidence in the data. Lakatos et al. (1973) also studied Ar in 15426, but mainly for exposure purposes. However, from ^{40}Ar, ^{39}Ar data intercepts, they determined that the spherules were constrained to be older than 2.5 b.y., younger than 4.4 b.y., hence were not formed in the Spur Crater impact.

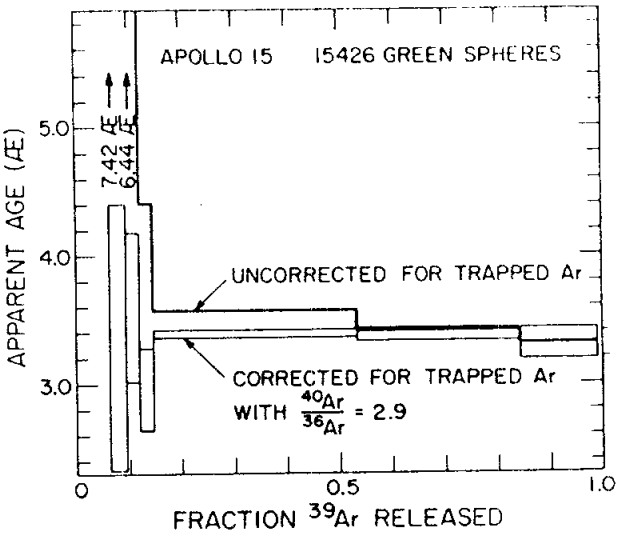

Figure 7. Ar-release and age (Huneke et al., 1973).

Barnes et al. (1973) analyzed a bulk green glass-enriched sample for $^{87}Sr/^{86}Sr$ and for Pb isotopes. The $^{87}Sr/^{86}Sr$ is 0.70301, giving a model age (I = 0.6990) of 6.642 m.y. ($\lambda\ ^{87}Rb = 1.39 \times 10^{-11}$), indicating complexities for the isotopic system. Pb isotopes also give very old model ages (Table 6) presumably because the Pb is unsupported surficial material (see Meyer et al., 1974).

TABLE 15426-6. Pb-isotopic ratios and model ages (Barnes et al., 1973)

Pb-ratios (after blank correction)				Model ages (b.y.)		
208/206	207/206	204/206	Pb207/Pb206	Pb206/U238	Pb202/U235	Pb208/Th232
1.1186	1.0683	0.01580	4.670	8.427	6.074	16.209

Lugmair and Marti (1977, 1978) analyzed three composites of green glass separates for Sm and Nd isotopes (Table 7). This system is not capable of supplying a direct crystallization age on glasses. The three composites have different physical characteristics (see Table 7); EG1 and EG2 were leached to remove volatile coatings. There is no real difference between the three subsamples. The data of Lugmair and Marti (1978) updates that of Lugmair and Marti (1977) in decreasing $^{147}Sm/^{144}Nd$ about 0.5%, changing $T_{IC}E$ from 3.35 ± 0.27 b.y. to 3.8 ± 0.4 b.y. (hence not so close to the Ar gas retention ages) (Fig. 8). Sm/Nd is only 4.6% higher than chondritic. Small changes in Sm/Nd produce large changes in T_{ICE}. If the age is 3.38 b.y., then ϵ_{JUV} is +0.4 ± 0.4, and if the age is 3.79 b.y., then ϵ_{JUV} is 0 ± 0.4. These are different (lower) than other mare basalts, and require an origin for green glass from nearly unfractionated reservoirs; an impact origin is unlikely. During melting of a "chondritic" source at 3.4 (or 3.8) b.y., the Sm/Nd was increased and a small Eu anomaly developed (Lugmair and Marti, 1977). Lugmair and Marti (1978) concluded that the lunar initial $^{144}Nd/^{143}Nd$ is consistent with an initially chondritic Moon.

TABLE 15426-7. Sm-Nd isotopic data (Lugmair and Marti, 1978)

Sample	$^{147}Sm/^{144}Nd$	$^{143}Nd/^{144}Nd$	Sm x 10^{-9} moles/g	^{144}Nd x 10^{-9} moles/g
EG1	0.2016	0.512842 ± 34	4.735	3.523
EG2	0.2015	0.512831 ± 18	4.897	3.645
YG1	0.2011	0.512823 ± 24	4.890	3.646

Samples: EG1 - mainly ideal spheres without internal surface exposed; leached; 15.28 mg
EG2 - mainly broken pieces; leached; 20.00 mg
YG1 - yellow-green devitrified glasses; unleached; 18.61 mg
(masses are for spiked aliquots)

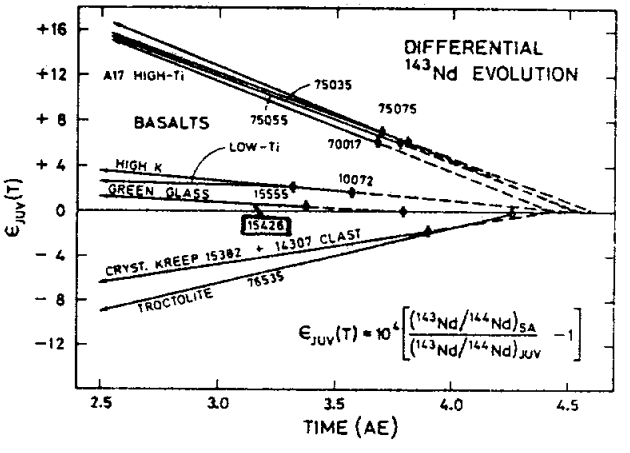

Figure 8. Differential ^{143}Nd evolution for 15426 green glass and other lunar materials (Lugmair and Marti, 1978).

A U fission track age (Storzer et al., 1973) for green spherules of 5.50 b.y. corresponds with an excess of 36.1%. If this results from Pu, and assuming a lunar $^{244}Pu/^{238}U$ of 0.013 at 4.58 b.y., a fission track age of 4.0 b.y. is calculated. In any case, whatever the source of excess tracks, the glass must be older than 3 b.y. (this is taken by Storzer et al., 1973, to suggest formation in a major, basin-forming impact).

TABLE 15426-8. Track data of Storzer et al. (1973)

	% solar flare irradiated	Density of cosmic ray tracks	Apparent exposure age (m.y.)
Green Glass	1.6	0.1 - 70	~2
Brown Glass	20	0.3 - 10	--
Feldspar	20	2 - 8	--

Spangler et al. (1984) used the laser probe Ar method to determine ages of five fragments of yellow volcanic glass from 15426 and 15427, finding an average age of 3.62 ± 0.07 b.y. There was no significant correction for trapped argon in the yellow glasses. Spangler and Delano (1984) used the same technique to determine ages for five fragments of yellow impact glasses in 15426 and 15427. They determined an age of 3.35 + 0.05 b.y. for the impact; there was a significant correction for trapped ^{40}Ar but a similar age was derived for each glass and the ages are considered reliable. Hence the ages of their source basalts are not young (i.e.,Eratosthenian), as had been predicted by Delano et al. (1981).

RARE GASES, TRACKS, AND EXPOSURE: Lakatos et al. (1973) tabulated He, Ne, and Ar isotopic data for single spherules and size separates from 15426 and other green glass materials. They found that spherules contain about 100 x less trapped inert gas than do normal bulk Apollo 15 fines, and have never been directly exposed to the solar wind; spherules in other fines contain about 10 x as much inert gas as those in 15426. The ^{21}Ne and ^{38}Ar exposure ages are 270-400 m.y.; ^{3}He exposure ages are always much less (less than 150 m.y.) because of ^{3}He losses. The trapped gases are not directly of solar wind origin and could be from solar-wind or an impacted precursor, or primordial lunar gas, which would then be similar to solar gas or the unfractionated component of gas-rich meteorites. The gas was trapped before formation of the clod. The $^{20}Ne/^{36}Ar$ ratio for spherules is very high. The ^{40}Ar-^{36}Ar systematics for materials from 15426 (and its residues, 15421) are different from green glasses in other fines.

Huneke et al. (1973) and Podosek and Huneke (1973) extensively discussed argon isotopic ratios which they determined and tabulated for 15426 green glasses. They found considerable trapped Ar in the near-surface regions, and it can be resolved into (at least) two components with separate origins--one shallow with $^{40}Ar/^{39}Ar$ >30; the other deeper (2 microns or so) with $^{40}Ar/^{39}Ar$ = 2.9. ^{40}Ar in both components is parentless. The ratio of trapped ^{40}Ar to ^{36}Ar is higher than in any lunar soil, and the trapped gas was implanted early. The derived exposure ages of ~ 300 m.y. differs from those of Lakatos et al. (1973) only in the choice of the production rate of ^{38}Ar. Spangler et al. (1984) determined Ar exposure ages of 275 to 300 m.y. for both green and yellow volcanic glasses in 15426 and 15427. Spangler and Delano (1984) determined Ar exposure ages of 274 ± 74 m.y. for yellow impact glasses from the same samples. Spangler and Delano (1984) noted two possibilities: either the clods formed more than 300 m.y. ago so have the same exposure, or 300 m.y. is an average for soils from St. 7.

Heymann (1975) plotted ($^{40}Ar/^{36}Ar$) trapped vs. $^{207}Pb/^{206}Pb$ (low temp. sites) for 15426 green glass in a discussion of records of ancient regolith, with the implication that 15426 is an ancient regolith from 3.5 to 4.0 b.y. ago.

Megrue (1972) and Megrue et al. (1973a,b) measured He, Ne, and Ar isotopes within individual green glass spheres from 15426 using a laser probe for gas release. Samples were sieved (<100 mesh and >60 mesh) and individual green (undevitrified) and black (devitrified) spherules picked from the coarser materials. They found differences in the proportions of cosmogenic and fractionated solar gases even within spherules and in the fine fractions. $^{20}Ne/^{36}Ar$ varies from 10 to 20 among spheres, and is higher than in soils. Devitrified spherules have only 1/2 to 1/4 the ^{4}He of non-devitrified spherules, and cosmogenic ^{21}Ne is 5 x as much in devitrified as in non-devitrified spherules. Both devitrified and non-devitrified spherules contain solar gases at depths greater than 5 microns. Megrue et al. (1973a) note that the $^{4}He(total)/^{36}Ar$ solar might result from different concentrations of radiogenic ^{4}He in spherules, or to selective fractionation of the gas when the original solids of the lunar surface were melted to produce the spherules (i.e., they assume an impact origin).

Lugmair and Marti (1978) noted an unusually large neutron fluence for $^{150}Sm/^{149}Sm$ for green glass spherules, consistent with a long near-surface residence time with a lower limit of 300 m.y.

Keith et al. (1972) provided cosmogenic nuclide disintegration count data for ^{26}Al, ^{22}Na, ^{54}Mn, ^{56}Co, and ^{46}Sc. They and Yokoyama et al. (1974) noted that the sample appears to be unsaturated in ^{26}Al, indicating an erosion rate high enough that ^{26}Al could not build up to saturation levels.

Fleischer and Hart (1972, 1973, 1974) measured particle track densities in green glass spherules, amber glass, and feldspar in 15426 (Fig. 9). The very abrupt cutoff of track densities shows that the clod has been "solid", i.e., unstirred, during its exposure to heavy cosmic rays, and contrasts with soils. The amber glass has a median track density 10 x that of the green glass in 15426 and is either older, added separately, or contains tracks from different particles (according to its track-determined U content, this amber glass is probably yellow impact glass). The cosmic ray tracks indicate that 15426 was brought to the surface 0.5 m.y. ago (and the rare gas spallation ages of 50-300 m.y. are subsurface exposures). The clod itself is older.

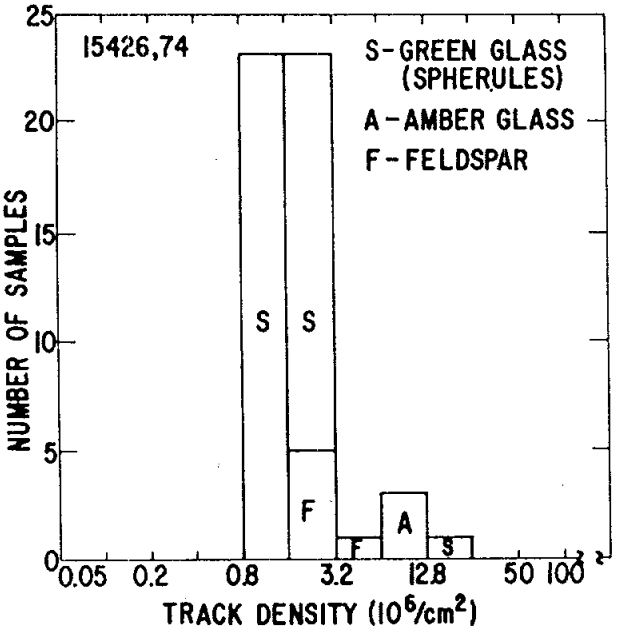

Figure 9. Track densities (Fleischer and Hart, 1972).

Bhandari et al. (1972, 1973) reported cosmic ray track data, finding a peak track density in glasses of 7 x 10^6 cm^{-2} for an interior chip. Track density frequencies are shown in Figure 10, which shows that track densities are lower than for regolith 15302 collected nearby. MacDougall et al. (1973) found etchable solar flare tracks in glass and feldspars, indicating a maximum of 300°C or a very short heating event since formation of the tracks. They apparently assume an impact origin, suggest that the glasses may not have completely outgassed at formation, and hence may be younger than the ^{40}Ar-^{39}Ar ages (this scenario is according to a fission track age of <0.7 b.y. for a green glass in 15086). This scenario is incompatible with both our understanding of impact melting and subsequent isotopic data for 15426.

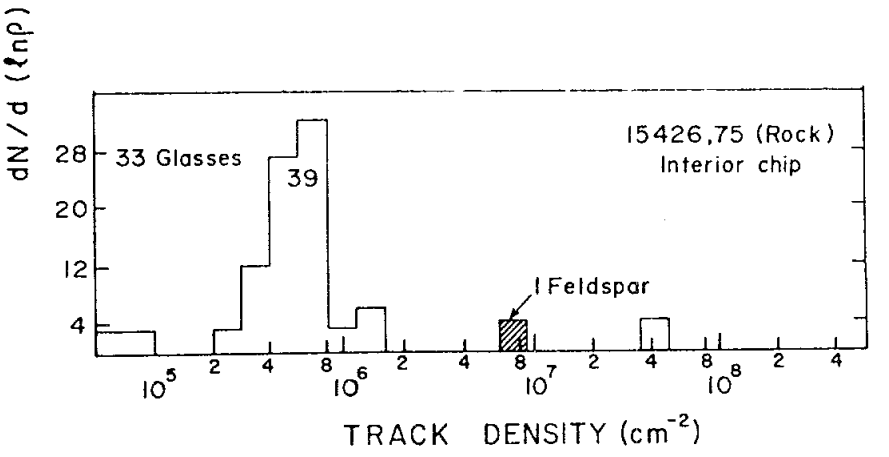

Figure 10. Track densities (Bhandari et al., 1973).

Storzer et al. (1973) studied cosmic ray and fission tracks (Table 8). Green spherules have a very low abundance of solar flare tracks compared with regoliths, and the 1.6% of solar flare-bearing particles observed might be soil contaminant. Solar flare tracks in the brown glasses and feldspars are higher (20%) and result from pre-clod irradiation. Combined 15426, 15421, and 15301 data give 4.5-5.5 x 10^5 tracks cm^{-2} on average. Assuming an average 5 cm burial gives a surface residence time of ~2 m.y. In 100 green spherules, 8.5 x 10^4 fission tracks cm^{-2} were found, with an average U of 0.049 ppm.

PHYSICAL PROPERTIES: Pearce et al. (1973) tabulated room temperature magnetic measurements for a green clod sample: J_s of 0.05 emu/g; X_ρ of 32.8 emu/g Oe; and J_{rs}/J_s of 0.08. They found a very low Fe^0 content, suggesting a process more oxidising than most lunar processes; in fact the Fe° content is very similar to most mare basalts.

Perry and Lowndes (1972) and Perry et al. (1972) measured infrared reflectance spectra on 15426, finding it spectroscopically different from soils and "also obviously richer in pyroxene than the Fra Mauro breccias". They calculated the real and imaginary parts of the dielectric constant. Perry et al. (1972) also produced a Raman spectrum for a green glass sphere, finding a doublet at 850 cm^{-1} from partial devitrification into olivine.

PROCESSING AND SUBDIVISIONS: Of the original three pieces ,1 is now 110.3 g and ,26 is 53.3 g. The latter is very pure green glass and is a restricted access sample. No other split is as large as 4 g. Most samples have been allocated from ,27, which is also a generally green glass-rich sample. A series of thin sections was made from ,2: ,4 is essentially a grain mount; and ,17 to ,25 are porous regolith breccia samples. Thin sections ,69; ,70; and ,72 were from a split of ,27 and are much richer in green glass, but also contain other materials. Sample ,3 was made into sieved fractions from which grain mounts were made; these are dominated by green glass.

15427 GREEN GLASS CLODS ST. 7 115.9 g

INTRODUCTION: 15427 is a group of extremely friable greenish clods which are the smaller pieces taken from the same sample bag as 15425, 15426, and the residue fines. The green material is the common Apollo 15 volcanic (pyroclastic) glass. The largest chip is shown in Figure 1. The samples are really regolith clods with green glass concentrations varying considerably from place to place. Two types of matrix dominate, one grayish-tan, the other grayish-green; both contain green glass spheres and light colored clasts. Green glasses from this sample and 15426 have been dated as about 3.4 b.y. old, yellow volcanic glasses as about 3.6 b.y. old, and yellow impact glasses as about 3.35 b.y. old. Rare gas exposure ages are about 300 m.y.

The clod pieces are grayish-tan and grayish-green, and are blocky, rounded, and very friable. They were removed from the same sample bag and processed as several small pieces. 15427 was collected with clods 15425 and 15426 and fines from the north rim of Spur Crater (see cataloging of 15425 for numbering and site characteristics). Data from all of these samples are most usefully considered together. Pieces of 15427 were originally numbered as 15923 and appear as such in some publications, e.g., LSPET (1972).

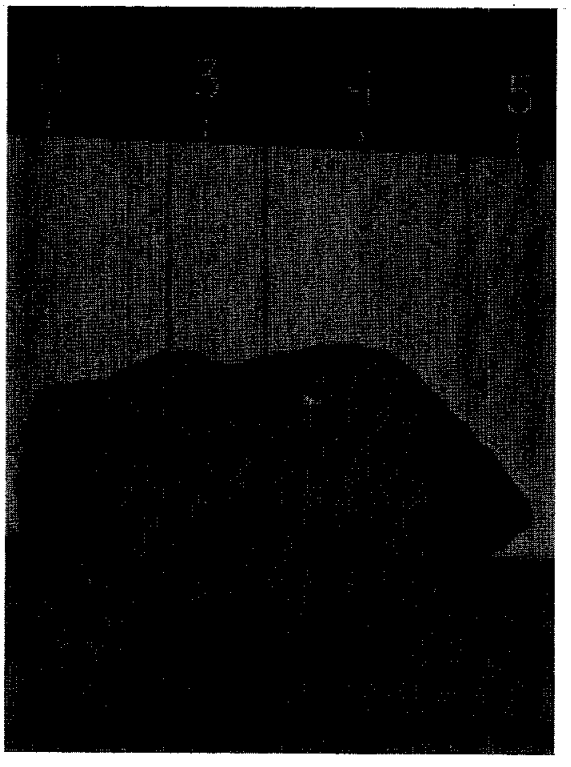

Figure 1. Sample 15427,22. S-71-52775

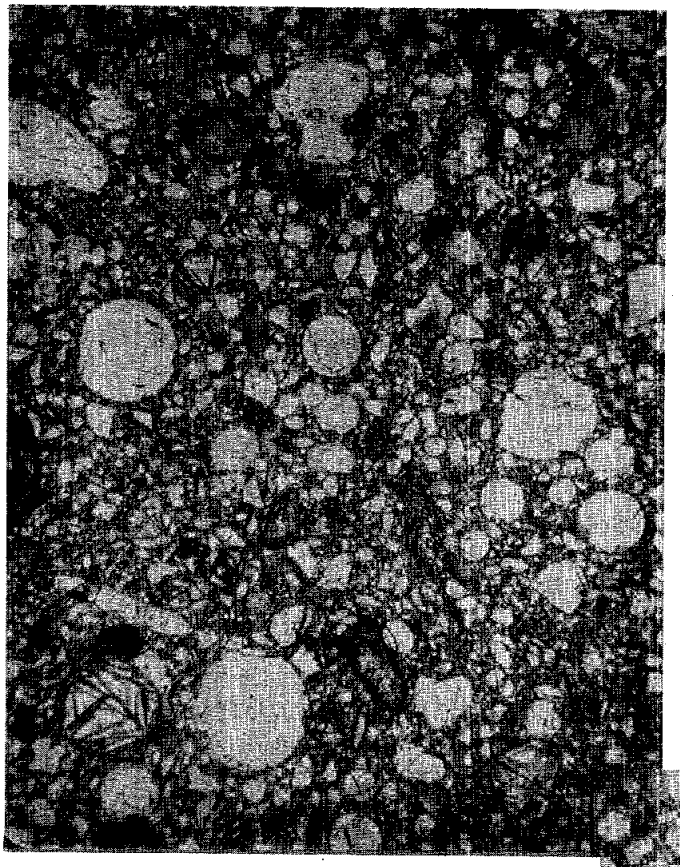

Fig. 2a

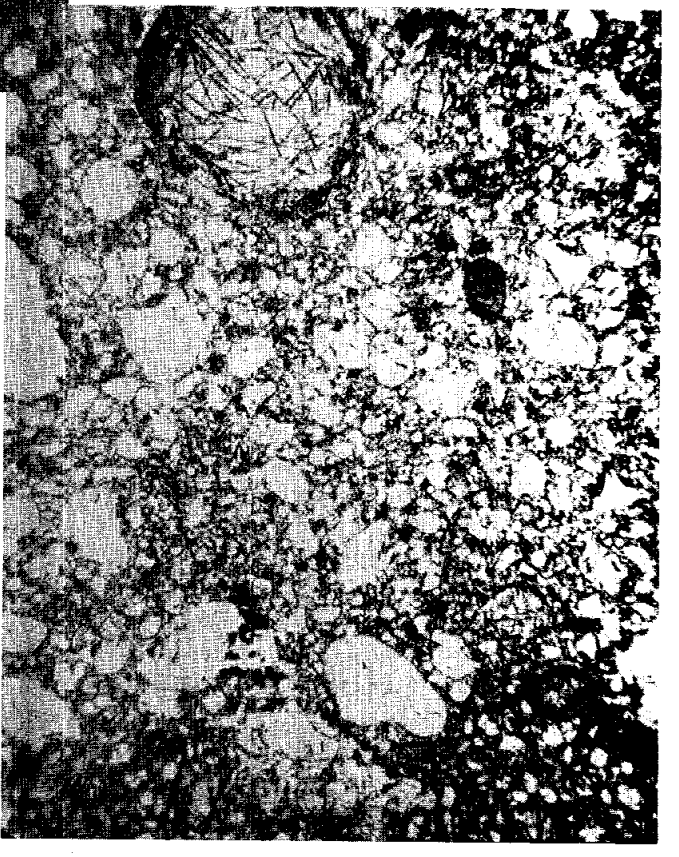

Fig. 2b

Figure 2. Photomicrographs of 15427,26. Transmitted light. Width about 2 mm. Both show green glass spherules and shards, including partly crystallized varieties, and heterogeneous yellow glasses.

PETROLOGY: Macroscopically 15427 is fine-grained and is striking in its abundance and visibility of green glass spherules. Like 15425 and 15426, there are considerable green glass concentration variations from place to place. There are too main types of matrix; one is grayish-tan, the other is grayish-green, and in at least one place, the contact between the two is sharp. Both types contain green glass spheres and light-colored clasts. One piece ,16 was described as having a pinkish gray matrix, with several irregular areas of green matrix making up less than 5%, with green glass spheres apparently composing less than 1% of the piece. Two sets of thin sections were made from two pieces, both of which were chosen to be green glass-rich pieces, hence are not representative of the bulk of the fragments. Most of the thin sections are dominated by green glass in various expressions, and heterogeneous, undevitrified yellow glasses (Fig. 2). Some plagioclase mineral grains with rare lithic and mafic mineral clasts are present. McKay et al. (1984) found an I_s/FeO of 20-30 for a tan matrix sample, indicative of an immature regolith. Gibson and Andrawes (1978) quoted a value of I_s/FeO of 0.3 from Morris (1976) but such a value does not appear in that source. Wood and Ryder (1977) provided a mode of thin section 15427,33, finding it to consist of about 90% green glass shards and spherules. Yellow heterogeneous glass is the most common (2.3%) non-green related component of the >25 micron fraction, but small amounts of lithic and mineral clasts of both highland and mare derivation are present. 15427,33 contains such a high proportion of green glass that it is likely to be an original deposit. Wood and Ryder (1977) provided average analyses of green and heterogeneous yellow glasses from this thin section and discussed the enigma of the green glass compositions. Nagle (1981) observed 15427,27 and compared it with samples of 15425 and 15426, and clods in 15007. He found that many green glass patches in 15427 are partly crystallized, as in 15425 but in contrast with 15426 (quenched) and 15007 (glassy). Agrell et al. (1973) described glasses from 15425, 15426, and 15427, and found 15427 to be like the others in containing abundant bright green glass spheres with subordinate brown spheres and glass fragments. They listed a microprobe analysis of a typical glass sphere in 15427 but in general do not specify observations from 15427. They ascribe to the green glass an impact origin, and interpreted an absence of high velocity micrometeorite impacts to indicate that the glasses, unlike many other types, were not exposed at the surface. Warner et al. (1972) analyzed glasses in 15427 and several other samples, finding many glass groups. Data from 15427 were not specified.

The green glasses have received the most intensive study, following early recognition of this glass type at the Apollo 15 site as common and significant. Apart from the studies listed above, Ridley et al. (1973b) analyzed green (and other) glasses in 15427,31, and an olivine (Fo_{76}) in a green glass. They discussed mainly green glass, and suggested that the Apennine Front might contain such an ultramafic rock or its glassy equivalent. They suggested green glass might be from a pyroxenitic layer at depth in the Moon, a source for mare basalts, although the Mg/Fe is too low. Delano (1979) included 15427 glasses in his precise microprobe analyses of green glasses for major elements and Ni. These analyses defined two main groups and five individual groups. Data for 15427 were not specified. Basu et al. (1979) studied green glass vitrophyres in 15427 and 15426 (and other regoliths), and provided an analysis of an olivine in one vitrophyre in 15427. Delano et al. (1984) hand-picked glasses from 15427 to find vesicular examples, identifying 24 vesicle-bearing green glass specimens, characterized with the microprobe. Arndt et al. (1984) studied green glass in a thin section of 15427, and compared the sizes and textures with those produced in cooling and heating of synthetic green glass melts. They found that ,27 contained 28% glassy spheres and 72% vitrophyres. Olivines are of three types: 1) lattice; 2) fibre; and 3) polyhedral, of which the latter are rare. 36% have only lattice, 48% have only fibre, 16% have both (with fibre interstitial to lattice). Those spheres with only lattice olivine have a 0.36 mm average diameter; with only fibre have 0.18 mm average diameter; with both, 0.32 average. On average vitrophyres have twice the diameter of glasses (0.22 mm vs. 0.094 mm) (Fig. 3). In actual fact, 49% of glasses and 38% of vitrophyres have elliptical, not circular cross sections. From experiments, the critical cooling rate for glass is 1°C/sec, and at 0.7 to 0.8°C/sec lattice olivines develop (Fig. 4). In free flight, all the spheres should be glassy (Fig. 5) hence Arndt et al. (1984) invoked suspension in a hot gas (for 10 minutes) to allow crystallization. The textures are not those of

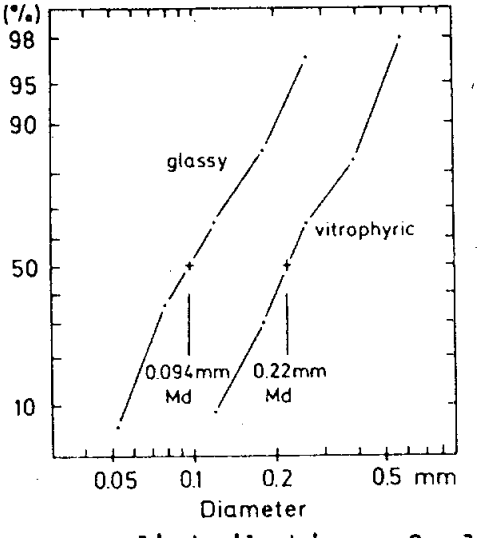

Figure 3. Size-frequency distribution of glassy and vitrophyric green glass beads in 15427,29 (average diameter of cross sections). (Arndt et al., 1984)

TABLE 15427-1. Chemical analyses of bulk materials

		,41	,2(a)	,71
Wt %	SiO2		45.18	
	TiO2		1.14	
	Al2O3		15.06	
	FeO		13.72	14.4
	MgO		12.14	
	CaO		11.11	9.9
	Na2O		0.36	0.37
	K2O		0.11	
	P2O5	0.036	0.09	
(ppm)	Sc			27.7
	V			
	Cr		2740	2580
	Mn		1400	
	Co			50.2
	Ni			191
	Rb		2.7	
	Sr		111	100
	Y		39	
	Zr		152	170
	Nb		10	
	Hf			3.9
	Ba			103
	Th		<2	1.7
	U	0.08		0.42
	Pb			
	La			10.2
	Ce			27
	Pr			
	Nd			16
	Sm			5.05
	Eu			0.919
	Gd			
	Tb			1.03
	Dy			
	Ho			
	Er			
	Tm			
	Yb			3.83
	Lu			0.540
	Li	4.5		
	Be			
	B			
	C			
	N			
	S		600	
	F	46		
	Cl	6.1		
	Br	0.196		
	Cu			
	Zn			
(ppb)	I	4.3		
	At			
	Ga			
	Ge			
	As			
	Se			
	Mo			
	Tc			
	Ru			
	Rh			
	Pd			
	Ag			
	Cd			
	In			
	Sn			
	Sb			
	Te			
	Cs			110
	Ta			550
	W			
	Re			
	Os			
	Ir			3.2
	Pt			
	Au			2.5
	Hg			
	Tl			
	Bi			
		(1)	(2)	(3)

References and methods:

(1) Jovanovic and Reed (1976); neutron and photon activation analysis
(2) LSPET (1972); XRF
(3) Korotev (1984, unpublished); INAA

Notes:

(a) Listed by its original designation of 15923.

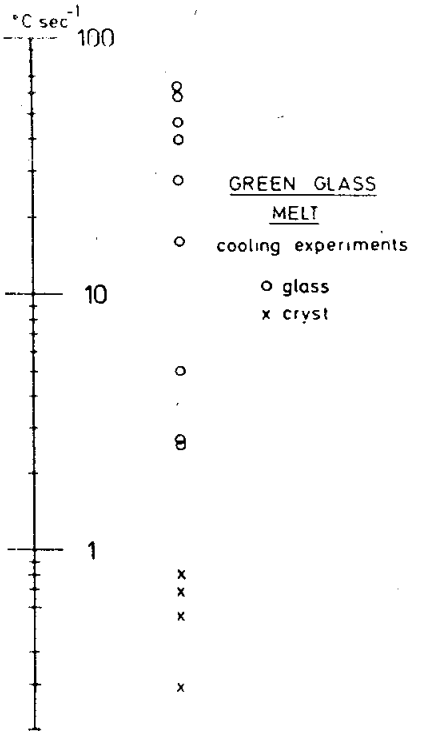

Figure 4. Cooling of synthetic green glass melt at predetermined linear rates from 1550°C to 660°C. (Arndt et al., 1984)

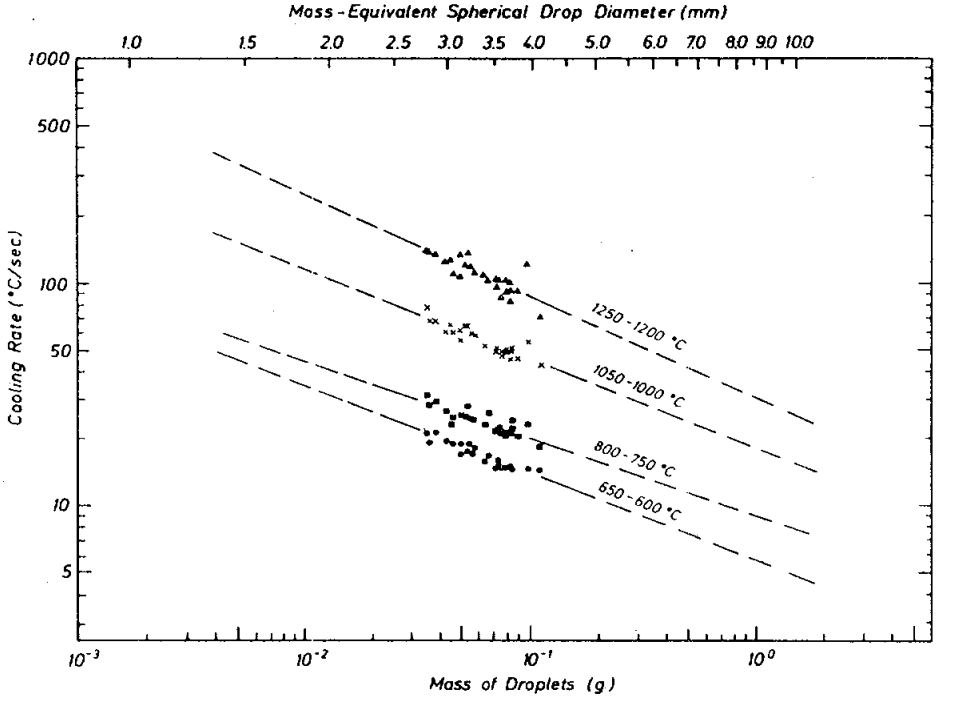

Figure 5. Free flight cooling rates of synthetic green glass melt droplets in different tempetrature ranges. (Arndt et al., 1984)

reheating or annealing, as shown by the experiments. Greagor and Lytle (1983) studied the Ti-site geometry in green glass in ,63, using x-ray absorption spectroscopy, by examination of the x-ray absorption near edge structure (XANES).

Delano (1980b) analyzed red volcanic glasses (TiO_2 approximately 13.8 wt %) in 15427,26, as well as in samples from 15318, 15425, and 15426, for major elements and Ni using the microprobe. Data for 15427 was not specified. Ni was always less than the detection limit of 50 ppm. Three subgroups were identified, related to each other by a prominent chemical trend. Experiments on this composition indicates that trend to originate from shallow (less than 5 Kb) fractionation, and the most primitive glass to have originated at about 480 Km depth.

Delano (1980a), Delano et al. (1981), and Spangler and Delano (1984) analyzed yellow impact glasses (TiO_2 about 4.8%) in 15427 as well as 15425, 15426, and 15378; chemical data for 15426 were not distinguished (see 15426 for a summary). This group is the same as the heterogeneous yellow glass of Wood and Ryder (1977), and that further investigated by Delano et al. (1982a,b).

A search for vesicular volcanic glasses found three of the yellow volcanic glasses to be vesicular (Delano et al., 1984).

Glass cooling rates were calculated by Fang et al. (1982), and for 15427 the calculated rate is 12°C sec^{-1}, compared to a measured rate of >5°C sec^{-1}. However, the composition listed for 15427 is much less magnesian than green glass, and is of unknown derivation, and the application of the results to 15427 is questionable--their essential conclusion was that the glasses formed in small bodies (i.e., spherules themselves) which were later assembled into the clod at temperatures which did not reach the liquidus.

CHEMISTRY: Chemical analyses of bulk clods are listed in Table 1. Rare earths are shown in Figure 6. That of LSPET was published under the former designation, 15923. This analysis and that of Korotev (1984, unpublished) are not of pure green glass clods, and have higher aluminum and incompatible elements, and lower magnesium and iron abundances than green glass. They are more similar to other Spur Crater regoliths but lower in incompatible element abundances. They agree fairly well but that of LSPET (1972) is a little less mafic. The analysis by Jovanovic and Reed (1976) has lower incompatibles (P and U), and suggests that a different kind of subsample, perhaps green glass-rich, was analyzed. Jovanovic and Reed et al. (1976) also listed data for F, Cl, and Br for leached and residue fractions separately. Gibson and Andrawes (1978) found that the amount of N released on crushing a sample is extremely small (less than 1 ngN/gm sample). Goldberg et al. (1975, 1976) studied F in green glasses, measuring the concentration changes with depth for handpicked green glass spheres. They found large surface enrichments of F, up to 3000 ppm in a layer less than or equal to

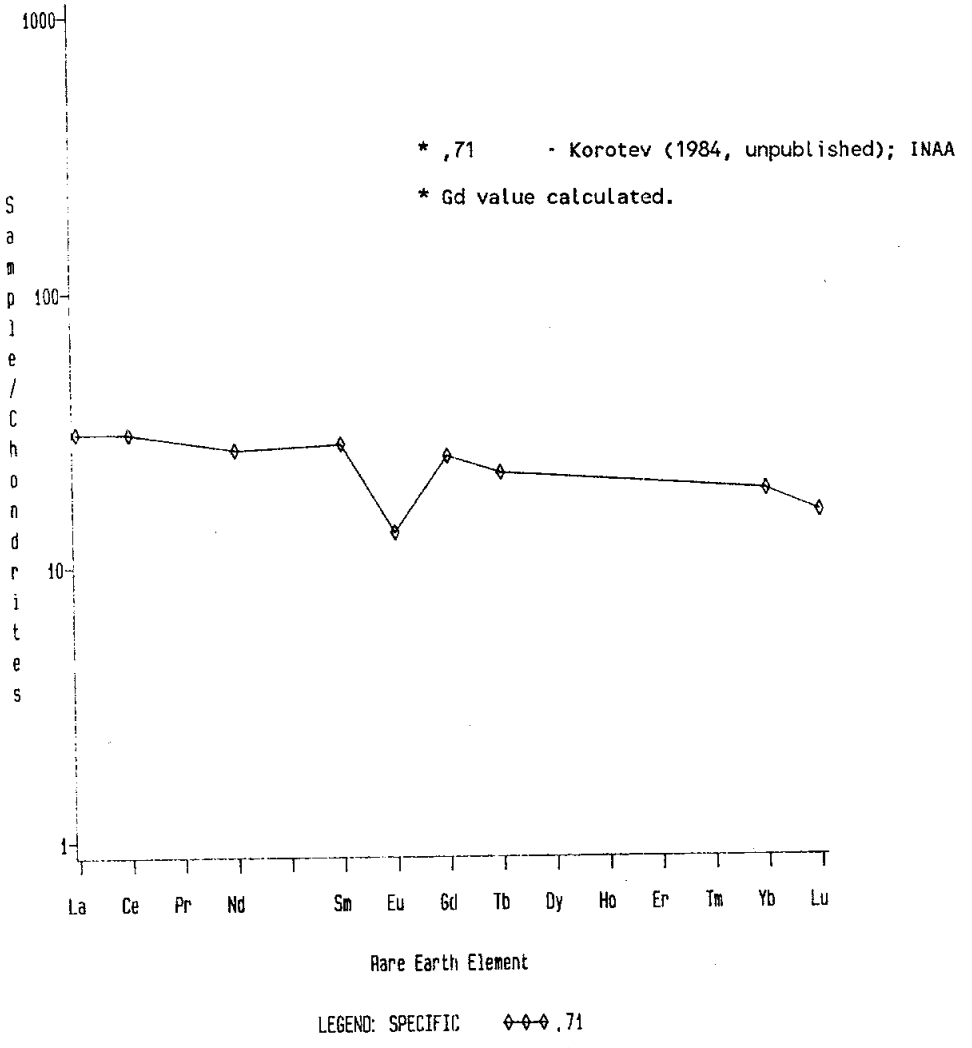

Figure 6. Rare earths in 15427 clod.

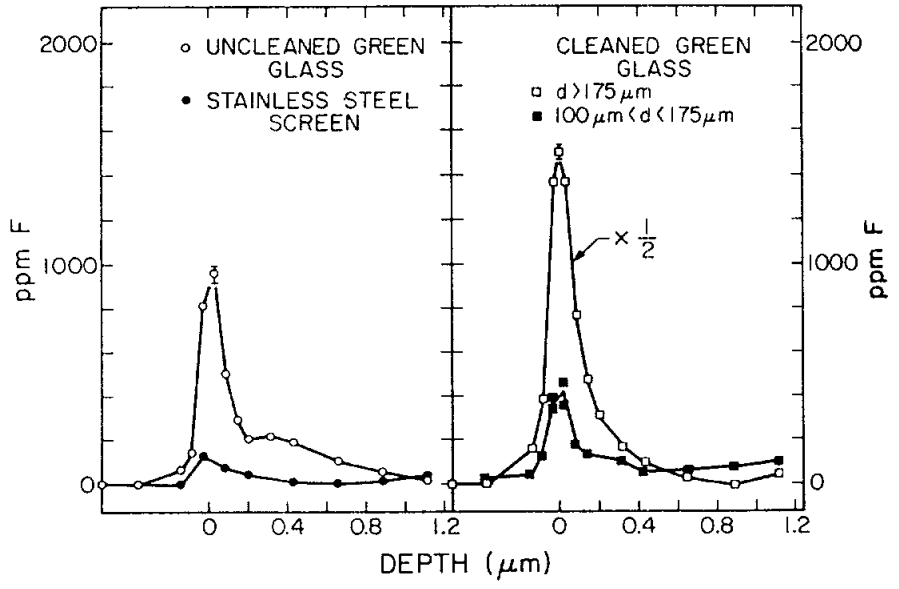

Figure 7. F-depth profiles for handpicked green glass separates from a 15427 clod and stainless steel screen behind which the green glasses were mounted. (Goldberg et al., 1976)

0.1 microns thick which cannot be terrestrial (Fig. 7). F was more enriched on particles larger than 175 microns than it was in the 100 to 175 micron fraction. F was highly localized and varied from grain to grain, with no preferential concentrations on devitrified grains as compared with clear spheres. Goldberg et al. (1976) found that F was more varied but higher on green glass than on Apollo 17 orange glass, and that other fragments (brown glass) do not have a high surface F. The bulk F determined for green glasses is about 50 ppm.

RADIOGENIC ISOTOPES AND GEOCHRONOLOGY: Spangler et al. (1984) used the laser microprobe for argon releases and dated six glasses from green glass group A (Delano, 1979) as an average 3.41 ± 0.12 b.y. old, and three from group D as an average 3.35 ± 0.018 b.y. old. The samples include examples from both 15426 and 15427. They also determined ages of yellow volcanic glass from 15426 and 15427 as an average of 3.62 ± 0.7 b.y. Spangler and Delano (1984) used the same technique to determine ages for five fragments of yellow impact glasses in 15426 and 15427, finding an average of 3.35 ± 0.05 b.y. corresponding to the age of the impact which produced them.

RARE GASES AND EXPOSURE: Spangler et al. (1984) determined Ar exposure ages of 275 to 300 m.y. for both green and yellow volcanic glasses in 15426 and 15427, and Spangler and Delano (1984) determined Ar exposure ages of 274 ± 74 m.y. for yellow impact glasses from the same samples. Spangler and Delano (1984) noted two possibilities: either the clods formed more than 300 m.y. ago so have the same exposure, or 300 m.y. is an average for soils from St. 7.

Bogard and Nyquist (1972) and LSPET (1972) provided noble gas data for 15427,2, listed as the number 15923,3. The sample has low abundances of noble gases, with the glass itself having the lowest abundances of ^{3}He, ^{4}He, ^{22}Ne, ^{36}Ar, ^{84}Kr, and ^{132}Xe of any of the Apollo 15 fines and glasses analyzed. The glass has lower $^{4}He/^{3}He$ than the other samples, and the ratios of $^{20}Ne/^{22}Ne$, $^{22}Ne/^{21}Ne$, $^{36}Ar/^{38}Ar$, and $^{36}Ar/^{40}Ar$ are higher than other samples. The isotopic ratios of Bogard and Nyquist (1972) show $^{22}Ne/^{36}Ar$ to be much higher than other A14 or A15 materials (2.45 cf. about 0.2 to 0.7) and also show the presence of either a trapped neon component with lower $^{20}Ne/^{22}Ne$ or a spallation neon with lower $^{21}Ne/^{22}Ne$. This component is not unique.

PROCESSING AND SUBDIVISIONS: 15427 originally consisted of many small pieces with masses up to 22 g. Several pieces numbered 15923 were renumbered as 15427. Most pieces have not been subdivided; the largest ,22 (22.0 g) and ,16 (17.7 g), are at Brooks. ,3, greenish matrix, was used to produce thin sections ,26; ,27; ,29-,34; ,54; ,56 via potted butt ,23 (now 4.8 g). ,7, also greenish matrix, had a daughter ,43 which was entirely used to make thin sections ,46-,52.

15435 REGOLITH CLOD ST. 7 206.8 g

INTRODUCTION: 15435 comprises 32 of the coarsest fragments (1 to 5 cm) of the clod which formed the pedestal for 15415 (Fig. 1). The clods are light olive gray, extremely friable, and nearly all appear to be loosely consolidated regolith. Finer-grained material was sieved and numbered as soil 15431 to 15434 (the original 826.8 g sample had been numbered 15925). Two non-regolith pieces, 15436 and 15437, were removed and numbered. These samples were collected on the north-northwest lip of Spur Crater.

PETROLOGY: Only one fragment, ,7, was made into thin sections. This is an unusual sample composed of banded glass, debris-laden glass, and rare intersertal basalt (KREEP?) fragments (Fig. 2). Green, light brown, orange, colorless, and red-brown glasses are present, as well as abundant tiny mineral fragments.

PROCESSING AND SUBDIVISIONS: Very little subdivision apart from the separation and numbering of individual pieces has been done. ,7 was made into a potted butt (2.26 g of which remains) and thin sections ,34 to ,47 made from it. The largest clods are ,10 (13.5 g); ,18 (49.1 g); and ,20 (58.3 g). ,18 is stored in Brooks.

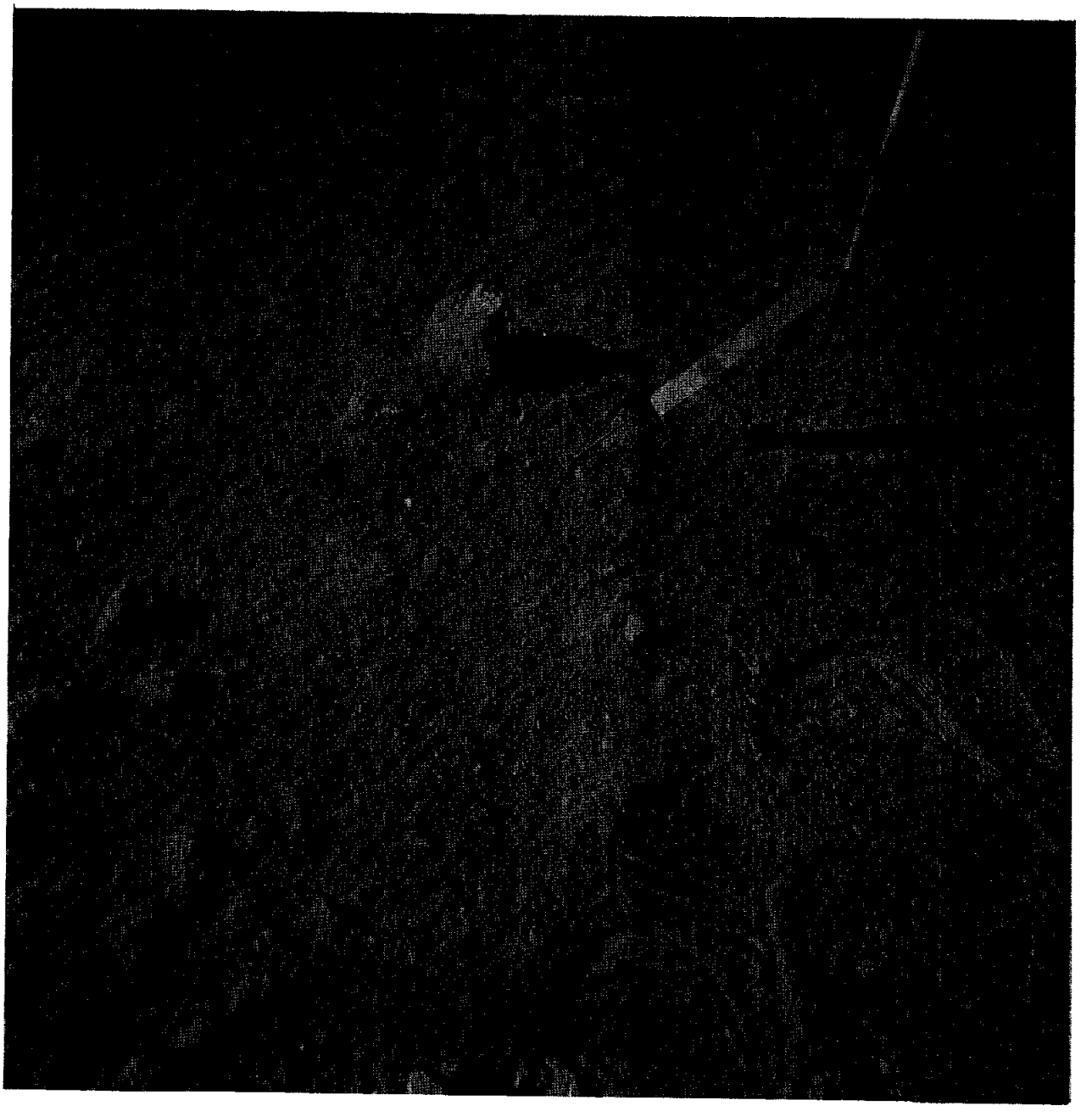

Figure 1. Sampling of samples 15415 and 15431 to 15437. Photo is AS15-86-11670.

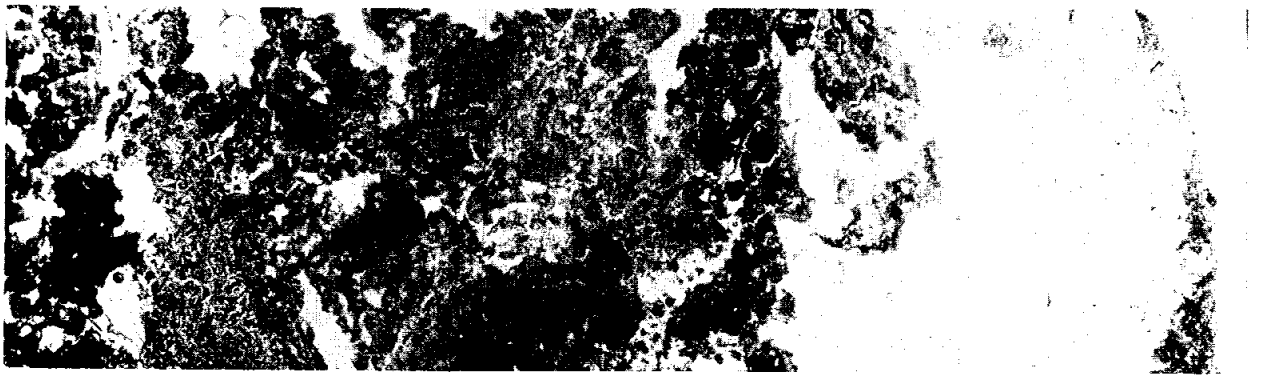

Figure 2. Photomicrograph of thin section 15435,36 showing glass (colorless), devitrified glass, dark glassy breccia, and subophitic/intersertal basaltic (impact?) melt streaks. Transmitted light. Height about 2 mm.

15436 FINE-GRAINED IMPACT MELT ST. 7 3.5 g

INTRODUCTION: 15436 is a dark colored vesicular impact melt (Fig. 1), which separated from the clod which formed the pedestal for 15415. It was thought to be an anorthosite (Phinney et al., 1972), but is deceptively covered with a thin coat of "white powder" (<< 1 mm thick)(see Warren and Wasson, 1978). The sample was collected on the north-northwest lip of Spur Crater (see Fig. 15435-1).

PETROLOGY: 15436 is a dense fine-grained impact melt with a micropoikilitic to microgranular texture (Fig. 2). It is not a glass as was stated by Warren and Wasson (1977). Clasts are mainly mineral fragments, with a few crystalline breccias, and the melt is feldspathic. The "white powder" which forms the coat appears to be actually a porous, corroded(?) part of the rock (Fig. 2c), not a foreign material, and grades outward into particulate materials.

PROCESSING AND SUBDIVISIONS: Two chips were removed from ,0 (Fig. 1). ,1 was potted and thin sections ,4 and ,5 made from it. ,0 is now 3.19 g.

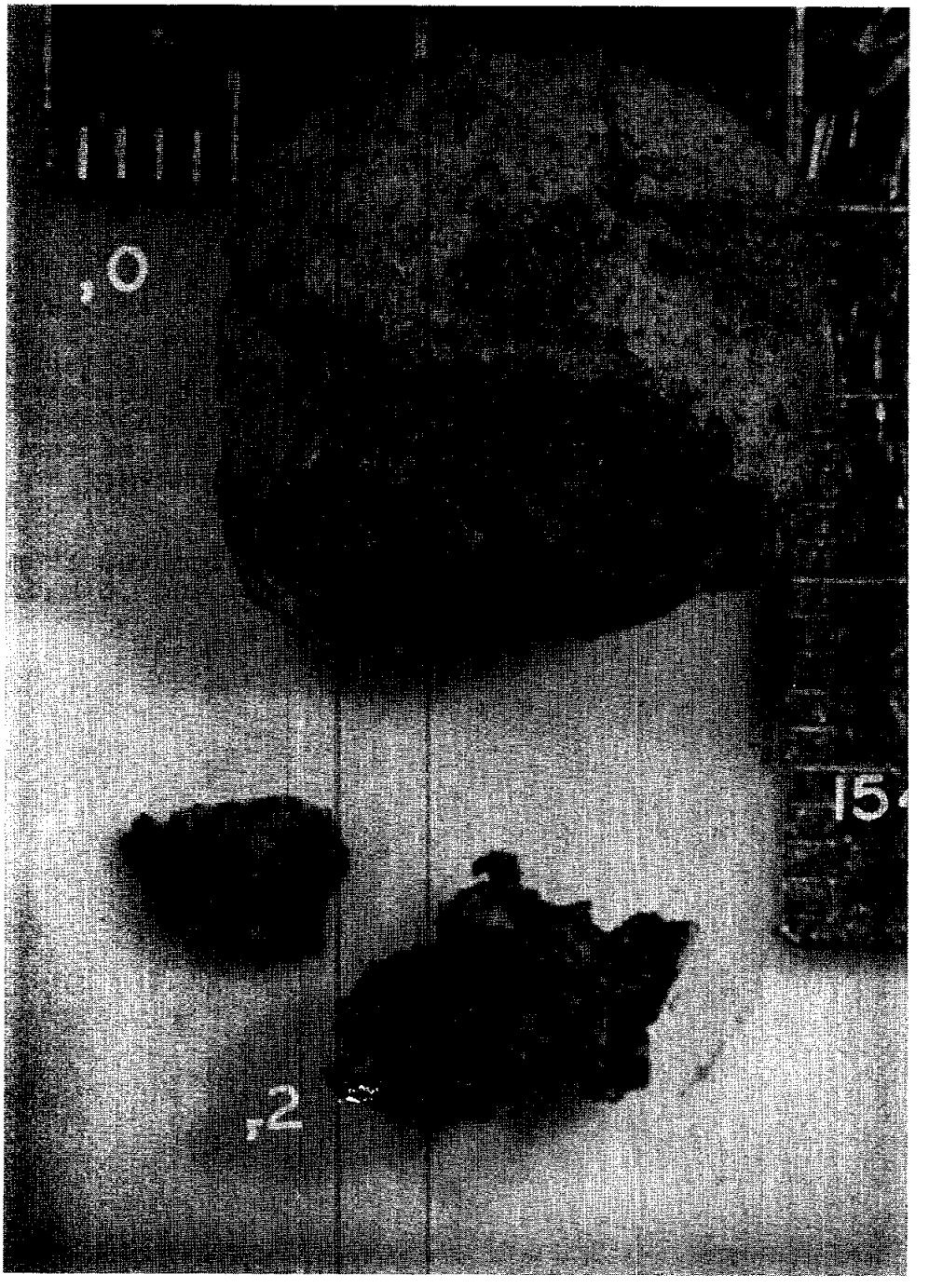

Figure 1. Post-split view of 15436. S-78-25499

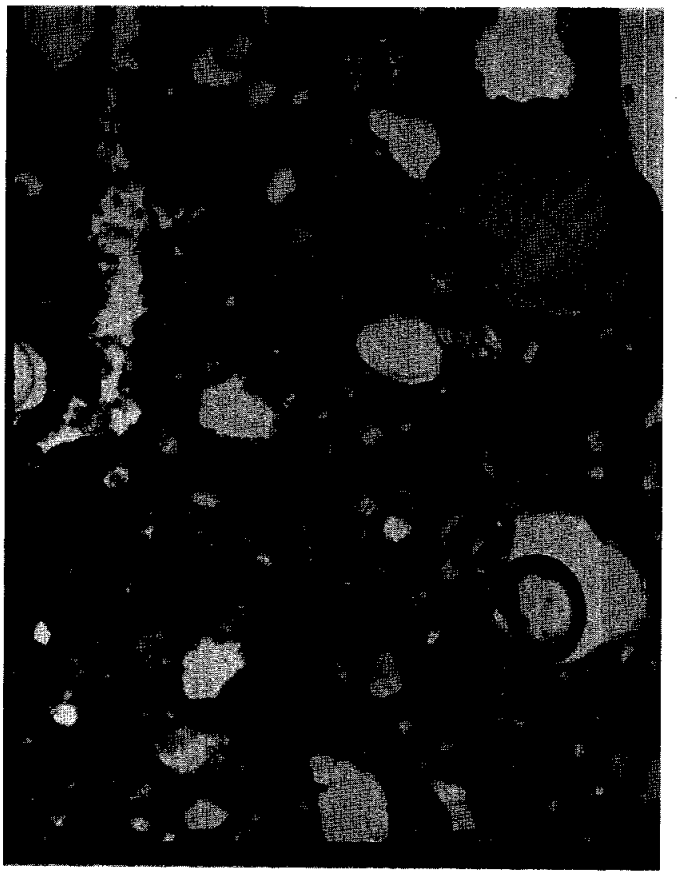

Fig. 2a

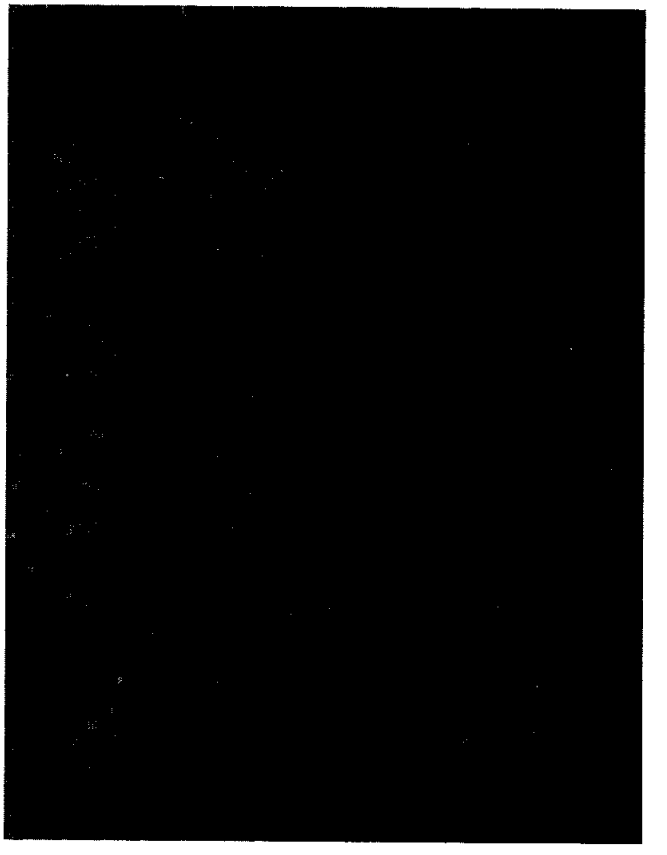

Fig. 2b

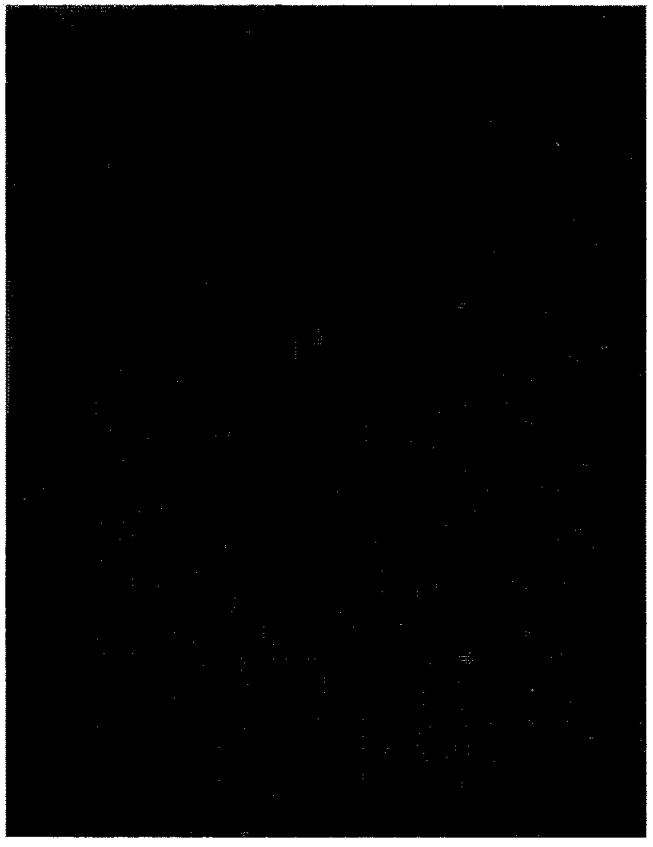

Fig. 2c

Figure 2. Photomicrograph of 15436,4 (a) general view showing large, exsolved orthopyroxene (top right) and numerous vesicles. Transmitted light. Width about 2 mm. (b) groundmass texture. Reflected light. Width about 160 microns. (c) porous edge of sample, showing continuity of melt towards exterior (to left) but increasing porosity. Reflected light. Width about 350 microns.

15437 FERROAN ANORTHOSITE ST. 7 1.0 g

INTRODUCTION: 15437 is a fragment of pristine ferroan anorthosite (Fig. 1) separated from the clod which formed the pedestal for 15415. It has a mineralogy unlike 15415. It is coherent, white, and a yellow grain of olivine(?) ~2 mm across is visible on one surface. The sample was collected on the north-northwest rim of Spur Crater (see Fig. 15435-1).

PETROLOGY: 15437 is an anorthosite (Phinney et al., 1972; Warren and Wasson, 1978). It was described by Warren and Wasson (1978). The grains are generally crushed to less than 0.2 mm (Fig. 2), but one 2 x 1 mm plagioclase is present, and a single yellow mafic grain about 2 mm across is visible macroscopically. According to Warren and Wasson (1978), the grains are barely annealed after cataclasis, but actually the sample appears to have been cataclasized, the fine material metamorphosed to a granular texture (Fig. 2), and then a second but minor cataclasis only partly disrupted the structure. The sample is 80% plagioclase ($An_{95.4}$ to $An_{96.6}$) and 20% olivine ($Fo_{66.7}$ to $Fo_{67.7}$), with one clinopyroxene grain ($En_{47}Wo_{40}$) containing exsolved orthopyroxene ($En_{72}Wo_2$). These homogeneous mineral compositions demonstrate a difference from 15415, which is more iron-rich and lacks olivine. Smith et al. (1980) made precise analyses of minor elements in five grains of olivine: FeO 25.3-30.7%; Al_2O_3 110-180 ppm, P_2O_5 0-40 ppm; CaO 390-480 ppm; TiO_2 0-300 ppm; Cr_2O_3 0-70 ppm; MnO 2010-3780 ppm. The ranges are similar to those in other ferroan anorthosites.

A small chromite plus mafic symplectite area occurs in thin section 15437,8.

CHEMISTRY: An analysis of bulk rock was made for major and trace elements, including siderophiles, by Warren and Wasson (1978) (Table 1, Fig. 3). The sample is free of meteoritic contamination and has very low levels of incompatible element abundances, hence is probably a chemically pristine igneous rock. The norm (82% plagioclase, 11% olivine, and 7% pyroxene) differs from the mode in its lower ol/px ratio.

PROCESSING AND SUBDIVISIONS: A small piece (,1) was chipped from ,0 and entirely used to make thin sections ,4 through ,8. Further chipping in 1978 produced some interior chips from which the chemical analysis and thin section ,10 was made.

TABLE 15437-1. Bulk rock chemical analysis

		,3
Wt %	SiO2	43.4
	TiO2	
	Al2O3	29.5
	FeO	4.3
	MgO	4.9
	CaO	16.9
	Na2O	0.227
	K2O	0.067
	P2O5	
(ppm)	Sc	3.0
	V	
	Cr	280
	Mn	456
	Co	12
	Ni	10.7
	Rb	
	Sr	
	Y	
	Zr	
	Nb	
	Hf	
	Ba	26
	Th	
	U	
	Pb	
	La	0.40
	Ce	1.5
	Pr	
	Nd	
	Sm	0.194
	Eu	0.60
	Gd	
	Tb	
	Dy	
	Ho	
	Er	
	Tm	
	Yb	0.13
	Lu	0.022
	Li	
	Be	
	B	
	C	
	N	
	S	
	F	
	Cl	
	Br	
	Cu	
	Zn	1.68
(ppb)	I	
	At	
	Ga	2600
	Ge	3304
	As	
	Se	
	Mo	
	Tc	
	Ru	
	Rh	
	Pd	
	Ag	
	Cd	1.1
	In	0.35
	Sn	
	Sb	
	Te	
	Cs	
	Ta	
	W	
	Re	0.016
	Os	
	Ir	0.036
	Pt	
	Au	0.024
	Hg	
	Tl	
	Bi	
		(1)

References and methods:

(1) Warren and Wasson (1978); INAA, RNAA, microprobe fused bead

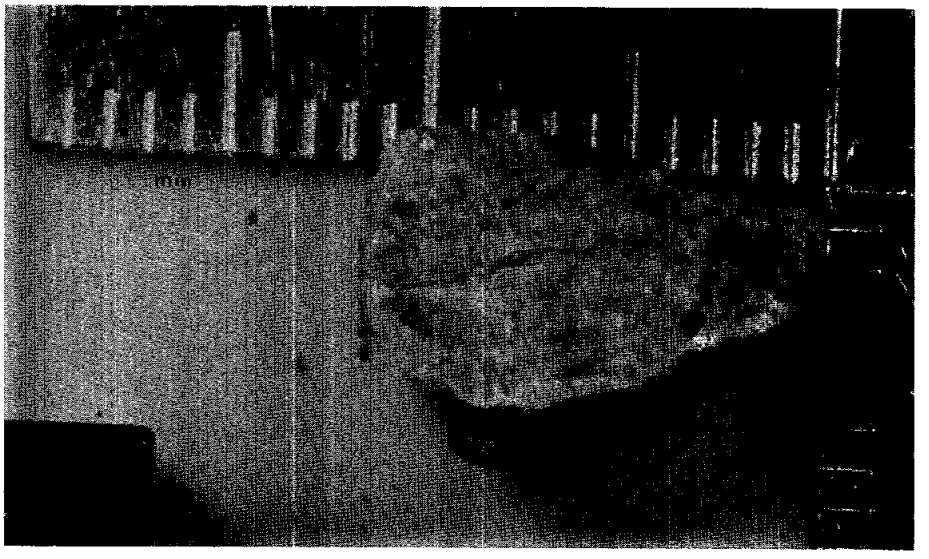

Figure 1. General view of 15437,0. S-78-25738

Fig. 2a

Fig. 2b

Fig. 2c

Figure 2. Photomicrographs of 15437. a) 15437,7, general view showing large grains in a finer-grained mortar. Crossed polarizers. Width about 2 mm; b) almost same view as (a), showing fine granular mafics. Transmitted light. c) 15437,8, showing granular mafic grains. Transmitted light. Width about 350 microns.

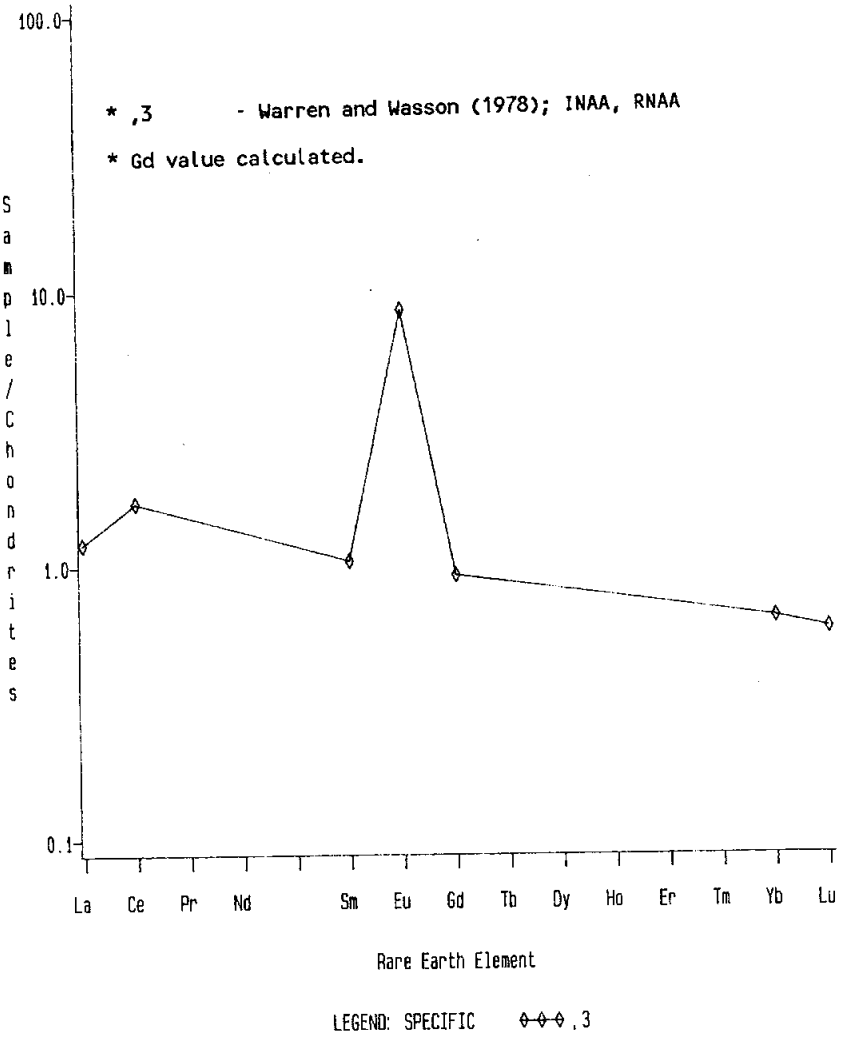

Figure 3. Rare earths in 15437 (Warren and Wasson, 1978).

15445 FINE-GRAINED IMPACT MELT WITH PRISTINE CLASTS 287.2 g

INTRODUCTION: 15445 is a very fine-grained impact melt of Mg-rich low-K Fra Mauro composition and contains clasts of metamorphic and plutonic pristine igneous rocks such as spinel troctolite and norite (Fig. 1) giving it its early designation of "black and white breccia". Clasts of surficial origin are absent. 15445 is very similar to 15455 which was collected nearby, and both rocks have been interpreted to be fragments of melt rock produced in the Imbrium event (Ryder and Bower, 1977). 15445 was studied in detail by the Imbrium Consortium (leader J.A. Wood) following some earlier studies. Imbrium Consortium reports are abbreviated here as ICR 1 (=1976) and ICR 2 (=1977).

15445 was found lying near a 1.5 x 0.6 m boulder that contained white clasts. It was collected because the astronauts believed it was likely to have once been a part of the boulder, which in turn was interpreted as Spur Crater ejecta (Bailey and Ulrich, 1975). The sample is tough, blocky, and angular, with a few zap pits on "T", "B", "N", and "S", with none on "E". The matrix is uniformly dark gray and fine-grained. Discontinuous veins of matrix of varied thickness cut some of the clasts. Vugs constitute perhaps 3% of the matrix.

PETROLOGY: 15445 consists of about 25% white lithic clasts in a dark gray, coherent, fine-grained impact melt matrix (Figs. 1 and 2). Locally the matrix contains tiny vesicles, and mineral fragments are ubiquitous. The lithic clasts tend to be pristine igneous, and do not include polymict breccia fragments or surface-derived fragments such as basaltic-textured clasts. Simonds et al. (1975) listed 15445 as a black and white rock "macroscopically similar to several Apollo 16 rocks" but 15445 does not have the mutually intrusive components nor the dimict nature of the Apollo 16 black and white rocks (now "dimict breccias"; Stoffler et al., 1980).

MATRIX: The matrix is an aggregate of mineral class and minerals that crystallized at least partly from a silicate melt, as demonstrated in particular by the presence of euhedral, skeletal olivines (Fig. 3a). It has been described by Ryder and Bower (1977) and in ICR 1 and ICR 2. Imbrium Consortium reports refer to the matrix as Lithology 45A. In a few areas, vesicles are elongated and roughly aligned, and elsewhere the matrix is roughly stratified (ICR 1). The siderophile element abundances are within the normal range for meteoritic contaminated highlands breccias (Gros et al., 1976) and the matrix is therefore most certainly a fragment-laden impact melt. Engelhardt (1979) lists the 15445 matrix as granular, in a group "without any signs of a sequential order of crystallization" whose members are "granoblastic products of solid state recrystallization", i.e., metamorphic.

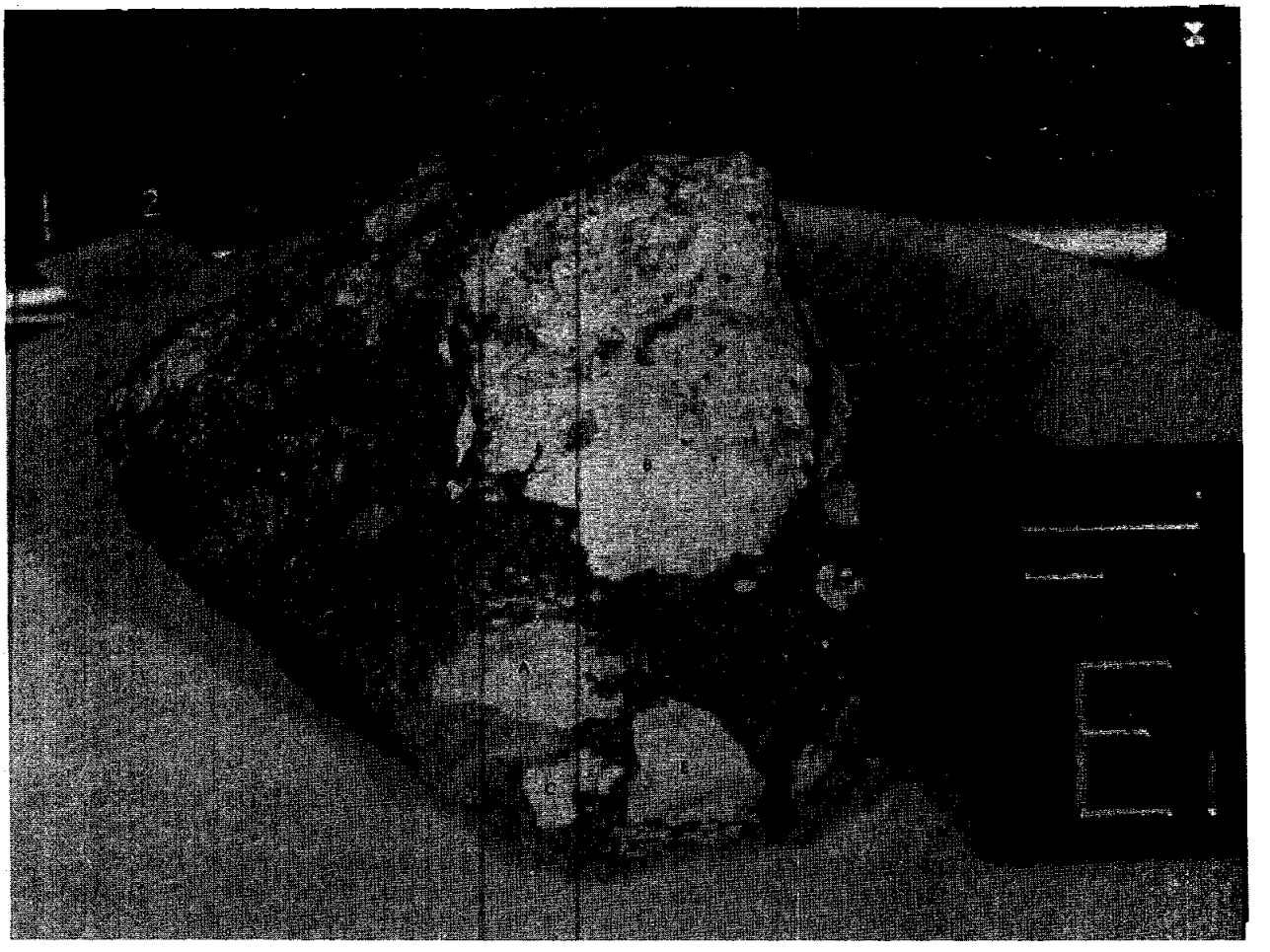

Figure 1. Macroscopic view of 15445, post-chipping (1972). Clast designations shown. Scale is in centimeters, cube is 2 cm. S-72-15938

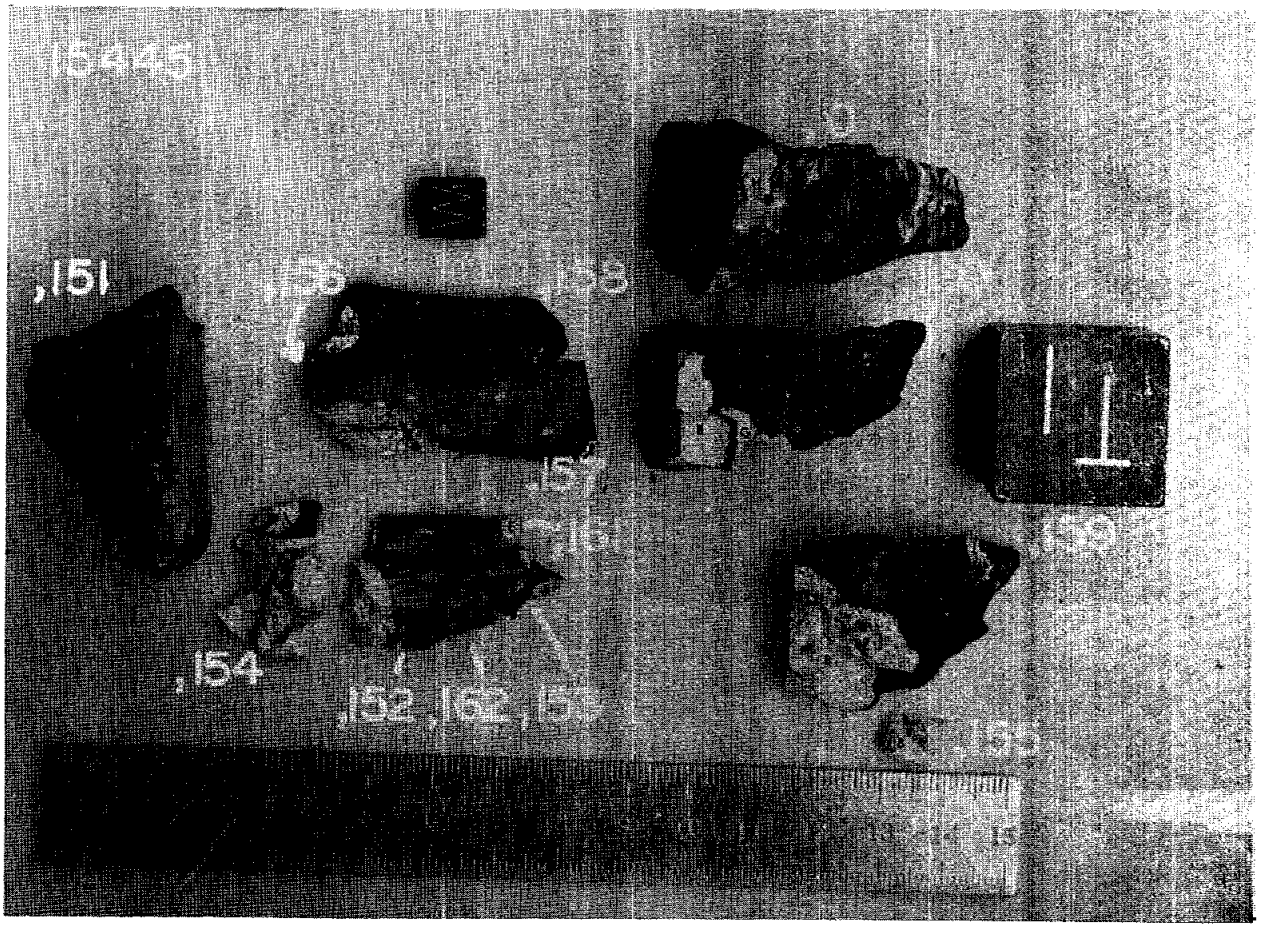

Figure 2. Dissection of slab sawn through 15445, with clast designations. Cube is 2 cm. S-75-33433

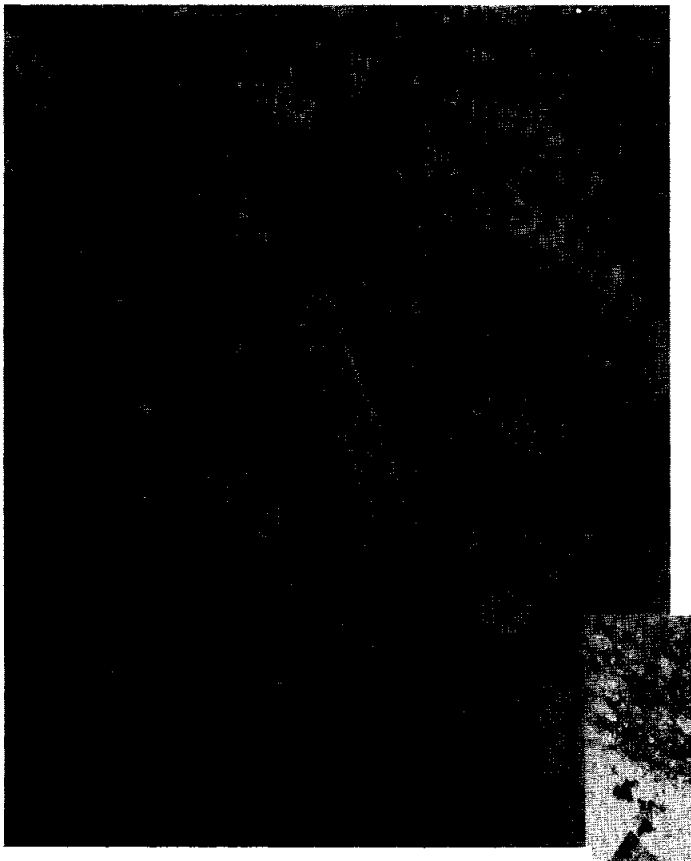

Fig. 3a

Fig. 3b

Figure 3. Photomicrographs of 15445. a) hollow euhedral olivine in matrix of 15445,133, indicating melt origin. Width about 125 microns. Transmitted light. b) spinel troctolite clast A (left) and matrix (right) in 15445,133. Width about 2 mm. Transmitted light. c) norite clast B (right) and matrix in 15445,133. Width about 2 mm. Transmitted light. d) polygonal olivine clast in 15445,147. Crossed polarizers. Width about 2 mm.

Fig. 3c

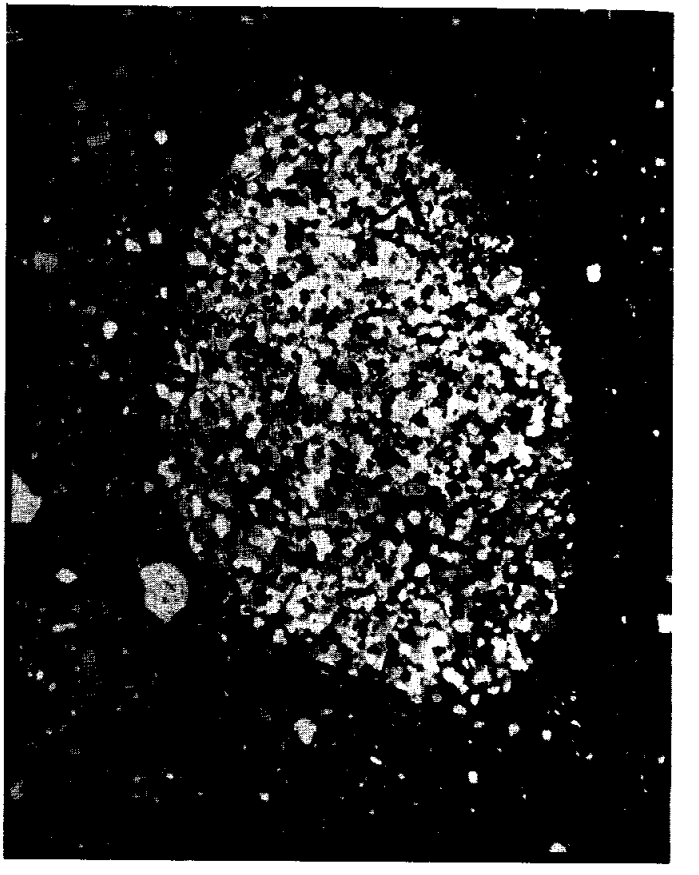

Fig. 3d

The finest mineral clastic material and coarsest melt mineral products overlap in grain size, and are difficult to distinguish. The melt phase (approximately 70% of the matrix) crystallized plagioclase, olivine, at least some low-Ca pyroxene, and opaque phases. Metal and sulfide grains are present, locally in the vesicles. Plagioclase grains less than 50 microns in diameter (dominantly melt-produced) have compositions An_{96-82} with a peak about An_{90}, and are more sodic than larger, clastic plagioclases (Fig. 4). Small olivines (less than about 50 microns) have compositions of Fo_{86-71}, peaked at about Fo_{79} (Fig. 4). Skeletal varieties are zoned, approximately Fo_{85-80}, and all small olivines are more Fe-rich than the obviously clastic olivines.

Mineral fragments form about 30% of the matrix. Most plagioclase fragments are An_{97-93}, with a range An_{97-65} (Fig. 4). No primary zoning of grains is apparent, but zoning from reaction with the matrix occurs in the outer few microns. Olivine fragments also show minor reaction border zoning, but no primary zoning. The total compositional range is Fo_{95-65} (Fig. 4), wider than observed in lithic clasts in 15445. Augite is a rare clastic phase. None of the augite clasts is larger than about 50 microns in diameter. Ridley et al. (1973) noted rare orthopyroxene in the matrix, but that study did not distinguish a melt phase. Essentially, low-ca pyroxene fragments are conspicuous by their absence, in contrast to the abundance of orthopyroxene in some of the lithic clasts in 15445. Other mineral fragments include pleonaste spinel and chromite.

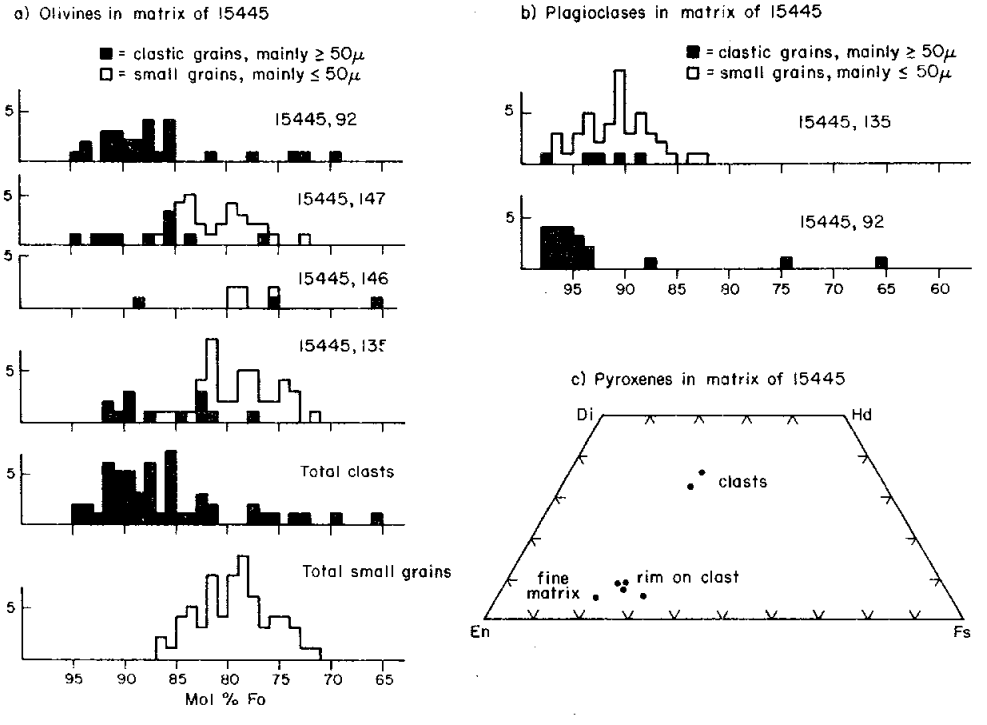

Figure 4. Compositions of minerals in matrix of 15445 (Ryder and Bower, 1977).

LITHIC CLASTS: Several types of lithic clasts occur in 15445. The larger ones all appear to be pristine plutonic igneous rocks. These were labelled as individual clasts and described in Ryder and Norman (1979). Specific clasts have been labelled A, B ...., etc. (not to be confused with type A, B of Ridley et al., 1973). Separate designations were used by the Imbrium Consortium. Comparisons of clast designations are listed in Table 15445-1.

1) Spinel Troctolite: Several of the clasts in 15445 consist of a cataclastic assemblage of olivine, plagioclase, aluminous spinel, and aluminous orthopyroxene, e.g., Clast A (Fig. 3b). The clasts are friable, once coarse-grained (>2 mm), notable for their Mg-rich olivine and Mg-Al spinel, and are generally believed to be from plutonic pristine igneous or metamorphic sources. Clast A at least is free of meteoritic contamination (Gros et al., 1976). The spinel troctolites have been described, with mineral analyses, by Ridley et al. (1973), Anderson (1973), Ridley (1977), Reid et al. (1977), Ryder and Bower (1977), Baker and Herzberg (1980), and in ICR 1 and ICR 2. Further detailed mineral analyses, particularly olivine, have also been reported by Steele and Smith (1975) (olivine; microprobe), and Steele et al. (1980) (plagioclases; ion microprobe). Steele et al. (1974) plotted armalcolite and olivine compositions. Clast A has been referred to as a peridotite (e.g., Anderson, 1973) but Ryder and Bower (1977) suggest a mode with 30 to 40% plagioclase, about 50% olivine, and 10 to 20% pleonaste.

TABLE 15445-1

CLAST DESIGNATION	LITHOLOGY (Imbrium Consortium)	RIDLEY et al. (1973)
Clast A	45E	Type B
Clast B	45D	Type A
Clast E	45B	-
Clast F	45C	Type B

Clast H contains about 65% olivine, 25% plagioclase, and 10% spinel (Baker and Herzberg, 1980). A few percent aluminous orthopyroxene is present in these spinel troctolite clasts, as well as opaque phases including rutile(?) and armalcolite.

The clasts are very magnesian, with olivines Fo_{92}. Plagioclases (An_{95-89}) are generally not as calcic as those in ferroan anorthosites, although Ridley et al. (1973) reported An_{98}. The orthopyroxenes (En_{92}) contain up to 5 wt% Al_2O_3 (e.g., Ridley et al, 1973). There is more grain-to-grain variation in Clast H than in Clast A (Baker and Herzberg, 1980) e.g., minor elements in orthopyroxene. The very low CaO contents (0.010-0.014%, Steele and Smith, 1975; 0.03%, Baker and Herzberg, 1980) are the lowest reported among lunar samples and require a slow cooling or a very low Ca potential. Smith et al. (1980) suggested equilibration at temperatures as low as 400° C for the CaO in these olivines, according to an empirical model. Most authors agree that the spinel troctolite clasts are probably from cumulates that underwent slow cooling and possibly some post-crystallization equilibration, although Bence and McGee (1976) have proposed that such assemblages are the residuum of partial melting deep in the crust. Anderson (1973) concluded that the petrology was consistent with initial igneous accumulation at moderate pressure (e.g., 2 Kb) followed by partial recrystallization during granulation at 950 ± 50° C and a pressure greater than or equal to 1.3 ± 0.5 Kilobars. Similarly, Herzberg (1978) used subsolidus thermodynamic calculations to estimate T and P_{min} of 960° C and nearly 2 Kb respectively (i.e., lower crust or upper mantle) for the 15445 spinel troctolite assemblage, and concluded that the phase equilibria require spinel accumulation.

MacDougall et al. (1973) studied grains from Clast A using high voltage electron microscopy (HVEM) techniques. No recrystallized zones, deformed crystals, multiple twinning, micro-fracturing, or other metamorphic features were observed in grains from the clast.

2) Norite: Clast B, the largest in 15445, consists of 60-65% plagioclase (An_{94-95}) and 35-40% low-Ca pyroxene (Fig. 5) (En_{77-81}, Ryder and Bower, 1977; En_{80-85}, Ridley et al., 1973). The clast is cataclasized (Fig. 3c) but is free of meteoritic contamination (Gros et al., 1976). It has been described by Ridley et al. (1973), Ryder and Bower (1977), and in ICR 1 and ICR 2. Macroscopically, its pyroxene is green. Mori et al. (1982) stated that they studied pyroxenes with ATEM, XRD, and microprobe techniques, but no data were reported.

The pyroxenes contain approximately 1.5% Al_2O_3, not unlike terrestrial plutonic norites. Silica and an opaque mineral (? ilmenite) (Ryder and Bower, 1977) and armalcolite and ilmenite (Ridley et al., 1973) have been reported as accessory phases. A minor vein system of Fe-metal (possibly secondary) cuts the pyroxene locally. Relict textures suggest that the norite was

Figure 5. Compositions of pyroxenes in norite clast B (Ryder and Bower, 1977).

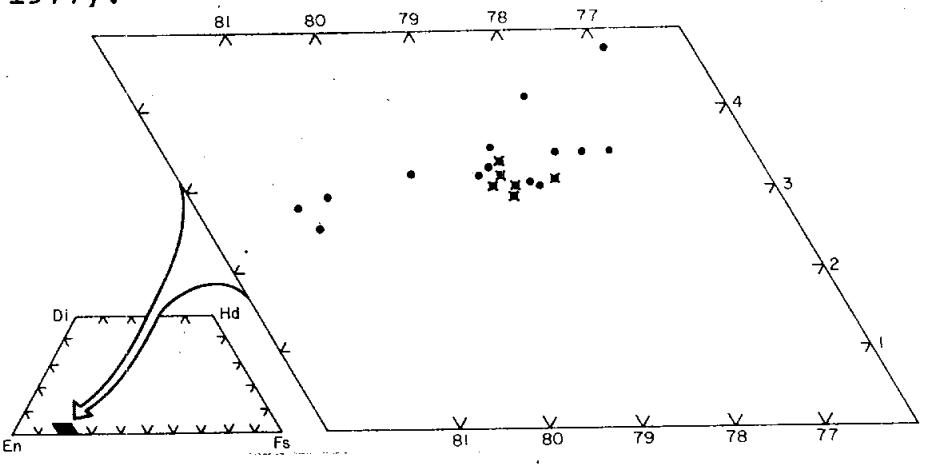

originally coarse-grained (>1 mm) and may have been poikilitic. The mineralogy is broadly similar to the 78235 norite and the 15455 norite, but it lacks the numerous minor phases present in the latter two samples. Other small fragments of norite occur in the sample, but low-Ca pyroxene is not a part of the monomineralic clast population of the matrix. James and Flohr (1982) list the norite as a member of the Mg-norite suite. MacDougall et al. (1973), using HVEM, found that crystals exhibited dislocations and twinning indicative of mild shock.

3) Anorthosite: A few small clasts consist entirely of brecciated and subsequently annealed plagioclase grains. The large size of some suggests that they are from anorthosites per se or very coarse-grained multiphase rocks.

4) "Gabbroic" Clasts: Marvin (ICR 1) observed rare "gabbroic" clasts containing yellow-brown pyroxene, but these clasts do not appear in thin sections.

5) Clast E: Clast E is unique and enigmatic. Macroscopically it is white, and free of pink spinel or green mafic minerals. One thin section (2 x 3 mm) consists of more than 95% plagioclase. A second thin section documented as from the clast is heterogeneous and consists of zones of crystalline plagioclase (An_{93-97}) + olivine (Fo_{82-84}), and crystalline plagioclase (An_{93-97}) + low-Ca pyroxene (En_{80-82}). The whole is injected by a brownish glass. Hence this is a complex clast. Warren and Wasson (1978) found a split from Clast E to be meteorite-free, but thought it to be polymict. While some of the discrepancies might result from erroneous documentation, the splits are clearly complex.

6) Others: Most other clasts are small and are monomineralic aggregates (Ryder and Bower, 1977). Polygonalized olivines (Fig. 3d) consist solely of olivine. The largest observed has a diameter of 3 mm. The two analysed have olivine of Fo_{87-88}. Spherulitic plagioclase masses up to 1 mm diameter, are mainly round and smooth. Some clearly recrystallized in situ from the rim inwards. Rare feldspathic granulites are small and have a typical triple-junction, polygonal texture.

TABLE 15445-2. Chemistry of 15445 Matrix

		,25	,25	,118	,123	,122	,125
Wt %	SiO2	44.6					
	TiO2	1.47	1.49				
	Al2O3	16.66	16.2				
	FeO	9.83	10.2	10.0			
	MgO	16.0	15.5				
	CaO	10.04	9.6				
	Na2O		0.55	0.54			
	K2O		.164				
	P2O5	0.21					0.17
(ppm)	Sc			17.6			
	V						
	Cr		1750				
	Mn	1085					
	Co			47.4			
	Ni			550	396		
	Rb	3.56			4.02		
	Sr	160					
	Y						
	Zr		315				
	Nb						
	Hf		10.5	7.4			
	Ba	237					
	Th			2.4			
	U		.800		.788		0.56
	Pb					13.3	
	La	22.1		20.4			
	Ce	57.6		54			
	Pr						
	Nd	35.7					
	Sm	10.1		10.3			
	Eu	1.85		1.64			
	Gd	11.9					
	Tb			2.4			
	Dy	13.2					
	Ho						
	Er	7.71					
	Tm						
	Yb	6.90		7.2			
	Lu	1.02		0.98			
	Li	14.1					
	Be						
	B						
	C						
	N						
	S	600					
	F						
	Cl						
	Br				.096		
	Cu						
	Zn				2.5		
(ppb)	I						
	At						
	Ga						
	Ge				630		
	As						
	Se				91		
	Mo						
	Tc						
	Ru						
	Rh						
	Pd				17.4		
	Ag				2.0		
	Cd				5.3		
	In				0.32		
	Sn						
	Sb				244		
	Te				4.7		
	Cs				177		
	Ta			1100			
	W						
	Re				0.668		
	Os				7.44		
	Ir				6.21		
	Pt						
	Au				6.02		
	Hg						
	Tl				0.59		
	Bi				0.24		
		(1)	(1)	(2)	(3)	(4)	(5)

References and Methods:

(1) Ridley et al. (1973); isotope dilution, XRF, AA. (also partial publication in Church et al. (1972); Nyquist et al. (1972b, 1973); Hubbard et al. (1974; Wiesmann and Hubbard (1975).
(2) Blanchard et al.; in ICR 2; INAA.
(3) Gros et al. (1977), in ICR 1; RNAA.
(4) Tatusmoto and Unruh, in ICR 1; isotope dilution.
(5) Jovanovic and Reed (1977) and ICR 1; INAA (U), colorimetry (P_2O_5).

CHEMISTRY: Chemical analyses of matrix and clasts are listed in Tables 2 to 5, and rare earths are plotted in Figure 6a,b,c. Jovanovic and Reed (1972) reported additional data on halogens and Te for matrix samples which were leached in the laboratory, as well as similar analyses for the leaches themselves. Keith et al. (1972) report gamma-ray-measured U (0.63 ± 0.08 ppm), Th (2.40 ± 0.18 ppm), and K (0.106 ± 0.014 ppm) abundances for the entire rock which are similar to those derived from analyses of the matrix alone (Table 3).

MATRIX:

The matrix of 15445 (Tables 2 and 3) is contaminated with meteoritic siderophiles (Gros et al., 1976) grouped as 1L by Hertogen et al. (1977), the same as the 15455 matrix. It has a magnesian low-K Fra Mauro composition with rare earth abundances higher than any of the lithic clasts contained within it (Fig. 6a). Ridley et al. (1973) noted that its composition is difficult to interpret in terms of mixing of Apennine Front materials, and it appears to represent a chemically distinct unit. It was interpreted by Ryder and Bower (1977) as melt created by the Imbrium impact. The high Pb (Unruh and Tatsumoto, 1976) requires a lot of pre-analysis contamination, but if the data are real then the non-radiogenic Pb is difficult to account for.

TABLE 15445-3. Microprobe defocussed beam analyses of matrix (Ryder and Bower, 1977; ICR 2)

Wt %	SiO_2	45.7	45.3
	TiO_2	1.56	1.70
	Al_2O_3	17.3	17.5
	FeO	7.9	9.5
	MgO	13.4	15.7
	CaO	11.5	9.7
	Na_2O	0.62	0.81
	K_2O	0.22	0.18
	P_2O_5	0.18	0.27
ppm	Cr	1230	1030
	Mn	850	1240

Fig. 6a

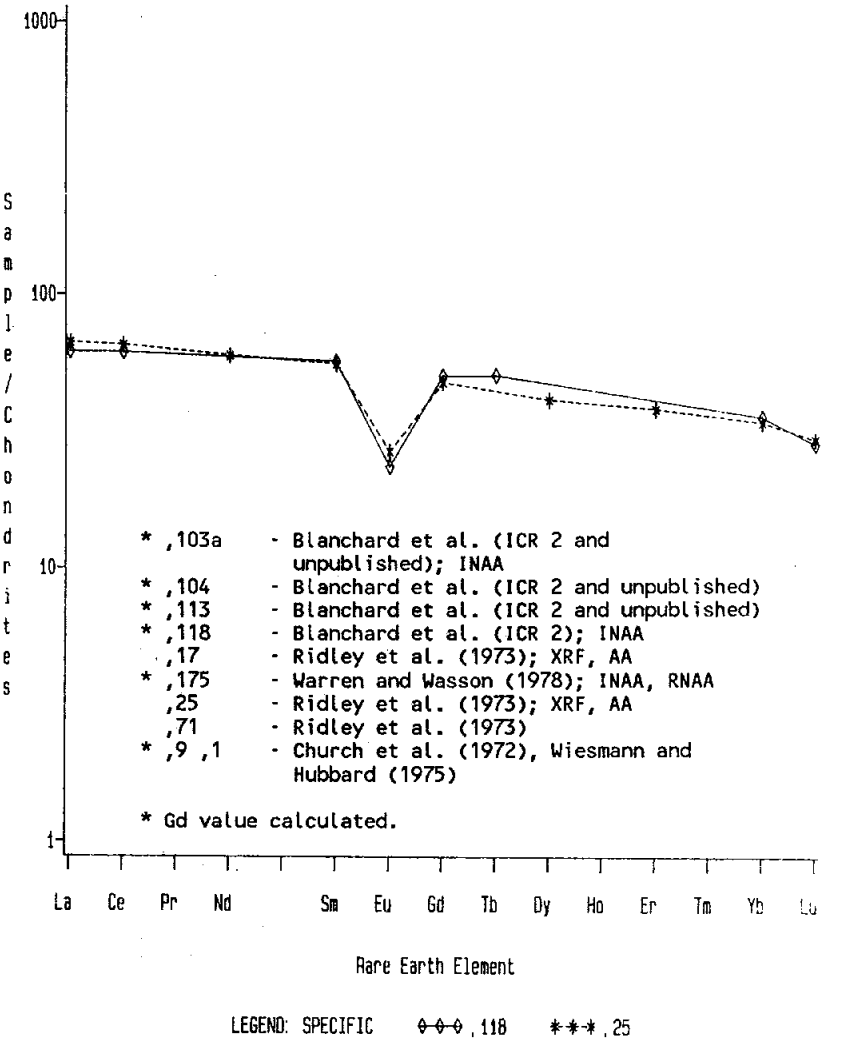
1000
100
10
1
Sample/Chondrites
La Ce Pr Nd Sm Eu Gd Tb Dy Ho Er Tm Yb Lu
Rare Earth Element
* ,103a - Blanchard et al. (ICR 2 and unpublished); INAA
* ,104 - Blanchard et al. (ICR 2 and unpublished)
* ,113 - Blanchard et al. (ICR 2 and unpublished)
* ,118 - Blanchard et al. (ICR 2); INAA
,17 - Ridley et al. (1973); XRF, AA
* ,175 - Warren and Wasson (1978); INAA, RNAA
,25 - Ridley et al. (1973); XRF, AA
,71 - Ridley et al. (1973)
* ,9 ,1 - Church et al. (1972), Wiesmann and Hubbard (1975)
* Gd value calculated.
LEGEND: SPECIFIC ◊-◊-◊ ,118 *-*-* ,25

Fig. 6b

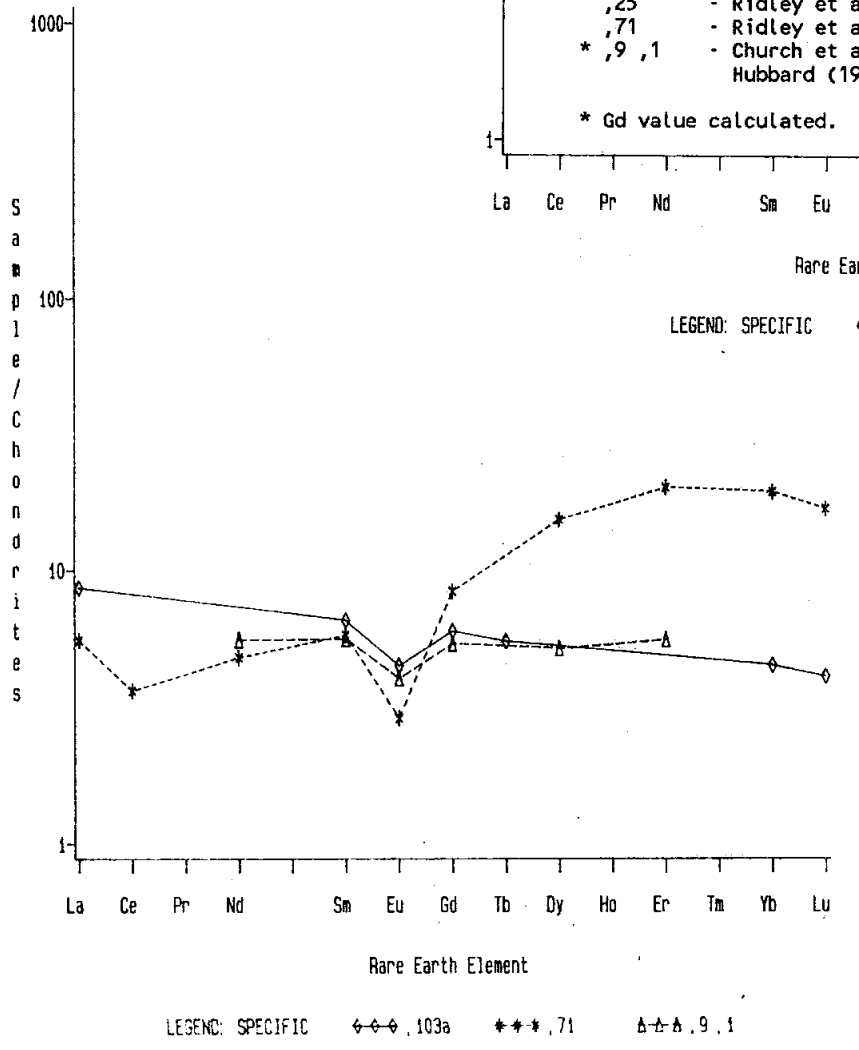
1000
100
10
1
Sample/Chondrites
La Ce Pr Nd Sm Eu Gd Tb Dy Ho Er Tm Yb Lu
Rare Earth Element
LEGEND: SPECIFIC ◊-◊-◊ ,103a *-*-* ,71 Δ-Δ-Δ ,9 ,1

Fig. 6c

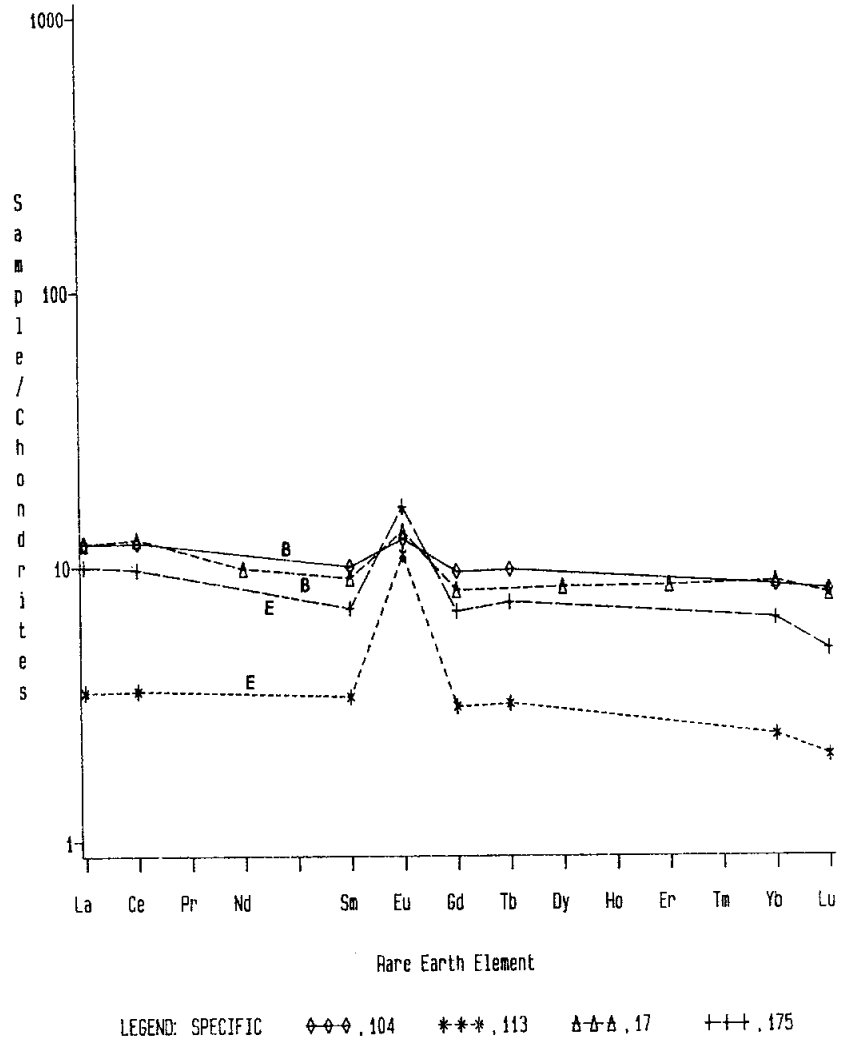

Figure 6. Rare earths in 15445. a) matrix; b) spinel troctolites; c) norite B and clast E.

LITHIC CLASTS:

1) Spinel Troctolites: The small size of the analyzed splits of the spinel troctolite samples are a disadvantage in their interpretation, but they do seem to be ultrabasic, with more than 30% MgO (Table 4). The rare earths for Clast G are substantially different from those for Clast A (Fig. 6b). The enriched heavy REEs (a unique pattern for a lunar sample) of Clast A reported by Ridley et al. (1973) were interpreted by the authors as indicating the former presence of garnet in the rock, but a second analysis of the same split (Wiesmann and Hubbard, 1975) showed no such enrichment and in fact appeared similar to the analysis of Clast G (or F) by Blanchard et al. (in ICR 1). Gros et al. (1976) note the very low siderophile content of Clast G (,102). According to Gros et al. in ICR 1, the levels are slightly enriched above the expected indigenous, an enrichment which could be explained by 5% matrix contamination. They suggested that the high Ni abundance they measured is spurious.

2) Norite: Clast B is an anorthositic norite according to its major elements (Table 5), and has a conspicuous positive Eu anomaly (Fig. 6c) consistent with plagioclase accumulation (Ridley et al., 1973). Hubbard et al. (1974) gave it "conditional membership" in an anorthositic series but gave no real discussion of it. Both Gros et al. (1976) and Tatsumoto and Unruh (ICR 1) and Unruh and Tatsumoto (1976) erroneously referred to this lithology as olivine and spinel-bearing i.e., spinel troctolite, and it is also erroneously referred to as 15455,107 in one place in the text of Gros et al. (1976). The norite is free of meteoritic contamination. The high Pb abundance, non-radiogenic, cannot be accounted for by their own possible laboratory contamination, but might be from previous sample handling, according to Unruh and Tatsumoto (1976).

3) Clast E: Chemical analyses by Blanchard et al. (ICR 2, and unpublished) and by Warren and Wasson (1978) are not in good agreement (Table 5), presumably because of small sample sizes and the apparent complexity of the clast. The analysis by Warren and Wasson is of a more mafic split; it is free of meteoritic contamination, but Ge is very high. The rare earth pattern is KREEPy, and Clast E may well be polymict. Wanke et al. (1983) plotted 15445 on a diagram of pristine rocks; the data appear to be that of Warren and Wasson (1978) for Clast E.

TABLE 15445-4. Chemistry of 15445 Spinel Troctolite Clasts

		Clast A			Clast G	
		,71	,9	,9,1	,102	,103a
Wt %	SiO2					37.5
	TiO2	.588		.154		0.25
	Al2O3	7.2				14.7
	FeO					6.4
	MgO	31.1		36.7		33
	CaO	1.9		4.76		4.8
	Na2O	0.10				0.14
	K2O			.0146		0.022
	P2O5					
(ppm)	Sc					3.43
	V					6900
	Cr					
	Mn					50.4
	Co				901*	820
	Ni				.66	
	Rb		.80			
	Sr		42.6			
	Y					
	Zr			35.5		
	Nb					
	Hf			<1		0.74
	Ba	25.0		23.6		
	Th					0.27
	U			.151	.024	
	Pb					
	La	1.84				2.86
	Ce	3.2				
	Pr					
	Nd	2.89		3.35		
	Sm	1.05		1.02		1.19
	Eu	0.196		0.275		0.31
	Gd	2.09				
	Tb					0.26
	Dy	4.88		1.65		
	Ho					
	Er	4.04		1.12		
	Tm					
	Yb	3.89				0.90
	Lu	0.573				0.136
	Li					
	Be					
	B					
	C					
	N					
	S					
	F					
	Cl				.0831	
	Br					
	Cu					
	Zn				13.4	
(ppb)	I					
	At					
	Ga					
	Ge				335	
	As					
	Se				1.3	
	Mo					
	Tc					
	Ru					
	Rh					
	Pd				<1.2	
	Ag				1.77	
	Cd				2.0	
	In				10.9*	
	Sn					
	Sb				18.9	
	Te				2.7	
	Cs				180	
	Ta					
	W					
	Re				.174	
	Os				.323	
	Ir				.340	
	Pt					
	Au				.319	
	Hg					
	Tl				2.7	
	Bi				.22	
		(1)	(2)	(3)	(4)	(5)

References and Method:

(1) Ridley et al. (1973); isotope dilution and ?
(2) Nyquist et al. (1972b, 1973); isotope dilution.
(3) Church et al. (1972) and Wiesmann and Hubbard (1975); isotope dilution.
(4) Gros et al. (1977) and in ICR 1; RNAA.
(5) Blanchard et al. in ICR 2 and unpublished; INAA
(6) Jovanovic and Reed (1977) and in ICR 1; thermal neutron activation for U; colorimetric for P_2O_5.

Notes:

* suspected by analyzers of contamination
(a) listed as Clast F, which it might be

TABLE 15445-5. Chemistry of 15445 Norite Clast B and Complex Clast E

		Norite B					Clast E	
		,17	,17	,106	,104	,107	,113	,175
Wt %	SiO2	48.7			47.7		43.4	45.58
	TiO2	0.15	0.140		0.27		.01	0.07
	Al2O3	23.76	20.8		23.0		33	30.43
	FeO	3.88	3.8		3.9		.55	2.32
	MgO	9.94	9.7		10.2		1.56	4.70
	CaO	13.26	12.6		12.8		17.3	16.38
	Na2O		0.33		0.32		.31	0.36
	K2O		.070		0.066		.045	
	P2O5	0.03						
(ppm)	Sc				7.1		1.90	4.3
	V							
	Cr		1560		1710		228	890
	Mn	600						292
	Co				10.3		2.64	10.1
	Ni					11	70	<90
	Rb		1.43			1.14		
	Sr		130					
	Y							
	Zr		115					
	Nb							
	Hf		4.1		1.36		0.60	1.2
	Ba		61.9					
	Th			0.893	.82		0.94	0.68
	U		.539	0.160		.135		0.18
	Pb			65.5				
	La		4.02		4.02		1.15	3.3
	Ce		11.1		10.8		3.1	8.6
	Pr							
	Nd		5.91					
	Sm		1.65		1.81		0.61	1.28
	Eu		0.929		0.87		0.77	1.14
	Gd		2.05					
	Tb				0.46		0.15	0.35
	Dy		2.69					
	Ho							
	Er		1.72					
	Tm							
	Yb		1.78		1.72		0.49	1.3
	Lu		0.268		0.28		0.069	0.17
	Li							
	Be							
	B							
	C							
	N							
	S							
	F							
	Cl							
	Br					.0679		
	Cu							
	Zn					1.5		0.81
(ppb)	I							
	At							
	Ga							4800
	Ge					5.1		3820
	As							
	Se					4.6		
	Mo							
	Tc							
	Ru							
	Rh							
	Pd					1.2		
	Ag					0.52		
	Cd					2.8		<9
	In					0.34		<150
	Sn							
	Sb					0.42		
	Te					<0.7		
	Cs					267		
	Ta				130		190	120
	W							
	Re					0.0099		0.70
	Os					0.018		
	Ir					0.072		0.14
	Pt							
	Au					0.022		<0.035
	Hg							
	Tl					3.5		
	Bi					0.25		
		(1)	(1)	(2)	(3)	(4)	(3)	(5)

References and Methods:

(1) Ridley et al. (1973); isotope dilution, XRF, AA. (also partial publication in Church et al. (1972); Nyquist et al. (1972b, 1973); Hubbard et al. (1974); Wiesmann and Hubbard (1975)).
(2) Tatsumoto and Unruh in ICR 1 and Unruh and Tatsumoto (1976); isotope dilution.
(3) Blanchard et al. in ICR 2 and unpublished.
(4) Gros et al. (1976) and in ICR 1; RNAA.
(5) Warren and Wasson (1978); INAA, RNAA, microprobe fused bead.

STABLE ISOTOPES: Clayton et al. (1973a, b) reported oxygen isotopic analyses of olivine from spinel troctolite Clast A, plagioclase and orthopyroxene from norite Clast B, and bulk matrix (Table 6).

The plag-opx fractionation in the norite, 0.35, is identical within experimental error of all previously reported fractionations of plag-px in lunar basalts and gabbros. It indicates equilibration at about 1200° C, but is fairly insensitive to temperature -- as low as 1050° C is also compatible with the data. The olivine in the spinel troctolite, if in equilibrium with the norite, also indicates 1000° C to 1200° C, hence there is no evidence of isotopic exchange following igneous crystallization. Metamorphic equilibration within the spinel troctolite cannot be ruled out. All the separated phases have δO^{18} values 0.2 to 0.3 o/oo lower than their counterparts in lunar mare basalts.

RADIOGENIC ISOTOPES/GEOCHRONOLOGY: Nyquist et al. (1972b, 1973) presented whole-rock Rb-Sr isotopic data (Table 7), without specific discussion, for matrix, spinel troctolite, and norite lithologies.

Tatsumoto and Unruh (ICR 1) and Unruh and Tatsumoto (1976) presented U, Th, Pb concentrations and isotopic abundances for both matrix and for plagioclase, orthopyroxene, and whole-rock splits of norite Clast B (Table 8). They erroneously referred to the norite as an olivine-spinel-bearing white clast, and hence to the green orthopyroxene as olivine. The matrix has a high lead content with $^{206}Pb/^{204}Pb$ of 27 i.e., very non-radiogenic. Such an isotopic composition requires a lot of contamination, but if the data are real, the non-radiogenic lead cannot be accounted for. All splits of the norite are also unusually non-radiogenic with $^{206}Pb/^{204}Pb$ of 20 to 24. Again, this could result from contamination during sample handling prior to analysis.

Bernstein (1983) reported ^{40}Ar-^{39}Ar stepwise release results for a matrix sample. The pattern is disturbed with no real plateau and a drop-off at 1100° C, similar to that obtained by Alexander and Kahl (1974) for a 15455 matrix sample. A weighted average gives an "age" of 3.76 ± 0.09 b.y. for 15445.

TABLE 15445-6. Oxygen isotopic analyses of 15445 (Clayton et al., 1973b)

SPLIT	ROCK TYPE	MINERAL	δO^{18} (SMOW)
,14	norite	plag	+5.67
,14	norite	opx	+5.32
,10	sp-troctolite	oliv	+4.89
,28	matrix	----	+5.63

RARE GASES/TRACKS/EXPOSURE: Drozd et al. (1977) analyzed the abundances of isotopes of Ne, Kr, and Xe in ,111, apparently a matrix chip. The sample is not rich in solar wind gases and does not contain more fission xenon then expected. They calculated a ^{21}Ne exposure age of 118 m.y. and a ^{81}Kr exposure age of 157 ± 22 m.y. Bernstein (1983) calculated a ^{38}Ar exposure age of 220 m.y. for a matrix sample.

Keith et al. (1972) counted cosmogenic radionuclide (^{26}Al, ^{22}Na, ^{54}Mn, ^{56}Co, and ^{46}Sc) disintegrations for the bulk rock. Yokoyama et al. (1974) could not decide if these data indicated saturation in ^{26}Al activity or not.

MacDougall et al. (1973) found no preserved solar flare tracks in the spinel troctolite or the norite clasts. They did not investigate the matrix.

PROCESSING AND SUBDIVISIONS: At the Lunar Receiving Laboratory in 1971, clasts were designated A, B, D, E, and F, and pieces of them and matrix were pried or chipped off for allocation (Fig. 7), leaving many chips. Subsequent mapping and processing for the Imbrium Consortium is detailed by Marvin (ICR 1). A slab, which broke along fractures, was cut through the sample, leaving end piece ,151 and ,0. ,0 was then split into ,0; ,159; and ,160, and the slab dismembered for allocation (Fig. 2). The sample is substantially dissected.

TABLE 15445-7. Rb-Sr Analyses of 15445 (Nyquist et al., 1973)

Split	Lithology	$^{87}Rb/^{86}Sr$	$^{87}Rb/^{86}Sr$	T_m [a]	T_{LUNI} [b]
,25	matrix	.0643 ± 7	.70322 ± 6	4.47 ± .11	4.57 ± .15
,17	norite	.0318 ± 4	.70122 ± 4	4.64 ± .15	4.85 ± .15
,9	sp-troctolite	.054 ± 12	.70238 ± 44	4.2 ± 1.6	4.4 ± 1.6

a) model age assuming I = 0.69910 (BABI plus lab bias)
b) model age assuming I = 0.69900
$\lambda = 1.39 \times 10^{-11} \times yr^{-1}$

TABLE 15445-8. U, Th, Pb Analyses of 15445 (Tatsumoto and Unruh, ICR 1)

Sample	Fraction	Weight[1] (microgram)	Run[2]	Concentrations: U (ppm)	Th (ppm)	Pb (ppm)	Atomic Ratios: $^{232}Th/^{238}U$	$^{238}U/^{204}Pb$	Lead Isotopic Composition, Observed Ratio[3]: $^{206}Pb/^{204}Pb$	$^{207}Pb/^{204}Pb$	$^{208}Pb/^{204}Pb$	Corrected Ratio[4]: $^{206}Pb/^{204}Pb$	$^{207}Pb/^{204}Pb$	$^{208}Pb/^{204}Pb$	$^{207}Pb/^{206}Pb$
15445,106 ~~olivine-spinel bearing white clast~~ Norite	whole rock	[illegible]	P						23.39	17.75	42.08	23.47	17.83	42.32	0.760
		434.6	C	0.160	0.993	65.5	5.78	0.166	22.43	17.55	--	22.43	17.55	--	0.782
	plagioclase (matrix)	814.6	P						21.24	17.73	40.93	21.32	16.61	41.19	0.788
		426.8	C	0.20[illegible]	1.17[illegible]	33.3	5.88	0.434	21.30	16.79	--	21.44	16.84	--	0.785
	[illegible] opx	[illegible]	P						20.84	16.58	[illegible]	21.03	[illegible]	40.01	[illegible]
		[illegible]	C	[illegible]	0.26[illegible]	[illegible]	[illegible]	[illegible]	[illegible]	[illegible]		[illegible]	[illegible]		[illegible]
15445,172 matrix	whole rock	134.0	P						26.98	20.11	45.98	27.10	20.72	46.28	0.746
		368.0	C	-	--	13.3	--	--	26.61	19.91	--	27.10	19.54	--	0.721

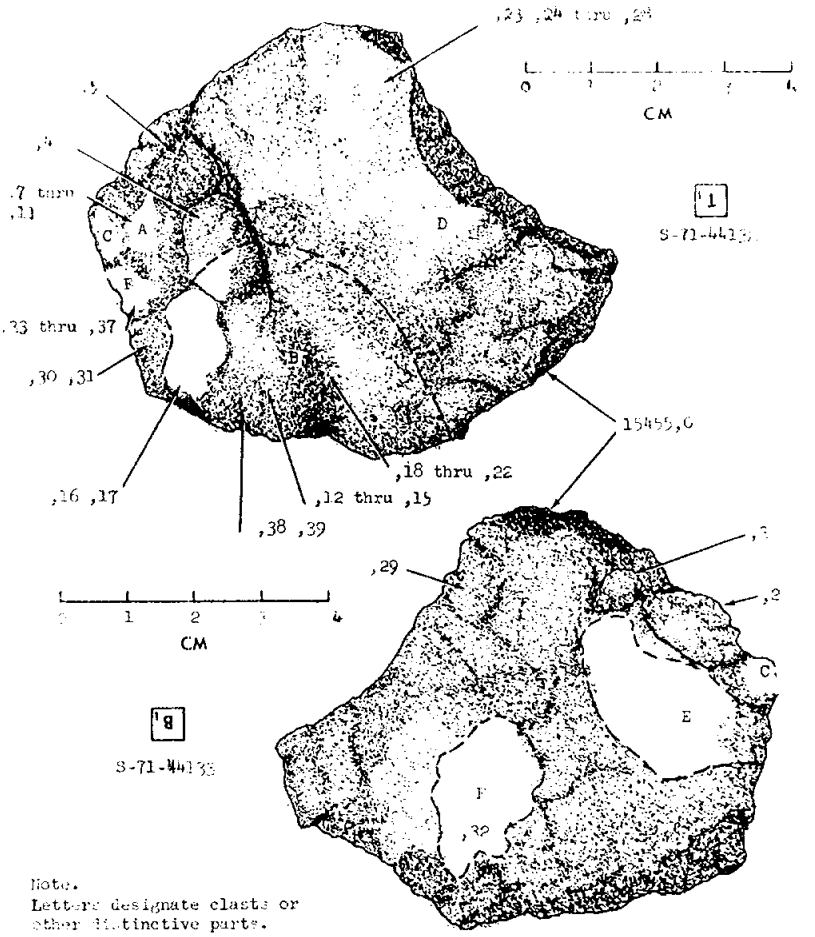

Figure 7. Original chipping and clast designations of 15445.

15455 FINE-GRAINED IMPACT MELT, WITH PRISTINE CLASTS 937.2 g

INTRODUCTION: 15455 is a very fine-grained impact melt of Mg-rich low-K Fra Mauro composition. It contains clasts of metamorphic and plutonic pristine igneous rocks, of which the dominant one is an anorthositic norite (Fig. 1), giving it its original name of "Black and White breccia." Clasts of surficial origin are absent. 15455 is very similar to 15445 which was collected nearby and both rocks have been interpreted to be fragments of melt rock produced in the Imbrium event (Ryder and Bower, 1977). 15455 was originally studied in a consortium led by L. Silver.

15455 was found lying about 15 meters from 15445 on the rim of Spur Crater, and was the largest of numerous rock fragments in an area of about 100 square meters that are characterized by the presence of high-albedo clasts (Swann et al., 1972). Like 15445, the sample is tough, blocky, and angular, with many zap pits on "N", "S", and "W", and few on "T" and "B". Vugs occupy 5 to 10% of the black matrix and average about 2 mm diameter. Veins of black aphanitic matrix are an ubiquitous feature of the norite clast (Figs. 1, 2).

PETROLOGY: 15455 consists of one large white anorthositic norite clast and several smaller white clasts in a dark gray, coherent, fine-grained impact melt matrix (Figs. 1 and 2). Locally the matrix contains vesicles and mineral fragments are ubiquitous. Veins of black aphanitic melt are common in the clasts, and appear to have altered the clasts for up to about 0.2 mm. The lithic clasts, in so far as they have been examined, appear to be pristine igneous or metamorphic varieties. Simonds et al. (1975) tabulated 15455 as a "black and white" breccia like some Apollo 16 rocks, but 15455 does not have the mutually intrusive forms and dimict nature of the Apollo 16 black-and-white (now "dimict breccias"; Stoffler et al., 1980).

MATRIX: James (1977) noted that the black material appeared to be fragment-laden melt that intruded the white material, and contained abundant xenoliths and xenocrysts in a very fine-grained igneous-textured groundmass (Fig. 3). Ryder and Bower (1977 and in Interdisciplinary Studies by the Imbrium Consortium, 1977) described the matrix as it occurs in a vein injected into a white clast--finer-grained than but otherwise similar to the 15445 matrix, including skeletal olivines. Most mineral fragments are olivines or plagioclases, with pink spinel, ilmenite, Fe-metal, troilite, and other minor phases. Pyroxene is virtually absent. Olivine and plagioclase compositions (Fig. 4) (Ryder and Bower, 1977; Reid et al., 1977) are similar to those in 15445. Fe-metal grains in the matrix have 5-9% Ni (Hewins and Goldstein, 1975; Ryder and Bower, 1977) and Co abundances in the meteoritic range. Heuer et al. (1972) and Christie et al. (1973) using HVEM techniques, found no glass in the matrix, which they described as a dark, non-porous, annealed microbreccia. They did find that many of the larger fragments

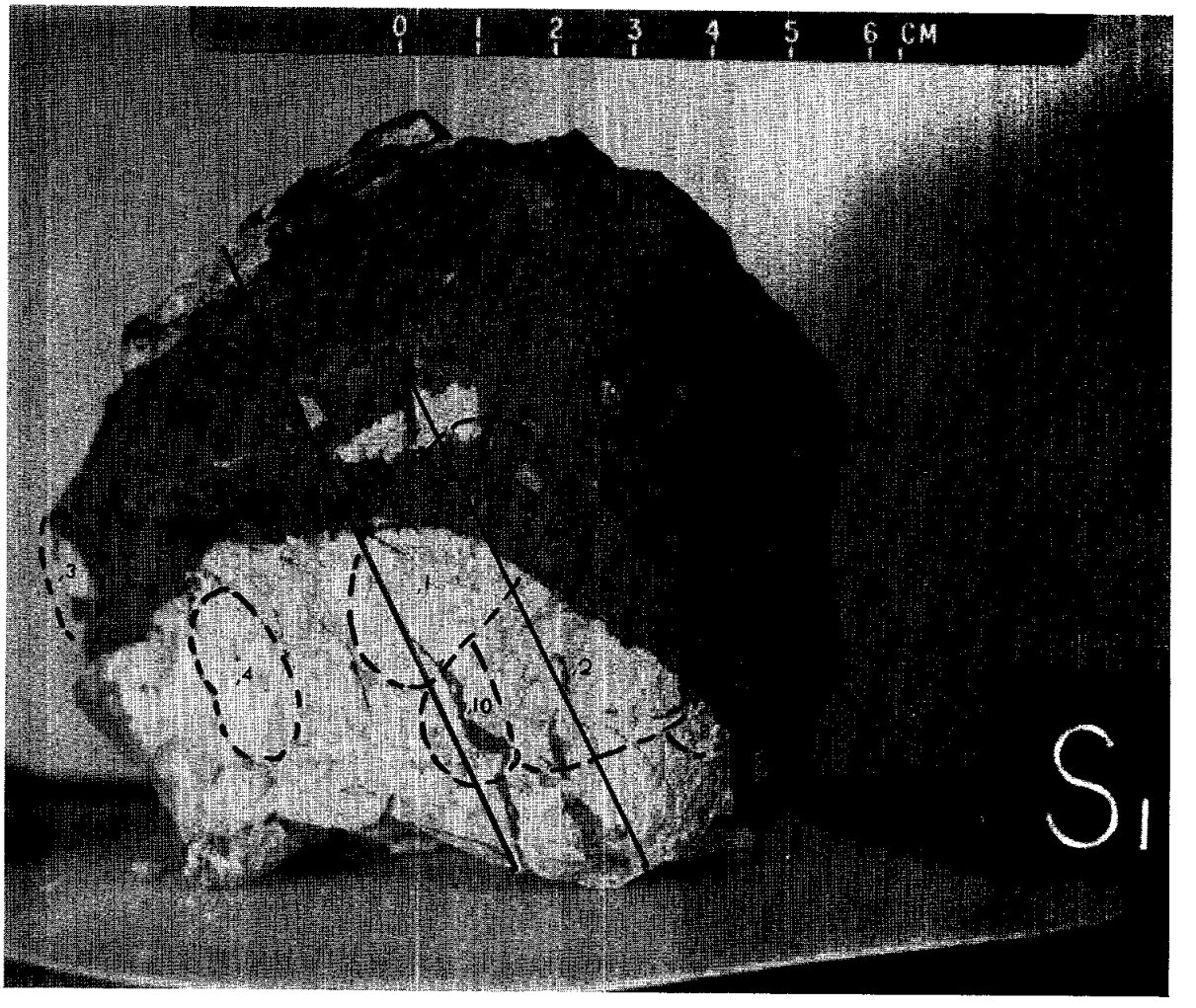

Figure 1. Macroscopic view of 15455, pre-cut but showing the future saw cut. Dashed areas are locations of documented loose pieces. S-71-46527

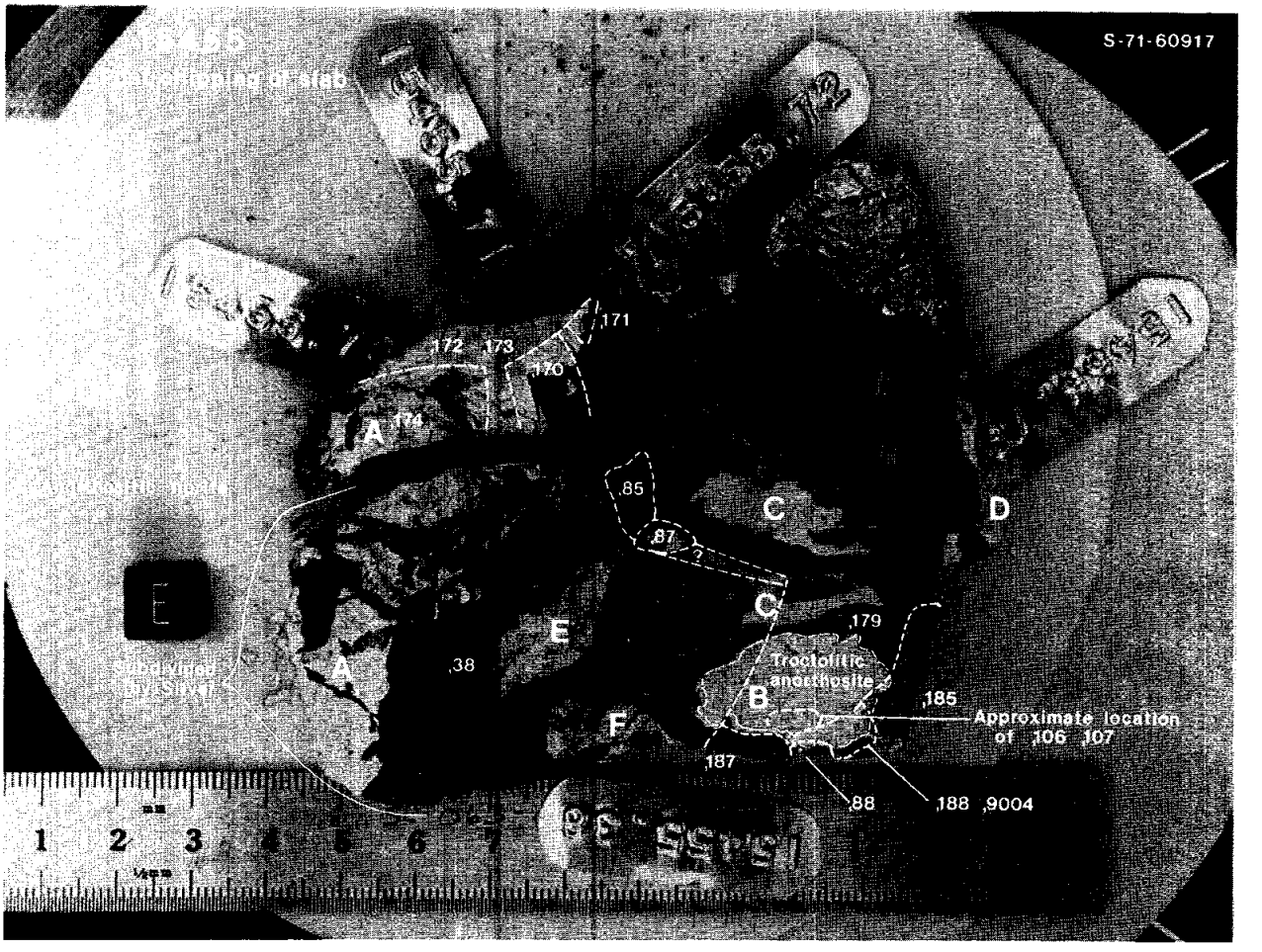

Figure 2. Chipping slab cut from 15455 showing lithologies and split numbering.

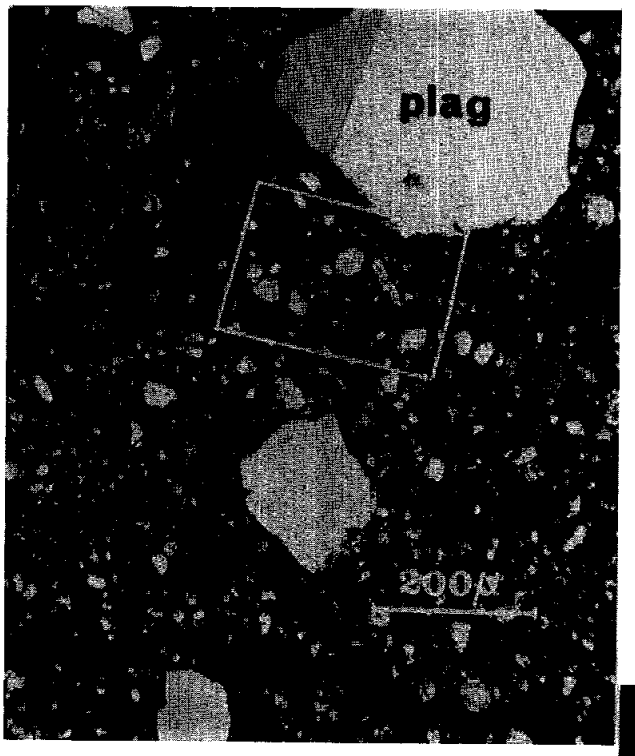

Fig. 3a

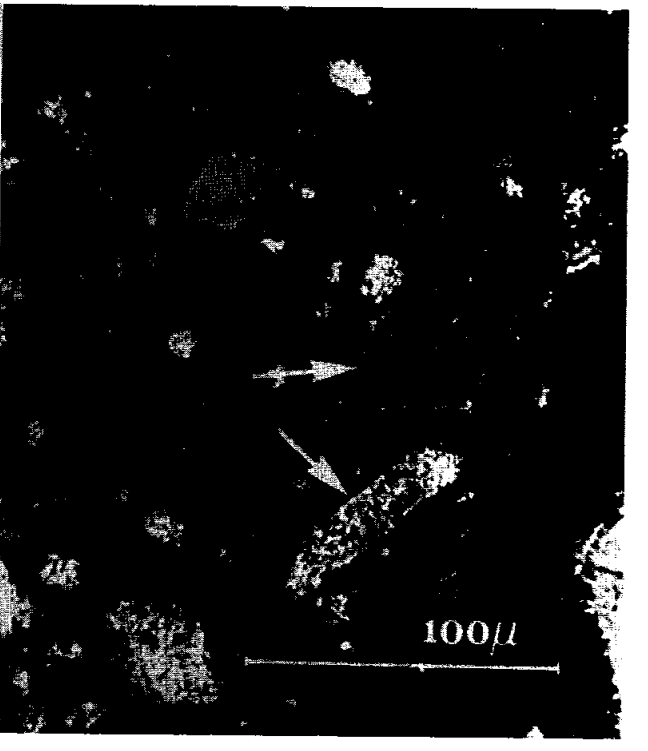

Fig. 3b

Figure 3. Photomicrographs of 15455. a) general matrix of 15455,28, showing clasts and fine melt groundmass. Rectangled area is Fig. 3b. Crossed polarizers. b) euhedral olivines (arrowed) in 15455,28 melt groundmass. Crossed polarizers. c) fine-grained vein-area of melt groundmass of 15455,28 with included small clasts. The main anorthositic norite clast which the vein splits is designated "norite". Transmitted light.

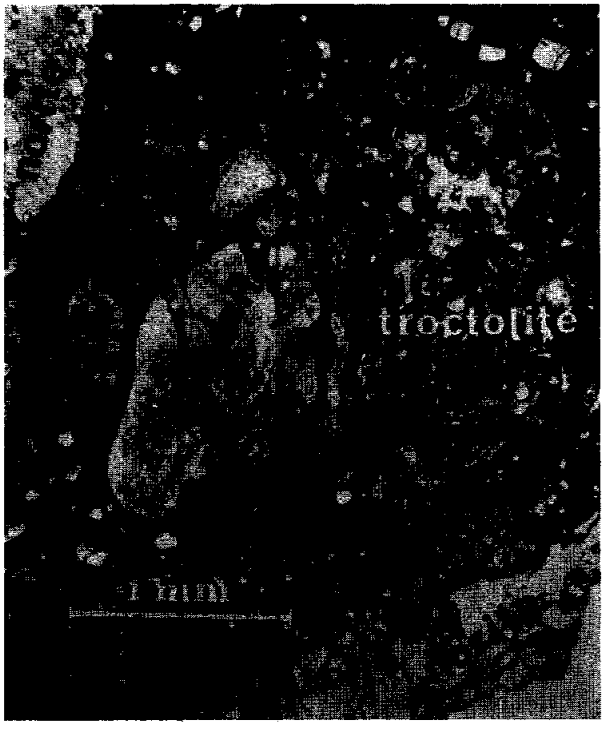

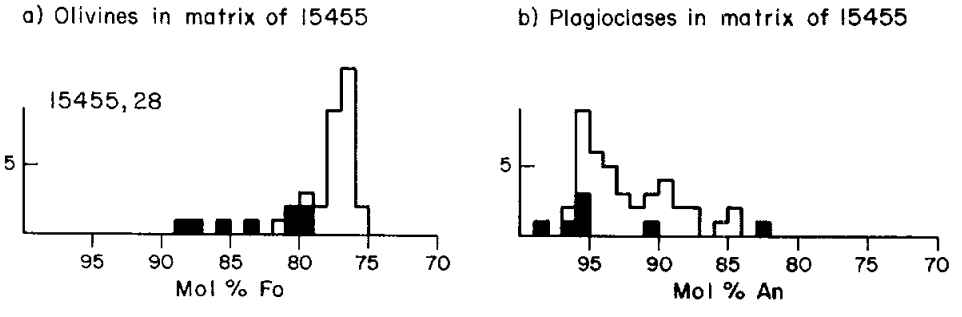

Figure 4. Compositions of minerals in matrix of 15455. Shaded are clastic grains larger than about 50 microns; unshaped are grains smaller than about 50 microns and are mainly melt grains (Ryder and Bower, 1977).

(>10 microns) in the matrix have internal deformation. Takeda and Ishii (1975) mention a thin section (,28) study but report no data. James (1977) noted that some xenocrysts are rounded and spherulitic devitrified maskelynite, with a history of shock more intense than the main anorthositic norite clast.

LITHIC CLASTS: Several lithic clasts occur in 15455. They appear to be pristine plutonic igneous rocks, but they have not been studied except for the large anorthositic norite, and a troctolite.

1) Anorthositic norite: The large norite clast (about 200 g) contains white plagioclase and pale green orthopyroxene. It was described by Ryder and Bower (1977). It had been found to be free of meteoritic contamination by Ganapathy et al. (1973). It consists of about 70% plagioclase and 30% orthopyroxene (Fig. 5). It is cataclasized and friable (see Phinney et al., 1977; Reid et al., 1977) but retains some originally coarse-grained zones, and areas of relict igneous texture. Heuer et al. (1972) and Christie et al. (1973) found it to be porous with a narrow zone of low porosity near the contact. It is bonded with glass of anorthositic composition, and shows no sign of recrystallization.

The plagioclase and orthopyroxene compositions are restricted (Ryder and Bower, 1977; Reid et al., 1977; Warren and Wasson, 1980) (Fig. 6) and similar to those in the 15445 norite- $En_{80-83}Wo_{1-3}$; An_{91-95}. Unlike the 15445 norite, the anorthositic norite of 15455 contains a variety of accessary phases--augitic diopside, silica, armalcolite, chromite, ilmenite, phosphate, zircon, baddelyite, Fe-metal, and troilite (Ryder and Bower, 1977), with many occurring together interstitially and probably representing trapped liquid. Fe-metal in the norite (referred to as the anorthositic facies of 15455) analyzed by Hewins and Goldstein (1975) was found to contain up to 10% Co. They believed that a correlation between Ni and Co in the metal was suggestive of an igneous fractionation trend.

Blanchard and McKay (1980) made mineral separate analyses (see CHEMISTRY section). Both Takeda and Ishii (1975) and Mori et al. (1982) reported studying the norite but provided no data.

2) Troctolitic anorthosite: This small clast (about 3 g) was analyzed by Ganapathy et al. (1973) and found to be free of meteoritic contamination. It is an egg-shaped white clast (Fig. 2) containing pale yellow mafic grains. Warren and Wasson (1979) found it to be a troctolite, comminuted to less than 350 microns grain size, but with monomineralic zones suggesting an original grain size up to 2 mm (Fig. 5). In thin section ,224 it is about 6/9 plagioclase, 2/9 olivine, and 1/9 pyroxene, with very uniform mineral compositions (Fig. 7) with pyroxenes and plagioclases similar to those in the norite. In ,169 it is about 75% plagioclase with the remainder mainly olivine, and with a feldspathic granulite texture (Ryder and Norman, 1979).

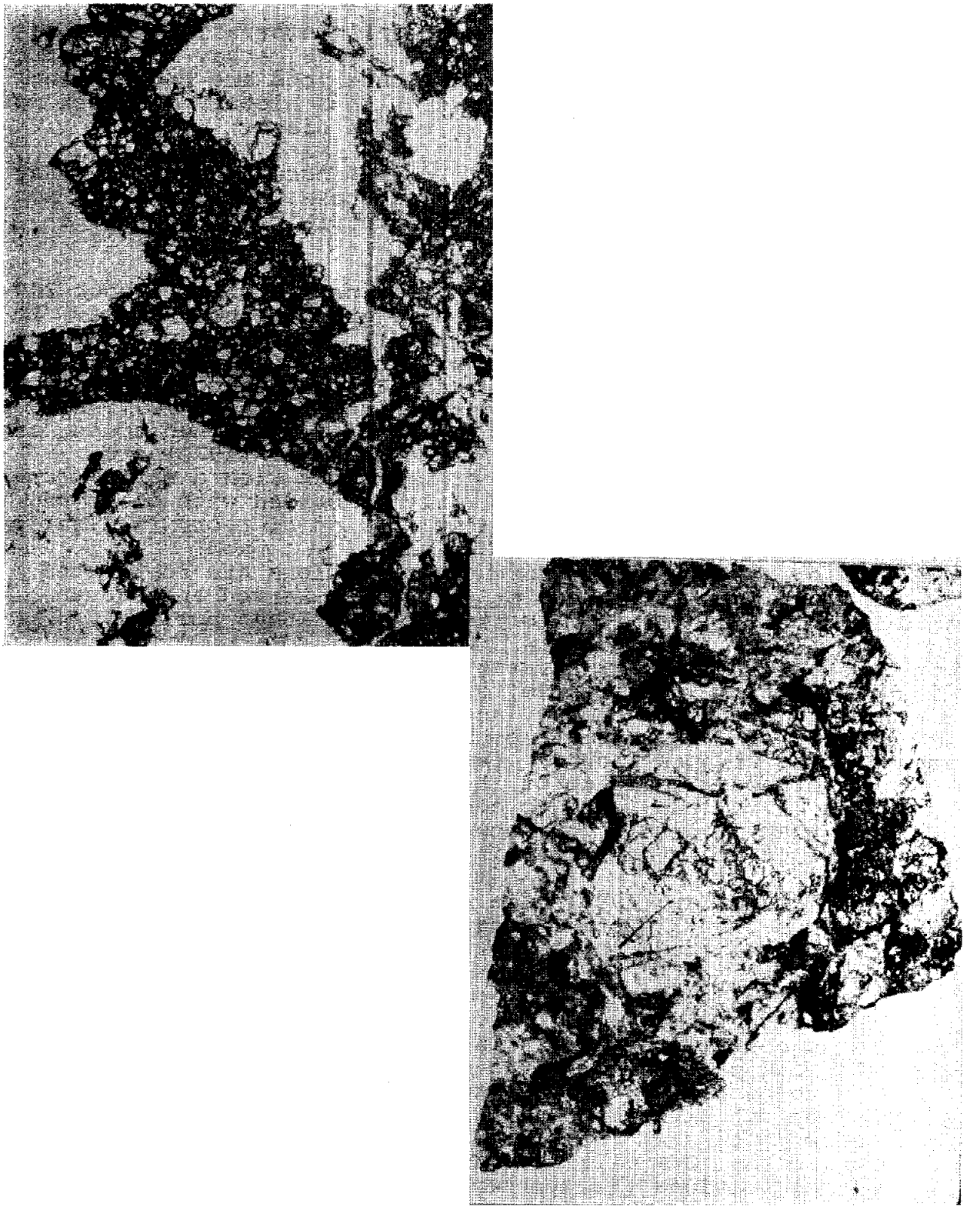

Figure 5. Photomicrographs of clasts in 15455. a) anorthositic norite in 15455,30. Width about 2 mm. Crossed polarizers. b) troctolitic anorthosite in 15455,169. Width about 2 mm. Crossed polarizers.

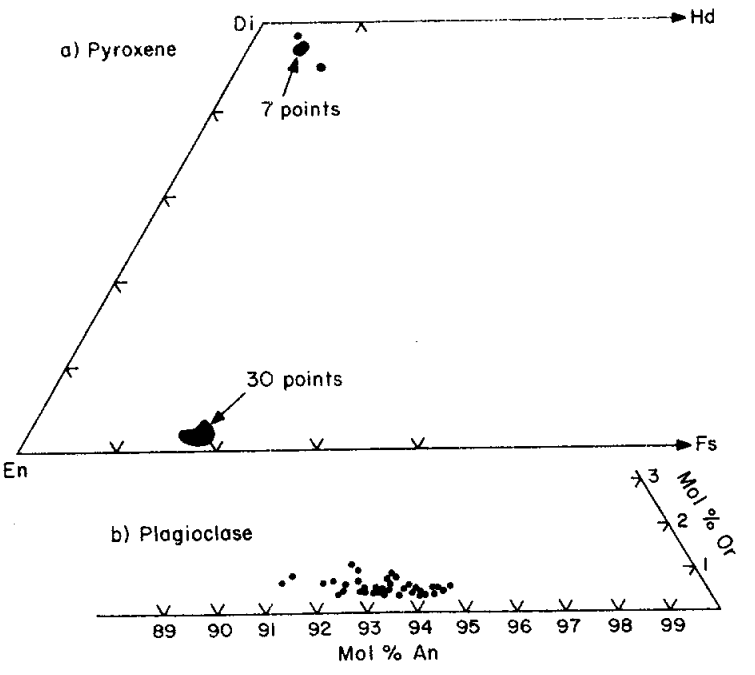

Figure 6. Compositions of minerals in anorthositic norite in 15455 (Ryder and Bower, 1977).

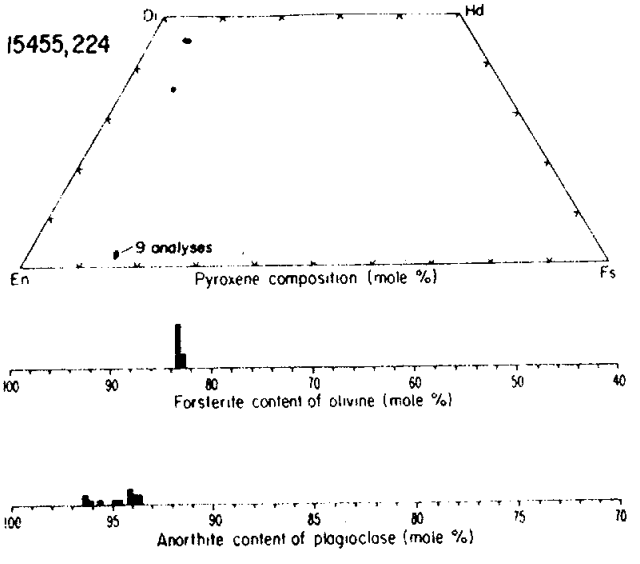

Figure 7. Compositions of minerals in troctolitic anorthosite in 15455 (Warren and Wasson, 1979).

3) Others: Most lithic clasts have not been separated and studied. A few in the matrix vein include anorthosite and troctolite (Ryder and Bower, 1977).

CHEMISTRY: Analyses for matrix, norite, and troctolitic anorthosite have been reported (Tables 1 - 4, Fig. 8).

MATRIX: Analyses are presented in Tables 1 and 2 and Figure 8. Those by Keith et al. (1972) and O'Kelley et al. (1972a, b, c) are gamma-ray measurements of the whole rock, though O'Kelley et al. stated that their analysis emphasizes the dark portion, i.e., matrix. The 15455 matrix is of low-K Fra Mauro composition (e.g., Taylor, 1973), similar to 15445.

Ganapathy et al. (1973) analyzed both vesicular and dense matrix, finding no real difference. Both contain siderophiles of meteoritic origin, which were assigned by Hertogen et al. (1977) to Group 1L, the same as 15445, and correlated with Imbrium. They match other KREEP-rich samples in pattern and absolute abundance for Ir, Re, Au, Ag, Zn, and Bi. Silver (1973) noted that U and Th were lower than other, regolith breccias at the Apollo 15 site and that 15455 was a rare type.

Modzeleski et al. (1972) reported analyses of carbon derived from CO, CO_2, and CH_4 as well as their total C abundance. Reed and Jovanovic (1972) and Jovanovic and Reed (1977) reported residue and leach analyses for Cl, Br, and I. They found that the non-leachable Cl was low. Moore et al. (1973) reported 39 ppm C for part of split ,63 which is a mixed norite and matrix sample, hence it is not known of what the analysis actually was.

LITHIC CLASTS:

1) Anorthositic norite: Several partial analyses for the norite phase have been reported (Table 3, Fig. 8). Those of Ganapathy et al. (1973) ("leucogabbro") and Warren and Wasson (1980) provided siderophile data demonstrating its lack of meteoritic contamination. Taylor et al. (1972, 1973) and Taylor (1973) analyzed the norite, but the CIPW norm has 20% olivine and only 7% pyroxene, and the low REE abundances and the REE pattern are those normally associated with plagioclase alone. The analyzed material was handpicked separates and may be unrepresentative of the norite as a whole (S.R. Taylor, pers. comm.). However, it is not quite as aluminous as that of Warren and Wasson (1980), which is slightly silica saturated. Bulk norite rare earth analyses are consistent with each other (Fig. 8) except for the S.R. Taylor analyses. They are high fractionated and have a positive Eu anomaly. They are similar to the 15445 norite abundances and pattern. Blanchard and McKay (1980) made analyses of mineral separates as well as bulk rock, and found it clear that the minerals had been in equilibrium with a highly evolved liquid with a distinct negative Eu anomaly. Silver (1976) noted the low Th/U ratio which is a result of plagioclase concentration.

TABLE 15455-1. Analyses of matrix of 15455

		,14	,183	,183	,38	,3	,0	,0	,183	,183	,66
Wt %	SiO2	47.3									
	TiO2	1.35									
	Al2O3	17.1									
	FeO	8.79									
	MgO	13.3								9.4	
	CaO	10.6									
	Na2O	0.58									
	K2O	0.17	0.143				0.108	0.127		0.132	
	P2O5					0.13					
(ppm)	Sc	13									
	V	39									
	Cr	1800									
	Mn										
	Co	22									
	Ni	184									
	Rb	2.7	2.91	2.7	2.2						
	Sr	141	161								
	Y	93									
	Zr	480	297								
	Nb	33									
	Hf	9.8									
	Ba	370	238								
	Th	5.31							2.855		
	U	1.37		0.715	0.875	0.14	0.53	0.53	0.770		
	Pb	3.0					2.0	2.0	1.857		
	La	32									
	Ce	81	62.0								
	Pr	11.5									
	Nd	47	38.6								
	Sm	12.8	10.6								
	Eu	1.82	1.91								
	Gd	15.5	12.6								
	Tb	2.41									
	Dy	16	13.4								
	Ho	3.76									
	Er	10.7	7.74								
	Tm	1.6									
	Yb	9.8	6.85								
	Lu	1.5	1.08								
	Li		13.6								
	Be										
	B										4.2
	C										
	N										
	S										
	F										
	Cl										
	Br			0.040	0.035						
	Cu	3.3									
	Zn			2.2	3.5						
(ppb)	I										
	At										
	Ga	3300									
	Ge			456	385						
	As										
	Se			89	92						
	Mo										
	Tc										
	Ru										
	Rh										
	Pd										
	Ag			1.6	1.6						
	Cd			2.5	2.3						
	In			0.35	0.34						
	Sn	220									
	Sb			1.5	1.9						
	Te			5.1	5.4	171					
	Cs	160		122	114						
	Ta										
	W										
	Re			0.41	0.63						
	Os										
	Ir			4.8	7.0						
	Pt										
	Au			4.6	5.8						
	Hg										
	Tl			0.41	0.32						
	Bi			0.21	0.17						
		(1)	(2)	(3)	(4)	(4)	(5)	(6)	(7)	(8)	(9)

References for Table 15455-1

Reference and methods:

(1) Taylor et al. (1972, 1973); Taylor (1973); spark source-mass spec/emission spec/microprobe
(2) Philpotts, unpublished; ID/MS
(3) Ganapathy et al. (1973); RNAA
(4) Reed and Jovanovic (1972), Jovanovic and Reed (1977); INAA, colorimetry
(5) Kelley et al. (1972a, b); gamma ray spectrometry
(6) Keith et al. (1972); gamma ray spectrometry
(7) Silver (1973); ID/MS
(8) Alexander and Kahl (1974); from argon isotopes from irradiation
(9) Modzeleski et al. (1972); vacuum pyrolysis/mass spec

TABLE 15455-2. Microprobe defocussed beam analysis of matrix (Ryder and Bower, ICR 2)

Wt %	SiO2	43.6
	TiO2	1.34
	Al2O3	20.5
	FeO	8.1
	MgO	14.0
	CaO	10.8
	Na2O	0.58
	K2O	0.14
ppm	Cr	1200
	Mn	600

TABLE 15455-3. Analyses of anorthositic norite

		,20	,183	,9015	,70A	,3	,70A	,70A	,228-1	,228-2	,65
Wt %	SiO2	44.4		47.7							
	TiO2	<0.07		0.1							
	Al2O3	26.2		27.0							
	FeO	4.2		2.8							
	MgO	10.9		6-9							
	CaO	14.3		14.8			10.2				
	Na2O	0.36		0.44							
	K2O	<0.06	0.058	0.08			0.053				
	P2O5					0.051					
(ppm)	Sc			5.33							
	V	16.0									
	Cr	440		1180							
	Mn			376							
	Co	10.0		27.2							
	Ni	12.0		21							
	Rb		1.09		1.1				1.133	1.065	
	Sr	270	124						137.9		
	Y	4.8									
	Zr	11.0		70							
	Nb	0.95									
	Hf	0.17		0.67							
	Ba	42.0	58.7	125							
	Th	0.23		0.59	0.195			0.665			
	U	0.05		0.18		0.073		0.258			
	Pb	1.00						0.592			
	La	3.0		4.8							
	Ce	6.7	10.5	11.8							
	Pr	0.95									
	Nd	3.73	6.66	7.4					7.79	5.379	
	Sm	0.88	1.86	1.74					2.13	1.502	
	Eu	1.67	1.03	1.38							
	Gd	0.95	2.21								
	Tb	0.14		0.35							
	Dy	0.84	2.59								
	Ho	0.17									
	Er	0.46	1.64								
	Tm	0.06									
	Yb	0.36	1.65	1.22							
	Lu	0.06	0.262	0.17							
	Li		6.08			8.4					
	Be										
	B										9.0
	C										
	N										
	S										
	F										
	Cl										
	Br				0.035						
	Zn			1.0	1.85						
(ppb)	I										
	At										
	Ga	2600									
	Ge			56	9.4						
	As										
	Se				8.3						
	Mo										
	Tc										
	Ru										
	Rh										
	Pd										
	Ag				1.7						
	Cd				1.0						
	In				0.05						
	Sn	670									
	Sb				0.079						
	Te				2.6	124					
	Cs				126						
	Ta			140							
	W										
	Re			6.3	0.0023						
	Os										
	Ir			0.020	<0.002						
	Pt										
	Au			0.023	0.009						
	Hg										
	Tl				0.054						
	Bi				0.14						
		(1)	(2)	(3)	(4)	(5)	(6)	(7)	(8)	(8)	(9)

TABLE 15455-4. Analyses of troctolitic anorthosite

		,106	,179
Wt %	SiO2	44.3	
	TiO2	0.08	
	Al2O3	21.9	
	FeO	5.8	
	MgO	16.1	
	CaO	11.6	
	Na2O	0.23	
	K2O	0.044	
	P2O5		
(ppm)	Sc	4.1	
	V		
	Cr	970	
	Mn	560	
	Co	25	
	Ni	26	
	Rb		0.54
	Sr		
	Y		
	Zr		
	Nb		
	Hf	0.86	
	Ba	77	
	Th	0.58	
	U	0.18	0.170
	Pb		
	La	3.2	
	Ce	8.1	
	Pr		
	Nd	4.4	
	Sm	1.23	
	Eu	0.82	
	Gd		
	Tb	0.25	
	Dy		
	Ho		
	Er		
	Tm		
	Yb	1.2	
	Lu	0.17	
	Li		
	Be		
	B		
	C		
	N		
	S		
	F		
	Cl		
	Br		0.030
	Cu		
	Zn	1.33	1.7
(ppb)	I		
	At		
	Ga	3100	
	Ge	14	11
	As		
	Se		9.6
	Mo		
	Tc		
	Ru		
	Rh		
	Pd		
	Ag		0.79
	Cd	2.9	0.91
	In	0.50	0.06
	Sn		
	Sb		0.22
	Te		7.5
	Cs		54
	Ta	140	
	W		
	Re	<0.010	0.0058
	Os		
	Ir	0.024	0.024
	Pt		
	Au	1.90	0.042
	Hg		
	Tl		0.058
	Bi		0.140
		(1)	(2)

References and methods: **References for Table 15455-3**

(1) Taylor et al. (1972, 1973), Taylor (1973); Spark source-mass spec/emission spec/microprobe.
(2) Philpotts J.A. (pers. comm.)
(3) Warren and Wasson (1980); INAA, RNAA, microprobe fused bead.
(4) Ganapathy et al. (1973); RNAA.
(5) Reed and Jovanovic (1972), Jovanovic and Reed (1977); INAA, colorimetry.
(6) Alexander and Kahl (1974); from Ar isotopes from irradiation.
(7) Silver (1973); isotope dilution/mass spec.
(8) Nyquist et al. (1979); isotope dilution/mass spec.
(9) Modzeleski et al. (1972); vacuum pyrolysis/mass spec.

Notes:

Taylor et al. (1972) reported Zr as 42 ppm and Sr as 218 ppm, both in error. Zr of 42 ppm would give a very high Zr/H_f ratio. Sr of 218 ppm is not compatible with the reported value of Sr/Eu. Taylor (1973) erroneously reported a value of Ti = 0.26%, and omitted "less than" symbols from TiO_2 and K_2O. The abundances in Taylor et al. (1972) were generally slightly revised in the later publications.

References and methods: **References for Table 15455-4**

(1) Warren and Wasson (1979); INAA, RNAA, microprobe fused beads.
(2) Ganapathy et al. (1973; RNAA.

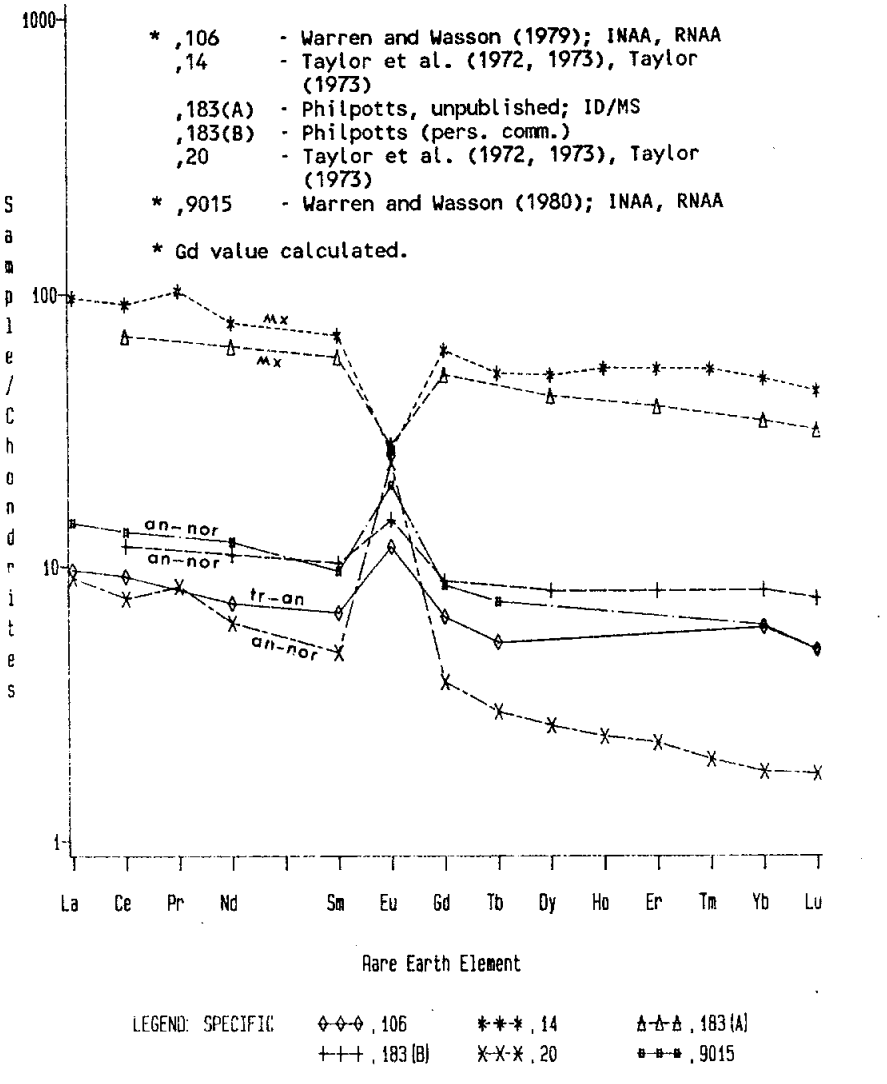

Figure 8. Rare earths in matrix and clasts in 15455.

Modzeleski et al. (1972) reported analyses of carbon derived from CO, CO_2, and CH_4 as well as their total C abundance. Surprisingly the norite contains more total C (9.0 v. 4.2 ppm) than the matrix. Reed and Jovanovic (1972) and Jovanovic and Reed (1977) provided analyses of residue and leach for Cl, Br, and I.

2) Troctolitic anorthosite: Ganapathy et al. (1973) found a clast of "anorthositic breccia" to be free of meteoritic contamination. A follow-up study by Warren and Wasson (1979) confirmed the pristinity of the clast (Table 4) and found it to be a troctolitic anorthosite. The norm has 58% feldspar, 29% olivine, and 13% orthopyroxene, and the rare earths are modestly fractionated in comparison with KREEP.

STABLE ISOTOPES: Epstein and Taylor (1972) made analyses for oxygen isotopes on both a matrix and norite sample, and a silicon isotopic analysis on the matrix (Table 5), without specific discussion. The isotopic values are similar to other lunar materials analyzed.

RADIOGENIC ISOTOPES/GEOCHRONOLOGY: Silver (1973) reported Pb isotopic compositions and Pb, U, and Th abundances for both matrix and anorthositic norite splits (Table 6). The Pb isotopic ratios differ from soils and other Apollo 15 breccias, and surprisingly show younger model ages distinct from any other Apollo 15 breccia.

Alexander and Kahl (1974) obtained ^{40}Ar-^{39}Ar data from both a matrix and an anorthositic norite split. No plateaus were obtained for either (Fig. 9). The norite suffered greater argon loss. By 700° C, the matrix released 43%, and the norite 63%, of its argon and has apparent younger ages for the 400° to 1100° C release. From the releases above 400° C, a minimum age of 3.82 b.y. is suggested for the norite, and a best estimate of the last major event affecting the matrix is 3.92 ± 0.04 b.y. A similar intermediate release age (~3.9 b.y.) for the norite was obtained by Bogard (unpublished data) (Fig. 9). Bernstein (1983) in a preliminary laser-probe ^{40}Ar-^{39}Ar study of the matrix obtained an imprecise age of 3.90 ± 0.25 b.y., and suggested that there had been incomplete degassing of plagioclase clasts during matrix formation. Nyquist et al. (1979) obtained Rb-Sr isotopic data for a norite sample (,228) (Table 7). An internal isochron yielded an age of 4.52 ± 0.10 b.y. ($\lambda = 1.39 \times 10^{-11}$ yr^{-1}) and an initial $^{87}Sr/^{86}Sr$ of 0.69903 ± 7. Further analyses (Nyquist, unpublished) modified this slightly to 4.58 ± 0.12 b.y. with initial $^{87}Sr/^{86}Sr$ of 0.69900 ± 6 (Fig. 10). The initial ratio is equivalent to LUNI as derived from Apollo 16 anorthosites, and would not be expected if the pyroxene data were artifacts, hence the isochron provides direct evidence for the early formation of the rock. A Sm-Nd analysis (Table 7) of bulk norite is consistent with that age, yielding calculated initial $^{143}Nd/^{144}Nd$ of 0.050596 ± 11 (at 4.52 b.y.) or 0.50591 ± 5 (at 4.56 b.y.), in agreement with eucrites. The model age (T_{ICE}) is 4.42 ± 0.34

TABLE 15455-5. Stable isotopes in 15455 (Epstein and Taylor, 1973)

Split	δO^{18}	δSi^{30}
white (norite)	5.83	--
dark (matrix)	5.90	-0.26

TABLE 15455-6. Pb isotopic ratios of 15455 (Silver, 1973)

SPLIT	TYPE	$\frac{Pb^{206}}{Pb^{204}}$	$\frac{Pb^{207}}{Pb^{204}}$	Pb ppm
,70A	An-norite	98.83	54.03	0.592
,183	matrix	185.26	103.98	1.857

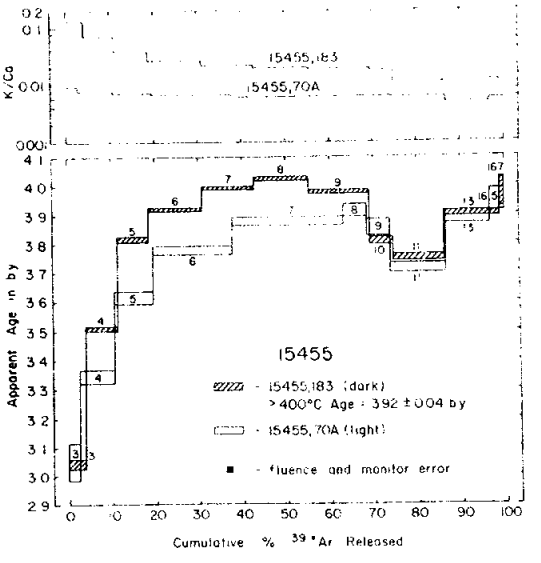

Fig. 9a

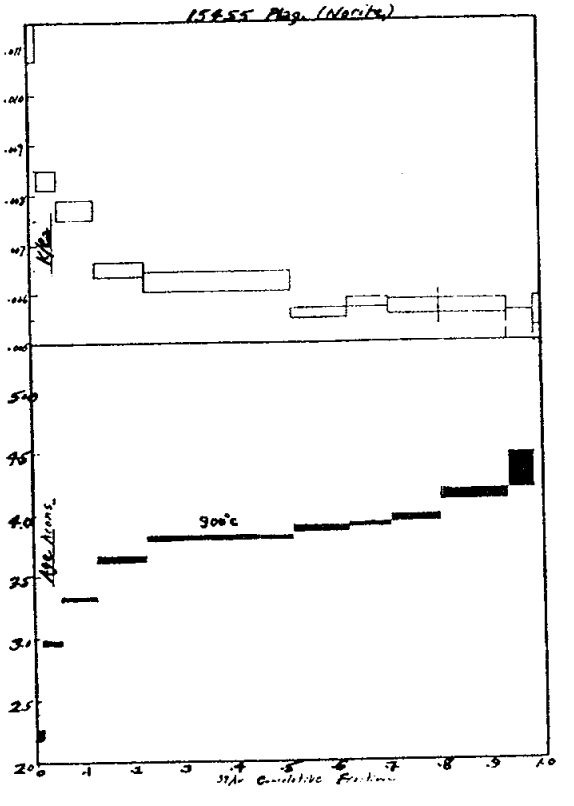

Fig. 9b

Figure 9. a) K/Ca and Ar release for 15455 samples. ,183 is matrix; ,70A is anorthositic norite (Alexander and Kahl, 1974); b) K/Ca and Ar release for 15455 anorthositic norite (Bogard, pers. comm.).

TABLE 15455-7. Sr and Nd isotopic data for the norite (Nyquist et al., 1979)

Sample	Wt (mg)	Rb (ppm)	Sr (ppm)	$^{87}Rb/^{86}Sr$(a)	$^{87}Sr/^{86}Sr$(b)	Sm (ppm)	Nd (ppm)	$^{147}Sm/^{144}Nd$(a)	$^{143}Nd/^{144}Nd$ (b)
W. R. 1	46	1.133	137.9	0.0237±2	0.70062±7	2.13	7.79		
W. R. 2	46	1.065				1.502	5.379	0.1689±3	0.511024±53
Plag	5.5	1.299	167.2	0.0225±2	0.70047±4	-	-	-	-
PX	7.6	0.485	15.03	0.0934±8	0.70508±6	-	-	-	-

(a) Uncertainties are for last digit.

(b) Uncertainties are for last digit and are $2\sigma_m$. Sr normalized to $^{88}Sr/^{86}Sr = 8.37521$; Nd normalized to $^{148}Nd/^{144}Nd = 0.24308$.

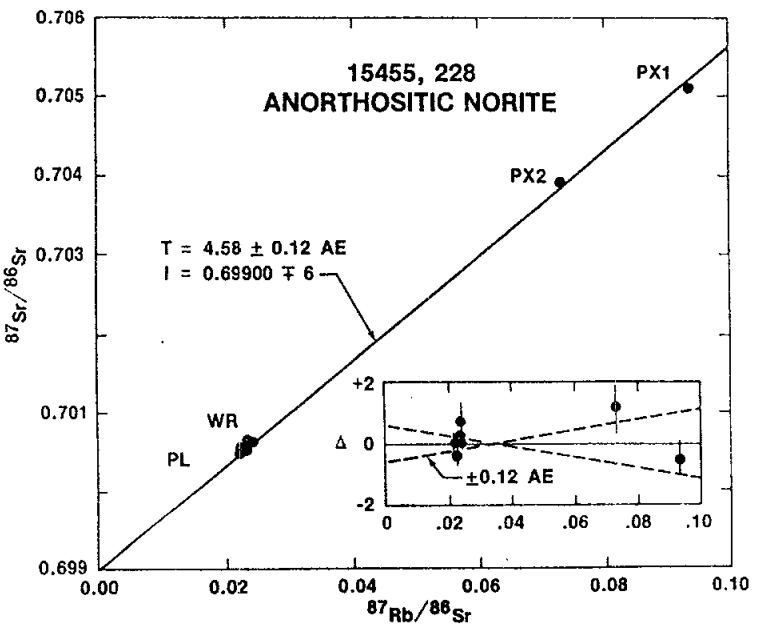

Figure 10. Rb-Sr isochron for 15455 anorthositic norite (Nyquist, pers. comm.).

b.y., and the ϵ value at 4.52 b.y. is +0.13 ± 1.1. Further Sm-Nd data (Nyquist, 1982 unpublished; Nyquist et al., 1981) for three whole rock splits show two with ϵ_{nd} of 0 at 4.4 b.y. but the other with ϵ_{nd} of +1.5 at 4.4 b.y. (Fig. 11). These three splits and a pyroxene datum give a Sm-Nd isochron age of 4.56 ± 0.26 b.y. with initial $^{143}Nd/^{144}Nd$ of 0.50596 ± 32, but a plagioclase datum falls well off this line (Fig. 12).

RARE GAS AND EXPOSURE: Alexander and Kahl (1974) derived a ^{38}Ar exposure age, from combined matrix and norite data, of 205 ± 21 m.y., an age representing a lower limit. Bernstein reported a ^{38}Ar exposure age of 190 m.y. for a matrix sample. Lightner and Marti (1974) reported Xe isotopic data for a matrix sample, without discussion. Keith et al. (1972) reported cosmogenic nuclide disintegration count data (^{26}Al, ^{22}Na, ^{54}Mn, ^{56}Co, and ^{46}Sc) for the bulk rock. Yokoyama et al. (1974) could not decide whether the sample was saturated in ^{26}Al or not.

PHYSICAL PROPERTIES: Cisowski et al. (1982) measured magnetic remanence in a matrix sample of 15455, finding a very low normalized intensity (NRM(200)/IRM_s(200) of about 4 x 10^{-3}. Housley et al. (1976) tabulated a matrix sample as having a very weak FMR intensity.

PROCESSING AND SUBDIVISIONS: 15455 was received as one large piece and 22 smaller pieces up to 3 g, including matrix and white clast material. Some of these fragments were locatable on the main piece (e.g., Fig. 1). Several whole fragments, mainly believed to be from the larger white clast, were allocated. Subsequently a slab (,38) was cut (Figs. 1, 2), exposing several white clasts. The sawing produced an intact end piece (,37) which is in remote storage. The other end piece is stored as several individual pieces (,39-,53) which have never been allocated. The slab itself was broken into a few pieces and the main part (,38 and ,70) allocated to the Silver Consortium for subdivision (Fig. 2).

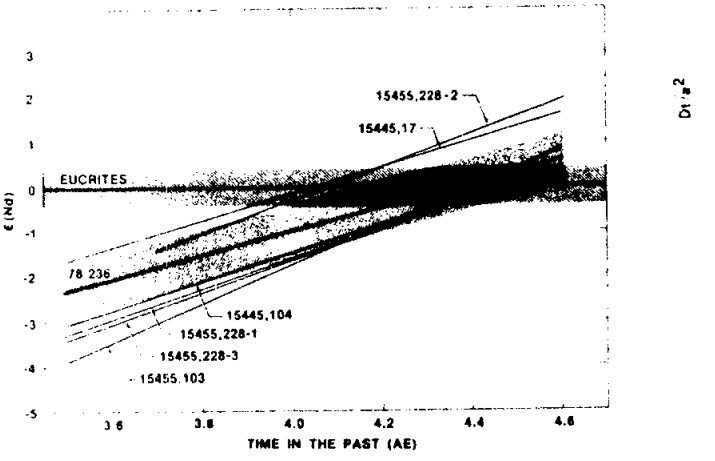

Figure 11. Nd evolution diagram for 15455 anorthositic norite samples, and 15445 and 78236 norite samples (Nyquist et al., 1981).

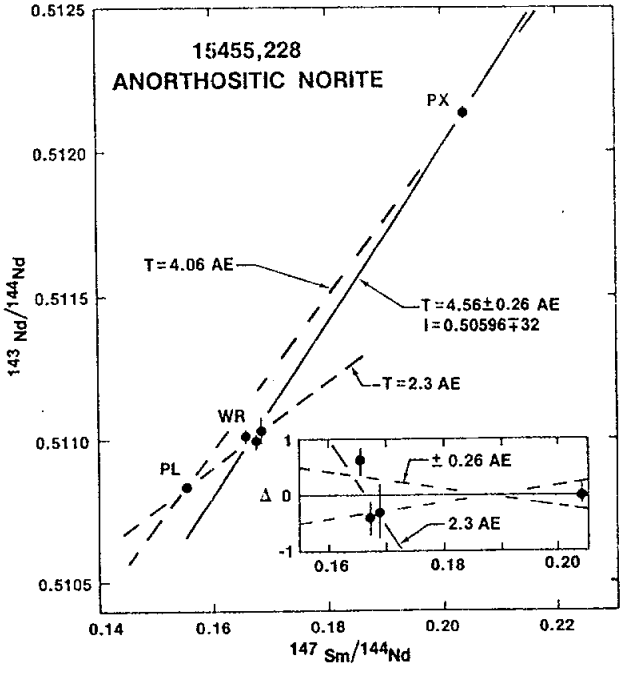

Figure 12. Sm-Nd "isochron" for 15455 anorthositic norite (Nyquist, pers. comm.).

15459 REGOLITH BRECCIA ST. 7 5854 g

INTRODUCTION: 15459 is a tough, glassy-matrix, glass ball-and glass shard-bearing regolith breccia. One large mare basalt clast in it has been dated as 3.3 b.y. old. 15459 is medium dark gray, blocky, and fractured (Fig. 2). It has fresh surfaces where it was broken off, zap pits elsewhere, and some vesicular splash glass coating as well as slickensides. Originally it was studied in a consortium headed by P. Gast.

The sample was collected on the northeast inner wall of Spur Crater, about 6 m southeast of the rim crest. It was taken from the center of a 30 x 30 x 15 cm rock (Fig. 1) that the CDR said looked as if it had "layering in it". A large fractured block lay immediately adjacent to it on the southeast (Fig. 1), and both it and 15459 were buried from one-third to one-half their height.

PETROLOGY: 15459 is a tough indurated breccia with small light-colored clasts dominant (Fig. 2). There is actually a diversity of clast types, including mare basalts, plutonic norites, impact melts, and numerous types of glass balls, shards, and schlieren (Figs. 3, 4). Light clasts appear to range from anorthosites or plagioclase to leucobasalts with pale green mafic minerals. Less abundant are gray lithic clasts and mafic mineral fragments. The glasses include black, green, and orange types. The matrix is dense and glassy, and thin glass veins and selvages on clasts are common.

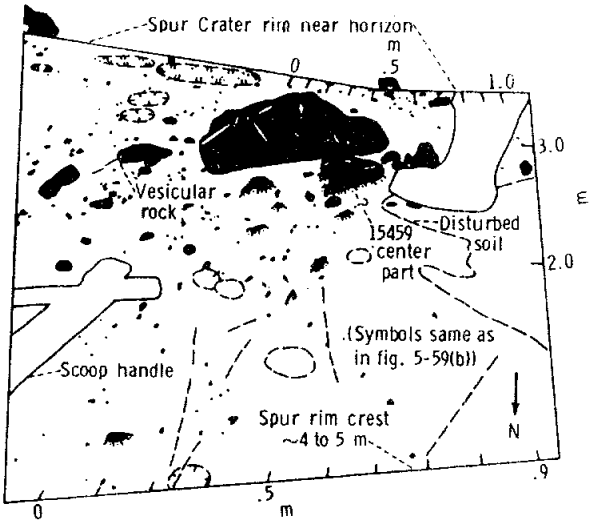

Figure 1. Presampling sample environment sketch map.

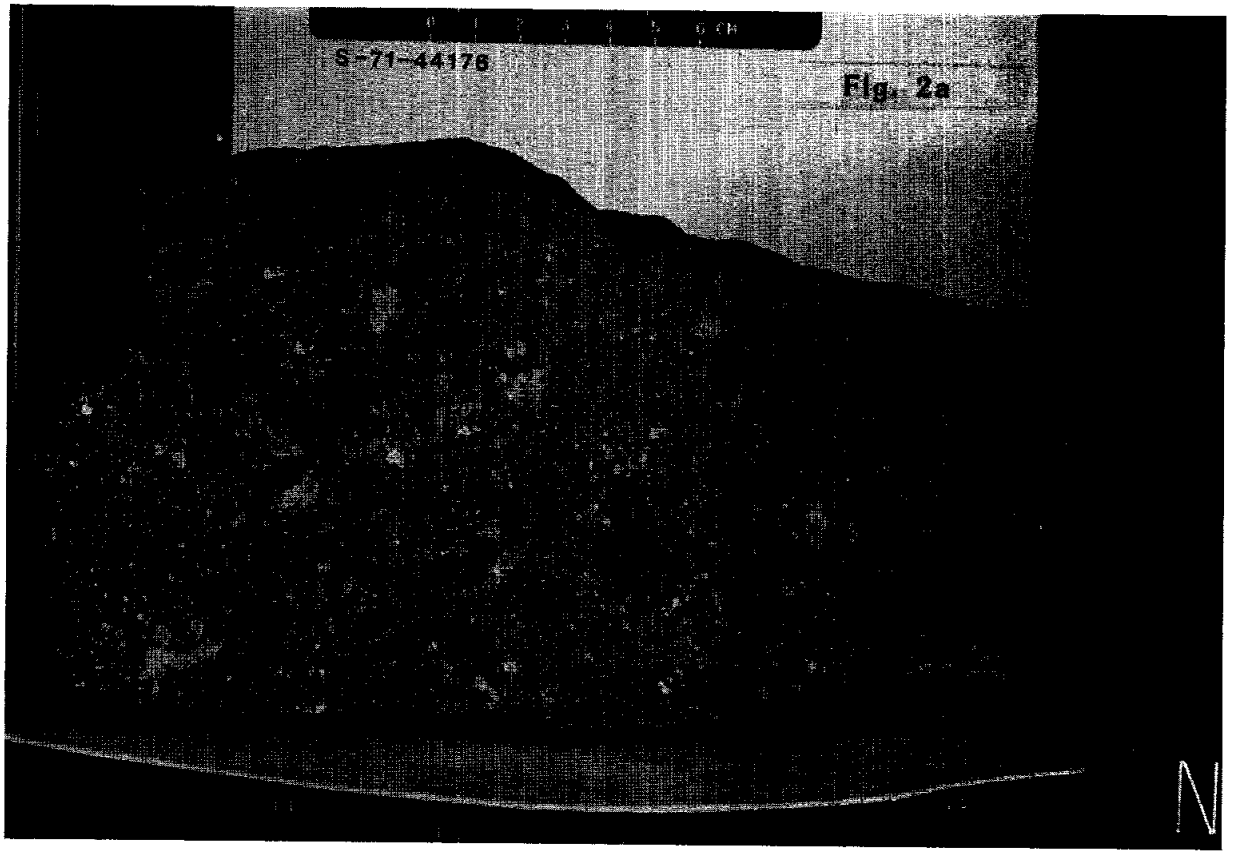

Figure 2. (a) 15459,0 presawing; (b) presawing, showing approximate locations of subsequent sawcuts; and (c) first post-sawcut, showing approximate location of section sawcut.

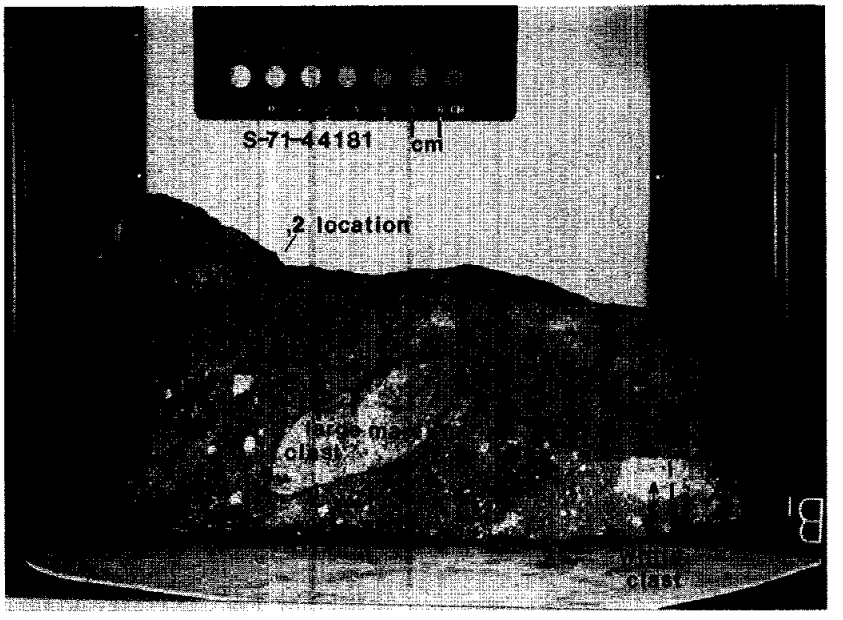

Fig. 2b

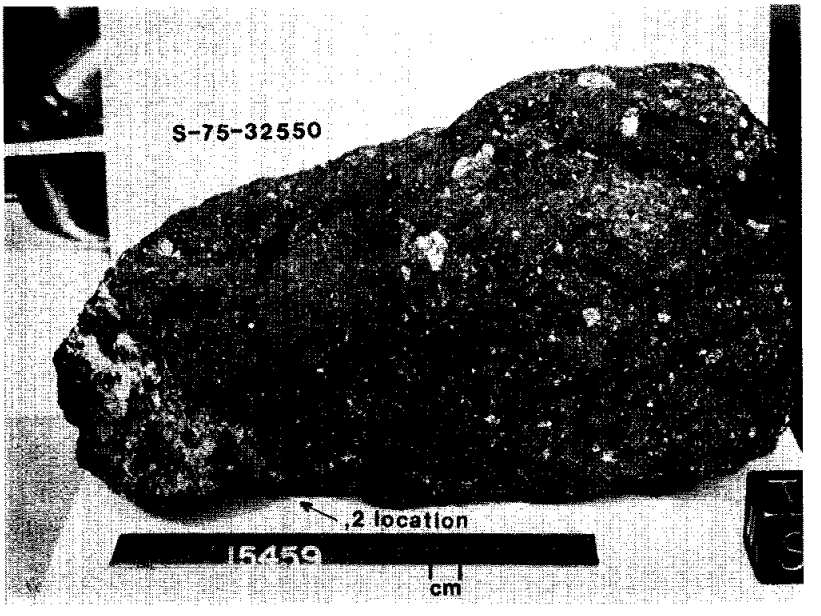

Fig. 2c

Fig. 3a

Fig. 3b

Figure 3. Photomicrographs of matrix in 15459,14, transmitted light.

Fig. 4a

Fig. 4b

Figure 4. Photomicrographs of clasts (a) 15459,124, large basalt, transmitted light; (b) as (a), crossed polarisers; (c) 15459,14 crushed basalt zone, transmitted light; (d) 15459,125, poikilitic impact melt clast, transmitted light; (e) 15459,125, matrix (right) and coarse norite (left), transmitted light.

Fig. 4c

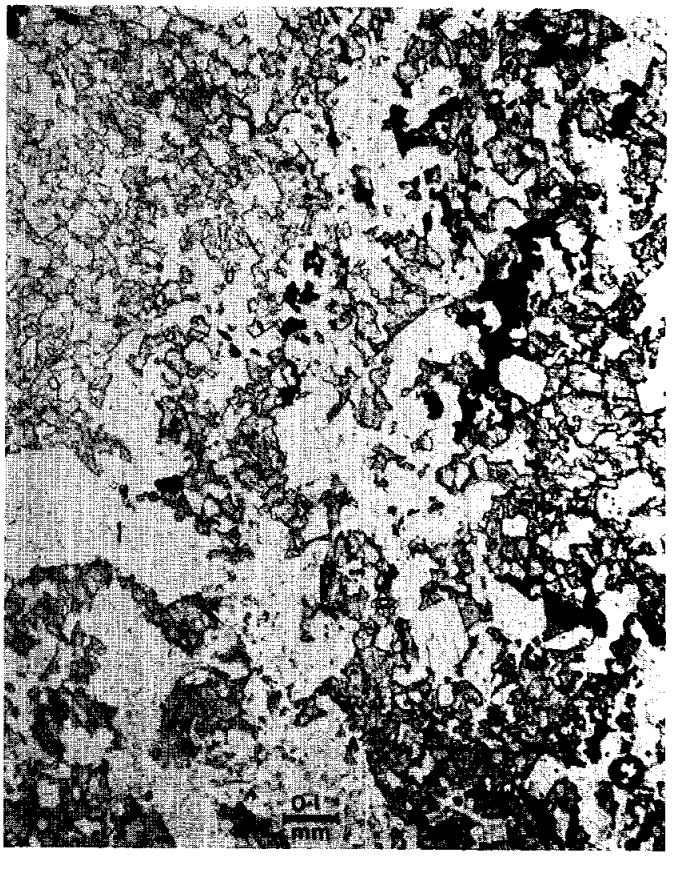

Fig. 4d

Fig. 4e

McKay and Wentworth (1983) found the sample to be compact, with a high fracture porosity, rare agglutinates, and common spheres, and with abundant shock features. Wentworth and McKay (1974) found its bulk density to be quite high, 2.84 g/cc. McKay et al. (1974) reported an I_s/FeO of 17-27 (25 in Korotev, 1984 unpublished), a submature index. According to Nagle (1982), 15459 shows the combination of characteristics expected in a rock produced by subcrater lithification, and its fabric is lineated rather than foliated.

Ridley (1975, 1977) briefly described the matrix and the glasses. The matrix contains numerous spherical glass particles of varied types, including Apollo 15 Green Glass, other mare types, and KREEP, for which Ridley (1977) provided group averages (Table 1). There are no glasses equivalent to the local quartz-normative basalts, nor to "highland basalt", and in fact highland glasses other than KREEP are rare. The glass group abundances are similar to those of soils around Spur Crater, as is the bulk composition, suggesting that 15459 is an indurated local soil.

Mare basalt clasts are common and include the prominent large clast (Fig. 2), but have not been much described in the literature. Ridley (1976, 1977) reported some data, referring to gabbros, and noted that they are similar to, but coarser grained than, local mare basalts. The pyroxene diagram shown in Ridley

TABLE 1. AVERAGE GLASS COMPOSITIONS IN 15459 MATRIX

	1	2	3	4	5	6	7	8	9
SiO_2	45.24	45.43	49.52	46.40	44.11	35.38	37.64	42.93	43.95
TiO_2	0.34	0.42	1.37	0.85	0.05	13.64	12.04	3.11	2.79
Al_2O_3	7.53	7.72	17.08	19.47	30.90	7.26	8.46	8.89	8.96
Cr_2O_3	0.45	0.43	0.19	0.17	0.03	0.64	0.48	0.46	0.46
FeO	19.51	19.61	9.37	8.34	3.53	21.42	19.93	21.72	21.10
MgO	17.55	17.49	9.07	12.49	3.51	12.10	10.49	12.37	12.30
CaO	8.23	8.34	10.65	11.39	17.23	7.66	8.81	8.68	9.02
Na_2O	0.13	0.12	0.63	0.53	0.13	0.52	0.54	0.39	0.27
K_2O	0.01	~0.01	0.50	0.18	0.01	0.14	0.13	0.08	0.05
Total	98.98	99.57	98.38	99.82	99.49	98.76	98.52	98.63	98.90

1, Green glass. 2, Average green glass composition in three Apollo 15 soils (Reid *et al.* 1972). 3, Medium-K kreep. 4, Low-K kreep. 5, 'Anorthositic' component. 6, High-Ti mare basalt. 7, 'Mare 4' glasses in Apollo 15 soils (Reid *et al.* 1972). 8, Mare glasses. 9, 'Mare 3' glasses in Apollo 15 soils (Reid *et al.* 1972).

Average abundances:	15459	A-15 soil
Green glass	43%	34%
Low-K kreep	13%	15%
Medium K kreep	20%	22%
'Anorthosite'	2%	
Mare	22% (High-Ti 2%)	22%

(1977) (Fig. 5) is of data from the large basalt clast, and shows pigeonite cores zoned to augite rims. Ridley (1976, 1977) also reported zoned olivine (Fo_{61-55}), plagioclase, spinel, and ilmenite in mare gabbros. The thin sections of the large clast show a coarse, pyroxene-rich mare basalt, sheared but not ground up (Fig. 4a,b). This large basalt has a chemistry (below) consistent with its being more mafic than typical mare basalts, and it is perhaps a pyroxene cumulate. It is the mare basalt which has been dated as 3.3 b.y. old (below). Other clasts of basalt are crushed (Fig. 4c). The "smeared" light zone, referred to in data packs as "anorthositic" are almost certainly the crushed basalts in the thin sections: chip ,2 (from which the thin sections which show cm-sized zones of crushed basalt were made) is from this zone (Fig. 2) and macroscopically the zone can be seen to contain laths of ilmenite. These crushed basalts do not appear to contain much olivine, but do contain cristobalite and patches of glassy mesostasis up to 1 mm across.

The other large clast (Fig. 2) is pale colored and fine-grained. There is some doubt as to its characteristics, because the chip taken for thin sections was not photographed, and the thin sections contain a poikilitic impact melt, a coarse norite, and matrix. The poikilitic impact melt dominates the relevant thin sections (Fig. 4d) and a later thin section specifically from the clast is a poikilitic impact melt. This clast type has been described by Ridley (1976, 1977) and Ridley and Adams (1976), in which it is described as poikiloblastic, and is also depicted by Reid et al. (1977). The clast contains unzoned, 1 mm-sized, orthopyroxene oikocrysts containing thin exsolution lamellae of augite. Pyroxene analyses (Fig. 6) are given in Ridley (1977) (some of the analyses appear to be erroneously listed by Ridley as cols. 11 and 12 instead of cols. 9 and 10), and are consistent with the compositions given by Reid et al. (1977) of $En_{71}Wo_{55}$ for oikocrysts. The oikocrysts contain chadacrysts of plagioclase (An_{92}) and olivine (Fo_{70}). There are also ilmenites (4% MgO), rare Al-Ti chromites, olivine fragments, and plagioclase clasts (cores homogeneous An_{92}, thin rims An_{69}). From a variety of px-ol "thermometers" Ridley (1977) and Ridley and Adams (1977) calculated equilibration temperatures close to solidus temperatures, hence prefer a metamorphic interpretation. (However, the characteristics and textures are very similar to some of the Apollo 17 "melt-sheet" rocks.) The x-ray diffraction data of Takeda (1973) is probably from this poikilitic clast (see below).

The coarse norite (Fig. 4e) contains exsolved and inverted pigeonites and plagioclases up to 1 mm across. According to Ridley (1976) the plagioclase is An_{88-92}, and to Ridley (1977) the pyroxene is ~$En_{60}Wo_{10}$ in bulk composition (Fig. 6) (again, note the apparent switching of cols. 9 and 10 with 11 and 12 in Table 4 of Ridley, 1977). Takeda (1973) studied this clast by microprobe and x-ray diffraction, concluding that the pyroxene is inverted pigeonite, estimating a bulk composition of $En_{57}Wo_{10}$ from microprobe data. However, he noted that probe analyses of the pyroxenes taken for x-ray diffraction are more magnesian

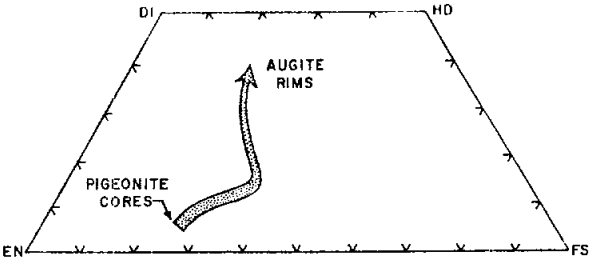

Figure 5. Zoning trends in pyroxenes in basalt 15459,124 (Ridley 1977).

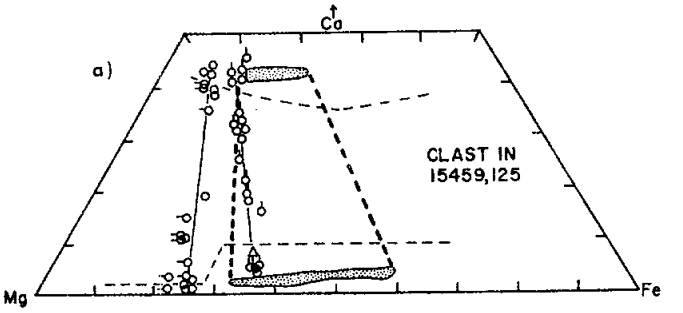

Composition of pyroxenes in clasts in breccia 15459. Solid lines are tie lines between coexisting Ca-rich and Ca-poor pyroxenes. Shaded areas are range in composition of exsolved pyroxenes in Apollo 16 breccias. Dashed lines are coexisting pyroxenes from the Skaergaard Intrusion. Circles with vertical bar are inverted pigeonites from a plutonic norite clast. Intermediate compositions represent analyses where the microprobe beam was unable to resolve host and lamellae. Triangle represents bulk analyses of inverted pigeonite. Circles with horizontal bars are exsolved orthopyroxene oikocrysts in a poikiloblastic clast. Circles represent coexisting orthopyroxene and augite chadacrysts in the same clast.

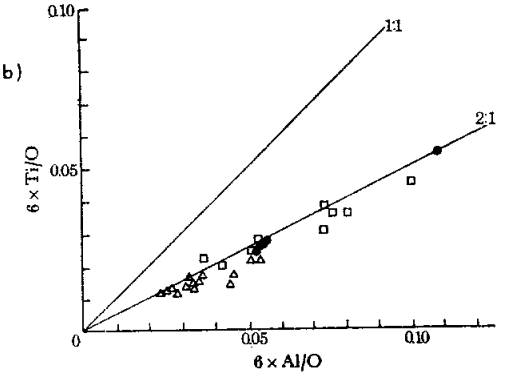

Ti-Al relations in pyroxenes plotted in figure a. Note the close adherence to Al:Ti = 2:1 line indicating the presence of $R^{2+}TiAl_2O_6$ component. △, exsolved inverted pigeonites in plutonic norite; □, exsolved orthopyroxene oikocrysts; ●, coexisting orthopyroxene-augite chadacrysts in a poikiloblastic clast.

Figure 6. Pyroxenes in 15459,125 (Ridley 1977).

TABLE 15459-2. Matrix

		,98	,74	,100	,99	,98	,0	,98	,97	,70	,1	,226
Wt %	SiO2				45.8				46.6			
	TiO2	0.9107			2.0a			0.911	1.02			1.11
	Al2O3				17.8				17.2			17.0
	FeO				11.0,11.1b			9.4	11.2			11.6
	MgO				11.8			10.0	11.4			12.3
	CaO							11.2	11.6			10.8
	Na2O				0.35			0.42	0.36,0.41			0.42
	K2O	0.1534					0.165	0.1530	0.16			
	P2O5									0.15		
(ppm)	Sc		23.0		21,20							22.0
	V		96.0									69
	Cr		2150		1800,1830				1900			2080
	Mn				1190				1000			1220
	Co		42.0		45,41							48.5
	Ni		232									213
	Rb		3.4			3.76		3.76	2.92			
	Sr		108			129.5		130				130
	Y		63.0						46.0			
	Zr	215	294.0		220c				240			220
	Nb		19.0						15.6			
	Hf	5.4	6.2		5.69,5.35				4.5			5.6
	Ba		230					157	160			157
	Th		3.71				2.9		2.52			2.4
	U	0.771	0.87				0.70	0.771	0.62	0.69		0.68
	Pb		3.3						3.5			
	La		19.0					14.7	15.0			14.2
	Ce		51.0					37.0	41.0			38
	Pr		6.5						5.3			
	Nd		27.0					22.9	20.9			21
	Sm		8.7					6.60	5.6			6.71
	Eu		1.18		1.1,1.3			1.15	0.83			1.08
	Gd		11.5						7.1			
	Tb		1.74		0.97				1.14			1.35
	Dy		10.8					9.14	7.3			
	Ho		2.68						1.83			
	Er		7.7					5.62	5.1			
	Tm		1.2						0.78			
	Yb		7.2					5.08	4.7			5.02
	Lu							0.858	0.73			0.696
	Li											
	Be											
	B											
	C			50						85		
	N											
	S											
	F									82		
	Cl									17		
	Br									0.387		
	Cu		4.4									
	Zn											
(ppb)	I									660		
	At											
	Ga		4100									
	Ge											
	As											
	Se											
	Mo											
	Tc											
	Ru											
	Rh											
	Pd											
	Ag											
	Cd											
	In											
	Sn		90						210			
	Sb											
	Te											
	Cs		150						130			180
	Ta				880,1100							680
	W								120			
	Re											
	Os											5.5
	Ir											
	Pt											1.3
	Au											
	Hg											
	Tl											
	Bi											
		(1)	(2)	(3)	(4)	(5)	(6)	(7),(13)	(8)	(9)	(10)	(14)

References for Tables 15459-2 through 15459-4

References and methods, Tables 2 to 4:

(1) Church et al. (1972); ID/MS
(2) S.R. Taylor et al. (1972, 1973); Spark source emission spec.
(3) Friedman et al. (1972); Combustion
(4) Janghorbani et al. (1973), Chyi and Ehmann (1973), Garg and Ehmann (1976); NAA
(5) Nyquist et al. (1972, 1973); ID/MS
(6) Keith et al. (1972); Gamma ray spec.
(7) Hubbard et al. (1973); ID/MS
(8) S.R. Taylor et al. (1973)
(9) Jovanovic and Reed (1975)
(10) Moore et al. (1972)
(11) Ganapathy et al. (1973); RNAA
(12) Stettler et al. (1973); MS
(13) Wiesmann and Hubbard (1975); ID/MS
(14) Korotev (1984 unpublished); INAA

Notes:

(a) authors reservations on accuracy.
(b) reactor NAA
(c) corrected value from Garg and Ehmann (1976)
(d) corrected value from Higuchi et al. (1975)

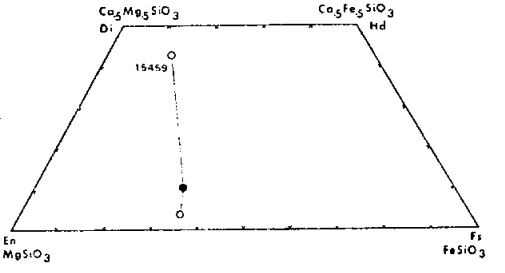

Figure 7. Pyroxenes in norite clast in 15459,125 (Takeda 1973).

TABLE 15459-3. Large mare clast

		,29	,28	,32	,31
WT %	SiO2	51.1			
	TiO2				2.0
	Al2O3	5.3			
	FeO	18.7b			
	MgO	24.2			17.3
	CaO			7.7	7.6
	Na2O				0.19
	K2O			0.0380	0.0389
	P2O5				
(ppm)	Sc	43			
	V				
	Cr	750			
	Mn	2050			
	Co	69	84		
	Ni				
	Rb		0.20		0.697
	Sr				54.9
	Y				
	Zr	48.6			
	Nb				
	Hf	1.17			
	Ba				46.7
	Th				
	U		0.107		0.16
	Pb				
	La				5.13
	Ce				14.2
	Pr				
	Nd				10.2
	Sm				3.25
	Eu	0.67			0.611
	Gd				4.40
	Tb	2.0			
	Dy				4.72
	Ho				
	Er				2.92
	Tm				
	Yb				2.21
	Lu				0.321
	Li				4.2
	Be				
	B				
	C				
	N				
	S				
	F				
	Cl				
	Br		0.033		
	Cu				
	Zn		0.93		
(ppb)	I				
	At				
	Ga				
	Ge		23		
	As				
	Se		66		
	Mo				
	Tc				
	Ru				
	Rh				
	Pd				
	Ag		0.34		
	Cd		3.2		
	In		0.85		
	Sn				
	Sb		0.042		
	Te		1.8		
	Cs		19d		
	Ta	990			
	W				
	Re		0.0105		
	Os				
	Ir		0.090		
	Pt				
	Au		0.081		
	Hg				
	Tl		0.08		
	Bi		0.39		
		(4)	(11)	(12)	(13)

For references and methods, see Table 15459-2.

($En_{68}Wo_9$ bulk). Ridley (1977) referred to the x-ray diffraction data as being from the poikilitic clast, and this is probably correct (despite Takeda's 1973 disavowal) because ,38 from which the grains were taken was mainly the poikilitic clast. The situation is quite confusing, because both the chemical data and the isotopic data (below) for fragments from the white clast appear to be unlike other poikilitic impact melts such as the Apollo 17 "melt-sheet" samples, and would be more compatible with a pristine noritic lithology.

Ridley (1976, 1977) also referred to another type of light-colored clast ("coarse norite with intergranular texture" or "diabasic-textured KREEP norite") which has zoned plagioclases and pyroxenes. The pyroxene zones from orthopyroxene (up to 4% Al_2O_3) to ferropigeonite, and plagioclase from An_{86-78}. They also contain Ti-Al chromites, Cr-Al ulvospinel, ilmenite, and rare armalcolite. Pyroxene compositional relationships are shown in Figure 8. This clasts(s) is evidently an Apollo 15 KREEP basalt.

McDougall et al. (1973) noted that glass spheres in 15459 are commonly shattered or heavily fractured, an apparent record of in situ shock or stress. The crystalline components show no evidence of post-breccia formation shock. From the preservation of solar flare tracks in olivine, they concluded that 15459 has never been above a temperature of ~400°C.

The only other published petrographic data on 15459 are by Muller et al. (1973) and Wenk et al. (1973), who found b- and c-type antiphase domains in a plagioclase grain, which is unidentified except for being $An_{94.7}$ and 0.5 mm across.

CHEMISTRY: Allocations for chemical analyses of the matrix and of the two larger clasts were made, and published data is listed in Tables 2-4. Rare earths are shown in Figure 9. In most cases there is little specific discussion of the analyses, even to the extent of what the analysis was of. Table 4 also lists an analysis of a second white clast analyzed by S.R. Taylor et al. (1973). In addition to the listed data, Janghorbani et al. (1973) also analyzed specifically for oxygen in the three lithologies (matrix 46.1%, basalt 43.0%, poikilitic melt 42.6%). Friedman et al. (1972) combined their two clast allocations (,30 and ,37) together for analysis, finding 22 ppm C; they also analyzed this combination for hydrogen (8 ppm), and found 38 ppm hydrogen in the matrix.

The matrix is aluminous and elevated in rare-earths compared with mare basalts and anorthositic lithologies. It corresponds roughly with low-K Fra Mauro which is a common glass composition within 15459 and Apollo 15 soils.

The mare basalt is much more magnesian than local large samples of mare basalt. Its rare-earth pattern is similar to other Apollo 15 mare basalts, both olivine and quartz-normative. The

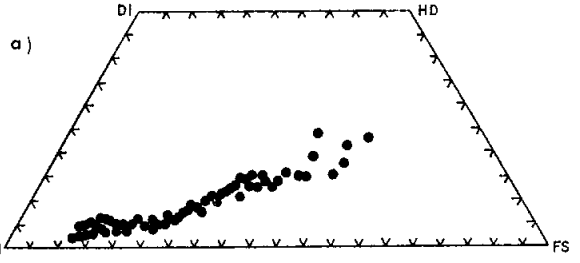

Variation in composition of pyroxenes in a diabasic-textured kreep norite clast 15459, 19. Note the continuity of pyroxene compositions from cores of aluminous bronzite to rims of intermediate pigeonite.

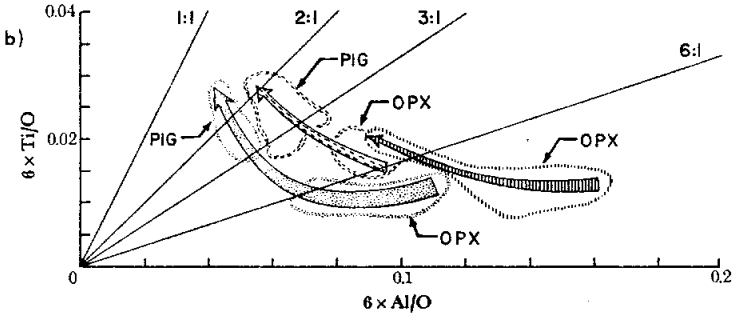

Ti-Al relations in pyroxenes plotted in figure a. Note the core bronzites have Al:Ti > 6:1 indicating the presence of $R^{2+}Al_2SiO_6$ component reflecting high alumina activity in the basalt melt. During crystallization the Al:Ti ratios approach 2 and in some crystals < 2 suggesting the presence of divalent Cr or trivalent Ti.

Figure 8. Pyroxenes in "diabasic-textured KREEP norite" in 15459,19 (Ridley 1977).

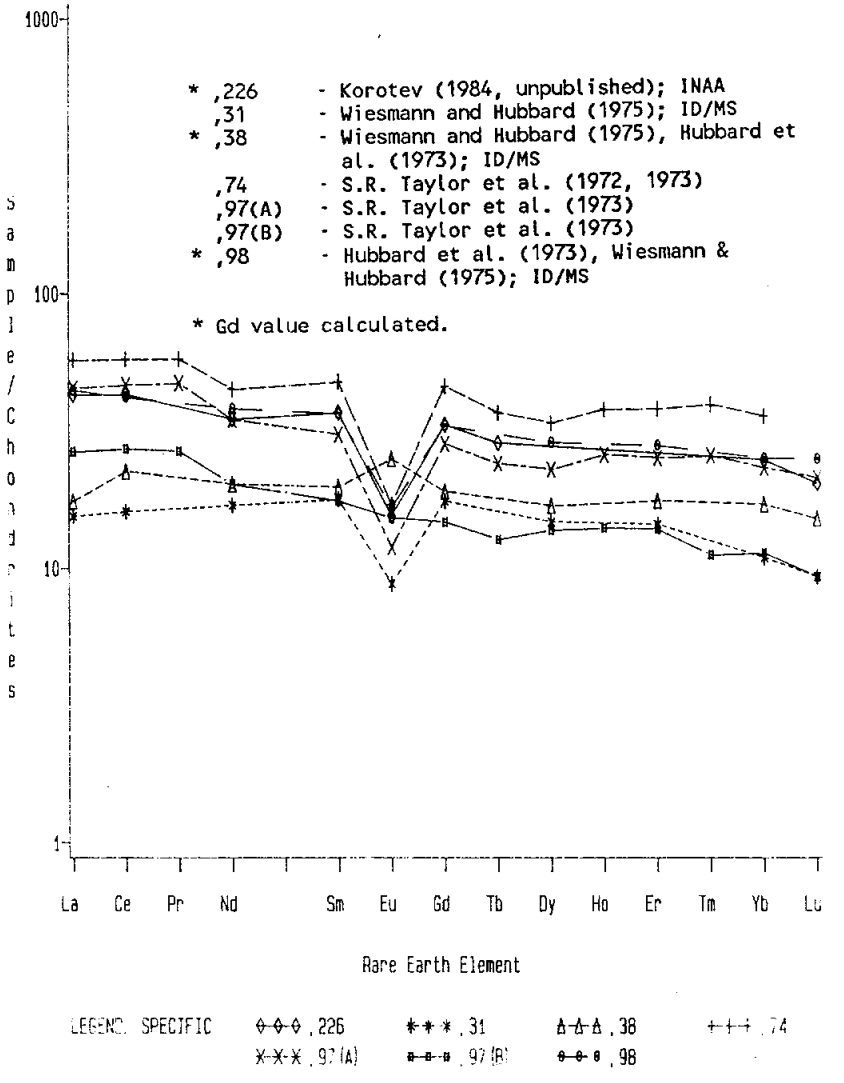

Figure 9. Rare earth elements in materials from 15459.

TABLE 15459-4. White clasts

		,36	,35	,38	,97
Wt %	SiO2	46.0			46.9
	TiO2	2.0a		1.7	0.32
	Al2O3	20.1			23.5
	FeO	7.9b			5.85
	MgO	14.6a		9.8	9.43
	CaO			12.5	13.7
	Na2O	0.38		0.73	0.41
	K2O			0.1046	0.08
	P2O5				
(ppm)	Sc	16			
	V				
	Cr	920			1640
	Mn	940			
	Co	19	20		
	Ni				
	Rb		0.27	1.69	0.78
	Sr			205.3	
	Y				30
	Zr	116c			
	Nb				
	Hf	2.97			1.6
	Ba			119.1	101
	Th				1.03
	U		0.420	0.35	0.29
	Pb				1.1
	La			5.80	8.8
	Ce			19.9	24.0
	Pr				3.0
	Nd			12.2	12.2
	Sm			3.60	3.2
	Eu	1.9		1.74	1.06
	Gd				3.7
	Tb	2.9			0.6
	Dy			5.37	4.4
	Ho				0.99
	Er			3.56	2.8
	Tm				0.34
	Yb			3.44	2.3
	Lu			0.523	0.32
	Li				
	Be				
	B				
	C				
	N				
	S				
	F				
	Cl				
	Br		0.048		
	Cu				
	Zn		2.1		
(ppb)	I				
	At				
	Ga				
	Ge		8.9		
	As				
	Se		50		
	Mo				
	Tc				
	Ru				
	Rh				
	Pd				
	Ag		0.48		
	Cd		7.8		
	In		0.63		
	Sn				120
	Sb		0.11		
	Te		6.4		
	Cs		100d		
	Ta	890			
	W				90
	Re		0.109		
	Os				
	Ir		2.2		
	Pt				
	Au		0.20		
	Hg				
	Tl		0.43		
	Bi		0.69		
		(4)	(11)	(13)(7)	(8)

For references and methods, see Table 15459-2.

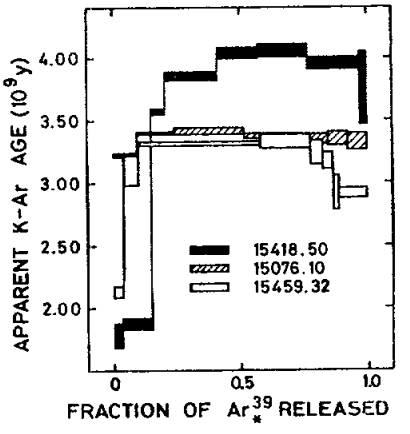

Figure 10. Ar release diagram (Stettler et al. 1973).

major element data are not complete enough to demonstrate whether the sample belongs to one of those two groups or to yet another. Wolf and Anders (1980) noted that it has "suspiciously high Ir, Re, Au and Ge contents, due either to its slight (<4%) contamination with matrix or to its mafic character." Hence they excluded the siderophile data from consideration with basalts in general.

The poikilitic clast chemistry is generally consistent with its mineralogy, including an Mg' of 75. The Ir content of 2.2 ppb suggests a meteoritic contribution. The rare-earth pattern, however, is quite unusual in having a positive Eu anomaly, and it is much flatter than a KREEP pattern. The other light clast analyzed by S.R. Taylor et al. (1973) has a pattern more like KREEP, but at low enough abundances to eliminate any significant Eu anomaly.

STABLE ISOTOPES: Friedman et al. (1972) reported hydrogen and carbon isotopic analyses for matrix and for a combination of the mare and poikilitic melt clasts (Table 5).

RADIOGENIC ISOTOPES AND GEOCHRONOLOGY: Stettler et al. (1973) determined a ^{40}Ar-^{39}Ar age of 3.33 ± 0.06 b.y. from the intermediate temperature release (Fig. 10). The release shows a high temperature drop-off. This age is the same as other Apollo 15 mare basalts.

Nyquist et al. (1972, 1973) reported whole rock Rb-Sr isotopic data for matrix (,98), mare basalt (,31), and the poikilitic clast (,38) (Table 6). The mare basalt data are consistent with a pyroxene-rich Apollo 15 mare basalt of 3.3 b.y. age. The light clast shows a very low $^{87}Sr/^{86}Sr$ ratio for its alumina content, quite different from most KREEP-rich impact melts.

EXPOSURE AND TRACKS: Stettler et al. (1973) determined a ^{38}Ar exposure age of 520 m.y. for the mare basalt sample. There is always a possibility that this basalt retains a record of exposure prior to incorporation into the breccia (see below). Keith et al. (1972) provided data on cosmogenic radionuclides (^{26}Al, ^{22}Na, ^{54}Mn, ^{56}Co, and ^{46}Sc). The ^{26}Al is saturated (Keith et al. 1972, Yokoyama et al. 1972), indicating an exposure of more than ~2 m.y. Track densities (Bhattacharya et al. 1975) for interior chips are in the range (6-20)x10^6 cm^{-2}, indicating a surface exposure age of less than 10 to 30 m.y.

McDougall et al. (1973) studied solar flare tracks in 15459, finding evidence for solar flare irradiation prior to breccia formation for the mare clast. The preservation of tracks in matrix olivines and their high densities in matrix plagioclases preclude heating above 400°C during the formation of the breccia.

PHYSICAL PROPERTIES: Collinson et al. (1972, 1973) reported magnetic data, including the effects of demagnetization, for two matrix splits (Fig. 11). 15459,95 is different from crystalline rocks in that it has no strong soft component, and a high inten-

TABLE 15459-5. H and C isotopes

	δD	$\delta^{13}C$
,100 matrix	-200	-25
,30 + ,37 comb.	-346	-22

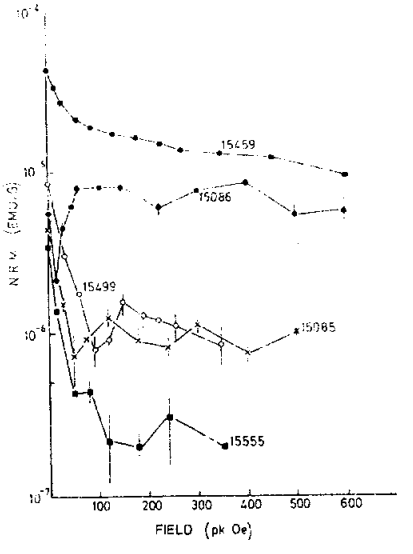

Alternating field demagnetization of Apollo 15 samples. Vertical bars indicate range of intensities obtained after repeated demagnetization.

Fig. 11a

Figure 11. Demagnetization of 15459 matrix samples (Collinson et al. 1973).

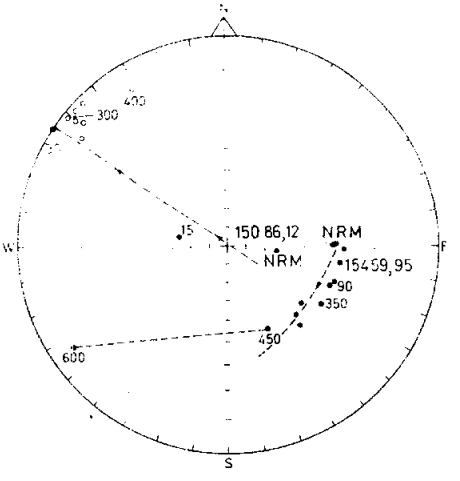

A.F. demagnetization of samples 15459,95 and 15086,12. The directions of NRM are referred to arbitrary axes in the rocks.

Fig. 11b

TABLE 15459-6. Rb-Sr isotopic data (Nyquist et al. 1973)

	Rb ppm	Sr ppm	$^{87}Rb/^{86}Sr$	$^{87}Sr/^{86}Sr$	T_{BABI} b.y.	T_{LUNI} b.y.
,98 matrix	3.76	129.5	0.0842 ± 10	0.70437 ± 14	4.37 ± .16	4.45 ± .16
,31 mare	0.697	54.9	0.0367 ± 6	0.70109 ± 6	3.80 ± .27	3.98 ± .27
,38 light clast	1.69	205.3	0.0239 ± 5	0.70067 ± 5	4.58 ± .24	4.86 ± .24

sity (10 x 10^{-6} emu/g) of hard NRM, stable above 100 Oe. Iron is the carrier (thermal demagnetization experiments). 15459 has a strong viscous remanent magnetism. The overall data are not inconsistent with the NRM being acquired by thermoremanence in a weak lunar field, but the detailed history is complicated. Brecher (1975, 1976) listed 15459 as a sample with an NRM showing directional change under demagnetization which is rotational in a plane, compatible with her model of "textural remanence". (In this model, the magnetic characters are produced by partial alignment of grain magnetic moments, not any ancient fields.)

Tittman et al. (1972) reported a Rayleigh wave (V_R) velocity of <1.95 km/sec parallel to fractures--this is a high value approaching that of synthetic basalts. Perpendicular to fractures, the V_R is much lower and shows steps reflecting the crossing of fractures (Fig. 12).

Chung and Westphal (1973) reported a density of 2.76 gm/cc, and tabulated and diagrammed (Fig. 13) electrical data. The electrical properties are typical of those for feldspar-rich lunar basalts.

Adams and McCord (1972) measured diffuse reflection spectra (0.35-2.5 m) to determine the wavelength position of the two crystal-field absorption bands for pyroxenes. The data is similar to some Apollo 14 breccias, and shows that on average 15459 has less calcic pyroxene (i.e., less augite) than mare basalts.

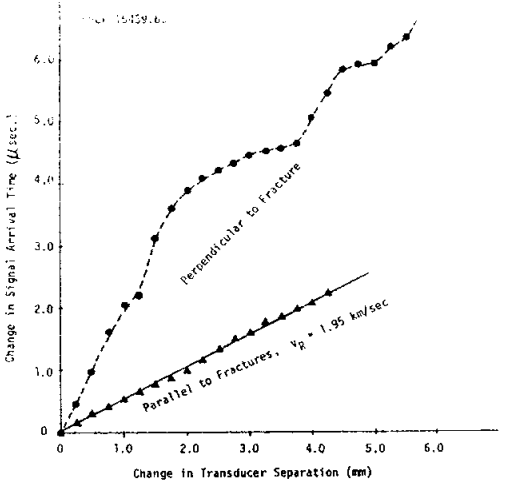

Sample data of change in signal arrival time versus change in transducer separation for rock 15459. The data were obtained by the impulse technique.[1] The reciprocal of the slope gives the Rayleigh wave group velocity.

Figure 12. V_R data for 15459 matrix (Tittman et al. 1972).

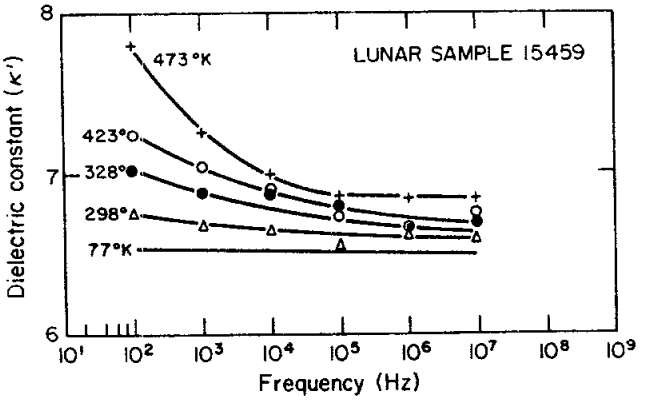

Dielectric constant of sample 15459,62 as a function of frequency and temperature.

3084

Fig. 13a

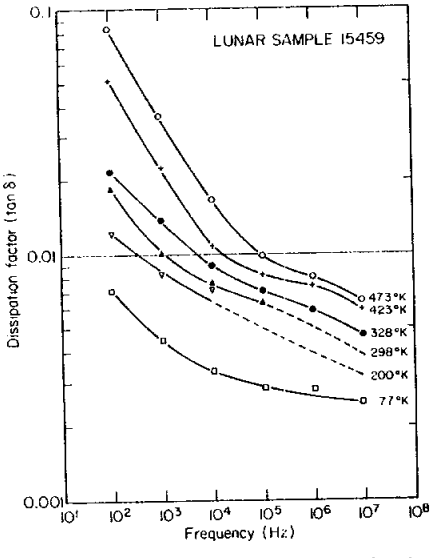

Dielectric losses in sample 15459,62 as a function of frequency and temperature.

Fig. 13b

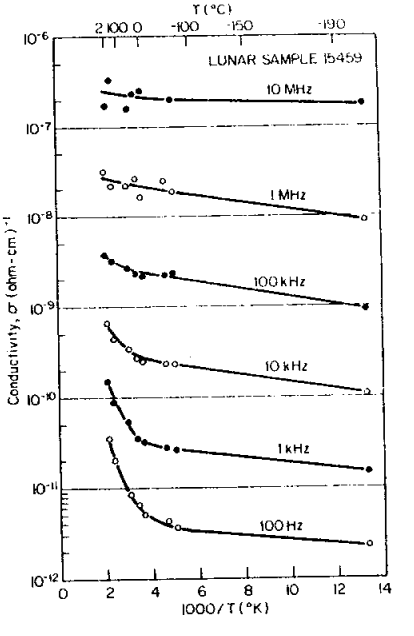

Electrical conductivity of sample 15459,62 as a function of frequency and temperature.

Fig. 13c

Figure 13. Electrical functions for 15459 matrix (Chung and Westphal 1973).

PROCESSING AND SUBDIVISIONS: Several small pieces were removed from 15459, including samples from the large mare basalt clast and the other large pale clast (Fig. 2). One piece ,6 (159.8 g) was removed from the west end and later was encapsulated for exhibition. A small piece was sawn off the west end and subdivided (Figs. 2, 14) and this cut was through the white clast. A later cut removed the west end (Fig. 2), which was numbered ,184 (1276 g) and placed in remote storage, and one of the other large pieces (,173, 85.6 g) removed in this operation also went for exhibition purposes. The main piece ,0 now has a mass of 3744 g.

Thin sections ,3; ,4, and ,13-,21 were made from ,2 (see Fig. 2). Thin sections ,122; ,124 and; ,224 sample the large mare basalt. Thin sections ,123 and ,125-,127 sample chips purportedly from the large white clast, contain matrix, poikilitic melt and (at least ,125) coarse norite. ,225 sampled the same white clast and appears to be of the poikilitic impact melt.

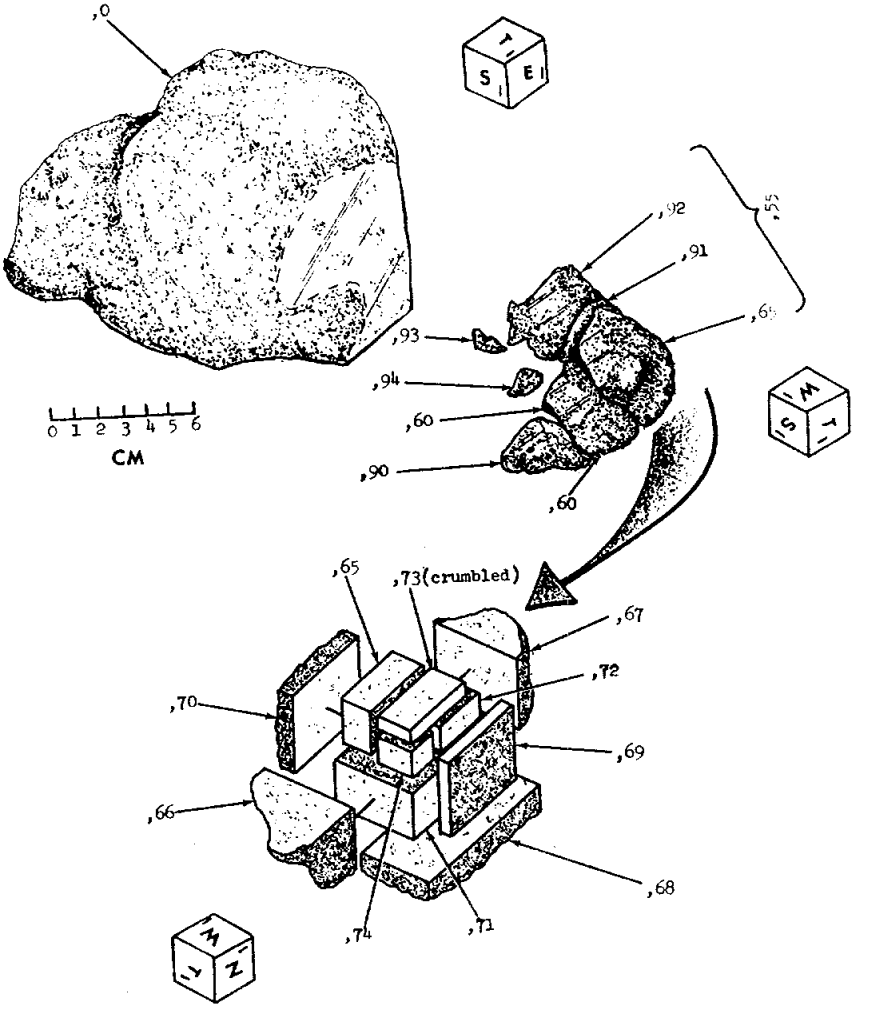

Figure 14. Initial sawing of 15459; several large chips had already been removed.

15465 GLASS WITH REGOLITH BRECCIA CLASTS ST. 7 376.0 g

INTRODUCTION: 15465 consists of a vesicular dark glass enclosing several pieces of regolith breccias (Figs. 1, 2), although most studies have referred to it as a glass-coated regolith breccia. The sample was first studied in a Consortium led by Haskin; the Consortium sample was ,7 which was mainly a large piece of a dominant regolith breccia clast (Fig. 2). The glass (hence rock formation age) is about 1.1 b.y. old (Husain, 1972). At least one individual clast is a chemically pristine highlands igneous fragment.

15465 is blocky and angular, and tough with delicate protrusions. The glass is a dark greenish-gray; the breccias are medium light gray. The surface is rough and hackly, and one block of breccia has many zap pits on one side, but the glass has no zap pits. 15465 was collected with 15466 just inside the north-northwest rim of Spur Crater.

Figure 1. Pre-split view of heterogeneous sample 15465. S-71-46427

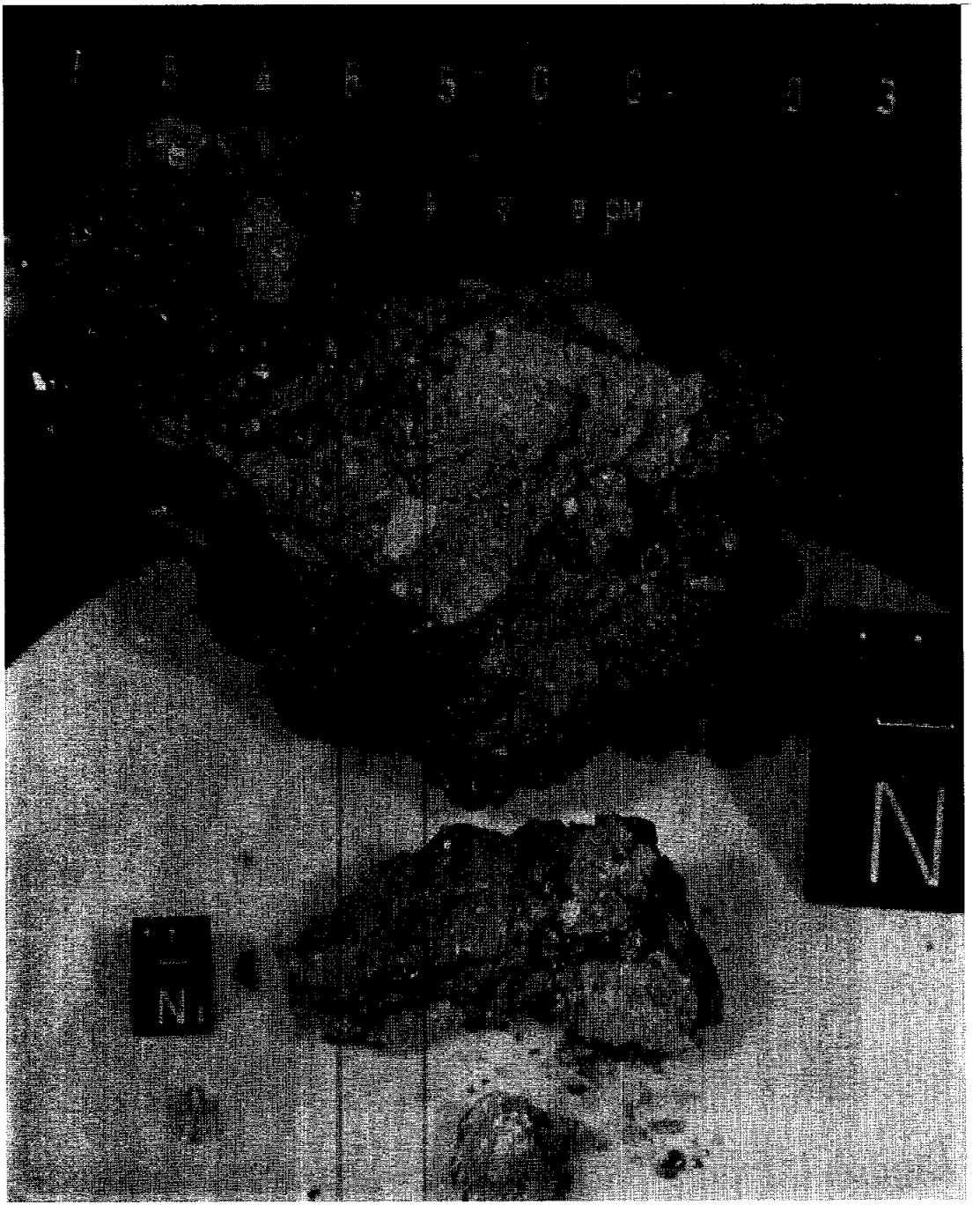

Figure 2. Post-split view, showing ,7 in foreground. S-71-60707

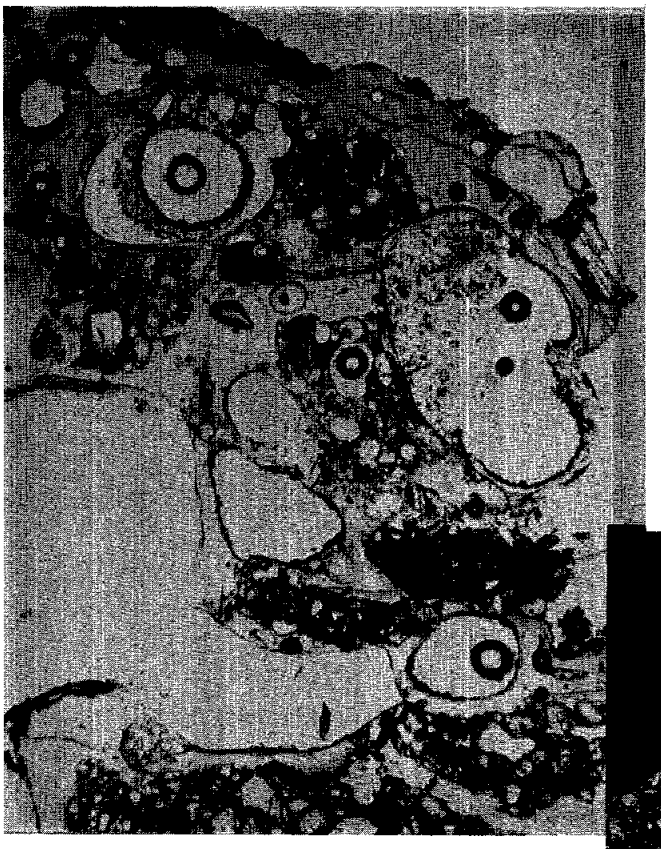

Fig. 3a

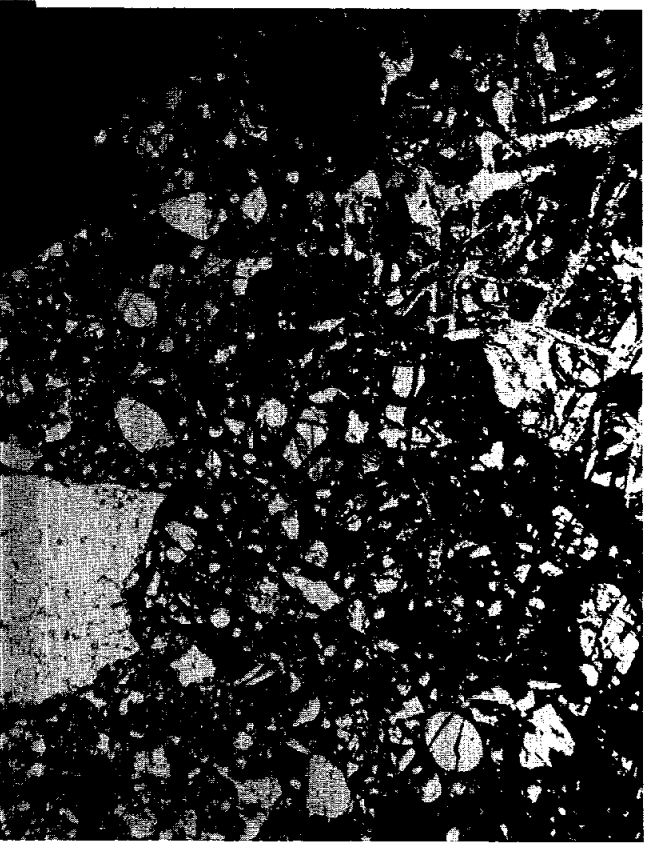

Fig. 3b

Figure 3. Photomicrographs of 15465. a) ,28, vesicular glass with small regolith breccia clasts. Transmitted light. width about 2 mm. b) ,28, regolith breccia fragment, showing dark glass fragment (upper left), KREEP basalt with conspicuous yellow/orange mesostasis (upper right), and glass spheres, etc. Transmitted light. Width about 2 mm. c) ,63 Clast ,59c of Warren and Wasson (1978) with two mafic grains (white, fractured) and plagioclase. Partly crossed polarizers. Widths about 800 microns. d) ,28, white cataclastic fragment, with some mafic grains (whitest). Transmitted light. Width about 2 mm.

Fig. 3c

Fig. 3d

PETROLOGY: 15465 has two dominant componets: vesicular glass, and regolith breccias (Figs. 3a, b). The glass appears to be the dominant component and engulfs the fragments of regolith breccias (Fig. 1), although the relationship has been frequently referred to as glass coating a breccia, including the Lunar Sample Information Catalog Apollo 15 (1971). Most petrographic reports (Delano, 1972; Cameron and Delano, 1973; Winzer, 1978) are of regolith breccia fragments.

The vesicular glass is greenish and has large clear patches (Fig. 3a). Faint flow-banding is present. The glass engulfs regolith breccias in varied stages of disaggregation; small fragments of breccia are well-disaggregated. Winzer et al. (1978) included 15465 in a study of glass coats on Apollo 15 breccias, but reported no data.

The regolith breccias are not identical, but there is a preponderance of porous breccias with prominent KREEP basalt fragments and yellow glass spheres along with their contingent of other glass, mineral, and lithic fragments. Delano (1972) and Cameron and Delano (1973) studied and analyzed 23 one-to-five millimeter chips from the Haskin Consortium sample ,7 (Fig. 2), which are brown glass matrix breccias (regolith breccias) and vesicular dark green glass described as splash glass. The breccias contain 5-10% rock fragments, 5-10% glass spheres and shards, 60-70% plagioclase fragments, 10-20% low-Ca pyroxene, and 5% high-Ca pyroxene. The matrices are composed of fine particles of brown glass. Of the rock fragments, 42.5% were KREEP basalts, with subophitic textures (referred to by Delano, 1972, as highland basalt) and a mineralogy like other KREEP basalts (Fig. 4). Recrystallized norites (with 19-26% Al_2O_3) composed 25% of the samples, mare basalts (many similar to 15555) composed 20% of the sample, and other lithologies (such as anorthosite, recrystallized polymict breccias, and shocked-igneous fragments) composed the remainder. Delano (1972) observed two types of mare basalt, one with poikilitic plagioclase, the other with porphyritic pyroxenes. (Remarkably, thin sections from other chips of the rock appear to lack mare basalt fragments.) The recrystallized norites have more calcic pyroxenes than the KREEP basalts (Fig. 4). Winzer (1978) described and analyzed several and varied lithic clasts in regolith breccia fragments, including apparent KREEP basalt fragments (clasts 8 and 9), inpact melt, and one fragment of a poikilitic cristobalite enclosing small ilmenites. McKay et al. (1974) found the Is/FeO ratio of a regolith breccia to be only 12, indicating a very immature regolith.

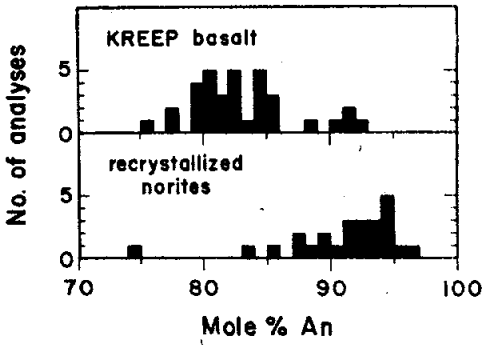

Plagioclase compositions from fifteen KREEP basalt fragments and nine recrystallized noritic fragments in 15465,7. No more than three analyses from any one rock fragment.

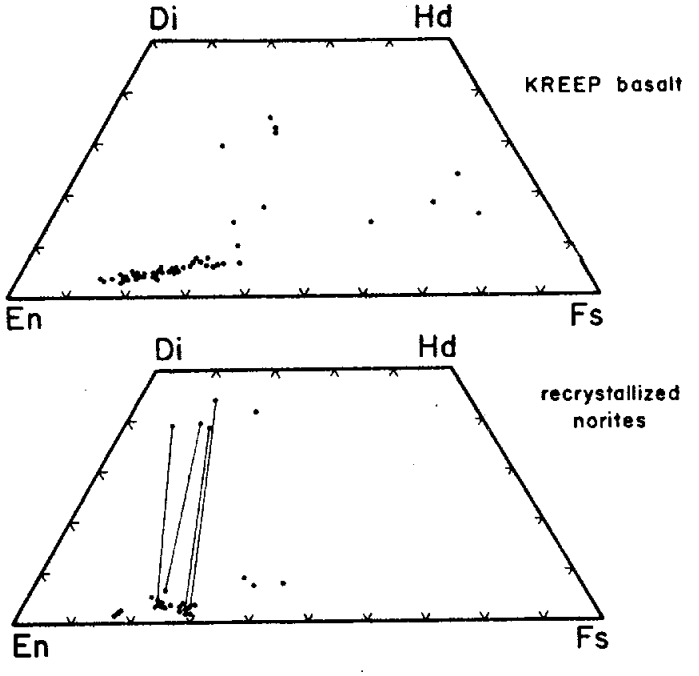

Pyroxene compositions from fifteen KREEP basalt fragments and nine recrystallized noritic fragments in 15465,7. Compositions are plotted in terms of mole proportions of Ca, Mg, and Fe. No more than four analyses from any one rock fragment. Tielines connect coexisting Ca-rich and Ca-poor pyroxenes in four recrystallized noritic fragments.

Figure 4. Compositions of minerals in KREEP basalt and recrystallized norite clast (Cameron and Delano, 1973).

Colorless, green, yellow, and rarely red/orange glass are present in 15465 regolith breccia fragments, and in some the proportion of yellow glass is high compared with many other regolith breccias. Delano (1972) found two groups of glass--emerald green similar to other Apollo 15 green glasses, and a high-K glass, which appears to be the host glass of the sample. Winzer (1978) mentions a green glass in 15465 with euhedral to subhedral crystals of olivine (Fo_{76}), which appears to have crystallized slowly.

Warren and Wasson (1978) described an anorthosite (,56c) which is pristine, but no thin sections are known to exist. A second clast ,59c, was described macroscopically as"plag-rich....cataclastic gabbro with original texture still intact." (Lunar Sample Information Catalog Apollo 15, 1972). Thin sections show it to be a cataclastic norite (Fig. 2c), rather fine-grained, without obvious relics or clasts. It has 65% plagioclase (An_{94-95}) and 30% unexsolved orthopyroxene (En_{79-82},$Wo_{2.4-3.7}$), 1-2% of a silica mineral, about 1% Ca-pyroxene, traces of rutile, and spinel. The sample may be pristine (Warren and Wasson, 1978). Another white clast in ,13 (e.g., thin sections ,28, Fig. 2d) is identified in the 15465 Data Pack as being the ,56c of Warren and Wasson (1978), but ,56c was apparently enclosed in glass; the white clast in ,28 (etc.) is enclosed in regolith breccia. This clast however is a plagioclase-rich, fine-grained highlands lithology, containing some mafic mineral grains.

Drever et al. (1973) studied radiate texture in a clast in 15465,29, but provided no information.

CHEMISTRY: Analyses of glass and bulk rock, of regolith breccias, and of clasts other than regolith breccias are listed in Table 1 to 3 respectively, and rare earth elements plotted in Figures 5 to 7, respectively. The glass and the regolith breccias are fairly similar in major elements, suggesting that the breccias were formed in a regolith from which the glass was also later made by impact. However, some of the regolith breccia analyses have higher rare earth element abundances. Analyses by Ehmann et al. (1975), Ali et al. (1976) and Stroube et al. (1977) have differences, albeit small, even though from the same splits and the same lab. Ali et al. (1976) had suggested that the glass and the breccia were different, for instance Cl was enriched in the glass. However, according to Stroube et al. (1977) that

TABLE 15465-1. Chemical analyses of glass and bulk rock of 15465

		,16(a)	,16	,16	,15	,15	,15	,46	,47	,47	,7,3	,0
wt %	SiO2										47.4	
	TiO2	1.1	1.1		1.1	1.1	1.4				1.40	
	Al2O3	17.8	17.8		15.1	14.9	15.9				17.0	
	FeO	12.9	11.5	11.5	11.9						11.4	
	MgO				10.2	10.0	11.1				10.5	
	CaO	6.9	10.4		10.2	10.3	11.5				12.1	
	Na2O	0.49	0.49	0.49	0.44						0.39	
	K2O			0.25	0.19						0.28	0.281
	P2O5											
(ppm)	Sc		23	22	22							
	V	54	53		71	77	78					
	Cr	2530(b)	2000	2300	2300							
	Mn	1200	1200		1300	1230	1320					
	Co	45	40									
	Ni											
	Rb											
	Sr											
	Y											
	Zr											
	Nb											
	Hf		8.3									
	Ba			280	220							
	Th		6.6									5.9
	U											1.46
	Pb											
	La			27	23							
	Ce											
	Pr											
	Nd											
	Sm			12	12							
	Eu		1.4	1.3	1.3							
	Tb											
	Dy											
	Ho											
	Er											
	Tm											
	Yb	9.8		7.2	6.8							
	Lu				1.08							
	Li											
	Be											
	B											
	C											
	N											
	S											
	F								>48, <53			
	Cl	146										
	Br											
	Cu											
	Zn									5.77		
(ppb)	I											
	At											
	Ga											
	Ge											
	As											
	Se											
	Mo											
	Tc											
	Ru							11				
	Rh											
	Pd											
	Ag											
	Cd											
	In											
	Sn											
	Sb											
	Te											
	Cs											
	Ta											
	W											
	Re											
	Os							13				
	Ir											
	Pt											
	Au											
	Hg									4.3		
	Tl											
	Bi											
		(1)	(2)	(2)	(2)	(2)	(2)	(3)	(4)	(5)	(6)	(7)

References and methods:

(1) Ali et al. (1976); INAA
(2) Stroube et al. (1977); INAA
(3) Jovanovic and Reed (1976); INAA
(4) Jovanovic and Reed (1977); INAA
(5) Reed et al. (1977); INAA
(6) Cameron and Delano (1973); microprobe
(7) Keith et al. (1972): gamma ray spectroscopy

Notes:

(a) apparently superceded by Stroube et al. (1977) in next column
(b) incorrectly reported as 2.53%

TABLE 15465-2. Chemical analyses of regolith breccia clasts in 15465

		,89	,16	,16(c)	,7	,11	,15	,16(c)	,47	,47	,47
wt %	SiO2		48.6								
	TiO2			1.22	1.38		0.99	1.22			
	Al2O3		16.3	15.0	16.3		15.9	15.0			
	FeO	11.7	11.6	10.2	11.2		11.7	11.1			
	MgO		19.1(a)		10.1		10.5				
	CaO	10.5	<6	10.4	10.9		11.6	10.6			
	Na2O	0.61	0.57	0.58	0.57		0.467	0.58			
	K2O						0.204				
	P2O5										
(ppm)	Sc	22.9		20	24.6		22				
	V			66			69	66			
	Cr	2280		1700	2690		2200	2090(b)			
	Mn		1250	1320	1200		1260	1300			
	Co	30			33.7		39	34			
	Ni	106			108						
	Rb										
	Sr	140			120						
	Y										
	Zr	530									
	Nb										
	Hf	14.8		10.8	14.8						
	Ba	417			450		220				
	Th	6.3									
	U	1.76									
	Pb										
	La	40.4			38.2		23				
	Ce	106			90						
	Pr										
	Nd	61			62						
	Sm	18.5			17.7		12				
	Eu	1.80		1.4	1.75		1.2				
	Gd										
	Tb	3.70			3.59						
	Dy										
	Ho										
	Er										
	Tm										
	Yb	12.6		11.4	12.0		6.8	11.4			
	Lu	1.76			1.72		1.05				
	Li										
	Be										
	B										
	C					45					
	N										
	S										
	F									41.8	
	Cl							76			
	Br										
	Cu										
	Zn										14
(ppb)	I										
	At										
	Ga										
	Ge										
	As										
	Se										
	Mo										
	Tc										
	Ru								3.7		
	Rh										
	Pd										
	Ag										
	Cd										
	In										
	Sn										
	Sb										
	Te										
	Cs	380			380						
	Ta	1680									
	W										
	Re										
	Os								6.6		
	Ir	2.7									
	Pt										
	Au	1.2									
	Hg										
	Tl										2.99
	Bi										
		(1)	(2)	(3)	(4)	(5)	(6)	(3)	(7)	(8)	(9)

References and methods:

(1) Korotev (1984 unpublished); INAA
(2) Ehmann et al. (1975); INAA
(3) Stroube et al. (1977); INAA
(4) Blanchard (1973 unpublished); INAA
(5) Moore et al. (1973); combustion, gas chromotography
(6) Ali et al. (1976); INAA
(7) Jovanovic and Reed (1976); INAA
(8) Jovanovic and Reed (1977); INAA
(9) Reed et al. (1977); INAA

Notes.

(a) unrealistically high
(b) listed erroneously as 2.09%
(c) probably revisions of a single analysis

TABLE 15465-3. Chemical analyses of non-regolith breccia clasts in 15465

		,56	,59
Wt %	SiO2	44.3	48.8
	TiO2	0.27	0.32
	Al2O3	34.0	21.9
	FeO	1.5	5.2
	MgO	0.83	10.54
	CaO	19.3	13.3
	Na2O	0.342	0.350
	K2O	0.022	0.097
	P2O5		
(ppm)	Sc	1.9	9.9
	V		
	Cr		1740
	Mn	110	59
	Co	7.5	15.5
	Ni	<4	110
	Rb		
	Sr		
	Y		
	Zr		
	Nb		
	Hf		2.4
	Ba		110
	Th		1.23
	U		0.35
	Pb		
	La	0.61	7.3
	Ce		21
	Pr		
	Nd		
	Sm	0.26	3.04
	Eu	0.8	0.99
	Gd		
	Tb		0.71
	Dy		
	Ho		
	Er		
	Tm		
	Yb		2.4
	Lu		0.36
	Li		
	Be		
	B		
	C		
	N		
	S		
	F		
	Cl		
	Br		
	Cu		
	Zn	0.98	10.2
(ppb)	I		
	At		
	Ga	4050	5710
	Ge	53	80
	As		
	Se		
	Mo		
	Tc		
	Ru		
	Rh		
	Pd		
	Ag		
	Cd	3.8	62
	In	0.34	<40
	Sn		
	Sb		
	Te		
	Cs		
	Ta		220
	W		
	Re		1.2
	Os		
	Ir	0.090	5.9
	Pt		
	Au	0.056	0.76
	Hg		
	Tl		
	Bi		
		(1)	(1)

References and methods:

(1) Warren and Wasson (1978); INAA

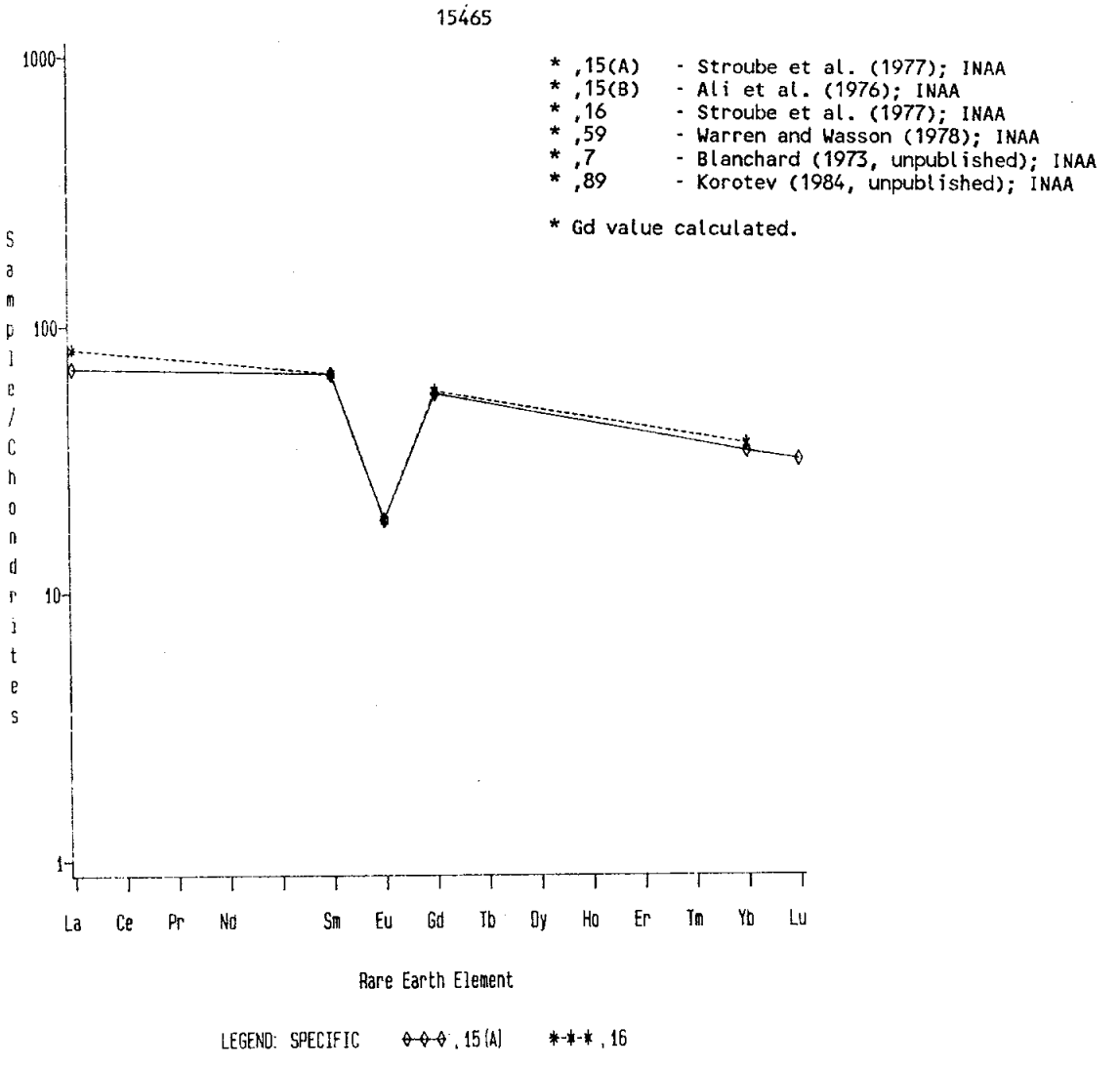

Figure 5. Rare earths in vesicular glass in 15465.

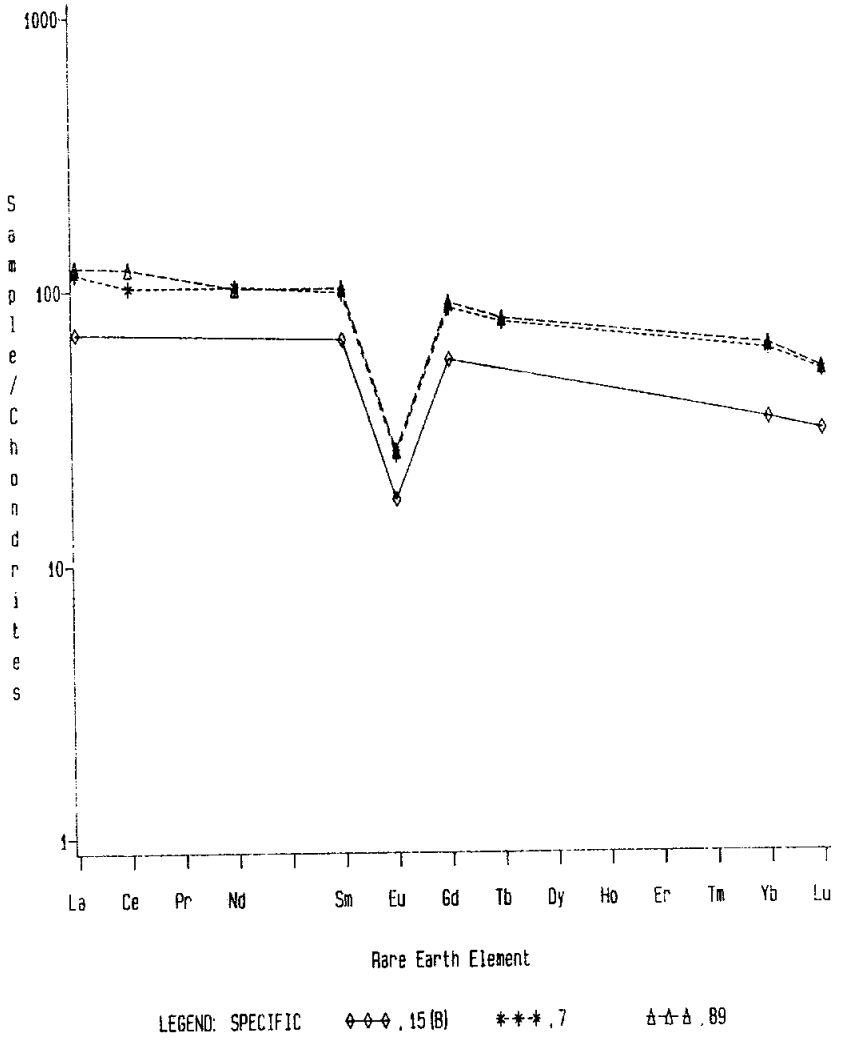

Figure 6. Rare earths in regolith breccia fragments in 15465.

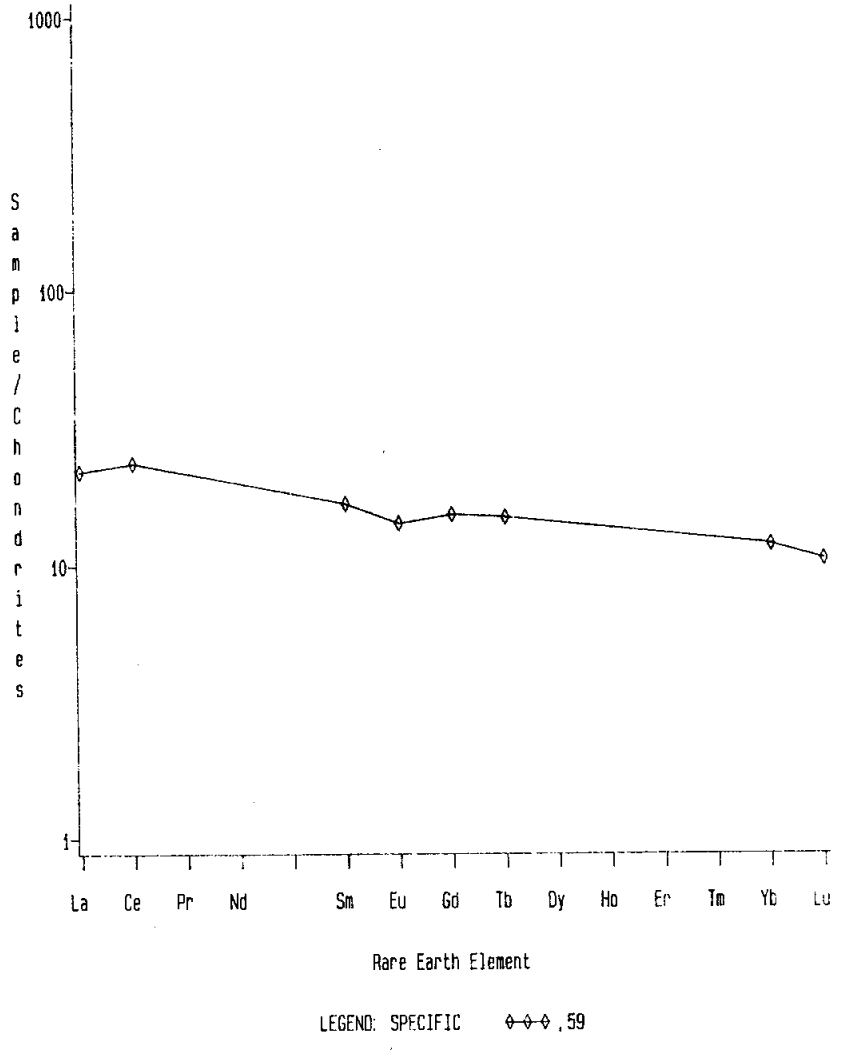

Figure 7. Rare earths in feldspathic clasts.

conclusion was erroneous and based on preliminary data for Cr and Ca. Jovanovic and Reed (1976, 1977) made some of their elemental analyses on leaches and residues; these are combined as a single bulk analysis in the Tables. The Moore et al. (1973) carbon value of 45 ppm for a regolith breccia sample is higher than basalts, but not as high as most fines (regolith) samples.

Warren and Wasson (1978) determined, mainly on the basis of incompatible and siderophile elements (Table 3), that clast ,56c, an anorthositic fragment, was a pristine igneous lithology, and that ,59c, a more noritic fragment, might have been a pristine igneous sample. However, the latter had rare earths with the KREEP pattern, and the high siderophiles were not easily explicable as merely matrix contamination.

STABLE ISOTOPES: Clayton et al. (1973) determined δO^{18} (°/oo) of 5.66 for whole rock (= regolith breccia?), 5.80 for glass, and 5.69 for a plagioclase, in separates from ,7, the Consortium sample. These values are not unusual for lunar samples.

RADIOGENIC ISOTOPES AND GEOCHRONOLOGY: Husain (1973) derived a minimum age of 1.09 ± 0.14 b.y. from a complex gas release (^{40}Ar-^{39}Ar method) for a glass sample (referred to as surface glass). They suggested this age to represent that of Aristillus or Autolycus. Schaeffer et al. (1976) and Plieninger and Schaeffer (1976) conducted a laser probe Ar study on interior breccia fragments from 15465. They found widely varied solar wind ^{36}Ar in different pieces, indicating that rock formation was not accompanied by appreciable redistribution of argon in the breccias; hence the original ages of constituents can be measured. A 3-isotope plot (Fig. 8) gives two distinct lines, one representing an age of 3.91 ± 0.04 b.y., the other an age of 1.9 ± 0.1 b.y. The latter is from basalt (stated to be mare basalts) and feldspar clasts. Some of the basalts, with a K-rich mesostasis, give individual ages of 1.0 ± 0.5 b.y., the same as rock formation. These "young" basalts are puzzling, requiring either young volcanism or uniform degassing around the time of 15465 formation. The 3.9 b.y. age represents highland basalts (=KREEP basalts), recrystallized norites, dark green glass spheres, other glass, and the groundmass (matrix) itself. The varied components make it not surprising that bulk breccia stepwide heating did not give a plateau (Husain, personal communication in Plieninger and Schaeffer, 1976). Plieninger and Schaeffer (1976) interpreted the 3.91 b.y. components to have been degassed during the Imbrium event.

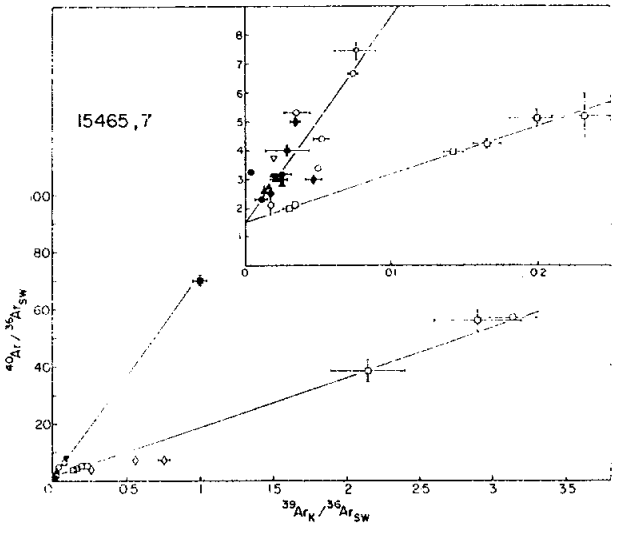

Three isotope plot of $^{40}Ar/^{36}Ar_{sw}$ against $^{39}Ar_K/^{36}Ar_{sw}$. The slopes of the two lines are used to determine the $^{40}Ar/^{36}Ar$ ratios in the presence of trapped ^{40}Ar. Symbols: ○ mare basalts, □ highland basalts, ● glass spherules, ▼ noritic clasts, ▲ groundmass, ◆ feldspar crystal clasts, ◇ K-rich basalts, and ○ glass fragments. The error bars represent the errors in the ^{40}Ar and ^{39}Ar measurements. Errors in the ^{36}Ar values used for normalization do not contribute to the errors in the best-fit lines which determine $^{40}Ar/^{36}Ar$ ratios.

Figure 8. 3-isotope argon plot for components of 15465 (Plieninger and Schaeffer, 1976).

EXPOSURE: Keith et al. (1972) provided disintegration count data for ^{26}Al, ^{22}Na, ^{54}Mn, ^{56}Co, and ^{46}Sc. According to Yokoyama et al. (1974) the ^{26}Al is a saturated value, indicating an exposure of more than about 2 m.y.

PROCESSING AND SUBDIVISIONS: Several pieces were originally chipped from ,0, including the Consortium Sample ,7 (Fig. 2, 9). Several thin sections were obtained from ,1; ,13; and ,17. (,1

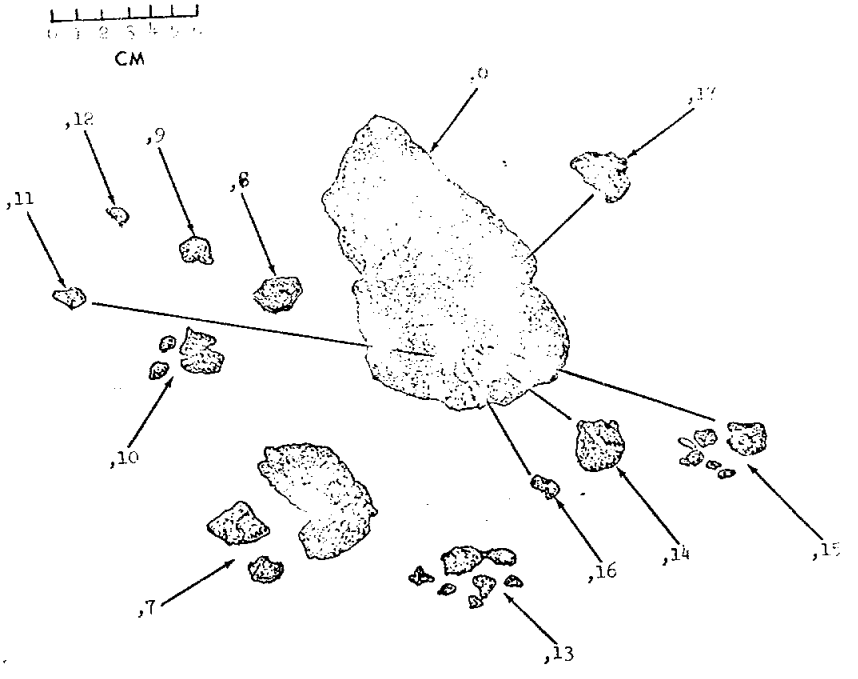

Figure 9. Original chipping of 15465.

had originally been numbered 15469 but was found to have broken off 15465 in transit.) Thin sections were cut from chip ,52 which was a granddaughter of ,9. Later chipping was done (Fig. 10) to acquire glass and interior chips, and a thin section was made from ,91, a daughter of ,44. Subsequently, more chipping acquired white clast material (,56; ,59; and ,61) and more thin sections were made. Most of the subdivisions of ,7, including the thin sections studied by Delano and Cameron, have not been documented.

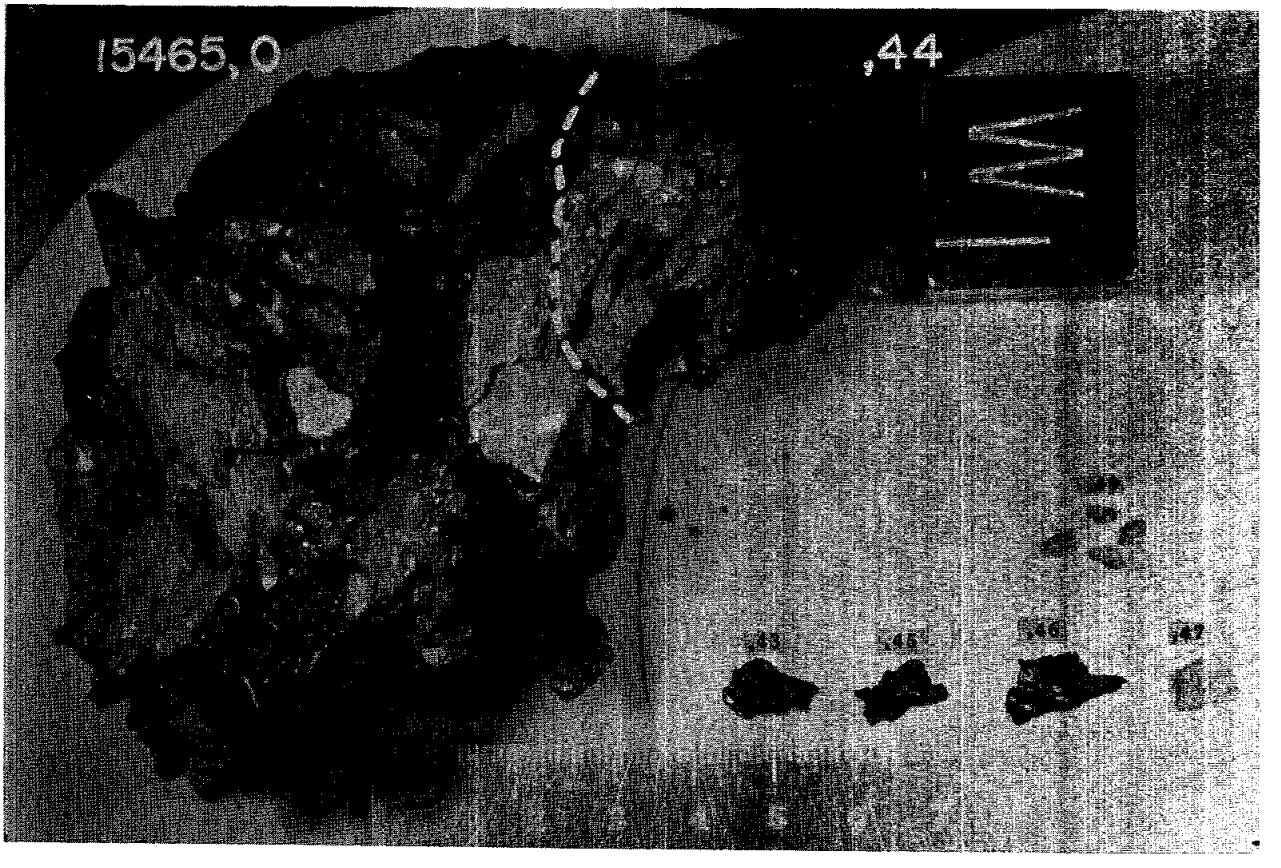

Figure 10. Origin of 15465,44 and smaller pieces. S-75-34267

15466 GLASS WITH REGOLITH BRECCIA CLASTS ST. 7 119.2 g

INTRODUCTION: 15466 is a vesicular glass with both chilled and broken surfaces. It contains numerous sharp-boundaried clasts which are mainly glassy regolith breccias (Fig. 1), and the rock is heterogeneous and tough. The glass is olive-gray and constitutes perhaps 90% of the rock. A few zap pits occur on one side ("S"). 15466 was collected with 15465 just inside the north-northwest rim crest of Spur Crater; the local surface is rather blocky.

PETROLOGY: 15466 consists largely of vesicular glass containing breccia clasts (Fig. 1). Macroscopically there appeared to be two types of breccia; the predominant one contained visible mare basalt clasts, the other contained none. Thin sections appear to support such a dichotomy. The breccias are regolith breccias containing glass spheres, shards, and lapilli, mineral fragments, and lithic fragments in opaque, glassy matrices (Fig. 2). Yellow glass spheres and shards are particularly prominent in thin sections from the chip ,4, and red glass is also present, whereas mare basalt debris appears to be absent. In contrast, thin sections from chip ,25 contain abundant coarse mineral fragments and basalt clasts, but yellow glass is rare to absent. The breccias are generally porous, but where engulfed in glass are locally sintered up to several millimeters from the glass (Fig. 2d).

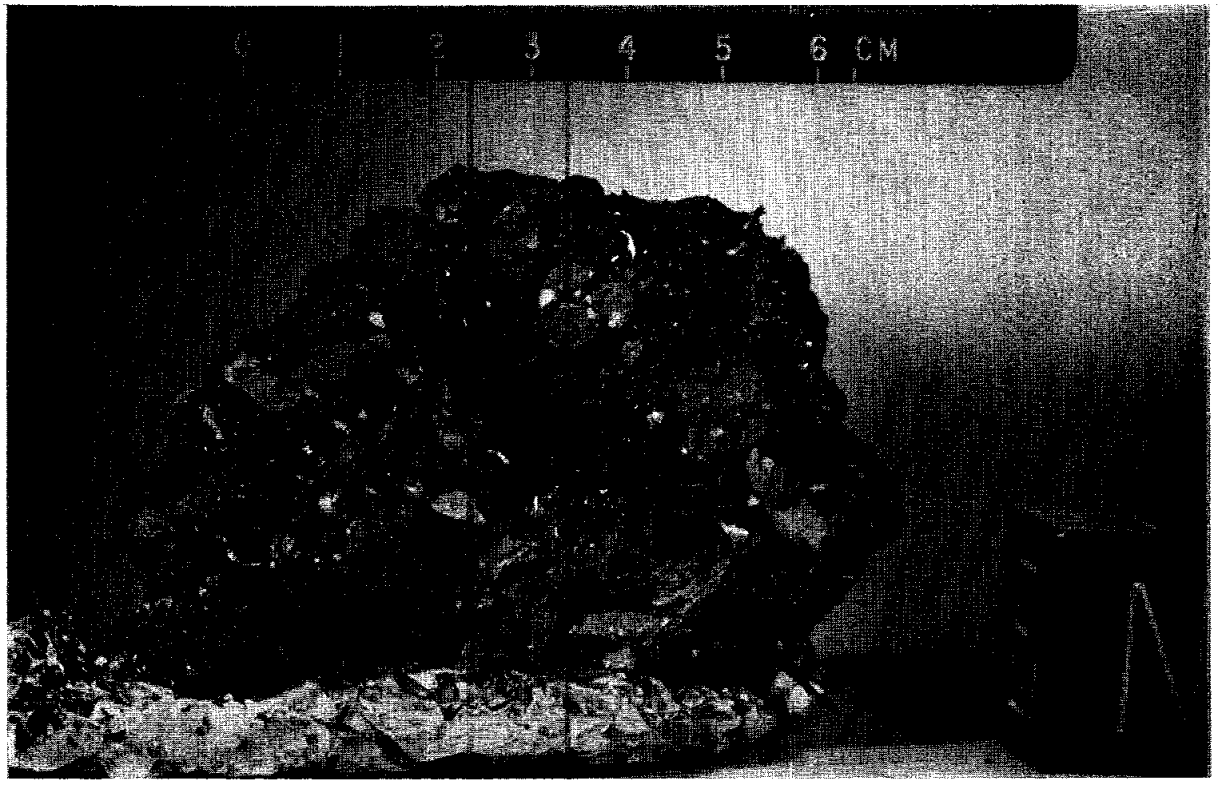

Figure 1. Pre-split view of 15466. S-71-46769

Fig. 2a

Fig. 2b

Figure 2 Photomicrographs of 15466. All transmitted light except d), reflected light. all widths 2 mm. a) 15466,9, showing dense regolith breccia with glass spheres and lithic (crystalline breccia) fragments, left, and vesicular glass host, right. b) 15466,9, showing dense matrix, glass spheres, and a large flow-structured glass fragment (lower left); c) 15466,28, showing large noritic fragment (upper left), and several mare basalt fragments (lower) in a regolith breccia matrix; d) 15466,9, showing high porosity away from glass (left), and low porosity towards glass (off to right).

Fig. 2c

Fig. 2d

Winzer et al. (1978), in a comparative study of glass coats, described the vesicular glass as a coat, and breccia fragments as the host breccia; this is incorrect. They also noted that the glass has a flow structure, very round vesicles, and droplets of iron metal/sulfide. They analyzed the glass with an energy-dispersive method (Table 1). Winzer (1977, 1978) described and analyzed (SEM/EDS) components of 15466, including green glass spheres, mineral fragments, impact melts, "ANT"-suite fragments, and including area scan (bulk) analyses of lithic clasts. Best and Minkin (1972) analyzed glass fragments and spheres, including green glasses ("peridotite") but did not specifically identify analyses from 15466.

CHEMISTRY: Little chemical work has been done on 15466, apart from the SEM/EDS data reported by Winzer (1977, 1978) and Winzer et al. (1978); that available is listed in Table 2. ,1 is a regolith breccia, but ,3 was dominantly glass, accounting for the gross differences in the carbon contents, which is not remarked on by the authors. The bulk rock (,0) gamma ray analysis has a K_2O content similar to that of the glass as analyzed by Winzer et al. (1978).

EXPOSURE: Keith et al. (1972) reported cosmogenic nuclide disintegration count data (^{26}Al, ^{22}Na, ^{54}Mn, ^{56}Co, ^{46}Sc); Yokoyama et al. (1974) were undecided as to whether the ^{26}Al was saturated or not.

TABLE 15466-1. SEM/EDS analysis of glass coat (Winzer et al., 1978)

%	SiO2	45.98 ± .39
	TiO2	1.42 ± .10
	Al2O3	17.15 ± .23
	FeO	11.41 ± .20
	MgO	11.51 ± .20
	CaO	11.12 ± .21
	Na2O	0.76 ± .27
	K2O	0.16 ± .07
ppm	Cr	2470 ± 550

TABLE 15466-2. Bulk rock chemical analyses

		,0	,3	,1
Wt %	SiO2			
	TiO2			
	Al2O3			
	FeO			
	MgO			
	CaO			
	Na2O			
	K2O	0.187		
	P2O5			
(ppm)	Sc			
	V			
	Cr			
	Mn			
	Co			
	Ni			
	Rb			
	Sr			
	Y			
	Zr			
	Nb			
	Hf			
	Ba			
	Th	3.5		
	U	0.86		
	Pb			
	La			
	Ce			
	Pr			
	Nd			
	Sm			
	Eu			
	Gd			
	Tb			
	Dy			
	Ho			
	Er			
	Tm			
	Yb			
	Lu			
	Li			
	Be			
	B			
	C		6.1	210
	N			
	S			
	F			
	Cl			
	Br			
	Cu			
	Zn			
(ppb)	I			
	At			
	Ga			
	Ge			
	As			
	Se			
	Mo			
	Tc			
	Ru			
	Rh			
	Pd			
	Ag			
	Cd			
	In			
	Sn			
	Sb			
	Te			
	Cs			
	Ta			
	W			
	Re			
	Os			
	Ir			
	Pt			
	Au			
	Hg			
	Tl			
	Bi			
		(1)	(2)	(3)

References and methods:

(1) Keith et al. (1972); gamma ray spectroscopy
(2) Modzeleski et al. (1972); vacuum pyrolysis, mass spectrometry
(3) Moore et al. (1972); pyrolysis, gas chromotography

PROCESSING AND SUBDIVISIONS: 15466 was split as shown in Figure 3. Chips ,1; ,2; and ,3 are small pieces from the pile in front, and ,4 is the chip between the two large fragments. ,0 consists of the two large pieces and most of the visible fines, and now has a mass of 110.35 g. Thin sections ,9; ,13; and ,14 were made from potted butt ,4. Thin section ,22 was made from a small piece of ,3 which was a small breccia fragment engulfed in glass. Thin sections ,27 and ,28 were made from chip ,25, which was taken with ,24 from the breccia clast shown by the arrow in Figure 3.

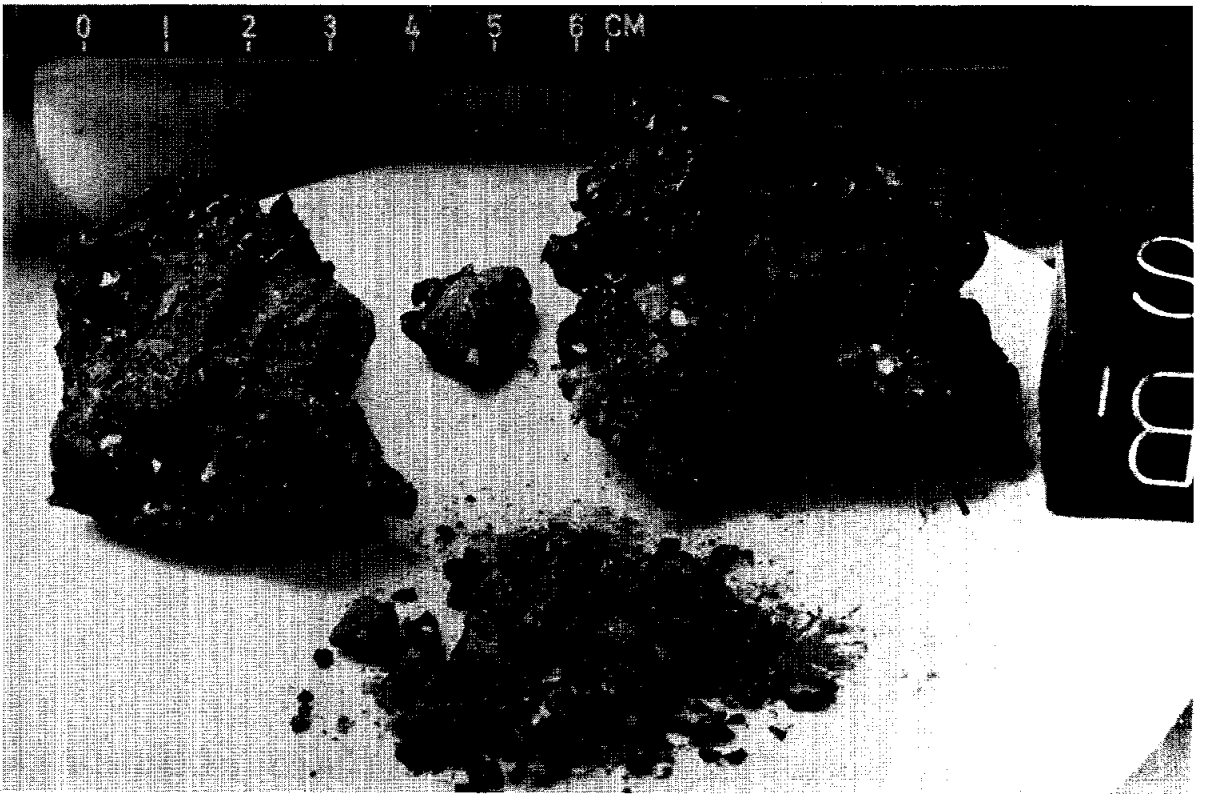

Figure 3. Post-chipping of 15466. S-72-15091

15467 REGOLITH BRECCIA/GLASS ST. 7 1.1 g

INTRODUCTION: 15467 is dominantly a regolith breccia, with vesicular glass cutting through it (Fig. 1). It is blocky, angular, and coherent. The breccia is medium gray and the glass is grayish black macroscopically. Its surface is irregular, and has no zap pits. 15467 was retrieved from the same bag as 15465 and 15466, hence was collected with them just inside the north-northwest rim crest of Spur Crater and may well have once been part of one of them.

PETROLOGY: The glassy regolith breccia contains glass balls, numerous mineral fragments, and conspicuous KREEP basalt fragments (Fig. 2). The glasses include minor amounts of red glass, but are mainly green or colorless. Lithic fragments include a small polygonal olivine as observed in 15445 and 15455; a plagioclase-pyroxene vitrophyre with an opaque glass which may be of mare origin; a coarse plagioclase and pyroxene radial intergrowth; and a small piece of poikilitic impact melt. The vesicular glass contains numerous breccia pieces (Fig. 2b), and is very pale colored. One large mineral clast is an ortho-pyroxene (Fig. 2a). The breccia evidently has varied sources. According to the I_s/FeO of 6 to 9 (McKay et al., 1974), revised to 9 with FeO data of Korotev (1984, unpublished), the breccia is very immature compared with typical Apollo 15 soils.

CHEMISTRY: An analysis of a breccia portion (no glass included) is given in Table 1, and its rare earths plotted in Figure 3. The incompatible elements are rather high, indicating a substantial KREEP component.

PROCESSING AND SUBDIVISIONS: 15467 was retrieved from the sample bag as two pieces (Fig. 4). A separate chip was made (,1) to produce thin section ,4. In 1983, 15467 was substantially chipped to produce interior breccia chips (,5 and ,6); the glass and breccia pieces constituting ,0 now have a mass of 0.748 g.

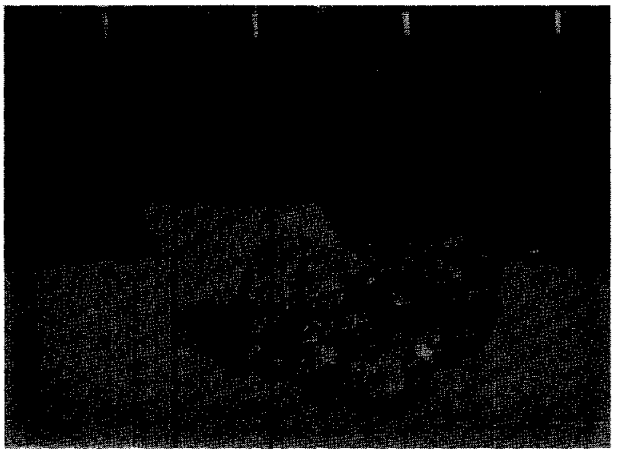

Figure 1. Main piece of 15467,0 prior to splitting. S-71-44910

Fig. 2a

Fig. 2b

Figure 2. Photomicrographs of 15467,4. Transmitted light. Widths about 2 mm. a) regolith breccia portion, showing KREEP basalt clast (center), large orthopyroxene fragment (bottom right), and glass and mineral pieces. b) vesicular glass portion, showing included regolith breccia pieces.

TABLE 15467-1. Bulk rock chemical analysis

		,5
Wt %	SiO2	
	TiO2	1.90
	Al2O3	15.7
	FeO	11.0
	MgO	9.6
	CaO	10.5
	Na2O	0.64
	K2O	
	P2O5	
(ppm)	Sc	22.6
	V	58
	Cr	2090
	Mn	1185
	Co	27.1
	Ni	63
	Rb	
	Sr	155
	Y	
	Zr	700
	Nb	
	Hf	18.3
	Ba	476
	Th	7.8
	U	2.3
	Pb	
	La	50.4
	Ce	132
	Pr	
	Nd	78
	Sm	22.8
	Eu	1.98
	Gd	
	Tb	4.39
	Dy	
	Ho	
	Er	
	Tm	
	Yb	15.6
	Lu	2.14
	Li	
	Be	
	B	
	C	
	N	
	S	
	F	
	Cl	
	Br	
	Cu	
	Zn	
(ppb)	I	
	At	
	Ga	
	Ge	
	As	
	Se	
	Mo	
	Tc	
	Ru	
	Rh	
	Pd	
	Ag	
	Cd	
	In	
	Sn	
	Sb	
	Te	
	Cs	440
	Ta	2110
	W	
	Re	
	Os	
	Ir	2.0
	Pt	
	Au	<5
	Hg	
	Tl	
	Bi	
		(1)

References and methods:

(1) Korotev (1984, unpublished); INAA

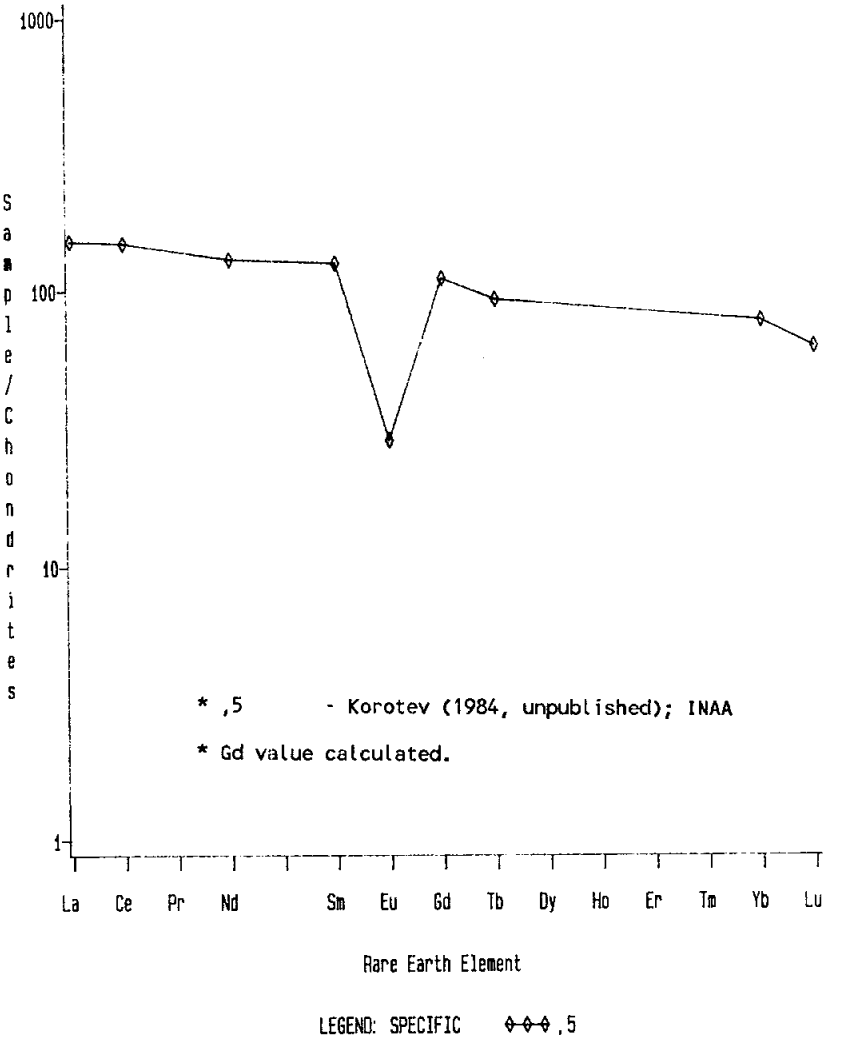

Figure 3. Rare earths in 15467 breccia.

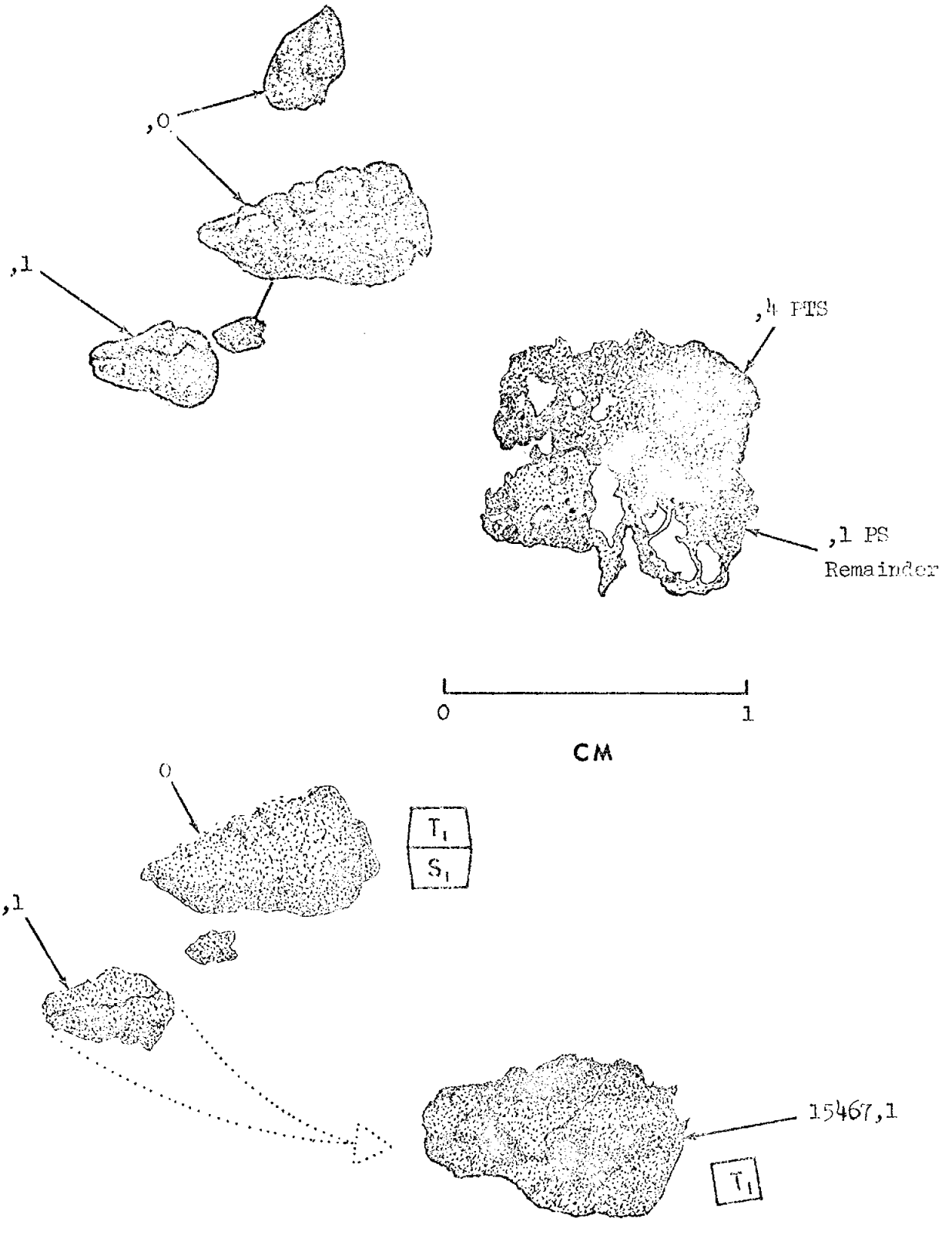

Figure 4. Original chipping of 15467.

15468 GLASSY BRECCIA ST. 7 1.3 g

INTRODUCTION: 15468 is a dark gray, very glassy breccia with an irregular surface (Fig. 1). The glass is very vesicular and encloses numerous regolith breccia fragments. The surface has no zap pits. The sample was retrieved from the same bag as 15465 and 15466, hence was collected with them just inside the north-northwest rim crest of Spur Crater and may well have once been part of one of them.

PETROLOGY: Thin section ,4 consists of a glassy regolith breccia almost completely surrounded by a very pale-colored vesicular glass. The breccia, which is not very porous, contains glass balls and shards and numerous mineral fragments, but is dominated by two KREEP basalt fragments (Fig. 2). The glass fragments are colorless (or very pale green) and pale brown where devitrified.

PROCESSING AND SUBDIVISIONS: ,0 was chipped to produce ,1 (to make thin section ,4), and now consists of 0.88 g of several pieces (Fig. 3).

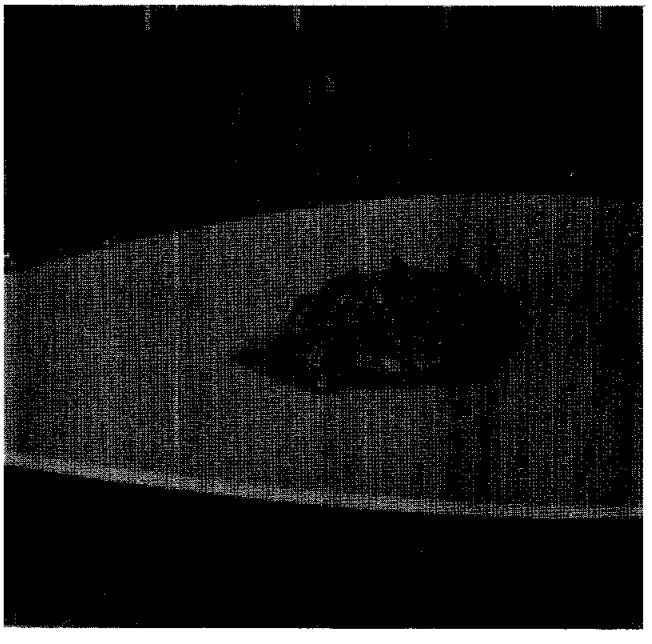

Figure 1. Pre-split view of 15468. S-71-44914

Figure 2. Photomicrograph of 15468,4 showing regolith breccia matrix, two KREEP basalt clasts, and vesicular glass (top). Transmitted light. Width about 2 mm.

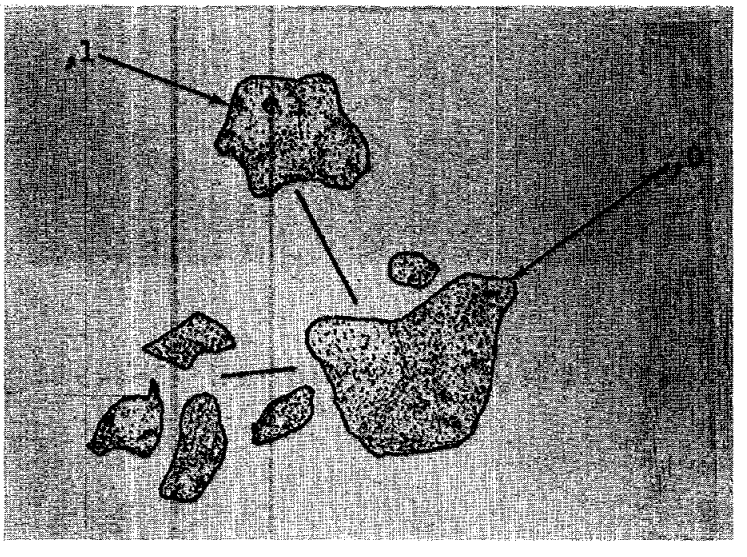

Figure 3. Chipping of 15468.

U.S. GOVERNMENT PRINTING OFFICE: 1991—561-014/40051